

Isabella Turbanti-Memmi
(Editor)

Proceedings of the 37th International Symposium on Archaeometry,

12th – 16th May 2008, Siena, Italy



 Springer

Proceedings of the 37th International Symposium on
Archaeometry

Isabella Turbanti-Memmi
Editor

Proceedings of the 37th International Symposium on Archaeometry

12th – 16th May 2008,
Siena, Italy

 Springer

Editor

Dr. Isabella Turbanti-Memmi
University of Siena
Dipartimento di Scienze della
Terra
Via Laterina 8
53100 Siena
Italy
memmi@unisi.it

ISBN 978-3-642-14677-0 e-ISBN 978-3-642-14678-7
DOI 10.1007/978-3-642-14678-7
Springer Heidelberg Dordrecht London New York

© Springer-Verlag Berlin Heidelberg 2011

This work is subject to copyright. All rights are reserved, whether the whole or part of the material is concerned, specifically the rights of translation, reprinting, reuse of illustrations, recitation, broadcasting, reproduction on microfilm or in any other way, and storage in data banks. Duplication of this publication or parts thereof is permitted only under the provisions of the German Copyright Law of September 9, 1965, in its current version, and permission for use must always be obtained from Springer. Violations are liable to prosecution under the German Copyright Law.

The use of general descriptive names, registered names, trademarks, etc. in this publication does not imply, even in the absence of a specific statement, that such names are exempt from the relevant protective laws and regulations and therefore free for general use.

Cover design: deblik, Berlin

Printed on acid-free paper

Springer is part of Springer Science+Business Media (www.springer.com)

PROCEEDINGS

37th International Symposium
on Archaeometry

May 12th – 16th 2008, SIENA, Italy

Editor

Isabella Turbanti Memmi

Associated Editors

Luis Barba Pingarron

Patrick Degryse

Henk Kars

Yannis Maniatis

Marco Martini

Josefina Perez-Antegui

Mark Pollard

Martine Regert

Thilo Rehren

Michael Tite

37th International Symposium on Archaeometry

SIENA, Italy May 12th – 16th, 2008

STANDING COMMITTEE

M.S. Tite (Oxford) President

Y. Maniatis (Athens) Chairman

L. Barba (Mexico City)

K.T. Biro (Budapest)

R.M. Farquhar (Toronto)

H. Kars (Amsterdam)

I. Turbanti Memmi (Siena)

P. Meyers (Los Angeles)

J.-F. Moreau (Chicoutimi)

J. Pérez-Arantegui (Zaragoza)

R. Tykot (Tampa)

Ch. Wang (Hefei)

S.U. Wisseman (Urbana)

*

LOCAL ORGANIZING COMMITTEE

Isabella Memmi Turbanti, Chairperson

Marco Giamello (Siena)

Gianluca Giorgi (Siena)

Elisabetta Gliozzo (Siena)

Giovanni Guasparri (Siena)

Emanuele Papi (Siena)

Alessandra Pecci (Siena)

ORGANIZING INSTITUTIONS



UNIVERSITA' DEGLI STUDI DI SIENA



With the organizing support of:



UNDER THE AUSPICES OF:



SPONSORS



Preface

On behalf of the Organizing Committee, I am pleased to present in these Proceedings volume the 95 papers that were accepted for publication, among the 125 submitted, following peer review.

We owe a great deal to the institutions and individuals who assisted us in making this Symposium possible. In particular, we would like to thank the University of Siena for providing the staff of the “Ufficio Congressi”, whose assistance was essential, and the Engineering and Humanities Faculties, who hosted the Symposium. I would also like to thank the members of the Organizing Committee, who gave me significant and much appreciated help.

This Conference could not have been carried out without the support provided by our sponsors (see next page). They included: Italian Ministry of Cultural Heritage, Regione Toscana, Fondazione Monte dei Paschi di Siena, Provincia and Comune di Siena, Fondazione Musei Senesi, Opera della Metropolitana di Siena, Associazione Italiana di Archeometria (AIAr), FEI, PANalytical, Thermo Scientific, Perkin Elmer, Bruker, Horiba Jobin-Yvon, Wiley-Blackwell, Springer, and Bancasciano.

The Symposium was held in Italy for the first time and the participants were more than 500, coming from all over the world. This huge participation demonstrates that archaeometric research is increasing, not only in quantity, but in quality as well.

The international team of convenors accepted 533 abstracts, which were compiled by approximately 1,400 authors. Eighty-one abstracts were selected for an oral presentation. The remaining 452 were posters, which was actually the highlight of the Symposium. The posters generated much discussion and allowed for more direct contact between authors and participants.

I would like to recognize the outstanding contributions of Elisabetta Gliozzo. She completed the painstaking work of editing the Abstract volume and coordinated the distribution and re-distribution of abstracts amongst the session convenors and authors.

In closing, let me remember and thank Riccardo Francovich, who passed away unexpectedly 2 years ago. Riccardo was a strong supporter of this conference, and he worked tirelessly and with enthusiasm to bring it about. If he were here today, he would certainly be pleased with what we have accomplished.

Siena, 2010

Isabella Turbanti-Memmi

Contents

Part I Ceramics, Glazes, Glass and Vitreous Materials (Technology and Provenance)	
Late Byzantine-Early Islamic Ceramic Technology, Transjordan	3
F.M. Alawneh and H.A. Béarat	
Provenance Study of Some Samples of “Compendiario” Majolica Found in Archaeological Excavations Carried Out in the Centre of Amsterdam	9
F. Amato, B. Fabbri, S. Gualtieri, J. Gawronski, and N. Jaspers	
Archaeometry of Bronze Age and Early Iron Age Italian Vitreous Materials: A Review	17
I. Angelini	
Chemical, Mineralogical and Textural Characterisation of Early Iron Age Vitreous Materials from the Golasecca Culture (Northern Italy)	25
I. Angelini, C. Nicola, G. Artioli, R. DeMarinis, M. Rapi, and M. Ubaldi	
Mapping Regional Ceramic Fabrics in Sagalassos (SW-Turkey), Dating from 500 BC–700 AD	33
D. Braekmans, B. Neyt, P. Degryse, J. Elsen, J. Poblome, and M. Waelkens	
Ethnoarchaeometric Study of the Traditional Cooking Ware Production Centre of <i>Pabillonis</i> (Sardinia): Investigating Raw Materials and Final Products	41
M.A. Cau, G. Montana, D. Pagliarello, and E. Tsantini	

Materials, Technology and Provenance of Ancient Ceiling Tiles from the Ceramic District in Riva San Vitale (Southern Switzerland)	49
G. Cavallo and M. Moresi	
An Investigation into the Ceramic Technology of the Two-Colour Tiles of “Prince Noir” Castle (Bordeaux, France, Thirteenth to Fourteenth Centuries AD)	55
B. Cicuttini, A. Ben Amara, and F. Bechtel	
Ceramic Production and Metal Working at the Trebbio Archaeological Site (Sansepolcro, Arezzo, Italy)	61
E. Gliozzo, A. Comini, A. Cherubini, A. Ciacci, A. Moroni, and I. Turbanti Memmi	
Many Potters – One Style: Pottery Production and Distribution in Transitional Late Byzantine–Early Islamic Palaestina Tertia	71
V.E. Holmqvist and M. Martínón-Torres	
Technological Features of Colonial Glazed Pottery from el Convento de Santo Domingo (Antigua, Guatemala). Similarities and Differences Between Colonial and Spanish pottery	77
J.G. Iñáñez and R.J. Speakman	
Applicability of Prompt Gamma Activation Analysis to Glass Archaeometry	83
Z. Kasztovszky and J. Kunicki-Goldfinger	
Colorants and Their Provenance of a Late Medieval Glass Goblet Found in Eger (Hungary)	91
A. Kocsonya, A. Váradi, I. Fórizs, I. Kovács, Z. Kasztovszky, and Z. Szőkefalvi-Nagy	
<i>Gnathia</i> and Red-Figured Pottery from Apulia: The Continuity of a Production Technology	99
A. Mangone, L.C. Giannossa, G. Colafemmina, R. Laviano, V. Redavid, and A. Traini	
North-Western European Forest Glass: Working Towards An Independent Means of Provenance	105
A.S. Meek, J. Henderson, and J.A. Evans	
Ceramic Production in the Indigenous Settlement of Entella (Western Sicily) During the Archaic Age	113
G. Montana, A. Corretti, A.M. Polito, and F. Spatafora	

Middle Guadiana River Basin (Badajoz, Spain and Alentejo, Portugal) Network Interactions: Insights from the Chemical Analysis of Bell Beaker Pottery and the Lead Isotope Analysis of Copper Items from the Third Millennium BC	119
C.P. Odriozola, M.A. Hunt-Ortiz, M.I. Dias, and V. Hurtado	
The Black Gloss Pottery in the Region of Ostia: Archaeology and Archaeometry	127
G. Olcese and C. Capelli	
Recognising Frit: Experiments Reproducing Post-Medieval Plant Ash Glass	133
S. Paynter and D. Dungworth	
Archaeometric Investigation of Early Iron Age Glasses from Bologna	139
A. Polla, I. Angelini, G. Artioli, P. Bellintani, and A. Dore	
Non Invasive Study of Nineteenth Century Iranian Polychrome Underglaze Painted Tiles by Fibre Optic Visible Reflectance Spectroscopy	145
I. Reiche, C. Boust, J.-J. Ezrati, S. Peschard, J. Tate, L. Troalen, B. Shah, B. Pretzel, G. Martin, S. Röhrs, and F. Voigt	
Neolithic Facies of Stentinello Culture: Analysis and Comparison of Ceramics from Capo Alfiere (Calabria) and Perriere Sottano (Sicily)	153
S. Scarcella, A. Bouquillon, and A. Leclaire	
Preliminary Archaeometric Data on Fineware from the Middle Neolithic Bükk Culture	159
V. Szilágyi, H. Taubald, T.K. Biró, S.J. Koós, P. Csengeri, M. Tóth, and Gy. Szakmány	
A Study of the Materials Used for the Inscriptions on Ceramic Vessels Excavated at Shang Dynasty Site in China	169
S. Wei, G. Song, and M. Schreiner	
A Discussion on Raw Materials Used for Ancient Chinese Porcelain	177
J. Zhu and C. Wang	

Part II Stone, Plaster and Pigments (Technology and Provenance)

Palaeolithic Paintings at Riparo Dalmeri, a Northern Italian Rock Shelter: Materials, Technologies, Techniques	187
R. Belli, G. Dalmeri, A. Frongia, S. Gialanella, M. Mattarelli, M. Montagna, and L. Toniutti	
“Ramses II in Majesty”: A Minero-Petrographic and Provenance Rock Study	193
A. Borghi, E. D’Amicone, M. Serra, G. Vaggelli, and L. Vigna	
Using Non-destructive X-Ray Fluorescence Analysis to Investigate the Prehistoric Use and Distribution of Hornfels in Southern Quebec ...	199
A.L. Burke and G. Gauthier	
Clinical Test Strips for Rapid Identification of Binder Materials in Rock Paintings	205
D. Fraser and R.A. Armitage	
Archaeometric Processing of Polished Stone Artefacts from the Ebenhöch Collection (Hungarian National Museum, Budapest, Hungary)	211
O. Friedel, B. Bradák, G. Szakmány, V. Szilágyi, and K.T. Biró	
The Colour of the Façades in Siena’s Historical Centre: Calcium Oxalate Films on Brickwork of the Fifteenth to Sixteenth Century Palaces	221
M. Giamello, F. Droghini, F. Gabbrielli, G. Guasparri, S. Mugnaini, G. Sabatini, and A. Scala	
Stone Beads from Late Bronze Age and Early Iron Age Settlements from South-Western Portugal: Analyses by X-Ray Diffraction	227
A.P. Gonçalves, A.M. Monge Soares, A.C. Silva, and L. Berrocal-Rangel	
Integrated Research on Sixteenth to Early Nineteenth Century Panel Paintings: Chromatographic and Spectroscopic Characterisation of Paint Layers	233
E. Kouloumpi, G. Lawson, and V. Pavlidis	
A Diptich by Marcellus Coffermans Analysed by Portable XRF	239
A. Križnar, M.V. Muñoz, F. de La Paz, M.A. Respaldiza, and M. Vega	
The Analysis of “San He Tu” from the Haizi and Weizi Emplacements at the Tianjin Dagu Site	247
N. Li, Z. Guo, Z. Zhang, and D. Wang	

Neolithic Obsidian Economy Around the Monte Arci Source (Sardinia, Italy): The Importance of Integrated Provenance/Technology Analyses ...	255
C. Lugliè, F.X. Le Bourdonnec, and G. Poupeau	
Mineralogical Characterization of the Weathering Crusts Covering the Ancient Wall Paintings of the Festival Temple of Thutmosis III, Karnak Temple Complex, Upper Egypt	261
H.H.M. Mahmoud, N.A. Kantiranis, and J.A. Stratis	
Scientific Characterization of Roman Age Over-Paintings at Luxor Temple, Upper Egypt: Preliminary Results	267
H.H.M. Mahmoud, N.A. Kantiranis, E. Pavlidou, and J.A. Stratis	
Gilding Techniques in Mural Paintings: Three Examples from the Romanesque Period in France	273
A. Mounier, F. Daniel, and F. Bechtel	
The Basalts of the Independent State of Samoa	279
L.A. Pavlish, R.G.V. Hancock, and A.C. D'Andrea	
Petrographic and Geochemical Investigation of Sarmatian Grinding Stones from the Űllő 5 Site, North Hungary	285
B. Péterdi, G. Szakmány, K. Judik, G. Dobosi, Z. Kasztovszky, and V. Szilágyi	
Brick-Lime Mortars and Plasters of a Sixteenth Century Ottoman Bath from Budapest, Hungary	293
F. Pintér, J. Weber, B. Bajnóczi, and M. Tóth	
Manufacturing Analysis and Non Destructive Characterisation of Green Stone Objects from the Tenochtitlan Temple Mayor Museum, Mexico	299
J.L. Ruvalcaba, E. Melgar, and Th. Calligaro	
Traces of Ancient Treatments on the Stone Materials of the Main Façade of the Siena Cathedral: Glazings (Calcium Oxalate Films s.s.) and Other Finishes	305
G. Sabatini, F. Droghini, M. Giamello, G. Guasparri, S. Mugnaini, and A. Scala	
Investigating Trade and Exchange Patterns in Prehistory: Preliminary Results of the Archaeometric Analyses of Stone Artefacts from Tell Gorzsa (South-East Hungary)	311
Gy. Szakmány, E. Starnini, F. Horváth, and B. Bradák	

Intra-site Obsidian Subsource Patterns at Contraguda, Sardinia (Italy)	321
R.H. Tykot, L. Lai, and C. Tozzi	
The Characterisation of Lime Plasters from Lamanai, Belize: A Diachronic Approach to the Study of Architectural Practices	329
I. Villasenor, E. Graham, R. Siddall, and C.A. Price	
Provenance Studies of Midwestern Pipestones Using a Portable Infrared Spectrometer	335
S.U. Wisseman, T.E. Emerson, R.E. Hughes, and K.B. Farnsworth	
Application of Micro-CT: 3D Reconstruction of Tool Marks on an Ancient Stone Bead and its Implication for Jade Drilling Techniques	343
Y. Yang, M. Yang, Y. Xie, and C. Wang	
Non Destructive In Situ Study of Mexican Codices: Methodology and First Results of Materials Analysis for the Colombino and Azoyu Codices	349
S. Zetina, J.L. Ruvalcaba, M. Lopez Cáceres, T. Falcón, E. Hernández, C. González, and E. Arroyo	
MissMarble, an Interdisciplinary Data Base of Marble for Archaeometric, Art History and Restoration Use	355
J. Zöldföldi, P. Hegedüs, and B. Székely	
Part III Micro-Nano Diagnostic and Ancient Technology	
Look Into the Objects: Why? Cultural Heritage Motivations of Neutron-Based Imaging Techniques	365
K.T. Biró and É. Durkovic, S. Farkas-Szóke, and The Ancient Charm Collaboration	
Nano-Scale Investigation of Some Dichroic/Opalescent Archaeological Materials	371
D. Dungworth and S. Paynter	
Sieneese “Archaic” Majolica: Characterisation of Enamels and Glazes by Analytical-Transmission Electron Microscopy (AEM-TEM)	377
G. Giorgetti, C. Fortina, I. Turbanti Memmi, and A. Santagostino Barbone	
From Micro- to Nano-Arrangement: Alteration Products in Archaeological Glass from Marine and Land-Based Environments	383
A. Silvestri, C. Viti, G. Molin, and G. Salviulo	

An Investigation of the Sulfur–Iron Chemistry in Timbers of the Sixteenth Century Warship, the <i>Mary Rose</i>, by Synchrotron Micro-X-Ray Spectroscopy	389
A.D. Smith, M. Jones, A. Berko, A.V. Chadwick, R.J. Newport, T. Skinner, M. Salomé, J. Frederick, and W. Mosselmans	
The Role of TOF-SIMS in the Characterisation of Inorganic and Organic Components in Paint Samples	395
A. Tognazzi, F. Benetti, R. Lapucci, and C. Rossi	
Part IV Bioarchaeology	
Provenance Study of Wood Found in Archaeological and Architectural Objects	405
S. Fossati, G.L.A. Pesce, and A. Decri	
Hormone Mass Fingerprinting: Novel Molecular Sex Determination of Ancient Human Skeletal Remains	411
L. Mark, Z. Patonai, A. Vaczy, N. Kajsza, and A. Marcsik	
Hair: An Untapped Forensic Resource	417
N.C. McCreesh, A.P. Gize, and A.R. David	
Archaeobotany as an <i>In-Site/Off-Site</i> Tool for Paleoenvironmental Research at Pulo di Molfetta (Puglia, South-Eastern Italy)	421
M. Primavera and G. Fiorentino	
Analysis of Archaeological Bones for the Purpose of Reconstructing the Paleodiet of Medieval Inhabitants	427
V. Rudovica, A. Viksna, G. Zarina, and I. Melne	
Integrating Stable Isotopes to the Study of the Origin of Management Strategies for Domestic Animals: $\delta^{13}\text{C}$ and $\delta^{18}\text{O}$ Results from Bioapatite Enamel of Cattle from the Tell Halula Site, Syria (7800–7000 BC)	435
C. Tornero and M. Saña	
Chemical Analysis of Hair Segments and Short-Term Dietary Variation: Results for the Ancient Site of Chongos (Peru)	441
R.H. Tykot, A. Metroka, M. Dietz, and R.A. Bergfield	
Distinguishing Between Reindeer Antler and Bone Using Raman Spectroscopy	447
J. Watson and C.C. Nordby	

Part V Food Preparation and Consumption in Antiquity

- Fish-Based Subproducts in Late Antiquity. Archaeometric and Archaeological Evidence from the Fish Factories at Traducta (Algeciras, Cádiz, Spain)** 453
S. Dominguez-Bella and D. Bernal Casasola

- Chemical Analyses of Floors at San Genesio (San Miniato, Pisa): A Medieval Tavern** 459
F. Inserra and A. Pecci

- Food Habits and Social Identity During the Archaic Age: Chemical Analyses of Organic Residues Found on Pottery Vessels from the Messapian Settlement of San Vito dei Normanni (South-Eastern Italy)** 465
F. Notarstefano, M. Lettieri, G. Semeraro, and L. Troisi

- Finding Food While Protecting Pots: A Non-Destructive Protocol for Absorbed Residue Analysis** 473
J.M. Vanderveen

Part VI Archaeochronometry

- ESR and U/Th Dating Methodologies Applied to Carbonates from Southern Italy** 481
J.J. Bahain, G. Burrafato, C. Falguères, A.M. Gueli, G. Stella, S.O. Troja, and A.R. Zuccarello

- The *Mezza Spiaggia* Tower (Cagliari, Italy): The Dating of Structures by the Metrological–Chronological Analysis of Masonry and the Petro-Geochemical Stratigraphy of Building Materials** 489
C. Giannattasio and S.M. Grillo

- Preliminary Results of Magnetic Archaeointensity Measurements in Brazil** 495
G.A. Hartmann, M.C. Afonso, and R.I.F. Trindade

- The Dating of a Sixteenth Century Settlement in the Vicinity of Quebec City (Canada) by Means of Elemental Analysis of Glass Beads Through Thermal and Fast Neutron Activation Analyses** 501
J.F. Moreau, B. Gratuze, R.G.V. Hancock, and M. Blet Lemarquand

Faster and More Accurate Processing of Samples for Microtephrochronology	509
J. Watson, C.A. Tryon, and M.C. Vicéns	
Part VII Recent Development in Radiocarbon Dating	
The Radiocarbon Dating of Mortars from <i>Wielka Waga</i>, The Great Scales Building in The Krakow Market Square	517
D. Nawrocka and J. Michniewicz	
Part VIII Field Archaeology	
Combination of Non-Destructive Methods for the Observation of the State of Subsurface Preservation of Ploughed Archaeological Sites: A Case Study from Oppidum Stradonice in Bohemia	527
R. Křivánek	
The Different Possibilities for Collaboration Between Geophysical and Archaeological Methods in the Context of the Research Project “Neglected Archaeology” of the Department of Archaeology of the University of West Bohemia in Pilsen	533
R. Křivánek	
Comparative Archaeometric Analysis by 3D Laser, Short Range Photogrammetry, and Hyperspectral Remote Sensing Applied to the Celtiberian City-State of Segeda	541
J.G. Rejas, M. Farjas, F. Burillo, R. López, M.A. Cano, M.E. Sáiz, T. Mostaza, and J.J. Zancajo	
Part IX Human-Environment Interaction	
Shell Mounds in Brazilian Coast: Integrating Archaeological and Environmental Studies	549
M.C. Afonso and M.C. Tenório	
Hydraulic Systems in the Po Plain (Northern Italy) During the Bronze Age: Archaeology and Geoarchaeology	555
M. Cremaschi and C. Pizzi	
Cultural Landscapes of South-Eastern Rhodope: The Transition from Byzantine to Modern Times	561
M. Kampa, M.K. Sioliou, P. Kaparti, E. Tsirimoná, and I. Ispikoudis	

**Part X Metals and Metallurgical Ceramics
(Technology and Provenance)**

XRF Analyses of Four Silver Gilded Hellenistic Epaulettes	569
E. Asderaki-Tzoumerkioti and A.G. Karydas	
The Use of Industrial Computed Tomography in the Study of Archaeological Finds	575
A. Berdondini, R. Brancaccio, V. D'Errico, A. Miceli, M. Bettuzzi, F. Casali, M.P. Morigi, M. Senn, and A. Flisch	
Arabic Coins as a Silver Source for Slavonic and Scandinavian Jewellers in the Tenth Century AD	579
N. Eniosova and R. Mitoyan	
Neutron-Based Analytical Methods for the Non-Invasive Characterisation of Iron Artefacts	585
E. Godfrey and W. Kockelmann	
Corrosion Studies and Lead Isotope Analyses of Musket Balls from Scottish Battlefield Sites	591
A.J. Hall, R. Ellam, L. Wilson, T. Pollard, and N. Ferguson	
Non-Destructive and Minimally Invasive Analyses of Bronze Seal Boxes from <i>Augusta Raurica</i> by Micro X-Ray Fluorescence Spectrometry, Raman Spectroscopy and FTIR Spectroscopy	599
K. Hunger, E. Hildbrand, V. Hubert, M. Wörle, A.R. Furger, and M. Wartmann	
A Multi-Disciplinary Approach to the Study of An Assemblage of Copper-Based Finds Assigned to the Prehistory and Proto-History of Fucino, Abruzzo, Italy	605
M.L. Mascelloni, G. Cerichelli, and S. Ridolfi	
Copper-Based Kettles from Brador: A Contribution to the Study of Eastern Settlements of New France on the Northern Shore of the Estuary of the Saint-Lawrence (Quebec, Canada)	611
J.-F Moreau and R.G.V. Hancock	
On the Gold Adornments from Apahida-Fifth Century AD, Transylvania, Romania	617
G. Niculescu, R. Oanță-Marghitu, and M. Georgescu	

Non Destructive In Situ Analysis of Gold and Silver Artifacts from Tomb 7 of Monte Alban, Oaxaca, Mexico	623
G. Peñuelas, J.L. Ruvalcaba, J. Contreras, E. Hernández, and E. Ortiz	
“Harvesting” the Ore: The Use of Iron Seepages in the Early Bloomery Furnace in Ireland	629
E. Photos-Jones and A.J. Hall	
Analysis of Gold Jewellery by PIXE and SEM–EDS: A Comparison of Ancient and Modern Productions	637
V. Virgili and M.F. Guerra	
Part XI Integrated Site Studies	
Reconstructing the Lost Moregine Site: A VR Based Approach to Simulate and Navigate an Inaccessible Archaeological Excavation ...	645
A.F. Abate, S.C. Nappo, T. Paduano, and S. Ricciardi	
The Study of the Fourth Millennium Mud-Bricks at Arslantepe: Malatya (Turkey): Preliminary Results	651
C. Alvaro, M. Frangipane, G. Liberotti, R. Quaresima, and R. Volpe	
Intra-Site Testing Using Magnetometry and Shovel Test Pits in the Podere Funghi near Poggio Colla (Florence, Italy)	657
R. Sternberg and S. Bon-Harper	

Contributors

A.F. Abate Dipartimento di Matematica e Informatica, Università degli Studi di Salerno, 84084 Fisciano, (SA), Italy, abate@unisa.it

M.C. Afonso Museu de Arqueologia e Etnologia, Universidade de São Paulo, São Paulo, Brazil

F.M. Alawneh Queen Rania's Institute of Tourism and Heritage, The Hashemite University, Zarqa, Jordan, firas-alawneh@hu.edu.jo

C. Alvaro Department of Historical, Archaeological and Anthropological Sciences, University of Rome "La Sapienza", P.le Aldo Moro 5, 00185 Roma, Italy, jovina@inwind.it

F. Amato CNR-ISTEC, National Research Council, Institute of Science and Technology for Ceramics, Faenza (Ravenna), Italy; University of Ferrara, Ferrara, Italy, francesca.amato@istec.cnr.it

I. Angelini Dip. di Geoscienze, Università degli Studi di Padova, Via Giotto 1, 35137 Padova, Italy, ivana.angelini@unipd.it

R.A. Armitage Department of Chemistry, Eastern Michigan University, Ypsilanti, MI 48197, USA

E. Arroyo Instituto de Investigaciones Estéticas, UNAM, Mexico City, Mexico

G. Artioli Dip. di Geoscienze, Università degli Studi di Padova, Via Giotto 1, 35137 Padova, Italy, gilberto.artioli@unipd.it

E. Asderaki-Tzoumerkioti 13th Ephorate of Prehistoric and Classical Antiquities, Athanassaki 1, 38222 Volos, Greece, e.asderaki@gmail.com

H.A. Béarat LECSSS, School of Materials, Arizona State University, Tempe 85287-1704, AZ, USA

J.J. Bahain Département de Préhistoire, Muséum National d'Histoire Naturelle, UMR 5198 du CNRS, 1 rue René Panhard, 75013 Paris, France

B. Bajnóczi Hungarian Academy of Sciences, Institute for Geochemical Research, Budaörsi út 45, 1112 Budapest, Hungary

F. Bechtel Institut de Recherche sur les Archéomatériaux, Centre de Recherche en Physique Appliquée à l'Archéologie, Maison de l'Archéologie, Esplanade des Antilles, Université de Bordeaux – CNRS, UMR 5060, F-33607 Pessac, France

R. Belli Dipartimento di Fisica, Università di Trento, Via Sommarive 14, 38050 Povo (TN), Italy, toniutti@science.unitn.it

P. Bellintani Soprintendenza per i Beni Archeologici della Provincia Autonoma di Trento, Via Aosta 1, 38100 Trento, Italy, paolo.bellintani@provincia.tn.it

A. Ben Amara Institut de Recherche sur les Archéomatériaux, Centre de Recherche en Physique Appliquée à l'Archéologie, Maison de l'Archéologie, Esplanade des Antilles, Université de Bordeaux – CNRS, UMR 5060, F-33607 Pessac, France

F. Benetti Department of Chemical and Biosystem Sciences, University of Siena, Via A. Moro 2, Siena, Italy; Inter-University Center of Colloid and Surface Science - CSGI, Via della Lastruccia 3, Sesto Fiorentino, Florence, Italy

A. Berdondini Department of Physics, Università di Bologna, C.Berti Pichat 6/2, 40127 Bologna, Italy, andrea.berdo@libero.it

R.A. Bergfield Department of Anthropology, University of Missouri-Columbia, Columbia, MO 65211, USA

A. Berko University of Kent, Canterbury CT2 7NH, UK

D. Bernal Casasola Department of History, Geography and Philosophy, University of Cádiz, Cádiz, Spain

L. Berrocal-Rangel Universidad Autónoma de Madrid, Ciudad Universitaria de Cantoblanco, 28049 Madrid, Spain

M. Bettuzzi Department of Physics, Università di Bologna, C.Berti Pichat 6/2, 40127 Bologna, Italy

K.T. Biró Hungarian National Museum, Budapest, Hungary, tbk@ace.hu

M. Blet Lemarquand Institut de Recherche sur les Archéomatériaux (IRAMAT), Centre Ernest Babelon, CNRS UMR5060, Université d'Orléans, Orléans, France, lemarquand@cnrs-orleans.fr

S. Bon-Harper Monticello Department of Archaeology, PO Box 316, Charlottesville, VA 22902, USA

A. Borghi Dipartimento di Scienze Mineralogiche e Petrologiche, Via V. Caluso, 35, 10125 Torino, Italy, alessandro.borghi@unito.it

A. Bouquillon Centre de Recherche et des Restauration des Musées de France, CNRS UMR 171, 6, rue des Pyramides, 75041 Paris, France

F.X. Le Bourdonnec Institut de Recherche sur les Archéomatériaux, UMR 5060, CNRS, Université Bordeaux-3, Maison de l'Archéologie, esplanade des Antilles, 33607 Pessac, France, françois.lebourdonnec@etu.u-bordeaux3.fr

C. Boust Laboratory of the Centre for research and restoration of the French Museums. (LC2RMF), UMR 171 CNRS French Ministry of Culture and Communication, Palais du Louvre, 14 quai François Mitterrand, 75001 Paris, France

B. Bradák Department of Physical Geography, Eötvös Loránd University, Pázmány P. sétány 1/c, 1117 Budapest, Hungary

D. Braekmans Section Geology, Earth & Environmental Sciences, Celestijnenlaan 200 E, bus 2408, 3001 Leuven, Belgium, dennis.braekmans@ees.kuleuven.be

R. Brancaccio Department of Physics, Università di Bologna, C.Berti Pichat 6/2, 40127 Bologna, Italy

F. Burillo Faculty of Humanities and Social Sciences of Teruel, University of Zaragoza (UZ), Zaragoza, Spain

A.L. Burke Département d'anthropologie, Université de Montréal, C.P. 6128, succursale Centre-ville Montréal, Montreal, QC, Canada H3C 3J7, adrian.burke@umontreal.ca

G. Burrafato LDL & BBCC, Laboratorio di Datazione tramite Luminescenza e di Metodologie Fisiche applicate ai Beni Culturali del Dipartimento di Fisica e Astronomia, Università di Catania and INFN Sezione di Catania, via Santa Sofia 64, 95123 Catania, Italy

Th. Calligaro Centre de Recherche et de Restauration des Musées de France, UMR 171 du CNRS, Paris, France

M.A. Cano Faculty of Humanities and Social Sciences of Teruel, University of Zaragoza (UZ), Zaragoza, Spain

C. Capelli Dipartimento per lo Studio del Territorio e delle sue Risorse, Università di Genova, Genova, Italy, capelli@dipteris.unige.it

F. Casali Department of Physics, Università di Bologna, C.Berti Pichat 6/2, 40127 Bologna, Italy

M.A. Cau Institució Catalana de Recerca i Estudis Avançats (ICREA), Universitat de Barcelona, Barcelona, Italy; Equip de Recerca Arqueomètrica de la Universitat de Barcelona (ERAUB), Barcelona, Italy, macau@ub.edu

G. Cavallo Lab. Tecnico Sperimentale, Environment Construction and Design Dpt, University of Applied Sciences of Southern Switzerland, P.O. Box 12, 6952 Canobbio, Switzerland, giovanni.cavallo@supsi.ch

G. Cerichelli Department of Chemistry, Chemical Engineering and Materials, University of L'Aquila, Via Vetoio (Coppito 1), 67010 Coppito, L'Aquila, Italy, cerichel@univaq.it

A.V. Chadwick University of Kent, Canterbury CT2 7NH, UK

A. Cherubini Department of Archaeology and History of Arts, University of Siena, Siena, Italy

A. Ciacci Department of Archaeology and History of Arts, University of Siena, Siena, Italy

B. Cicutti Institut de Recherche sur les Archéomatériaux, Centre de Recherche en Physique Appliquée à l'Archéologie, Maison de l'Archéologie, Esplanade des Antilles, Université de Bordeaux – CNRS, UMR 5060, F-33607 Pessac, France, cicuttinibeatrice@yahoo.fr

G. Colafemmina Department of Chemistry, University of Bari, Via Orabona 4, Bari, Italy

A. Comini Department of Archaeology and History of Arts, University of Siena, Siena, Italy

J. Contreras Escuela Nacional de Conservación, Restauración y Museografía, INAH, Mexico D.F., Mexico

A. Corretti Laboratorio di Storia, Archeologia e Topografia del Mondo antico, Scuola Normale Superiore di Pisa, Pisa, Italy

M. Coutinho Afonso Museu de Arqueologia e Etnologia, Universidade de São Paulo, São Paulo, Brazil, marisa.afonso@usp.br

M. Cremaschi Dipartimento di Scienze della Terra “A. Desio”, Università degli Studi di Milano, Milano, Italy, mauro.cremaschi@unimi.it

P. Csengeri Herman Ottó Museum, Miskolc, Hungary

E. D’Amicone Soprintendenza Archeologica per il Piemonte e del Museo Antichità Egizie, Via Accademia delle Scienze, 6, 10123 Torino, Italy

A.C. D’Andrea Department of Archaeology, Simon Fraser University, Burnaby, BC, Canada V5A 1S6

V. D’Errico Department of Physics, Università di Bologna, C.Berti Pichat 6/2, 40127 Bologna, Italy

G. Dalmeri Museo Tridentino di Scienze Naturali, via Calepina 14, 38100 Trento, Italy

F. Daniel Institut de Recherche sur les Archéomatériaux (IRAMAT), Centre de Recherche en Physique Appliquée à l’Archéologie, UMR 5060-IRAMAT, Université de Bordeaux/CNRS, 33607 Pessac Cedex, France, fdaniel@u-bordeaux3.fr

A.R. David The KNH Centre for Biomedical Egyptology, F Floor The Mill, The University of Manchester, PO Box 88, Manchester M60 1QD UK

A. Decri Institute of the History of Material Culture (ISCUM), c/o Museum of St. Agostino, Piazza Sarzano, 35r 16128 Genoa, Italy

P. Degryse Section Geology, Earth & Environmental Sciences, Celestijnenlaan 200 E, bus 2408, 3001 Leuven, Belgium

R. DeMarinis Università degli Studi di Milano, Dip. di Scienze dell’Antichità, Via Festa del Perdono 7, I-20122 Milano, Italy, raffaele.demarinis@unimi.it

F. de La Paz Museo de Bellas Artes, Plaza del Museo 9, 41001 Seville, Spain

M.I. Dias Instituto Tecnológico e Nuclear, Estrada Nacional 10, 2686-953 Sacavém, Portugal

M. Dietz Department of Anthropology, University of Missouri-Columbia, Columbia, MO 65211, USA

G. Dobosi Hungarian Academy of Sciences, Institute of Geochemical Research, Budapest, Hungary

S. Dominguez-Bella Department of Geology, University of Cádiz, Cádiz, Spain, salvador.dominguez@uca.es

A. Dore Museo Civico Archeologico di Bologna, Via dell'Archiginnasio 2, 40124 Bologna, Italy, anna.dore@comune.bologna.it

F. Droghini Dipartimento di Scienze Ambientali, U.R. Conservazione del Patrimonio Culturale Lapideo, Università degli Studi di Siena, Via Laterina 8, 53100 Siena, Italy

D. Dungworth English Heritage, Fort Cumberland, Fort Cumberland Road, Eastney, Portsmouth PO4 9LD, UK

É. Durkovic Department of Archaeology, ELTE University, Budapest, Hungary

R. Ellam Scottish Universities Environmental Research Centre, East Kilbride, UK

J. Elsen Section Geology, Earth & Environmental Sciences, Celestijnenlaan 200 E, bus 2408, 3001 Leuven, Belgium

T.E. Emerson Illinois Transportation Archaeological Research Program, University of Illinois at Urbana, Champaign, IL, USA

N. Eniosova Department of Archaeology, Moscow State University, Lomonosovsky prospect 27-4, 119992 Moscow, Russia, eniosova@inbox.ru

J.A. Evans NERC Isotope Geosciences Laboratory, Keyworth NG12 5GG UK

J.-J. Ezrati Laboratory of the Centre for research and restoration of the French Museums. (LC2RMF), UMR 171 CNRS French Ministry of Culture and Communication, Palais du Louvre, 14 quai François Mitterrand, 75001 Paris, France

I. Fórizs Institute for Geochemical Research of the Hungarian Academy of Sciences, Budapest, Hungary

B. Fabbri CNR-ISTEC, National Research Council, Institute of Science and Technology for Ceramics, Faenza (Ravenna), Italy

T. Falcón Instituto de Investigaciones Estéticas, UNAM, Mexico City, Mexico

C. Falguères Département de Préhistoire, Muséum National d'Histoire Naturelle, UMR 5198 du CNRS, 1 rue René Panhard, 75013 Paris, France

M. Farjas E.T.S.I. in Topography, Geodesy, and Cartography, Polytechnic University of Madrid (UPM), Madrid, Spain

S. Farkas-Szöke Hungarian National Museum, Budapest, Hungary

K.B. Farnsworth Illinois Transportation Archaeological Research Program, University of Illinois at Urbana, Champaign, IL, USA

N. Ferguson Department of Archaeology, Centre for Battlefield Archaeology, University of Glasgow, Glasgow, UK

G. Fiorentino Laboratory of Archaeobotany and Paleoecology, Department of Cultural Heritage, Salento University, Via D. Birago, 64 - 73100 Lecce, Italy, charcoal@unile.it

A. Flisch Empa – Swiss Federal Laboratories for Materials Testing and Research, Ueberlandstrasse 129, 8600 Duebendorf, Switzerland

C. Fortina Dipartimento di Scienze della Terra, Università di Pavia, Pavia, Italy

S. Fossati Institute of the History of Material Culture (ISCUM), c/o Museum of St. Agostino, Piazza Sarzano, 35r 16128 Genoa, Italy, dendrolab@iscum.it

M. Frangipane Department of Historical, Archaeological and Anthropological Sciences, University of Rome “La Sapienza”, P.le Aldo Moro 5, 00185 Roma, Italy

D. Fraser Chemistry Department, Lourdes College, 6832 Convent Blvd, Sylvania, OH 43560 USA, dfraser@lourdes.edu

J. Frederick Diamond Light Source, Didcot OX11 0DE, UK

O. Friedel Department of Petrology and Geochemistry, Eötvös Loránd University, Budapest, Hungary, tolleetlege@gmail.com

A. Frongia Dipartimento di Ingegneria dei Materiali e T.I, Università di Trento, Via Mesiano 77, 38050 Povo (TN), Italy

A.R. Furger Augusta Raurica, Giebenacherstrasse 17, CH-4302 Augst, Switzerland

F. Gabbrielli Dipartimento di Archeologia e Storia delle Arti, Università degli Studi di Siena, Via Roma 56, 53100 Siena, Italy

G. Gauthier Département de chimie, Université de Montréal, Montreal, QC, Canada

J. Gawronski Bureau Monumenten en Archeologie, Afdeling Archeologie, Amsterdam, The Netherlands

M. Georgescu National Research Institute for Conservation and Restoration, 12 Calea Victoriei, 030026 Bucharest, Romania

S. Gialanella Dipartimento di Ingegneria dei Materiali e T.I, Università di Trento, Via Mesiano 77, 38050 Povo (TN), Italy

M. Giamello Dipartimento di Scienze Ambientali, U.R. Conservazione del Patrimonio Culturale Lapideo, Università degli Studi di Siena, Via Laterina 8, 53100 Siena, Italy, giamello@unisi.it

C. Giannattasio Department of Architecture, University of Cagliari, Via Corte d'Appello, 87 - 09124 Cagliari, Italy, cgiannatt@unica.it

L.C. Giannossa Department of Chemistry, University of Bari, Via Orabona 4, Bari, Italy

G. Giorgetti Dipartimento di Scienze della Terra, Università di Siena, Siena, Italy, giorgettig@unisi.it

A.P. Gize School Earth Atmospheric Environmental Sciences, University of Manchester, Manchester M13 9PL, UK

E. Gliozzo Department of Earth Sciences, University of Siena, Siena, Italy, gliozzo@unisi.it

E. Godfrey STFC Rutherford Appleton Laboratory, Isis Neutron Facility, Harwell OX11 0QX UK, evelyne.godfrey@stfc.ac.uk

A.P. Gonçalves Instituto Tecnológico e Nuclear, Estrada Nacional 10, 2686-953 Sacavém, Portugal, apg@itn.pt

C. González Biblioteca Nacional de Antropología e Historia, INAH, Mexico City, Mexico

E. Graham University College, London, UK

B. Gratuze Institut de Recherche sur les Archéomatériaux (IRAMAT), Centre Ernest Babelon, CNRS UMR5060, Université d'Orléans, Orléans, France, gratuze@cnsr-orleans.fr

S.M. Grillo Department of Geo-engineering and Environmental Technologies
Piazza d'Armi, University of Cagliari, 16 - 09123 Cagliari, Italy, grillo@unica.it

S. Gualtieri CNR-ISTEC, National Research Council, Institute of Science and
Technology for Ceramics, Faenza (Ravenna), Italy

G. Guasparri Dipartimento di Scienze Ambientali, U.R. Conservazione del Patri-
monio Culturale Lapideo, Università degli Studi di Siena, Via Laterina 8, 53100
Siena, Italy

A.M. Gueli LDL & BBCC, Laboratorio di Datazione tramite Luminescenza e di
Metodologie Fisiche applicate ai Beni Culturali del Dipartimento di Fisica e Astro-
nomia, Università di Catania and INFN Sezione di Catania, via Santa Sofia 64,
95123 Catania, Italy

M.F. Guerra Centre de Recherche et de Restauration des Musées de France, UMR
171 CNRS, Palais du Louvre, Paris, France, maria.guerra@culture.gouv.fr

Z. Guo Department of Scientific History and Archaeometry, Graduate University
of Chinese Academy of Sciences, Beijing 100049 People's Republic of China

A.J. Hall Department of Archaeology, University of Glasgow, Glasgow, UK,
a.hall@archaeology.arts.gla.ac.uk

R.G.V. Hancock Department of Medical Physics and Applied Radiation Sciences
and department of Anthropology, McMaster University, Hamilton, ON, Canada
L8S 4K1, ronhancock@ca.inter.net

G.A. Hartmann Departamento de Geofísica, Instituto de Astronomia, Geofísica
e Ciências Atmosféricas, Universidade de São Paulo, São Paulo, Brazil,
gelvam@iag.usp.br, gelvam@gmail.com

P. Hegedüs Arany János út 1, 7754 Bóly, Hungary

J. Henderson Department of Archaeology, The University of Nottingham,
Nottingham NG7 2RD, UK

E. Hernández Instituto de Investigaciones Estéticas, UNAM, Mexico City,
Mexico

E. Hildbrand Swiss National Museum Zurich, Collection Centre, Lindenmoos-
strasse 1, CH-8910 Affoltern a.A, Switzerland

V.E. Holmqvist Institute of Archaeology, University College London, 31–34
Gordon Square, London WC1H 0PY UK, v.holmqvist@ucl.ac.uk

F. Horváth Móra Ferenc Museum, Roosevelt tér 1-3, 6720 Szeged, Hungary

V. Hubert Swiss National Museum Zurich, Collection Centre, Lindenmoosstrasse 1, CH-8910 Affoltern a.A, Switzerland

R.E. Hughes Illinois State Geological Survey, University of Illinois at Urbana, Champaign, IL, USA

K. Hunger Swiss National Museum Zurich, Collection Centre, Lindenmoosstrasse 1, CH-8910 Affoltern a.A, Switzerland, katja.hunger@slm.admin.ch

M.A. Hunt-Ortiz Departamento de Prehistoria y Arqueología, Universidad de Sevilla, C/María de Padilla S/N, 41004 Sevilla, Spain

V. Hurtado Departamento de Prehistoria y Arqueología, Universidad de Sevilla, C/María de Padilla S/N, 41004 Sevilla, Spain

J.G. Iñáñez Museum Conservation Institute, Smithsonian Institution, 4210 Silver Hill Road, Suitland, MD 20746, USA, inanezj@si.edu

F. Inserra Archaeometric Laboratory, Department of Archaeology and History of Art, University of Siena, via Roma, 56, 53100 Siena, Italy, fernandainserra@hotmail.it

I. Ispikoudis Laboratory of Rangeland Ecology (286), Aristotle University of Thessaloniki, 54124 Thessaloniki, Greece

N. Jaspers Bureau Monumenten en Archeologie, Afdeling Archeologie, Amsterdam, The Netherlands

M. Jones The Mary Rose Trust, Portsmouth PO1 3LX, UK

K. Judik Hungarian Academy of Sciences, Institute of Geochemical Research, Budapest, Hungary

R. Křivánek Institute of Archaeology of the Academy of Sciences of the Czech Republic, Prague, v.v.i., Letenská 4, 118 00 Prague 1, Czech Republic; Department of Archaeology, University of West Bohemia in Pilsen, Sedláčkova 15, 306 14 Pilsen, Czech Republic, krivanek@arup.cas.cz

N. Kajsza Institute of Biochemistry and Medical Chemistry, University of Pécs, Szigeti str.12, 7624 Pécs, Hungary

M. Kampa Laboratory of Rangeland Ecology (286), Aristotle University of Thessaloniki, 54124 Thessaloniki, Greece, mariakampa97@hotmail.com

N.A. Kantiranis Department of Mineralogy-Petrology-Economic Geology, Aristotle University, 54124 Thessaloniki, Greece

P. Kaparti Laboratory of Rangeland Ecology (286), Aristotle University of Thessaloniki, 54124 Thessaloniki, Greece

A.G. Karydas Institute of Nuclear Physics, NCSR “Demokritos”, 153 10 Aghia Paraskevi, Athens, Greece, karydas@inp.demokritos.gr

Z. Kasztovszky Institute of Isotopes, Hungarian Academy of Sciences, Konkoly Thege str. 29-33, 1121 Budapest, Hungary, kzsolt@iki.kfki.hu

S.J. Koós Herman Ottó Museum, Miskolc, Hungary

W. Kockelmann STFC Rutherford Appleton Laboratory, Isis Neutron Facility, Harwell OX11 0QX, UK

A. Kocsonya KFKI Research Institute for Particle and Nuclear Physics of the Hungarian Academy of Sciences, Budapest, Hungary

E. Kouloumpi Laboratory of Physicochemical Research, National Gallery – Alexandros Soutzos Museum, 1 Michalacopoulou Street, 11601 Athens, Greece, elenikouloumpi@nationalgallery.gr

I. Kovács KFKI Research Institute for Particle and Nuclear Physics of the Hungarian Academy of Sciences, Budapest, Hungary

A. Križnar Centro Nacional de Aceleradores (CNA), University of Seville, Avda. Thomas A. Edison 7, Parque tecnológico Cartuja '93, 41092 Seville, Spain, akrižnar@us.es

J. Kunicki-Goldfinger Institute of Nuclear Chemistry and Technology, Dorodna 16, 03-195, Warsaw, Poland; School of History and Archaeology, Cardiff University, 10 3EU, Cardiff, UK

R. López Faculty of Humanities and Social Sciences of Teruel, University of Zaragoza (UZ), Zaragoza, Spain

M. López Cáceres Biblioteca Nacional de Antropología e Historia, INAH, Mexico City, Mexico

L. Lai Department of Anthropology, University of South Florida, Tampa, FL 33620, USA

R. Lapucci Studio Art Centers International - SACI, Via Sant'Antonino 11, Florence, Italy

R. Laviano Department of Geomineralogy, University of Bari, Via Orabona 4, Bari, Italy

G. Lawson Faculty of Health and Life Sciences, De Montfort University, Hawthorn Building, Leicester 1 9BH, UK

A. Leclaire Centre de Recherche et des Restauration des Musées de France, CNRS UMR 171, 6, rue des Pyramides, 75041 Paris, France

M. Lettieri Istituto per i Beni Archeologici e Monumentali (CNR-IBAM), Complesso Ecotekne, Via Monteroni, 73100 Lecce, Italy

N. Li Chinese Academy of Cultural Heritage, Beijing 100029 People's Republic of China

G. Liberotti Department of Chemistry, Chemical Engineering and Materials, University of L'Aquila, Monteluco di Roio, 67100 L'Aquila, Italy

C. Lugliè Dipartimento di Scienze Archeologiche e Storico-Artistiche, Università di Cagliari, Piazza Arsenale 1, 09124 Cagliari, Italy, luglie@unica.it

H.H.M. Mahmoud Department of Conservation, Faculty of Archaeology, Cairo University, Giza 12613 Egypt; Laboratory of Analytical Chemistry, Aristotle University, 54124 Thessaloniki, Greece

A. Mangone Department of Chemistry, University of Bari, Via Orabona 4, Bari, Italy, fabia@chimica.uniba.it

A. Marcsik Department of Anthropology, University of Szeged, Egyetem str. 2, 6722 Szeged, Hungary

L. Mark Institute of Biochemistry and Medical Chemistry, University of Pécs, Szigeti str.12, 7624 Pécs, Hungary, laszlo.mark@aok.pte.hu

G. Martin Science Section, Conservation Department, Victoria and Albert Museum, South Kensington, London SW7 2RL, UK

M. Martínón-Torres Institute of Archaeology, University College London, 31–34 Gordon Square, London WC1H 0PY, UK

M.L. Mascelloni Department of Chemistry, Chemical Engineering and Materials, University of L'Aquila, Via Vetoio (Coppito 1), 67010 Coppito, L'Aquila, Italy, mascelloni@hotmail.com

M. Mattarelli Dipartimento di Fisica, Università di Trento, Via Sommarive 14, 38050 Povo (TN), Italy

N.C. McCreesh The KNH Centre for Biomedical Egyptology, F Floor The Mill, The University of Manchester, PO Box 88, Manchester M60 1QD UK, natalie.mccreesh@postgrad.manchester.ac.uk

A.S. Meek Department of Archaeology, The University of Nottingham, Nottingham NG7 2RD UK, acxam@nottingham.ac.uk

E. Melgar Museo del Templo Mayor, INAH, Mexico City, Mexico

I. Melne National History Museum of Latvia, Riga, Latvia

A. Metroka Department of Anthropology, University of South Florida, Tampa, FL 33620, USA

A. Miceli Department of Physics, Università di Bologna, C.Berti Pichat 6/2, 40127 Bologna, Italy; Empa – Swiss Federal Laboratories for Materials Testing and Research, Ueberlandstrasse 129, 8600 Duebendorf, Switzerland

J. Michniewicz Institute of Geology, Adam Mickiewicz University, Makow Polnych 16, 61-606 Poznan, Poland, danamich@amu.edu.pl

R. Mitoyan Department of Geochemistry, Moscow State University, Moscow, Russia, mitoyan@geol.msu.ru

G. Molin Dipartimento di Geoscienze, University of Padova, Padova, Italy

A.M. Monge Soares Instituto Tecnológico e Nuclear, Estrada Nacional 10, 2686-953 Sacavém, Portugal

M. Montagna Dipartimento di Fisica, Università di Trento, Via Sommarive 14, 38050 Povo (TN), Italy

G. Montana Dipartimento di Chimica e Fisica della Terra ed Applicazioni alle Georisorse e ai Rischi Naturali (CFTA), Università di Palermo, Via Archirafi, 36, 90123 Palermo, Italy, gmontana@unipa.it

J-F Moreau Laboratoire d'Archéologie and Département des sciences humaines, Université du Québec à Chicoutimi, Chicoutimi, QC, Canada G7H 2B1, jfmoreau@uqac.ca

M. Moresi Department of Geomineralogy, University of Bari, via Orabona 4, 70124 Bari, Italy

M.P. Morigi Department of Physics, Università di Bologna, C.Berti Pichat 6/2, 40127 Bologna, Italy

A. Moroni Department of Environmental Sciences, University of Siena, Siena, Italy

W. Mosselmans Diamond Light Source, Didcot OX11 0DE, UK

T. Mostaza Higher Polytechnic School of Ávila, University of Salamanca (USAM), Salamanca, Spain

A. Mounier Institut de Recherche sur les Archéomatériaux (IRAMAT), Centre de Recherche en Physique Appliquée à l'Archéologie, UMR 5060-IRAMAT, Université de Bordeaux/CNRS, 33607 Pessac Cedex, France

M.V. Muñoz Museo de Bellas Artes, Plaza del Museo 9, 41001 Seville, Spain

S. Mugnaini Dipartimento di Scienze Ambientali, U.R. Conservazione del Patrimonio Culturale Lapideo, Università degli Studi di Siena, Via Laterina 8, 53100 Siena, Italy

S.C. Nappo Dipartimento di Matematica e Informatica, Università degli Studi di Salerno, 84084 Fisciano, (SA), Italy, scnappo@alice.it

D. Nawrocka Institute of Geology, Adam Mickiewicz University, Makow Polnych 16, 61-606 Poznan, Poland, danutamich@go2.pl

R.J. Newport University of Kent, Canterbury CT2 7NH, UK

B. Neyt Section Geology, Earth & Environmental Sciences, Celestijnenlaan 200 E, bus 2408, 3001 Leuven, Belgium

C. Nicola Università degli Studi di Milano, Dip. di Scienze della Terra, Via Botticelli 23, I-20133 Milano, Italy, chiara.nicola@unimi.it

G. Niculescu National Research Institute for Conservation and Restoration, 12 Calea Victoriei, 030026 Bucharest, Romania, niculescu.geo@gmail.com

C.C. Nordby Culture Historical Laboratory, Department of Archaeology, Tromsø Museum, University of Tromsø, N-9037 Tromsø, Norway

F. Notarstefano Dipartimento di Beni Culturali, Università del Salento, via D. Birago 64, 73100 Lecce, Italy, florinda.notarstefano@ateneo.unile.it

R. Oanță-Marghitu National History Museum of Romania, 12 Calea Victoriei, 030026 Bucharest, Romania, rodicamarghitu@yahoo.com

C.P. Odriozola Instituto de Ciencia de Materiales de Sevilla, Centro Mixto Universidad de Sevilla-CSIC, Avd. Américo Vespucio 49, 41092 Sevilla, Spain, carlos@icmse.csic.es

G. Olcese Facoltà di Lettere e Filosofia, Dipartimento di Scienze storiche, archeologiche e antropologiche dell'antichità, Università di Roma "La Sapienza", Roma, Italy, gloria.olcese@uniroma1.it

E. Ortiz Instituto de Investigaciones Antropológicas, UNAM, Mexico city, Mexico

B. Péterdi Geological Institute of Hungary, Geological Museum of Hungary, Stefánia u. 14, 1143 Budapest, Hungary, peterdi@mafi.hu

T. Paduano Dipartimento di Matematica e Informatica, Università degli Studi di Salerno, 84084 Fisciano, (SA), Italy, t.paduano@libero.it

D. Pagliarello Dipartimento di Chimica e Fisica della Terra (CFTA), Università di Palermo, Palermo, Italy

Z. Patonai Institute of Biochemistry and Medical Chemistry, University of Pécs, Szigeti str.12, 7624 Pécs, Hungary; Institute of Forensic Medicine, University of Pécs, Szigeti str.12, 7624 Pécs, Hungary

V. Pavlidis Allied Health Sciences, De Montfort University, Hawthorn Building, Leicester 1 9BH, UK

E. Pavlidou Department of Physics, Aristotle University, 54124 Thessaloniki, Greece

L.A. Pavlish Department of Physics, University of Toronto, Toronto, ON, Canada M5S 1A7

S. Paynter English Heritage, Fort Cumberland, Fort Cumberland Road, Eastney, Portsmouth PO4 9LD UK, sarah.paynter@english-heritage.org.uk

S. Paynter English Heritage, Portsmouth PO4 9LD, UK

G. Peñuelas Escuela Nacional de Conservación, Restauración y Museografía, INAH, Mexico D.F., Mexico

A. Pecci Archaeometric Laboratory, Department of Archaeology and History of Art, University of Siena, via Roma, 56, 53100 Siena, Italy, alepecci@gmail.com

G.L.A. Pesce Institute of the History of Material Culture (ISCUM), c/o Museum of St. Agostino, Piazza Sarzano, 35r 16128 Genoa, Italy

S. Peschard Laboratory of the Centre for research and restoration of the French Museums. (LC2RMF), UMR 171 CNRS French Ministry of Culture and Communication, Palais du Louvre, 14 quai François Mitterrand, 75001 Paris, France

E. Photos-Jones Analytical Services for Art and Archaeology (SASAA) Ltd, Glasgow, UK; Department of Archaeology, University of Glasgow, Glasgow, UK

F. Pintér Scientific Laboratory – Federal Bureau for Monument Protection, Arsenal Objekt 15, Tor 4, 1030 Vienna, Austria, farkas.pinter@bda.at

C. Pizzi Dipartimento di Archeologia, Università degli Studi di Padova, Padova, Italy

J. Poblome Sagalassos Archaeological Research Project, Blijde-Inkomststraat 21, bus 3314, 3000 Leuven, Belgium

A.M. Polito Dipartimento di Chimica e Fisica della Terra ed Applicazioni alle Georisorse e ai Rischi Naturali (CFTA), Università di Palermo, Via Archirafi, 36, 90123 Palermo, Italy

A. Polla Dip. di Scienze della Terra, Università degli Studi di Milano, Via Botticelli 23, 20133 Milano, Italy, angela.polla@unimi.it

T. Pollard Department of Archaeology, Centre for Battlefield Archaeology, University of Glasgow, Glasgow, UK

G. Poupeau Institut de Recherche sur les Archéomatériaux, UMR 5060, CNRS, Université Bordeaux-3, Maison de l'Archéologie, esplanade des Antilles, 33607 Pessac, France; Département de Préhistoire, UMR 5198, CNRS, Muséum national d'histoire naturelle, Musée de l'Homme, 17 place du Trocadéro, 75016 Paris, France, gpoupeau@u-bordeaux3.fr

B. Pretzel Science Section, Conservation Department, Victoria and Albert Museum, South Kensington, London SW7 2RL, UK

C.A. Price University College, London, UK

M. Primavera Laboratory of Archaeobotany and Paleoecology, Department of Cultural Heritage, Salento University, Via D. Birago, 64 - 73100 Lecce, Italy

R. Quaresima Department of Chemistry, Chemical Engineering and Materials, University of L'Aquila, Monteluco di Roio, 67100 L'Aquila, Italy

S. Röhrs Conservation and Scientific Research, The British Museum, Great Russell Street, London WC 1 B3 DG, UK

M. Rapi Università degli Studi di Milano, Dip. di Scienze dell'Antichità, Via Festa del Perdono 7, I-20122 Milano, Italy, marta.rapi@unimi.it

V. Redavid Department of the Science of Antiquity, University of Bari, Piazza Umberto, Bari, Italy

I. Reiche Laboratory of the Centre for research and restoration of the French Museums. (LC2RMF), UMR 171 CNRS French Ministry of Culture and Communication, Palais du Louvre, 14 quai François Mitterrand, 75001 Paris, France

J.G. Rejas National Institute of Aeronautics and Space Technology (INTA), Madrid, Spain, rejasaj@inta.es

M.A. Respaldiza Centro Nacional de Aceleradores (CNA), University of Seville, Avda. Thomas A. Edison 7, Parque tecnológico Cartuja '93, 41092 Seville, Spain

S. Ricciardi Dipartimento di Matematica e Informatica, Università degli Studi di Salerno, 84084 Fisciano, (SA), Italy, sricciardi@unisa.it

S. Ridolfi Ars Mensurae, Roma, Italy, stefano@arsmensurae.it

C. Rossi Department of Chemical and Biosystem Sciences, University of Siena, Via A. Moro 2, Siena, Italy; Inter-University Center of Colloid and Surface Science - CSGI, Via della Lastruccia 3, Sesto Fiorentino, Florence, Italy

V. Rudovica Department of Analytical Chemistry, University of Latvia, Riga, Latvia

J.L. Ruvalcaba Instituto de Física, Universidad Nacional Autónoma de México (UNAM), Mexico City, Mexico, sil@fisica.unam.mx

M.E. Sáiz Faculty of Humanities and Social Sciences of Teruel, University of Zaragoza (UZ), Zaragoza, Spain

M. Saña Laboratory of Archaeozoology, Prehistory Department, Universitat Autònoma de Barcelona. Edifici B – Campus UAB, 08193 Bellaterra, Barcelona, Spain

G. Sabatini Dipartimento di Scienze Ambientali, U.R. Conservazione del Patrimonio Culturale Lapideo, Università degli Studi di Siena, Via Laterina 8, 53100 Siena, Italy, sabatini@unisi.it

M. Salomé ESRF, BP 220, 38043 Grenoble CEDEX 9, Grenoble, France

G. Salviulo Dipartimento di Geoscienze, University of Padova, Padova, Italy

A. Santagostino Barbone Opificio delle Pietre Dure, Firenze, Italy

A. Scala Dipartimento di Scienze Ambientali, U.R. Conservazione del Patrimonio Culturale Lapideo, Università degli Studi di Siena, Via Laterina 8, 53100 Siena, Italy

S. Scarcella Ecole des Hautes Etudes en Sciences Sociales, 58, Boulevard de Reuilly, 75012 Paris, France, simonascarcella@yahoo.it

M. Schreiner Institute of Natural Sciences and Technology in Arts, Academy of Fine Arts in Vienna, Vienna, Austria

G. Semeraro Dipartimento di Beni Culturali, Università del Salento, via D. Birago 64, 73100 Lecce, Italy

M. Senn Empa – Swiss Federal Laboratories for Materials Testing and Research, Ueberlandstrasse 129, 8600 Dübendorf, Switzerland

M. Serra Dipartimento di Scienze Mineralogiche e Petrologiche, Via V. Caluso, 35, 10125 Torino, Italy

B. Shah Science Section, Conservation Department, Victoria and Albert Museum, South Kensington, London SW7 2RL, UK

R. Siddall University College, London, UK

A.C. Silva Direcção Regional de Cultura do Alentejo, R. de Burgos, 5, 7000-863 Évora, Portugal

A. Silvestri Dipartimento di Geoscienze, University of Padova, Padova, Italy, alberta.silvestri@unipd.it

M.K. Sioliou Laboratory of Rangeland Ecology (286), Aristotle University of Thessaloniki, 54124 Thessaloniki, Greece

T. Skinner The National Museums of Scotland, Edinburgh EH1 1JF UK

A.D. Smith STFC, Daresbury Laboratory, Warrington WA4 4AD UK, andrew.d.smith@stfc.ac.uk

G. Song Institute of Natural Science and Technology in Archaeology, Graduate University, Chinese Academy of Science, Beijing, China

F. Spatafora Regione Siciliana, Soprintendenza BB. CC. AA. di Palermo (Servizio per i Beni Archeologici), Palermo, Italy

R.J. Speakman Museum Conservation Institute, Smithsonian Institution, 4210 Silver Hill Road, Suitland, MD 20746, USA

E. Starnini Department of Archaeology and Classical Philology, University of Genova, Via Balbi 4, 16126 Genova, Italy

G. Stella LDL & BBCC, Laboratorio di Datazione tramite Luminescenza e di Metodologie Fisiche applicate ai Beni Culturali del Dipartimento di Fisica e Astronomia, Università di Catania and INFN Sezione di Catania, via Santa Sofia 64, 95123 Catania, Italy

R. Sternberg Department of Earth and Environment, Franklin & Marshall College, Lancaster, PA 17603 USA, rob.sternberg@fandm.edu

J.A. Stratis Laboratory of Analytical Chemistry, Aristotle University, 54124 Thessaloniki, Greece, jstratis@chem.auth.gr

B. Székely Institute of Photogrammetry and Remote Sensing, Vienna University of Technology, Vienna, Austria

Z. Szőkefalvi-Nagy KFKI Research Institute for Particle and Nuclear Physics of the Hungarian Academy of Sciences, Budapest, Hungary

G. Szakmány Department of Petrology and Geochemistry, Eötvös Loránd University (ELTE), Budapest, Hungary

Gy. Szakmány Department of Petrology and Geochemistry, Eötvös Loránd University, Pázmány P. sétány 1/c, 1117 Budapest, Hungary, gyorgy.szakmany@geology.elte.hu

V. Szilágyi Institute of Isotopes, Hungarian Academy of Sciences, Budapest, Hungary, szilagyi@iki.kfki.hu

J. Tate Department of Conservation and Analytical Research and Department of World Cultures, National Museums Scotland, Chambers Street, Edinburgh EH1 1JF UK

H. Taubald Department of Geochemistry, Eberhard Karls University of Tübingen, Tübingen, Germany

M.C. Tenório Museu Nacional, Universidade Federal do Rio de Janeiro, Rio de Janeiro, Brazil

A. Tognazzi Department of Chemical and Biosystem Sciences, University of Siena, Via A. Moro 2, Siena, Italy; Inter-University Center of Colloid and Surface Science - CSGI, Via della Lastruccia 3, Sesto Fiorentino, Florence, Italy, tognazzi@unisi.it

L. Toniutti Dipartimento di Fisica, Università di Trento, Via Sommarive 14, 38050 Povo (TN), Italy

M. Tóth Hungarian Academy of Sciences, Institute for Geochemical Research, Budaörsi út 45, 1112 Budapest, Hungary

C. Tornero Laboratory of Archaeozoology, Prehistory Department, Universitat Autònoma de Barcelona. Edifici B – Campus UAB, 08193 Bellaterra, Barcelona, Spain, carlos.tornero@uab.cat

C. Tozzi Dipartimento di Scienze Archeologiche, Università di Pisa, 56126 Pisa, Italy

A. Traini Department of Chemistry, University of Bari, Via Orabona 4, Bari, Italy

R.I.F. Trindade Departamento de Geofísica, Instituto de Astronomia, Geofísica e Ciências Atmosféricas, Universidade de São Paulo, São Paulo, Brazil

L. Troalen Department of Conservation and Analytical Research and Department of World Cultures, National Museums Scotland, Chambers Street, Edinburgh EH1 1JF, UK

L. Troisi Dipartimento di Scienze e Tecnologie Biologiche ed Ambientali (Di.S. Te.B.A.), Laboratorio di Chimica Organica, Università del Salento, Complesso Ecotekne, Via Monteroni, 73100 Lecce, Italy

S.O. Troja LDL & BBCC, Laboratorio di Datazione tramite Luminescenza e di Metodologie Fisiche applicate ai Beni Culturali del Dipartimento di Fisica e Astronomia, Università di Catania and INFN Sezione di Catania, via Santa Sofia 64, 95123 Catania, Italy

C.A. Tryon Department of Anthropology, New York University, 25 Waverly Place, New York, NY 10003 USA; Human Origins Program, Department of

Anthropology, National Museum of Natural History, Smithsonian Institution, Washington, DC 20013, USA, christian.tryon@nyu.edu

E. Tsantini Equip de Recerca Arqueomètrica de la Universitat de Barcelona (ERAUB), Barcelona, Italy

E. Tsirimona Laboratory of Rangeland Ecology (286), Aristotle University of Thessaloniki, 54124 Thessaloniki, Greece

I. Turbanti Memmi Department of Earth Sciences, University of Siena, Siena, Italy, memmi@unisi.it

R.H. Tykot Department of Anthropology, University of South Florida, Tampa, FL 33620, USA, rtykot@cas.usf.edu

M. Uboldi Museo Civico Archeologico di Como, uboldi.marina@comune.como.it

A. Váradi István Dobó Castle Museum, Eger, Hungary

A. Vaczy Institute of Biochemistry and Medical Chemistry, University of Pécs, Szigeti str.12, 7624 Pécs, Hungary

G. Vaggelli CNR – Istituto di Geoscienze e Georisorse, Via V. Caluso, 35, 10125 Torino, Italy

J.M. Vanderveen Department of Sociology and Anthropology, 1700 Mishawaka Avenue, South Bend, IN 46634-7111, USA, jmvander@iusb.edu

M. Vega Museo de Bellas Artes, Plaza del Museo 9, 41001 Seville, Spain

M.C. Vicéns Aspex Corporation, 175 Sheffield Drive, Delmont, PA 15626, USA, mvicens@aspexcorp.com

L. Vigna Soprintendenza Archeologica per il Piemonte e del Museo Antichità Egizie, Via Accademia delle Scienze, 6, 10123 Torino, Italy

A. Viksna Department of Analytical Chemistry, University of Latvia, Riga, Latvia, arturs.viksna@lu.lv

I. Villasenor University College, London, UK

V. Virgili CNR - Dipartimento Patrimonio Culturale, Innovation Relay Centre CIRCE, Rome, Italy

C. Viti Dipartimento di Scienze della Terra, University of Siena, Siena, Italy

F. Voigt Department of Conservation and Analytical Research and Department of World Cultures, National Museums Scotland, Chambers Street, Edinburgh EH1 1JF, UK

R. Volpe Department of Chemistry, Chemical Engineering and Materials, University of L'Aquila, Monteluco di Roio, 67100 L'Aquila, Italy

M. Wörle Swiss National Museum Zurich, Collection Centre, Lindenmoosstrasse 1, CH-8910 Affoltern a.A, Switzerland

M. Waelkens Sagalassos Archaeological Research Project, Blijde-Inkomststraat 21, bus 3314, 3000 Leuven, Belgium

C. Wang Department of Scientific History and Archaeometry, Graduate University of the Chinese Academy of Sciences, Beijing, People's Republic of China

D. Wang Tianjin Dagu Emplacement Site Managing Institute, Tianjin 300000, People's Republic of China

M. Wartmann Augusta Raurica, Giebenacherstrasse 17, CH-4302 Augst, Switzerland

J. Watson Museum Conservation Institute, Smithsonian Institution, 4210 Silver Hill Road, Suitland, MD 20746 USA, watsonj@si.edu

J. Weber Institute of Art and Technology – Conservation Sciences, University of Applied Arts Vienna, Salzgries 14/1, 1010 Vienna, Austria

S. Wei Institute of Natural Sciences and Technology in Arts, Academy of Fine Arts in Vienna, Vienna, Austria, sywei66@hotmail.com

L. Wilson Technical Conservation Group, Historic Scotland, Edinburgh, UK

S.U. Wisseman Illinois Transportation Archaeological Research Program, University of Illinois at Urbana, Champaign, IL, USA; Program on Ancient Technologies and Archaeological Materials, University of Illinois at Urbana, Champaign, IL, USA, wisarc@illinois.edu

Y. Xie Institute of Archaeology of Shanxi Province, Shanxi Province, China

Y. Yang Department of Scientific History and Archaeometry, Graduate University of Chinese Academy of Sciences, Beijing, China

M. Yang School of Mechanical Engineering and Automation, Beijing University of Aeronautics and Astronautics, Beijing, China

J. Zöldföldi Institute of Geoscience, University of Tübingen, Wilhelmstrasse 56, 72074 Tübingen, Germany, zoeldfoeldi@yahoo.de

J.J. Zancajo Higher Polytechnic School of Ávila, University of Salamanca (USAM), Salamanca, Spain

G. Zarina Institute of the History of Latvia, University of Latvia, Riga, Latvia

S. Zetina Instituto de Investigaciones Estéticas, UNAM, Mexico City, Mexico

Z. Zhang Chinese Academy of Cultural Heritage, Beijing 100029, People's Republic of China

J. Zhu Department of Scientific History and Archaeometry, Graduate University of the Chinese Academy of Sciences, Beijing, People's Republic of China, jzhu@gucas.ac.cn

A.R. Zuccarello LDL & BBCC, Laboratorio di Datazione tramite Luminescenza e di Metodologie Fisiche applicate ai Beni Culturali del Dipartimento di Fisica e Astronomia, Università di Catania and INFN Sezione di Catania, via Santa Sofia 64, 95123 Catania, Italy, agnese.zuccarello@ct.infn.it

Part I
Ceramics, Glazes, Glass and Vitreous
Materials (Technology and Provenance)

Late Byzantine-Early Islamic Ceramic Technology, Transjordan

F.M. Alawneh and H.A. Béarat

1 Introduction

Administratively, the territories of Transjordan (a neutral term for what is now Jordan) have always belonged to different provinces. During the Late Byzantine or Early Islamic periods, the administrative borderlines were imposed by geographic rather than political considerations. They were generally running from east to west (Hitti 1970; Watson 2001). Hence, we can distinguish three major regions in Transjordan: northern, central and southern. While the northern one certainly had privileged relations with north Palestine and Syria, the central region had close relations with Palestine, and the southern played an important role in relations with south Arabia and Egypt. In times of peace as well as in times of war, Transjordan has therefore played an important role as a platform for trade and warfare in both north-south and east-west directions.

It is quite possible that different patterns of cultural interactions simultaneously existed in Transjordan during this period. For instance, it can be postulated that change might have been much faster in the south than in the centre or north. In the south, one may also expect to see an enhanced interaction of the local culture with the Egyptian and South Arabian cultures, whereas in the northern area, a more complicated model of interaction might have been in place between the local culture and those of Palestine, Syria, Byzantium, and probably Sasanid Mesopotamia. Whether one wants to associate prosperity or decline with this historical transition (Schick 1995; Walmsley 2001; Watson 2001; Whitcomb 2001), cutting-edge evidence can certainly be provided by the scientific study of the material culture of the societies under consideration, and without having to

F.M. Alawneh (✉)

Queen Rania's Institute of Tourism and Heritage, The Hashemite University, Zarqa, Jordan
e-mail: firmas-alawneh@hu.edu.jo

H.A. Béarat

LECSSS, School of Materials, Arizona State University, Tempe 85287-1704, AZ, USA

suffer from a biased reading of these changes. Needless to say, the ceramic traditions of the Islamic World in general and of the Levant in particular, during these early times, have not yet received fair scientific attention meant to elucidate the role it had to play in later technological development. Therefore, the choice of Transjordan for the study of the ceramic of the Late Byzantine-Early Islamic transition period is being driven by this motivation and favored by the variation in the socio-cultural landscape and well-contrasted geological/geographical settings of the selected regions.

This transition period has never been systematically studied previously. Only a few studies regarding pottery analysis were carried out, both internationally and locally. The integration of geochemical, mineralogical and petrological data would be an effective and representative approach for characterizing ceramics and clay material. Chemical and/or mineralogical analyses of ancient ceramics aim, above all, at characterizing the products.

2 Samples and Methodology

The samples studied in this project consisted of archaeological ceramics sherds drawn from twelve sites situated in the three major geographical areas: (1) northern, (2) central, and (3) southern (Fig. 1). The samples belonged to the transition period, dated from the middle of the sixth to the middle of the eighth century AD, and were collected in collaboration with the archaeologists who had excavated the sites. Twenty potsherds were considered the minimum sample size necessary to characterize a single site, but in some cases availability was limited by the quantity of artifacts recovered from the excavation. A primary criterion for selecting transition period sherds focused on the presence of vertical levels. Samples from the Late Byzantine and Early Islamic levels were incorporated into the study whenever it was possible. Due to the complexity of differentiating between the two levels, archaeologists tend to assign some of the samples to the “transition” period rather than associating them with a specific dated level (Amr 2005, Personal communication).

A total of 228 samples were considered in this study (Table 1). Sherds included red, black, gray, yellow, pink, stamped, painted and glazed pottery. As part of the ceramic study, a program of analysis for clay materials collected in the proximity of the selected archaeological sites was also included. In total, eight clay samples were collected from the different geographical areas. These samples are being used for comparative purposes in order to identify possible source areas of the sherds. The collected clays were fired in oxidizing atmosphere at different temperatures, ranging from 500°C to 1,100°C. These firing experiments were used to define the technological characteristics of each clay material and compared with archaeological samples to further classify these ceramics according to their manufacturing technologies.

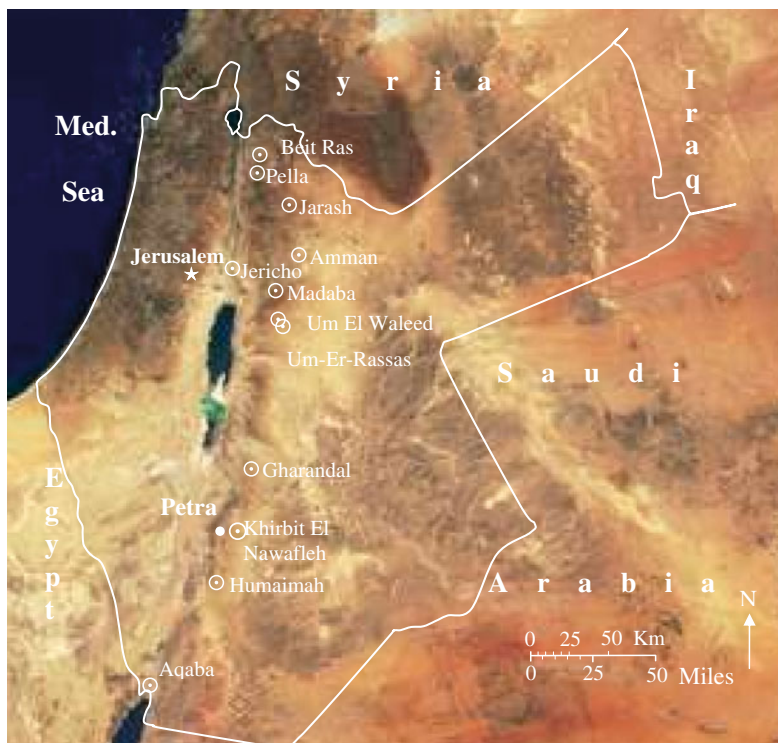


Fig. 1 Map of the Southern Levant with the archaeological sites selected for the study indicated by the sign ⊙

3 Results and Discussion

The multifaceted analytical study of the pottery from Jordan generated different types of datasets. Compositional analysis with PIXE provided quantitative elemental compositions of the pottery and the clay materials. Phase analysis with XRD provided qualitative as well as semi-quantitative mineralogical compositions of the potsherds and allowed the technical study of the clay materials. Textural/morphological study with PLM of thin sections from representative samples provided information on the nature, amount, and grain size distribution of the inclusions, as well as the ceramic matrix.

In order to assess the validity of pottery classification, and better understand their fabrication technology, the ceramic sherds of three sites were characterized by XRD.

Observation of the diffraction patterns for samples from these sites reveals important similarities. By reviewing the mineral assemblages in Table 1, and using petrographic results, one can notice the similarity among them. Thus, for

Table 1 List of archaeological sites included in the study area, their identified mineral assemblages and their respective locations. *Ca* Calcite, *Di* Diopside, *Do* Dolomite, *Ge* Gehlenite, *He* Hematite, *Il* Illite, *Pl* Plagioclase, *Py* Pyroxene, *Qz* Quartz

Site name	Abbreviation	Geographical location	Mineral assemblages
Amman	AM	Middle	Qz, Pl, He, Ca, Il Qz, Pl, Ge, Kf
Aqaba	AQ	South	Qz, Pl, Ge, Py, He Qz, Pl, He, Ge, Ca
Beit Ras	BR	North	Qz, Il, Pl, He Qz, Pl, Ge, Ca, He
Gharandal	GH	South	Qz, Pl, Ca Qz, Py, Ge, Pl, Kf
Humaimah	HM	South	Qz, Pl, Ca, Py, Ge Qz, Ge, Pl, Ca, He
Jarash	JA	North	Qz, Pl, He, Ca Qz, Di, Py, Ge, Pl, Kf
Jericho	JE	Middle	Qz, Pl, Kf, Il Qz, Ge, Pl, He, Py
Khirbit El Nawafleh	KN	South	Qz, Pl, Ge, Py, He Qz, Pl, Ca, Il
Madaba	MA	Middle	Qz, Pl, Ca Qz, Py, Pl, Di, Ge
Pella	PE	North	Qz, Pl, He, Ca, Il Qz, Pl, Di, Py, He
Um Er Rasas	UR	Middle	Qz, Ge, Pl, Py, He Qz, Ca, Il
Um El Waleed	UW	Middle	Cl, Ta, Do Qz, Ge, Pl, Py, Kf

the different groups, the following results can be concluded: for instance, group Ia shows that the potter tended to add the same inclusion ratio ($\approx 50\%$) in samples FA102-JA and FA196-PE, or he might have used the same clay source, which had this natural distribution of inclusions. Inclusions in this group have the same size distribution and morphology (0.1–0.4 mm in size), are rounded to sub-rounded, and occasionally present some sharp edge grains. The phase analysis results for group Ia showed the same phases. For group Ib samples, the proportion of the inclusions is less than 23%. The mineral assemblages are quartz, plagioclase, calcite, hematite, gehlenite, K-feldspar and pyroxene. Inclusions tend to have small size grains. Group II consisted of samples with the same dark matrix, and smaller inclusion ratio ($\approx 3\%$), with rounded to sub-rounded shape. The same technology appears to have been used on samples belonging to the same chemical group. This explanation could in turn be attributed to the hypothesis that people throughout the transition period kept the same trend and used almost the same technological aspect in ceramic manufacture. This conclusion was drawn for samples classified by archaeologists as belonging to the Early Islamic period or to the transition period. Unfortunately, none of the samples studied from this region can be ascribed with certainty to the Late Byzantine level. Thus, the previous conclusion concerns only the transition period and the Early Islamic finds.

The presence or absence of specific mineral phases in a ceramic product gives information on the production technology. For an initial clay material of given chemical and mineralogical composition, the mineral assemblage detected with XRD is strongly influenced by firing temperature and atmosphere (Philpotts and Wilson 1994). An estimation of the firing temperature may therefore be carried out on the basis of the mineral assemblage, as the occurrence or absence of specific mineral phases, at a given bulk composition, provides constraints on the maximum firing temperature. It should be noted that the time and conditions of the firing process do not necessarily result in a mineral assemblage which is in a state of thermodynamic equilibrium, and this aspect must be remembered in any attempt to predict the firing conditions (Maggetti 1982). However, a preliminary rough estimation of the firing temperature for each of the above mineral assemblages and an interpretation of the mineralogical composition are still useful as starting points. In order to explore this possibility, experiments were carried out on samples JA1-clay, JA2-clay, and PE-clay, from the Jarash and Pella sites areas. The clay samples were fired under oxidizing condition over a large temperature range.

For Jarash clay, the original clay (JA1) contains the following phases: illite-montmorillonite, calcite, dolomite plagioclase and quartz. As temperature goes up and reaches 500°C, the illite-montmorillonite mixed layer is completely decomposed. At 600°C and before the temperature reaches 600°C, dolomite and calcite peaks could still be seen, while at 700°C and over the peaks were decomposed. When temperature reaches 800°C, illite peaks start to decompose and low firing phases are absent. The intensity of clay peaks decreases over 800°C and disappears around 900°C. Over 900°C, new firing phases of pyroxene and hematite begin to crystallize. In addition, some primary phases also exhibit clear changes. Illite starts to undergo a decomposition process that is completed between 850°C and 900°C. In contrast, the illite (110) reflection is not essentially affected below 900–950°C and is stable up to 1,000–1,050°C (Maggetti 1981). On the other hand, plagioclase shows an increasing intensity of the peaks that must be related to the crystallization of plagioclase minerals, anorthite and albite.

4 Conclusion

Overall, the technology employed seems to be very similar in the northern, central and southern regions. Pottery was made following roughly similar criteria, regardless of its domestic function. This can be regarded as a preliminary indication, provided by the analysis of mineralogical and petrographic data. Petrographic analysis, for instance, shows the presence of similar inclusions in samples of the same chemical groups.

The combination of chemical, phase, and petrographic analyses is an adequate approach to the characterization of archaeological ceramics. Measurement of major and minor element concentrations proved satisfactory in this case for establishing similarities and differences among sherds and clays.

Based on these analytical results, one can draw a number of preliminary conclusions on the nature of raw materials employed, ceramic technologies, distribution of products, and hence on the implicit socio-cultural and economic exchange trends within Transjordan during that period. The conclusions are being drawn for the individual sites and geographical regions, and for adjacent regions as well.

Based on the mineral assemblages observed with XRD and the color of the sherds, it is concluded that potters of the two groups favored firing in oxidizing atmosphere. Firing temperatures varied from about 700 to 900°C for Beit Ras samples, from 800 to 1,000°C in Jarash, and 800°C to higher than 1,000°C in Pella. However, a slight difference between the production technologies used for the two groups has been noticed. It consists of variation in ceramic thickness. Samples 188, 189 and 190 were thick ceramics, while samples from the other group were thinner.

References

- Hitti PK (1970) *History of the Arabs: from the earliest times to the present*, 10th edn. MacMillan St. Martin's Press, London
- Maggetti M (1981) Composition of Roman pottery from Lousonna (Switzerland). In: Hughes MJ (ed) *Scientific studies in ancient ceramics*, British Museum Occasional Paper 19. London, pp 33–49
- Maggetti M (1982) Phase analysis and its significance for technology and origin. In: Olin JS, Franklin AD (eds) *Archaeological ceramics*. Smithsonian Institution, Washington, pp 121–133
- Philpotts AR, Wilson N (1994) Application of petrofabric and phase equilibria analysis to the study of a potsherd. *J Archaeol Sci* 21:607–18
- Schick R (1995) *The Christian Communities of Palestine from Byzantine to Islamic Rule: a historical and archaeological study*. The Darwin Press, Princeton, NJ
- Walmsley A (2001) Fatimid, Ayyubid and Mamluk Jordan and the Crusader Interlude. In: MacDonald B et al (eds) *The archaeology of Jordan*. Sheffield, Sheffield Academic Press, pp 515–559
- Watson P (2001) The Byzantine period. In: MacDonald B et al (eds) *The archaeology of Jordan*. Sheffield Academic, Sheffield, pp 461–502
- Whitcomb D (2001) Umayyad and Abbasid periods. In: MacDonald B et al (eds) *The archaeology of Jordan*. Sheffield Academic, Sheffield, pp 503–513

Provenance Study of Some Samples of “Compendiario” Majolica Found in Archaeological Excavations Carried Out in the Centre of Amsterdam

F. Amato, B. Fabbri, S. Gualtieri, J. Gawronski, and N. Jaspers

1 Introduction

Since 2006, the CNR-ISTEC in Faenza (Italy) and the Bureau of Monuments and Archaeology in Amsterdam (The Netherlands) are involved in an international research project on European tin-glazed ceramics from the early modern period. The project deals with the study of imported “compendiario” majolica found as a result of archaeological excavations in the Netherlands, in contexts dating from the first half of the seventeenth century. In the upcoming years, the cooperation will expand to English and French scientific institutions.

At the end of the sixteenth century, during the Mediterranean grain crisis, the Dutch merchants and shippers that controlled the major part of the international grain trade in the Baltic area (Lindblad 1998) entered the Italian markets (Grendi 1971). The archaeological contexts in the Netherlands dating from this period show a sudden increase in imported ceramics, in majority (presumably) of Italian origin (Hurst et al. 1987; Jaspers 2007a; Ostkamp 2003). By analysing ceramic assemblages, archaeologists try to reconstruct historic commercial contacts, even if the exact provenance is not actually always known. For example, some of the imports appeared to be French (Jaspers 2007b; Rosen 2002, 2003) rather than Italian, while others are often falsely attributed to Faenza (Baart 1985, 1991; Baart et al. 1990; Hurst et al. 1987). Without reliable results concerning the provenance of the

F. Amato (✉)

CNR-ISTEC, National Research Council, Institute of Science and Technology for Ceramics, Faenza (Ravenna), Italy

and

University of Ferrara, Ferrara, Italy

e-mail: francesca.amato@istec.cnr.it

B. Fabbri and S. Gualtieri

CNR-ISTEC, National Research Council, Institute of Science and Technology for Ceramics, Faenza (Ravenna), Italy

J. Gawronski and N. Jaspers

Bureau Monumenten en Archeologie, Afdeling Archeologie, Amsterdam, The Netherlands

materials, it is impossible to use this type of archaeological data for historical interpretations. By means of archaeometric analyses carried out on shards found in the Netherlands, the present research aims to shed more light on the origins of these majolica productions.

2 Experimental

Twenty-five representative fragments of imported “compendiario” majolica have been selected for laboratory analyses among the materials recovered from excavations in Amsterdam. Except for a fragment of a vase on a pedestal, all the samples belong to the category of open shape vessels, mostly plates and bowls. Some of them are completely white (called “bianchi” and labelled ADb1-6), while others are polychrome – yellow, orange and blue – fragments in “compendiario” style, consisting of different types of garlands positioned around a scene, usually with a *putto* figure (labelled ADc7-26). According to the Dutch art historians and archaeologists, samples ADc26 is of local production.

Observations on thin sections by means of optical microscopy (OM) have been carried out in order to characterise the microstructure and the morphology of pastes and glazes, while scanning electron microscopy combined with energy dispersive spectroscopy (SEM-EDS) has been used to determine their chemical compositions. Some samples have also been analysed by means of X-Ray Diffraction (XRD) for the individuation of the crystalline phases in the ceramic pastes.

3 Results and Discussion

3.1 Pastes

Observations on thin sections show that all the pastes consist of a very fine, isotropic and homogeneous groundmass. On the basis of the inclusions present, two groups of pastes can be recognised:

- Group A (ADb02, ADb03, ADb04, ADb05, ADb06, ADc21 and ADc26) with a-plastic inclusions in the ranges of silt ($<63\ \mu\text{m}$), very fine sand ($63\text{--}125\ \mu\text{m}$) and coarse sand ($500\text{--}1,000\ \mu\text{m}$), with a maximum size of about $700\ \mu\text{m}$ (Fig. 1a). The minerals are quartz (mono- and poly-crystalline grains), feldspar and biotite;
- Group B (all the other samples), in which coarse inclusions are absent (Fig. 1b).

The chemical composition (Table 1) evinces high contents of polluting elements, such as phosphorous (P_2O_5) and sulphur (SO_3), which are related to the interaction with the channel environment (Fabbri and Gualtieri 1999; Maritan and Mazzoli 2004; Tennent et al. 1996). It is also easily discernible that the chemical data are spread in a wide range of values, especially for CaO and MgO. In any case, on the

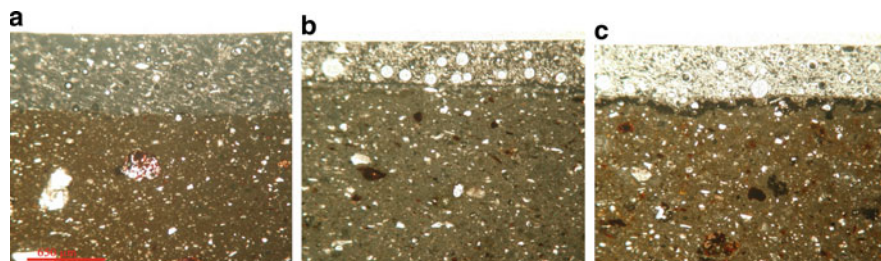


Fig. 1 Representative thin sections: (a) paste A covered by a glaze with high opacifying power (type 1); (b) paste B covered by a glaze with medium opacifying power (type 2); (c) paste B covered by a glaze with low opacifying power (type 3)

Table 1 Chemical composition of pastes (wt% oxides)^a

	SiO ₂	Al ₂ O ₃	TiO ₂	Fe ₂ O ₃	MgO	CaO	Na ₂ O	K ₂ O	P ₂ O ₅	SO ₃
“Bianchi”										
ADb01	59.95	13.43	0.69	5.17	4.24	13.19	1.48	1.77	1.95	3.18
ADb02	56.40	11.25	0.57	3.91	2.66	22.81	1.28	1.13	1.58	4.69
ADb03	52.18	10.87	0.60	4.30	1.67	28.19	1.37	0.82	1.36	5.85
ADb04	55.62	11.18	0.61	3.96	1.49	25.48	1.07	0.58	1.48	3.96
ADb05	54.70	12.61	0.86	5.16	1.88	22.20	1.10	1.50	0.50	1.85
ADb06	59.43	12.71	0.79	4.37	0.89	20.52	0.41	0.88	1.04	3.71
“Compendiario”										
ADc07	56.76	12.73	0.58	5.23	4.45	17.85	1.09	1.31	1.86	3.44
ADc08	50.67	12.18	0.62	7.02	5.59	21.22	1.83	0.88	0.69	6.04
ADc09	54.90	12.38	0.39	6.01	4.94	18.34	1.27	1.78	1.78	2.67
ADc10	57.71	12.73	0.90	5.10	5.03	15.61	1.70	1.22	0.38	1.78
ADc11	58.21	14.04	0.43	2.87	6.51	14.23	2.19	1.53	0.54	2.54
ADc12	56.94	12.47	0.49	5.41	5.85	14.93	1.02	2.89	0.34	4.01
ADc13	54.09	13.39	0.65	4.47	4.54	19.84	1.08	1.94	0.47	2.79
ADc14	52.92	11.71	0.67	4.39	3.15	25.01	1.12	1.03	0.37	1.97
ADc15	55.69	13.75	0.30	2.17	4.42	20.62	2.35	0.70	1.88	3.11
ADc17	56.85	13.36	0.64	6.05	6.68	13.69	1.10	1.63	0.60	3.62
ADc18	53.83	13.47	0.74	5.69	7.16	16.55	1.29	1.17	0.82	4.18
ADc19	52.96	13.52	0.73	5.71	7.35	17.92	1.03	0.82	0.74	3.28
ADc20	56.50	14.00	0.54	5.87	5.59	13.87	1.77	1.67	0.43	2.63
ADc21	55.33	13.26	0.61	4.83	3.70	18.86	1.28	2.17	0.35	3.70
ADc22	53.61	14.62	0.80	7.05	4.40	17.66	1.20	0.86	0.49	0.93
ADc23	58.54	12.81	0.82	5.24	4.49	14.23	2.50	1.37	0.56	2.55
ADc24	51.79	13.62	0.73	5.06	3.93	21.65	1.23	1.99	0.52	1.73
ADc25	58.32	13.32	0.72	4.95	5.23	14.44	1.33	1.69	0.93	1.52
ADc26	57.80	10.77	0.47	4.04	2.13	23.06	0.86	0.88	1.12	2.32

^aThe data have been normalised by excluding P₂O₅ and SO₃

basis of calcium and magnesium contents, it is possible to individuate two or three groups of samples:

1. Very high calcium content (20–28% CaO) and low magnesium content (<3% MgO); seven samples belong to this group, six of which included in the optical group A;

2. Medium (13–17% CaO) or high (17–22% CaO) calcium content and high magnesium content (>3% MgO); 18 samples, mainly included in the optical group B.

This indicates that the raw materials should have contained high amounts of calcite, or calcite and dolomite. The presence of newly formed phases such as pyroxene and gehlenite in the mineralogical compositions, together with the isotropy of the groundmass, allows us to define a range of firing temperature of 900–950°C (Cultrone et al. 2001).

3.2 Glazes

In thin sections, the glaze layers (150–350 µm in thickness), present on both recto and verso surfaces, are distinguishable into three different groups, corresponding to degrees of “opacifying power”.

This subdivision depends on the concentration and dimensions of the tin oxide crystals and on the presence and dimensions of bubbles (Fig. 1a–c): type 1 with high opacity and small bubbles – maximum 100 µm (Fig. 2a); type 2 and 3, with medium and low opacity, respectively, both with big bubbles – up to 250 µm (Fig. 2b).

The chemical compositions of the glazes (Table 2) show that all samples are characterised by high amounts of SiO₂ (≈53%) and PbO (≈24%), approximately in a 2:1 ratio. The tin oxide varies from 5 to 13%, with a decreasing trend among the glazes of type 1, 2 and 3.

Comparing the results of pastes and glazes (Table 3), it is clear that the so-called “bianchi” samples mainly show a paste with high CaO/MgO ratio, coated by a high “opacifying” glaze. On the contrary, the “compendiario” ones have a paste with low or intermediate CaO/MgO ratio, coated by a glaze with medium-low “opacifying power” (types 2-3). There are some exceptions, like ADb01, which is grouped together with the “compendiario” samples. It is also worth noting that the supposed local “compendiario” ADc26 does not cluster with samples of the same type.

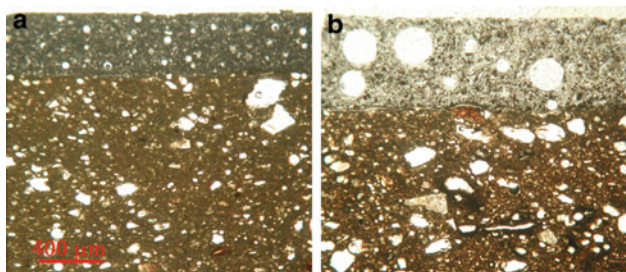


Fig. 2 Thin sections with details of the different types of glazes: (a) type 1 with high opacity and small bubbles; (b) type 3 with low opacity and big bubbles

Table 2 Chemical composition of glazes (wt% oxides)

	SiO ₂	Al ₂ O ₃	TiO ₂	Fe ₂ O ₃	MgO	CaO	Na ₂ O	K ₂ O	SnO ₂	PbO
“Bianchi”										
ADb01	51.59	4.42	0.11	0.39	0.59	1.38	2.41	3.16	7.55	28.10
ADb02	48.91	1.90	0.07	0.71	0.83	2.49	2.37	3.71	12.87	26.14
ADb03	49.73	2.06	0.56	0.45	1.04	2.99	2.37	3.88	12.27	24.64
ADb04	55.57	1.97	0.00	0.39	1.21	1.86	2.52	3.24	10.85	22.41
ADb05	49.28	5.57	0.21	0.56	1.19	2.15	3.52	4.45	7.62	25.45
ADb06	48.89	4.97	0.00	0.52	0.15	0.76	1.31	3.43	10.86	29.00
“Compendiario”										
ADc07	55.01	3.86	0.00	0.31	0.76	2.09	2.40	3.78	6.86	24.96
ADc08	51.29	4.13	0.06	0.29	0.51	1.71	2.06	3.20	6.13	30.63
ADc09	55.92	4.51	0.00	0.13	0.68	1.89	2.15	4.80	6.32	23.60
ADc10	55.52	4.01	0.04	0.19	0.70	1.76	2.26	3.81	5.88	25.83
ADc11	56.63	5.09	0.12	0.05	0.57	1.18	4.46	2.43	5.41	24.00
ADc12	52.11	4.30	0.15	0.52	0.33	2.10	1.43	3.83	7.13	28.11
ADc13	56.41	5.58	0.00	0.69	0.34	1.35	1.44	4.19	8.21	21.75
ADc14	54.65	4.89	0.02	0.20	0.83	3.14	1.98	5.73	5.82	22.73
ADc15	58.91	5.99	0.03	0.17	1.26	1.93	4.94	3.00	5.75	18.00
ADc17	54.70	3.41	0.08	0.44	0.69	2.01	1.61	3.46	10.44	23.17
ADc18	52.47	3.82	0.03	0.56	0.70	2.17	2.37	3.07	11.56	23.25
ADc19	52.11	4.01	0.78	0.58	0.86	2.74	2.24	2.23	12.27	22.17
ADc20	50.87	3.99	0.03	0.47	1.17	3.14	3.12	3.24	8.78	25.19
ADc21	54.84	4.85	0.00	0.46	0.21	1.16	1.88	4.51	8.97	23.51
ADc22	49.86	4.93	0.08	0.45	0.69	2.04	2.73	3.95	10.19	25.08
ADc23	51.36	3.58	0.00	0.40	0.52	1.78	2.30	2.57	9.27	28.22
ADc24	62.81	6.18	0.16	0.74	0.33	0.79	1.50	4.74	6.77	15.98
ADc25	56.39	4.29	0.00	0.82	0.82	1.99	2.13	3.69	5.42	24.46
ADc26	49.85	2.05	0.13	0.54	0.91	4.66	2.14	2.77	9.75	27.21

Table 3 Groups of samples based on thin section observations and chemical analyses

Glaze		Paste (CaO/MgO)		
Opacity	SnO ₂ %	<3.5	3.5–5	>7
High	11.2 ± 1.5		ADc21	ADb2, ADb3, ADb4, ADb6
Medium	9.1 ± 1.9	ADb01, ADc17, ADc18, ADc19, ADc23	ADc7, ADc9, ADc13, ADc22	ADb5, ADc26
Low	6.3 ± 1.1	ADc10, ADc11, ADc12, ADc20, ADc25	ADc8, ADc15, ADc24	ADc14

4 Conclusions

The “bianchi” and “compendiario” samples constitute two different archaeometric groups, and different explanations can be hypothesised for their origin: (1) presence in the area of several workshops specialised in one or the other type of ceramic production and using raw materials originating from different sources; (2) the recovered products are examples of commercial exchange between The Netherlands and different European countries; (3) the use of different raw materials in

order to obtain different products: a less fine body with high covering power glaze for the “bianchi” samples and vice versa for the “compendiario” samples; (4) a different period of production of the two typologies, with the use of different raw materials due to the exhaustion of argillaceous deposits.

The individuation of a defined production period and the small range of “bianchi” production resulting from the historical investigation allow us to exclude the last hypothesis. The third hypothesis can also be rejected, because the use of different recipes to obtain a better glaze (as for the “bianchi”) is attested, while the same situation is not common for pastes. It seems ineffectual to use different pastes in order to obtain similar products, like the “bianchi” and the “compendiario” ceramics are. Therefore, the existence of different workshops or imports from other countries are the most probable hypotheses. The next step in this project will consist of the comparison of these results with data from previously conducted studies on ceramic fragments from various Italian production centres; this could help in the individuation of their production sites.

References

- Baart JM (1985) Ceramiche italiane rinvenute in Olanda e le prime imitazioni olandesi. Paper read at Rapporti ceramici tra Italia ed Europa settentrionale, 28–30 maggio 1983, Albisola
- Baart JM, Krook W, Lagerweij AC (1990) Italiaanse en Nederlandse witte faience (1600–1700). Mededelingenblad Nederlandse vereniging van vrienden van de ceramiek 138:4–48
- Baart JM (1991) Italian pottery from the Netherlands and Belgium. In: Wilson T (ed) *Italian renaissance pottery*, London, pp 232–240
- Cultrone G, Rodriguez-Navarro C, Sebastian E, Cazalla O, De la Torre MJ (2001) Carbonate and silicate phase reactions during ceramic firing. *Eur J Mineral* 13:621–634
- Fabbi B, Gualtieri S (1999) Caratterizzazione e tecniche di intervento per il restauro di ceramiche con rivestimento vetroso solforato. In: Mascolo G (ed) *Atti II Convegno “Materiali e Tecniche per il restauro”*. Idea Stampa Editore, Cassino (FR), pp 135–146
- Grendi E (1971) I nordici e il traffico del porto di Genova: 1590–1666. *Rivista storica italiana* 83(1):23–71
- Hurst JG, Neal DS, van Beuningen HJE (1987) Pottery produced and traded in north-west Europe 1350–1650. *Rotterdam Papers. Het Nederlandse Gebruiksvoorwerp*, Rotterdam
- Jaspers NL (2007a) Met de Franse slag. Franse compendiariofaience uit Nederlandse bodem (ca. 1600–1660). *Vormen uit Vuur* 199:2–16
- Jaspers NL (2007b) Schoon en werkelijk aangenaam. Italiaanse importkeramiek uit de 16de en 17de eeuw in Nederlandse bodem. *Doctoraalscriptie, Archeologie van de Middeleeuwen en de Moderne tijd*, Universiteit van Amsterdam, Amsterdam
- Lindblad JT (1998) Nederlanders en de Oostzee, 1600–1850. In: Daalder R., van Eyck van Heslinga E, Lindblad JT, Rogaar P, Schonewille P (eds) *Goud uit graan. Nederlanders en het Oostzeegebied 1600–1850*, Zwolle, 8–27.
- Maritan L, Mazzoli C (2004) Phosphates in archaeological finds: implications from environmental conditions of burial. *Archaeometry* 46(4):673–683
- Ostkamp S (2003) Majolica en faience uit een beerput op het bedrijfsterrein aan het Oosteinde. Een greep uit het assortiment van De Porceleyne Fles (1660–1680). In: Schledorn LA, van Aken-Fehmers MS, Eliëns TM (eds) *Geschiedenis van een nationaal product. De Porceleyne Fles*, Zwolle, pp 14–47

- Rosen J (2002) Diffusion de la technique et production de majolique en France aux XVIe et XVIIe siècles. In: Veeckman J, Jennings S, Dumortier C, Whitehouse D, Verhaeghe F (eds) *Majolica and glass from Italy to Antwerp and beyond. The transfer of technology in the 16th-early 17th century*, Antwerpen, pp 333–346
- Rosen J (2003) L’émancipation des sources gravées: de la majolique italienne à la faïence française (1540–1645). In: Rosen J (ed) *Majoliques Européennes. Reflets de l’Estampe Lyonnaise (XVI–XVII siècles)*. Actes des journées d’études internationales. Estampes et Majoliques, Rome/Lyon, pp 126–141
- Tennent NH, Baird T, Gibson LT (1996) The technical examination and conservation of blackened delftware from anaerobic sites. In: *Archaeological conservation and its consequences*, Stockholm, 182–187

Archaeometry of Bronze Age and Early Iron Age Italian Vitreous Materials: A Review

I. Angelini

1 Introduction

In the past 7 years, several research projects aimed at the characterisation of Italian Bronze Age (BA) vitreous materials were carried out in collaboration with Museums, National and Regional Institutions (Soprintendenze), and University Archaeological Departments. Over 130 objects, mainly ornamental beads, have been selected based on typology and chronology. The samples were analysed using different analytical techniques, methodologies and experimental conditions specifically adapted to small BA vitreous material beads (Angelini et al. 2002, 2004, 2005; Artioli et al. 2008). The results of the archaeometric studies reveal a remarkably dynamic picture of the development of glass technology and diffusion; the compositional variations being strongly related not only to the age, but also to the geographic context of the materials.

Further, it is worth noting that there is a surprising scarcity of data concerning the transition between the Final Bronze Age (FBA) and the Iron Age (IA). Recently, four new projects focused on Italian Early Iron Age (EIA) vitreous materials have been planned, aimed at covering the analytical information gap. The results of two projects, related to seventy EIA beads from Northern Italy, are presented for the first time in Angelini et al. (2010) and Polla et al. (2010). The other projects, concerning 135 vitreous material objects dated to the EBA-EIA from Sicily and Sardegna (Nicola et al. 2008) are still in progress, and only preliminary results will be reported.

I. Angelini

Dip. di Geoscienze, Università degli Studi di Padova, Via Giotto 1, 35137 Padova, Italy
e-mail: ivana.angelini@unipd.it

2 Vitreous Materials Texture and Compositions: Changes from Eba to Eia in Continental Italy

Prehistoric vitreous materials exhibit a high variability both in terms of chemical composition and in terms of texture. They are important indicators of changes in glass production. The difference in the amount of glass/crystals may be quantified by computerised 2-D image processing (DIP) of SEM-BSE images. The parameter X_M (i.e., the glass matrix area/total area excluding porosity) is particularly useful for the classification of vitreous materials (Angelini et al. 2002, 2004) into faience, glassy faience, and glass. The different material types have a specific evolution in time.

2.1 Faience of the Early Bronze Age (EBA, 2100–1700/1650 BC)

Vitreous materials of EBA age are found exclusively in Northern Italy. Only faience beads with simple typologies (biconical and segmented beads) have been found (Bellintani et al. 2006). Unfortunately, in most cases the glaze is heavily weathered; 13 samples from three different sites have been analysed, but only three show surviving glass (Angelini et al. 2006a, b). The glaze has a consistent Low Magnesium High Potassium (LMHK, Fig. 1) composition, similar to the one of

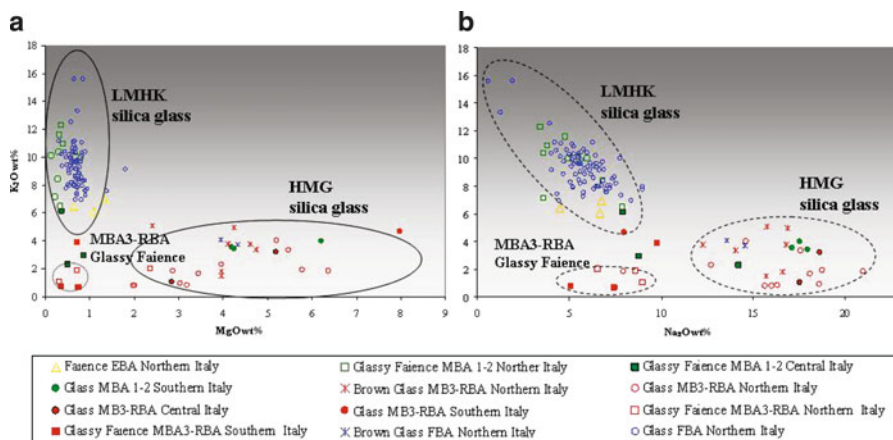


Fig. 1 Summary plots of BA glass chemical data. (a) K₂O vs MgO (wt%); (b) K₂O vs Na₂O (wt%). Colours are related to different age: yellow = EBA, green = MBA1-2, red = MBA3-RBA, blue = FBA. Symbols are related to different materials: triangles = faience, squares = glassy faience, circles = glasses, stars = HMBG glasses. Empty symbols = objects from Northern Italy; full symbols with black border = objects from Central Italy; full symbols = objects from Southern Italy. (Reference list and unpublished data)

coeval European faience samples, whereas the minor and trace elements indicate local productions (Angelini et al. 2006a; Tite et al. 2008).

2.2 *Glassy Faience and Glass of the Middle Bronze Age 1–2 (MBA1-2, 1700/1650–1450 BC)*

Faience samples from this period are no longer present in Northern Italy, and only glassy faience ornaments with special local typology (conical buttons) have been found (Bellintani et al. 2006). All the 11 analysed objects from six different localities have a glass phase with LMHK composition (Fig. 1, data from Angelini et al. 2002, 2005 and unpublished data). In Central Italy, a few conical buttons have been found, showing a LMHK glass, but with a Na/K ratio different from the Northern Italian ornaments (Fig. 1, Angelini et al. 2005). At Prato di Frabulino, biconical glassy faience beads (analyses by Santopadre and Verita 2000, not reported in Fig. 1) and a spacer (Bellintani et al. 2006) have also been discovered. These ornaments show an LMHK composition similar to the composition of the FBA glasses.

During this period, “true” glasses made their first appearance in Central and Southern Italy (Angelini et al. 2002, 2005). They are composed of High Magnesium Glass (HMG), generally coloured by copper. In Sicily, a few faience beads with simple typologies are reported, though analyses are still lacking (Bellintani et al. 2006).

Because of the local typology and the LMHK compositions, the MBA1-2 glassy faience samples are supposed to indicate a local production, whereas the HMG glass objects are considered to have a Near Eastern origin.

2.3 *Glassy Faience and Glass of the Middle Bronze Age 3: Recent Bronze Age (MBA3-RBA, 1450–1200 BC)*

During this period, HMG glass beads with simple typologies are present everywhere in the Italian peninsula (Fig. 1; Bellintani et al. 2006). The beads are mainly composed of Cu-blue glass, whereas white glass is used essentially for decorations. Well preserved white glasses are rare, and the only certain analytical data obtained show a glass with scarce amounts of colouring metals, high level of Ca and several pyroxene crystal inclusions. Although direct evidence of production sites is not yet available for this phase, the presence of a peculiar class of HMG brown glasses (HMBG) having a unique composition and texture has been identified in Northern Italy, suggesting the existence of small glass making or glass working centres. The HMBG samples are characterised by a glass phase very rich in Fe (FeO in the range of 3–10 wt%), Ca and Al, with abundant augitic pyroxenes and copper-iron sulphide inclusions (Fig. 1; Angelini et al. 2005; Artioli et al. 2008).

In the MBA3-RBA, glassy faience and possibly faience are present especially in Southern Italy (Bellintani et al. 2006). The situation is extremely confused because of the scarce analytical data available on Southern Italian objects (Fig. 1), so that even the nature of the materials is often doubtful. These beads are of various typologies related to the Eastern Mediterranean area, the Near East and Egypt (Bellintani et al. 2006). They also show high variability in terms of glass composition (Fig. 1): all but one (an HMG glass phase) contain low amounts of K, Mg and Ca, and thus no clear correlation between typology, provenance and composition is possible. In two glassy faience beads (Angelini et al. 2005; Santopadre and Verita 2000), the use of Co as colorant is attested for the first time in Italy. The trace elements associated with Co (Sb, Pb and Ni) indicate a similarity to Aegean beads (Tite et al. 2005), thus suggesting a possible origin for these objects (Angelini et al. 2005; Tite et al. 2005).

2.4 Final Bronze Age Glass (FBA, 1200–900 BC)

In the Final Bronze Age (FBA), there is a critical change in terms of glass composition: LMHK glass, largely diffused in Northern Italy, starts to be massively produced (Fig. 1). The archaeological investigations of the Frattesina site and nearby areas produced clear evidence of a number of glass production workshops in FBA Italy (Henderson 1988; Brill 1992; Towle et al. 2001; Angelini et al. 2004). Similar glass beads have been found at eight other Italian sites (Angelini et al. 2002, 2006b, 2007 and unpublished data) and at several coeval European sites. To date, there are no clear results that may support the hypothesis of the existence of different production centres. The statistical analysis of the chemical data by Principal Components Analysis (PCA) shows that the chemical differences are mainly related to the colouring components. In the Co-blue beads, a weak correlation between the chemistry and typology of the beads is observed (Angelini et al. in press), indicating the possibility of the presence of different production centres.

The wide diffusion of LMHK glass coincides with the disappearance of imported HMG vitreous materials, and only two HMBG glass samples can be dated to this period (Fig. 1). Interestingly, the colouring agents used in the FBA differ from the ones of the MBA3-RBA: Co is associated with different trace metals (mainly Ni), possibly indicating a different Co source, and red glass appears for the first time, obtained by the in situ reduction of copper to metal microparticles (Angelini et al. 2004, 2007). With few exceptions, the use of faience and glassy faience is largely discontinued.

2.5 Early Iron Age Glass (EIA, 900–600 BC)

At the very beginning of EIA, the archaeological records attest the presence of entirely new materials and varied object typologies. The EIA glass strongly differs

in macroscopic texture and colour from the previous materials and also from the subsequent Roman glasses.

The FBA LMHK composition has been encountered only in rare Golasecca beads dated to the ninth century BC (Fig. 2). In the coeval Villanovan Bologna area, the few glass beads present show an LMG-like glass composition.

Northern Italian EIA glasses have essentially LMG and HMG compositions, although they show a remarkable degree of compositional variation. New components are used in glass production, including: (1) lead antimonate as yellow colorant; (2) Ca antimonate in the white opaque glass; (3) high amounts of Fe, and sometimes Mn, in the dark blue/black glass; (4) Pb in opaque dark blue/black glass objects which show numerous crystals and metallic inclusions, but no Pb-antimonate particles (Angelini et al. 2010; Polla et al. 2010). The compositional variability of the glass is likely to be related both to different origins of the materials and to the glass recycling process.

	North Italy	Central Italy	South Italy	Sardinia
EBA	Blue faïence LMHK			(?)
MBA 1-2	Glassy Faïence LMHK (Conical Buttons)	Glassy Faïence LMHK (Conical Button, higher Na/K); & Glassy Faïence LMHK beads & few HMG glass	HMG blue & Faïence (?)	(?)
MBA 3-RBA	HMG brown Glass (HMBG)			Faïence and Glass showing age-typology-composition relations different from the ones of continental Italy. Mainly HMG and LMG glass (to date no LMHK observed). Numerous black faïence with high Mn and Fe.
	HMG blue glass & Glassy Faïence (different typologies, no conical buttons)	HMG blue glass & Glassy Faïence (different typologies, no conical buttons)	HMG blue glass & Faïence (?) & numerous Glassy Faïence (different compositions and typologies, no conical buttons)	
FBA	LMHK glass	Few Glass (?)	Few Glass (?)	
EIA : IX cent. BC	Few LMHK glass beads with simple typology in the Golasecca area.			
	Few glass beads with composition similar to LMG (but low Ca, high Fe)	(?)	(?)	
EIA: VIII-VI cent. BC	Complex and variable compositions and typologies (HMG, LMG and similar composition with some chemical variations). In the Golasecca area: Glassy Faïence/Glass with high Pb	Glass (?) & (?)	(?)	

Fig. 2 Summary of the age, location and compositional changes of EBA-EIA vitreous materials. *Red lines* mark abrupt compositional changes related to the geographical distribution. *Hatching lines* indicate supposed changes, though no chemical data are available, or partial compositional change, for example in Central Italy between MBA-1 and MB3-RBA: LMK samples disappear, but HMG samples are still observed. *Question marks* indicate open problems

3 Short Note on the Prehistoric Vitreous Materials from Italian Islands

In Sardinia, vitreous materials are present from the MBA3-RBA onward, thus somehow later than in continental Italy (Bellintani et al. 2006). Among the investigated materials, fragments of glassy faience are rare, whereas glass and faience are the most frequent occurrences.

All the analysed samples of glass have HMG, LMG or similar compositions. To date, no fragments of LMHK glass have been found (Fig. 2). Some technological innovations, such as the use of lead antimonate, seem to appear earlier in Sardinia than in Northern and Central Italy. These two factors suggest that Sardinian vitreous materials were preferentially imported from the Near East and Egypt rather than from the Italian mainland (Nicola et al. 2008). No chemical data are currently available for the Sicilian materials.

4 Conclusions

The brief overview on BA-EIA vitreous materials reported here is summarised in Fig. 2. The resulting picture is clearly more complex than expected before this investigation. Although a few open questions remain (question marks in Fig. 2), it is now possible to outline a satisfactory compositional stratigraphy of these materials. The red lines in Fig. 2 show at least four abrupt changes of composition in time, whereas the green lines are related to the geographic changes.

A few hypotheses may explain the observed changes in the production and trade of vitreous materials; for example, the arrival, diffusion and disappearance of HMG glass are commonly related to the history of the Mycenaean culture. Nevertheless, the cultural, social and economic background influencing the early use, the abandonment, the rediscovery and the final discontinuation of the LMHK glass production is to date largely unknown. In the EIA, the production of glass became more and more complex.

Acknowledgements The author is grateful to all the archaeologists involved in the projects for fundamental contributions and discussions. Special thanks are due to the archaeometric collaborators: Prof. Gilberto Artioli, Prof. Gianmario Molin, Dr. Angela Polla and Dr. Chiara Nicola.

References

- Angelini I, Artioli G, Bellintani P, Diella V, Polla A, Residori G (2002) Project “Glass materials in the protohistory of North Italy”: a first summary. In: D’Amico C (ed) *Atti II Congresso Nazionale di Archeometria*, 2002. Pàtron Editor, Bologna, pp 581–595
- Angelini I, Artioli G, Bellintani P, Diella V, Gemmi M, Polla A, Rossi A (2004) Chemical analyses of Bronze Age glasses from Frattesina di Rovigo, Northern Italy. *J Archaeol Sci* 31:1175–1184

- Angelini I, Artioli G, Bellintani P, Polla A (2005) Protohistoric vitreous materials of Italy: from early faience to final bronze age glasses. In: Cool H (ed) *Annales of 16th AIHV Congress*, London, pp 32–36
- Angelini I, Artioli G, Polla A, De Marinis RC (2006a) Early Bronze Age faience from North Italy and Slovakia: A comparative archaeometric study. In: *Proceedings of the 34th International Symposium on Archaeometry*, 3–7 May 2004, Zaragoza, Spain; 371–378, <http://www.dpz.es/ifc/libros/libros.htm>
- Angelini I, Nicola C, Artioli G (2006b) Studio analitico dei materiali vetrosi. In: *Navigando lungo l'Eridano. La necropoli Golasecchiana di Morano Po*, Marica Venturino Gambari ed., Ministero per i Beni e le attività Culturali, Soprintendenza per i Beni Archeologici del Piemonte, Casale Monferrato, pp 77–82
- Angelini I, Polla A, Artioli G (2007) I vaghi in vetro provenienti dalla necropoli di Ponte Nuovo (Gazzo Veronese): indagini archeometriche e confronto con materiali coevi. *Notizie Archeologiche Bergomensi* 13, 2005. Museo archeologico di Bergamo, Bergamo, pp 141–152
- Angelini I, Nicola C, Artioli G, deMarinis RC, Rapi M, Uboldi M (2010) Chemical, mineralogical and textural characterization of the Early Iron Age vitreous materials from the Golasecca culture (Northern Italy). In: Turbanti-Memmi I (ed) *Proceedings of 37th International Symposium on Archaeometry*, 12th – 16th May 2008, Siena, Italy. Springer, Hiedelberg
- Angelini I, Polla A, Giussani B, Bellintani P, Artioli G (2009) Final bronze age glasses in northern and central Italy: is Frattesina the only glass production center?. In: *Proceedings of the 36th International Symposium on Archaeometry*, Quebec City, Canada, 2–6 May, 2006, 329–337, CELAT, Université du Laval
- Artioli G, Angelini I, Polla A (2008) Crystals and phase transitions in protohistoric glass materials. *Phase Transitions* 81(2&3):233–252
- Bellintani P, Angelini I, Polla A, Artioli G (2006) Origini dei materiali vetrosi italiani: esotismi e localismi. *Atti della XXXIX Riunione Scientifica I.I.P.P.*, Firenze, Italy, 25–27 November 2004, Vol III. pp 1495–1532
- Brill RH (1992) Chemical analyses of some glasses from Frattesina. *J Glass Stud* 34:11–22
- Henderson J (1988) Electron probe microanalysis of mixed-alkali glasses. *Archaeometry* 30: 77–91
- Nicola C, Angelini I, Artioli G, Bellintani P, Fadda MA, and Usai A, (2008) Materiali vetrosi della Cultura Nuragica: studi archeometrici preliminari, V Congresso Nazionale di Archeometria, Scienza e Beni Culturali – Siracusa – 26–29 Febbraio 2008. Abstracts Volume, 146
- Polla A, Angelini I, Artioli G, Bellintani P, Dore A (2010) Archaeometric investigation of early iron age glasses from Bologna. In: Turbanti-Memmi I (ed) *Advances in archeometry*. Springer, Hiedelberg
- Santopadre P, Verita M (2000) Analyses of production technologies of Italian vitreous materials of the Bronze Age. *J Glass Stud* 42:25–40
- Tite MS, Hatton G, Shortland AJ, Manatis Y, Kavoussanaki D, Panagiotaki M (2005) Raw materials used to produce Aegean Bronze Age glass and related vitreous materials. In: Cool H (ed) *Annals of 16th AIHV Congress*, London, pp 10–13
- Tite MS, Shortland AJ, Angelini I (2008) Faience production in northern and western Europe. In: Tite MS, Shortland AJ (eds) *Production technology of faience and related early vitreous materials*, Monograph No 72. Oxford University School of Archaeology, Oxford, pp 129–146
- Towle A, Henderson J, Bellintani P, Gambacurta G (2001) Frattesina and Adria: report of scientific analyses of early glass from the Veneto. *Padusa* 37:7–68

Chemical, Mineralogical and Textural Characterisation of Early Iron Age Vitreous Materials from the Golasecca Culture (Northern Italy)

I. Angelini, C. Nicola, G. Artioli, R. DeMarinis, M. Rapi, and M. Uboldi

1 Introduction and Description of Samples

During the last 3 years, a systematic archaeometric investigation of the protohistoric glass materials from the Como area has been carried out. This research is part of a long-term project aimed at defining a high-resolution chemical chronology of protohistoric Italian glass (Angelini et al. 2004, 2005), and the Como project specifically seeks to yield data that would cover the gap regarding the transition from the Bronze Age to the Iron Age. The investigated materials are all from the “P. Giovio” Archaeological Museum in Como. A set of beads made of vitreous material were carefully selected for analyses on the basis of their age, bead typology, and nature of the glass material. The beads are from Early Iron Age cemeteries of the Como area, except for one bead found in a grave of the Canegrate

I. Angelini (✉) and G. Artioli

Università degli Studi di Padova, Dip. di Geoscienze, Via Giotto 1, I-35137 Padova, Italy
e-mail: Ivana.angelini@unipd.it, gilberto.artioli@unipd.it

C. Nicola

Università degli Studi di Milano, Dip. di Scienze della Terra, Via Botticelli 23, I-20133 Milano, Italy
e-mail: chiara.nicola@unimi.it

R. DeMarinis and M. Rapi

Università degli Studi di Milano, Dip. di Scienze dell'Antichità, Via Festa del Perdono 7, I-20122 Milano, Italy
e-mail: raffaele.demarinis@unimi.it, marta.rapi@unimi.it

M. Uboldi

Museo Civico Archeologico di Como
e-mail: uboldi.marina@comune.como.it

Culture at Appiano Gentile. The archaeological and age data of the beads are reported in the following table:

<i>Phase</i>	<i>Age</i>	<i>Number, typology and archaeological note on the analysed objects</i>
Recent Bronze Age (RBA)	Thirteenth century BC	An exceptional bead, with a very particular typology has been studied in the present paper. It is a brown bead with blue and white eyes decoration, from Appiano Gentile (Canegrata Culture).
Golasecca I A1 (G.IA1),	Ninth century BC	During this phase, vitreous materials are rare in the area. Three small annular beads from Ca' Morta grave 289, monochrome of blue transparent glass, have been sampled.
Golasecca IB (G.IB)	Mid-eighth – beginning of the seventh century BC	Few vitreous objects from this phase have been found to date. The only bead analysed is a monochrome bead of violet-blue colour, from Ca' Morta grave 102.
Golasecca IC (G.IC)	Seventh century BC	For this study, we have selected the exceptional assemblage from a female grave (Ca' Morta III/1921) dating to the mid-seventh century BC, composed of: Six glass beads. For the first time, we encountered beads with eyes decoration, formed of three concentric circular yellow threads, some also with a zig-zag motif around the hole, a type mostly spread in the Japodic-Liburnic area (Northern Dalmatia) (Haevernick 1987, map 7). Two blue cylindrical beads with white irregular ring decorations are also present in the grave.
Golasecca IIA (G.IIA)	End of the seventh – beginning of the sixth century BC	Two objects that belong to this phase, the beads from Ca' Morta graves 24 and 30, have been sampled. They are eye beads with three concentric circular yellow threads showing a compact and translucent glass phase.
Golasecca IIA-B (G.IIA-B)/ Golasecca IIB (G.IIB)	Around the middle of the sixth century BC/end of the sixth – beginning of the fifth century BC	During the G.IIA-B phases, larger beads decorated with three concentric circular yellow threads on three sides become very frequent (the following analysed samples: Ca' Morta graves 4, 229, 232, 256, the Baserga Situla grave and probably also Civiglio Pregosa belong to these phases). This bead type is again recorded in the G.IIB, as shown by finds from Ca' Morta graves 261, 277, 294, and the Brunate grave from the Pissarottino site; a total of 17 beads with this typology have been analysed.

Two beads with yellow striped decorations from Rondineto have also been analysed. They belong to an old discovery without a reported archaeological context, probably dated to the Late Iron Age.

Analytical data on Italian Early Iron Age glass samples are extremely scarce in the literature, and they are generally limited to few Etruscan objects lacking a precise archaeological context (Brill 1999; Towle et al. 2001). Therefore, in the present work, the results will be discussed without a comparison with other coeval materials.

2 Experimental Techniques

The 36 selected beads were micro-sampled for the analyses. 60 micro-samples, representative of the different glass textures and colours, were taken. One of the body samples and a large number of the decorations (about 10) show extensive weathering. In the following plots, only the samples not affected by weathering are reported and discussed. The symbols used in the diagrams are relative to the provenance of the sample, whereas the colours are related to the typology (see the legend of Fig. 1).

The mean chemical composition of the glass phase was obtained by Electron Probe Microanalysis with Wavelength Dispersive Spectroscopy (EPMA-WDS), whereas the morphology, the texture and the nature of the glass inclusions have been studied by Scanning Electron Microscopy with Energy Dispersive Spectroscopy (SEM-EDS). The identification of the mineral phases present in the vitreous material as unreacted or newly formed crystalline phases (Artioli et al. 2008) was performed by non-invasive X-Ray diffraction (XRD) analysis, whereas the textural study was performed by Digital Image Processing (DIP) of the backscattered electron SEM images. The methodologies, technical details and experimental conditions employed are described in more detail in previous papers (Angelini et al. 2004, 2005).

3 Results and Discussion

The major compositional classes of the analysed glass samples may be identified in the K_2O vs. MgO diagram (Fig. 1). The results neatly show that the Bronze Age glasses differ completely in chemical composition from the Iron Age glasses. All three glass types (white, blue and brown) present among the RBA eye beads from Appiano Gentile are HMG glasses (Fig. 1). It is worth noting that these types of glass are well known and diffused in Italy during the Middle Bronze Age 3 (MBA3) – RBA. In particular, the samples of brown glass show typical augitic crystals characteristic of the HMG brown glasses (HMBG), which are possibly materials derived from Italian local productions (Angelini et al. 2005; Artioli et al. 2008; Tite et al. 2008). The three annular blue beads dating to the ninth century BC are fully comparable with the data available for Final Bronze Age (FBA) objects; they belong to the typical European LMHK recipe (Fig. 1), and are consistently coloured by Cu (Brill 1999; Angelini et al. 2004; Tite et al. 2008). The beads date to the

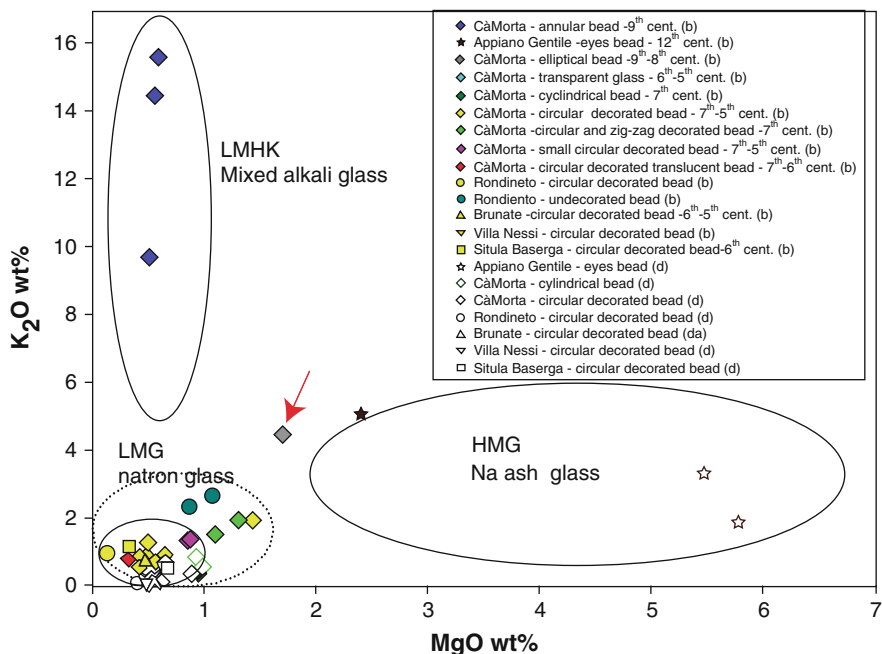


Fig. 1 K₂O vs MgO (wt%). The samples of glass from the beads' bodies are reported with full symbols, while the ones from the decorations are reported with empty symbols. Colours correspond to different ages, whereas the different symbols are related to the provenance (as summarised in the legend)

period between the seventh and the fifth centuries BC, and they invariably display a K/Mg ratio similar to LMG glasses (presented in Fig. 1 as a circled line), although some of them show higher Mg and K contents (Fig. 1, dotted line). It is interesting to note that the only bead dated to the eighth century BC (CM 102) exhibits an average composition with respect to the glass types discussed above (Fig. 1, point with the arrow). Although it is theoretically possible to obtain such a composition by a mixing of HMG and LMHK glasses, a few observations seem to rule out this hypothesis: (1) the LMHK glasses of the FBA are generally coloured by Cu or Co and white LMHK glasses are extremely rich in crystal inclusions (Artioli et al. 2008; Artioli and Angelini in press); no crystal inclusions or appreciable amounts of Cu and Co are present in CM 102, which is coloured in pale violet by Mn (MnO 0.36 wt%). (2) The ratio $\text{Na}_2\text{O}/\text{K}_2\text{O} = 2.9$ is quite comparable with the use of Na plant ashes, and it is too high to be the result of a substantial mixing of Na-poor LMHK glass. (3) The level of Al is quite high ($\text{Al}_2\text{O}_3 = 4.16$ wt%), and therefore is it possible that the low increase in K may derive from the use of impure sand.

The decorations are mainly made of yellow opaque glass. Only the two cylindrical beads from the G.I.C period show white opaque glass decorations. Both coloured glasses contain a large amount of crystal inclusions: Pb antimonate in the yellow glass, and Ca antimonate in the white one. The two glass types are also

very different in terms of the chemical composition of the glass phase; in particular, the white glass samples have higher levels of Ca and Mg, whereas the yellow ones show a high Pb content.

All the beads dated to the period between the seventh and the fifth centuries BC have similar Mg content (Fig. 1), but differ markedly in terms of the contents of the other principal elements. The chemical separation between bead typologies is barely visible in the K_2O/MgO diagram (Fig. 1), but the distinction becomes evident by plotting the $FeO-CaO-K_2O$ ternary diagram (Fig. 2). The globular beads made of clear transparent glasses (dated to the G.IIB, red in Figs. 1–3) have a typical LMG composition. The cylindrical beads show an LMG-type glass chemistry, although they are sufficiently distinct to form a separate cluster (dark green rhombi in Fig. 2). The two undated and undecorated beads from Rondineto also cluster together, because of the similar levels of Ca, Fe and K: about 2 wt% (dark green circles in Fig. 2). In this ternary diagram, the remaining globular beads dating from the seventh to the sixth century BC group in the same area. Within this area, a correlation between several different typologies and compositions is appreciable, especially for the zigzag-decorated and small eye beads (pale green and fuchsia rhombi in Fig. 2, respectively).

Two main groups of globular dark-blue and black beads (seventh to sixth century BC) are clearly distinguished (Fig. 3):

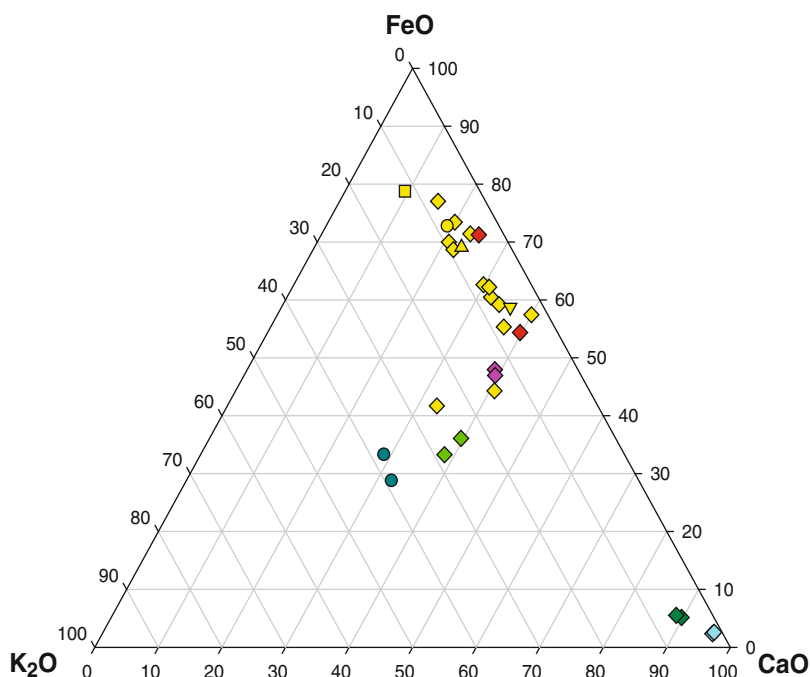


Fig. 2 Ternary diagram: $FeO-CaO-K_2O$ (wt%) of samples from the bodies of globular beads dated from the seventh to the fifth centuries BC; symbols as in Fig. 1

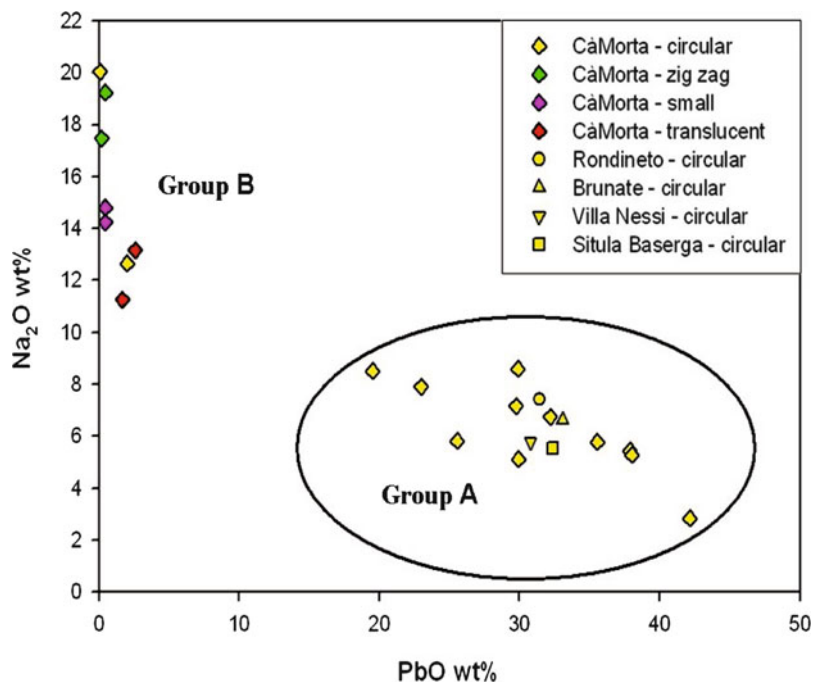


Fig. 3 Na₂O vs PbO (wt%). The diagram shows the data of samples from the bodies of globular beads dated from the seventh to the fifth centuries BC, and with similar K₂O, MgO and CaO amounts

A – a group of high-Pb glasses, composed of objects having the same typology: beads with eye decorations, formed by three concentric circular yellow threads. The black body is Pb-rich and contains small Pb-rich droplets, and it is completely devoid of Pb antimonate crystals, which are otherwise very frequent in the yellow decorations.

B – a second heterogeneous group of beads, with different typologies, characterised by the use of Na as main fluxing element and often coloured with Co.

The two groups also differ strongly in their microstructure: group A shows a very heterogeneous glass with abundant inclusions of different mineralogical nature; group B consistently shows a minor amount of inclusions, generally composed of SiO₂ and, possibly, metals.

4 Conclusions

The main results of the present work provide evidence for a radical change in glass composition at the end of the ninth century BC within the materials of the Gola-secca Culture. The analysed RBA and ninth century BC glasses from the same area

show typical HMG and LMHK compositions, respectively, as normally observed in the other Italian glasses of the RBA and FBA (Brill 1999; Angelini et al. 2004, 2005; Tite et al. 2008). For the first time, an HMBG glass of possible Italian production (Angelini et al. 2005; Tite et al. 2008; Artioli et al. 2008) has been found associated with HMG blue and white glasses (generally referred as imported glass) in the same object.

The only analysed bead from the eighth century BC shows a composition different from all the other glasses, testifying that the LMHK recipe was no longer in use. However, the small number of vitreous objects dated to this period and the absence of literature data on coeval materials precludes at this stage the formulation of reliable hypotheses concerning the raw materials, the production processes, or the provenance of the glass.

In Northern Italy, the use of antimonate to produce coloured opaque glass is first attested in the seventh century BC, and is generally related to the glass used in the decorations of the beads, as clearly emphasised by the analyses of the Golasecca samples. In the yellow glass, the colour is due to the Pb antimonate crystal inclusions, whereas Ca antimonate is used to produce opaque white glass.

The chemical composition of the beads dated to the period between the seventh and the fifth centuries BC is a function of the age and the typology. The LMG glasses indicate possible imports from the Eastern Mediterranean or the Near East, although the substantial variability in the making and typology of the beads, coupled with the lack of comparable data, does not exclude a local production. In particular, we have identified the earliest use of Pb vitreous materials in Italy: they appear at the end of the seventh century BC and form a compositionally homogeneous class. They are beads with eye decorations formed by three concentric circular yellow threads, and are dated to the G.IIA–G.IIB periods. These glasses are also characterised by the presence of a high amount of crystal inclusions in the glass matrix. The mineralogical nature of the inclusions suggests the use of impure and poorly selected sands as raw materials.

Acknowledgements The Museo Civico Archeologico “P. Giovio” in Como is kindly acknowledged for making the samples available for the investigation.

References

- Angelini I, Artioli G, Bellintani P, Diella V, Gemmi M, Polla A, Rossi A (2004) Chemical analyses of Bronze Age glasses from Frattesina di Rovigo, Northern Italy. *J Arch Sci* 31:1175–1184
- Angelini I, Artioli G, Bellintani P, Polla A (2005) Protohistoric vitreous materials of Italy: from early faience to final bronze age glasses, In: Cool H (ed) *Annales of 16th AIHV Congress de l' Association Internationale pour l'Histoire du Verre*, London, pp 32–36
- Artioli G, Angelini I, Polla A (2008) Crystals and phase transitions in protohistoric glass materials. *Phase Transitions* 81(2 &3):233–252

- Artioli G, Angelini I (in press) Evolution of vitreous materials in Bronze Age Italy. Charter 5.4. In: Janssens K (ed) *Modern methods for analysing archaeological and historical glass*. University of Antwerp, Belgium
- Brill RH (1999) *Chemical analyses of early glass*. Corning Museum of Glass, New York
- Haevernick Th E (1987) *Glassperlen der vorrömischen Eisenzeit II*, Marburger Studien z. Vor- u. rühgeschichte 9, Marburg/Lahn
- Tite MS, Shortland AJ, Angelini I (2008) Faience production in northern and western Europe, Chapter 7. In: Tite MS, Shortland AJ (ed) *Production technology of faience and related early vitreous materials*. Oxford University School of Archaeology Monograph No. 72, Oxford, 129–146
- Towle A, Henderson J, Bellintani P, Gambacurta G (2001) Frattesina and Adria: report of scientific analyses of early glass from the Veneto. *Padusa* 37:7–68

Mapping Regional Ceramic Fabrics in Sagalassos (SW-Turkey), Dating from 500 BC–700 AD

D. Braekmans, B. Neyt, P. Degryse, J. Elsen, J. Poblome, and M. Waelkens

1 Introduction

Since the start of the excavations at Sagalassos in 1990, interdisciplinary research has been carried out with the purpose of reconstructing the economic history of the site. One of the most important finds was the discovery that Sagalassos was an important regional centre for pottery manufacture from at least the late Hellenistic period into early Byzantine times (Poblome 1999; Degeest 2000). In order to understand regional ceramic production and identify the clay raw materials used, an integrated approach of typological, petrographic and geochemical methods is used in the present study.

2 Materials and Methods

2.1 Materials

The ceramic assemblage presented in this study includes material from Sagalassos itself ($n = 33$), the so-called “fabric 4” sherds, which are mainly used for cooking and storage functions. These sherds can be dated to the late Roman period (550–650 AD) based on seriation data (Degeest 2000). A second group of samples ($n = 129$) was collected from the site of Tepe Düzen (excavated by H. Vanhaverbeke), a mainly Classical-Hellenistic (proto-)urban settlement (tentatively dated to

D. Braekmans (✉), B. Neyt, P. Degryse, and J. Elsen
Section Geology, Earth & Environmental Sciences, Celestijnenlaan 200 E, bus 2408, B-3001, Leuven, Belgium
e-mail: dennis.braekmans@ees.kuleuven.be

J. Poblome, and M. Waelkens
Sagalassos Archaeological Research Project, Blijde-Inkomststraat 21, bus 3314, B-3000, Leuven, Belgium

the fifth to third centuries BC) located at approximately 1.5 km from Sagalassos. For correlation purposes, reference samples are included. This reference material consists of the locally produced red slipped tableware, referred to as “Sagalassos Red Slip Ware”; the raw material used for these tablewares and a commonly used mineral resource (ophiolitic origin) were located at the Potters’ Quarter of Sagalassos (Ottensmeyer et al. 1993; Poblome 1999; Poblome et al. 2001; Poblome 2006; Degryse and Waelkens 2008). Despite the chronological discrepancy, the selected assemblages provide information pertaining to the mechanisms of a regional economy and the diachronic organisation of production.

A full typological and diachronic overview of the Classical-Hellenistic ceramics at Tepe Düzen will be presented in the near future. The ceramic assemblages of this site show generic typological features of the period, along with some minor Greek, Achaemenid and Cypriot influences. At Tepe Düzen, tablewares are regularly typologically related to the so-called echinus bowl with incurving rim. The majority of the material has a common, daily use and can therefore be described as belonging to the category of technomic wares (Rice 1987). Cooking wares are generally represented by vessels with a simple rounded rim, whereas for storage vessels the rim can be (slightly) thickened and curved.

From a macroscopic perspective, both assemblages can be divided in several groups, based on inclusion type, fabric colour, texture, inclusion size and frequency, hardness, fracture and surface treatment (Peacock 1977).

In addition to ceramics, clay raw materials were also sampled ($n = 70$). The main geological units that are found in the area of Sagalassos are autochthonous limestone and an overthrust allochthonous nappe complex, comprising limestone and ophiolite. Flysch deposits have also developed (Degryse and Waelkens 2008). A lake basin with more recent sediments lies in the western part of the territory. In the different valley systems in between, clay deposits are found. The clay samples studied are representative of the larger clay deposits in the territory.

2.2 *Methods*

In addition to the petrography of the ceramics, both sherds and clays were chemically analysed (Table 1), using XRF for major elements and ICP-MS for trace elements. All chemical data were recalculated to a hundred percent.

3 Results

3.1 *Petrography*

An extensive petrographic investigation is being carried out for the entire area of Sagalassos (approximately 1,200 km²) (Vanhaveerbeke and Waelkens 2003). The

Table 1 Results of chemical analyses of ceramics and clay. Main elements in wt%, trace elements in ppm

Sample	Location	SiO ₂	Al ₂ O ₃	Fe ₂ O ₃ (T)	MnO	MgO	CaO	Na ₂ O	K ₂ O	TiO ₂	P ₂ O ₅	Total
Classical – Hellenistic 5th–3rd century BC	Sagalassos	55.07	15.83	7.95	0.11	6.88	8.82	1.10	3.12	0.85	0.25	99.99
	Sagalassos	58.00	18.99	7.21	0.17	2.89	5.50	2.03	3.97	0.79	0.44	99.99
	Tepe	68.90	15.28	6.04	0.13	1.41	2.92	0.73	3.23	0.79	0.59	100.03
Late Roman 5th–6th AD	Düzen	53.78	19.08	8.89	0.16	3.28	8.13	1.57	3.25	0.94	0.91	100.00
	Tepe	56.38	24.91	5.99	0.12	1.15	2.60	3.27	4.23	0.78	0.58	100.01
	Düzen	59.47	15.34	6.02	0.13	1.36	13.13	0.79	2.53	0.77	0.44	99.99
Clay materials	Sagalassos	62.61	16.59	8.02	0.21	2.40	5.03	0.91	3.01	1.03	0.19	100.00
	Sagalassos	64.97	17.34	7.27	0.16	2.55	1.54	1.68	3.37	0.89	0.24	100.00
	Seydiköy	65.15	16.45	6.58	0.17	2.48	2.86	1.83	3.39	0.82	0.28	100.01
	Tepe	53.65	28.35	8.35	0.16	1.72	2.23	1.32	2.94	0.87	0.42	100.01
	Düzen	58.97	20.52	8.84	0.21	3.28	2.50	1.10	3.21	1.01	0.36	100.00
References	Düzen	54.26	12.91	7.20	0.11	5.92	15.67	0.99	2.01	0.76	0.16	99.99
	Çanakl?	54.01	18.93	9.41	0.15	5.83	6.33	1.01	3.21	0.93	0.22	100.04
	Çanakl?	54.43	16.72	8.60	0.10	6.72	8.41	1.01	2.80	0.91	0.28	100.00
	SRSW	55.90	17.24	8.37	0.13	5.15	7.91	1.18	2.92	0.90	0.31	100.00
	Çanakl? clay	60.10	17.65	7.74	0.19	3.94	3.94	1.34	3.85	0.99	0.25	100.00
Ophiolite clay pq												

(continued)

Sample	Location	SiO ₂	Al ₂ O ₃	Fe ₂ O ₃ (T)	MnO	MgO	CaO	Na ₂ O	K ₂ O	TiO ₂	P ₂ O ₅	Total
Sample	Location	Ba	Sr	Zr	Cr	Ni	Cu	Zn	La	Th		
Classical – Hellenistic 5th-3rd century BC												
SA07DB25	Sagalassos	368	233	158	350	300	60	120	34.7	11.1		
SA07DB42	Sagalassos	2,158	1,937	373	180	130	130	90	227	47.8		
SA07DB21	Tepe	1,111	356	229	120	70	40	120	87.7	20		
	Düzen											
SA07DB37	Tepe	1,534	1,424	314	330	200	50	140	128	27.4		
	Düzen											
SA07DB45	Tepe	2,892	2,835	506	60	50	30	90	241	61.2		
	Düzen											
Late Roman 5th–6th AD												
SA06BN001	Sagalassos	1,103	923	297	340	100	40	110	116	23.4		
SA06BN015	Sagalassos	975	844	272	290	170	50	110	102	20.5		
SA06BN030	Sagalassos	1,281	1,200	322	410	220	60	140	140	29.5		
SA07BNS05	Seydiköy	1,438	1,698	329	350	150	50	80	106	23.3		
SA07BNS25	Tepe	1,551	1,091	508	70	70	60	140	330	81		
	Düzen											
SA07BNS31	Tepe	1,188	963	309	150	100	50	110	173	31.8		
	Düzen											
SA07BNS42	Çanakl?	297	284	144	280	200	40	60	27.7	7.9		
SA07BNS47	Çanakl?	763	479	191	190	220	50	100	66.9	17.2		
SRSW		420	209	160	209	337	55	131	36	19		
Çanakl? clay		371	130	206	120	82	30	127	71	27		
Ophiolite clay pq		2,023	2,726	320	95	65	32	231	312	56		

References

material presented in this study, however, concerns the ceramics produced within the connecting valleys of Ağlasun and Çanaklı (within a 7 km radius of Tepe Düzen and Sagalassos), in order to ascertain the possibility of identifying a regional production.

Petrographic analyses of the thin sections of ceramics from the Classical-Hellenistic site of Tepe Düzen resulted in the distinction of several larger petrographic ware groups (Fig. 1a, b). Within each group, variations can be discriminated.

A first main ceramic group has mineral inclusions of quartz, feldspar, basalt clasts, biotite, pyroxene, amphibole, chert, opaque minerals and fine sandstone (all ranging between 250–1,000 μm in size), in different proportions, alongside a moderate (20–30%) amount of pores and micropores. A second major petrographic group shows similar characteristics, but an abundant amount of limestone fragments is added as temper. A third group consists of a quartz-rich ware with some pyroxenes, K-feldspars (sanidine, anorthoclase), grog and a minor amount of organic shell fragments (100–250 μm). A fourth petrographic group has large amounts (40–50%) of metamorphic rock (schist) and quartzite inclusions, together with some large (1–2 mm) talc inclusions and, in minor amounts, quartz, K-feldspar (sanidine, anorthoclase), sandstone and biotite (250–750 μm).

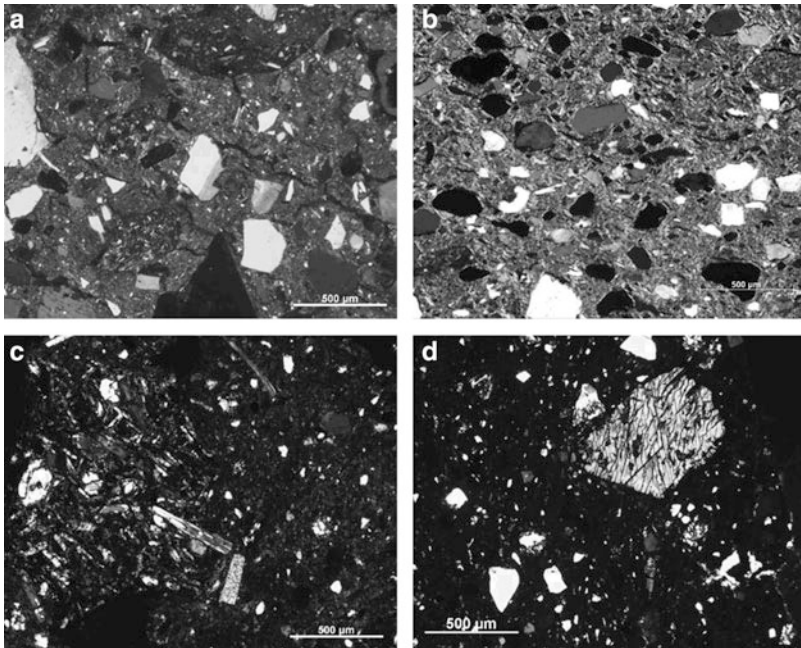


Fig. 1 (Crossed polars): (a) Common ware VIII-1: variation of group 1: basalt clasts, quartz, feldspar and biotite in sherd matrix. (b) Common ware V-3: variation of group 3: quartz-rich fabric with smaller amounts of feldspar, grog and several opaque minerals. (c) Late Roman Fabric 4: basalt clasts in sherd matrix. (d) Late Roman Fabric 4: amphibole fragment in a chert-rich variation

The study of the thin sections of Late Roman “fabric 4” sherds (Fig. 1c, d) has shown no major differences in terms of mineralogical composition.

The most abundant mineral inclusions are feldspar, pyroxene, amphibole, biotite, chert, basalt clasts and grog fragments. Quartz, opaque minerals, apatite and sphene are present in minor amounts. Of the 33 studied samples, only seven are believed to be produced with a different raw material than the main group (a quartzite-rich group and a group with schist fragments).

As mentioned above, the major geological units found on the territory are limestones, ophiolitic *mélange* and *flysch*. The abundant presence of K-feldspar (sanidine, anorthoclase), pyroxene, amphibole, chert and basalt clasts may point at an ophiolitic origin of the raw material. Some of the sherds contain some siltstone/sandstone fragments, an aspect which may indicate a local *flysch* origin. The fabrics which contain metamorphic inclusions (e.g. quartzite and schist) are most likely originating from non-local clay deposits. There is no record of quartzite or schist lithologies in the area, and thus a ceramic fragment containing such rock fragments is most likely produced with material from outside this territory.

The petrographic study of the ceramic assemblages resulted in the formulation of general considerations regarding the provenance area, but an unambiguous attribution to potential sources would likely be biased, due to the possible (un)intentional mixing of resources or the very heterogeneous nature of the raw material. A general remark concerning this categorisation of fabrics is that a fairly significant heterogeneity can be observed within each of the identified groups.

3.2 *Elemental Analysis*

A summary of the results of elemental analyses is provided in Table 1. Earlier studies on provenancing showed that examples of Sagalassos red slip ware, the locally produced tableware, which are found in large amounts at Sagalassos, are produced with material found in the valley near the modern-day village of Çanaklı (Ottenburgs et al. 1993). As shown in the table, the composition of this SRSW (reference sample 1) is very similar to the reference Çanaklı clay (reference sample 2). These clays underwent little preparation before they were used for making ceramics (Poblome et al. 2001).

For the coarse wares studied, a comparison is not as straightforward. It is clear that a simple bulk study can provide some clues about provenance, but does not provide enough detail. As expected from the petrographic study, the Classical-Hellenistic sherds show a much wider range in terms of chemical composition than the Late Roman “fabric 4” sherds. There are some similarities between the composition of individual clays and sherds – for example the clay found at Şeydiköy (SA07BNS05) has a similar composition to one of the “fabric 4” sherds (SA06BN030) – but no proof of provenance can yet be provided. More research focusing on mineralogy needs to be performed in order to be able to identify more robust links between the clays and ceramics.

4 Discussion

An important aspect of material studies entails clarifying the transition from observable facts to the archaeologically invisible processes of the past. In the present case, the correspondence between the macroscopic identification and petrography seems to be meaningful, although some cases of petrographic similarity and macroscopic heterogeneity could be observed within the assemblage. It is reasonable to assume that these variations are not the product of compositional differences, but result from technological, functional, socio-cultural or typo-chronological considerations in the production process. These observations argue that a macroscopic classification methodology, in the applicable field, incorporates compositional data; emphasis needs to be firmly placed upon the identification of clasts and fabric characteristics. A preliminary typological study of the ceramic material reveals that most “wares” are multifunctional. The lack of correspondence between the compositional data and the complete functional spectrum is also worth noting. This aspect stands in contrast to the situation verified for the “fabric 4” samples, which seem to have a nearly unique relation with storage and cooking functionalities.

Regarding the question of provenance, at this stage of the research most fabrics seem to be related to the geological setting of the region. Taken into account the distance feedback model (Arnold 1985), this aspect supports a possible matching of raw materials within a radius with a maximum range of 7–9 km. Most of the ware groups from Tepe Düzen identified in this study correspond to the fairly homogeneous mineralogical signature of the local geology. However, from a petrographic point of view, some wares cannot be ascribed to local resources. The multifunctional aspect of the different ware groups suggests the absence of specialised clay preparation at Tepe Düzen. The preliminary data seem to indicate a fairly unspecialised mode of production. Following Peacock’s classification of different modes of production, it is possible to suggest an individual workshop mode, where pottery production develops into a primary source of subsistence (Peacock 1982). Towards the Hellenistic period, production processes seem to become more developed. Taking into account the more homogeneous petrographic compositions and a more systematic tableware production that requires consistent clay preparation, this change can well represent the beginning of a well-organised artisanal production. At a later stage, the organisation of production within the studied area is indicative of its development into a regional centre of production (on manufactory level) for the mass produced tableware from the Potters’ Quarter of Sagalassos (Poblome 1999; Poblome 2006). Whether the small variations in chemical and mineralogical composition of Late Roman “fabric 4” wares should be interpreted as indicating the use of different source material or just the use of one heterogeneous source material is not yet clear.

It is also possible to take the hypothesis one step further: ceramics attested from other Classical-Hellenistic sites (to be published in the near future) in this area show a similar production pattern with the one identified at Tepe Düzen. This study suggests a system of peer polities (Renfrew 1986) of self-sufficient local and

regional production entities during the Classical period, where the continuous use of the same fabrics over a relatively extensive period can be observed, in use for the entire functional spectrum of ceramics.

At this stage of the research, reconstructing a regional economy in all its aspects remains a highly speculative endeavour. However, the data of this provenance study represent a stepping stone for the achievement a wider understanding in terms of the mechanisms of regional development, especially when combined with insights on a wider chronological scale and broader sample area.

Acknowledgements The research was supported by the Belgian Programme on Interuniversity Poles of Attraction (IAP VI/22). The text also presents the results of a project by the Research Fund of the K.U.Leuven (BOF- GOA07/2).

References

- Arnold D (1985) *Ceramic theory and cultural process*. Cambridge University Press, Cambridge
- Degeest R (2000) The common wares of Sagalassos: typology and chronology. *Studies in Mediterranean Archaeology* 3. Brepols, Turnhout
- Degryse P, Waelkens M (2008) Sagalassos VI Geo- and Bio-Archaeology at Sagalassos and in its Territory. Universitaire Pers, Leuven
- Ottensmeyer F, Viaene W, Jorissen C (1993) Sagalassos ware IV. Study of the clays. In: Waelkens M (ed) *Sagalassos 1, First General Report on the Survey (1986–1989) and Excavations (1990–1991)* (Acta Archaeologica Lovaniensia Monographiae 5). Universitaire Pers, Leuven, pp 163–169
- Peacock DPS (1977) *Pottery and early commerce. Characterization and trade in Roman and later ceramics*. Academic, London
- Peacock DPS (1982) *Pottery in the Roman world: an ethnoarchaeological approach*. Longman, London
- Poblome J (1999) Sagalassos red slip ware. Typology and chronology. *Studies in Eastern Mediterranean Archaeology* 2. Brepols, Turnhout
- Poblome J (2006) Made in Sagalassos. Modelling regional potential and constraints. In: Menchell S, Paquinucci M (eds) *Territorio e produzioni ceramiche: paesaggi, economia e società in età romana*. Pisa University Press, Pisa
- Poblome J, Bounegru O, Degryse P, Viaene W, Waelkens M, Erdemgil S (2001) The Sigillata Manufactories of Pergamon and Sagalassos. *J Roman Archaeol* 14:143–165
- Renfrew C (1986) Introduction. Peer polity interaction and socio-political change. In: Renfrew C, Cherry JF (eds) *Peer polity interaction and socio-political change*. Cambridge University Press, Cambridge, pp 1–18
- Rice PM (1987) *Pottery analysis: a sourcebook*. University of Chicago Press, Chicago
- Vanhaverbeke H, Waelkens M (2003) The Chora of Sagalassos. The evolution of the settlement pattern from prehistoric until recent times. *Studies in Eastern Mediterranean Archaeology* 5. Brepols, Turnhout

Ethnoarchaeometric Study of the Traditional Cooking Ware Production Centre of *Pabillonis* (Sardinia): Investigating Raw Materials and Final Products

M.A. Cau, G. Montana, D. Pagliarello, and E. Tsantini

1 Introduction

Ceramic Ethnoarchaeology (Longacre 1991; Costin 2000) has been particularly useful, among other aims, for understanding all the stages and parameters involved in pottery production, such as raw materials selection or paste recipes used by the potters. Moreover, analysing modern pottery-making communities that exploit their natural resources can provide an insight into the raw materials available in the area that could have also been used in the past. Ethnoarchaeological case studies were also used in order to test hypotheses in provenance studies (Arnold et al. 1991; Arnold et al. 2000). More recently, Buxeda i Garrigós et al. (2003) have proposed the term “ethnoarchaeometry” for this type of approach.

Within the Late Roman Cooking Wares (LRCW) commercialised in the Western Mediterranean, some fabrics, such as Fabrics 1.2, 1.6/1.7 and 1.9 (Fulford and Peacock 1984), have been proposed to have a Sardinian origin (Fulford and Peacock 1984; Cau 2003; Cau et al. 2002). This aspect represented the motivation behind a specific project aimed at exploring the nature of cooking pottery on the

M.A. Cau (✉)

Institució Catalana de Recerca i Estudis Avançats (ICREA), Universitat de Barcelona, Barcelona, Italy

and

Equip de Recerca Arqueomètrica de la Universitat de Barcelona (ERAUB), Barcelona, Italy
e-mail: macau@ub.edu

G. Montana and D. Pagliarello

Dipartimento di Chimica e Fisica della Terra (CFTA), Università di Palermo, Palermo, Italy
e-mail: gmontana@unipa.it

E. Tsantini

Equip de Recerca Arqueomètrica de la Universitat de Barcelona (ERAUB), Barcelona, Italy



Fig. 1 Location of Pabillonis (Sardinia, Italy) and some images from Piras' workshop

island and the raw clays, as well as the production technologies that have been traditionally used for their manufacture.

Traditional cooking wares in Sardinia are relatively well recorded. In particular, the pottery making tradition of *Pabillonis* (Fig. 1) is known to be the most representative and diffused, and for this reason it was studied in great detail (Annis and Geertman 1987; Annis and Jacobs 1989/1990).

Starting from this work, a field survey in the area of *Pabillonis* was undertaken in order to locate the raw materials used. Moreover, representative samples from final products were also collected in a traditional workshop. All the materials (clays and pots) were analysed in order to determine their chemical, petrographical and technological characteristics. The final aim was to reconstruct the paste recipe used by the local potters for cooking vessels. In addition, this approach can also provide a feedback related to the characteristics of the production to be used in the study of the LRCWs of alleged Sardinian origin.

2 Geological Sketch of the Area

The territory of *Pabillonis* is part of the *Campidano* graben and is characterised by alluvial and colluvial deposits composed of gravels, silt and sandy clay (Holocene), together with Plio-Pleistocene conglomerates, sand and mud deposits cropping out in river terraces and/or alluvial cones (Carmignani et al. 2001). The *Flumini Malu* River grinds detritic materials from the rocks which outcrop about 10 km to the east of the village of *Pabillonis*. These are sedimentary formations mainly consisting of polygenic continental conglomerates and sandstones with reddish clayey matrix; micaceous metasandstone and quartzites interbedded with phyllites and rare metaconglomerates. The detritic materials eroded by the *Flumini Bellu* belong for the most part to the Upper Carboniferous-Permian Plutonic Complex (outcropping

west of *Pabillonis*). This is composed of granodiorites, tonalites and cordierite-bearing granitoid rocks. Micaceous materials (Middle Cambrian–Lower Ordovician) are also ground down, especially near the village of *Guspini*. The Oligocene–Miocene calc-alkaline volcanic cycle (*Monte Arcuentu*), mainly consisting of andesites, andesitic basalts and latites, is simply skimmed over by the *Flumini Bellu*. In contrast, the same deposits are deeply worn away by *Rio Montevecchio*, which flows alongside the *Flumini Bellu* (about 5 km to the north). The lava products of the *Mount Arci* volcanic complex (Pliocene–Pleistocene; mainly trachibasalts, basaltic andesites, trachytes, phonolitic trachytes, rhyolites and rhyodacites with perlitic structure, and obsidians) lie only to some extent in the drainage basin of a small tributary river (*Rio Setti*) which meets the *Flumini Malu* north-east of *Pabillonis* (approximately 2 km).

3 Materials and Methods

A total of 25 sherds were collected in the workshop of G. Piras. All of the samples were broken and discarded fragments of pottery from the workshop and some showed signs of previous use. Except for three tile and brick sherds, the rest of the samples are typical casseroles from Piras' workshop, with relatively thin walls and a lead glaze on the inner part of the vessel and partially on the external surface.

The clayey materials collected near *Pabillonis* were indicated in some cases by G. Piras, the last traditional potter living in the area. He took us to *Arrubius Campo*, located about 1.5 km south-west of *Pabillonis* over the right bank of the *Bellu* River, where two samples were collected (labelled AC1 and AC2). Another sample (labelled PDC) originates from *Domu Campu*, a location used in the past for clay extraction, situated about 1 km west of the village. Clay was also collected from *Morimenta Mogoro* (samples labelled MRM) and *Terramaini* (labelled TRM), which are both located a few kilometres away from the village.

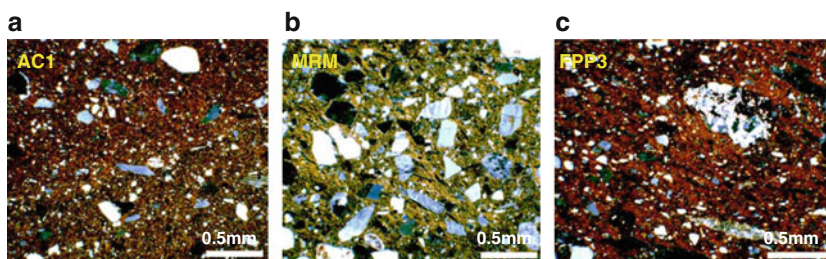
All materials were characterised using a combination of techniques, including X-Ray Fluorescence (XRF) for the chemical characterisation, X-Ray Diffraction (XRD) for the bulk mineralogical composition, and thin-section analyses by optical microscopy (OM) for the petrographic characterisation. Moreover, raw clays were studied in terms of grain size distribution (granulometric analysis) and also in terms of mineralogical composition of clay-sized fraction ($<2\ \mu\text{m}$) by XRD performed on oriented preparations. SEM and EDS microanalyses were carried out on pottery samples in order to explore the microstructure and sintering stage, as well as the composition of the glaze. Raw clays were pressed into wood moulds in order to obtain experimental briquettes which, after drying at 60°C , were fired in a muffle oven at final temperatures ranging from 700 to $1,000^\circ\text{C}$. This procedure was followed in order to obtain specimens of “fired clay pastes”, which could then be properly compared under the polarising microscope (thin section) with local pottery products.

4 Results

4.1 The Cooking Wares from the Workshop

The chemical results for the 22 samples of cooking wares recovered from Piras' workshop allow defining a reference group indicating a quite homogeneous production (Fig. 2, Table). Chemical results were explored with statistical techniques using S-Plus. In order to explore the data further, elemental concentrations were log-ratio transformed (Aitchison 1986, 1992; Buxeda i Garrigós 1999) using Zn as divisor.

The Compositional Variation Matrix (CVM) (Buxeda i Garrigós 1999; Buxeda i Garrigós and Kilikoglou 2003) calculated using the subcomposition normally analysed in our laboratory (Buxeda i Garrigós et al. 2003), except for MnO due to analytical imprecision, and considering only the cooking ware samples, gives a value of $vt = 1.1359$, relatively high for a monogenetic composition. After a detailed examination of the CVM, the most variable elements appear to be P_2O_5 ($\tau.i. = 11.1529$) and Pb ($\tau.i. = 9.5394$). The latter corresponds to a clear contamination



Cooking Ware RG, n=22	Fe ₂ O ₃	Al ₂ O ₃	MnO	P ₂ O ₅	TiO ₂	MgO	CaO	Na ₂ O	K ₂ O	SiO ₂					
mean	7,17	21,66	0,06	0,13	0,75	1,27	0,47	0,86	4,12	63,26					
std. deviation	0,59	1,67	0,02	0,11	0,11	0,17	0,16	0,18	0,20	2,22					
Clays	Fe ₂ O ₃	Al ₂ O ₃	MnO	P ₂ O ₅	TiO ₂	MgO	CaO	Na ₂ O	K ₂ O	SiO ₂					
TRM	5,06	14,22	0,12	0,09	0,69	1,73	3,02	0,91	2,49	65,40					
AC1	6,65	16,53	0,19	0,10	0,73	0,88	0,28	0,51	3,19	65,52					
AC2	7,05	17,03	0,08	0,10	0,68	0,93	0,28	0,42	3,16	63,54					
PDC	7,24	18,64	0,06	0,09	0,77	1,22	0,48	0,60	3,95	59,65					
MRM	3,55	12,83	0,09	0,05	0,44	1,02	1,13	1,06	2,91	72,31					
Cooking Ware RG, n=22	Ba	Rb	Th	Nb	Pb	Zr	Y	Sr	Ce	Ga	V	Zn	Cu	Ni	Cr
mean	666	197	19	20	422	247	39	84	97	30	126	196	31	43	87
std.deviation	64	13	2	2	223	16	5	11	12	3	19	26	5	6	7
Clays	Ba	Rb	Th	Nb	Pb	Zr	Y	Sr	Ce	Ga	V	Zn	Cu	Ni	Cr
TRM	527	90	12	14	41	192	28	130	62	16	111	89	29	38	131
AC1	567	149	15	18	61	253	29	79	114	22	142	104	25	36	112
AC2	559	155	14	17	61	218	27	72	73	22	146	125	27	41	117
PDC	696	193	18	21	80	220	43	76	90	26	150	228	42	42	83
MRM	566	100	9	11	23	134	20	107	53	15	81	55	12	21	97

Fig. 2 Thin section microphotographs (crossed Nicol, scale bar = 0.5 mm) of the local clays and the studied pottery: (a) Arrubius Campu (AC1); (b) Morimenta Mogoro (MRM); (c) cooking pot sample FPP-3. Below: Table with the mean and standard deviation for the reference group (RG) of the cooking ware production at Piras' workshop (Pabillonis, Sardinia) and raw chemical data of the clays (major and minor elements concentrations are expressed in oxide wt%, and trace elements in ppm)

deriving from the glaze covering. If these two elements are excluded, the v_t value decreases to 0.3420, the most variable elements now being CaO and Na_2O .

The petrographic study revealed that the packing is between 15 and 20%. The sorting is serial, with a slight tendency to bimodal. The grain size is variable, with abundant coarse silt, common very fine sand (0.004–0.1 mm), subordinate to common medium sand (0.25–0.5 mm), and to rare coarse sand (>0.5 mm). The inclusions are mainly of very abundant angular and subangular quartz, frequent K-feldspars (sometimes altered to sericite), common to subordinated plagioclase (some of volcanic origin and with different degrees of alteration). Lithic fragments are common and they are mostly acidic crystalline fragments (granitoid rocks). Rare quartzarenite and quartz-siltite fragments with slightly metamorphosed iron oxide matrix are also present. Sporadic mica flakes, clinopyroxene and some volcanic fragments of andesite type are also visible.

According to the XRD, OM and SEM results, the Equivalent Firing Temperature (EFT) ranges between 850 and 1,000°C. The mineralogical compositions detected by XRD on the studied pottery samples allowed us to infer different intervals of firing temperatures: (a) $\leq 800^\circ\text{C}$, (b) $\leq 850/900^\circ\text{C}$ and (c) $\leq 950/1,000^\circ\text{C}$. Moreover, the observation performed by SEM revealed the development of a typical non-calcareous ceramic microstructure and confirmed the equivalent firing temperatures estimated by XRD.

A fine structured lead glaze can be observed over the surface, with an irregular width oscillating between 0.1 and 0.15 mm (100–150 μm). Based on thin section and SEM observation, it seems clear that the lead glaze was applied to a previously fired body.

4.2 The Clays

From a chemical point of view, all the clays from the area of *Pabillonis* are low calcareous clays with relatively high K_2O content (see Table in Fig. 2). The petrographic observations of the clay samples fired at 700°C show an abundance of monocrystalline and polycrystalline quartz in all samples. In general, the particles with size bigger than 0.25 mm are subrounded or even rounded (fluvial sand). K-feldspars, grains and fragments from granitoid and/or gneissic rocks, as well as low-grade metamorphites (argillites, micaceous metasiltites and metarenites) are common to sporadic. The frequency of amphibole, biotite and volcanic inclusions is even more sporadic, with only one exception, sample TRM, where clinopyroxene, geminated plagioclase, and rock fragments with vitrophyric texture are quite abundant.

5 Conclusions

The ethnoarchaeometric study has allowed the characterisation of a reference group for the pottery from Piras' workshop and its technology. The pottery corresponds to a highly standardised, low calcareous, mainly well-fired glazed ceramic production.

Taking into consideration the analyses of the raw materials, potential sources for *Pabillonis* raw materials can be located in certain areas of the Quaternary alluvial sediments on the left side of the River *Bellu*. The clays from *Terramaini* (TRM) and *Morimenta Mogoro* (MRM) can be clearly excluded as potential raw material sources for the studied *Pabillonis* production. There are no compositional similarities between the Late Roman Cooking Wares of possible Sardinian provenance and the ceramic materials and clays of the area of *Pabillonis*. This negative result is important, as it allows the exclusion of this area as a potential source for the LRCWs under study in the framework of the current project. However, the results of chemical and petrographic comparisons between the *Pabillonis* products and Neolithic ceramic fabrics found at different locations within a 10 km radius of the site (Bertorino et al. 2000) show remarkable consistency. This aspect indicates the continuity of a local ceramic tradition over a wide chronological range.

Acknowledgments We are grateful to the village of *Pabillonis* that hosted us very kindly. In particular, we would like to thank G. Piras and his family for sharing their knowledge with us, and the mayor of the village (Dott. Marco Dessì) for his support. Special thanks are also due to Sara Santoro, co-director of the project, to the entire team working on the Sardinian materials, and to B. Annis and P. van Dommelen for their interest in our research. This research is part of the Spanish–Italian Action (HI2005-0067) funded by Ministerio de Educación y Ciencia and MIUR and also of the project *Poblamiento y cerámica en las Islas Baleares durante la Antigüedad tardía: el caso de Mallorca* (CERPOANTAR), HUM2005-0996/HIST, funded by Ministerio de Educación y Ciencia, now Ministerio de Ciencia e Innovación, also with FEDER funding.

References

- Aitchison J (1986) The statistical analysis of compositional data. Chapman and Hall, London
- Aitchison J (1992) On criteria for measures of compositional difference. *Math Geol* 24 (4):365–379
- Annis B, Geertman H (1987) Production and distribution of cooking ware in Sardinia. *Newslett Depart Pottery Technol Leiden* 5:154–196
- Annis MB, Jacobs L (1989/1990) Cooking Ware from Pabillonis (Sardinia) Relationships between raw materials, manufacturing techniques and the function of the vessels. *Newslett Depart Pottery Technol* 7/8: 75–131
- Arnold DE, Neff H, Glascock MD (2000) Testing assumptions of neutron activation analysis: communities, Workshops and Paste Preparation in Yucatán Mexico. *Archaeometry* 42: 301–316
- Arnold DE, Neff H, Bishop RL (1991) Compositional analysis and “Sources” of pottery: an ethnoarchaeological approach. *Am Anthropol* 93:70–90
- Bertorino G, Lugliè C, Marchi M, Melis RT (2000) Insediamenti all’aperto della Sardegna centro-occidentale nel Neolitico Antico: ambiente e produzioni ceramica. *Boll Acc Gioenia Sci Nat* 33(357):121–134
- Buxeda i Garrigós J (1999) Alteration and contamination of archaeological ceramics: the perturbation problem. *J Archeol Sci* 26:295–313
- Buxeda i Garrigós J, Cau Ontiveros MA, Kilikoglou V (2003) Chemical variability in clays and pottery from a traditional cooking pot production village: testing assumptions in Pereruela. *Archaeometry* 45(3):1–17

- Buxeda i Garrigós J, Kilikoglou V (2003) Total variation as a measure of variability in chemical data sets. In: van Zelst L, Bishop RL, Henderson J (eds) *Patterns and process* Smithsonian Institution, Washington, DC, pp. 185–198
- Carmignani L, Oggiano G, Barca S, Conti P, Salvatori I, Eltrudis A, Funedda A, Pasci S (2001) Geologia della Sardegna. In: *Memorie Descrittive della Carta Geologica d'Italia*, Vol. LX, Istituto Poligrafico e Zecca dello Stato
- Cau Ontiveros MA (2003) *Cerámica tardorromana de cocina de las Islas Baleares. Estudio arqueométrico* BAR International Series, 1182, Archaeopress, Oxford
- Cau Ontiveros MA, Iliopoulos I, Montana G (2002) Pots and volcanoes: provenance of some Late Roman Cooking Wares in the Western Mediterranean. *Archaeometry* 2000 México, México
- Costin CL (2000) The use of ethnoarchaeology for the archaeological study of ceramic production. *J Archaeol Method Theory* 7(4):377–403
- Fulford MG, Peacock DPS (1984) *Excavations at Carthage: the British Mission*, vol I, 2, The avenue du président Habib Bourguiba, Salammbô: the pottery and other ceramic objects from the site. University of Sheffield, Sheffield
- Longacre W (1991) *Ceramic ethnoarchaeology*. University of Arizona Press, Tucson

Materials, Technology and Provenance of Ancient Ceiling Tiles from the Ceramic District in Riva San Vitale (Southern Switzerland)

G. Cavallo and M. Moresi

1 Introduction

The Riva San Vitale village is a district with a long ceramic tradition devoted to the production of bricks, floor and ceiling tiles (Eberhardt-Meli 2005); the advantage of the site was related to the availability of clay deposits close to Lake Ceresio. The earliest document referring to the production activities in these buildings and sometimes to decorative materials as well dates back to the mid-thirteenth century AD, when the term *fornace* (kiln) is mentioned in the archive of the St. Fedele cathedral in Como. From this time until the second half of the nineteenth century, before the construction of the St. Gottardo tunnel, each village in this area had its own kiln, and produced ceramics that represented the object of an intense trade with Italy. The advent of the mechanical mould, the Hoffmann kiln, and cement caused the decline of this tradition.

The materials analysed in the present study were ancient ceiling tiles belonging to the owner of two historical kilns. No previous information was available about the origin of the raw materials, the provenance of the tiles and the firing process. The surfaces of the tiles exhibit engraved signs, a few of them indicating the dates 1634 and 1754, others a cross, one the palindrome *SATOR AREPO TENET OPERA ROTAS* (Fig. 1; for the significance, see Camilleri 2004; Giordano and Kahn 1979), one the vegetal motif of the palm, and, in a few cases, an illegible inscription.

The main goals of this research were the petrographic, mineralogical and chemical characterisation of the ceiling tiles and a comparison with the raw materials, allowing for a better understanding of the probable link between the artefacts and the production technology.

G. Cavallo (✉)

Lab. Tecnico Sperimentale, Environment Construction and Design Dpt, University of Applied Sciences of Southern Switzerland, P.O. Box 12, 6952 Canobbio, Switzerland
e-mail: giovanni.cavallo@supsi.ch

M. Moresi

Department of Geomineralogy, University of Bari, via Orabona 4, 70124 Bari, Italy



Fig. 1 The ceiling tile ref. 13 showing the palindrome of the “magic squared”

2 Materials and Methods

The description of the samples is reported in Table 1. Optical microscopy carried out on thin-sections in transmitted light was employed to study the fabric and the composition of each sample. X-Ray Diffraction Powder (XRD) was used for studying the mineralogical composition of the collected samples. The analysis was performed using a Philips X' Pert Pro diffractometer type PW 3040/60; X-ray tube with Cu anti-cathode, generator settings 40 kV 40 mA, speed $1^\circ 2 \theta/\text{min}$, measurements range: $2^\circ\text{--}65^\circ$.

X-Ray Fluorescence (XRF) was used to determine the quantitative chemical composition of the major elements. XRF analyses were carried out on powder pills using a solution of *elvacite* 15% in acetone as binder. *Elvacite* is a polymer resin added in order to have the individual grains stick together. After the acetone vaporizes, a grain-coated conglomerate of grains is formed (Dietrich and Schwandner 2000). The grain size of the powder was less than 10–20 μm (Leoni et al. 2004). An automatic spectrometer Philips PW 1480 was used; X-ray tube with Cr anode (70 kV, 30 mA). LOI (Loss on Ignition) was determined as loss in weight following heating at $1,000^\circ\text{C}$, after elimination of hydration water at 110°C . The precision is better than 5%.

3 Experimental

3.1 Petrography

Samples ref. 11, 13, 19, 20, 21, 24, 25 are very similar. The matrix is a mixture of two types of clays (dark grey, corresponding to Ca-rich clays, and red, corresponding to Ca-poor clays) exhibiting a characteristic layering. The non-plastic

Table 1 Description of the samples

Ref.	Description
11	Red ceiling tile
12	Dark yellow ceiling tile with the date 1634
13	Red ceiling tile with the inscription <i>SATOR AREPO TENET OPERA ROTAS</i>
15	Dark yellow ceiling tile
19	Dark red ceiling tile with the date 1754
20	Very dark red ceiling tile with an illegible inscription
21	Dark yellow ceiling tile with the symbol of the palm
22	Dark yellow ceiling tile
23	Very dark red ceiling tile with the symbol of the cross
24	Very dark yellow ceiling tile with the symbol of the cross
25	Dark red ceiling tile with a writing inscription and the symbol of the cross

fraction is concentrated inside the red matrix: grains of mica schists, metamorphic quartz, quartz plus plagioclases and biotite are the main constituents. Differences between the samples are present in terms of grain size. The grain size of samples 19, 20, 21, 24 is equal (about 50 μm), the shape of the main mineralogical phases is the same, and they do not show any preferred orientation; samples 11, 13, 25 show different grain size, ranging from 50 to 500 μm , and the shape of the non-plastic fraction is different, showing preferred orientation. The percentage of the non-plastic fraction ranges between 30 and 50%. All these samples have plastic inclusions, optically isotropic, with a diameter ranging from 2 mm to 1 cm, appearing darker than the matrix, and sometimes including a non-plastic fraction; these natural clay inclusions, also called “clay pellets” (Whitbread 1986), show a continuity with the matrix. Samples ref. 12, 15, 22, 23 are very similar. Their mixture is very heterogeneous, the colour is pale, and the non-plastic fraction is small and due to quartz and feldspars.

3.2 X-Ray Diffraction (XRD)

The XRD results are reported in Table 2. Quartz and feldspars correspond to the non-plastic fraction; only samples 11 and 12 contain some 10 \AA -micas (muscovite and biotite). Traces of calcite have been detected in sample 12. Pyroxenes (all the samples), gehlenite (samples 11, 12, 13) and Fe-oxides attributable to hematite (samples 11, 13, 19, 20, 24, 25) are the newly-formed phases due to firing.

3.3 X-Ray Fluorescence (XRF)

The results of the chemical analysis by means of XRF are listed in Table 3. The comparison between the chemical and mineralogical data allows pointing out that the SiO_2 content is clearly related to quartz and CaO to gehlenite and pyroxenes;

Table 2 Mineralogical phases (XRD)

Ref.	Qtz	Fd	10Å-M	Cal	Ge	Py	Fe-ox
11	+++	++	+	–	Tr	Tr	Tr
12	–	++	+	Tr	++++	Tr	–
13	++	++	–	–	+	Tr	Tr
15	+	++	–	–	–	+++	–
19	++++	++	–	–	–	Tr	Tr
20	++++	++	–	–	–	Tr	Tr
21	++++	++	–	–	–	++	–
22	++	++	–	–	–	+++	–
23	t	++	–	–	–	+++	–
24	+++	++	–	–	–	Tr	Tr
25	++	++	–	–	–	Tr	Tr

++++ very high, +++ high; ++ abundant; + small; Tr traces; - absent or not detected

Qtz Quartz, Fd Feldspars, 10Å-M 10Å-Micas (muscovite and biotite), Cal Calcite, Ge Gehlenite; Py Pyroxenes; Fe-ox Fe-oxides

Table 3 Chemical analysis (XRF) – wt%

Ref.	SiO ₂	TiO ₂	Al ₂ O ₃	Fe ₂ O ₃	MnO	MgO	CaO	K ₂ O	Na ₂ O	P ₂ O ₅	LOI	Σ
11	54.97	0.75	16.05	6.85	0.09	5.05	8.34	2.91	1.00	0.11	3.88	100.00
12	41.99	0.61	10.47	5.46	0.12	6.83	25.36	2.07	0.60	0.19	6.30	100.00
13	49.67	0.70	13.98	6.01	0.10	5.17	12.52	2.64	1.02	0.14	8.05	100.00
15	49.63	0.81	14.81	7.09	0.10	5.78	15.70	3.33	1.06	0.15	1.54	100.00
19	67.28	0.72	13.90	5.25	0.09	2.88	4.67	2.46	1.68	0.17	0.90	100.00
20	68.72	0.86	16.22	4.88	0.05	1.99	1.49	2.77	1.74	0.15	1.13	100.00
21	61.65	0.57	11.09	4.60	0.08	3.77	13.20	1.88	0.99	0.13	2.04	100.00
22	48.29	0.68	12.67	6.04	0.10	7.13	19.13	2.56	0.97	0.15	2.28	100.00
23	44.38	0.65	15.10	6.02	0.10	6.20	19.26	2.47	0.56	0.14	5.12	100.00
24	58.52	0.82	16.49	7.12	0.10	4.14	7.41	3.15	0.96	0.18	1.11	100.00
25	57.36	0.77	15.72	6.60	0.12	5.55	8.08	2.93	1.10	0.20	1.57	100.00

LOI Loss on ignition

calcite content is low. Feldspars do not show a direct correlation with chemical elements, probably due to their variable composition (Ca and/or Na plagioclases, K-feldspars). Fe₂O₃ content is not related to any specific mineralogical phases, depending on the presence of pyroxenes, some phyllosilicates and Fe-oxides, generally poorly crystallized; only samples 11, 13, 19, 20, 24, 25 show weak reflections attributable to hematite.

4 Discussion

The petrographic examination allows the classification of samples in two main groups: artefacts produced using two different types of clay, corresponding to carbonatic and silicatic raw materials, and artefacts having an isotropic groundmass mixed with a low percentage of sand. These latter samples are characterised by a high concentration of newly-formed pyroxenes, as shown by XRD.

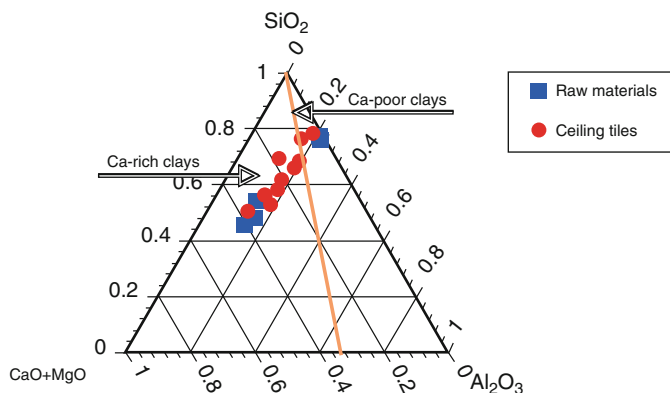


Fig. 2 A $(\text{Al}_2\text{O}_3) \text{ C} (\text{CaO}+\text{MgO}) \text{ S} (\text{SiO}_2)$ diagram showing the relationship between the raw materials (Cavallo et al. 2007) and the ceiling tiles

The CaO weight percentages are high (except for samples ref. 19 and 20), in accordance with the high content of calcite in the raw materials (Cavallo et al. 2007). Only sample 12 contains calcite at trace level, probably due to a secondary contribution. This indicates that the firing temperatures were always higher than the ones of calcite decomposition (about 700–750°C). In samples ref. 11, 12, and 13, where gehlenite and pyroxenes are co-existing, the firing temperatures were probably around 850–900°C. Samples ref. 11 and 12 show peaks of 10Å-micas (muscovite and biotite); at these temperatures, 10Å-micas display a crystalline lattice still partially preserved. For all the remaining samples, where the newly-formed phases are represented by pyroxenes, the firing temperatures should have been higher than 900°C, probably around 1,000°C (Cultrone et al. 2001).

The chemical data have been reported on the ACS diagram (Fig. 2), together with the chemical data related to the raw materials collected from locations around the village (Cavallo et al. 2007). The $\text{SiO}_2/\text{Al}_2\text{O}_3$ ratios of the raw materials and ceiling tiles are similar. The non-plastic fraction shows a homogenous composition.

Differences can be established taking into consideration the CaO + MgO content, caused by the variation of CaO due to its variable content in the raw materials. The CaO content in the ceiling tiles is intermediate between the maximum and minimum content observed in the raw materials. This is due to a mixture of two different types of clays (Ca-rich and Ca-poor clays), as also observed under the microscope.

5 Conclusions

The results indicate that the ceiling tiles were hand-made with silica-based sands, generally using two types of clays (calcareous and non-calcareous clays of glacio-fluvial origin). The chemical analysis indicates that the $\text{SiO}_2/\text{Al}_2\text{O}_3$ ratio is similar

between the raw materials and the artefacts, whereas the content of CaO + MgO in the artefacts is widely variable, depending on the relative quantity of the two types of clays in the mixture. This aspect becomes clear upon examining the thin sections, where the two fractions are distinguishable by colour: grey colour associated with carbonatic clay, and red for the one containing a major quantity of silicates and Fe oxides.

The mineralogical analysis shows the absence of calcite and the presence of gehlenite and pyroxenes as newly-formed phases. The firing temperature may be estimated to around 850°C for the artefacts where gehlenite is prevailing and to more than 900°C where the pyroxenes are the main newly-formed phases. The non-plastic fraction is consistent with the local deposits of clay, suggesting a local source for the raw materials and the use of the kilns located in the same village. The red colour of the ceiling tiles is due to Fe-oxides (poorly crystalline hematite) formed during firing under an oxidising atmosphere; the dark yellow colour is generally associated with the presence of newly-formed pyroxenes and is due to the high content of carbonates in the original clay.

References

- Camilleri R (2004) Il quadrato magico. In: Rizzoli (Ed), Milano, 1–231
- Cavallo G, Moresi M, Vassalli G (2007) La produzione di materiali da costruzione tra il XIX e la prima metà del XX secolo a Riva San Vitale (Ticino, Svizzera) In: Proceedings of the IX giornata di Archeometria edited by Comune di Pordenone and CNR-ISTEC Faenza, pp 41–49
- Cultrone G, Rodriguez-Navarro C, Sebastian E, Cazalla O, De La Torre MJ (2001) Carbonate and silicate phase reactions during ceramic firing. *Eur J Mineral* 13:621–634
- Dietrich V, Schwandner F (2000) Preparation of glass beads and powder pills for XRF analysis of silicic and calcareous rocks. ETH Zürich
- Eberhardt-Meli S (2005) Artigiani della Terra. Dadò Ed, Locarno, pp 27–57
- Giordano G, Kahn I (1979) Gli Ebrei a Pompei. Procaccini Ed, Napoli, pp 75–82
- Leoni L, Menichini M, Saitta M (2004) Ricalibrazione di una metodologia in Fluorescenza X per l'analisi di minerali e rocce su campioni in polvere. *Atti Soc tosc Sci nat, Mem, Series A* 109:13–20
- Whitbread IK (1986) The characterisation of argillaceous inclusions in ceramic thin sections. *Archaeometry* 28:79–88

An Investigation into the Ceramic Technology of the Two-Colour Tiles of “Prince Noir” Castle (Bordeaux, France, Thirteen to Fourteenth Centuries AD)

B. Cicuttini, A. Ben Amara, and F. Bechtel

1 Introduction

Two-colour tiles were produced in abundance in France and England during the thirteenth and fourteenth centuries AD. They replaced the mosaic, hand-incised and counter-relief tiles that had been developed since the twelfth century. These tiles proved very successful and many regional styles of decoration for religious and secular opulent edifices. Two-colour tiles are usually made by applying a pattern impression on an unfired, clayey tile. The impression is then filled with a slip, and, finally, the surface is covered with glaze.

The tiles examined in this study originate from the “Prince Noir” Castle, located in Lormont, near Bordeaux (France). The main purpose of the present study is to determine the various manufacturing aspects of the tile production process, while at the same time testing the suitability of a non-destructive procedure using SEM-EDS (LV – Low Vacuum mode) for glaze analysis.

2 The Site and Materials

The story of the “Prince Noir” Castle began around 1060 with a first edifice built by Guillaume VIII, Duke of Aquitaine. The castle became a royal residence in 1154, when Henry Plantagenet, Eleanor of Aquitaine’s husband, acceded to the throne of England, becoming King Henry II. Since the royal family was rarely there, the archbishops of Bordeaux benefited from the use of the castle, until they were granted ownership in 1453. Despite the fact that the castle was occupied by both

B. Cicuttini (✉), A.B. Amara, and F. Bechtel

Institut de Recherche sur les Archéomatériaux, Centre de Recherche en Physique Appliquée à l’Archéologie, Maison de l’Archéologie, Esplanade des Antilles, Université de Bordeaux – CNRS, UMR 5060, F-33607 Pessac, France
e-mail: cicuttinibeatrice@yahoo.fr



Fig. 1 Some representative samples of the collection that includes two-colour and plain tiles. Different colours of glazes and several distinct patterns have been selected

royalty and the church for centuries, its medieval story is still largely unknown. Subsequently, the castle went through many transformations, with the most recent alterations dating to the seventeenth century. Today, there is no visible evidence of the medieval period in the castle (Solé 1990).

The tile collection consists of 55 items: 41 two-colour tiles and 14 plain tiles (Fig. 1).

They have been discovered out of context, although in two well-defined areas, as a result of several works carried out around the castle, e.g. construction of the motorway, uprooting of trees, and preliminary archaeological investigations. For this reason, it is difficult to identify the date or the person in charge of the pavement (French or English, civil or religious); however, this material is assigned to the middle of the thirteenth century (Norton 1992). The site is currently undergoing restoration and no other tiles have been found so far.

Among the items in this collection, we were able to observe patterns and colours that are unusual for the area: a pattern with four veined leaves or budding flowers (common in the north of France), and green or black colours. As this collection appears to be an isolated one, i.e. not typical of the region, we advance the hypothesis that these tiles have been imported especially for use in the “Prince Noir” Castle.

3 Methodology

Homogenized powders of red bodies and thick sections (obtained by sawing perpendicularly to the surface of the sample) were obtained in order to study all the components of the tiles (the two clays and the glaze). The sampling has been carried out in the least destructive way possible. The description of the texture was performed on a thick section, under white light, by scanning electron microscopy (Jeol, JSM-6460LV).

The initial analysis, for both the sections and the powder, was performed using energy-dispersive X-ray spectrometry (EDS), in order to determine the chemical composition of the white paste and the glaze. The composition of the glaze was also analysed directly on the tile surface in low vacuum mode (pressure: 20 Pa). The data obtained from the sections and from the analysis carried out on the surface have been compared in order to determine the suitability of non-destructive analysis on this type of material. The results obtained represent the mean of 5–10 analyses, which have been standardized to 100%.

4 Texture and Chemical Composition of the Bodies

In general, the paste used for the filling of the impression is fine. It is white, or pale “honey” and pale grey, depending on the body colour (red or grey, respectively). “The colour of the pastes shows a certain degree of heterogeneity and small amounts of minerals can be recognized (quartz, feldspars, etc.). These observations show that the preparation of the clay was not very accurate. The chemical composition results of four samples show that the white paste is composed of 68-73% SiO₂, 19-22% Al₂O₃, 3-4% K₂O, and 3% Fe₂O₃. The pale grey and “honey” colours are due to the presence of iron and the firing atmosphere (reducing or oxidizing).

The same approach was used to observe the texture of the ceramic body. The observations show the use of very heterogeneous pastes, an aspect which implies an imprecise preparation of the clay. The ceramic bodies are red or grey. The colour of the tile is linked to the colour of the body: a red paste for a “honey” tile, grey for a green tile, and a principally grey paste with red edges for a black tile. We have also identified veins or zones that vary in darkness, and the presence of cracks. These cracks may be due to the drying or packing of clay during the manufacture of the tiles. Minerals observed in the body are rugged, up to 500 µm in size, and uniformly distributed. The chemical compositions of 12 body samples (obtained from powder, and representing the mean of ten analyses) indicate that the pastes are mainly composed of silica (60-71% SiO₂), aluminum (15-23% Al₂O₃), iron (6-9% Fe₂O₃), and potassium (3-4% K₂O). The pastes are not calcareous and are rich in iron. The iron is responsible for the colour of the body: red under oxidizing conditions, grey under a reduced firing atmosphere.

5 Non-Destructive Analysis of the Glaze by SEM–EDS: Low Vacuum Mode

When observed with a magnifying binocular microscope, glazes appear translucent. Their thickness ranges from 120 to 400 µm when they are well preserved. Two different SEM-EDS procedures were used to study the chemical composition of the glazes from nine ceramic fragments:

- High Vacuum (HV), for the analysis of thick sections of glazes (5–7 areas per sample).
- Low Vacuum (LV, pressure: 20 Pa), for the analysis of glaze surfaces (6–8 areas per sample), trying to avoid damaged zones.

The analysis by SEM-EDS (HV) shows that glazes are mainly composed of lead (32–69% PbO), silica (26–49% SiO₂), aluminum (4–13% Al₂O₃) and iron (1–5% Fe₂O₃). From an archaeological point of view, this indicates that the craftsmen used lead glazes. The identification of the colouring agents allows us to hypothesize the presence of Fe³⁺ for “honey” coloured glazes (oxidized firing) and Fe²⁺ for “honey-green” coloured glazes (reduced oxygen firing), as no copper was detected. This result indicates that the “honey” coloured tiles and the green tiles have not been fired in the same batch. We have generally noticed that the “honey-green” glazes were richer in silica and poorer in lead than the green or black glazes. The black glazes are distinguished by the presence of iron, in addition to copper (2–3% CuO). The adding of copper to the iron already present in the glaze results in a very dark colour, close to black, for the glaze. This observation shows that the black colour of these tiles was the intended result desired by the craftsmen.

From a physical point of view, the comparison between section and surface analyses shows different results. For seven samples, the results are relatively satisfactory, showing consistency between the two procedures. The histogram (Fig. 2) shows a slight difference between the two methods.

For the main elements, the difference reaches 3% at most. In the majority of cases, analysis deviations intersect between both procedures. However, two tiles show variability between the two procedures (up to 8% for lead and 3% for aluminum). This can be explained by the presence of damaged surfaces on the tiles concerned.

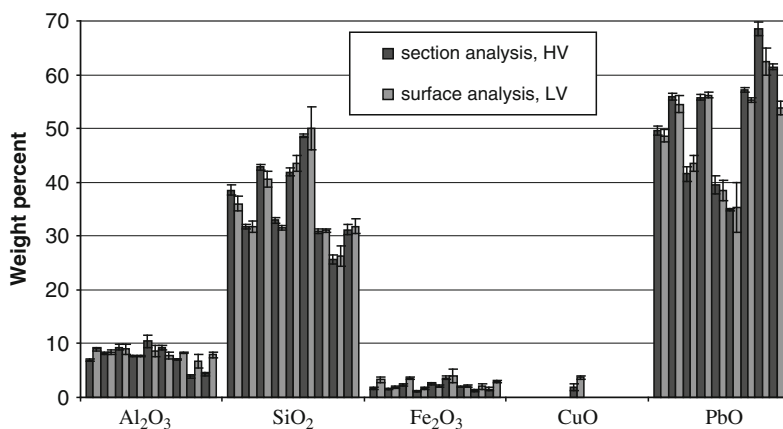


Fig. 2 Chemical composition of the glazes by SEM-EDS in HV (section) and LV (surface) modes

6 Technological Implications

Generally, we observed that the preparation of the clay which is rich in iron but poor in calcium has failed. The clay appears to have undergone a deficient kneading process, which led to fissures during drying and/or firing. The size of the unfired clayey tile was uneven. White pastes (possibly kaolin clay) were decanted. The glazing mixture may have been composed of lead ore, fine sand and clay. The quantity of clay would have been 2.5–4 times the aluminum detected in the glazes (4–13% Al_2O_3) (Tite et al. 1998).

The firing might have reached a temperature higher than 800°C . We can assume that tiles containing less flux were placed in the hotter part of the kiln. We can also assume that “honey-green” tiles are due to a bad circulation of oxygen in the kiln. For green and “honey” glazes, iron seems to be intrinsic to the raw material (a clay rich in iron, the same one used to produce the tiles?) and due to diffusion from the body. The green colour is only due to the presence of iron and shows the mastery of craftsmen. Nevertheless, it seems that control over the production process was not complete, if we consider the “honey-green” tiles. Green tiles were common during the Middle Ages, but mainly as plain tiles; they were rare for two-colour tiles. Indeed, if the glaze is too dark, the pattern is unreadable. Thus, great skill appears to have been necessary in order to produce green two-colour tiles (Norton 1992). It is important to emphasize that the existing literature, published by archaeologists or historians of art, appears to attribute the colour of green glazes to the presence of copper too readily. The present study shows that craftsmen were able to obtain this colour without using copper. Lastly, the deliberate addition of copper in the glaze in order to obtain black tiles indicates that the craftsmen wanted to produce tiles of varied colours.

7 General Conclusions

The identification of manufacturing aspects and processes provides real insight into the know-how of the craftsmen, who displayed real diversity in their production. Nevertheless, this expertise is not evident in the entire region of Bordeaux. The observation of patterns and the determination of manufacturing aspects tend to suggest an import of the material from the North of France (Artois?), where similar patterns were found (Cicuttini et al. 2007).

On the other hand, we have seen that the surface analysis of glazes by SEM-EDS in LV mode can provide good results if the sample is well preserved. However, it is necessary to increase the number of analysed areas in order to minimize the effect of anomalies due to the degradation of the surface. To conclude, the analysis of glazed surfaces by Low Vacuum SEM-EDS may represent an efficient tool in the non-destructive study of medieval tiles.

Acknowledgements The authors would like to thank Mr Lafon and Mr Gsell (Association des Amis du Vieux Lormont) for their collaboration on this study. This research project has been supported by the “Conseil Régional d’Aquitaine”.

References

- Cicuttini B, Mérat A, Ben Amara A, Bechtel F (2007) Etude stylistique et technologique des carreaux de pavement du château de Lormont (Gironde, XIIIe - XIVe s.), In: Actes du 4ème Congrès international d’Archéologie Médiévale et Moderne – Medieval Europe Paris 2007, 3-8 september 2007, Paris, France
- Norton C (1992) Carreaux de pavement du Moyen Age et de la Renaissance, éditions Paris-Musées. Collections du Musée Carnavalet, Paris
- Solé J-L (1990) Le château de Lormont au cours des siècles, faits de guerre et description. Publications des Amis du Vieux Lormont, France
- Tite MS, Freestone I, Mason R, Molera J, Vendrell-Saz M, Wood N (1998) Lead glazes in antiquity – methods of production and reasons for use. *Archaeometry* 40(2):241–260

Ceramic Production and Metal Working at the Trebbio Archaeological Site (Sansepolcro, Arezzo, Italy)

E. Gliozzo, A. Comini, A. Cherubini, A. Ciacci, A. Moroni,
and I. Turbanti Memmi

1 Introduction

Located in the extreme eastern portion of present Tuscany, the archaeological area of Trebbio-Spinellina (Sansepolcro, Arezzo; Fig. 1) is situated between Umbrian and Etruscan territories, in a culturally complex area where Picenian and Sabinian influences are also present (Migliorati 2003; Zamarchi Grassi and Scarpellini Testi 1992).

Along the left bank of the River Tiber (i.e. the main commercial “road”), the district was characterised by an intense artisanal activity, mainly devoted to ceramic production. In particular, regarding the period between the eighth and the sixth centuries BC, the concentration of wastes at “Casa Bandinelli”, the kilns at Trebbio-Spinellina, and the diffusion of waste products at the confluence of the Afra and Tiber rivers testify to a long-lasting ceramic production (Catucci 1993; Alberti and Laurenzi 2001; Alberti et al. 2001). The presence of water, the abundance of suitable clays in the alluvial deposits of the Tiber Valley, coupled with the nearby availability of both wood and mineral ores in the Monti Rognosi territory (Antonelli 1961; Antonelli and Dottorini 1966; Bini et al. 1974; Rossellini 1987) both favoured human settlement and stimulated the development of numerous manufacture activities.

The archaeological site of Trebbio-Spinellina was the object of archaeological excavations from 2002 to 2005 (Acconcia et al. 2008; Ciacci and Moroni Lanfredini

E. Gliozzo (✉), and I. Turbanti Memmi
Department of Earth Sciences, University of Siena, Siena, Italy
e-mail: gliozzo@unisi.it, memmi@unisi.it

A. Comini, A. Cherubini, and A. Ciacci
Department of Archaeology and History of Arts, University of Siena, Siena, Italy

A. Moroni
Department of Environmental Sciences, University of Siena, Siena, Italy

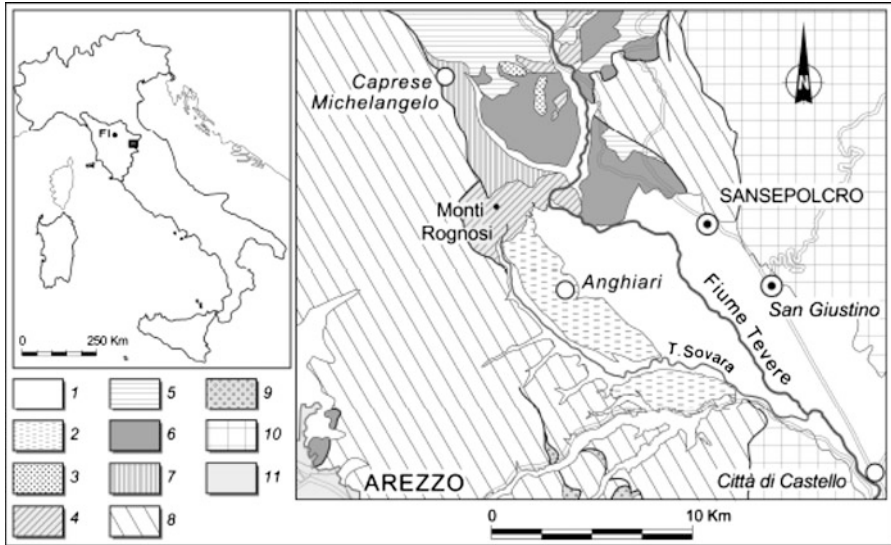


Fig. 1 The Trebbio-Spinellina area (Sansepolcro, Arezzo, Italy). *Legend:* (1) Sands, pebbles and mud (alluvial, eolian, lacustrine, palustrine, lagoonal, shore Quaternary deposits); (2) Conglomerates, sandstones, siltstones, clays and limestones of fluvial lacustrine environment (Ruscinian-Villafranchia); (3) Calcarenites, marls, mudstones, calcareous and glauconitic sandstones (Middle Eocene-Late Serravallian); (4) Ophiolites (Jurassic peridotites, gabbros, basalts, ophiolites and ophiolitic breccias, plagiogranites); (5) Helminthoid tertiary flysch: limestones, marls and sandstones with olistostromes (Paleocene-Middle Eocene); (6) Shales, sandstones, conglomerates (Cretaceous-Paleocene); (7) Breccias and polygenic conglomerates with clasts of ophiolites, limestones, radiolarites, sandstones and shales, quartz-mica bearing sandstones, feldspathic sandstones and ophiolite-rich sandstones (Cretaceous-Middle Eocene); (8) External sandstone flysch (Chattian-Aquitainian sandstones, siltstones and marls with olistostromes); (9) Shales and marls, quartz-rich calcilutites and nummulites calcarenites (Early Cretaceous-Oligocene); (10) Sandstone-marly flysch (Late Burdigalian-Early Messinian sandstones, siltstones and marls with olistostromes); (11) Urban

2006; Ciacci 2008). The investigations brought to light several structures, related both to ceramic production and metal working, dated between the ninth century BC and the beginning of the Archaic period (sixth century BC). Ceramic production is testified by the presence of ceramic kilns, partially corresponding to type I/a of Cuomo di Caprio's typology (Cuomo di Caprio 1971–1972, 2007; Comini 2008). Numerous pottery fragments were also collected on-site, including a significant number of large *pythoi* (Fig. 2a). The external, convex side of the bottom of numerous *pythoi* showed traces of vitrification and alteration. Usually these dark traces were approximately circular and localised right in the middle of the large pottery fragments (Fig. 2b). The occurrence of metal working activities at the site is indicated by the presence of metal slags and ceramic fragments with clear traces of fire (Fig. 2c).

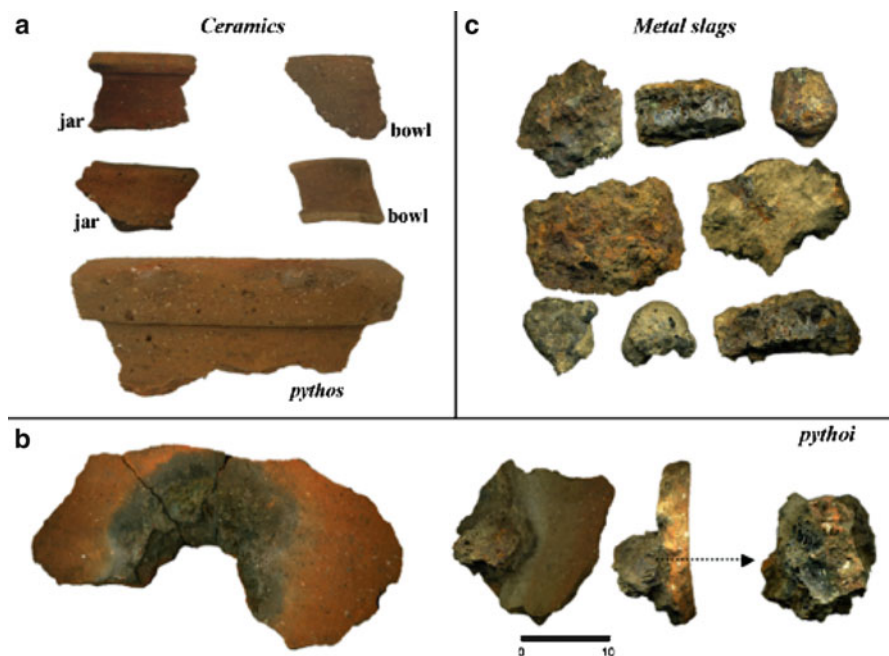


Fig. 2 Representative pictures of analysed ceramics and metal slags

2 Materials and Method

The present archaeometric study is aimed at characterising archaeological objects and local clayey sediments in order to reconstruct the patterns of ceramic and metal production at the Trebbio-Spinellina site. Local ceramics such as *pythoi*, jars, bowls and lids were sampled and analysed in order to characterise the composition of the ceramic bodies and investigate the production technology (Table 1). Greater attention has been devoted to the study of the large *pythoi*, as they were frequently associated to metal production. Metal slags of coarse-unshaped type (see Serneels 1993) were also sampled, based on their morphology and dimensions (Table 1). Fragments of ceramics and metallic slags were analysed by means of optical microscopy, X-ray diffraction and X-ray fluorescence.

In addition, clayey sediments outcropping in the vicinity of the archaeological site were sampled and investigated, in order to gain an insight into the locally available raw materials (Table 1). A total of six samples were collected close to the archaeological site (S-TSP 4–6) and along the banks of the River Tiber (S-TSP 1–3). X-ray diffraction and X-ray fluorescence were used to characterise these samples; a few samples were further investigated by means of optical microscopy.

The instruments used were the following: scanning electron microscope (SEM) Philips XL 30 SEM equipped with an Energy Dispersive Spectrometer (EDS)

Table 1 Sample list and description

	Sample	Description	Type	Stratigraphic unit	
CERAMICS	TSP 1	<i>Pythos</i>	vitrified portion	212	
	TSP 2	<i>Pythos</i>	vitrified portion	212	
	TSP 3	<i>Pythos</i>	traces of fire	212	
	TSP 7	<i>Pythos</i>	traces of fire	212	
	TSP 9	<i>Pythos</i>	Type 4	212	
	TSP 10	<i>Pythos</i>	Type 3	212	
	TSP 11	<i>Pythos</i>	Type 9	212	
	TSP 12	<i>Pythos</i>	Type 1	135 (filling of kiln C)	
	TSP 21	<i>Pythos</i>	Type 7	Kiln C	
	TSP 13	Bowl	Type 11	181	
	TSP 15	Bowl	Type 1	116	
	TSP 18	Bowl/lid	Type 8/9	243	
	TSP 16	Lid	Type 7	127	
	TSP 14	Jar	Type 2	127	
	TSP 19	Jar	Type 7	243	
	TSP 20	Jar	Type 1	212	
	TSP 22	Jar	Type 9	135 (filling of kiln C)	
	TSP 8	Perforated floor	traces of fire	212	
	METALS	TSP 4	Metal slag	–	212
		TSP 23	Metal slag	–	116
		TSP 24	Metal slag	–	116
		TSP 25	Metal slag	–	116
TSP 26		Metal slag	–	116	
TSP 27		Metal slag	–	116	
TSP 28		Metal slag	–	Surface	
TSP 29		Metal slag	–	Surface	
TSP 30		Metal slag	–	Surface	
TSP 31		Metal slag	–	Surface	
TSP 32		Metal slag	–	212	
ROCKS				North	East
	S-TSP 1	Clayey sediment	43° 32' 22.8"	12° 08' 18.6"	
	S-TSP 2	Clayey sediment	43° 32' 24.3"	12° 08' 19.4"	
	S-TSP 3	Clayey sediment	43° 32' 32.3"	12° 08' 23.3"	
	S-TSP 4	Clayey sediment	43° 32' 38.9"	12° 08' 21.5"	
	S-TSP 5	Clayey sediment	43° 32' 35.8"	12° 08' 39.0"	
	S-TSP 6	Clayey sediment	43° 32' 40.8"	12° 08' 41.8"	

EDAX-DX4 operating at 20 kV; X-ray Philips PW 1710 Bragg-Brentano diffractometer, using Cu-K α radiation, in the 5–70° 2 θ range, with a scan speed of 1.2°/min; operating conditions were 45 kV and 25 mA; X-ray fluorescence (XRF) Philips MagicX Pro (loss on ignition was also determined by heating samples to 1,050°C for 2 h). Bulk chemical and mineralogical analyses require 6 g and 1 g of material, respectively; however, considering the coarse texture of the ceramic materials, 20 g were ground, powdered and divided by quartation in order to reach a representative dataset.

3 The Characterisation of Ceramics, Metal Slags and Local Clayey Sediments

3.1 Ceramics

All samples are characterised by a Ca-poor, Mg- and Fe-rich composition (Table 2).

CaO contents never exceed 5.5 wt%, being generally less than 3 wt%. MgO contents range between 2 wt% and 9.6 wt%. CaO and MgO contents are linearly correlated: the former are in a range of 1.9–2.5 wt% with MgO < 4 wt%, of 2.7–3.3 wt% with MgO < 6 wt%, and of 4.9–5.5 wt% with MgO > 6 wt%. Fe₂O₃ contents vary from 6.1 to 9.6 wt%, reaching however 12 wt% in the lid TSP 16. A significant variability is observable in the contents of minor elements as well. It is worth noticing that Ni and especially Cr values are frequently higher than 200 ppm, reaching 545 and 1,138 ppm, respectively, in one *pythos* sample (TSP 2). The results of mineralogical analyses (XRD and optical microscopy) can be summarised as follows: quartz and feldspars are ubiquitous; clay minerals (i.e. smectites) and micas (mainly muscovite) are often abundant, hematite is always present, while calcite and clinoamphiboles have been sporadically observed. Both magmatic and metamorphic rocks are present, while microfauna is generally absent.

3.2 Local Clayey Sediments

Local clayey sediments outcropping nearby the archaeological site show a heterogeneous CaO content, ranging from 1.3 to 16.1 wt% (Table 2). Sediments outcropping in the vicinity of the archaeological site (STSP 4–6) are poorer in Ca than those outcropping close to the river banks (STSP 1–3). Based on major, minor and trace element contents, the former are more homogeneous and characterised by higher SiO₂, Al₂O₃, Fe₂O₃, Na₂O, K₂O, V, Zn, Rb, Y, Zr, Nb, Ba, La, Th, and U contents than the latter. It is important to note that Ni and Cr contents reach 132 and 248 ppm, respectively. Mineralogical analyses (XRD and optical microscopy) allowed us to distinguish two groups of sediments, based on the relative calcite contents. Micas, clay minerals, quartz and feldspars are present in both groups; hematite is sporadic.

3.3 Metallic Slags

Metallic slags can be divided into three main groups, characterised by a different chemical composition (Table 2) and mineralogical association. The first group includes most of the examined samples (TSP 24–26, 30–31), and contains quartz,

Table 2. Bulk chemical analyses (XRF). Oxides expressed in wt%, minor and trace elements expressed in ppm

Sample	SiO ₂	TiO ₂	Al ₂ O ₃	Fe ₂ O ₃	MnO	MgO	CaO	Na ₂ O	K ₂ O	P ₂ O ₅	LOI	V	Cr	Co	Ni	Cu	Zn	Rb	Sr	Y	Zr	Nb	Ba	La	Pb	Ce	Th	U	
TSP 1	Pythos	57.38	0.65	18.94	7.56	0.06	5.53	3.22	1.38	1.27	1.75	2.06	110	253	25	230	-	87	75	233	24	165	12	753	20	21	37	9	3
TSP 2	Pythos	54.93	0.65	16.28	9.43	0.27	5.44	2.76	1.42	1.41	0.99	6.13	126	1,138	59	545	-	102	75	392	26	162	12	553	30	26	52	8	3
TSP 3	Pythos	57.03	0.67	19.92	7.75	0.11	8.30	4.90	1.20	1.58	0.00	0.00	70	180	25	288	39	114	72	347	23	130	12	1,286	18	24	45	9	4
TSP 7	Pythos	49.12	0.49	20.05	7.42	0.11	6.97	4.98	1.67	0.61	4.18	4.13	75	227	26	325	-	129	36	423	22	110	8	1,313	23	18	39	6	0
TSP 9	Pythos	58.21	0.66	18.27	8.04	0.06	4.31	2.72	0.94	1.70	0.43	4.48	133	267	23	158	23	135	108	143	24	144	13	528	25	25	46	11	4
TSP 10	Pythos	55.33	0.89	19.65	9.27	0.17	2.15	2.01	0.42	1.84	1.90	6.15	167	195	26	141	-	163	113	227	37	180	19	966	42	30	76	15	4
TSP 11	Pythos	60.17	0.62	18.12	6.68	0.06	3.62	2.19	1.14	2.06	1.29	3.83	112	196	18	149	-	123	114	184	26	138	12	968	24	24	0	9	4
TSP 12	Pythos	55.66	0.66	16.48	9.55	0.28	5.49	2.79	1.44	1.43	1.00	4.92	120	1,084	56	519	-	97	72	183	25	153	11	539	29	21	44	8	3
TSP 21	Pythos	52.34	0.58	18.16	7.03	0.06	6.45	5.41	1.35	1.14	1.61	5.69	98	269	25	235	-	72	69	212	25	141	11	688	29	21	42	9	3
TSP 13	Bowl	60.53	0.70	17.80	6.80	0.14	3.60	2.15	1.26	2.18	1.14	3.50	93	227	23	152	18	115	106	215	27	162	14	828	31	23	44	10	4
TSP 15	Bowl/lid	50.57	0.50	18.52	7.07	0.12	6.27	5.06	1.68	0.85	3.07	5.17	68	480	29	381	-	96	37	349	17	108	7	985	18	15	37	5	1
TSP 16	Lid	56.29	0.74	18.41	12.01	0.14	2.85	1.85	1.00	1.78	1.81	2.88	132	250	37	220	-	117	96	170	32	198	15	959	37	39	58	14	4
TSP 14	Jar	58.21	0.76	17.36	7.78	0.15	3.16	2.10	0.86	1.88	2.01	5.52	121	267	28	154	-	106	97	210	34	197	15	944	34	26	43	11	3
TSP 19	Jar	47.32	0.26	19.22	6.15	0.09	9.63	5.50	1.44	0.41	3.10	6.65	43	302	22	419	22	136	26	400	18	70	4	782	10	14	22	4	0
TSP 20	Jar	58.36	0.76	17.17	7.44	0.13	2.06	2.51	0.90	2.18	3.56	4.68	108	170	22	120	-	134	113	336	35	199	15	1,131	29	29	41	12	3
TSP 22	Jar	57.52	0.77	17.55	7.97	0.15	2.91	2.38	0.84	1.95	3.20	4.50	109	229	26	150	31	124	94	262	32	197	15	1,226	35	27	59	11	3
TSP 8	Perforated floor	56.36	0.64	18.21	8.17	0.12	4.90	3.33	1.24	1.62	3.47	1.65	113	255	24	222	-	140	89	327	32	162	12	1,331	29	28	46	11	3
TSP 4	Metal slag	19.16	0.21	3.89	67.21	0.13	0.99	5.83	0.57	1.13	0.90	0.00	35	60	186	327	27	5	57	49	4	33	6	365	8	56	20	11	3
TSP 23	Metal slag	46.47	0.41	11.64	27.16	0.13	2.97	6.57	1.43	2.11	0.73	0.23	86	176	80	173	50	49	91	213	14	152	10	397	18	73	35	14	2
TSP 24	Metal slag	13.16	0.18	2.77	77.57	0.14	0.77	3.77	0.38	0.53	0.73	0.00	83	104	217	317	151	8	27	33	3	24	6	327	11	27	18	3	4
TSP 25	Metal slag	14.36	0.20	3.12	76.54	0.13	0.87	3.13	0.41	0.62	0.63	0.00	68	127	216	303	110	8	14	29	2	21	5	269	13	13	28	1	4
TSP 26	Metal slag	22.95	0.28	4.91	65.89	0.15	0.86	2.98	0.53	0.86	0.59	0.00	58	73	187	250	164	3	216	35	6	77	6	316	19	224	39	56	0
TSP 27	Metal slag	40.25	0.47	9.98	35.15	0.16	3.63	6.97	0.90	1.89	0.60	0.00	73	250	111	207	57	25	39	93	8	44	7	373	9	19	42	3	4
TSP 28	Metal slag	23.82	0.28	5.60	57.12	0.15	1.60	7.59	0.91	2.10	0.83	0.00	39	72	160	209	889	3	23	73	4	31	6	363	13	16	35	1	4
TSP 30	Metal slag	24.86	0.28	5.02	55.81	0.12	1.34	9.89	0.71	1.55	0.42	0.00	42	96	157	226	28	2	83	72	5	41	6	270	9	81	33	12	2
TSP 31	Metal slag	16.98	0.22	3.62	70.51	0.08	0.81	5.75	0.57	1.06	0.40	0.00	40	54	191	241	23	1	90	40	4	40	6	239	14	92	41	21	1
TSP-32	Metal slag	11.70	0.16	2.72	81.07	0.09	0.55	2.06	0.41	0.51	0.73	0.00	36	48	225	296	551	0	238	25	6	74	6	261	11	251	19	62	0
STSP-1	Clayey sed.	45.80	0.44	10.55	3.65	0.13	4.11	15.82	0.77	1.64	0.14	16.80	66	248	20	130	-	62	63	426	21	104	8	344	17	17	25	6	2
STSP-2	Clayey sed.	45.57	0.45	10.69	3.79	0.13	4.20	16.08	0.73	1.59	0.12	16.50	70	219	20	132	-	62	67	433	21	113	8	315	13	20	45	6	2
STSP-3	Clayey sed.	57.46	0.45	12.56	3.29	0.06	2.53	10.12	1.31	2.21	0.21	9.67	65	112	12	50	-	61	99	278	19	121	9	376	18	24	25	5	3
STSP-4	Clayey sed.	62.62	0.70	15.37	5.57	0.15	2.85	2.42	1.23	2.42	0.18	6.35	106	139	18	75	-	88	117	133	28	191	14	447	27	27	43	9	5
STSP-5	Clayey sed.	65.25	0.66	15.39	5.09	0.11	2.89	1.32	1.42	2.50	0.24	4.99	96	127	16	61	-	88	120	110	26	195	14	489	28	26	43	8	5
STSP-6	Clayey sed.	61.81	0.66	15.21	5.19	0.11	3.05	3.25	1.19	2.56	0.27	6.55	102	127	16	63	-	92	121	143	27	176	14	469	22	26	38	9	5

fayalite, magnetite and wustite. Samples TSP 24 and 25 also contain hematite, while samples TSP 30 and 31 show the presence of kirschsteinite. Chemical analyses suggest a distinction between samples TSP 24–26 and TSP 30–31, mainly based on minor element contents. The Pb content in sample TSP 26 deserves further attention. The second group includes TSP 28 and TSP 32, characterised by Cu contents higher than 500 ppm and the following mineralogical association: quartz, fayalite, wustite, and minor contents of magnetite. Sample TSP 32 also shows significant Pb contents. The third group includes samples TSP 23 and TSP 27, characterised by Fe_2O_3 contents lower than 40 wt% and MgO contents ranging between 3 and 3.6 wt%. The mineralogical association is mainly represented by quartz and plagioclase, with minor contents of fayalite, wustite and monticellite.

4 Discussion

The chemical and mineralogical composition of ceramic materials is comparable to that of local clayey sediments, although excluding those outcropping close to the river bank. Even considering that fluvial meandering and erosional phenomena produced a heterogeneous context that probably does not coincide with the one present in antiquity, the high contents of CaO in the samples of clayey sediments collected from this area exclude any direct comparison with the composition of the ceramic samples. As for ceramics, the significant variability observed in minor and trace element contents is mainly due to the different proportion of lithic inclusions within the ceramic body. It is thus worth considering that, although an oversampling (20 g instead of 7 g) was performed in the analyses, the heterogeneity of the artefacts could have affected the results obtained by bulk analyses for these coarse ceramic materials (inclusions of 0.5–1.5 cm are frequent). The high Cr and Ni contents are probably related to the presence of lithic fragments from the ophiolitic complex.

The three groups of metal slags can be referred to different stages and types of productions. The first and third group seem to be related to iron production, considering that the former includes proper metallic slags, while the latter shows vitrified by-products, resulting from the heating of clay materials. Based on the copper and lead contents, the second group seems to indicate a “mixed” production, where iron was only one of the metals worked on-site. Sample TSP 26, showing high Pb contents, could also be included in this group. In terms of the working conditions, the contemporaneous presence of oxidised (e.g. hematite), reduced (e.g. fayalite, wustite) and oxidised/reduced (e.g. magnetite) mineralogical phases provides evidence of non-equilibrium systems. In two samples, the modest presence of kirschsteinite could suggest the occurrence of high temperatures and fairly reducing conditions (Gustafson 1974). On the other hand, the rare presence of hematite can be interpreted as representing an alteration product or, alternatively, as a relic of a process taking place under variable (i.e. oxidising/reducing) conditions. As for quartz and plagioclase, these phases are not to be considered components of the

metallic slag, but as contributions to the total slag originating from the kiln structure or from the sand employed during processing.

5 Conclusions

This study represents the first attempt aimed at characterising an Etruscan production of both ceramics and metals in Tuscany. The characterisation of ceramic and metal objects at the Trebbio site allowed the reconstruction of an production activity using various types of local raw materials. Local sediments were suitably selected (Ca-poor clays), coherent lithic materials were opportunely added to the clay, iron and copper sources available in the area were certainly exploited. Ceramics were low fired (clay minerals are still present), but were highly resistant to thermal shock, due to the numerous added lithic inclusions. The compositions of metal slags indicate a multifunctional activity. Smelters presumably used ores from different sources and worked different types of metals, such as iron and copper. Both ore minerals were available in the ophiolitic complex of Monti Rognosi, where copper smelting is archaeologically attested at the “La Fabbrica” site beginning with the Etruscan period. Native copper, cuprite, bornite, chalcopyrite and magnetite were mined in this territory, an important source for metal production until the early Roman period.

References

- Acconcia V, Arrighi S, Ciacci A, Moroni Lanfredini A (2008) Risultati delle campagne di scavo al Gorgo del Ciliegio e al Trebbio in Alta Valtiberina (Sansepolcro-AR) - Anni 2001–2003 (Atti Montefiascone 2005)
- Alberti D, Laurenzi GP (2001) Rinvenimenti dell'età del Ferro nell'Alta Valtiberina, In: Atti della XXXIV Riunione Scientifica dell'Istituto Italiano di Preistoria e Protostoria della Toscana
- Alberti D, Laurenzi GP, Moroni LA (2001) Evidenze dell'età del Ferro al Trebbio in Alta Valtiberina (AR). *Rassegna di Archeologia* 18A:91–101
- Antonelli C (1961) Itinerari mineralogici I Monti Rognosi *Natura*. *Riv Sci Nat* 52:46–52
- Antonelli C, Dottorini C (1966) I Monti Rognosi e il loro rame. *L'Universo* 46:117–126
- Bini C, Faraone D, Giaquinto S (1974) Indagini petrografiche e chimiche su ofioliti della Toscana; nota I: il complesso dei Monti Rognosi (Arezzo). *Periodico di mineralogia* 43:591–654
- Catucci M (1993) Sansepolcro (Ar): la fornace di Casa Bardinelli. *Rassegna di Archeologia* 11:245–286
- Ciacci A (2008) Il Trebbio: un sito per la produzione ceramica lungo il corso dell'Alto Tevere, In: *Piana fiorentina, Valdarno e aree limitrofe. Studi recenti e nuovi dati dalla ricerca archeologica* (Atti Montefiascone 2005)
- Ciacci A, Moroni Lanfredini A (2006) Sansepolcro (AR).Trebbio. In: *Notiziario della Soprintendenza per i Beni Archeologici della Toscana*. 370–374
- Comini A (2008) Le fornaci del Trebbio (Sansepolcro-AR): considerazioni tipologiche e contesti di riferimento, In: *Piana fiorentina, Valdarno e aree limitrofe. Studi recenti e nuovi dati dalla ricerca archeologica* (Atti Montefiascone 2005)

- Cuomo di Caprio N (1971–1972) Proposta di classificazione delle fornaci per ceramica e laterizi nell'area italiana. *Sibirium* 11:371–461
- Cuomo di Caprio N (2007) La ceramica in *Archeologia*. Roma
- Gustafson WI (1974) The stability of andradite, hedenbergite and related minerals in the system Ca-Fe-Si-OH. *J Petrology* 15:455–496
- Migliorati C (2003) Il confine orientale dell'Etruria nell'età antica: l'Alta valle del Tevere tra Etruschi ed Umbri. *Annali Liceo Ginnasio Plinio il Giovane* 2:39–68
- Rossellini A (1987) I Monti Rognosi. La loro geologia, la loro storia, il loro rame. *Notiziario Gr Mineral Fiorent* 14:20–28
- Serneels V (1993) Archéométrie des scories de fer. Recherches sur la sidérurgie ancienne en Suisse occidentale. *Cahiers d'Archéologie Romande* 61.
- Zamarchi Grassi P, Scarpellini Testi M (1992) Osservazioni preliminari sulle testimonianze archeologiche in epoca etrusca e romana. In: Gruppo Ricerche Archeologiche Sansepolcro (eds) *Nuovi contributi per una carta archeologica della Valtiberina*. Arezzo, pp 19–24

Many Potters – One Style: Pottery Production and Distribution in Transitional Late Byzantine–Early Islamic Palaestina Tertia

V.E. Holmqvist and M. Martínón-Torres

1 Introduction

This article examines the ceramic economies of the late Byzantine–early Islamic southern Palestine (sixth to ninth centuries AD), the area of the Byzantine province *Palaestina Tertia*. The region was affected by economic stagnation already before the end of the Byzantine period, and we currently know very little of its socio-economic situation after the Muslim invasion in ca. AD 630. The administrative changes left the area relatively remote and rarely mentioned in the early Arabic written sources. Nevertheless, an increasing number of studies show evidence for peaceful political transition and cultural continuation in the area under the Umayyad rule (Schick 1998; Rosen 2000; Walmsley 1992). It is possible that the economic decline mainly affected only the largest urban centres, which transformed into rural and agricultural villages (Fiema 2001; Graf 2001; King 1992).

This study seeks to assess the effect that the political and cultural transition had on the local ceramic economies, regional and inter-regional ceramic trade and transportation, and examines the uniformity and survival of the local ceramic productions and traditions, and looks for shared production and exchange of ceramics. There are currently no known post-Byzantine ceramic workshops in the area. In addition to ceramic traditions clearly regional to southern Palestine, there seem to be certain stylistic and functional features introduced in the course of the transitional period that are shared in household ceramics across Palestine.

2 Archaeological Materials and Analytical Methods

The research material included ceramic artefacts from five archaeological sites: the monastery of Jabal Harûn near Petra (JH), the village site of Khirbet edh-Dharîh in southern Jordan (DH), the port city of ‘Aqaba/Aila on the Red Sea coast (A), the city

V.E. Holmqvist (✉) and M. Martínón-Torres

Institute of Archaeology, University College London, 31–34 Gordon Square, London WC1H 0PY, UK
e-mail: v.holmqvist@ucl.ac.uk

of Elusa in the Negev (E) and the farmhouse site of Abu Matar in Beersheva (AM) (Frösén et al. 2004; Gilead et al. 1994; Goldfus and Fabian 2000; Parker 2003; Villeneuve 1990). The underlying aim was to obtain a broad sample including rural, urban, and religious sites across the area of the former Byzantine province.

A total of 136 sherds were prepared as powder pellets and analysed for their bulk chemical compositions employing a polarising ED-XRF spectrometer (Spectro Lab Xpro 2000). Hierarchical cluster analysis of the data was used to identify groups based on these results, and these groups were confirmed via microchemical and textural analyses by optical and electron microscopy. Fifty-four polished blocks were prepared and analysed by SEM-EDS (using a Philips XL30 with an Oxford Instruments EDS) to study ceramic body compositions, mineralogical inclusions, paste vitrification and other technological aspects.

3 Results and Discussion

Due to space limitations, raw data and a more detailed discussion will be published elsewhere, while only a brief overview is advanced here. Cluster analysis of the XRF data included the following elements: Mg, Al, Si, K, Ca, Ti, V, Cr, Mn, Fe, Co, Ni, Cu, Zn, Rb, Sr, Zr and Ba. The dendrogram shown in Fig. 1 demarcates five compositional groups, which will be discussed in turn.

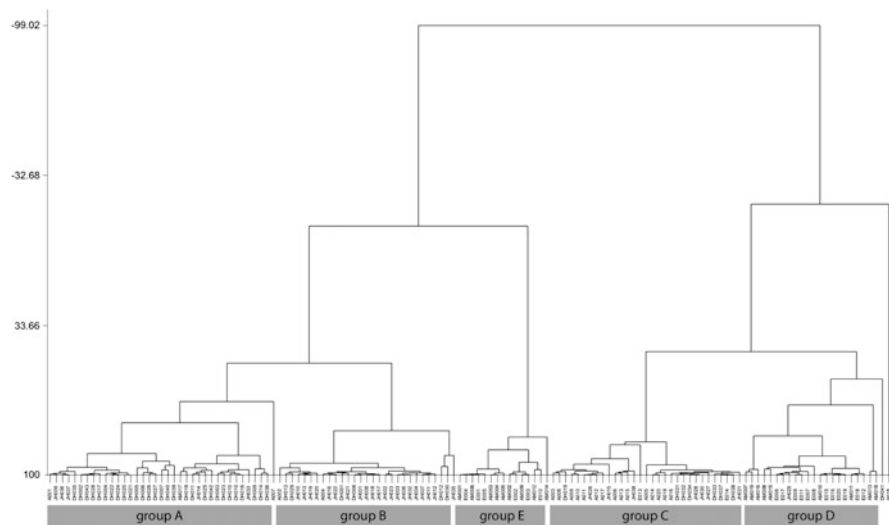


Fig. 1 Dendrogram resulting of the cluster analysis of the XRF data, using the Ward-linkage method and squared Euclidean distances

Groups A and B might be better considered subgroups of the same broad fabric: group A is dominated by DH sherds, whereas group B includes predominantly ceramics from JH. Both subgroups have a considerable similarity (>50%), which is corroborated by the comparable compositions of the ceramic bodies as analysed by SEM-EDS. These are typically non-calcareous clays, with their petrography characterised by the presence of quartz, ilmenite, relatively abundant clay pellets and iron oxides, and rare apatite. The slight compositional segregation between the two groups, mostly derived from variable CaO contents, may suggest that these two sites in southern Transjordan, separated by approximately 75 km, had different suppliers of pottery, possibly at the local level, although these are likely to have exploited similar clay resources within the same region. It is plausible that local potters operated in the vicinities of both sites, and that their products were exchanged in small, regional markets. Other than ceramics from DH and JH, these two subgroups include a few sherds of cooking vessels found in the port of 'Aqaba. The potential presence of JH/DH ceramics in this southern port may well be explained by the important flow of materials that took place in the opposite direction, i.e. from 'Aqaba to the north (see below). Finally, of all of the archaeological samples from the Negev analysed, only one jar appears to originate from these Transjordanian sites.

Group C includes all of the 'Aqaba/Aila-type amphorae from the port of 'Aqaba, known to have been produced there locally at least until the seventh century (Melkawi et al. 1994). These are all calcareous ceramics, with abundant potassium and sodium feldspars together with biotite, augite and iron oxides. Interestingly, this group also includes a good number of amphorae recovered in the sites of JH and DH, and one amphora identified in the Negev city of Elusa (Fig. 2). Thus these results provide the first evidence of the use of these amphorae for inland transportation, using land routes of up to several hundred kilometres.

The provenance of the highly calcareous ceramics forming group D can be ascribed to the site of Elusa, as this group includes all of the ceramic wasters from a workshop in Elusa that ceased to operate in the sixth century. Ceramics in this group include a variety of forms – although excluding cooking pots – found both in Elusa and the Beersheva farmhouse of Abu Matar. Only three sherds in this group were identified in the assemblages of JH and DH, again indicating that, even though ceramic exchange took place between the Negev and southern Transjordan, this is likely to have been of a minor importance, and both regions could ensure a supply of ceramics at the local or regional level.

Finally, group E is solely composed of cooking pots from the Negev (both in E and AM), made from a non-calcareous clay containing characteristic Mn-rich pellets. This attests to the common practice of employing non-calcareous clays for cooking vessels (Tite and Kilikoglou 2002), but it also denotes that these two sites shared cooking pot production or purchased them from the same market, although we cannot, at the moment, say with certainty where the pots were produced.



Fig. 2 Aila/Aqaba-amphora sherds recovered from 'Aqaba (*above left*), Elusa (*above right*), Khirbet edh-Dharih (*below left*) and Jabal Harûn (*below right*)

4 Conclusions

The results suggest material exchange on local, regional, inter-regional and long-distance level in the transitional late Byzantine–early Islamic southern Palestine. The local rural markets were places for farmers, pastoralists and craftsmen to gather and exchange their products, such as pottery, metal and other common goods, but it is difficult to provide evidence for such open-air markets by the means of archaeology (Graf 2001). Jabal Harûn, Khirbet edh-Dharih and 'Aqaba in southern Transjordan, and Elusa and Beersheva in the Negev, respectively shared cooking vessels and other pottery types from the same manufacturers, attesting to local trade. This sheds further light on the commerce of the rural areas during the Byzantine and post-Byzantine periods, and supports the idea of rural markets, combined market places of villages located nearby, and their increasing importance during the so-called

de-urbanisation of the seventh century, when long-distance trade and urban markets decreased.

The results show that the Aila-amphorae display a wide distribution network and were transported as far inland as Khirbet edh-Dharih in Transjordan and Elusa in the Negev, both located ca. 200 km from their production centre in 'Aqaba. This dovetails with the suggestion that the main roads running from 'Aqaba towards north and west were still used in the eighth century, with 'Aqaba as a centre junction, connecting Sinai, the Negev and Transjordan (Avner and Magness 1998; Frenkel 1996; Whitcomb 1995).

The transitional period ceramic workshops in southern Palestine remain unidentified, but the existence of distinct fabric groups for each site (or pair of nearby sites) allows us to suggest that these groups are local to the sites in question, perhaps produced in newly established workshops currently unknown to us. In this sense, the situation would be comparable to that of the northern Palestine, where newly established Umayyad ceramic workshops were founded in the former Byzantine centres, such as Bet Shean and Jerash (Bar-Nathan and Mazor 1993; Schaefer 1986; Walmsley 1992).

Although some ceramic varieties are unquestionably specific to certain areas of Palestine, stylistic comparisons indicate that shared stylistic traditions were also followed across Palestine. More effort should be put into investigating cultural transmission and homogenisation in transitional-early Islamic Palestine. This evidence, however, suggests that different potters adapted similarly to the new cultural influences and responded similarly to the changed consumer demands, possibly arising from new customs, diets, and dishes. There seem to be common stylistic traits for products that were manufactured, as revealed by compositional data, in different production centres and workshops: many potters – one style.

Acknowledgements This article was written with the support of the following institutions and individuals: Osk Huttunen Foundation, the “Centres of Excellence in Research” programme 2006–2011 of the Academy of Finland, Thilo Rehren, Steven Rosen, Jaakko Frösén, Zbigniew Fiema, S. Thomas Parker, Francois Villeneuve, Haim Goldfus, Peter Fabian, Isaac Gilead and Zeidoun al-Muheisen.

References

- Avner U, Magness J (1998) Early islamic settlement in the southern Negev. *Bull Am Schools Orient Res* 310:39–57
- Bar-Nathan R, Mazor G (1993) City center (South) and Tel Iztabba Area, excavations and surveys in Israel, vol 11: The Bet She'an excavation project (1989–1991):33–51
- Fiema ZT (2001) Byzantine petra – a reassessment. In: Burns TS, Eadie JW (eds) *Urban centers and rural contexts in late antiquity*. Michigan State University Press, East Lansing, pp 111–131
- Frenkel Y (1996) Roads and stations in Southern Bilad al-Sham in the 7th–8th Centuries. *ARAM* 8:177–188

- Frösén J, Fiema ZT, Lavento M, Danielli C, Holmgren R, Latikka J, Rajala A, Mikkola E, Lahelma A, Holappa M, Juntunen K (2004) The 2003 Finnish Jabal Harūn Project: Preliminary Report. *Annu Dep Antiquities Jordan* 48:97–116
- Gilead I, Rosen SA, Fabian P (1994) Horvat Matar (Bir Abu Matar) – 1990/1991. *Excavations Surv Israel* 12:97–99
- Goldfus H, Fabian P (2000) Haluza (Elusa). *Excavations Surv Israel* 111:93–94
- Graf DF (2001) Town and countryside in Roman Arabia during late antiquity. In: Burns TS, Eadie JW (eds) *Urban centers and rural contexts in late antiquity*. Michigan State University Press, East Lansing, pp 219–240
- King GRD (1992) Settlement patterns in islamic Jordan: The umayyads and their Use of the land. *Studies Hist Archaeol Jordan* 4:269–375
- Melkawi A, Amr K, Whitcomb D (1994) The excavation of two seventh century pottery Kilns at Aqaba. *Annu Dept Antiquities Jordan* 38:447–467
- Parker ST (2003) The Roman 'Aqaba project: The 2002 campaign. *Annu Dept Antiquities Jordan* 47:321–333
- Rosen SA (2000) The decline of desert agriculture: a view from the classical period Negev. In: Gilbertson D, Barker G (eds) *The archaeology of drylands: living at the margin*. Routledge, London, pp 45–62
- Schaefer J (1986) An umayyad potter's complex in the North Theatre, Jerash. In: Zayadine F (ed) *Jerash Archaeological Project 1981–1983 I*. The Department of Antiquities of Jordan, Amman, pp 411–459
- Schick R (1998) Palestine in the early Islamic period: luxuriant legacy. *Near Eastern Archaeol* 61 (2):74–108
- Tite MS, Kilikoglou V (2002) Do we understand cooking pots and is there an ideal cooking pot? In: Kilikoglou V, Hein A, Maniatis Y (eds) *Modern trends in scientific studies of ancient ceramics (BAR International Series 1011)*. Archaeopress, Oxford, pp 1–8
- Villeneuve F (1990) The pottery from the oil-factory at Khirbet edh-Dharih (2nd Century A.D.), A Contribution to the Study of the Material Culture of the Nabataens. *ARAM* 2(1&2):367–384
- Walmsley A (1992) The social and economic regime at Fihl (Pella) and neighbouring centres, between the 7th and 9th Centuries. In: Cavinet P, Rey-Coquais J-P (eds) *La Syrie de Byzance a l'Islam VIIe–VIIIe Siècles*. Institute Francais de Damas, Damas, pp 249–261
- Whitcomb D (1995) The Misr of Ayla: new evidence for the early Islamic city. *Studies Hist Archaeol Jordan* 5:277–288

Technological Features of Colonial Glazed Pottery from el Convento de Santo Domingo (Antigua, Guatemala). Similarities and Differences Between Colonial and Spanish pottery

J.G. Iñáñez and R.J. Speakman

1 The Convent of Santo Domingo (Antigua, Guatemala)

According to historic documentation, production of majolica at Santiago de Guatemala began no later than 40 years after the foundation of the city in 1543. In terms of majolica production and quality, we can consider the seventeenth century as the high point for majolica production in Antigua. Historic documents reflect the existence of more than 16 majolica masters in the city, who produced Guatemalan majolica pottery that is typified by black-on-white patterns, with green, yellow, and/or blue decorative elements (Luján 1975). Although the first priests of the Dominican order arrived in Antigua in 1559, the convent of Santo Domingo was not built until the mid-seventeenth century. The convent, which was home to more than 80 priests, was recognized as one of the most significant religious centers in Guatemala at that time, and consequently a significant number of majolica tiles, plates and pots were used in its construction and in everyday-life. Unfortunately, the convent was adversely impacted by earthquakes in 1773; the resulting structural damage forced the Dominicans to abandon the site and move to Nueva Guatemala de Asunción, where the capital of the former Capitanía General de Guatemala had moved to in 1776.

2 Goals and Methodology

The main objective of this work is the archaeometric characterization of colonial glazed pottery from the seventeenth century found in the archaeological excavations conducted at the site of the convent of Santo Domingo, both for provenancing issues and for technological features assessment. In order to achieve our aims, 7 majolica sherds out of a sample of 16 ceramic sherds were selected and their glazes

J.G. Iñáñez (✉) and R.J. Speakman

Museum Conservation Institute, Smithsonian Institution, 4210 Silver Hill Road, Suitland, MD 20746, USA

e-mail: inanezj@si.edu

studied by means of laser ablation inductively coupled plasma mass spectrometry (LA-ICP-MS) and scanning electron microscopy (SEM).

The instrumentation used in this analysis was a Perkin Elmer Elan 6000 inductively coupled plasma-mass spectrometer (ICP-MS). A Cetac LSX-200 Plus Nd:YAG 266 nm laser was used for the direct introduction of solid samples to the ICP. Ablations consisted of patterns of parallel lines, conducted twice in order to remove surface contamination; analysis of the actual sample matrix occurred during the second pass of the laser over the ablation area. For the pre-ablation, laser was operated at 20 Hz using a spot size of 100 μm at a speed of 100 $\mu\text{m/s}$. The second ablation was performed at 5 Hz using a spot size of 25 μm at a speed of 30 $\mu\text{m/s}$. Twenty scans were made for each of the isotopes measured. Each sample was analyzed for Ag, Al, As, Au, Ba, Bi, Ca, Cd, Co, Cr, Cu, Fe, Hg, In, K, Mg, Mn, Na, Ni, P, Pb, Rb, Sb, Si, Sn, Sr, Th, Ti, U, Zn, and Zr. The normalization approach used is modified from that suggested by Gratuze and others (Gratuze 1999; Neff 2003; Speakman and Neff 2005). Data generated from the analyses, expressed as counts per second, were referred to an internal standard (in this case Al) to normalize for different count rates between samples and standards. Quantitative data were then obtained by comparing the normalized signal in the unknown samples to the normalized signals for standard reference materials SRM612, SRM621, and Brill Glasses A, B, C, and D. Because of low analytical precision for As, Au, Bi, Cd, Hg, Ni, P, Sb, and Zn these elements were removed from consideration during the statistical treatment of the data. Because our focus is on the white glazed areas, data for Co and Mn were not used, since they are the main components of blue and black decorations on Spanish ceramics, and likely would distort the statistical treatment. To achieve a better understanding of the technological features of the Guatemalan colonial pottery, these latter sherds were compared with a sample set of 24 ceramics from Spain: Talavera de la Reina (4), Puente del Arzobispo (7), and Seville (13). Statistical treatment in this work was performed using the Aitchison's procedures for dealing with compositional data (Aitchison 1986; Aitchison et al. 2000).

3 Chemical Characterization

Principal Component analysis was performed to explore the chemical differences between the Guatemalan glazes and the Spanish productions. The first five principal components account for more than 92% of the cumulative variation in the dataset (Fig. 1).

Examination of the LA-ICP-MS data generated for the white glazes reveals four groups that correspond to archaeological provenance – Santo Domingo (SDM), Seville, Talavera, and Puente (see Iñáñez 2007 for additional information on Spanish ceramics and deeper discussion, available on line at <http://www.tdx.cat/TDX-0205107-115739>), and one individual not matching any reference group (Fig. 1).

Thus far, chemical data indicates the use of different PbO, alkali, and SiO₂ proportions by potters in Guatemala to make the glazed coating when compared with the Spanish productions. Guatemalan majolica glaze generally shows higher

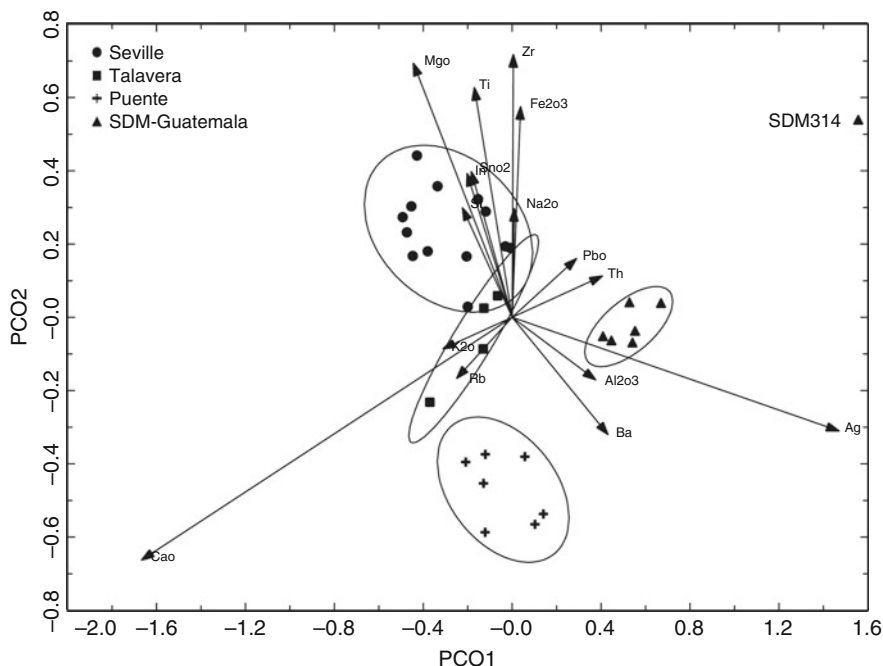


Fig. 1 Plot of the first two components according to the Principal Components Analysis using logarithm ratios and SiO₂ as divisor. Plot shows the three different Spanish compositional groups and the Compositional Group of Convento de Santo Domingo (SDM), Guatemala. Ellipses represent a confidence interval of 90%

PbO and lower SiO₂ and K₂O concentrations. Moreover, higher Ag also is detected amongst the Guatemalan colonial pottery, possibly as a result of the lead and silver ore processing. Silver is therefore a discriminating element between Spanish and Guatemalan productions. Seemingly, the amount of SnO₂ used for opacifying the glazed coating might point out some differences between the Spanish and Guatemalan pottery (Table 1).

However, significant differences on the chemical composition of sample SDM314 – mainly on CaO, SiO₂, and PbO contents – may indicate a different glaze recipe or, perhaps, even a different production. Therefore, SDM314 should remain labelled as unknown until future studies might reveal the existence of multiple recipes and/or provenance groups in the ceramics from the Convento of Santo Domingo de Antigua.

4 Technological Characterization

Double firing is the most common firing process for majolica ware according to European majolica making tradition. SEM examination of the samples from Antigua shows that crystal growth at the interface matrix-glaze area is less than 10 μm. This finding supports a double firing process hypothesis (Fig. 2, left) given the very

Table 1 Mean and standard deviations calculated for the chemical compositions of the groups from Convento de Santo Domingo, Seville, Talavera, and Puente

	SDM Guatemala (n = 6)		Seville (n = 13)		Talavera (n = 4)		Puente (n = 7)		SDM314
	Average	St. dev.	Average	St. dev.	Average	St. dev.	Average	St. dev.	
Al ₂ O ₃ (%)	7.49	0.70	2.84	0.83	4.45	1.59	5.96	1.16	5.89
CaO (%)	0.29	0.16	2.06	0.87	2.58	1.54	3.01	0.85	n.d.
Fe ₂ O ₃ (%)	0.71	0.09	0.94	0.32	0.35	0.10	0.24	0.04	0.57
K ₂ O (%)	1.21	0.17	3.33	1.35	3.61	0.95	3.73	0.31	0.93
MgO (%)	0.17	0.04	0.85	0.33	0.49	0.29	0.13	0.04	0.11
Na ₂ O (%)	1.04	0.24	1.41	0.38	1.22	0.56	0.73	0.24	0.84
PbO (%)	42.91	4.83	32.20	8.82	23.76	7.37	26.91	8.40	53.70
SiO ₂ (%)	42.58	4.49	48.65	6.41	56.76	3.46	53.87	7.87	34.09
SnO ₂ (%)	3.28	0.72	6.61	2.29	5.82	2.90	0.35–12.01 ^a		3.62
Ag	88	31	0–15 ^a		2–9 ^a		6–55 ^a		158
Ba	603	82	180	82	388	93	537	101	494
Cu	32–2,142 ^a		54–2,334 ^a		250	48	41–518 ^a		338
In	64	14	141	49	141	55	73	32	70
Mn	597	61	58–1,286 ^a		165–355 ^a		97	53	535
Rb	57	5	139	71	151	11	202	23	43
Sr	61	7	138	60	109	36	68	22	45
Th	6	0	2	1	4	1	2	1	5
Ti	835	86	2,051	556	1,211	577	396	67	677
Zr	41	2	80	47	29	6	15	4	57

All values are expressed as ppm ($\mu\text{g g}^{-1}$) except those expressed as oxide weight %

n.d. element not determined

^aMinimum and maximum value

low interaction between glaze coat and paste, in agreement with relevant literature (Molera et al. 1997; Tite et al. 1998).

Moreover, Guatemalan glaze coating averages a thickness around 250 μm , which might be considered as a “typical” thickness for those productions. Although some specimens from Seville and Talavera also studied by SEM showed differences in their glaze coating thickness, most of the ceramics from the Spanish production centers exhibit glaze coating ranging from 150 to 300 μm (Iñáñez 2007).

Compositions of pigments composing the chromatic decoration applied on the white opaque glaze also have been characterized. Interestingly, the black decoration is not made from Mn, as is common for most Medieval and Renaissance majolica produced in Spain. In contrast, black decoration on Guatemalan-produced majolica is made of a Fe-based compound (Fig. 2, right). Identification of the specific compound is ongoing.

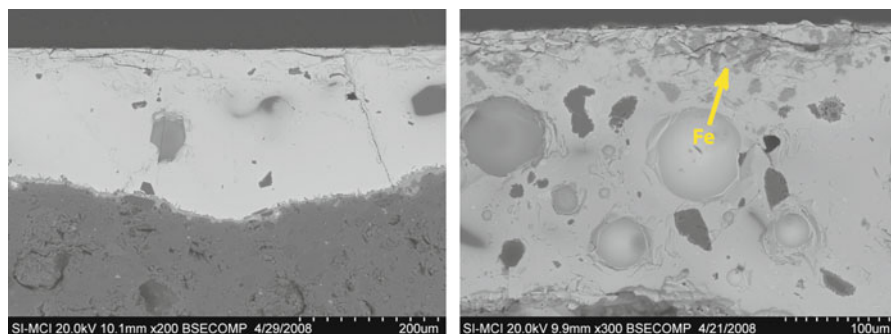


Fig. 2 *Left* SEM-backscattered electron microphotography of the white area of sample SDM314 showing the interface glaze-matrix at 200 \times . *Right* SEM-backscattered microphotography of sample SDM301 of the black pigment area at 300 \times with indication of Fe-particles

5 Conclusions

Differentiation of Spanish colonial from Spanish majolica might be possible through the analysis of glaze composition. Additionally, Ag concentrations on lead-tin glazes may be linked to a Guatemalan origin, perhaps related to the lead ores, or to the silver extraction technology during that period in the Americas; however more in depth studies must be undertaken. Although Guatemalan majolica production is apparently similar to that of Spanish majolica, some differences can be highlighted, such as the differential use of PbO, SnO₂, and SiO₂ in their glazing technology. Furthermore, the fact that ancient craftsmen used a Fe-based compound for producing black decoration – which is in contrast with the Spanish tradition – might be related to a secular pottery-making tradition still in existence during the colonial period in Guatemala, revealing the existence of a new hybrid recipe. Future studies, with an increased number of samples, will determine more robustly the differences pointed out in this paper.

Acknowledgements Authors are indebted to James Blackman and Ronald L. Bishop for providing the samples analyzed in this study. In addition, Javier G. Iñáñez is also indebted to the Smithsonian Institution postdoctoral fellowship program, and to the IOF Marie Curie Program of the European Commission for their support. Authors are grateful to Dr. Isabella Memmi for her comments on this paper.

References

- Aitchison J (1986) The statistical analysis of compositional data: monographs on statistics and applied probability. Chapman and Hall, London
- Aitchison JA, Barcelo-Vidal C, Martin-Fernandez JA, Pawlowsky-Glahn V (2000) Logratio analysis and compositional distance. *Math Geol* 32(3):271–275

- Gratuze B (1999) Obsidian characterization by laser ablation ICP-MS and its application to prehistoric trade in the Mediterranean and the near East: sources and distribution of Obsidian within the Aegean and Anatolia. *J Archaeol Sci* 26(8):869–881
- Iñáñez JG (2007) *Caracterització arqueomètrica de la ceràmica vidrada decorada de la Baixa Edat Mitjana al Renaixement dels principals centres productors de la Península Ibèrica: Tesis Doctorals en Xarxa, v. 0205107-115739*, Universitat de Barcelona, Barcelona
- Luján L (1975) *Historia de la mayólica en Guatemala*. Instituto de Antropología e Historia, Ciudad de Guatemala
- Molera J, Vendrell-Saz M, García M, Pradell T (1997) Technology and colour development of hispano-moresque lead-glazed pottery. *Archaeometry* 39(1):23–39
- Neff H (2003) Analysis of Mesoamerican plumbate pottery surfaces by laser ablation-inductively coupled plasma-mass spectrometry (LA-ICP-MS). *J Archaeol Sci* 30(1):21–35
- Speakman RJ, Neff H (2005) *Laser ablation ICP-MS in Archaeological Research*. University of New Mexico Press, Albuquerque
- Tite MS, Freestone IC, Mason I, Molera J, Vendrell M, Wood N (1998) Lead glazes in antiquity – methods of production and reasons for use. *Archaeometry* 40(2):241–260

Applicability of Prompt Gamma Activation Analysis to Glass Archaeometry

Z. Kasztovszky and J. Kunicki-Goldfinger

1 Introduction and Objectives

Chemical (elemental and isotopic) analysis is a basic tool in provenance, as well as in conservation studies of historical glass. In addition to the widely applied Electron Probe Microanalysis (EPMA), X-ray Fluorescence Analysis (XRF) and Inductively Coupled Plasma Mass Spectrometry (ICP-MS), the less known Prompt Gamma Activation Analysis (PGAA) is a powerful method for investigating fragments of or entire glass objects. In 2004, we have initiated a research project with the purpose of investigating the elemental compositions of historical glass objects which were unearthed in Poland. PGAA and EPMA were applied for quantitative analysis of major components, as well as of some minor elements. The non-destructive feature of PGAA, as well as its very low ($0.3 \mu\text{g g}^{-1}$) detection limit for boron is highly valuable in the context of this project, as we already discussed in Kasztovszky et al. (2005). The boron concentration can provide important technological information for glass archaeometry. However, it is very difficult to detect trace element levels by the use of traditional non-destructive methods. In this respect, PGAA seems to be a complementary tool to the other analytical methods already well known and used in glass archaeometry.

Z. Kasztovszky (✉)

Institute of Isotopes, Hungarian Academy of Sciences, Konkoly Thege str. 29-33, 1121 Budapest, Hungary

e-mail: kzsolt@iki.kfki.hu

J. Kunicki-Goldfinger

Institute of Nuclear Chemistry and Technology, Dorodna 16, 03-195, Warsaw, Poland
and

School of History and Archaeology, Cardiff University, 10 3EU, Cardiff, UK

2 Investigated Objects

In two series of investigations, 44 historical glass fragments were examined (Table 1). Most of the analysed objects originated from the post-medieval period (typically from the sixteenth or seventeenth centuries). Only objects nos. 1, 4–9, 23 and 24 were from the eighteenth century, and there were two other single objects from different periods, one medieval (no. 21), and one from the nineteenth century (no. 22). Most of them were excavated from the cesspits unearthed during the archaeological works carried out in the area of the Old Town in Elbląg (Poland); two pieces (nos. 1, 20) were found in the Old Town in Poznań (Poland), and three others (nos. 21–23) belong to private collections: one medieval piece of stained glass, one nineteenth century example of stained glass and one engraved plate glass, respectively. One eighteenth century bottle (no. 24) was found at a Baltic Sea underwater site. The objects mostly represent *façon-de-Venise* (nos. 2, 3, 11–20, 25–44) or Baroque style vessels (nos. 1, 4–9). However, a few examples of various plate glass pieces (nos. 21–23), one example of Roemer (no. 10), and one fragment of an ordinary container bottle (24) were also included in the project. Most of them were white, more or less tinted. Only a few fragments were coloured: nos. 21 and 24 were green, no. 22 was amber and no. 20 was blue. Additionally, some glass reference materials – SU 4001, 4002 and 4003; Corning B, C, D; NIST 610, 612 and 614 – have also been analysed.

3 Experimental

The PGAA measurements were carried out at the external cold (20 K) neutron beam of the 10 MW Budapest Research Reactor. The beam intensity was $5 \times 10^7 \text{ cm}^{-2}\text{s}^{-1}$. The objects were placed into a sample holder chamber which can be evacuated. The maximum applied beam size was $2 \times 2 \text{ cm}^2$, but the irradiated area can be reduced to a few mm^2 by ${}^6\text{Li}$ collimators. Since the neutrons can penetrate deeper layers of the object, average concentrations for the entire irradiated volume can be obtained. It is not necessary to take sub-samples from the objects, as any kind of sample can be placed into the beam. Furthermore, the induced radioactive products decay fast, and thus the method can be considered non-destructive. More details can be found in Révay et al. (2004).

Prompt Gamma Activation Analysis is based on the detection of prompt- and decay γ -photons, emitted in the (n,γ) nuclear reaction. The γ -spectra from the bulk material are collected by an HPGe-BGO detector system. The spectrum fit is performed with the “HYPERMET PC” software. The elements are identified by their characteristic γ -energies, while the quantitative analysis is carried out according to peak intensities. The standardisation is based on our prompt k0-library, as described in Révay et al. (2001).

In principle, every chemical element can be detected, although with different sensitivities. The sensitivities depend on the neutron capture cross-sections. The

Table 1 Elemental composition of the analysed glass, measured with PGAA

No.	Inv. No. ^a	Object ^b	Style/ dating ^c	SiO ₂	Al ₂ O ₃	Na ₂ O	K ₂ O	CaO	MgO	P ₂ O ₅	Cl	H ₂ O	B ₂ O ₃	TiO ₂	MnO	Fe ₂ O ₃	CoO	CuO	As ₂ O ₃	BaO	PbO	SnO ₂	SO ₃
1	NMP/xx	Beaker	D.L.	1.5	0.6	0.03	0.2	1.4	1.2	1.0	0.01	0.02	0.0002	0.01	0.05	0.1	0.005	0.1	0.1	0.5	0.3	2.0	0.1
2	EM/XXXI/3661	Baroque	Baroque	78.5	<	1.19	13.5	6.40	<	<	0.16	<	0.0000	<	<	<	<	<	0.2	<	<	<	<
		Beaker	fdV	63.7	1.60	14.2	5.32	8.90	3.8	<	0.80	0.13	0.0196	0.13	0.84	0.66	0.01	<	<	<	<	<	<
3	EM/XXXI/1900	Goblet	fdV	69.3	<	5.06	19.5	3.10	<	<	0.27	0.70	0.0601	0.06	0.84	0.27	<	.	<	<	<	<	<
4	EM/IIIG/6894	Goblet	Baroque	78.1	<	<	13.6	7.10	<	<	0.09	0.05	0.0160	0.01	0.27	0.13	<	<	0.8	<	<	<	<
5	EM/XXII/10377	Goblet	Baroque	77.5	<	14.1	0.34	6.80	<	<	0.14	0.03	0.0000	0.04	0.12	0.05	<	<	0.2	<	0.7	<	<
6	EM/XXX/1730	Goblet	Baroque	69.2	<	0.79	19.0	10.7	<	<	0.10	0.06	0.0453	0.04	0.14	<	<	<	<	<	<	<	<
7	EM/XXX/2432	Beaker	Baroque	75.7	<	<	13.8	9.90	<	<	0.22	0.10	0.0197	0.02	0.12	0.12	<	<	0.2	<	<	<	<
8	EM/XXX/2758	Goblet	Baroque	76.5	<	<	14.1	8.20	<	<	0.11	0.10	0.0223	0.03	0.19	0.00	<	<	0.8	<	<	<	<
9	EM/XXX/2017	Goblet	Baroque	71.4	<	<	18.5	9.30	<	<	0.07	0.11	0.0318	0.01	0.43	0.22	<	<	<	<	<	<	<
10	EM/XXIV/359	Roemer	Post-me- dieval	65.5	<	2.15	5.71	22.2	3.0	<	0.33	0.05	0.0465	0.11	0.37	0.43	0.01	<	<	<	<	<	<
11	EM/XXX/2866	Goblet	fdV	62.4	<	<	20.3	13.3	3.0	<	0.15	0.07	0.0465	0.05	0.78	<	<	<	<	<	<	<	<
12	EM/XXIII/5176	Goblet	fdV	61.8	<	4.77	23.9	8.30	<	<	0.23	0.13	0.0598	0.16	0.39	0.20	0.01	<	<	<	<	<	<
13	EM/XXII/476	Goblet	fdV	61.3	<	<	11.4	16.7	2.7	2.6	0.04	0.02	0.0437	0.08	1.02	0.28	0.01	0.02	<	3.8	<	<	<
14	EM/5301	Goblet(?)	fdV	64.9	<	1.97	17.1	14.0	<	<	0.30	<	0.0432	0.06	0.59	<	<	<	<	<	<	<	<
15	EM/XX/4833	Goblet	fdV	63.8	<	1.77	15.1	15.1	3.0	<	0.28	<	0.0459	0.07	0.73	<	0.01	<	<	<	<	<	<
16	EM/XXII/590	Goblet	fdV	64.5	<	1.35	17.5	12.5	3.0	<	0.23	0.09	0.0334	0.06	0.53	0.16	<	<	<	<	<	<	<
17	EM/XXX/1813	Goblet	fdV	66.9	1.80	2.53	8.80	16.5	3.3	<	0.55	0.06	0.0520	0.10	0.87	0.31	0.01	<	<	<	<	<	<

(continued)

36	EM/XXII/ 7181	Goblet	fdV	58.7	1.92	0.29	10.8	16.8	2.8	1.7	0.01	0.10	0.0406	0.08	0.81	0.27	0.01	<	4.8	0.6	<	0.30
37	EM/XXII/ 6085	Beaker(?)	fdV	56.2	1.39	0.23	11.7	20.7	3.5	3.3	0.05	0.07	0.0504	0.07	1.04	0.33	<	<	1.1	<	<	0.38
38	EM/XXII/ 6071	Goblet	fdV	56.3	1.64	0.11	16.7	16.0	2.7	2.9	0.04	0.15	0.0397	0.08	1.32	0.41	<	<	0.9	0.5	<	<
39	EM/XXII/ 8788	Goblet	fdV	52.2	2.82	0.50	7.57	26.4	3.9	2.6	0.01	0.09	0.0717	0.18	1.71	0.65	0.02	<	0.1	0.8	<	0.34
40	EM/XXII/ 10053	Goblet	fdV	59.6	0.93	0.07	17.0	16.1	2.9	<	0.04	0.06	0.0530	0.07	0.90	0.21	<	<	0.6	<	<	0.30
41	EM/XXII/ 10839	Goblet	fdV	63.9	2.06	2.40	9.86	17.1	2.6	<	0.43	0.18	0.0417	0.11	0.86	0.31	0.01	<	<	<	<	<
42	EM/XXII/ 10268	Goblet	fdV	60.3	1.50	0.08	10.8	19.1	3.0	2.1	0.02	0.06	0.0439	0.09	1.30	0.31	<	<	0.8	0.3	<	<
43	EM/XXII/ 5384	Goblet	fdV	59.0	1.77	0.39	11.3	18.9	3.3	2.6	0.09	0.09	0.0458	0.12	1.12	0.48	<	<	0.6	<	<	<
44	EM/XXII/ 591	Goblet	fdV	57.4	0.97	0.26	22.7	12.5	2.5	<	0.05	0.07	0.0406	0.04	0.69	0.12	<	<	0.6	<	<	0.30

The concentration data are expressed in wt% and normalized to 100%

^aEM-Museum in Elblag, NMP-National Museum in Poznan, PMM-Polish Maritime Museum, PO-private owner, xx-without inventory number

^bAll pieces colourless (white), unless otherwise noted

^cfdV-façon de Venise (16th–17th centuries), Baroque-eighteenth century

best elements in terms of the detection limit are B, Cd, Sm and Gd; the worst are C, N, O, F, Sn and Pb. The detection limits can be lowered by increasing the acquisition time. In general, for glass, we can quantify most major components and some trace elements by using this method.

4 Results and Discussion

Using PGAA, we were able to quantify the concentrations of Si, Na, K, Ca, Mg and H, as well as the traces of B, Cl, Co, Ti, Fe, Mn, Sm and Gd in most cases. Occasionally, Al, P, S, Co, Cu, As, Ba, Sn and Pb were also identified. However, these elements were below our detection limits in most samples. On a set of samples (both historical ones and standards), we have checked the reliability of PGAA by comparing it with EPMA. As we have previously shown in Kasztovszky et al. (2005), the agreement between PGAA and EPMA results is good. Nevertheless, the elevated PGAA sensitivities for H, B, Cl, Sm or Gd represent an advantage of this method. PGAA results regarding the chemical composition of the analysed glasses are shown in Table 1. The components are given in oxide forms and the concentrations are in wt%.

Figure 1 shows a possible manner of using PGAA results for the technological interpretation of the examined objects. Due to the limited space available for this paper, which is aimed at supplying more information about the method than about the objects, it is impossible to provide here a final technological interpretation.

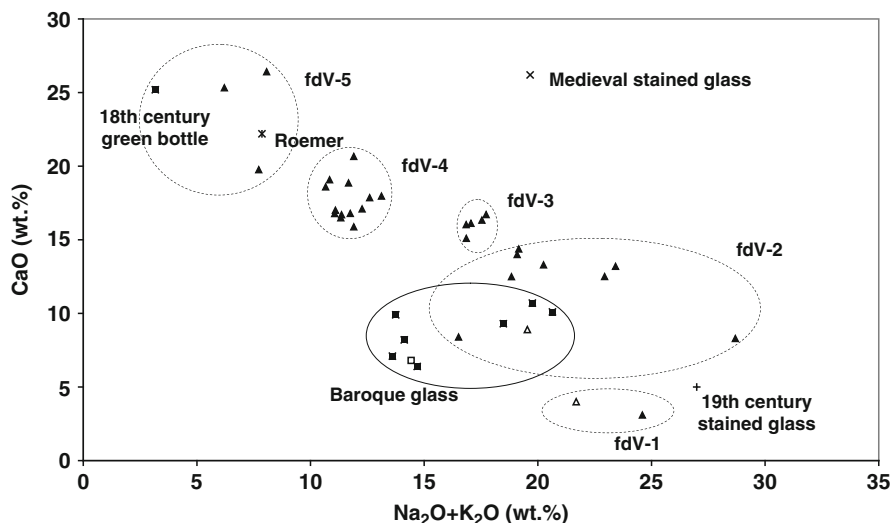


Fig. 1 Plot scatter of CaO versus the sum of alkaline oxides. The groups distinguished among the analysed glasses are shown. FdV vessels are marked as *triangles* and the samples of eighteenth century glass as *squares* (in both cases, a white background means that the glass was found to be sodic). A few single items, such as the medieval and the nineteenth century stained glass, as well as the one analysed Roemer, are distinguished by other symbols

However, on this plot of CaO against the sum of alkali oxides we can distinguish five groups of the *façon-de-Venise* (fdV) vessels. Most of them are potassium glasses; however, two of them were made of sodium glass. Moreover, a group of Baroque glasses have been distinguished, including one sodium and two potassium glasses. It was also possible to separate the following single items: the eighteenth century green bottle, the nineteenth century object and the medieval pieces of stained glass. The only Roemer type vessel analysed appeared to fall into the group fdV-5. However, we must remember that this grouping constitutes only the first step of the final interpretation of the glasses and does not necessarily indicate a real differentiation of various glassmaking technologies.

In the present paper, we wanted to show that PGAA may be successfully applied in glass archaeometry as a fully eligible method. The discussion of the possible origin and technology of these glasses, along with their typological study, constitutes a subject of forthcoming studies.

The real benefit of the method resides in the possibility to analyse boron even in large objects without taking any samples. For the present group of analysed items, the boron concentrations of Baroque glasses, as well as of the single nineteenth century item, was found to be much lower (0.023 wt% on average) than of the majority of fdV vessels (0.047 wt% on average). Among fdV vessels, two high sodium glasses have similar boron concentrations to those of Baroque glasses. This aspect seems to indicate that these two glasses have a different origin from the rest of the fdV glasses.

5 Conclusions

PGAA proved to be an efficient non-destructive analytical method valuable for glass archaeometry. It seems to be particularly useful in cases when no sample can be taken from the object. PGAA provides bulk composition results, thus representing quite a unique procedure as compared to other non-destructive methods, which are mostly surface methods. PGAA is also unique in the determination of low levels of B and in H detection.

Acknowledgement PGAA experiments have been carried out at the Budapest Neutron Centre, within the context of the EU FP6 framework; contract nr. RII3-CT-2003-505925. The authors are grateful to Grażyna Nawrońska and Piotr Wawrzyniak for their invaluable help in collecting the samples. The authors also express their gratitude to the Boards of different museums, which have provided us with the objects available for the examination. These were the Archaeological-Historical Museum in Elbląg, the National Museum in Poznań, and the Polish Maritime Museum in Gdańsk (all of them in Poland).

References

- Kasztovszky ZS., Kunicki-Goldfinger JJ, Dzierżanowski P, Nawrońska G, Wawrzyniak P (2005) PGAA and EPMA as complementary non-destructive methods for analysis of boron content in historical glass. 8th International conference on non-destructive investigations and microanalysis

- for the diagnostics and conservation of the cultural and environmental heritage, Lecce, Italy, 15–19 May 2005. Proceedings published on CD-ROM
- Révay ZS, Molnár GL, Belgya T, Zs K, Firestone RB (2001) A new gamma-ray spectrum catalog and library for PGAA. *J Radioanal Nucl Chem* 248(2):395–399
- Révay ZS, Belgya T, Zs K, Weil JL, Molnár GL (2004) Cold neutron PGAA facility at Budapest. *Nucl Instrum Methods Phys Res B* 213:385–388

Colorants and Their Provenance of a Late Medieval Glass Goblet Found in Eger (Hungary)

A. Kocsonya, A. Váradi, I. Fórizs, I. Kovács, Z. Kasztovszky,
and Z. Szókefalvi-Nagy

1 Archaeological and Art-Historical Introduction

An interesting and unique glass drinking cup can be found in the Medieval Archaeological Collection of the István Dobó Castle Museum in Eger, originating from Károly Kozák's (OMF – National Inspectorate of Historic Monuments¹) excavations at Eger Castle, from a site located to the south of the Romanesque Cathedral. The find came to light on October 14, 1977.

The bowl of the glass was reconstructed from its fragments. A thin rib runs around the top third of the conical upper part of the fragile pale blue glass. Above this rib there are three handles on which green rings are threaded, one on each handle. Since the bottom of the glass was missing, a reappraisal of the object appeared necessary and led to the assumption that the glass had a foot, thus giving it the form of a goblet (Fig. 1).

Formerly this cup was recorded as an “Antique Roman glass”. However, no Roman glass drinking cups of a conical type known so far take the form of the Eger glass, but interesting parallels can be found among the sixteenth and seventeenth century glassware and its formal imitators. Two dominant styles of glass-making are known in medieval Europe: the Forest glass (or *Waldglas*, in German) and Venetian glass. The former type was produced in North-Western Europe made in workshops known as “glass-houses”, in forest areas, while Venetian glasses were made

¹Since 2001: National Office of Cultural Heritage (KÖH) <http://www.koh.hu>

A. Kocsonya (✉), I. Kovács and Z. Szókefalvi-Nagy
KFKI Research Institute for Particle and Nuclear Physics of the Hungarian Academy of Sciences,
Budapest, Hungary
e-mail: kocksonya@rmki.kfki.hu

A. Váradi
István Dobó Castle Museum, Eger, Hungary

I. Fórizs
Institute for Geochemical Research of the Hungarian Academy of Sciences, Budapest, Hungary

Z. Kasztovszky
Institute of Isotopes of the Hungarian Academy of Sciences, Budapest, Hungary

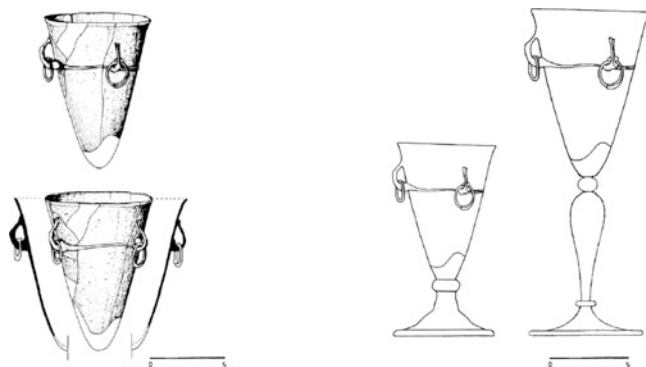


Fig. 1 The Eger glass cup and assumptions about its stem

in Venice, primarily on the island of Murano. The Venetian style glass-making soon became widely-known and it had a considerable effect on the glass manufacturing of several other countries, significantly influencing regional traditions.

Both Venetian type glasses and formal imitations made of *Waldglas* can be found among the analogous artefacts from the sixteenth to seventeenth century, which form two relatively uniform groups. The Murano style Ringglas (Kämpfer and Beyer 1966) products are either completely colourless, or the coloured and colourless parts are alternated, while the cups of the continental glasses are painted. The Eger drinking cup does not fit into any of these groups. It is neither colourless like the Venetian ones, nor painted like the *Waldglas* products.

Thus, our glass is a curiosity among the *Ringglas* products, making it difficult to assign it to any known glass manufacturer. In order to verify this hypothesis concerning the age and the origin of the cup, some instrumental analyses of the find were carried out.

2 Materials of the Ancient and Medieval European Glassware

Whereas Roman and earlier glasses (of Si/Na/Ca composition) were rather uniform over a wide area and period of time, medieval glasses (of Si/K/Ca composition) are characterized by a variety of compositions. Analysis of ancient Roman glasses have shown that natural soda was used exclusively as the flux in glass production, mainly in the form of natron. At the end of the first millennium AD, as the supply of natural soda was diminishing, it was replaced by plant ash and wood ash. The latter type was the one more frequently used outside of Venetian glass making. Therefore the chemical composition of wood ash glasses presents a very wide variation, and thus the analysis of glasses can provide meaningful information about the origin and age of the object.

3 Instrumental Analysis of the Goblet by EPMA

The first instrumental analysis of the object was performed by Electron Probe Microanalysis (Tóth et al. 2001). The purpose of this measurement was to determine the composition of the glass.

Small grains were removed from the surface of the bowl and the rings as well. Although more grains were taken from the bowl, only one of them turned out to be reliable; unfortunately, the other grains came from the glue, which was used in the course of the restoration. The removed grains were glued onto an aluminium block which was previously covered by an electrically conducting layer.

The electron probe analysis revealed that the studied goblet is made of a wood ash-silica glass, a composition which is typical of medieval glass (Table 1.).

The compositions of the different points of the green rings are rather homogeneous the green rings contain significant amount (~1.5%) of CuO. Depending on its oxidation state and its substitution in the octahedral or tetrahedral sites, copper yields green or blue colour. One can assume that the green colour of the rings is caused by the Cu content.

Comparison of its chemical composition with other published data (Wedepohl 2000) support the hypothesis of a late medieval origin. We can conclude that the object is a continental, Venetian-inspired *Ringglas* type product, presumably made in the fifteenth to sixteenth century.

The sensitivity of EPMA, however, was not sufficient for providing direct information about the blue colorant of the body.

4 External Beam PIXE Analysis: What Colorants Were Applied?

Clear colours of glass products were often produced by deliberate addition of metal oxides. We assumed that the blue colorant of the goblet was cobalt, but its concentration was below the detection limit of EPMA.

Further analyses of the colorants were performed by external beam PIXE (Particle Induced X-ray Emission) spectrometry (Gyódi et al. 1999), a method having higher elemental sensitivities than the electron microprobe. The external

Table 1 Results of the EPMA analysis of the Eger goblet and some similar objects

Glass type	SiO ₂	K ₂ O	CaO	Na ₂ O	MgO	Al ₂ O ₃	P ₂ O ₅	Cl	MnO	FeO	CuO	Sum
Green ring P1	62.8	13.5	15.3	0.9	2.6	1.1	1.1	0.1	0.5	0.4	1.8	100.3
Green ring P2	62.6	13.2	15.0	0.8	2.3	1.3	1.0	0.2	0.5	0.4	1.2	98.5
Green ring P3	62.6	13.3	15.3	1.1	2.3	1.2	1.0	0.3	0.7	0.4	1.6	99.0
Blue body	63.2	12.6	15.3	1.8	2.3	1.5	0.8	0.3	0.4	0.6	–	98.8
Sopron, 16th c.	61.8	11.7	17.1	1.9	2.8	1.5	2.2		0.9	0.9		100.7
Buda, 15th c.	67.4	11.9	15.0	0.3	2.2	1.4	1.0		0.4	0.3		99.8

Table 2 Metal concentrations in different parts of the goblet measured by external-beam PIXE

Position	Mn	Fe	Co	Cu
Green rings	0.3%	0.2%	<0.005%	0.40%
Blue parts	0.4%	0.5%	0.04%	0.01%

beam version of PIXE is especially suitable for non-destructive analyses of art and archaeological objects, because even large artefacts can be directly analysed without any sampling or sample preparation. Both the external beam and conventional PIXE analyses were performed at the 5 MV Van de Graaff accelerator of the KFKI Research Institute for Particle and Nuclear Physics.

The composition was measured at 14 positions: 12 points on the blue body and two points on the green rings. Since the diameter of the beam was approximately 2 mm, the analysed areas were similar.

The compositions of both the blue body and the green rings proved to be rather homogeneous. The measured amount of copper in the green rings is in agreement with the previous EPMA results. In the blue parts of the goblet significant amount of cobalt is detected, while no cobalt is detected in the green rings. This result shows that the blue colorant of the body of the goblet body is cobalt (Table 2). It can be also seen that an approximately ten times lower Co concentration than that of Cu giving the rings their green colour is sufficient for producing the blue colour of the body.

5 Conventional PIXE Analysis: What Trace Elements Are Detectable in the Colorant?

Raw materials often contain a great variety of impurities, which may be characteristic of their origins. Thus the careful analysis of these impurities can indicate the raw materials' origin and development processes.

Three cobalt-mines are known in medieval Europe (Gratuze et al. 1998). The ores from these mines are characterized by different chemical association (Table 3):

The characteristic trace elements present in cobalt ores may enable us to identify the provenance of the ore; as such our next goal was to determine the origin of the cobalt ore used as blue colorant.

The concentration of cobalt in the glass is rather low, only 0.04%, and therefore the concentrations of the trace elements associated with it may be even lower. Since the detection limits of the external beam PIXE facility were not sufficient for determining these trace elements, this called for the application of a more sensitive analytical method. The conventional PIXE method (Johansson and Johansson 1976) has significantly lower detection limits; however the size of the samples that can be analysed with this method is limited. Fortunately a small fragment of the goblet which was not yet attached back to the artefact in the course of the restoration was available. This fragment was just appropriate in size to fit into the measuring chamber.

The elements detected in the blue fragment show significant similarity with those present in the third cobalt ore in Table 3 (Fig. 2, Table 4). All trace elements in this ore were detected, while some trace elements associated with the other two ores are missing. This result indicates that the cobalt ore used as a blue colorant originates most probably from the mine of Schneeberg in the German Erzgebirge.

The significant amount of arsenic indicates that it may not only indicate an impurity in the cobalt ore, but may have been used in the composition of the glass, since As were also applied as decolouring agent (Ryan and Sanderson 1963). The overdose of As may have produced the opalescent character of the glass, another feature of this artefact that makes it a curiosity among similar objects.

Table 3 Known cobalt ores and their chemical associations in the medieval Europe

Chemical association	Mine
Co–Zn–Pb–In	Freiberg(?), Erzgebirge
Co–Ni–Mo	Unknown location, Erzgebirge
Co–As–Ni–Bi–Mo–W–U	Schneeberg, Erzgebirge

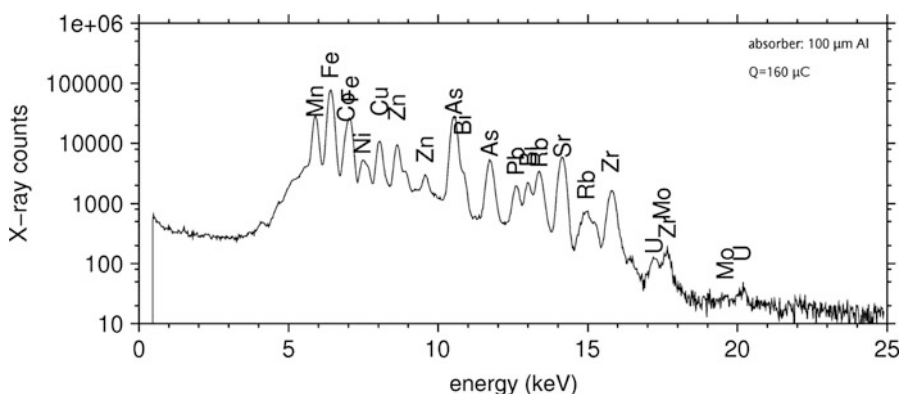


Fig. 2 PIXE spectrum of the blue fragment

Table 4 Trace element concentrations and limits of detection (LOD) in the blue body of the goblet measured by conventional PIXE

Element Z Symb.	Conc. (ppm)	LOD (ppm)	Element Z Symb.	Conc. (ppm)	LOD (ppm)
25 Mn	2,148.5 ± 13.9	8.7	37 Rb	275.4 ± 3.9	3.1
26 Fe	3,754.3 ± 20.3	14.5	38 Sr	686.1 ± 5.6	1.1
27 Co	359.2 ± 9.5	16.3	40 Zr	119.7 ± 5.7	12.1
28 Ni	105.6 ± 2.1	2.4	42 Mo	4.4 ± 2.8	3.9
29 Cu	275.6 ± 2.3	1.6	82 Pb	261.7 ± 34.9	102.3
30 Zn	225.1 ± 2.1	1.6	83 Bi	320.4 ± 11.3	7.7
33 As	1,045.9 ± 67.4	5.7	92 U	55.8 ± 8.5	11.5

6 Bulk Analysis by PGAA

The X-ray emission spectrometry methods applied thus far provide information about an area of approximately $\sim 50 \mu\text{m}$ thickness near the surface layer. To obtain information about deeper areas a further examination by a bulk analysis method was necessary.

Prompt Gamma Activation Analysis (PGAA) is a widely applicable technique for multi-elemental analyses of very different samples (Kasztovszky et al. 2005). The method is non-destructive, any type of sample can be placed into the beam. In principle, every chemical element can be detected, although at different sensitivities. The measurement was done at the $1 \cdot 10^8 \text{ cm}^{-2} \text{ s}^{-1}$ external cold (20 K) neutron beam of the 10 MW Budapest Research Reactor.

The measured composition (Table 5) is in good agreement with the PIXE and EPMA results. Such an agreement proves, that the sample is homogeneous in volume, since the composition measured in the bulk matter and in the layer near the surface are identical.

Furthermore, some other trace elements were also determined by the PGAA analysis: H, B, Nd, Sm, Gd.

7 Conclusions

While in its first description this object was identified as “Roman glass”, based on several archaeological analogies with Venetian glassware, the medieval origin of the goblet was subsequently assumed. Moreover drinking cups decorated with rings

Table 5 The composition of the blue fragment measured by PGAA

Z	El	Conc.
1	H	$350 \pm 11.2 \text{ ppm}$
5	B	$114.4 \pm 1.72 \text{ ppm}$
11	Na	$12,800 \pm 320 \text{ ppm}$
12	Mg	$12,000 \pm 840 \text{ ppm}$
13	Al	$6,000 \pm 600 \text{ ppm}$
14	SiO ₂	$64 \pm 0.64\%$
17	Cl	$2,000 \pm 600 \text{ ppm}$
19	K ₂ O	$13.5 \pm 0.28\%$
20	CaO	$16 \pm 0.58\%$
22	Ti	$500 \pm 20 \text{ ppm}$
25	MnO	$0.35 \pm 87.5\%$
26	Fe ₂ O ₃	$0.55 \pm 0.01\%$
27	Co	$400 \pm 12.8 \text{ ppm}$
28	Ni	$140 \pm 11.2 \text{ ppm}$
29	Cu	$320 \pm 35.2 \text{ ppm}$
33	As	$1,000 \pm 80 \text{ ppm}$
60	Nd	$60 \pm 7.2 \text{ ppm}$
62	Sm	$0.56 \pm 0.03 \text{ ppm}$
64	Gd	$0.8 \pm 0.06 \text{ ppm}$

made with *Waldglas* are also known in North-Western Europe. The primary purpose of the instrumental analyses described above was the verification of the assumption of medieval origin.

The material of the Eger glass goblet is similar to continental glasses, but, by alternating the blue and green colours, it imitates the Murano style. The object was shown to be a late medieval cup of a *Ringglas* type. The Eger glass goblet is a fine example of Venetian-inspired (material, form, colour, ornament) forest glass. Due to its opalescence, the goblet is not a perfect object, and therefore it was probably not an imported commercial product. The artefact was most probably a product of a Hungarian glass workshop that adopted the Venetian style and was active in a period from the sixteenth century until the first third of the seventeenth century. One can assume that the Eger glass goblet may be a product of a local glass workshop located close to Eger in the Bükk Mountains, where the *Waldglas* manufacturing techniques and the addition of decolouring agents were known, but the artefact also inspired by Venetian style *Ringglas* products. The cobalt used for the production of blue coloured glass probably originated from the mine of Schneeberg in the German Erzgebirge.

Four different types of instrumental analyses of the object were performed. The results of the different methods were in good agreement with each other. The complementary application of the different analytical methods provided more comprehensive information about the examined object.

References

- Gratuze B, Uzonyi I, Elekes Z, Kiss ÁZ, Mester E (1998) A study of Hungarian medieval glass compositions: Preliminary results. In: Proceedings of the 31st International Symposium on Archaeometry. Budapest, Hungary
- Gyódi I, Demeter I, Hollós-Nagy K, Kovács I, Szókefalvi-Nagy Z (1999) External-beam PIXE analysis of small sculptures. *Nucl Instrum Methods Phys Res B* 150:605–610
- Johansson SAE, Johansson TB (1976) Analytical application of particle induced X-ray emission. *Nucl Instrum Methods B* 137:473–516
- Kämpfer F, Beyer KG (1966) *Viertausend Jahre Glas*. Süddeutscher Verlag, München
- Kasztovszky ZS, Kunicki-Goldfinger JJ, Dzierzanowski P, Nawrołska G, Wawrzyniak P (2005) PGAA and EPMA as complementary non-destructive methods for analysis of boron content in historical glass (oral) 8th International conference on non-destructive investigations and micro-analysis for the diagnostics and conservation of the cultural and environmental heritage. Lecce, Italy, 15–19 May 2005. 12. 09. Proceedings published on CD-ROM
- Ryan JA, Sanderson JR (1963) Arsenic in glass. *Talanta* 10:127
- Tóth M, Bertóti I, Mohai M, Fórizs I, Vozil I (2001) Material analysis of the bronze statuette of Imhotep. *Bull Mus Hong B Arts* 95:35–44
- Wedepohl KH (2000) The change in composition of medieval glass types occurring in excavated fragments from Germany, *Annales du 14e Congrès de l'Association Internationale pour l'Histoire du Verre*, Italia, Venezia-Milano 1998; *AIHV. Lochem* 2000:253–257

***Gnathia* and Red-Figured Pottery from Apulia: The Continuity of a Production Technology**

A. Mangone L.C. Giannossa G. Colafemmina, R. Laviano V. Redavid, and A. Traini

1 Introduction

Samples of *Gnathia* pottery from Egnazia, one of the most important archaeological sites in Southern Italy (Cassano et al. 2007), were examined with different complementary techniques. The conventional name of “*Gnathia*” pottery refers to the black gloss ware, typical of Hellenistic Age Apulian production, which had a wide circulation throughout the Mediterranean basin (Webster 1968; Green 2001). Over-painted decorations (usually in white, yellow and red), incisions and ribbings characterise this ceramic class. Questions concerning the technological and functional relationships of *Gnathia* with red-figured pottery, the typological and chronological classification of samples, and the location of workshops are still unsolved. This lack of data is due to the methodology followed to date in studies and classifications of this type of pottery, based almost exclusively on stylistic criteria used to define the most valuable figured pottery.

Finds from Egnazia show an articulated typology of shapes in keeping with red-figured pottery and the use of peculiar morphologies of the class, such as objects used for pouring, mixing and drinking wine during the *symposium* – *hydria*, *oinochoe*, *epichysis*, *pelike*, kraters, bowls, *skyphos* and hemispherical cups. In contrast, the ornamentation has a craftmade dimension which makes it difficult to find an excellent artistic production, and the uniformity of decorative designs is proof of a tendency to schematize and standardize production. All of these aspects

A. Mangone (✉), L.C. Giannossa, G. Colafemmina, and A. Traini
Department of Chemistry, University of Bari, Via Orabona 4, Bari, Italy
e-mail: fabia@chimica.uniba.it

R. Laviano
Department of Geomineralogy, University of Bari, Via Orabona 4, Bari, Italy

V. Redavid
Department of the Science of Antiquity, University of Bari, Piazza Umberto, Bari, Italy



Fig. 1 An examined *Gnathia* pottery vase from Egnatia

emphasize the need for a substantial revision of the methodological approach formerly used for the study of *Gnathia* pottery.

The examined finds, dating essentially from a period between the second half of the fourth and the third century BC, originate from the “western necropolis”, one of the most important *extra moenia* necropoleis in the city, fundamental in the study of *Gnathia* pottery from chronological, social and ritual points of view. Decorative motifs include typical phytomorphic designs, such as vine and ivy branches, composed in repetitive schemes (Fig. 1), typical of the Middle and Late phases of production (Green 1976), and also less typical designs, such as the head of a woman among volutes and a rhomboidal grid over-painted in white.

Relatively little archaeometric analysis, directed exclusively to identifying the location of the production centres, has been carried out on *Gnathia* pottery. Only the chemical and sometimes mineralogical compositions of the ceramic bodies of a small number of fragments from different sites have been analysed to date (Prag et al. 1974; Hatcher et al. 1980; Jones 1986; Grave et al. 1997). Thus, these results cannot be considered representative for the entire production. No information about the technological process is currently available.

The aim of the present research is to define the technological aspects of this ceramic production and to confirm the close relationship existing between *Gnathia* and Apulian red-figured pottery from a technological point of view, not only from a morphological and decorative one (Lanza 2005).

2 Experimental

The fragments were examined with polarized-light Optical Microscopy (OM), Scanning Electron Microscopy (SEM) with Energy Dispersive Spectrometry (EDS), X-ray Diffraction (XRD) and High Resolution Magic Angle Spinning Nuclear Magnetic Resonance (CP-MAS NMR).

The orthoscopic analysis of mineralogical textures was performed with an optical microscope (Carl Zeiss) on polished thin sections. On the same sections, SEM analyses (EVO-50XVP (LEO)) and microanalyses (Oxford-Link EDS instrument equipped with a PENTAFET Si(Li) detector and with a 0.4 mm-thick Super Atmosphere Thin Window (SATW)) were carried out. The X-ray diffraction analysis was performed using a Philips X'Pert Pro X-Ray diffractometer (working conditions: CuK α Ni-filtered radiation, 40 kV, 40 mA, divergence slit 1°, anti-scatter slit 0.5°, receiving slit 0.2 mm, speed 0.5° in 2 θ per minute). CP-MAS NMR studies were carried out with a Varian Inova I400 spectrometer equipped with an AutoMAS Varian probe of 5 mm operating at 79.4 MHz for ^{29}Si and 104.2 MHz for ^{27}Al . The spinning rates were between 7 and 10 kHz, and the line broadenings were up to 30 Hz for broad-line spectra.

3 Results and Discussion

The ceramic bodies of the examined finds show a fine texture paste with remarkable amounts of micas, quartz, feldspar and iron oxides (Fig. 2a), which leads us to advance the hypothesis of a use of raw materials originating from alluvial or eluvial deposits (Cinquelpalmi et al. 2003), characterised by the presence of “*terra rossa*”, quartz and calcite due to superficial erosion.

Moreover, a comparison of the chemical and mineralogical characteristics of the ceramic bodies of *Gnathia* pottery artefacts originating from two different sites – Egnatia and Monte Sannace, another important site of Peucetia – demonstrates the use of different raw materials, compatible with the characteristics of clay deposits which can be found near the two sites, but of the same technological process. This confirms the hypothesis that different production centres sharing an in-depth technological knowledge of the same production process were distributed across the studied area. In fact, the coarse texture of the ceramic bodies, made up mainly of carbonate flakes, but also containing quartz and mica flakes, characterises the artefacts from Monte Sannace (Fig. 2b). This is compatible with the use of raw materials originating from “*argille subappennine*” deposits, characterised by the presence of abundant clay minerals (illite, smectite, chlorite and kaolinite), carbonates and lesser quantities of quartz, feldspars and micas (Dell’Anna and Laviano 1991).

In both cases, an engobe layer – 35–100 μm thick – is present on the ceramic body and underneath the black gloss, showing finer texture and larger quantities of

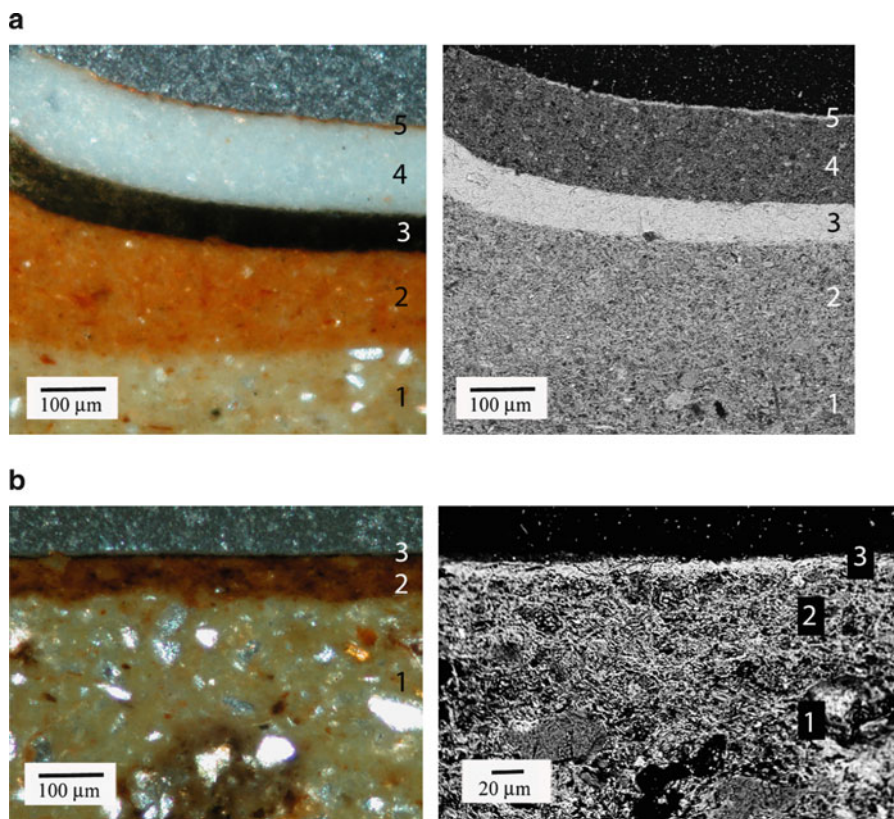


Fig. 2 (a) *Gnathia* pottery from Egnatia. *Left*: crossed polars optical microscopy of thin section of a shard showing fine textured clay body (1), *engobe* layer (2), *black gloss* (3), *white* (4) and *yellow* (5) decorations. *Right*: SEM–BSE photomicrograph of the same thin section with highlighted characteristic differences of the overlapping layers. (b) *Gnathia* pottery from Monte Sannace. *Left*: crossed polars optical microscopy of thin section of a shard showing coarse textured clay body (1), *engobe* layer (2) and *black gloss* (3). *Right*: SEM–BSE photomicrograph of the same thin section

Al, K and Fe as compared to the ceramic body. The characteristics of this layer, probably obtained by decanting the clay used for the body, are very similar to that of the “*ingobbio rosso*” of late Peucetian red-figured pottery (Mangone et al. 2008).

Nevertheless, the *ingobbio rosso* in the red-figured pottery from Peucetia is used to cover the greyish coarse grained ceramic body of large vases with a fine grained iron rich clay, in order to obtain the smooth red surface which allowed the artisan to add the red figures on the vase. On the other hand, *Gnathia* ceramic bodies, even though greyish in colour, are completely covered with black gloss, except for samples featuring a paint-free pedestal, and thus the covering of all samples with *engobe* can be explained simply as a standard traditional practice in this case.

Black gloss was obtained, as for Apulian red-figured pottery, from a clay different from the one used for the ceramic body, probably the finest fraction, easily separated

by decantation, of the so-called “*terre rosse*”. *Terre rosse*, which are very common throughout Apulia, are characterised by a silty clay granulometry and by a mineralogical composition including mainly partially crystalline Fe and Al oxides and hydroxides, clay minerals (illite and kaolinite) and traces of quartz, feldspars, micas, pyroxenes and other minerals (Dell’Anna 1967). The finest fraction, richer in kaolinite and illite, as well as in Fe and Al oxides, imparted its technological and chemical properties to the gloss. The dull aspect of this gloss could be due to its lower thickness as compared to that of the red-figured pottery, 10–15 vs. 30–40 μm , respectively.

As regards the over-painted colours, their morphology, chemical composition and production technology are also the same as for Apulian red-figured pottery. In particular, kaolinite, homogenised with low melting albite and K-feldspar, is the raw material for the white pigment, a mix of black gloss and white pigment is the raw material for the yellow decoration, and a mix of iron oxides, hydroxides and clay minerals, probably the same as the one used for the *ingobbio rosso*, is the raw material for the dark red pigment.

Pigments were applied before firing and underwent the entire oxidising-reducing-oxidising cycle, as highlighted by NMR analyses on the white pigment. Spectra of ^{29}Si and ^{27}Al of kaolinite standard, fired at different temperatures, ranging from 100°C up to 1,000°C, were performed. The resulting spectra show that their respective chemical shifts change as temperature increases, and, in the case of ^{29}Si , a new peak appears as shoulder at 94 ppm. The comparison between the spectra of standards and of the white sample allowed us to identify the firing temperature of the sample. The ^{29}Si signal of the white sample can be deconvoluted in two Gaussian peaks arising from Si bonded to one Al atom through the oxygen (≈ 107 ppm) and Si with a Q^4 environment with two neighbouring Al atoms (≈ 94 ppm) (Lambert et al. 1989).

This spectrum is very similar to that of the kaolinite standard fired at temperatures higher than 900°C. In addition, the ^{27}Al NMR spectrum shows the typical pattern of aluminosilicates fired at temperatures higher than 900°C and can be accounted for by three Gaussian peaks, due to different coordination, the $-\text{Al}^{\text{IV}}$ peak at ≈ 56 ppm representative of metakaolinite, the peak at 4 ppm characteristic of the Al^{VI} , and the broad and weak peak at ≈ 34 ppm typical of Al^{V} or Al^{IV} sites hardly distorted (MacKenzie et al. 1985).

Analytical results corroborate the hypothesis that the production technology of Hellenistic ceramic in Apulia, although following the broad outline of the Attic technological process – elutriation of clay to obtain the black gloss, three stages of firing, etc. – does however present peculiar features, probably deriving from the different raw materials available in Apulia and/or from a familiarity, rather than a real and proper continuity, with the Attic pottery tradition.

Moreover, in spite of a general standard trend of the iconographic system, related to an advanced phase of the production, archaeometric results for *Gnathia* pottery samples from Egnazia suggest a good technological cycle, from the recovery of raw materials to the manufacturing and firing process, with firing temperatures in the range of 900–1,050°C, as it is possible to infer from the concurrent results obtained by XRD spectra of ceramic bodies and NMR spectra of white over-painted decorations.

References

- Cassano MR et al (2007) Ricerche archeologiche nella città di Egnazia Scavi 2004–2006: relazione preliminare. In: Pani M (ed) *Epigrafia e territorio Politica e società. Temi di antichità romane VIII*. Edipuglia, Bari, pp 7–136
- Cinquelpalmi A, Laviano R, Muntoni IM (2003) Pottery production in the middle bronze age village of Egnazia (South-Eastern Italy): raw materials provenance and firing techniques, In: Di Pierro S, Serneels V, Maggetti M (eds) *Proceedings of “Ceramic in the Society: 6th European Meeting on Ancient Ceramics”* 3–6 October 2001 – Fribourg, 65–74
- Dell’Anna L (1967) Ricerche su alcune terre rosse della regione pugliese. *Periodico di Mineralogia* 36(2):539–592
- Dell’Anna L, Laviano R (1991) Mineralogical and chemical classification of Pleistocene clays from the Lucanian basin (Southern Italy) for the use in the Italian tile industry. *Appl Clay Sci* 6:233–243
- Grave P, Robinson E, Barbetti M, Yu Z, Bailey G, Bird R (1997) Analysis of South Italian pottery by PIXE-PIGME. *Mediterranean Archaeol* 9(10):113–125
- Green JR (1976) *Gnathia pottery in the Akademisches Kunstmuseum Bonn*. Verlag Philipp von Zabern, Mainz
- Green JR (2001) Gnathia and other overpainted wares of Italy and Sicily: a survey. In: Geny E (ed) *Céramique hellénistiques et romaine, III*. Presses Universitaires, Paris, pp 57–103
- Hatcher H, Hedges REM, Pollard AM, Kenrick PM (1980) Analysis of Hellenistic and Roman fine pottery from Benghazi. *Archaeometry* 22(2):133–151
- Jones RE (1986) *Greek and Cypriot pottery: a review of scientific studies*. The British School at Athens, Athens
- Lanza E (2005) *Ceramica di Gnathia al Museo di Antichità di Torino*. Società archeologica s.r.l, Mantova
- Lambert JF, Millman WS, Fripiat JJ (1989) Revisiting kaolinite dehydroxylation: a ^{29}Si and ^{27}Al MAS NMR study. *J Am Chem Soc* 111(10):3517–3552
- MacKenzie KJD, Brown IWM, Meinhold RH, Bowden ME (1985) Outstanding problems in the kaolinite-mullite reaction sequence investigated by ^{29}Si and ^{27}Al Solid State NMR: I, meta-kaolinite. *J Am Chem Soc* 68:293–297
- Mangone A, Giannossa LC, Ciancio A, Laviano R, Traini A (2008) Technological features of apulian red figured pottery. *J Archaeol Sci* 35(6):1533–1541
- Prag AJNW, Schweizer F, Williams JLL, Schubiger PA (1974) Hellenistic glazed wares from Athens and southern Italy: Analytical techniques and implications. *Archaeometry* 16 (2):153–187
- Webster TBL (1968) Towards a classification of Apulian Gnathia. In: *Bulletin of institute of classical studies, XV*. University of London, 1–33

North-Western European Forest Glass: Working Towards An Independent Means of Provenance

A.S. Meek, J. Henderson, and J.A. Evans

1 Introduction

This paper presents the preliminary findings of a long-term project to establish an independent means of provenancing forest glasses. Here we present an overview of the compositional analysis carried out on samples from around England. However, the project will eventually expand to include samples from across north-western Europe and include multi-element isotope analysis. Previous studies have attempted to provenance glass based on compositional analysis and have found characteristic groupings. However a great number of these do not stand close scrutiny when compared to the results of more advanced scientific techniques. This study will be the first to apply multi-isotope analysis to the problem of forest glass provenance.

2 Forest Glass Production

Forest glass was produced in North-western Europe from around 1000 to 1700 AD, and the first evidence of its use in England is in the twelfth century. Forest glass is potassium-rich and is produced using the ash of wood or bracken, and impure sand. During its early use in England a lack of production evidence points to a continental origin for this glass. However, by the thirteenth century documentary evidence points to the establishment of a large number of glasshouses producing forest glass in the Weald and Staffordshire.

By the early sixteenth century the evidence of glass production in the UK wanes. There is a large quantity of archaeological evidence for its use but not for its production. One 1542 reference implies that there was no English-made window

A.S. Meek (✉) and J. Henderson
Department of Archaeology, The University of Nottingham, Nottingham, NG7 2RD, UK
e-mail: acxam@nottingham.ac.uk

J.A. Evans
NERC Isotope Geosciences Laboratory, Keyworth, NG12 5GG, UK

glass available to glaziers (Godfrey 1975). There was clearly no problem obtaining the necessary raw materials in England, what was lacking was the skill. The time was ripe for an influx of glassmakers skilled in the art of window and high quality vessel production. A large number of highly skilled Huguenot glassmakers entered England during this period due to religious persecution elsewhere in northern Europe. The immigration of foreign glassmakers greatly increased following the massacre of Huguenots in Paris in 1572 (Vose 1980).

At the start of the seventeenth century there were frequent documented complaints regarding wood shortages and the consequent raising of fuel prices. Furthermore, overproduction in certain areas, such as the Weald, led to falling glass prices. Some glassmakers became migratory, seeking out wood and new markets, resulting in numerous short-lived sites from Herefordshire to the North Riding of Yorkshire dating to the late sixteenth century. Their spread drew greater attention to wood shortages throughout the country. On the 23rd of May 1615 James I made a Royal proclamation banning the use of wood as a fuel in glass production. This led to the production of forest glass in England using coal as a fuel, which necessitated new glass recipes and the redesign of the furnaces.

3 Scientific Analysis

3.1 *Compositional Analysis*

Many excavation reports of forest glass production sites include a few compositional analyses of the glass found. However, these are generally limited to a small number of samples and often restricted to major element determination. Several more extensive studies have been undertaken (e.g. Merchant et al. 1997; Welch 1997), but even these generally only cover one region or site. Due to the small number of analyses of production waste, it is difficult to assign provenance to the glasses based on their compositions. This study involves the analysis of 223 raw glass samples with the most up-to-date techniques to provide a high degree of accuracy and precision.

3.2 *Isotopic Analysis*

In recent years advancements in analytical techniques has provided Nd and Sr isotopic analysis using Thermal Ionisation Mass Spectrometry (TIMS) as a new technique in archaeological science. While still more time consuming and expensive than compositional analysis, many studies have shown isotopic analysis to be far superior in archaeological provenance studies. Even though major elements make up the largest proportion of a sample, their variation in composition across different

locations is often limited. On the other hand, isotope ratios depend on the compositions and geological history of the source rock and are potentially more useful in fingerprinting artefacts made in different places (Li et al. 2006).

In addition to compositional analysis this project will also involve the determination of strontium, neodymium and oxygen isotopes. England has a highly variable geology and therefore should allow this technique to provide signatures specific to regions, or even sites. Forest glass production provides this opportunity due to the low value and probable local sourcing of raw materials. No isotopic analyses of forest glass have been published. There have, however, been a few recent studies of glass from other regions and time periods which have provided us with some very promising results (e.g. Brill et al. 1999; Freestone et al. 2003; Henderson et al. 2005; Degryse and Schneider 2008).

4 Sites

The results presented in this paper come from forest glass production waste excavated at twelve production sites across Britain. These sites range in time period from the first half of the fourteenth century to the middle of the seventeenth century. Importantly, for the isotopic analyses, they are located on varying geologies (Fig. 1).

5 Methodology

A JEOL JXA-8200 electron microprobe with four wavelength-dispersive spectrometers located in the Department of Archaeology at The University of Nottingham was used for compositional analysis. Small pieces were broken from each glass sample ensuring that they included some unweathered glass. These samples were set in 1" epoxy resin blocks, polished to a 0.25 μm diamond paste finish and carbon coated to prevent surface charging and distortion of the electron beam during analysis. A defocused electron beam (to prevent affecting the sodium and other volatiles) with a diameter of 50 μm was fired at the surface at an accelerating voltage of 20 kV. Emitted X-rays were counted for 20 s for each peak and 10 s for background. For magnesium, X-rays were counted for 20 s for each peak and 20 s for background. Calibration with mixed mineral and pure metal standards was carried out.

6 Results

Samples from all of the sites shown in Fig. 1 were analysed by electron microprobe for 25 major, minor and trace elements. A total of 223 samples from the twelve sites were analysed. The plot reproduced here is aluminium oxide (Al_2O_3) vs. magnesium oxide (MgO) (Fig. 2). It is a useful way of explaining compositional differences

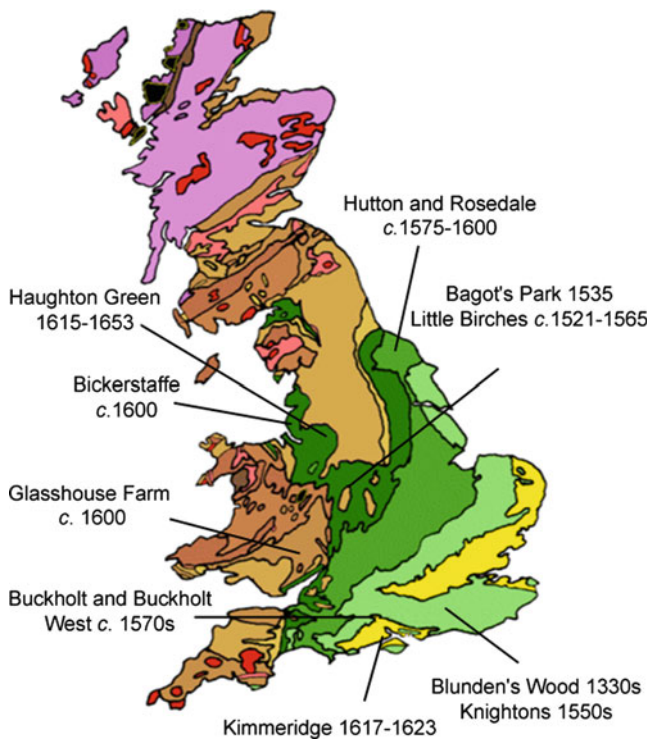


Fig. 1 Sites presented on a simplified geological map

since the bulk of the aluminium comes from the silica source and the magnesium from the alkali, in this case wood ash. The plot shows that each production site is generally represented by a small group. While not always distinct, the data for each site still generally form groups with limited distributions. Discussed below are the differences between results for samples from three chronological periods and a detailed discussion of the samples from Rosedale.

6.1 Early Pre-1500 Group

Blunden's Wood was the only site which produced glass of this date that has been analysed and it has a distinctive composition. It has the lowest aluminium levels and some of the highest magnesium levels. This distinction is more likely to be due to the use of specific silica and wood sources rather than related to chronological factors or greatly different glassmaking recipes.

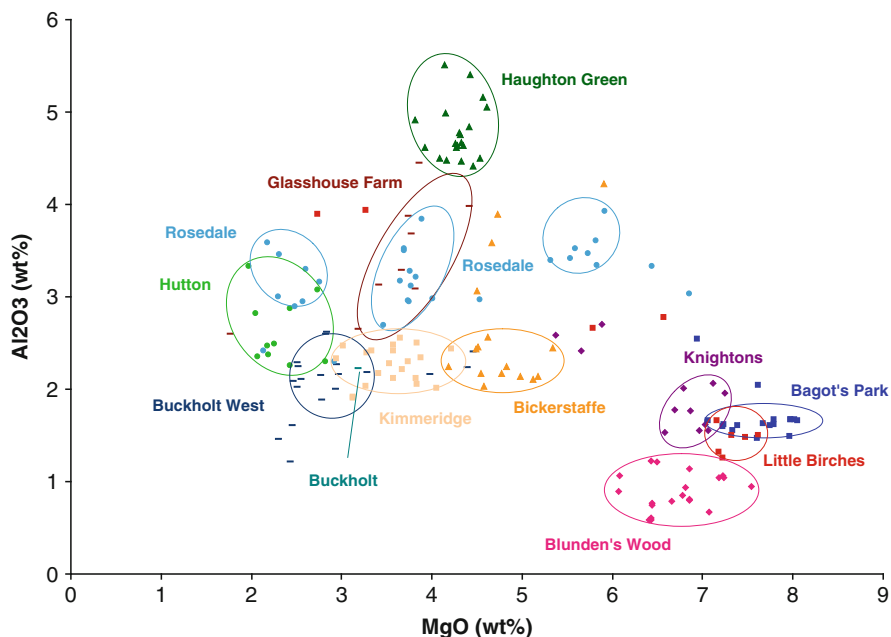


Fig. 2 Compositional analysis of glass from 12 British production sites

6.2 Transitional 1500–1567 group

The three sites in this group, Knights, Bagot's Park and Little Birches, have very similar compositions. Together with Blunden's Wood they form a high-MgO, low- Al_2O_3 group. This similarity, which is also seen in a number of other major and minor components of the glass, implies that glassmakers in Staffordshire and the Weald were using similar ingredients and/or production processes at this time. There is also the possibility that something occurred around the mid to late sixteenth century that caused the recipes used to alter. These sites all predate the arrival of the Huguenot glassmakers in 1567, so perhaps the difference in recipe is a result of their introduction of new production methods and recipes.

6.3 Late 1567–1615 group

This group consists of six sites, Buckholt and Buckholt West, Hutton, Rosedale, Glasshouse Farm and Bickerstaffe. There are some similarities between the compositions from each of these sites. However, they do not form a coherent group like the glasses from the earlier periods. Ignoring the high-MgO Rosedale group, the glass in

this group have far lower MgO compositions compared to those in the early/transitional group.

The samples from Rosedale fall into three groups: low, medium and high MgO. Each group has a relatively similar level of Al_2O_3 (2–4%). There are two possibilities that could explain these results. Firstly, there may have been three sources of alkali used at this site and one sand source used in combination with these three alkalis. Alternatively, the high-MgO and low-MgO groups could relate to different recipes or firing regimes (Rehren 2008) with the mid-MgO group resulting from a mixture of the two. There is also therefore the possibility that the low-MgO glass was produced at the nearby site of Hutton and the high-MgO glass at Rosedale. The middle grouping could result from secondary melting of the low-MgO glass from Hutton and subsequent mixing with the high-MgO glass at Rosedale.

6.4 Coal Fired Post-1615 Group

The two sites in this group, Kimmeridge and Haughton Green, have very different compositions. Although, there is some overlap in their MgO levels, it is Haughton Green's very high Al_2O_3 that makes it distinct. These two sites were controlled by the same company and similarities in composition were expected. These differences are promising in terms of the isotopic analysis. The differences are geographically constrained, possibly implying that the raw materials are from contrasting geological locations.

7 Conclusions

The results of this study have demonstrated that there is some hope for provenancing forest glasses based on compositional analysis. However, this is not an independent provenance since the reasons for the differences between sites are not necessarily linked to the location of production. The isotopic analyses will link the glasses to the origins of the raw materials used to make them. Assuming that the model of relative proximity of the raw materials to the place of manufacture holds then an independent provenance can be assigned. Overall the elemental analyses carried out have provided unexpectedly informative results. Using simple major and minor element bi-plots it has been possible to discern surprisingly distinct groupings. The compositions of these forest glasses are far more site-specific than would have been expected based on the highly variable compositions of the impure raw materials (Sanderson and Hunter 1981). This is very encouraging for the isotopic work on forest glasses that we are carrying out.

References

- Brill RH, Clayton RN, Mayeda TK, Stapleton CP (1999) Oxygen isotope analyses of early glasses. In: Brill RH (ed) *Chemical analysis of early glasses*, vol 1. Corning Museum of Glass, New York, pp 303–322
- Degryse P, Schneider J (2008) Pliny the Elder and Sr–Nd isotopes: tracing the provenance of raw materials for Roman glass production. *J Archaeol Sci* 35(7):1–8
- Freestone IC, Leslie KA, Thirlwell M, Gorin-Rosin Y (2003) Strontium isotopes in the investigation of early glass production: Byzantine and Early Islamic glass from the Near East. *Archaeometry* 45(1):19–32
- Godfrey ES (1975) *The development of english glassmaking*. Clarendon, Oxford
- Henderson J, Evans JA, Sloane HJ, Leng MJ, Doherty C (2005) The use of oxygen, strontium and lead isotopes to provenance ancient glasses in the Middle East. *J Archaeol Sci* 32:665–673
- Li B-P, Jian-Xin Z, Greig A, Collerson KD, Yue-Xin F, Xin-Min S, Mu-Sen G, Zhen-Xi Z (2006) Characterisation of Chinese Tang sancai from Gongxian and Yaozhou kilns using ICP-MS trace element and TIMS Sr–Nd isotopic analysis. *J Archaeol Sci* 33:56–62
- Merchant I, Henderson J, Crossley D, Cable M (1997) Medieval glass-making technology: the corrosive nature of glass. In: Sinclair A, Slater E, Gowlett J (eds) *Archaeological sciences 1995. Proceedings of a conference on the application of scientific techniques to the study of archaeology*, Liverpool, July 1995. Oxbow Books, Oxford, pp 31–37
- Rehren Th (2008) A review of factors affecting the composition of early Egyptian glasses and faience: alkali and alkali earth oxides. *J Archaeol Sci* 35:1345–1354
- Sanderson DCW, Hunter JR (1981) Compositional variability in vegetable ash. *Sci Archaeol* 23:27–30
- Vose RH (1980) *Glass*. Collins, London
- Welch C (1997) Glassmaking in Wolseley, Staffordshire. *Post-Medieval Archaeol* 31:1–60

Ceramic Production in the Indigenous Settlement of Entella (Western Sicily) During the Archaic Age

G. Montana, A. Corretti, A.M. Polito, and F. Spatafora

1 Archaeological Background and Aims

Indigenous fine tablewares (both plain and with painted geometric patterns/decorations) were widely diffused in western and central Sicily between the seventh and the fifth centuries BC (Gargini 1995; Spatafora 1996; Trombi 1999; Campisi 2003). However, the considerable recurrence of shapes and decorative subjects inhibits the identification of specific production centres merely on the basis of stylistic and morphological analyses. Therefore, the extent of the distribution of objects manufactured in different workshops cannot be fully appreciated, and the network of ceramic trade in Archaic Sicily is acknowledged only in terms of the relationships between the Phoenician and Greek colonies and the native hinterland. To date, any kind of transaction patterns involving only indigenous centres still remains unknown.

The ancient town of Entella is situated in the Sicani Mounts area, in a strategic location allowing the control of the E–W and N–S routes (Fig. 1a); it can be considered one of the most important indigenous settlements of Western Sicily (Spatafora 1996). An industrial quarter was discovered on the southern slope of the plateau, in the area of the necropolis (Guglielmino 2000). Pottery kilns and waste disposal sites were brought to light here; the dating of the imported Greek wares indicated that the large geometrically painted tableware was mainly produced in the sixth century BC (Fig. 1b). In this paper, a representative set of local ceramic artefacts from Entella (20 samples) was

G. Montana (✉) and A.M. Polito

Dipartimento di Chimica e Fisica della Terra ed Applicazioni alle Georisorse e ai Rischi Naturali (CFTA), Università di Palermo, Via Archirafi, 36, 90123 Palermo, Italy
e-mail: gmontana@unipa.it

A. Corretti

Laboratorio di Storia, Archeologia e Topografia del Mondo antico, Scuola Normale Superiore di Pisa, Pisa, Italy

F. Spatafora

Regione Siciliana, Soprintendenza BB. CC. AA. di Palermo (Servizio per i Beni Archeologici), Palermo, Italy

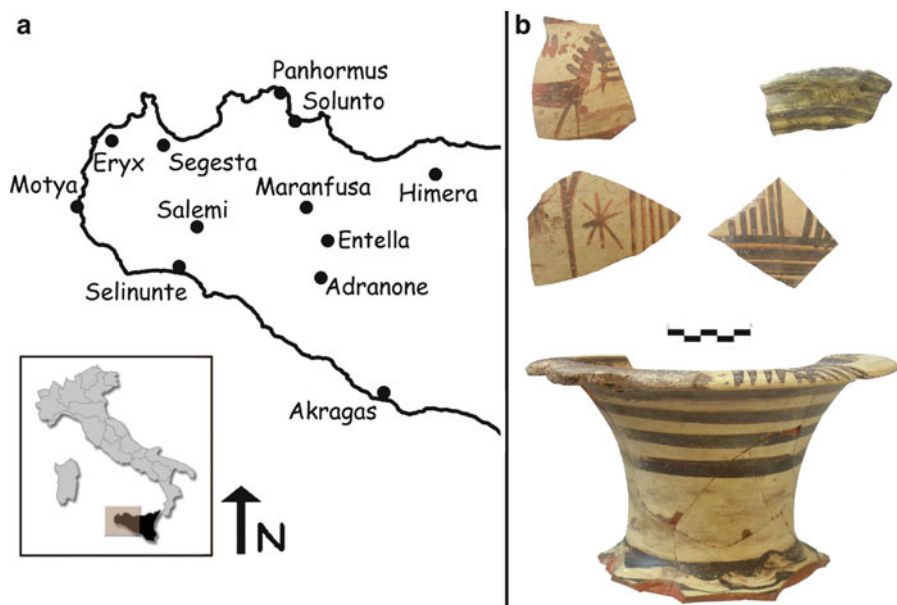


Fig. 1 Map of the study area (a); representative ceramic forms included in the present study (b)

analysed by thin section petrography and wavelength dispersive X-ray fluorescence (WDXRF) spectroscopy, and compared with the raw clays outcropping in the vicinity of the site (24 samples). A detailed description of the procedure followed for the XRF analysis of ceramic sherds and raw clays can be found in Hein et al. (2002). The aim of this experimental work was to establish the settlement of Entella as one of the most important production centres of geometrically painted tableware in the area during the Archaic Age.

2 Results and Discussion

Clayey deposits, potentially appropriate for ceramic manufacture, outcrop extensively in the area around the site of Entella. They belong to three different stratigraphic horizons, dating from the Middle Miocene to the Middle-Upper Pliocene. In particular, *San Cipirrello* clays are Serravallian-Lower Tortonian materials, with extremely abundant calcareous microfauna. *Terravecchia* clays, which surround the hill of Entella, belong to Tortonian–Messinian levels; they are not particularly rich in fossil fauna and are characterised by the presence of tiny mica flakes in the coarse silt fraction. The Pliocene clayey materials from the *Marnoso-Arenacea Formation* (M.A.B.) outcrop at least 5 km to the east of Entella and have a notable content of calcareous microfossils as well. Regarding their grain size distribution, all these raw materials have an average content of sand fraction

Table 1 Mean values of major (in wt%) and trace elements (ppm) concentrations obtained by XRF. Reported values are normalized versus loss on ignition (LOI)

	Entella tableware		S. Cipirrello clays		Terravecchia clays		M.A.B. clays	
	Mean (n = 20)	St. dev.	Mean (n = 8)	St. dev.	Mean (n = 8)	St. dev.	Mean (n = 8)	St. dev.
SiO ₂ (wt%)	59.23	1.27	40.93	1.73	55.18	1.04	49.62	1.92
TiO ₂	0.92	0.05	0.73	0.05	1.08	0.02	0.89	0.05
Al ₂ O ₃	17.88	0.86	15.02	0.68	20.52	0.64	16.54	1.12
P ₂ O ₅	0.15	0.01	0.14	0.01	0.15	0.00	0.19	0.02
Fe ₂ O ₃	8.34	0.42	5.80	0.55	8.44	0.16	6.94	0.76
MgO	2.41	0.18	2.38	0.07	2.83	0.09	3.44	0.22
MnO	0.10	0.01	0.07	0.01	0.09	0.01	0.08	0.01
CaO	6.96	0.90	32.10	2.98	7.70	0.25	19.92	2.68
Na ₂ O	0.97	0.07	0.28	0.04	1.06	0.33	0.38	0.09
K ₂ O	2.67	0.09	2.31	0.11	2.69	0.05	2.00	0.09
Rb (ppm)	110	14	69	11	91	3	81	18
Sr	234	48	847	129	272	8	638	138
Zr	338	25	211	12	325	19	189	56
Cr	145	37	194	17	131	36	100	9
Ni	24	5	46	5	28	8	32	4
Ba	351	33	191	15	359	17	288	69
La	26	3	22	5	27	3	35	3
Ce	74	9	61	13	75	4	88	4
Cu	28	9	17	3	31	1	14	2
Zn	126	16	69	20	104	8	41	5
V	173	15	76	19	176	12	145	15

around 10 wt%; however, the *Marnoso-Arenacea* clays have a relatively higher silt fraction (Montana et al. 2006). The chemical analysis (Table 1) emphasized the remarkable calcium oxide content of the *San Cipirrello* clays (around 32 wt% as an average value normalized against loss on ignition), coupled with a very high content of strontium. *Terravecchia* clays, in contrast, have the lowest CaO content and, at the same time, are characterised by slightly higher concentrations of sodium and potassium oxides, as well as by the presence of barium and rubidium among the trace elements.

These latter elements clearly have a geochemical relationship with potassium. *Marnoso-Arenacea* clays, in addition to a high CaO content, show a relatively higher concentration of magnesium oxide. Experimental firings of briquettes at 900°C allowed us to observe several textural and mineralogical features related to the natural sandy fraction of these clays. They were also useful for the assessment of specific chemical markers, such as the abundance of strontium in *San Cipirrello* clays, due to the large quantity of foraminifera, or the higher potassium, titanium, aluminum, rubidium and barium contents in *Terravecchia* clays, due to the presence of K-feldspars and white mica flakes.

The fabric observed under the polarizing microscope in all the analysed ceramic samples, representative of local productions of geometrically painted tableware, is characterised by aplastic temper packing ranging from 10% (area) to 20%. Size

distribution is mainly serial, with a bimodal affinity whenever (sporadically) a medium sand component (0.25–0.5 mm) is also present, while the prevailing temper size falls in the class of very fine sand (0.06–0.1 mm). From the compositional point of view, grains of monocrystalline quartz are prevalent. Common subordinate components are polycrystalline quartz, K-feldspar, plagioclase and mica flakes, the latter being homogeneously distributed in the groundmass. The calcareous component is relatively modest and represented by microfossils, which are more or less decomposed, depending on the firing temperature. The mineralogical features described above fit well with the average chemical composition of the set of ceramic samples (values are shown in Table 1), which, first of all, is characterised by a good homogeneity, as expressed by the more than acceptable standard deviation values, especially with regard to the major constituents. We can also emphasize the relatively high concentrations of aluminum, iron and potassium oxides, and, in contrast, the moderate CaO content. Rubidium, barium and zirconium show quite elevated contents in comparison with the rest of the trace elements.

Subsequently, the data for the ceramic manufactures of Entella were combined with that related to the local raw materials, the latter ones after having been experimentally fired, and compared in terms of petrographic features. All the investigated clays show similar textural features: they fall in the same range of temper packing (5 up to 15–20% area), with a clear prevalence of very fine and fine sand grains (Fig. 2a). However, the composition of this fine sand fraction is different: in the *San Cipirrello* clays, it is mainly composed of calcareous microfossils (which react with the groundmass after firing); in the *Marnoso-Arenacea* clays, the calcareous component is still abundant even if subordinate with respect to the quartz grains; in the *Terravecchia* clays, quartz predominates and the calcareous component is greatly restricted. Moreover, this latter raw material shows two mineralogical peculiarities compatible with the microfabric of local ceramic artefacts: common to abundant mica flakes scattered homogeneously in the groundmass, and the frequent presence of feldspar grains. Thus, the *Terravecchia* clay, after the experimental firing, exhibits similar textural and mineralogical features to the local ceramic manufactures. The use of local Upper Miocene clays from the *Terravecchia* formation in the archaic production of tableware at Entella is even more evident when comparing chemical data. The compositional convergence between the ceramic artefacts from Entella and the *Terravecchia* clays is easily discernible even by a simple comparison between mean contents of major and trace elements in the analysed ceramic samples and in the three varieties of local clays. Furthermore, the multivariate elaboration of the chemical data, concerning both major and trace elements, also indicated a chemical correspondence between the *Terravecchia* clays and the local ceramic productions. The results of a Principal Component Analysis undertaken using the S-plus software are shown in Fig. 2b. Sample scores are plotted on the two-dimensional plane defined by the first two components, which stand for 87% of the total variance. It thus once again appears clear that *Terravecchia* clays and the Archaic manufactures from Entella emerge as a very well confined compositional group.

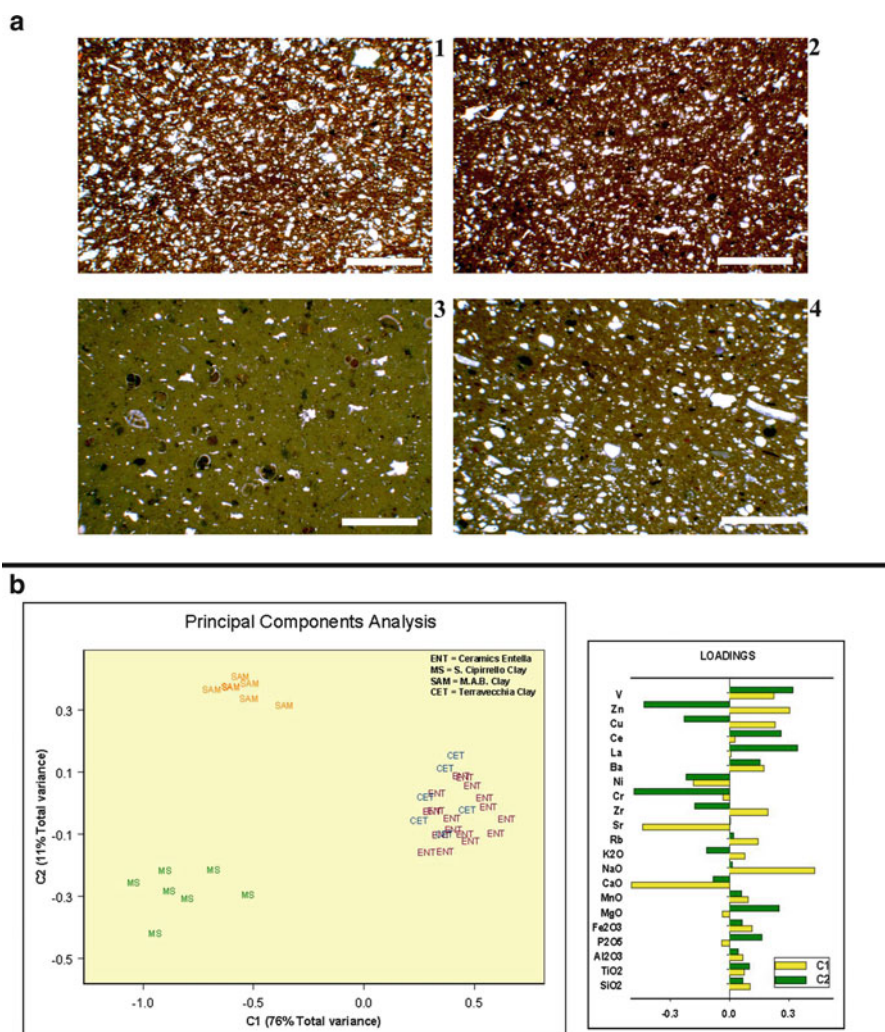


Fig. 2 (a) photomicrographs (crossed nicol, scale bar = 0.5 mm) showing the ceramic paste of Entella (frame 1) compared to local clays fired at 900°C (frame 2 = Terravecchia, frame 3 = S. Cipirello, frame 4 = MAB clays); (b) projection of the factor scores on the 2-D plane defined by the first two components and factor loadings obtained through Principal Component Analysis (PCA) considering all the elements

3 Conclusive Remarks

Our archaeometric approach, integrating data related to the territory and its geology, petrography and chemistry has led to: (a) a characterisation of the microscopic fabric and of the chemical composition of the studied class of painted tableware; (b) a recognition of the *Terravecchia* clays as the clayey raw material used for

pottery manufacture. Therefore, the petrographic examination and the chemical analysis of a representative number of selected samples, coupled with the study of local clayey raw materials, allowed us to define the compositional markers of the tableware produced in Entella during the Archaic Age (seventh to early fifth century BC). Consequently, this makes possible a relatively straightforward recognition of Entella manufactures in further studies of geometrically painted artefacts discovered in other sites of western Sicily. This aspect will allow for a better definition of trade patterns among native settlements. Moreover, this would also allow for a better determination of the main trade routes, as well as for the study of settlements which were supplied from different, still unknown, production centres. On a local level, the identification of the locations where clayey raw materials were exploited could also lead us to advance hypotheses about the territorial influence of Entella in its surrounding area.

References

- Campisi L (2003) La ceramica indigena a decorazione geometrica dipinta. In: Spatafora F (ed) Monte Maranfusa, un insediamento nella media valle del Belice, l'abitato indigeno, Soprintendenza ai Beni Culturali e Ambientali. Servizio Beni Archeologici, Palermo, pp 157–228
- Gargini M (1995) La ceramica indigena a decorazione geometrica dipinta, In: Nenci G (ed.) Entella I, Pisa, 111–161
- Guglielmino R (2000) Entella: un'area artigianale extra-urbana di età tardo-arcaica, In Atti delle Terze Giornate Internazionali di Studi sull'Area Elima. Pisa, 701–713
- Hein A, Tsolakidou A, Iliopoulos I, Mommsen H, Buxeda I, Garrigos J, Montana G, Kilikoglou V (2002) Standardization of elemental analytical techniques applied to provenance studies of archeological ceramics: an interlaboratory calibration study. *The Analyst (Royal Society of Chemistry)* 127(4):542–553
- Montana G, Caruso A, Lavore AL, Polito AM, Sulli A (2006) Definizione composizionale delle "argille ceramiche presenti nella Sicilia nord-occidentale: inquadramento geologico e ricadute di carattere archeometrico. *Il Quaternario* 19(2):277–296
- Spatafora F (1996) La ceramica indigena a decorazione impressa e incisa nella Sicilia centro-occidentale: diffusione e pertinenza etnica. *Sicilia Archeologica* 29:91–110
- Trombi C (1999) La ceramica indigena dipinta della Sicilia. In: Barra Bagnasco M, De Miro E, Pinzone A (eds.) Origine e incontri di culture nell'antichità Magna Grecia e Sicilia. Stato degli Studi e prospettive di ricerca, Atti dell'Incontro di Studi (Messina 2-4 dicembre 1996), Catanzaro, 275–293

Middle Guadiana River Basin (Badajoz, Spain and Alentejo, Portugal) Network Interactions: Insights from the Chemical Analysis of Bell Beaker Pottery and the Lead Isotope Analysis of Copper Items from the Third Millennium BC

C.P. Odriozola, M.A. Hunt-Ortiz, M.I. Dias, and V. Hurtado

1 Introduction

Several settlement networks from the Iberian Copper Age period are located alongside the Guadiana River (Iberian Peninsula) – i.e. Perdigões, Reguengos de Monsaraz, Portugal (Dias et al. 2005; Valera 2006), or Tierra de Barros, Badajoz, Spain (Hurtado 1995, 1999). In this context, a clear relation has been found between the sites in terms of spatial organization (hierarchical, where La Pijotilla could be considered as a central place in a core-periphery system), a restricted stylistic distribution of the so-called Guadiana ‘eyed idol’ figurines (Hurtado 2008), or the distribution of bone based inlaid Bell Beaker pottery (Hurtado and Odriozola 2008; Odriozola in press).

Since the 1970s, the Beaker Network paradigm (Clarke 1976) has been systematically used to explain the broad and fast expansion of the so-called “Beaker phenomenon” all over Europe and the north of Africa, linked to the long distance trade of prestige items (copper items, ivory, amber, etc). However, little if any evidence of exchanged Bell Beaker (BB) pottery or copper items has been found after years of research, except for stylistic inferences. It is known that a style can be easily copied just by visual examination of the finished product; this is likely the easiest way to explain style dispersion, but does not justify hypotheses regarding vessel or copper artefact exchanges or transactions.

Research carried out within the I + D Project (MAT2005-00790) and within the GRICES-CSIC Project (2005-PT0030).

C.P. Odriozola (✉)

Instituto de Ciencia de Materiales de Sevilla, Centro Mixto Universidad de Sevilla-CSIC, Avd. Américo Vespucio 49, 41092 Sevilla, Spain
e-mail: carlos@icmse.csic.es

M.A. Hunt-Ortiz and V. Hurtado

Departamento de Prehistoria y Arqueología, Universidad de Sevilla, C/María de Padilla S/N, 41004 Sevilla, Spain

M.I. Dias

Instituto Tecnológico e Nuclear, Estrada Nacional 10, 2686-953 Sacavém, Portugal

Our goal is to examine elite interactions and exchanges of BB pottery and copper production related items among the main sites of the Guadiana River Middle Basin (GRMB), in order to obtain a broad picture of prestige items' consumption and distribution patterns within GRMB. This will be accomplished by chemical composition analyses of Bell Beaker pottery and lead isotope analyses of items related to metallic production.

2 Materials and Methods

For this research study, X-ray Fluorescence (collected on a pellet – 50 μm particles size, diluted with powdered wax (0.1:0.061 ratio), and pressed at 40 Tm – using a Pananalytical Axios analyzer) was used to determine the elemental composition of 103 sherds from four sites (La Pijotilla, San Blas, Porto Torrão and Perdigões), belonging to two differentiated settlement networks. This was done in order to determine compositional groups. The pottery selected for this study consisted of a homogeneous group of domestic household bowls (not expected to be exchanged) and a series of so-called “prestige pottery”, comprised mainly of Bell Beaker pots of Corded Zone Maritime (CZM), Maritime and Regional incised types, combed wares and what are referred to as “symbolic wares” in the Portuguese archaeological literature, mainly characterized by a decoration consisting of inverted triangles, and, in most of the cases, filled with impressed dots.

Compositional data for major and minor elements were log-transformed (to base 10) in order to normalize data prior to the statistical analysis. Hierarchical Cluster (HC) on Ward's method and Principal Component Analysis (PCA) were developed on the normalized compositional data, in order to determine the number of compositional clusters in the data set, following well-established procedures (Baxter 1994; Glascock 1992). No outlier detection or variable selection method was used to perform this analysis.

For the lead isotopic analyses, six copper metallurgy related samples from the site of San Blas were submitted to Thermal Induced Mass Spectrometry, following well-established procedures (Hunt Ortiz 2003). These analyses were complemented by the characterization of samples obtained from mineral deposits exploited in modern times and containing copper minerals, located in the proximity of San Blas: the Novillero Viejo mine, close to the site, and the Norte Alconchel mine. The lead isotopic results obtained were compared with those previously carried out on metallic items from the site of La Pijotilla (Hunt Ortiz 2003).

3 Results

Although the number of samples analysed with lead isotopes is still limited, some interpretations on possible exchange networks can be pointed out from the available results. Regarding the site of San Blas, the copper production was not based on a

single mineral deposit. The mineral deposit isotopically characterised in the vicinity of San Blas, Novillero Viejo (the closest mine), had a different isotopic composition from the archaeometallurgical samples from San Blas, although the Alconchel Norte mine showed isotopic consistency with one of the slag samples (n° 9) from San Blas.

At a regional level, the comparison of the lead isotopic compositions between San Blas and La Pijotilla samples showed a clear isotopic consistency among archaeometallurgical samples from the two sites (Fig. 1).

With regard to the pottery samples, six significant tendencies in compositional variation can be observed on the Ward’s method HC output (Fig. 2a), where sherds recovered at each specific site generally cluster together. However, a small number of

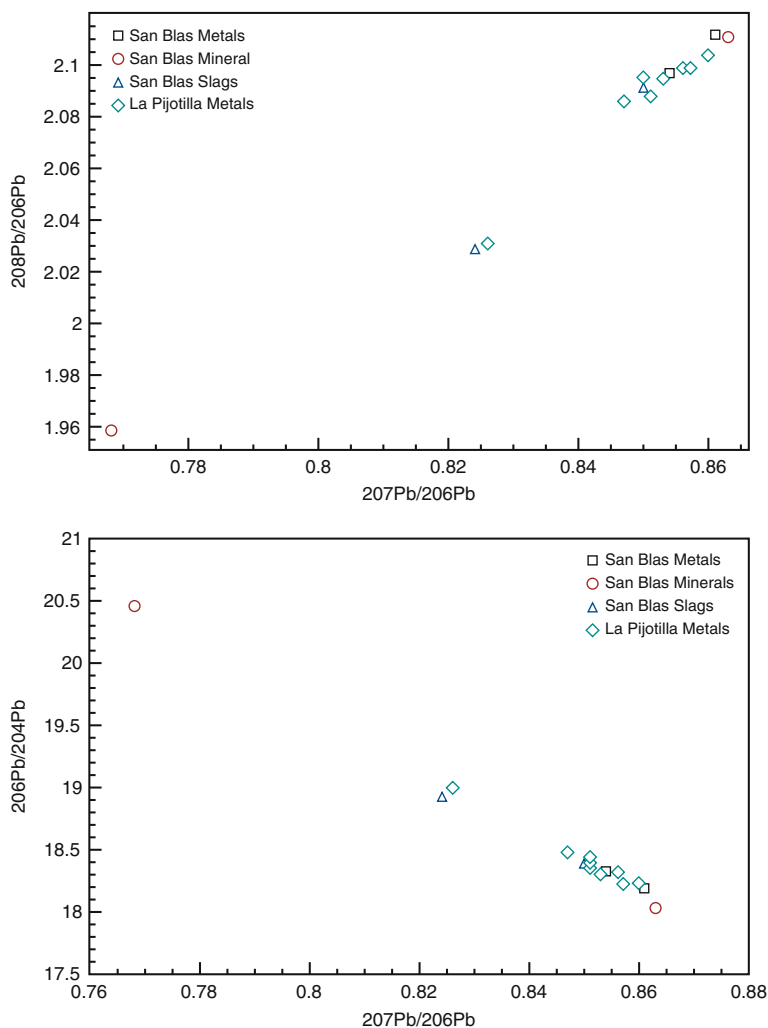


Fig. 1 Lead Isotope plots: San Blas versus La Pijotilla

samples clusters into these groups; thus, it can be assumed that producers/consumers were exchanging some pots between sites, possibly as part of a trade/exchange network, since it seems unlikely that potters from different sites could have used raw materials that were geochemically similar, and/or prepare the paste in a similar way.

The varimax rotated PCA scores of the normalised data of the first two components (Fig. 2b) corroborate the tendencies observed in the HC, clustering together in the HC, as well as in the PCA. These groupings appear to reflect differences in geographical location and geology of clay sources, along with potters' behaviour. Thus, the pottery found at the site of San Blas possesses distinct geochemical signatures from that found at La Pijotilla, Porto Torrao or Perdigões, as can be seen in the mean concentrations and standard deviation of each cluster group (as summarized in Table 1).

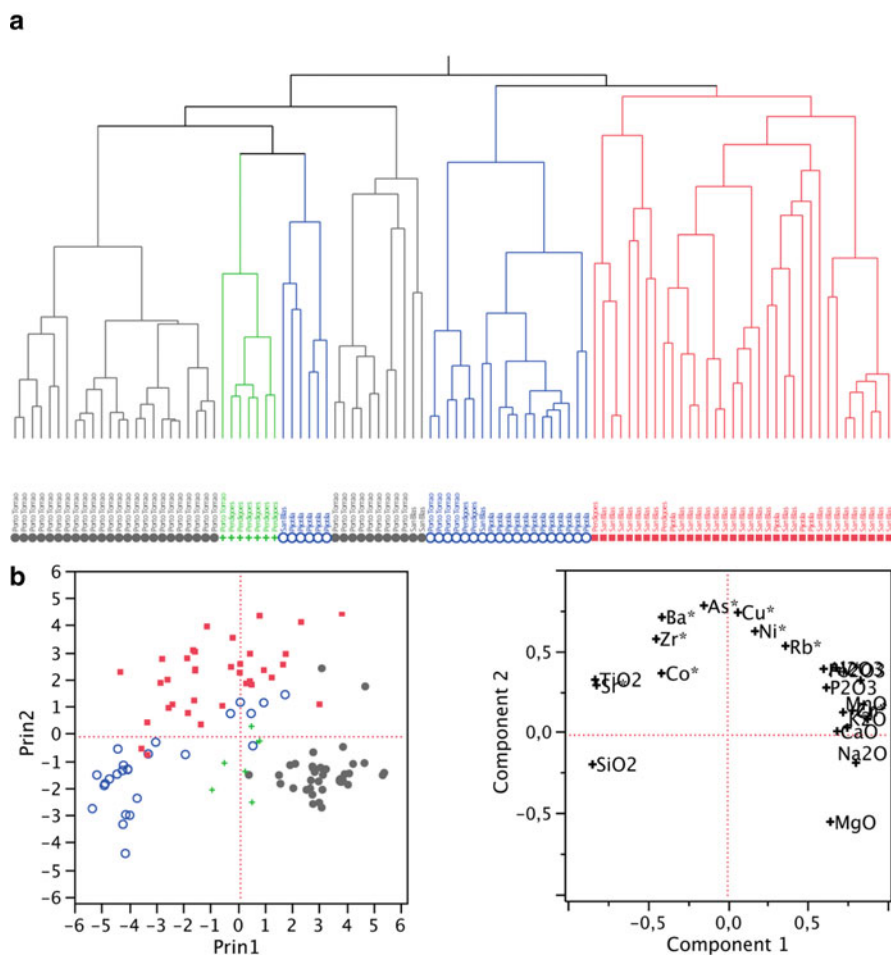


Fig. 2 (a) Ward's method HC, (b) PCA score and loading plots

Table 1 Mean major element concentrations for each of the cluster groups, expressed in oxide wt% (shadowed data are expressed in ppm)

	Porto Torrão 1		Perdigões		La Pijotilla 1		Porto Torrão 2		La Pijotilla 2		San Blas	
	\bar{X}	SD	\bar{X}	SD	\bar{X}	SD	\bar{X}	SD	\bar{X}	SD	\bar{X}	SD
SiO ₂	50.99	3.39	52.00	1.95	54.66	3.07	48.99	1.44	67.22	9.21	55.97	6.78
Al ₂ O ₃	18.48	1.16	16.89	1.11	17.49	1.13	18.59	1.32	13.79	2.18	18.55	1.91
Fe ₂ O ₃	8.38	1.08	8.53	1.57	10.95	1.30	11.38	1.73	5.33	2.65	8.38	2.70
MnO	0.11	0.02	0.10	0.03	0.12	0.02	0.13	0.02	0.07	0.05	0.10	0.06
MgO	2.20	0.55	2.72	0.76	0.12	0.04	2.40	0.63	0.07	0.05	0.19	0.39
CaO	2.20	0.55	2.72	0.76	2.61	0.79	2.40	0.63	1.61	0.91	1.72	0.73
Na ₂ O	5.97	0.76	4.10	0.45	3.09	0.82	5.93	0.64	2.86	2.45	2.61	0.80
K ₂ O	1.64	0.24	1.08	0.28	1.49	0.31	1.94	0.35	0.81	0.46	1.34	0.76
TiO ₂	0.67	0.27	1.68	0.21	2.05	0.52	0.56	0.15	1.99	0.46	2.08	0.73
P ₂ O ₅	0.83	0.21	0.82	0.16	1.29	0.37	1.76	0.48	0.81	0.59	0.93	0.21
As	0.18	0.09	1.51	1.37	0.46	0.24	0.15	0.09	0.66	1.06	2.58	1.80
Ba	2.92	0.97	4.43	0.53	8.17	4.26	3.00	1.32	6.27	1.49	10.94	4.75
Co	888.83	168.66	1,419.00	408.16	1,526.33	854.01	621.67	212.36	1,242.73	345.36	1,499.26	710.69
Cr	30.46	4.49	22.29	2.81	35.17	8.06	42.67	8.67	18.33	8.85	26.34	12.53
Cu	110.54	36.00	120.00	40.52	91.17	26.23	95.11	48.26	114.40	100.54	284.17	161.57
Ni	58.04	17.68	20.29	13.76	50.83	45.29	81.89	28.48	55.13	36.95	187.63	164.22
Rb	65.17	11.92	46.43	10.21	67.33	24.88	53.00	9.19	51.93	10.15	75.31	25.19
Sr	42.63	7.74	73.14	8.84	86.17	19.84	37.00	3.39	80.67	20.24	97.89	52.59
V	206.63	25.02	134.71	33.87	182.50	82.06	238.22	35.78	122.00	100.46	199.49	81.90
Zn	208.00	66.41	154.86	28.42	200.00	54.09	467.89	159.56	105.87	80.09	158.06	62.07
Zr	35.38	8.38	61.86	11.47	104.67	13.11	58.78	45.16	69.07	19.35	91.86	34.16

4 Discussion

The six clusters found on the data set are believed to reflect local clay deposits and/or manufacturing traditions. However, the multiple compositional groups appearing in a ceramic assemblage of a single site (La Pijotilla or Porto Torrao) may represent either differences due to exchange, or differences in technical behaviour, which is more likely. If we look at the statistical analysis, it is clear that none of these compositional groups correspond to exchanged vessels. Nevertheless, there is an interesting 14% of pottery samples that does not cluster with the rest of the samples recovered at one site. Thus, this percentage of pottery may have been exchanged from its production site to other locations within social or trade networks. The pottery exchange follows a main east-west axis, while the west-east axis is only present between La Pijotilla and San Blas.

Regarding the isotopic composition of the mineral deposits and copper metallurgy related samples (metal objects and by-products), the diversity of sources for copper mineral procurement, involving different geological areas (not necessarily the closest mines were exploited), can be clearly observed. The lead isotope analysis of samples from the sites of San Blas and La Pijotilla also shows that exchange networks were in place.

5 Conclusions

The detection of a significant 14% of exchanged pottery seems to constitute reliable evidence of local network exchange flows or inter village alliances. Thus, pottery was probably being exchanged within and between settlement networks, but we cannot say at the moment if these exchanges were made directly between settlements, within an inter-settlement network exchange framework, i.e. between La Pijotilla and Porto Torrao, or if San Blas, Perdigões, and/or other settlements were acting as intermediary agents between both of them in a nodal exchange system.

The consistence in isotopic composition between the metal related archaeological samples from San Blas and La Pijotilla (with no evidence of copper smelting at this last site) points to San Blas as a production site, with a complex mineral procurement network, supplying metallic artefacts to La Pijotilla. This evidence provides a closer insight into the settlement network scale exchange systems, supporting the hypothesis of La Pijotilla as a central redistributive place, as previously argued by V. Hurtado (1995).

The interactions between San Blas and La Pijotilla could involve the exchange of copper items processed at San Blas, and the distribution of BB pottery from La Pijotilla to San Blas at an early stage of this network.

The picture of GRMB is complex: we have direct evidence of the exchange of metal objects from San Blas to La Pijotilla, and also evidence of La Pijotilla producing and distributing BB pottery to San Blas, Perdigões and Porto Torrao.

Although it was thought that copper resources were mined, processed and exchanged within local settlement networks, it appears that, like BB pottery, metal was also involved in broader exchange networks that included further settlement networks.

References

- Baxter MJ (1994) *Exploratory multivariate analysis in archaeology*. Edinburgh University Press, Exeter
- Clarke DL (1976) *Glockenbechersymposium, Oberreid, 18–23 März 1974*. Bussum, Unieboek, pp 459–77
- Dias MI, Valera AC, Prudencio MI (2005) Pottery production through the third millennium BC on a local settlement network in Fornos de Algodres, central Portugal. In: M Isabel Prudencio, M Isabel Dias, JC Warenbrough (eds) *Understanding people through their pottery*. Proceedings of the 7th European Meeting on Ancient Ceramics (EMAC'03) (42), pp 41–50
- Glascocock MD (1992) Neutron activation analysis in chemical characterization of ceramic pastes in archaeology. In: Neff H (ed) *Prehistory Press, Madison*, p 11–26.
- Hunt Ortiz MA (2003) *Prehistoric mining and metallurgy in South-West Iberian peninsula*. British Archaeological Reports, BAR International Series 1188. Archaeopress, Oxford
- Hurtado V (1995) Interpretación sobre la dinámica cultural en la Cuenca Media del Guadiana (IV–III milénios ANE). *Extremadura Arqueológica* V:53–80
- Hurtado V (1999) Los inicios de la complejización social y el campaniforme en Extremadura. *SPAL* 8:47–83
- Hurtado V (2008) Ídolos, estilos y territorios de los primeros campesinos en el sur peninsular. In: Cacho Quesada C et al (eds) *Acercándonos al pasado*. Prehistoria en 4 actos. Museo Arqueológico Nacional, CSIC, Madrid
- Hurtado V, Odriozola C (2008) Landscape, identity and material culture in “Tierra de Barros” (Badajoz, Spain) During the 3rd millennium BC. In: Salisbury RB, Thurston T (eds) *Reimagining regional analyses: the archaeology of spatial and social dynamics*. Cambridge Scholar Press, New York
- Odriozola, CP (in press) The two sides of the Guadiana: Inlaid pottery from 3rd millennium BC alongside the Guadiana River (Spain and Portugal). In: Biró TK (ed) *Vessels: inside and outside*. Papers presented at EMAC '07, 9th European Meeting on Ancient Ceramics. Budapest, Hungarian National Museum
- Valera AC (2006) A margem esquerda do Guadiana (região de Mourão), dos finais do 4º aos inícios do 2º milénio AC. *ERA-Arqueologia* 7:136–210

The Black Gloss Pottery in the Region of Ostia: Archaeology and Archaeometry

G. Olcese and C. Capelli

1 Introduction, Material and Questions

Archaeometric data on black gloss pottery (BGP) from the area of Ostia, as well as from central Italy, are scarce (Morel and Picon 1994; Olcese and Picon 1998; Niro Giangiulio 1999; Gliozzo and Memmi Turbanti 2004). The production was probably distributed among several workshops, as suggested by preliminary analyses on other contexts of Latium (Olcese 1998).

Recent excavations carried out by the Soprintendenza Archeologica di Ostia in the *Ager Portuensis* brought to light several Republican sites dated to a period between the fourth and the second centuries BC (Morelli et al. 2004; Morelli et al. 2008) (Fig. 1).

The excavated contexts, mainly unpublished, contain BGP associated with Greco-Italic amphorae (Olcese and Thierrin-Michael 2007) and local common wares. Among the BGP documented in the *Ager Portuensis*, the forms most frequently attested are the bowls Morel 2783 and 2784, and in minor quantities Morel 2621 (third century BC), which have an impressed decoration on the inside of the base (palmettes or rosettes), of the *petites estampilles* type or of the “Etruria/Latium” workshops.

Due to the lack of any identified workshops or kilns involved in the production of BGP and to the difficulty in making clear distinctions among this type of pottery on the basis of macroscopic characteristics, archaeometric analyses on samples from the *Ager Portuensis* have been carried out in the framework of the FIRB Project “Reconstructing the trade in the Mediterranean sea in the Hellenistic and

G. Olcese (✉)

Facoltà di Lettere e Filosofia, Dipartimento di Scienze storiche, archeologiche e antropologiche dell'antichità, Università di Roma “La Sapienza”, Roma, Italy
e-mail: gloria.olcese@uniroma1.it

C. Capelli

Dipartimento per lo Studio del Territorio e delle sue Risorse, Università di Genova, Genova, Italy
e-mail: capelli@dipteris.unige.it

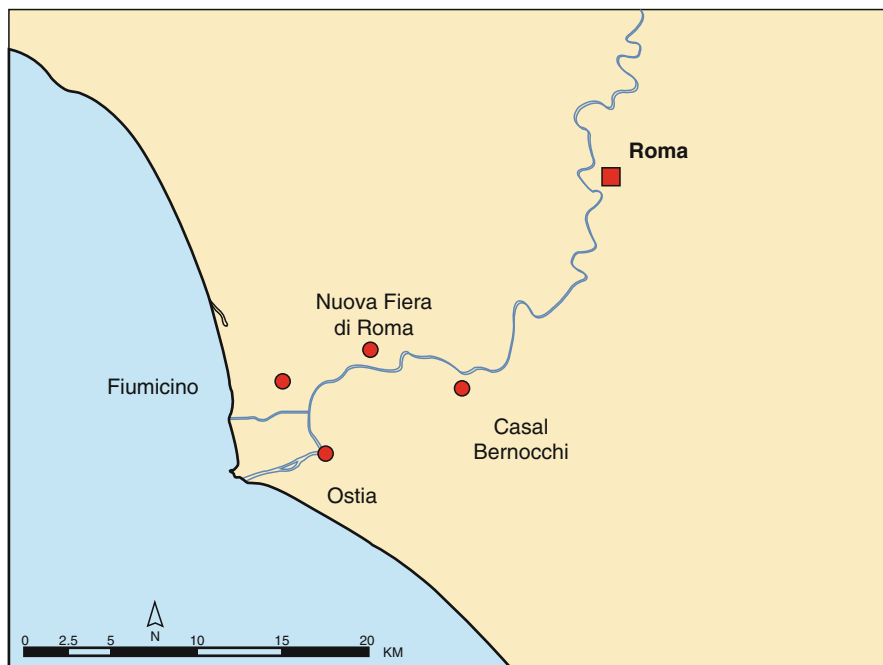


Fig. 1 Schematic map showing the location of Ostia and *Ager Portuensis*

Roman periods through new scientific and technological approaches” (<http://www.immensaequora.org>).

Chemical analyses by X-ray Fluorescence (WDS) of ten major and 13 trace elements have been performed by a Philips PW 1480/10 spectrometer on 40 samples (in glass tablets) at the laboratories of CNR/IGG, Rome. Moreover, petrographic analyses (thin section observation under polarising microscope) have been carried out on 38 samples.

This study was aimed at contributing to answer the following questions: (a) was there one or many production centres of BGP? (b) what are the characteristics of the BGP from the *Ager Portuensis*? (c) was there a local production of BGP?

2 Analytical Results

The integration of chemical and petrographic analyses has allowed the identification of a relatively homogeneous group ($n = 29$), consisting mainly of samples recovered in Ostia. The group includes large bowls – Morel 2538, 2621, 2775, 2783, 2784 (beginning of the third century BC) and the bowls Morel 1312, 2534, and 2788 (second century BC) (Fig. 2).

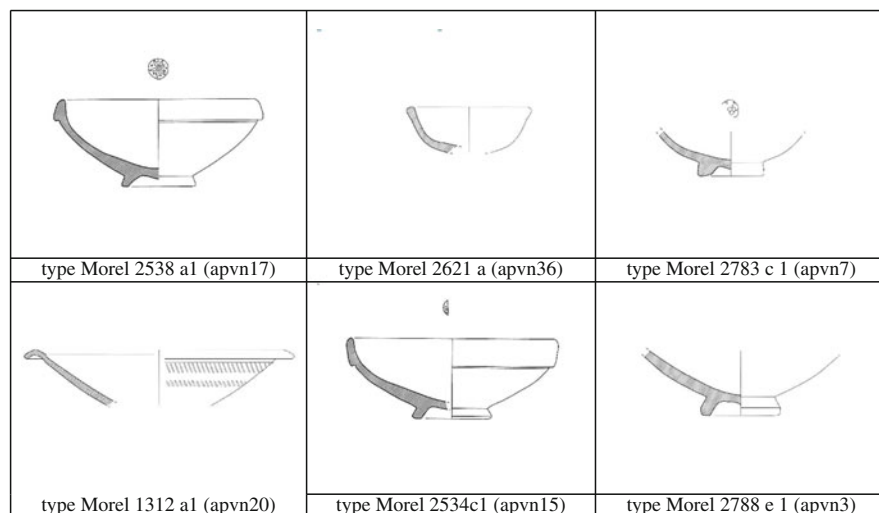


Fig. 2 Main types of black gloss pottery from *Ager Portuensis*

The objects in this group are slightly different in morphological features and macroscopic characteristics of the black gloss from BGP samples of the same types found in other distant or neighbouring areas.

The mean values of the chemical data of the “Ostia-*Ager Portuensis*” group are listed below.

		Oxide wt%												
		SiO ₂	TiO ₂	Al ₂ O ₃	FeO	MnO	MgO	CaO	Na ₂ O	K ₂ O	P ₂ O ₅			
m		55.64	0.81	18.30	7.21	0.16	2.73	10.91	1.03	2.42	0.27			
σ		2.21	0.03	0.69	0.38	0.03	0.19	2.01	0.16	0.20	0.03			
		ppm												
		Rb	Sr	Y	Zr	Zn	Th	Pb	Cr	Ni	V	Ce	Ba	La
m		121	401	27	208	98	20	35	111	62	124	108	613	65
σ		26	56	2	21	9	3	6	9	6	21	10	40	14

Under the microscope, the “Ostia-*Ager Portuensis*” group fabrics are characterised by a generally oxidised Fe-rich clay matrix and numerous fine-grained aplastic inclusions (<0.1–0.2 mm in size), mainly consisting of quartz, mica and feldspar grains (Fig. 3a).

Microfossils ± limestone fragments (partially or totally dissociated by firing) are often present, sometimes abundant. Titanite, amphibole, clinopyroxene and chert, claystone, and volcanic rock fragments are accessory components. Several subgroups are recognisable due to variability in grain size of inclusions, relative ratio of the various components, firing temperature, oxidation degree, and, in most cases, coating features (for the black gloss technology, see Maggetti et al. 1981;

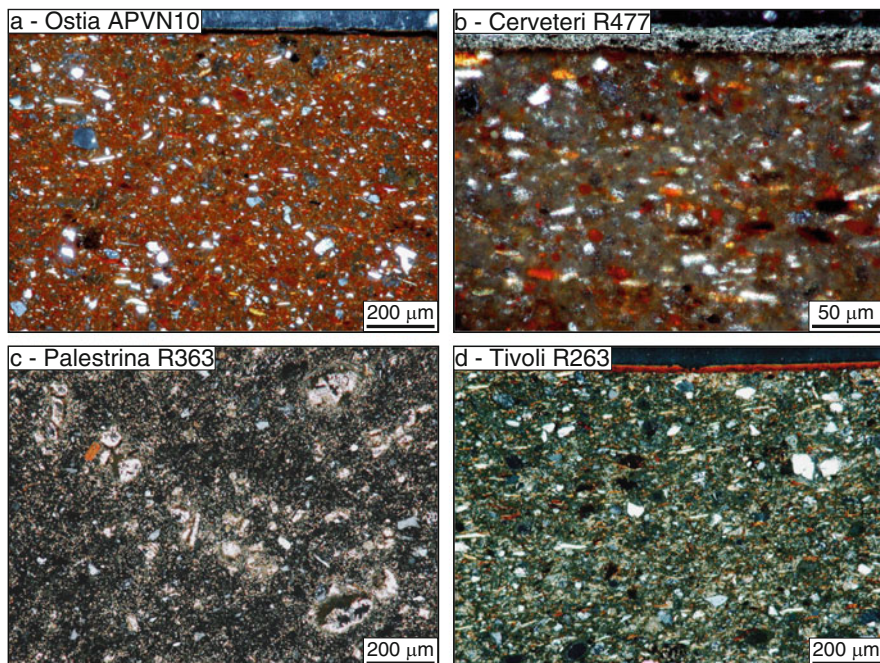


Fig. 3 (a–d) Microphotographs (crossed polars) of representative samples of the groups discussed in the text

Gliozzo et al. 2004). This variability is possibly related to different productions/workshops in one geological/production area.

In terms of chemical composition, the “Ostia-Ager *Portuensis*” group differs from the BGP analysed samples recovered in other sites of Latium (Rome, Cerveteri, Segni, Tivoli, and Palestrina; for the reference groups, see Olcese 1998).

Preliminary thin section analyses on a few representative samples from Cerveteri, Palestrina and Tivoli confirm the textural and mineralogical differences from the “Ostia-Ager *Portuensis*” group. The main petrographic features of these samples are listed below.

Cerveteri (two samples): very fine-grained inclusions (<0.1 mm) formed by mica (dominant), quartz, feldspar and accessory titanite; no volcanic elements have been found (Fig. 3b).

Palestrina (one sample): Ca-rich poorly oxidised matrix; abundant fine-grained inclusions (<0.1 mm) formed by calcareous microfossils (dominant), quartz, feldspar, subordinate mica, accessory clinopyroxene, amphibole, titanite, and chert fragments (Fig. 3c).

Tivoli (one sample): Ca-rich clay matrix; very abundant fine-grained inclusions (<0.1 mm), formed by calcareous microfossils, sponge spiculae, quartz, micas, feldspars, and accessory amphibole, epidote, tourmaline, melanitic garnet, and volcanite fragments (Fig. 3d).

3 Conclusive Remarks

New data about the BGP from the area of Ostia were obtained through an integrated archaeological, chemical and petrographic approach. A possibly “local” group has been identified. The fabrics of the “Ostia-*Ager Portuensis*” group contain inclusions related to the alkali-potassic volcanites outcropping in southern Tuscany, Latium and Campania, which on one hand excludes a provenance from Northern Etruria, and, on the other hand, does not exclude a local/regional production.

The “Ostia” group differs in both chemical and petrographic features from characteristic samples of neighbouring sites of Latium. In addition to this, the majority of BGP samples from Ostia and *Ager Portuensis* show a chemical composition different from samples from other production centres in Campania (Morel and Picon 1994; Olcese et al. 1996), as well as in northern Etruria (Gliozzo and Memmi Turbanti 2004).

References

- Gliozzo E, Memmi TI (2004) Black gloss pottery: production sites and technology in northern Etruria, Part I: provenance studies. *Archaeometry* 26(2):201–225
- Gliozzo E, Kirkman IW, Pantos E, Memmi TI (2004) Black gloss pottery: production sites and technology in northern Etruria, Part II: gloss technology. *Archaeometry* 26(2):227–246
- Maggetti M, Galetti G, Schwander H, Picon M, Wessicken R (1981) Campanian pottery: the nature of black coating. *Archaeometry* 23(2):199–207
- Morel JP, Picon M (1994) Les céramiques étrusco-campaniennes: recherches en laboratoire. In: *Ceramica romana e archeometria: lo stato degli studi*, Atti delle Giornate Internazionali di Studio, Castello di Montegufoni (Firenze). 26–27 aprile 1993, a cura di Olcese, G., Firenze, pp 23–46
- Morelli C, Olcese G, Zevi F (2004) Scoperte recenti nelle saline portuensi (*Campus salinarum romanarum*) e un progetto di ricerca sulla ceramica ostiense in età repubblicana. In: Gallina Zevi A. and Turchetti R., (a cura di) *Anciennes routes maritimes méditerranéennes, Méditerranée occidentale antique: les échanges*, Rubbettino Editore ANSER, 43–55
- Morelli C, et al. (2008) The landscape of the *Ager Portuensis*, Rome: some new discoveries, 2000–2002. In: Lock G, Faustoferri A (a cura di) *Archeologia e territorio nell’Italia centrale: in ricordo di John A. Lloyd*. University of Oxford School of Archaeology, Oxford, 213–231
- Niro Giangiulio M (1999) La ceramica a vernice nera di età ellenistica. In: Chiaramonte Trerè C (a cura di) *Tarquinia, scavi sistematici dell’abitato. I materiali*, Roma
- Olcese G (1998) Ceramiche a vernice nera di Roma e area romana: i risultati delle analisi di laboratorio, Indagini archeometriche relative alla ceramica a vernice nera: nuovi dati sulla provenienza e la diffusione, In: *Atti del Seminario internazionale di Studio*, Milano 22–23 novembre 1996. Edizioni New Press, Como, 141–152
- Olcese G, Picon M (1998) Ceramiche a vernice nera in Italia e analisi di laboratorio: fondamenti teorici e problemi aperti, In *Atti del Seminario internazionale di Studio*, Milano 22–23 novembre 1996. Edizioni New Press, Como, pp 31–37
- Olcese G, Picon M, Thierrin-Michael G (1996) Il quartiere ceramico sotto la chiesa di Santa Restituta a Lacco Ameno d’Ischia e la produzione di anfore e di ceramica ellenistica. *Bollettino di Archeologia* 39–40:7–29
- Olcese G, Thierrin-Michael G (2007) Greco-italic amphorae in the region of Ostia: archaeology and archaeometry, EMAC ’07, Budapest, 24–27 ottobre 2007 (abstract p. 106; text in press)

Recognising Frit: Experiments Reproducing Post-Medieval Plant Ash Glass

S. Paynter and D. Dungworth

1 Introduction

Archaeological excavation on the site of a seventeenth-century coal-fired glasshouse at Vauxhall, London, recovered a quantity of opaque, light purple to pale blue/green material. Although the material itself was highly crystalline, the bulk composition matched samples of the transparent, pale-green glass made at the glasshouse, confirming that it was glassworking waste of some kind. The material was reported as frit (Tyler and Wilmott 2005) but alternative interpretations have also been proposed (Dungworth 2007). The authors therefore examined samples of the material with a scanning electron microscope (Fig. 1) but the conclusive identification of the material was hindered by uncertainty about what frit should look like, particularly after being buried for hundreds of years.

The glass made at Vauxhall was of a type common from the late sixteenth century onwards, when glass workers from Lorraine and Normandy came to England (Kenyon 1967). This type of glass contains more lime but less potash than earlier English glass, so is sometimes referred to as “high-lime low-alkali” or HLLA glass (Mortimer 1997). Previous studies analysing archaeological glass, potential raw materials and experimentally replicated glass, suggest that HLLA glass was produced from plant ashes and a source of silica, such as sand or quartz pebbles (for example O’Brien et al. 2005; Sanderson and Hunter 1981; Smedley and Jackson 2002; Stern and Gerber 2004; Turner 1956).

The composition of plant ashes varies greatly with many factors, including the species of plant. Historical accounts of glass production from plant ashes refer to beech and oak ash amongst others (for example Hawthorne and Smith 1979; Hoover and Hoover 1950) and the ratios of elements in the ashes of these hard wood species,

S. Paynter (✉) and D. Dungworth
English Heritage, Fort Cumberland, Fort Cumberland Road, Eastney, Portsmouth PO4 9LD, UK
e-mail: sarah.paynter@english-heritage.org.uk

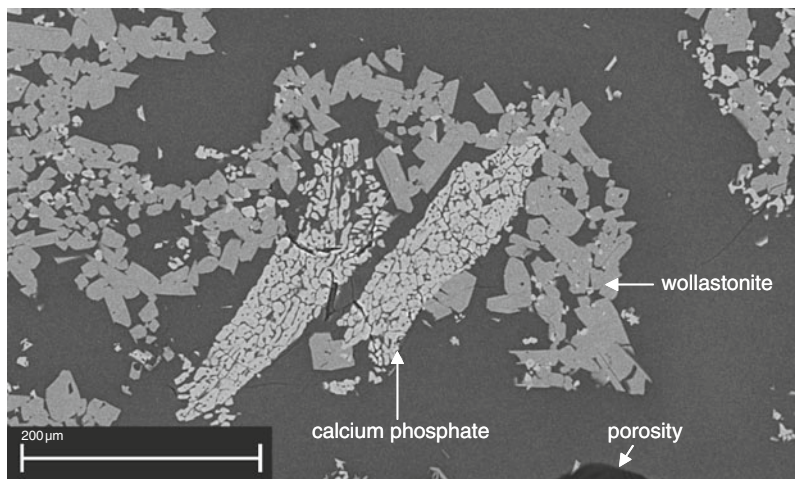


Fig. 1 Vauxhall glass waste: the microstructure comprised a glassy matrix (*dark grey*) surrounding the crystalline phases wollastonite (*mid-grey*) and calcium phosphate (*light grey*), porosity (*black*) and weathered crystals (not shown in image), but no surviving quartz

which are dominated by calcium compounds, are most comparable with the ratios detected in HLLA glass. The same accounts often describe a fritting or calcining step in glass production. Although there are inconsistencies between the accounts, they often describe mixing before and during fritting. The process also appears to be lengthy, requiring a day or more. The temperatures used for fritting were less than those used for melting the glass, with the process generally taking place in a Calcar built for the purpose, or in an upper hearth of the furnace. During fritting, moisture and gases were driven off and reactions between the batch materials were initiated (Smedley et al. 1998; Verità 2005) but the temperatures were insufficient to form a homogenous glass. Although vitrification and the formation of lumps are described in some accounts, the product is described as white rather than completely glassy and transparent, and Theophilus warns against allowing the batch to agglomerate (Hawthorne and Smith 1979). Therefore fritting temperatures in the region of 750–900°C (Smedley et al. 1998; Turner 1956; Verità 2005) have been suggested, although the conditions would be expected to vary for different glass compositions.

Archaeological evidence of the fritting process remains elusive, and although material from archaeological investigations has on rare occasions been claimed as frit (Kenyon 1967; Tyler and Wilmott 2005), such interpretations are often contentious. For example, Crossley (1967) asks

Whether the fused glass ‘frits’ found at Knighton’s and St. Weonards were not waste. Modern frit is not usually heated beyond a loose granular formation which if dropped on site would soon cease to be easily recognisable.

2 Aims

The goal of this research was to experimentally recreate HLLA glass from plant ashes and sand including a fritting stage in the process, so that the appearance and microstructure of a frit could be characterised. The experimental frit is described and compared to the archaeological material from the Vauxhall glasshouse.

3 Experimental Methods

The experimental glass was produced using ash from a 0.3 m thick oak branch, which was cut from a tree in the Weald in the south of England, which was an important medieval and post-medieval glassmaking area (Kenyon 1967). The complete branch was burnt in a grate at approximately 800°C and the ash was therefore from mixed heartwood, sapwood and bark. Beach sand from the south of England was used, sieved through a 0.5 mm sieve, with the majority of grains approximately 0.2 mm in diameter. The compositions of the oak ash and sand were determined by XRF analysis and used to estimate the proportions of each needed to produce an HLLA type glass. The oak ash XRF data were in the form of weight percent oxides by convention, and compared well with literature data (for example Stern and Gerber 2004). XRD analysis showed that, although the ash was dominated by lime immediately after burning, over time this reacted to form portlandite ($\text{Ca}(\text{OH})_2$) and then calcium carbonate; the latter was the dominant form when the ash was actually used. This is consistent with the data of Sanderson and Hunter (1981), which suggest that only about 42 wt% of the ash contributes to the glass composition and the rest is lost during heating, for example as water and carbon dioxide. Taking this into account, the proportions required to produce a glass of HLLA type composition were calculated as about 1:1 ash to sand by weight; this was the ratio used to make the experimental glass batches described here. The batches were heated to a series of trial fritting temperatures, starting at 800°C, and held at temperature for at least 7 h. Batches were heated to temperatures of up to 1,350°C in order to melt them.

4 Analytical Methods

After heating to different temperatures, the experimental glass batches were examined using scanning electron microscopy (SEM). The crystalline phases present were identified using an X-ray diffractometer (XRD). This short paper focuses on the microstructures produced; however samples of the batches and raw materials (ash and sand) were also analysed using an energy dispersive spectrometer (EDS) attached to the SEM and using an X-ray fluorescence (XRF) spectrometer; the results of these analyses will be published separately.

5 Results

The experiments investigated a wide range of influences on the fritting process, including time, temperature, sand particle size, stirring and small additions of other raw materials. Each of these variables impacted on the microstructures that developed under different conditions but, due to space constraints, these aspects of the results will be reported elsewhere. The emphasis of this paper is on the microstructures and phases that developed, which were of similar types in all cases.

After heating to 800°C for 7 h the batch remained powdery. SEM examination (Fig. 2) of the batch revealed quartz grains (dark-grey) surrounded by a thin layer of potassium- and calcium-rich glass (mid-grey) and then an outer layer of an alkali calcium phosphate silicate phase (light grey). Surrounding these reacting grains, although hardly visible in the SEM image, are the lime-dominated remains of the oak ash. The batch was analysed at intervals over the weeks following the experiment, during which time the lime reacted to form portlandite, eventually returning to calcium carbonate. In an archaeological context, however, this heterogeneous, powdery material would be easily dispersed, as it contains insufficient glass matrix to provide cohesive strength, and it would become difficult to recognise. Most of the components, with the exception of the quartz grains, would also be highly susceptible to weathering through processes such as the leaching of the alkalis. Therefore the absence of material fitting this description in the archaeological record is not surprising.

Batches heated to 1,050°C for 7 h became lightly cemented with wollastonite also forming. As the temperature approached 1,300°C, sufficient glass had formed for a sample to be taken on a gathering iron, although the high proportion of crystalline phases and bubbles in the mixture caused samples to appear opaque

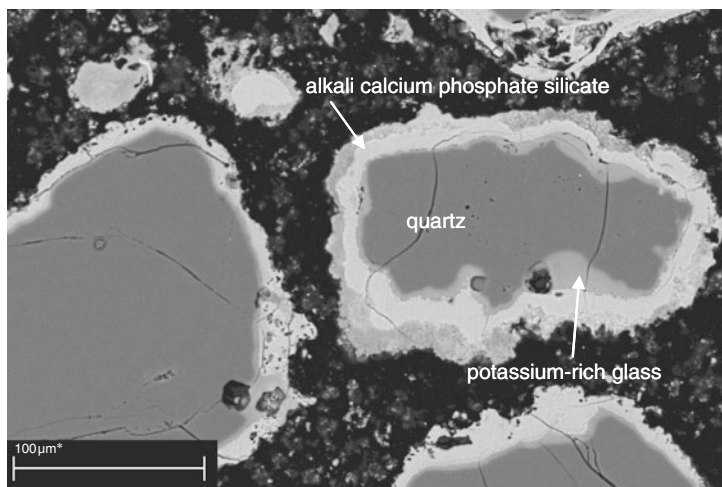


Fig. 2 Experimental glass batch after 7 h at 800°C, see text for description of microstructure

white. This heterogeneous material contained occasional quartz grains, cristobalite, wollastonite and considerable porosity. The increased proportion of glass would give these more vitrified materials improved cohesive strength and the crystalline phases present would also be less susceptible to weathering, therefore these materials would be more likely to survive in a recognisable form.

For a 1:1 ratio of oak ash to sand, a temperature of 1,350°C was required to melt the batch, consistent with the results of other researchers for experimental and archaeological glasses of comparable composition (Cable and Smedley 1987; Stern and Gerber 2004). The composition of the glass produced was very similar to archaeological HLLA glass, with the exception of a small but important difference in the alkali content, the significance of which will be discussed elsewhere.

6 Conclusions

Although the overall composition of the material from Vauxhall matches the HLLA glass made at the site, the material is compositionally heterogeneous and contains several crystalline phases, in common with the experimental fritted batches described in this paper. However there are differences between the archaeological material and the experimental frit, which indicate that the two were produced in different ways. Some quartz persisted to high temperatures in our experimental batches whereas no quartz survived in the archaeological material and there was a large proportion of glass in the latter, perhaps as a result of the addition of cullet and/or prolonged heating times and durations for some components of the batch. Yet, a phosphorus-rich constituent was added to the Vauxhall glass batch at a late stage, as precipitated calcium phosphate crystals survived in localised regions (Fig. 1). Therefore the archaeometric investigation of the material from the Vauxhall glasshouse indicates that it is probably an intermediate between the fritting stage and the final HLLA glass product. Whether a material with such a significant glassy proportion is ultimately referred to as “frit” depends on the definition of frit being used; for some, this would be inconsistent with the friable material described in documentary accounts and a more precise term such as “partially made glass” would be preferred.

References

- Cable M, Smedley JW (1987) Liquidus temperatures and melting characteristics of some early container glasses. *Glass Technol* 28(2):94–98
- Crossley DW (1967) Glassmaking in Bagot’s Park, Staffordshire, in the sixteenth century. *Post-Medieval Archaeol* 1:44–83
- Dungworth D (2007) Review of John Baker’s Late 17th-century Glasshouse at Vauxhall. *Post-medieval Archaeol* 41(1):208–209
- Hawthorne JG, Smith CS (1979) *Theophilus, on divers arts*. Dover Publications, New York

- Hoover HC, Hoover LH (1950) *Georgius Agricola, De Re Metallica*. Dover Publications, New York
- Kenyon GH (1967) *The glass industry of the Weald*. Leicester University Press, Leicester
- Mortimer C (1997) Appendix 1: Analysis of the glass, In Welch C.M., *Glass-making in Wolseley, Staffordshire*. *Post-Medieval Archaeol* 31:38–43
- O'Brien C, Farrelly J, Paynter S (2005) *The 17th-century glasshouse at Shinrone, Co Offaly, Ireland*, Unpublished Centre for Archaeology Report 39/2005. English Heritage, Swindon
- Sanderson DCW, Hunter JR (1981) Compositional variability in vegetable ash. *Sci Archaeol* 23:27–30
- Smedley JW, Jackson CM, Booth CA (1998) Back to the roots: the raw materials, glass recipes and glassmaking practices of Theophilus. In: McCray P, Kingery WD (eds) *The prehistory and history of glassmaking technology, Ceramics and civilization* 8. American Ceramic Society, Westerville, pp 145–65
- Smedley JW, Jackson CM (2002) Medieval and post-medieval glass technology: batch measuring practices. *Glass Technology*, 43(1):22–27
- Stern WB, Gerber Y (2004) Potassium-calcium glass: new data and experiments. *Archaeometry* 46(1):137–156
- Turner WES (1956) Studies in ancient glasses and glassmaking processes. Part V. Raw materials and melting processes. *J Glass Technol* 40:277T–300T
- Tyler K, Wilmott H (2005) *John Baker's late 17th-century glasshouse at Vauxhall*, MoLAS Monograph 28. Museum of London Archaeology Service, London
- Verità M (2005) Comments on W. B. Stern and Y. Gerber, 'Potassium-calcium glass: new data and experiments', *Archaeometry*, 46(1)(2004):137–56. *Archaeometry* 47(3):667–669

Archaeometric Investigation of Early Iron Age Glasses from Bologna

A. Polla, I. Angelini, G. Artioli, P. Bellintani, and A. Dore

1 Introduction

1.1 Glass Beads from the Villanovan Graves of Bologna: The Archaeological Context

There is very little evidence of glass objects in the necropolises of the Bologna area during the Villanovan I period (ninth century BC). None of the few existing glass objects have the typical diagnostic typologies, such as the small blue beads on fibulae, which appear late in the period. During the Villanovan II phase (820–770 BC), a new style of rather precious fibulae appears, together with pins carrying glass beads of ever increasing dimensions. A further remarkable variation in the typology of the glass artefacts occurs during the Villanovan III phase (770–680 BC). The beads of this period, commonly inserted on metallic pins with composite head and fibulae with glass coated bows, are rather peculiar of the Bologna area. The decorated beads of this age have different typologies: mostly they show simple- or stratified-eye motifs, and sometimes wave patterns. In the Villanovan III phase, an increasing use of coloured glass is evident: opaque and transparent yellow glass,

A. Polla (✉)

Dip. di Scienze della Terra, Università degli Studi di Milano, Via Botticelli 23, I-20133, Milano, Italy

e-mail: angela.polla@unimi.it

I. Angelini and G. Artioli

Dip. di Geoscienze, Università degli Studi di Padova, Via Giotto 1, 35137 Padova, Italy

e-mail: ivana.angelini@unipd.it; gilberto.artioli@unipd.it

P. Bellintani

Soprintendenza per i Beni Archeologici della Provincia Autonoma di Trento, Via Aosta 1, 38100 Trento, Italy

e-mail: paolo.bellintani@provincia.tn.it

A. Dore

Museo Civico Archeologico di Bologna, Via dell'Archiginnasio 2, 40124 Bologna, Italy

e-mail: anna.dore@comune.bologna.it

transparent light blue glass, and colourless glass are found to be progressively more diffused. Variations in the decorations are also attested, such as the eye motif with concentric circles pattern. A specific group of large triangle-shaped beads having spiral glass wires circling around the top represents a category extensively diffused from Northern Europe to the Near East, with a substantial concentration in the Aegean region, which is probably the original production area.

In summary, first, the well-known Final Bronze Age glass workshops of the Frattesina area seem to present no continuation during the Early Iron Age, based on the typology of artefacts. This is attested by the disappearance of the popular Late Bronze Age bead typologies and by the very scarce occurrence of glass beads during the ninth century BC, both in Bologna and in the Veneto area (Este).

Second, during the Villanovan phases of Bologna, particularly starting from the eighth century BC, some of the diagnostic typologies suggest a possible glass import from Southern Italy and/or from the Aegean, and of local production and/or working. To date, there is insufficient analytical data in the literature on coeval European materials to warrant a precise comparison (Brill 1999; Towle et al. 2001).

2 Materials

The samples analysed in the present work are 34 carefully selected beads from the necropolises of Bologna, all dated to the period between the ninth and the seventh centuries BC. The investigated beads differ in typology: annular, toroidal and globular beads; and in the type of decorations: wave, spiral, point and eye beads. The colours of the glass are: blue, amber, yellow, black, red, and white. Generally, pale blue and amber glass objects are transparent, whereas dark blue, black, yellow, white and red ones are opaque.

3 Experimental Techniques

3.1 SEM-EDS and EPMA Chemical Analysis

Microsamples have been taken from the surface of the beads, embedded in epoxy resin, polished and carbon coated in order to be analysed using Scanning Electron Microscopy with Energy Dispersive Spectroscopy (SEM-EDS). The chemical composition of the glass phases and of the large crystal inclusions were carried out by Electron Probe Microanalysis (EPMA).

3.2 *Image Analysis*

Backscattered electron images obtained by SEM were used to study the fabric and texture of the glasses and to identify the different inclusions.

In the opaque glass, crystal inclusions are present, generally uniformly dispersed in the matrix, except for few yellow glass specimens showing a band distribution. All the opaque yellow glasses contain lead antimonate crystals, whereas in the white decorations calcium antimonate crystals are present. Antimonate crystals in both glass types are present as single particles or as crystal aggregates, with size in the order of 1–60 μm .

In the coloured opaque glass, the crystals are generally uniformly dispersed in the matrix, except in few yellow glass specimens showing a band distribution. The red decorations are characterised by the presence of dispersed Cu–Fe particles of very small size, in the order of 1–2 μm ; only in one red sample the inclusions are arranged in layered structures.

Transparent blue glasses are generally rather homogeneous and show rare crystalline inclusions (mostly quartz); occasionally, thin alteration layers due to depletion in alkali elements are visible. In the opaque blue glasses, there are different kinds of inclusions, such as calcium antimonate, (Na,Ca)-silicates, and lead antimonate crystals.

Digital Image Processing (DIP) has been applied to the SEM backscattered images in order to quantify the relative proportion between the glassy matrix and the inclusions: all the analysed samples fall into the class of true glasses (Angelini et al. 2004; Polla et al. 2006).

4 Results and Discussion

The beads show numerous different typologies, and a few are unique pieces, such as one cylindrical bead and one large triangular bead with spiral decoration. The archaeometric data obtained have been studied both as a function of the age and of the typology of the glass.

The analytical results show a wide range in the chemical composition of the samples; this makes their classification difficult from the point of view of elemental chemistry. It is possible to identify a few parameters that can be used to divide the samples into different groups, although it is not yet possible to define a univocal time-composition relationship that can be used to follow and rationalise the technological developments of the period.

4.1 *Main Elements Chemistry*

The MgO/K₂O diagram (Fig. 1), generally used to classify the different classes of prehistoric glass materials, shows a substantial number of points outside the

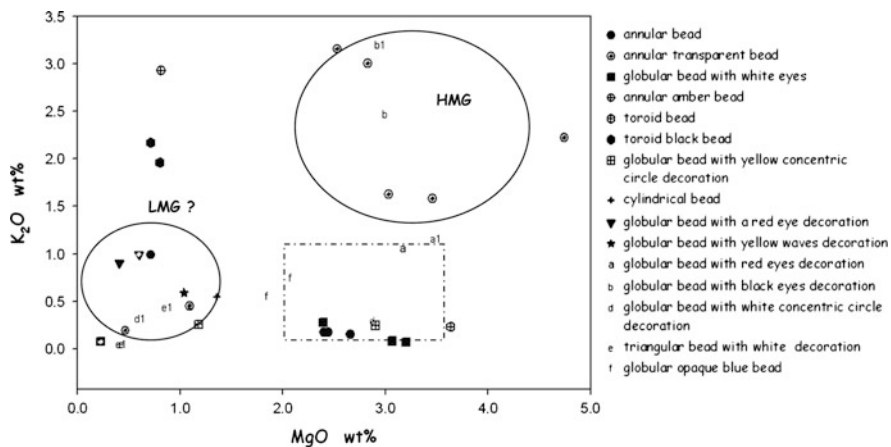


Fig. 1 MgO vs K₂O (wt%). The samples from the beads bodies with decoration are reported with the full symbols and letter of the alphabet, while the decorations are reported with the full symbols and letter with l

commonly recognised LMG (Low Magnesium Glasses), HMG (High Magnesium Glasses) and LMHK (Low Magnesium High Potassium glasses) compositional fields (Angelini et al. 2004, 2005).

The group of samples comparable to the HMG class is mainly composed of blue transparent beads and one globular blue bead with black decorations.

In the highlighted area (enclosed by dashed-dotted line in Fig. 1), several samples of different typology are clustered (globular, toroidal, annular and eye beads), mostly having a blue body with white and yellow decorations. These samples are close to the HMG field, though they consistently show a slightly lower K₂O content, a higher content of Al₂O₃ (4–6 wt%), and the presence of Mn, Co and Ni in variable amounts.

The group of samples comparable to LMG is actually spread on an area considerably larger than the usual field of LMG glass. These samples are chemically heterogeneous and include materials having a much lower percentage of CaO (2–4 wt%) than the typical LMG glass. Most white glasses used for bead decorations fall in this group. Even if the white glasses are opacified with Ca antimonate, the glass matrix far from the crystal inclusions systematically has a low Ca amount, as shown by a large number of point analyses.

Outside these three main areas (LMG, HMG, and HMG with low K₂O, Fig. 1), some of the samples have rather unusual compositions: two large globular or “toroidal” black beads are characterised by a high Na₂O content (19–20 wt%), one annular amber bead is rich in Al₂O₃ (8.5 wt%) and Na₂O (22 wt%), and two blue opaque beads contain lead antimonate in the PbO-rich glass matrix.

4.2 Pigments and Decorations

The coloured glass used for decorations can be adequately described and classified on the basis of the FeO–PbO–CaO (Fig. 2) diagram. It is worth noting that when glass materials of similar colour are used in the body and in the decorations, they usually carry a different chemical signature. For example, the yellow decorations have a higher PbO content (28–36 wt%) than the similarly coloured yellow bodies (PbO 19–34 wt%). In these samples, the lead antimonate particles were used for the characteristic opaque yellow coloration.

The coloration of opaque blue glasses enriched in PbO seems related to the presence of low percentages of other elements, Cu and Fe. In the investigated samples, Cu is rarely used as the main pigmenting agent, and only very few HMG and LMG samples are characterised by an appreciable Cu content (about 1 wt%). This is a remarkable difference with respect to the Bronze Age blue glasses, which are generally very rich in copper. Some of the Villanovan dark blue samples contain Co in trace amounts, and a number of them also show a considerable amount of iron

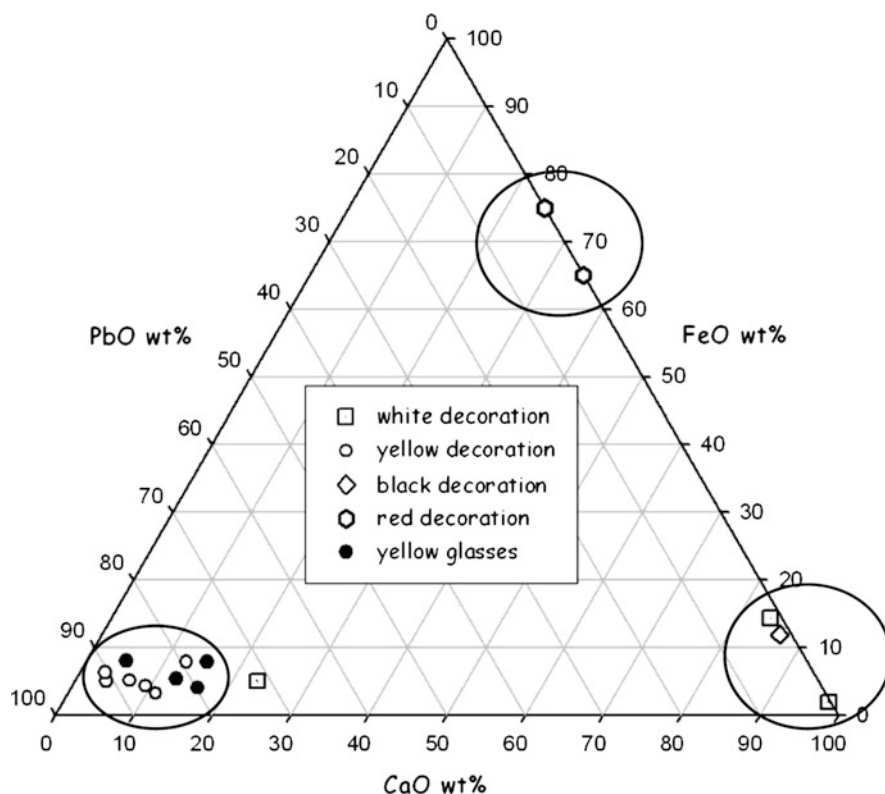


Fig. 2 CaO–FeO–PbO (wt%) ternary plot of glass decorations and yellow glasses

(FeO even up to 12 wt%). For these samples with mixed cations, it is impossible to interpret the origin of the colour without detailed spectroscopic investigation.

5 Conclusions

The present investigation shows the chemical and textural complexity of the materials studied. As a matter of fact, the analysed Early Iron Age materials are completely different from the previous glass known from the Final Bronze Age, as they show entirely different typologies and chemical composition.

The glass samples from the Early Iron Age show significant variability in terms of major element composition (Na, K, Mg, Al) and in the colorant elements (Cu, Co, Fe).

Yellow glass objects appear for the first time in Northern Italy, and their vitreous matrix is characterised by a peculiarly high lead concentration.

The identification of the raw materials used for the production of glass is complicated by their very heterogeneous chemical composition. A more extensive database of different bead typologies and ages is necessary in order to allow an overall interpretation of the data. The recycling of earlier materials seems to be a possible explanation for the high chemical variability of the glass.

Acknowledgements The Museo Civico Archeologico di Bologna is kindly acknowledged for making the samples available for the investigation.

References

- Angelini I, Artioli G, Bellintani P, Diella V, Gemmi M, Polla A, Rossi A (2004) Chemical analyses of Bronze age glasses from Frattesina di Rovigo, Northern Italy. *J Archaeol Sci* 31:1175–1184
- Angelini I, Artioli G, Bellintani P, Polla A, (2005) Protohistoric vitreous materials of Italy: from early faience to Final Bronze Age glasses *Annales du 16e Congrès de l'Association Internationale pour l'Histoire du Verre*, 7–13 September 2003, London, UK, 32–36
- Brill RH (1999) *Chemical analyses of early glass*. Corning Museum of Glass, New York
- Polla A, Angelini I, Artioli G (2006) Analisi d'immagine digitale su materiali vetrosi. *Atti XXXIX Riunione Scientifica I.I.P.P.* pp 1621–1626
- Towle A, Henderson J, Bellintani P, Gambacurta G (2001) Frattesina and Adria: report of scientific analyses of early glass from the Veneto. *Padusa* 37:7–68

Non Invasive Study of Nineteenth Century Iranian Polychrome Underglaze Painted Tiles by Fibre Optic Visible Reflectance Spectroscopy

I. Reiche, C. Boust, J.-J. Ezrati, S. Peschard, J. Tate, L. Troalen, B. Shah, B. Pretzel, G. Martin, S. Röhrs, and F. Voigt

1 Introduction

This paper presents the first results of the application of fibre optic visible reflectance spectroscopy to a group of fourteen underglaze polychrome painted tiles from nineteenth century Iran. The measurement of the entire range of colours appearing on the tiles is aimed at investigating the practices of the Persian master potter Ali Muhammad Isfahani (AMI), who was active in his workshop in Tehran between 1884 and 1893, according to his signed works. In an earlier study, an analytical approach for the non destructive investigation of underglaze painted ceramics was developed, combining microanalytical X-ray methods for the determination of the chemical composition of the glaze (micro X-ray fluorescence, XRF or micro proton induced X-ray and gamma-ray emission, microPIXE/PIGE) with microRaman and visible reflectance spectroscopy, intended to identify more particularly the types of colorants and pigments used (Reiche et al. 2009).

As the visual examination of the tiles from this period reveals, a much broader range of colours was used as compared to previous centuries, so that new types and mixtures of pigments were expected. Combined with information regarding the glaze

I. Reiche (✉), C. Boust, J.-J. Ezrati, and S. Peschard
Laboratory of the Centre for research and restoration of the French Museums. (LC2RMF), UMR 171 CNRS French Ministry of Culture and Communication, Palais du Louvre, 14 quai François Mitterrand, 75001 Paris, France
e-mail: ina.reiche@culture.gouv.fr

J. Tate, L. Troalen, and F. Voigt
Department of Conservation and Analytical Research and Department of World Cultures, National Museums Scotland, Chambers Street, Edinburgh EH1 1JF, UK

B. Shah, B. Pretzel, and G. Martin
Science Section, Conservation Department, Victoria and Albert Museum, South Kensington, London SW7 2RL, UK

S. Röhrs
Conservation and Scientific Research, The British Museum, Great Russell Street, London WC 1 B3 DG, UK

and body compositions, we hoped that characterising these pigments would help in dating the objects with more accuracy, and in ascribing them to individual workshops. However, Persian tiles sometimes exhibit transparent glaze layers which may be up to 1 mm thick over the pigment or coloured glaze layers, and the determination of the colouring species is not straightforward using the generally applied X-ray based methods, such as X-ray fluorescence spectroscopy. The X-ray techniques present inherent limitations because, without taking samples, they cannot always reach the coloured layers under the transparent glaze and provide information about the molecular composition and valence state of the colouring material, information which, in contrast, may be obtained with optical methods such as visible spectroscopy.

2 Material and Experimental Equipment

The fourteen tiles analysed in the present study come from the National Museums Scotland, Edinburgh (NMS), the Victoria and Albert Museum, London (V&A), the Middle East Department (ME) of the British Museum, London (BM), and a private collection (PC). The range of objects selected covers tiles signed by AMI (group A), tiles known to have been bought from his workshop according to written sources (group B), samples ascribed to him for stylistic reasons (group C), and tiles dating from the second half of the nineteenth century but originating from a different Iranian production centre, probably Isfahan (group D) (Table 1).

A portable spectro-photo-goniometer was used to investigate the visible light reflectance spectra of the coloured area of the tiles (Dupuis et al. 2002). This instrument is a custom-made device that was assembled at the C2RMF and designed to function in a non-contact mode, in order to avoid doing damage to the works of art. It is based on a back-scattering geometry, with an angle of incidence equal to the angle of reflection. An angle of 22° is used primarily to minimise specular reflection for varnished objects. The distance between the device and the object is maintained at 7.5 cm, with a measuring spot of 1–6 mm in diameter on the object's surface. Spectra were collected for the range of 400–800 nm.

The spectrophotometer was used to obtain spectral data with 5 nm resolution at several locations on the object. The equipment is well suited for in situ analyses, even though it has a relatively low sensitivity in the short-wavelength range.

3 Results of Fibre Optic Visible Reflectance Spectroscopy

On the fourteen tiles examined, a great variety of colour shades could be distinguished, ranging from light yellow to black over green, blue, blue green, different purple and red hues. The spectroscopic examination of these tiles from British collections revealed a similar range of colorants to those characterised in nineteenth century Persian tiles from German and French collections, which were part of a previous research project (Reiche et al. 2009). These are: uranyl ions (UO_2)²⁺, Fe^{3+} and Pb–Sn–Sb oxides for yellow shades; Fe^{3+} for green-brown; Cr^{3+} for dark green,

Table 1 Material selected for this study

No.	Tile Inv. no/Size	Collection	Provenance	Date	Group
1	510.1889/44.5 × 55.5 × 3.5 cm	V&A, London	Tehran	1884	A
2	511.1889/44.5 × 56.5 × 3.5 cm	V&A, London	Tehran	1884	A
3	1888.105/45.5 × 45.2 cm	NMS, Edinburgh	Tehran (V&A Museum Archive: Enclosure to Reg. No 5441-1887)	1887	B
4	Tile with Market Scene	Private collection	Probably Tehran	1880s	C
5	Tile with Banquet Scene (1)	Private collection	Probably Tehran	1880s	C
6	1890.239/34.9 × 47.0 cm	NMS, Edinburgh	Probably Tehran (Scarce 1976: 286)	1880s	C
7	559.1888/diameter 131.0 cm	V&A, London	Tehran	1887	A
8	Portrait tile of Sir Robert Murdoch Smith	Private collection	Tehran	1887	A
9	565.1888/44.5 × 44.5 cm	V&A, London	Tehran (V&A Museum Archive: Enclosure to Reg. No 5441-1887)	1887	B
10	LOST OK (18.1886)/ 27.5 × 22.0 × 2.3 cm	V&A, London	Probably Isfahan	c. 1880-5	D
11	G.313/25.0 × 16.0 × 2.0 cm	ME, BM, London	Probably Isfahan	1880s	D
12	G.314/30.5 × 30.5 × 2.5 cm	ME, BM, London	Probably Isfahan, signed Muhammad Ibrahim	1890s	D
13	G.315/34.0 × 26.5 × 2.5 cm	ME, BM, London	Probably Isfahan	1870s	D
14	1922.0201.1/22.0 × 16.0 × 0.7 cm	ME, BM, London	Probably Isfahan	1890s	D

A – Tile signed and dated by Ali Muhammad Isfahani (AMD), B – Tile proved to have been made by him or his workshop according to written sources, C – Tile art-historically ascribed to his workshop, D – Tile originating from a different workshop

which can be mixed with uranyl yellow to result in a green-yellow colour; Co^{2+} for blue; Cu^{2+} for cerulean blue (turquoise), or mixed together probably with another chemical species for blue–green; Au^0 for red and pink; Mn^{3+} for different purple shades; a mixture of Mn^{3+} with Co^{2+} for blue grey purple; and a mixture of Cr/Mn/Fe oxides of variable composition for brown and black (Figs. 1 and 2). Table 2 summarises the different colorants found for each colour on the fourteen tiles.

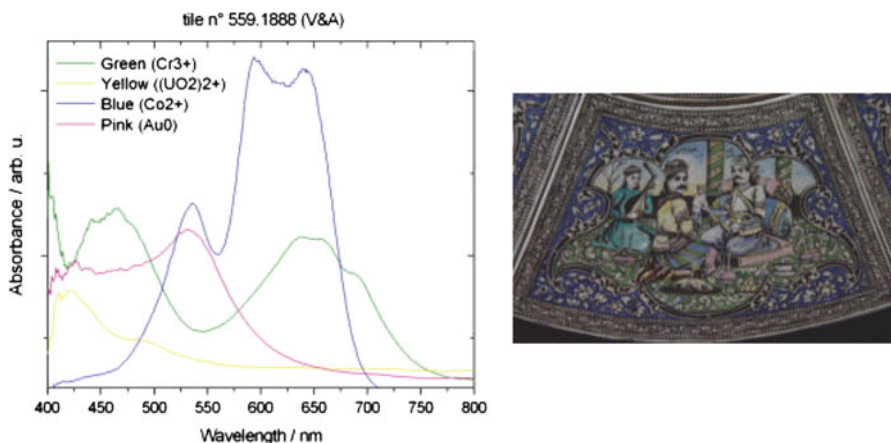


Fig. 1 *Left*: Visible spectra of *green*, *blue*, *yellow* and *pink* on the tile inv. n° 599.1888, corresponding to Cr^{3+} , $(\text{UO}_2)^{2+}$, Co^{2+} ions and Au^0 particles in the glaze, respectively. *Right*: lower part of the tile panel inv. N° 559.1888 investigated on display in the V&A Museum, London, © Trustees of V&A

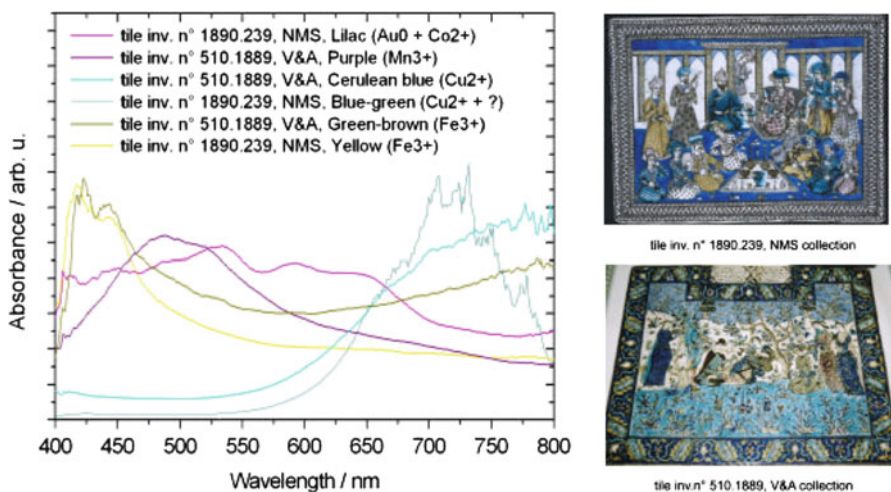


Fig. 2 *Left*: Visible spectra of *lilac*, *purple*, *cerulean blue*, *blue-green*, *green-brown* and *yellow* corresponding to Au^0 and Co^{2+} , Mn^{3+} , Cu^{2+} , Cu^{2+} and an unidentified species, and Fe^{3+} with another colorant and only Fe^{3+} ions in the glaze, respectively. *Right*: tiles investigated, above inv. n° 1890.239, NMS, Edinburgh, © Trustees of NMS, and below inv. n° 510.1889, V&A Museum, London, © Trustees of V&A

Table 2 Identified colour shades with the corresponding colorant on the investigated tiles from the V&A, NMS, BM and a private collection (PC)

Colour	Tile	Group A			Group B			Group C			Group D				
		510.1889 (V&A)	511.1889 (V&A)	559, 1888 (V&A)	Sir Murdoch Smith portrait (PC)	1888, 105 (NMS)	565.1888 (V&A)	Market (PC)	Banquet (PC)	1890.239 (NMS)	311 (18.1886) (V&A)	LOST OK (18.1886) (V&A)	G.313 (BM, ME)	G.314 (BM, ME)	G.315 (BM, ME)
Yellow	(UO ₂) ²⁺	-	-	x	x	x	-	-	-	-	-	-	-	-	x
Yellow	Fe ³⁺	?	?	-	-	-	?	?	?	?	?	?	?	?	-
Yellow	Pb-Sn-Sb oxide	?	?	-	-	-	?	?	?	?	?	?	?	?	-
Green-brown (bottle green)	Fe ³⁺ + other ion?	x	x	-	-	-	-	-	-	-	-	-	-	-	-
Green, green-yellow	Cr ³⁺	-	-	x	x	x	-	-	-	-	-	-	x	-	x
Blue	Co ²⁺ (Td)	x	x	x	x	x	x	x	x	x	x	x	x	x	x
Cerulean blue	Cu ²⁺ (Oh)	x	x	x	x	-	-	-	-	x	x	x	-	-	-
Blue green	Cu ²⁺ (Oh) + other ion?	-	-	-	-	-	x	x	x	-	-	-	-	-	-
Lilac	Au ⁰ + Co ²⁺	-	-	-	x?	x	-	-	-	x	-	-	-	-	-
Blue grey purple	Mn ³⁺ + Co ²⁺	-	-	-	x?	-	-	-	-	-	-	-	-	-	-
Purple	Mn ³⁺	x	x	-	-	x	x	x	-	-	x	x	x	-	x
Pink	Au ⁰	-	-	x	x	x	-	-	-	x	-	-	x	x	-
Grey-purple	Cr/Mn/Fe oxide + Mn ³⁺	x	-	-	-	-	-	-	-	-	-	-	-	-	-
Brown	Cr/Mn/Fe oxide of variable composition	x	x	x	x	x	x	x	x	x	x	x	x	x	x
Black	Cr/Mn/Fe oxide of variable composition	-	-	-	-	-	-	-	-	-	-	-	x	-	-

4 Discussion and Conclusions

This study highlights the potential of visible reflectance spectroscopy for the non-invasive identification of the colorants used for polychrome underglaze painted ceramics. The present research demonstrated the use of colorants and mixtures that were not employed by Persian potters in the previous centuries (Reiche et al. 2009). These are especially uranyl (UO_2)²⁺ ions for yellow or orange hues, and Cr^{3+} ions for green colours. Mixtures of different colouring agents, such as gold ruby glass produced by Au^0 nanoparticles or Mn^{3+} purple with blue Co^{2+} ions, seem also to have been used to produce lilac or blue/grey/purple, respectively. These first results seem to indicate that AMI used a limited colour palette in the early 1880s, based on colorants like Fe^{3+} , Pb–Sn–Sb oxides, Co^{2+} , Cu^{2+} , Au^0 and Mn^{3+} . As from the second half of the 1880s, the colour palette used by AMI seems to have been considerably enlarged, the earliest and most certain evidence for this coming from the two attributed tiles dated to 1887, which show additional Cr^{3+} and UO_2 ²⁺-based colorants, as well as mixtures of Au^0 with Co^{2+} .

However, it is obvious that the detection of a specific colouring agent alone is not sufficient to establish an attribution criterion of the tiles to a particular nineteenth century Persian workshop (e.g., that of AMI). For instance, uranium-based yellow and chromium-based green were also found in tiles attributed to other production centres, such as Isfahan. There is therefore a need to develop this work by further high precision analytical research combining different chemical and spectroscopic methods for the study of the glaze, colorants and ceramic body of these and other tiles. It is also expected that the comparison of the results obtained for the tiles analysed in this study with those obtained on raw material samples originating from the workshop of AMI in Tehran and preserved today in the V&A Museum, London (Troalen et al. in press) will advance our understanding of the pigments used by AMI and assist in the establishment of discrimination criteria between different workshops. Research on these samples is in progress in order to clarify this issue.

Acknowledgements The authors would like to thank the Franco-Britain ALLIANCE Programme 2007–2008, supported by the French Ministry of Foreign Affairs (EGIDE, no. 15125NJ) and the British Council (Alliance, project no 07.003), as well as Lucia Borgio, Mariam Rosser-Owen, Tim Stanley (V&A), Ulrike Al-Khamis (NMS), and David Saunders (BM) for their support of this programme. We owe particular thanks to the owners of the tiles in the private collection for allowing our examination.

References

- Dupuis G, Elias M, Simonot L (2002) Pigment identification by fiber-optics diffuse reflectance spectroscopy. *Appl Spectrosc* 56:1329–1336
- Reiche I, Röhrs S, Salomon J, Kanngießner B, Höhn Y, Malzer W, Voigt F (2009) Development of a nondestructive method for underglaze painted tiles – demonstrated by the analysis of Persian objects from the nineteenth century. *Anal Bioanal Chem* 393(3):1025–1041

- Scarce JM (1976) Ali Mohammed Isfahani, Tilemaker of Tehran. *Oriental Art* NS 22(9):278–288
- Troalen L, Reiche I, Röhrs S, Pretzel B, Burgio L, Shah B, Peschard S, Boust C, Tate J, Martin G and Voigt F (2009) 'To acquire a good name': Specimens of nineteenth century Persian tilemaking from the Teheran workshop of the master potter Ali Muhammad Isfahani, In: *Sources and Serendipity – Testimonies of Artists*. Practice. London (Archetype Publications): 119–127

Neolithic Facies of Stentinello Culture: Analysis and Comparison of Ceramics from Capo Alfiere (Calabria) and Perriere Sottano (Sicily)

S. Scarcella, A. Bouquillon, and A. Leclaire

1 Introduction

The cultural facies of Stentinello developed within the context of the culture of “Impressed Ceramics” that spread from the Near East towards the central Mediterranean, certifying the expansion of this Neolithic civilisation. The diffusion of the facies of the Stentinello culture covered a vast area, from southern Calabria to the whole of Sicily (Tiné 2002), in a period around the fifth millennium BC.

The ceramic decorated in Stentinello style is distinguishable from the “impressed ceramic” due to its complex decorations, which are not limited to impressions of natural tools, but are also undertaken using ceramic punches for reproducing the decorative motives on the vase. In ceramics belonging to the Stentinello style, the use of coloured inlays to emphasize the decorations is remarkable.

In most settlements of the Early and Middle Neolithic period in southern Calabria and Sicily, both examples of “impressed ceramic” and objects belonging to the Stentinello culture have been found. However, most of these settlements were excavated at the beginning of the twentieth century. At that time, the techniques of excavation were not sufficiently developed to allow for an optimal recording of the archaeological data, and today it is difficult to understand the relationship between the “Impressed Ceramic” phase and that of Stentinello, as well as between their characteristics, especially with regards to ceramic production.

The aim of the present research is to evaluate the technological features of the ceramic assemblages from two settlements, Capo Alfiere in Calabria and Perriere Sottano in Sicily, in order to appraise the continuity or the disruption of ceramic production during the two different phases of the Neolithic period in this area of the Mediterranean. Furthermore, an exploration of the homogeneity of the chemical

S. Scarcella (✉)

Ecole des Hautes Etudes en Sciences Sociales. 58, Boulevard de Reuilly, 75012 Paris, France
e-mail: simonascarcella@yahoo.it

A. Bouquillon and A. Leclaire

Centre de Recherche et des Restauration des Musées de France, CNRS UMR 171. 6, rue des Pyramides, 75041 Paris, France

features of the analysed ceramics will outline the complexity of the ceramic production and the existence of possible relationships of exchange with neighbouring villages. Finally, a comparison of the ceramic complexes analysed will establish the differences and similarities between the two, and thus allow a discussion as to whether a general trend in ceramic production existed, or if every human group had a specific handicraft specialization.

2 Sampling and Analytical Methods

The first group of 23 samples originated from the settlement of Capo Alfiere. The samples were excavated according to a stratigraphic methodology which can distinguish samples of the earlier “Impressed Ceramic” phase from those belonging to the Stentinello phase (Morter 1992) (Table 1).

The sixteen samples from the site of Perriere Sottano originated from a survey conducted in the early 1980s (Recami et al. 1983). Their attribution to the “Impressed Ceramic” phase or Stentinello phase is based on the different decorations visible on the artefacts. The objective of the sampling was to include sherds that represent both decorative styles present in the ceramic assemblages, “Impressed Ceramic” and Stentinello, in order to allow for a technological and typological comparison.

All analyses were carried out in the Centre de Recherche et de Restauration des Musées de France. Thin sections were prepared for petrographic analysis. The bulk chemical composition was determined by using particle induced X-Ray emission (PIXE) on the AGLAE particle accelerator (Calligaro et al. 2005). The size of the beam spot was 50 μm in diameter; scanning was performed on 1 mm^2 surfaces to average compositions. Two detectors were used for the detection of low and high energy X-rays, respectively. The quantitative interpretation of data was obtained using the GUPIX code, and various standards were used to adjust the parameters. As the textures of the ceramic bodies were often heterogeneous, the sherds were sampled with a tungsten carbide micro-drill and pellets of 5 mm in diameter were formed after grinding and homogenisation of the powder. The inlays were investigated by EDX coupled with a scanning electron microscope, in order to allow an examination of the textures, as well as a qualitative chemical analysis of the material.

Table 1 Capo Alfiere – Distribution of the studied samples. Calibrated data using CALIB 5.0.1 (Stuiver and Reimer 1993)

	Stratigraphy	CAL BC 2σ (95.4%)	Number of samples
Neolithic-Stentinello	IIC	4444–4042	6
	IIB	4449–4072	6
	Ia	4679–4351	7
Neolithic-Impressed Ceramic	Ib	5200–4552	4

3 Composition of Ceramic Bodies and Inlays from Capo Alfiere and Perriere Sottano

The 23 sherds from Capo Alfiere shared common petrographic characteristics: abundant clay matrix tempered with quartz grains, feldspars, micas, detritic rock fragments and some minerals, such as pyroxene and amphibole. An accurate observation distinguished two groups among the samples, according to the granulometry of the temper and the relative proportions of feldspars vs. quartz (Fig. 1a).

In the first group (17 samples), the temper was dominated by quartz, and the mean granulometry was 200 μm , while in the second group (six samples), feldspars were more abundant and the non-plastic grains were coarser.

The chemical compositions (Table 2) show that the pastes were all silica and alumina-rich, but poor in CaO (<2%).

There was no obvious chemical difference between the pastes belonging to the two petrographic groups, except a slight increase of Na₂O, CaO and Fe₂O₃ for the

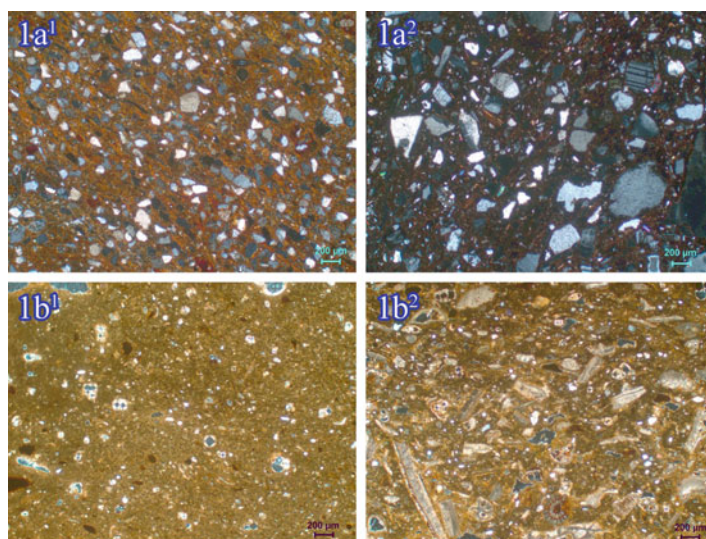


Fig. 1 Thin sections of samples from Capo Alfiere (a1, a2) and Perriere Sottano (b1, b2). © C2RMF – Photo Scarcella S

Table 2 Mean chemical composition and standard deviation of the ceramic samples from Capo Alfiere – data expressed in oxide wt%

Capo Alfiere	Na ₂ O	MgO	Al ₂ O ₃	SiO ₂	P ₂ O ₅	SO ₃	ClO	K ₂ O	CaO	TiO ₂	MnO	Fe ₂ O ₃
Gr. A	0.98	1.00	16.90	68.69	0.31	0.02	0.01	3.69	1.71	0.73	0.06	5.77
Sd	0.13	0.20	0.93	1.80	0.17	0.02	0.01	0.34	0.39	0.14	0.03	0.79
Gr. B	1.18	1.04	19.38	64.59	0.22	0.03	0.01	3.20	2.45	0.88	0.09	6.73
Sd	0.27	0.16	0.44	2.53	0.04	0.02	0.00	0.29	0.68	0.20	0.05	1.08

second group. No relationship was found between the petrography and typological features of samples, indicating that the “Impressed ceramic” samples and those belonging to the Stentinello culture were made of the same raw materials.

In the samples from Perriere Sottano, the mineralogical and chemical compositions were completely different from those described for the previous site: many of the samples were characterised by the presence of micrite associated with bioclasts (foraminifera, fragments of shells), quartz and iron oxide concentrations. It should be noted that the relative proportion of the different components was variable from sample to sample (Fig. 1b). Analyses of the chemical composition confirm this heterogeneity. For example, CaO amounts ranged from 4.78 to 37.40%, whereas SiO₂ conversely varied between 38.45 and 47.11%. In accordance with these results, we identified four groups based on the chemical compositions, using CaO as the discriminating element (Table 3). There is no relationship between these groups and typological features of the samples.

Eight fragments from Capo Alfiere and three from Perriere Sottano were chosen for investigating the mineralogical and chemical composition of the inlays. According to petrographic observations, all inlays were composed of micritic calcitic paste, associated to a greater or lesser extent with clay. However, the white inlays of Perriere Sottano and Capo Alfiere seem to be different. Although calcite is the dominant mineral in both cases, the habitus of the mineral is different: fine micritic paste is characteristic for the samples from Perriere Sottano, while better crystallised calcium carbonate can be found in those from Capo Alfiere (Fig. 2). This could

Table 3 Mean chemical composition and standard deviation of the ceramic samples from Perriere Sottano – data expressed in oxide wt%

Perriere Sottano	Na ₂ O	MgO	Al ₂ O ₃	SiO ₂	ClO	K ₂ O	CaO	TiO ₂	MnO	Fe ₂ O ₃
Gr. 1	0.45	1.43	12.11	70.13	0.19	2.83	4.78	0.84	0.09	6.33
Sd	0.11	0.23	1.94	2.44	0.13	0.37	1.54	0.12	0.04	1.03
Gr. 2	0.47	1.84	11.78	62.65	0.16	2.71	12.53	0.86	0.13	6.13
Sd	0.08	0.51	1.75	0.98	0.09	0.36	1.88	0.16	0.02	1.09
Gr. 3	0.30	1.63	13.11	47.11	0.22	2.58	25.68	0.98	0.10	7.32
Sd	0.05	0.12	1.00	2.95	0.10	0.40	2.54	0.10	0.06	2.32
Gr. 4	0.30	1.47	10.97	38.45	0.19	2.17	37.40	0.83	0.06	7.23
Sd	0.10	0.10	0.36	1.58	0.14	0.42	3.35	0.17	0.01	2.50

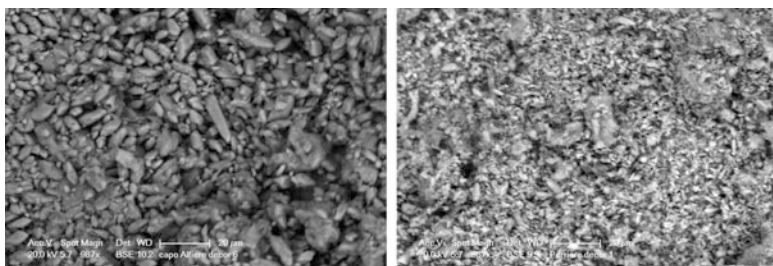


Fig. 2 Microstructure of calcium carbonate grains in white inlays from Capo Alfiere (a) and Perriere Sottano (b) SEM – backscattered electron mode © C2RMF – Photo Bouquillon A

be due either to different preparation of the raw material, or to different conditions of burial allowing for secondary crystallisation. Red and yellow inlays, only found on Capo Alfiere ceramics, are coloured by thin iron oxide grains and probably by an iron-rich clay associated with calcium carbonate.

4 Discussion

One can easily differentiate the ceramics from Capo Alfiere from those originating from Perriere Sottano because of their completely different mineralogical and chemical compositions. This is most likely due to the fact that each village probably exploited the nearest clay outcrops.

Furthermore, it is also possible to distinguish between the two villages due to their use of technical knowledge, i.e., for the white inlays, the initial mixtures and forms of the calcium carbonate crystallisations are different between the sites. Moreover, in Perriere Sottano, the only colour used for decorations was white, whereas samples from Capo Alfiere display a more diversified palette, including white, yellow, orange and red colours. This feature suggests a more sophisticated preparation of the decorations for the latter samples.

One of the main lines of inquiry focused on the continuity or disruption of the ceramic production between the “Impressed Ceramics” and the Stentinello phases. In Capo Alfiere, it was impossible to distinguish between the mineralogical and chemical characteristics of the older production and Stentinello. This may suggest that the same raw materials were consistently used from the beginning of the Neolithic, from period Ib to period IIc. In Perriere Sottano, it was also not possible to find mineralogical and chemical differences between the sherds decorated according to the “Impressed Ceramic” style and those of Stentinello style.

Finally, did exchanges between neighbouring sites exist? The mineralogical and chemical heterogeneity of the sherds from Perriere Sottano suggests the existence of different workshops in this area, or of exchanges between production centres located in this region of Sicily, which is near the Etna Volcano, close to the sea, and with easy access to the rest of the island. On the other hand, the ceramic assemblage from Capo Alfiere was characterized by a more homogeneous bulk composition, probably linked to local material. Exchange patterns between villages were certainly less prevalent in this case. This may be explained by the geographical location of Capo Alfiere, which is located on the coast of Calabria and is surrounded by a mountain chain that is difficult to cross.

In conclusion, different materials were used in the production of vessels from each investigated site, and the decoration style seemed to be the only common feature between the two settlements. The technical data collected confirm that both sites belonged to the same cultural root, but also suggest a handicraft specialization in each village.

5 Directions for Future Research

Three different research directions will be explored in the future:

1. Mineralogical investigations by X-ray diffractometry on all previously studied samples, in order to determine the mineralogical composition of the ceramic bodies, and to estimate firing temperatures for calcitic pastes
2. Comparison of the mineralogical and chemical compositions of raw clays collected from areas close to the settlements with the data collected on the ceramic sherds
3. Comparison with the data already studied from other contemporaneous sites, e.g. Acconia (Calabria), or whose study is in progress, e.g. Skorba (Malta), in order to acquire a better understanding of ceramic production during the Early Neolithic in the central Mediterranean.

Acknowledgments To Professor Guilaine for his support, to the PIXE team, to the Museo Archeologico di Crotona and Museo Civico di Ramacca for permitting this study, and to the Fondazione Monte dei Paschi di Siena for the financial grant.

References

- Calligaro T, Dran JC, Salomon J (2005) Non destructive analytical tools at the Centre for research and restoration of museums of France : present status and future trends. In: Adriaens A, Cassar J, Degriygn C (eds) Benefits of non-destructive techniques for conservation. pp 77–86
- Morter J (1992) Capo Alfiere and the middle Neolithic period in eastern Calabria, southern Italy, unpublished Ph - University of Texas at Austin
- Recami E, Mignosa C, Baldini LR (1983) Nuovo contributo sulla preistoria della Sicilia. *Sicilia Archeologica* 16:45–82
- Stuiver M, Reimer PJ (1993) Extended C14 data base and revised CALIB 3.0 C 14 age calibration program. *Radiocarbon* 35:215–230
- Tiné V (2002) Le facies a ceramica impressa dell'Italia meridionale e della Sicilia, In: Fugazzola Delpino MA, Pessina A, Tiné V (eds.) *Le ceramiche impresse nel Neolitico antico*. pp 131–166

Preliminary Archaeometric Data on Fineware from the Middle Neolithic Bükk Culture

V. Szilágyi, H. Taubald, T.K. Biró, S.J. Koós, P. Csengeri, M. Tóth, and Gy. Szakmány

1 Introduction

This paper deals with the preliminary petro-mineralogical and geochemical characterization of a special Neolithic fineware type which could have been an object of long distance trade. The results presented here represent the first steps of a longer project.

The Middle Neolithic Bükk culture (c. 5000 BC) is one of the descendants of the Central European (Early) Neolithic culture complex known as Linear Band Pottery culture (Kalicz 1970; Visy et al. 2003). In the late phase of this culture (sixth millennium BC), the originally very homogeneous archaeological complex split and a group seemingly specialised in artisan activities moved to mountainous areas, inhabiting also the foothill regions and higher altitudes, as well as the cave sites, of the North Hungarian Mid-Mountain range. The territory of the Bükk culture extended over present day North-Eastern Hungary, South-Eastern Slovakia and South-Western Ukraine (Fig. 1).

V. Szilágyi (✉)

Institute of Isotopes, Hungarian Academy of Sciences, Budapest, Hungary
e-mail: szilagyv@iki.kfki.hu

H. Taubald

Department of Geochemistry, Eberhard Karls University of Tübingen, Tübingen, Germany

T.K. Biró

Hungarian National Museum, Budapest, Hungary

S.J. Koós and P. Csengeri

Herman Ottó Museum, Miskolc, Hungary

M. Tóth

Institute of Geochemical Research, Hungarian Academy of Sciences, Budapest, Hungary

G. Szakmány

Department of Petrology and Geochemistry, Institute of Geography and Earth Sciences, Eötvös Loránd University of Budapest, Budapest, Hungary

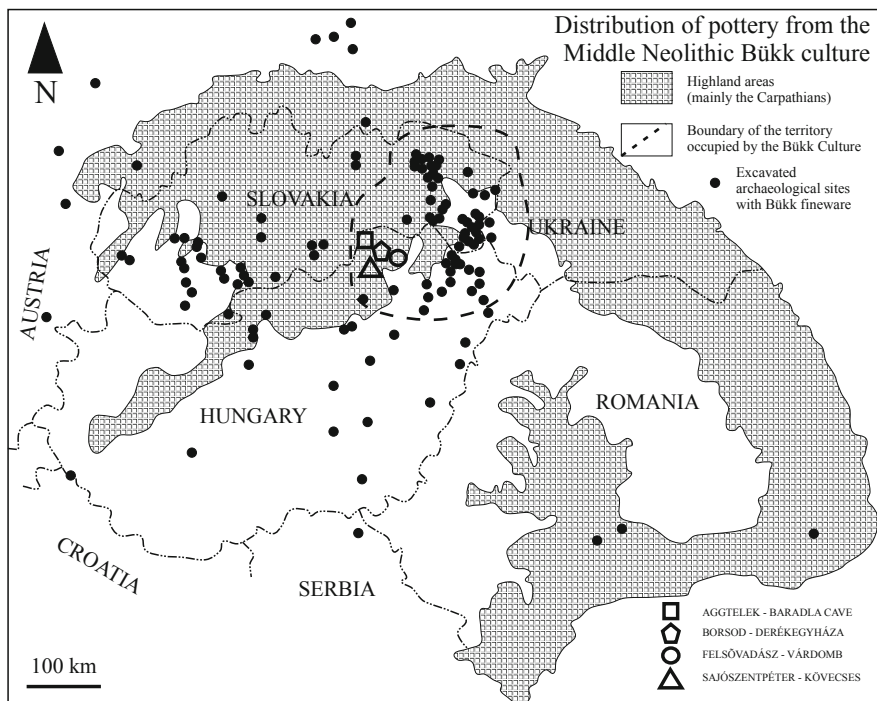


Fig. 1 Distribution of Bükk Culture fineware in and around the Carpathian Basin, and the localities of archaeological sites involved in the present archaeometric investigation

Caves and open-air sites yielded relics of Neolithic settlements with special fine pottery (egg-shell thin walls, fine incrustated decoration). This artistic product of handicraft can be found in archaeological sites located far away (even up to 100 km) from the territory of the Bükk culture (Kalicz and Makkay 1977). This indicates that the pottery can be considered a trade good spreading beyond the boundary of the tribal territory of the culture.

After investigating a very limited sample group of this type of fine pottery, we would like to provide preliminary data on it and give suggestions for a detailed project on the long distance trade of Bükk fineware. Our aim here was to obtain preliminary information about the composition of any special raw materials or individual recipes applied in the making of fine Bükk pottery.

2 Samples and Methods

The investigated ceramic assemblages are derived from four archaeological sites, all of them important settlements of the Bükk culture: the Aggtelek-Baradla cave (ABC), Borsod-Derékegyháza (BD), Felsővadász-Várdomb (FV) and Sajószentpéter-Kövecses

(SK). The Baradla cave is one of the classic localities of the Bükk culture excavated in Hungary (and also in Slovakia) by a range of researchers, including J. Nyáry, O. Kadić, L. Márton, J. Korek, and recently G. Rezi-Kató (Kalicz and Makkay 1977; Holl 2007). In addition to the cave site, the open-air sites of Felsővadász-Várdomb (located on a hilltop; Koós 1986a and 1986b; Csengeri 2001; Csengeri 2004; Biró in press), Borsod-Derékegyháza (on a hill slope; Tompa 1929; Kalicz and Makkay 1977) and Sajószentpéter-Kövecses (on a hilltop; Csengeri 2003) were selected for the preliminary overview.

The sample set consists of 29 ceramic and 22 local soil/sediment samples. Together with the fineware, coarse potteries related to the Bükk culture were also collected from each site because of their possible local origin. Our investigations were carried out on fragments and not on complete vessels; therefore, the grouping of the archaeological samples was based on the texture and finishing of the shards. The 15 pieces of fineware were fine-grained (maximum grain size <1 mm), with thin walls (maximum 5–6 mm) and varied decoration (with or without polishing, incision/incrustation or slip). Some of the pieces were plant tempered. The 14 coarse “domestic” ceramics had coarser grain size (maximum grain size >1 mm) and thicker walls (>6 mm). Decoration was absent or plastic (embossed). Sample codes are presented in Table 1.

The local soil/sediment samples (for sample codes, see Table 1) were obtained by approx. 2 m deep manual/hand drillings near the territory of the archaeological sites. The location of the drillings was selected taking into consideration the geological setting (in each case Miocene-Quaternary alluvial-proluvial-deluvial sediment types) and the topography (elevated and depressed areas). The selection of samples from the lithological columns was made on the basis of grain size and workability (plasticity, drying shrinkage) in terms of ceramic making. Detailed descriptions of the samples are given at <http://www.ace.hu/daad/daad2/furas2006.html>.

The archaeometric study involved microscopic petrographic observations (Department of Petrology and Geochemistry, Eötvös University of Budapest), mineralogical characterisation by XRD (Institute of Geochemical Research, HAS) and major and trace element measurements using XRF (Department of Geochemistry, University of Tübingen). For a detailed description of these methods, see Gherdán et al. (2007). In order to observe the similarities and differences from an archaeometric point of view, the same methodology was applied on archaeological and comparative raw material samples.

3 Petrography

At the ABC site, the four Bükk fineware sherds could be separated into two groups. Samples RAG-04 and RAG-06 have micaceous, silty clay paste, fine-grained (50–80 μm), compact fabric with serial distribution of grain size and contain exclusively mineral fragments (quartz, with undulatory extinction, muscovite, feldspar) as non-plastics. Samples RAG-05 and RAG-07 have a similar non-plastic

Table 1 Brief description and chemical composition of ceramic and comparative soil/sediment samples examined in the framework of the archaeometric investigation (Abbreviations: cw coarseware, fw-I-II fineware, first or second class, C clay, Si silt, Sa sand)

Sample code	Dep.	SiO ₂	TiO ₂	Al ₂ O ₃	Fe ₂ O ₃	MnO	MgO	CaO	Na ₂ O	K ₂ O	P ₂ O ₅	LOI	Rb	Sr	Ba	Zr	Nb	Y	La	Ce	Nd	Sm	Eu	Yb	V	Cr	Co	Ni	Zn	Sum
RAG-01	cw	54.85	0.92	19.61	6.24	0.03	0.86	2.66	0.28	3.04	3.57	7.43	136	102	886	247	19	50	39	95	44	8.0	0.8	4.6	123	92	9	-	744	99.49
RAG-02	cw	61.28	0.84	18.39	5.25	0.07	0.86	2.54	0.23	2.81	1.74	5.43	138	102	1,270	241	18	44	25	181	39	10.0	1.0	4.0	128	69	25	56	195	99.44
RAG-03	cw	65.98	0.73	15.33	6.36	0.12	0.73	2.24	0.34	2.33	0.91	4.70	122	136	1,094	200	14	30	15	64	18	4.8	0.7	2.6	102	72	17	81	76	99.76
RAG-04	fw-I	63.62	0.91	16.72	4.22	0.06	1.07	2.05	0.57	2.94	1.62	5.61	133	166	1,289	269	20	42	26	85	38	6.8	0.9	3.8	114	74	13	44	171	99.78
RAG-05	fw-II	60.76	0.88	21.03	4.94	0.01	1.35	1.47	0.25	4.15	0.53	4.38	186	66	703	203	18	40	34	103	40	6.5	0.6	3.8	142	89	7	50	135	99.34
RAG-06	fw-I	57.52	0.91	16.58	4.63	0.02	0.91	3.65	0.77	2.49	6.08	6.10	120	218	864	268	20	41	37	91	38	4.8	0.8	3.7	111	77	8	-	403	99.66
RAG-07	fw-II	59.58	1.18	23.22	4.83	0.03	1.50	1.51	0.34	3.29	0.85	3.30	190	96	568	257	23	54	53	124	54	7.7	0.7	4.9	195	114	18	43	225	99.63
AG-01	C	61.13	1.04	18.88	6.47	0.02	0.96	0.71	0.46	3.31	0.56	5.61	174	71	451	260	24	39	37	89	39	7.9	0.7	3.5	147	94	8	46	178	99.15
AG-02	SIC	73.50	0.97	12.49	4.51	0.02	0.70	0.51	0.50	2.34	0.25	3.52	114	59	357	415	26	47	29	92	49	5.2	0.5	3.9	93	69	6	62	111	99.31
AG-03	SIC	54.48	0.95	16.54	6.35	0.12	1.12	5.39	0.70	2.37	1.92	9.29	124	109	390	333	24	53	38	96	52	6.3	0.8	4.6	116	93	18	36	300	99.24
AG-04	SaC	68.84	0.92	12.19	4.80	0.04	1.21	2.58	0.44	2.11	0.77	5.68	110	93	341	420	24	46	35	91	47	8.0	0.8	3.8	93	74	9	59	139	99.57
AG-05	SIC	64.21	0.90	11.55	4.59	0.03	0.70	5.04	0.36	1.75	4.59	5.65	90	186	350	411	24	47	39	95	41	6.9	0.9	3.9	88	68	5	-	326	99.38
AG-06	C	67.65	1.02	14.93	5.29	0.08	1.15	0.83	0.81	2.34	0.18	5.11	119	86	422	411	25	55	37	95	49	8.7	0.9	4.7	111	89	15	88	75	99.38
AG-07	SIC	69.00	1.04	14.28	5.40	0.10	1.01	0.76	0.60	2.00	0.15	4.92	116	76	367	469	27	59	40	106	49	9.9	1.0	5.0	112	83	18	95	76	99.26
AGF-04	SIC	69.24	1.09	12.79	4.62	0.16	0.80	0.94	0.66	1.93	0.15	6.88	109	80	448	427	29	55	39	106	48	7.7	0.9	4.7	104	78	18	78	63	99.26
AGF-09	Si	72.40	1.00	12.07	4.50	0.13	0.73	0.59	0.57	1.82	0.14	5.22	99	68	391	411	27	50	29	99	41	7.1	0.8	4.2	96	78	17	72	52	99.16
AGF-14	C	70.80	1.03	12.77	4.72	0.13	0.76	0.55	0.52	1.88	0.15	5.71	105	68	402	373	27	48	35	96	43	6.6	0.7	4.1	102	78	18	70	52	99.02
RBD-01	cw	67.47	0.69	16.13	5.79	0.08	1.70	1.79	1.18	2.78	0.27	1.74	126	129	672	179	13	35	33	87	33	5.7	0.8	3.2	113	80	14	62	86	99.63
RBD-02	fw-I	68.02	0.82	15.88	5.71	0.12	1.80	1.07	1.06	2.87	0.26	2.11	136	113	683	271	20	38	28	88	30	6.9	0.8	3.3	130	100	15	85	85	99.70
RBD-03	fw-II	68.85	0.82	15.58	5.54	0.10	1.44	0.80	1.11	3.17	0.28	2.02	132	102	617	285	19	39	36	84	35	5.4	0.7	3.3	111	86	14	82	77	99.71
BD1-05	SIC	66.63	0.91	15.18	5.54	0.10	1.13	0.80	0.83	2.11	0.13	6.37	127	82	459	369	24	47	37	101	41	6.7	0.7	4.0	116	93	17	93	61	99.72
BD1-12	SIC	68.41	0.92	14.50	5.30	0.11	1.08	0.79	0.87	1.97	0.09	5.75	114	82	446	391	24	47	35	93	39	7.4	0.8	3.9	112	96	16	97	62	99.79
BD1-17	SIC	70.34	0.95	13.59	4.78	0.11	1.02	0.77	0.91	2.03	0.08	5.10	110	82	425	418	26	48	36	101	47	6.6	0.7	4.0	102	85	16	94	60	99.68
BD2-03	SIC	67.83	0.84	12.95	4.55	0.12	1.10	1.17	1.03	2.25	0.28	7.62	115	95	480	326	20	43	32	86	33	5.8	0.7	3.7	93	74	15	75	71	99.73
BD2-07	SIC	70.96	0.82	12.24	4.63	0.14	1.07	1.35	1.08	2.08	0.19	5.42	105	98	439	376	21	45	35	95	39	6.4	0.8	3.8	89	77	14	89	59	99.97
BD2-09	SIC	68.15	0.83	13.76	4.92	0.12	1.26	1.26	0.97	2.42	0.37	6.30	123	106	472	318	21	42	38	92	34	6.6	0.8	3.6	97	79	14	83	85	100.34
RFV-01	fw-I	67.81	0.83	14.18	4.76	0.08	1.59	1.03	0.97	2.85	0.20	5.46	126	102	516	281	18	25	28	81	29	6.5	0.8	2.8	115	88	13	38	78	99.75
RFV-02c	fw-I	69.47	0.76	13.23	4.64	0.04	1.42	1.04	0.73	2.79	0.30	4.87	113	103	586	248	17	29	27	77	35	3.8	0.6	2.6	107	89	13	67	81	99.33
RFV-03	fw-II	85.23	0.38	7.03	2.44	0.09	0.77	0.65	0.40	1.30	0.10	1.27	66	51	276	103	-	5	19	-	11	3.9	0.5	1.6	61	38	3	6	15	99.67
RFV-04	fw-I	84.59	0.42	7.53	2.44	0.02	0.62	0.48	0.37	1.33	0.17	1.89	61	56	327	131	-	11	21	-	21	3.4	0.4	2.0	54	38	5	6	17	99.84
RFV-05	cw	68.29	0.82	15.39	4.56	0.08	1.46	1.17	0.45	2.92	0.52	4.76	116	139	635	198	16	28	27	72	31	5.8	0.8	2.7	124	94	15	69	82	100.41

composition and similar silty clay paste to the previous ones, but the paste is less micaceous, the fabric is less compact, and they show plant tempering.

At the FV site, six Bükk fineware sherds were analysed and could be classified into two groups. Samples RFV-01, -02c, -04 and FVD-V/5a have micaceous, silty (limonitic) clay paste, fine-grained (average 50–90 μm), compact fabric with serial distribution of grain size and contain mineral fragments (quartz, muscovite, feldspar) as non-plastics. Samples RFV-03 and FVD-V/5b have a coarser grained (average 100 μm) fabric than the first two samples, with weakly hiatal (almost serial) distribution of grain size, less micaceous clay paste and metamorphic rock fragments as non-plastics.

At the BD site, the two Bükk fineware sherds proved to be different. Sample RBD-02 is characterized by micaceous, silty clay paste, fine-grained (70–90 μm), compact fabric with serial distribution of grain size, and contains mineral fragments (quartz, muscovite, biotite) as non-plastics. Sample RBD-03 has similar paste and fabric, but different non-plastic composition, with tuff related glass clasts.

At the SK site, the investigated three Bükk fineware sherds (Ssztp-01-03) were similar. These have micaceous, silty clay paste, fine-grained (50–60 μm) fabric with serial distribution of grain size, and contain mineral fragments (quartz, muscovite, feldspar) as non-plastics.

To sum up, Bükk fine pottery could have been manufactured by applying carefully selected or well elaborated (cleaned? washed?) fine-grained raw materials. However, with the exception of the SK site, the fine potteries proved to be heterogeneous in terms of their fabric and/or composition. It was possible to distinguish a first class (with micaceous, silty clay paste, fine-grained, compact fabric with serial distribution of grain size and mineral non-plastics) and a second class (with plant tempering or coarser grained paste) subgroup within the Bükk fineware.

4 Geochemical Data

A total of 23 ceramic and 22 soil/sediment samples were analyzed by XRF for their major and 17 trace elements composition. For provenance investigations, those major and trace element ratios were selected which are constant under conditions of soil forming and ceramic making processes. The sediments/soil samples suggest a trend on the Zr/V vs. $\text{TiO}_2/\text{Al}_2\text{O}_3$ bivariate correlation diagram (Fig. 2).

On this trend line, the enrichment of incompatible elements is highest in ABC cave samples, intermediate in BD samples and lowest in FV samples. The ceramics are in the lower left side (depleted in incompatible elements) of the trend. The petrographically selected first class Bükk fineware samples are close to each other, while the second class Bükk fineware items are a bit different and show more diversity in their composition. This feature can suggest a possible relationship between the sources of the first class Bükk fineware samples (workshop context?).

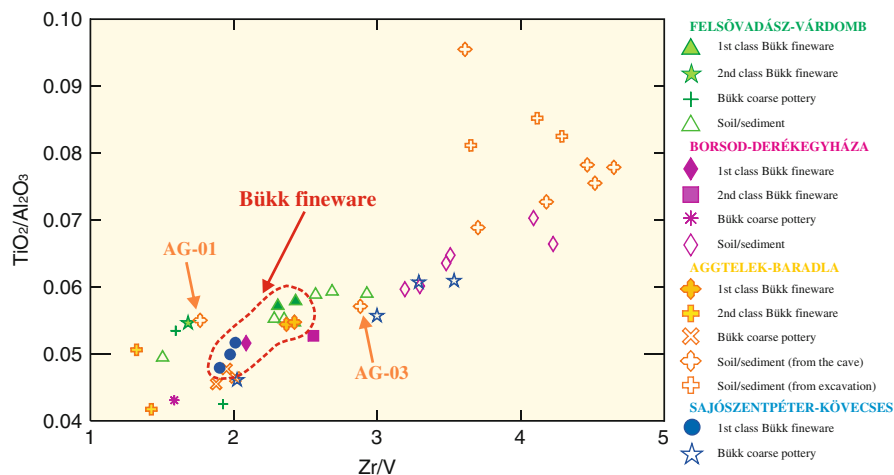


Fig. 2 Zr/V vs. $\text{TiO}_2/\text{Al}_2\text{O}_3$ element ratio diagram of the pottery and comparative soil/sediment samples from the four investigated sites

Regarding the possible source of material for these pots, the closest soil/sediment samples in terms of composition are FV samples and some ABC cave samples (e.g. AG-01 and AG-03).

5 XRD Data

The XRD analyses were carried out on samples from the ABC and BD sites (four Bükk fine ceramics and three soil/sediment samples). A semi-quantitative estimation was performed on the basis of peak area calculations; because of the limited space available here, the results are added in the order of quantity of each phase and “greater than” signs are used to express the relative differences.

Bükk fineware samples from ABC present an XRD pattern (quartz $\gg 10\text{\AA}$ (illite) $>$ plagioclase $>$ K-feldspar) which allows us to estimate a medium level (750–850°C) firing temperature. The XRD analysis on Bükk pottery from Borsod-Derékegyháza detected mineral phases (quartz $\gg 10\text{\AA}$ (illite-sericite) $>$ K-feldspar, plagioclase $>$ hematite) which indicate a medium level (750–850°C) firing temperature. The mineralogical composition of Bükk fineware does not suggest a special (high) firing temperature or atmosphere.

As – on the basis of the XRF analyses – the most probable raw material for the first class Bükk fineware was derived from some of the cave samples (e.g. AG-03) of ABC, a detailed XRD analysis of the sediments from there was carried out. The clayey sediment of the cave is a vermiculitic silty clay, sometimes with separable carbonatic nodules (quartz $\gg 10\text{\AA}$ (sericite-muscovite) $>$ calcite (detrital), plagioclase $>$ K-feldspar $>$ vermiculite $>$ hematite). This characteristic of a possible

paste phase of a ceramic requires some kind of tempering of the swelling clay. It is thus not very probable that the clay of the cave itself could be appropriate for pottery making.

6 Discussion

Based on the petrological, geochemical and mineralogical analyses, it is clear that the archaeologically selected Bükk fineware group can be distinguished from Bükk coarse pottery even by its material. In addition, the archaeological category of Bükk fine pottery, which was formerly believed to be homogenous, has at least two quality classes in terms of the raw material used in almost all of the archaeological sites involved in this study. The first class Bükk pieces of fineware are made of naturally or elaborated (washed?) fine-grained raw material, while the second class Bükk fineware is made of a raw material that is slightly coarser grained, but still quite fine, and which is sometimes even tempered.

At the ABC site, both the first class and the plant tempered second class Bükk pieces of fineware could be made with raw material of local origin, but then the vermiculitic clay from the cave, which is not a common raw material, would have had to be used. At the FV site, both the first class and the second class, slightly coarser grained, Bükk fineware could be made with raw material of local origin, but a clay paste different from that of the first class one was utilized for the second class pottery making. At the BD site, the first class Bükk fineware is probably made with raw material of non-local origin, while the raw material of second class Bükk fine potteries, containing tuff clasts, is local. At the SK site, the first class Bükk fineware could have been made with local raw materials.

7 Conclusion

As a result of our research, we obtained preliminary data on the Middle Neolithic high quality pottery manufacturing of the Bükk Culture. Although this petrological-geochemical-mineralogical investigation was performed only on a limited set of samples, it became clear that it is important to employ a complex methodology in the characterization of Bükk fineware, in order to distinguish its quality classes, and to find the parameters of the most probable raw materials.

Our results show that detailed systematic investigations on a large sample set of Bükk fineware could expose the origin (workshops) and recipes (special manufacturing technology) of this high quality pottery making.

Acknowledgements This research was partly carried out in the framework of a DAAD-MÖB German-Hungarian bilateral project (2005–2006) concerning “Archaeometrical analysis of Neolithic pottery and comparison to potential sources of raw materials in their immediate environment”

(www.ace.hu/daad/daad2). The authors are grateful for the financial support of the project No. K 62874 of the Hungarian Scientific Research Fund and the Mecenatura Grant of the National Office for Research and Technology. This paper could not be developed into its present state without the comments of the anonymous referee, who improved the manuscript in many ways and gave us directions for further research.

References

- Biró TK (in press) Lithic implements of the Stone Age site. In: Settlement of the Bükk Culture at Felsővadász-Várdomb (in Hungarian). Borsod-Abaúj-Zemplén Megye Régészeti Emlékei, Miskolc
- Csengeri P (2001) Data on the pottery handicraft of Bükk Culture. Artefacts of Felsővadász-Várdomb site, (in Hungarian). Herman Ottó Múzeum Évkönyve 40:73–105
- Csengeri P (2003) Bükk culture's settlement at Sajószentpéter, Kövecses, (Preliminary Report, in Hungarian), In Régészeti kutatások Magyarországon 2001. Kulturális Örökség Minisztériuma and Magyar Nemzeti Múzeum, Budapest, pp 31–46
- Csengeri P (2004) Data on neolithic settling history of the Cserehát (in Hungarian). In: Nagy E, Dani J, Hajdú ZS (eds) ΜΩΜΩΣ II. Hajdú-Bihar Megyei Múzeumok Igazgatósága, Debrecen, pp 45–59
- Gherdán K, Gy S, Tóth M, Biró TK, Kiss V (2007) Archaeometric studies on early Bronze age pottery from Vörs-Máriaasszony-sziget. *Archeometriai Műhely* 2007(2):21–31
- Holl B (2007) Archaeological research of the Baradla Cave, (in Hungarian). *Archeológiai Értesítő* 132:267–288
- Kalicz N (1970) Clay gods. The Neolithic period and the copper age in Hungary, Hereditas. Corvina, Budapest, 87
- Kalicz N, Makkay J (1977) Die Linienbandkeramik in der Großen Ungarischen Tiefebene. *Studia Archaeologica* 7:385
- Koós J (1986a) Archäologische Beiträge zur Geschichte der Bükker Kultur in Nordost-Ungarn. In Chopovský (ed) *Urzeitliche und frühhisrotische Beseidlung der Ostslowakei in Bezug zu den Nachbararbeiten*. Nitra, Archäologisches Insitut der Slowakischen Akademie der Wissenschaften, pp 103–107
- Koós J (1986b) Report of excavations at Felsővadász-Várdomb, 1982–1984, (in Hungarian). Herman Ottó Múzeum Közleményei 24:18–20
- Tompa F (1929) Die Bandkeramik in Ungarn. *Archaeologica Hungarica* 5–6:43–44
- Visy ZS, Nagy M, Kiss BZs (eds) (2003) *Hungarian archaeology at the turn of the millenium*. Budapest, p 482

A Study of the Materials Used for the Inscriptions on Ceramic Vessels Excavated at a Shang Dynasty Site in China

S. Wei, G. Song, and M. Schreiner

1 Introduction

The Xiao Shuang Qiao site is located west of the city of Zhengzhou, Henan Province, China, and was excavated during the last few years. According to radiocarbon dating, the site dates back to the Middle Shang period (1400 BC). It represents another urban centre of the Shang Dynasty, perhaps the “AO” capital of Zhong Ding, King of Shang. Its discovery is extremely important for Chinese archaeology, covering a previously unknown period of the Shang Dynasty. At this site, apart from the great findings, such as a high platform foundation of a palace formed of rammed earth, dwellings, sacrificial pit clusters, ditches, refuse pits, and metal craft remains, a number of pottery ritual vessels with inscriptions written on them were also excavated. These written characters are from an earlier period than the oracle bone inscriptions of Shang and the bronze inscriptions of Shang and Zhou (Song 1996). They are of great significance not only in terms of the interpretation of the artefacts from this particular site, but also for the study of the origin and changes in ancient Chinese writing.

The inscriptions can be classified in three categories: numerals, insignia and pictographs. Most of the inscriptions are well preserved; however, some of them are not so clearly readable, due to long-time ageing. A debate ensued in Chinese archaeology about whether they are writing characters, and about the types of materials that were used for the inscriptions. To answer those questions, a comprehensive scientific study addressing these inscriptions appears essential. In the present study, firstly, different photography techniques have been applied in order to reveal the unclear inscriptions, helping us recognize the original writing and

S. Wei (✉) and M. Schreiner

Institute of Natural Sciences and Technology in Arts, Academy of Fine Arts in Vienna, Vienna, Austria

e-mail: sywei66@hotmail.com

G. Song

Institute of Natural Science and Technology in Archaeology, Graduate University, Chinese Academy of Science, Beijing, China

making it possible to interpret the meaning of the characters. In addition, X-ray fluorescence (XRF) has been applied in order to identify the pigments used for the inscriptions. For the identification of binding media used in artworks, pyrolysis gas chromatography-mass spectrometry (Py/GC/MS) and gas chromatography-mass spectrometry (GC/MS) are the most valuable techniques (Mills and White 1977; Andreotti et al. 2006).

In ancient times, only organic materials from natural sources, including oils, proteinaceous materials, waxes and resins, etc., could be used as binding media. The differentiation of oils can be carried out on the basis of the ratio of saturated fatty acids, palmitic acid to stearic acid (P/S) (Mills and White 1977; Schilling and Khanjian 1996), while the type of protein can be classified according to the relative abundances of stable amino acids (Bonaduce et al. 2008; Gimeno-Adelantado et al. 2002). Resins (De la Cruz-Cañizares et al. 2005; Van der Doelen et al. 1998) and waxes (Regert et al. 2001; Evershed et al. 2003) are identified according to their mark compounds. In order to identify the materials used as binding media in the inscriptions, an analysis protocol has to be designed that can cover the entire range of the natural organic materials mentioned above.

In this study, a two-step GC/MS analysis method has been used: the first step consists of using GC/MS to analyse oils, resins and waxes after derivatization by trimethyl sulfonium hydroxide (TMSH) (Wei 2007); the second step consists of using the residue from the first stage of the analysis after it is hydrolysed and then derivatized with ethyl chloroformate (ECF) for the identification of proteinaceous material. This method is suitable for the analysis of extremely small amounts of samples, with minimum sample preparation/transferring.

2 Experimental

2.1 *Samples and the Identification of the Pigments Used for the Inscriptions*

Six potsherds with inscriptions were analysed. The strategies of this investigation are directed at performing the minimum sampling possible. First of all, the potsherds with inscriptions were documented by photographing them; subsequently, the images have been processed with the Photoshop software to reveal the unclear characters. One image of the inscriptions before and after processing with Photoshop is shown in Figure 1; it is evident that after using the Photoshop software, the inscription is more clearly readable.

A portable XRF instrument was used for the analysis of the pigments from the inscriptions. The instrument was developed in the Institute of Science and Technology in Art, Academy of Fine Arts in Vienna, and it allows non-destructive and local analysis of sub-millimetre samples with minor/trace level sensitivity. A polycapillary lens is used to focus the primary X-ray beam down to a level of

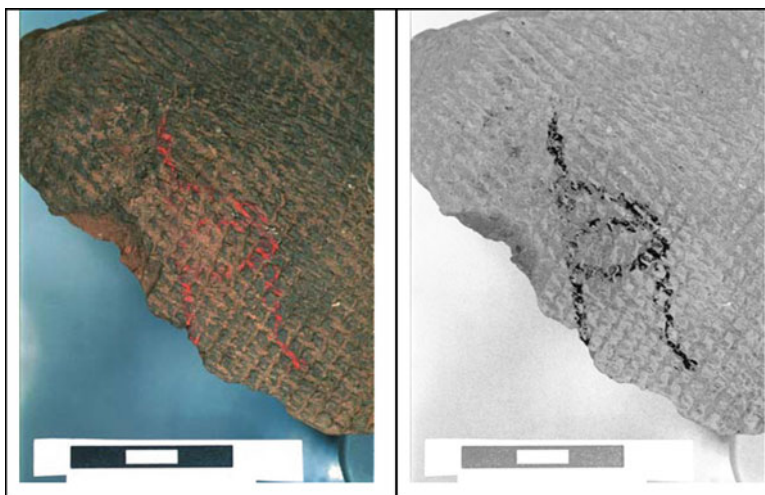


Fig. 1 The inscription on a potsherd before (*left*) and after (*right*) using Photoshop techniques to reveal the character

70–100 μm in diameter. XRF was used to analyse both the inscription area and the area without an inscription. Mercury was identified in the inscription area for all the six sherds, but not in the areas not showing an inscription, indicating the use of cinnabar as red pigment. Interestingly, in one sherd with a pictograph, apart from the mercury, reasonable amounts of lead were also detected, indicating that red lead mixed with cinnabar was probably used for the drawing. In any case, a Raman spectroscopy study appeared necessary for confirming these results.

2.2 The Instrumentation and Procedures for the Identification of Binding Media

Both pyrolysis gas chromatography-mass spectrometry (Py-GC-MS) and gas chromatography-mass spectrometry (GC-MS) measurements were carried out. A double shot pyrolyzer PY-2010iD (Frontier Lab, Japan) and a gas chromatograph-mass spectrometer GC-MS-QP2010 Plus (Shimadzu, Japan) were employed. The Shimadzu GC-MS real time analysis software was used for GC-MS control, peak integration and mass spectra evaluation. Pyrolysis was performed at 600°C for 10 s. The pyrolyzer interface was set at 320°C and the injector at 250°C, respectively.

A capillary column SLB-5MS (5% diphenyl/95% dimethyl siloxane) with 0.25 mm internal diameter, 0.25 μm film thickness, and 30 m length (Supelco) was used in order to provide an adequate separation of components. The chromatographic conditions were as follows: the oven initial temperature was 50°C, with a gradient of 10°C/min up to 320°C, a temperature which was maintained

for 12 min. The carrier gas was helium (He, purity 99.999%). The electronic pressure control was set to a constant flow of 1.0 ml/min, in splitless mode. Ions were generated by electron ionisation (70 eV) in the ionisation chamber of the mass spectrometer. The mass spectrometer was set from m/z 40 to 750, with a cycle time of 0.5 s. EI mass spectra were acquired by total ion monitoring mode. The temperatures of the interface and the source were 280°C and 200°C, respectively. Standards NIST 05 and NIST 05s from the Library of Mass Spectra were used for identifying compounds.

For Py-GC-MS analysis, a small amount of sample (about 0.1 mg) was directly placed into the sample cup for hydrolysis and then analysed by GC-MS. The sample preparation for the GC-MS analysis was carried out as follows: a scalpel was used to remove a sample of approximately 0.3 mg from the sherd, from the areas with and without an inscription; 50 μ l of chloroform were added, and shaken thoroughly; then, 25 μ l of TMSH reagent were added, and ultra sonicated for 1 h; finally, 2 μ l of the solution were injected into the GC-MS for the identification of oils, resins and waxes. The sample residues from the first step were evaporated to dryness, 60 μ l of 6N HCl were added under argon to hydrolyse for 24 h, subsequently derivatized with ECF and subjected to GC-MS analysis for the identification of proteinaceous materials.

3 Results and Discussion

The complete ion chromatogram of one inscription sample is shown in Fig. 2. In the chromatogram, a wide range of compound classes, including short, middle and long chain fatty acids, as well as long chain esters and alkanes have been detected and identified (Table 1).

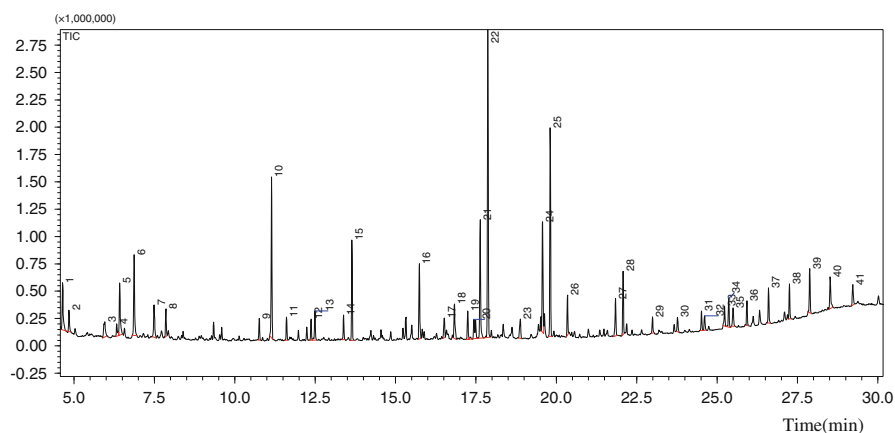


Fig. 2 TIC of the sample from the inscription on the potsherd (above, Fig. 1), derivatized with TMSH, analyzed with GC-MS. The identified compounds are listed in Table 1

Table 1 Compounds identified in the sample from the inscription on the potsherd

Peak No.	RT	Area%	Compound identified
1	4.64	2.63	Methyl 2-(methylthio)acetate
2	4.84	0.89	Hexanoic acid, methyl ester
3	5.95	1.42	Decane
4	6.32	0.77	Heptanoic acid, methyl ester
5	6.42	2.76	2-ethyl-1-Hexanol
6	6.87	4.00	Unidentified
7	7.49	1.87	<i>N</i> -[-[benzoyloxy]-phenyl]-Benzamide
8	7.8	1.19	Octanoic acid, methyl ester
9	10.76	0.9	2-methyl-Undecanoic acid,
10	11.14	6.88	2,4,4-Trimethyl-1-pentanol
11	11.61	0.97	2,2,4,4-tetramethyl-Pentanoic acid, methyl ester
12	12.37	0.9	Octanedioic acid, dimethyl ester
13	12.49	1.39	Dimethyl phthalate
14	13.38	1.00	Dodecanoic acid, methyl ester
15	13.64	4.13	Nonanedioic acid, dimethyl ester
16	15.7	3.52	Myristic acid, methyl ester
17	16.52	1.11	Tetradecanoic acid, 12-methyl-, methyl ester
18	16.83	1.88	Octadecanoic acid, 17-methyl-, methyl ester
19	17.24	1.33	7-Hexadecenoic acid, methyl ester
20	17.4	1.99	Tetradecanoic acid, 12-methyl-, methyl ester
21	17.63	5.64	7-Hexadecenoic acid, methyl ester
22	17.87	15.18	Palmitic acid, methyl ester
23	18.88	1.19	Trans-9-Hexadecen-1-ol
24	19.57	5.41	10-Octadecenoic acid, methyl ester
25	19.81	8.94	Stearic acid, methyl ester
26	20.35	1.68	Palmetic acid, butyl ester
27	21.84	1.88	1-Phenanthrenecarboxylic acid, methyl ester
28	22.08	2.7	Stearic acid, butyl ester
29–41	22.99–29.22		Long chain alkanes
32, 34, 35			Unidentified

Heptanoic acid, dodecanoic acid, octanedioic acid (suberic acid) and nonanedioic acid (azelaic acid) could represent oxidization products from plant oil, while 7-hexadecenoic acid (C16:1), palmitic acid (C16:0), 10-octadecenoic acid (C18:1) and stearic acid (C18:0) are the original fatty acids in the oils. The peak area ratio of palmitic acid to stearic acid (P/S) is 1.6 and the ratio of azelaic acid to palmitic acid (A/P) is 0.2, a feature which leads us to conclude that drying oil is present in the sample. However, for the area without an inscription, similar analysis results were found, with a wide range of compound classes, including short, middle and long chain fatty acids. This aspect makes the interpretation of the results more complicated. Drying oils could originate from the binding media used for the inscription, or from the potsherd itself, since the pot may have been used for cooking in ancient times, and include residues of oils (Evershed et al. 2003).

The detection of palmitic acid butyl ester, stearic acid butyl ester and a series of alkanes only in the areas of the samples with an inscription (and not in the areas without an inscription) indicate that wax may have been used as a binder. The

presence of dimethyl phthalate is due to subsequent contamination. In the second procedure, having as its purpose the analysis of proteinaceous materials, no amino acids were detected. By Py/GC/MS analysis, small amounts of palmitic acid and stearic acid were detected, which, however, cannot clearly indicate which materials are present in the samples. Interestingly, mercury was identified by the Py/GC/MS analysis, an aspect which is in agreement with the existing literature (Chiavari and Mazzeo 1999). This result confirmed the use of cinnabar as the main pigment employed for the inscription, consistent with the data obtained with the XRF analysis.

4 Conclusion

From this scientific study, it can be concluded that cinnabar was the main pigment employed for the red inscriptions. In one area with a pictograph, red lead was mixed with cinnabar in order to produce the pigment used for the drawing. It is interesting to learn that the knowledge of using cinnabar and red lead could date back to the Mid-Shang period. The binding media used for the inscriptions are probably drying oil or wax. The scientific study of archaeological objects certainly contributes to the better understanding of the activities and technologies developed in ancient times, and offers complementary information to the archaeological and historical knowledge.

References

- Andreotti A, Bonaduce M, Colombini MP, Gautier G, Modugno F, Ribechini E (2006) Combined GC/MS analytical procedure for the characterization of glycerolipid, waxy, resinous, and proteinaceous materials in a unique paint microsample. *Anal chem* 78(13):4490–4500
- Bonaduce I, Blaensdorf C, Dietemann P, Colombini MP (2008) The binding media of the polychromy of Qin Shihuang's Terracotta Army. *J Cult Herit* 9(1):103–108
- Chiavari G, Mazzeo R (1999) Characterization of paint layers in Chinese archaeological relics by pyrolysis-GC-MS. *Chromatographia* 49(5–6):268–272
- De la Cruz-Cañizares J, Doménech-Carbó MT, Gimeno-Adelantado JV, Mateo-Castro R, Bosch-Reig F (2005) Study of *Burseraceae* resins used in binding media and varnishes from artworks by gas chromatography–mass spectrometry and pyrolysis-gas chromatography–mass spectrometry. *J Chromatogr A* 1093(1–2):177–194
- Evershed RP, Dudd SN, Anderson-Stojanovic VR, Gebhard ER (2003) New chemical evidence for the use of combed ware pottery vessels as beehives in Ancient Greece. *J Archaeol Sci* 30(1):1–12
- Gimeno-Adelantado JV, Mateo-Castro R, Doménech-Carbó MT, Bosch-Reig F, Doménech-Carbó A, De la Cruz-Cañizares J, Casas-Catalán MJ (2002) Analytical study of proteinaceous binding media in works of art by gas chromatography using alkyl chloroformates as derivatising agents. *Talanta* 56(1):71–77
- Mills J, White R (1977) Analyses of paint media. *Natl Gallery Tech bull* 1:57–59

- Regert M, Colinart S, Degrand L, Decavallas O (2001) Chemical alteration and use of beeswax through time: accelerated ageing tests and analysis of archaeological samples from various environmental contexts. *Archaeometry* 43(4):549–569
- Song G (1996) The excavation of Xiao Shuang Qiao Site in 1995. *Hua Xia Kao Gu*, 10–25
- Schilling MR, Khanjian HP (1996) Gas chromatographic determination of the fatty acid and glycerol content of lipids, I. In: Bridgland J (ed) *The effects of pigments and aging on the composition of oil paints in ICOM Committee for Conservation Preprints, 11th Triennial Meeting*, Edinburgh, Scotland, 1–6 September. James & James (Science Publishers) Ltd., pp 220
- Van der Doelen GA, Van den Berg JK, Boon JJ, Shibayama N, René de la Rie E, Genuit WJL (1998) Analysis of fresh triterpenoid resins and aged triterpenoid varnishes by high-performance liquid chromatography–atmospheric pressure chemical ionisation (tandem) mass spectrometry. *J Chromatogr A* 809(1–2):21–37
- Wei S (2007) A study about natural organic binding media used in artworks and their ageing behaviour by GC/MS and GC/FID, PhD thesis, Vienna Technology University

A Discussion on Raw Materials Used for Ancient Chinese Porcelain

J. Zhu and C. Wang

1 Introduction

The Chinese civilisation has a long and rich history of millennia. An important aspect of Chinese civilisation, the invention and development of porcelain is one of the most significant contributions that ancient Chinese culture made to human civilisation. Scientific research on ancient ceramics is carried out in the context of many fields of study, including ceramics technology, geology and material science. In all these different fields, there are some small but significant differences in terms of the meaning conferred to some basic terms and concepts related to Chinese ceramics. Regardless of the reasons for citing literature from different fields of study or explaining data, it is necessary to check this terminology carefully, in order to avoid misunderstanding and confusion. During the last 50 years of technology research, there is still confusion about certain concepts. One of them regards the different understandings pertaining to about porcelain clay and porcelain stone, as raw materials used for making Chinese porcelain. In this paper, some issues related to this aspect will be discussed.

2 Concept and Dispute

As compared to porcelain clay, the concept of “porcelain stone” is clear and comprehensible. Generally, porcelain stone is a product of granite or other rocks, caused by an air-slaking effect, and is suitable for producing porcelain. The main minerals of porcelain stone are quartz and mica (sericite), which constitute a multi-component fit for porcelain manufacture. Thus, about 3000 years ago, the ancient Chinese used this material to make ware.

J. Zhu (✉) and C. Wang

Department of Scientific History and Archaeometry, Graduate University of the Chinese Academy of Sciences, Beijing, People's Republic of China
e-mail: jzhu@gucas.ac.cn

Generally speaking, there are two major opinions about porcelain clay among researchers of ancient Chinese ceramics. The first opinion is that, as the air-slaked product called porcelain stone, porcelain clay is a type of sericite clay which is suitable for porcelain manufacture and can be solely used to make porcelain. The mines of porcelain stone and of porcelain clay are often associated. On the weathered shell of mined porcelain stone, a weathered residue of porcelain clay can always be found. The difference between the two is related to the degree of weathering (Fang et al. 1990; Wang 1986).

The second opinion is that porcelain clay is the synonym of kaolin, distinct from porcelain stone. For example, in his paper “Raw materials used for porcelain in China”, Prof. Yanyi Guo thought that porcelain clay is kaolin and has a high concentration of Al_2O_3 , but porcelain stone is a different kind of clay (Guo 1984; Li 1998).

We believe the first opinion is more reasonable due to some evidence, as follows:

Firstly, there is a strict definition in geology according to which porcelain clay is generally thought of as the weathered product of porcelain stone. There is a gradual transition in the mine between porcelain stone and porcelain clay. On the surface of the mine, porcelain clay can be found; when digging deeper, because of the decrease in the degree of weathering, the mine displays a gradual transition to porcelain stone.

Secondly, the ancient literature records support our point of view. The Qing dynasty illustrations and articles in “The illustrated book of porcelain” document that porcelain material is the result of refining stones for obtaining clay. Other ancient books, such as “The record of Jingdezhen ceramics”, offer similar records. Thus, porcelain clay originates from naturally crumbled stone, and presents a homology to porcelain stone. Both of them represent the same type of material.

We suggest porcelain clay should be defined as a ground-like or mud-like rock, composed by quartz and a series of minerals of sericite-hydromica, featured with high Potassium, high Silicon, poor Aluminium and low Iron, according to the recommended guidelines of ISO (ISO704:196). This definition is more scientific and understandable for future research.

3 Discussion and Conclusion

The theory that before the Tang Dynasty (AD 618–907), the porcelain body recipe mainly includes only one type of raw material is widely accepted. Furthermore, it is almost common knowledge for ancient Chinese ceramics scholars that porcelain clay or stone were only distributed in Southern China, and that the raw material for porcelain in Northern China is mainly kaolin. Because the raw material used for making the ceramics body and the fuel were often chosen locally in porcelain manufacture, previous theories held that the porcelain produced in Southern China has a characteristic high Silicon content in the porcelain body, and the porcelain

produced in Northern China has a characteristic high Aluminium content in the porcelain body (Wang 1986). For a long time, many scholars thought that kaolin exists mainly in Northern China, and that porcelain clay (or stone) exists mainly in Southern China (Guo et al. 1980). The history of the development of ancient Chinese ceramics was constructed based on this hypothesis; according to this framework of interpretation, unknown porcelains could be differentiated using the Si/Al ratio of the raw material to identify whether it originated from the north or south of China. However, whether based on either theory or practice, this assumption lacks sufficient scientific support.

Thus, according to the data from geological investigations and the samples we tested, we found that the profile of the raw material and its chemical composition are not so simple. Firstly, porcelain clay or stone are also widely distributed in Northern China. Some of the sites and corresponding chemical components of typical porcelain clay or stone are listed in Table 1.

Secondly, kaolin is more easily geologically formed under conditions corresponding to the climate and geological environment in Southern China (Fig. 1). Thus, the kaolin reserve in Southern China is higher than the one in Northern China. For example, the kaolin reserve in Guangdong Province (far south of China) is the highest in China, accounting for 30% of the entire kaolin reserve in China.

In particular, the porcelain stone in Zhouyang (Table 1 No.9), Henan province, is a by product of the Xinyang porcelain vein, and its content of R_2O ($K_2O + Na_2O$) is as high as 5%. It appears as greyish white blocks, and its degree of Mohs hardness is around 3, which makes it possible to be easily comminuted. The firing experiments indicated that this material could alone be fired into proper porcelain wares, and meanwhile, that the production process had the advantages of being an easy process, resulting in a porcelain with good formation properties and high rate of qualification (Ren 1986).

The porcelain mine in Laiwu, Shangdong province (case n. 2 in Table 1), is veined, and there is a distinct boundary between the ore body and the surrounding rocks, making it convenient to be explored. There are two types of this ore: one is mylonitized trondhjemite ore, the average chemical composition of which is 74.53% SiO_2 , 14.98% Al_2O_3 , 0.54% Fe_2O_3 and 0.12% TiO_2 ; the other one is aplite ore, the average chemical composition of which is 75.81% SiO_2 , 14.21% Al_2O_3 and 0.56% Fe_2O_3 . According to the amount of D-degree porcelain stone ore approved by the Shangdong Mineral Resources Committee, the intrinsic amount usable as an economic resource should be around 310,000 tons. According to the tests carried out by the Shangdong Institute of Ceramics, this ore was an ideal material for making domestic ceramics.

Therefore, it is clear that the porcelain stone (clay) resource abounds in Northern China. As for porcelain stone (clay), the further weathering of the parent rock will result in kaolin or other minerals of the kaolinite family. Accordingly, in geology the porcelain stone is usually regarded as non-completely-weathered parent kaolin and is categorized as part of the group of kaolinite materials. As geological categories are usually broad, kaolinite materials with high Silicon (the ratio of Si to Al is above 2.5) can be sometimes found in the geological material, among

Table 1 Chemical composition of porcelain clay in Northern China (wt%)

Provenance	SiO ₂	Al ₂ O ₃	Fe ₂ O ₃	TiO ₂	K ₂ O + Na ₂ O
1 Renli, Wulian county, Shandong	78.0	12.4	0.9	0.08	4.01
2 Xiangshan, Laiwu city, Shandong	74.53–75.81	14.21–14.98	0.54–0.56	–	6.78–7.57
3 Pengyang, Zibo city, Shandong	83.95	9.19	0.39	0.23	4.39
4 Chapeng, Shunyi county, Beijing	75	13.6	1.2	–	5–7
5 Ertaizi, Huairou county, Beijing	68.58	13.73	1.29	0.07	1.61
6 Zhoukoudian, Fangshan, Beijing	64.18	23.51	2.45	–	–
7 Yangeryu, Yangeryu, Beijing	70	18	1.56	–	–
8 Ying county, Shanxi	74.96–76.10	14.10–14.54	0.54–0.83	0.05–0.08	6.83–7.8
9 Zhoudang, Xinyang city, Henan	80.06	15.15	<0.41	–	5
10 Miaoling, Hailin, Heilongjiang	74.5–76.0	11.98–13.95	–	–	–
11 Xiaoshiren, Jiangyuan, Jilin	74	14	1.3	0.1	6.50
12 Hafu, Lishu county, Jilin	76.83	13.42	1.03	0.08	3.68
13 Shuangyang county, Jilin	75	15	1.0	–	–
14 Qianxinqiu, Faku county, Liaoning	74	14	1.2	–	–

Except for 8 and 9, data are from unpublished geological investigation reports in the National Archives of China

- Li Shiliang et al. 1989. Porcelain mineral resources of Renli, Wulian, Shandong, record 81667. Shandong Provincial Bureau of Geology & Mineral Resources
- Hao Jianjun et al. 1999. Porcelain mineral resources of Xiangshan, Laiwu, Shandong, record 88665. Shandong Provincial Bureau of Geology & Mineral Resources
- Wang Xuewu et al. 1991. Porcelain mineral resources: Zhoucun, Zibo, Shandong, record 94555. Shandong Provincial Bureau of Geology & Mineral Resources
- Liang Tao et al. 1997. Porcelain mineral resources: Chapeng, Shunyi, Beijing, record 86181. China National Materials Group Corporation
- Zhao Bo et al. 1989. Felsite and porcelain mineral resources: Pengyang, Huairou, Beijing, record 76897. Beijing Institute of Geological Investigation
- Li Fupei et al. 1989. Porcelain mineral resources: Fangshan, Zhoukoudian, Beijing, record 18967. Beijing Bureau of Building Materials
- Chen Shijin et al. 1959. Porcelain mineral resources: Yangeryu, Zhoukoudian, Beijing, record 19029. Beijing Bureau of Building Materials
- Wang Xiaojun and Shuai Guofang. 1995. Study of Yin county pottery stone. Journal of Chemical Technology of Nanjing University 17:122–25
- Ren Cuiping. 1986. Discovery of a porcelain mineral with high-silicon. Journal of Zhengzhou University (Natural Science Edition) 1:103–6
- Chen Xilin, Pu Baotian, Lu Changqiao, et al. 1988. Porcelain mineral resources: Hailin, Miaolin, Heilongjiang, record 79607. Heilongjiang Provincial Bureau of Geology & Mineral Resources
- Zhou Guanwu, Song Zhuqin, Song Shulin, et al. 1997. Porcelain mineral resources: Xiaoshiren, Dashiren, Jilin, record 86963. East-North Institute of Coalfield Geological Reconnaissance and Design (Changchun)

12. Yang Huaqin, Qu Jie, Wang Rencheng, et al. 1985. Porcelain mineral resources: Hafu, Lishu, Jilin, record 69196. Jilin Building Material and Geological Prospecting Team
13. Qu Wengui et al. 1960. Mineral and Geological investigation report in south area of Jinlin province. Record 24224. Changchun Bureau of industry
14. Peng Liren, Gao furen, Zhang Wei et al. 1983. Particular Porcelain mineral resources investigation: Qian xinqiu ,Faku, Liaoning. Record 72389. Liaoning Provincial Bureau of Geology & Mineral Resources

which the major parts can be attributed to porcelain stone. However, there is still a lot of work that needs to be done concerning the concept, definition and distribution of porcelain stone, and providing a definition that is consistent with the concept will be of help for further studies.

As discussed above, the porcelain stone (clay) resource also exists in Northern China. Thus, the distribution of kaolin deposits in China should also be analyzed with regards to the dynamics and the geological background of sedimentary rock. In fact, the research on this respect is rather mature so far (Tao 1984).

There are different classification criteria or kaolinitic bed. In terms of ore-forming geological background represented by parent rock, ore-bearing rock series and ore-bearing space, the kaolinite ore deposits can be classified as some types, including fine-grained weathered acid rock vein, weathered pegmatite granite, weathered tuff, cavity filling of paleokarst denudation plain type, alteration pattern of cavity filling of paleokarst denudation plain type, altered marginal migmatite, clastic and coal-bearing sedimentary formations. According to the ore formation dynamics, the kaolinite ore deposits can be divided into weathering residue, weathering leaching, hydrothermal sedimentation and sedimentation.

Regardless of the classification, the formation of kaolinite can basically take two forms: one type of kaolinite is formed after the parent rocks (dike rock, porphyry

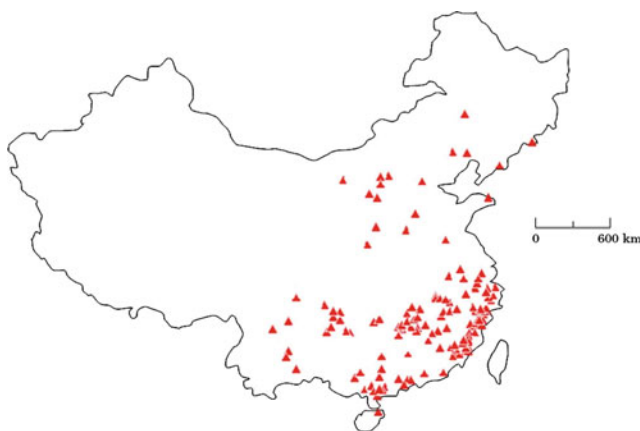


Fig. 1 The distribution of kaolin deposits in China

and carbonatite) experienced weathering, leaching and alteration, and the other one is formed after transportation and sedimentation. The former type represent the major forming pattern of kaolinite, and its parent rock is widely distributed in the acid rocks in the east and south of China, such as granite, pegmatite, fine-grained acid ore dike rock and tuff. This is due to the fact that the Chinese continental plate is adjacent to the Pacific plate, and the massive invasion of Mesozoic acid magma and volcanic eruption resulted in the formation of ore deposits that are related to the respective hydrothermal alteration, and also of the parent rocks of weathered ore deposits, which provided the premise of the massive Cenozoic weathered ore deposits. Meanwhile, the moist and hot climate in Southern China is appropriate for the development of kaolinite. In other words, the formation of kaolinite tends to be favoured by the geographic and climatic conditions prevalent in the south of China. As a result, kaolinite generally tends to be distributed more in the south than in the north. The investigation of the ore resources can verify this as well. A large amount of kaolinite ore can be found in Guangdong province. In 1996, the amount of recoverable deposit was 442,150,000 tons (B+C degrees sum up to 117,910,000 tons), representing 30.9% of the total national deposit. Following next are the Shanxi, Fujian, Jiangxi, Guangxi, and Hunan provinces, and their amounts of recoverable deposits are 26.8%, 11.0%, 7.7%, 7.6% and 3.7% (Ren 1986).

The assumption that porcelain clay or stone are distributed mainly in Southern China and kaolin is mainly distributed in Northern China is popular among researchers of Chinese ceramics and was of great importance for constructing the history of the development of ancient Chinese ceramics. According to this assumption, the Si/Al ratio can be used to differentiate between unknown ceramics, and establish if they were produced in Northern or Southern China. However, this assumption is not self-evident, lacks theoretical support and contradicts factual evidence; as a result, the history of the development of ancient Chinese ceramics might need to be reconsidered. Factual evidence demonstrates that there are sufficient porcelain stone resources in Northern China for firing porcelain; if the porcelains with higher Silicon content from Northern China had been previously classified as products fired in Southern China, the history of porcelain in Northern China would have been misunderstood. More work on the concept, definition and distribution of porcelain is needed in the future, as it would greatly contribute towards the development of research on ancient Chinese ceramics.

Acknowledgements This work has been supported by the National Natural Science Foundation of China Grant 10875169,10979075 and Cultural heritage conservation science and technology research projects (No. 20070116).

References

- Fang Yeseng, Fang Jinman, Liu Changrong (1990) Mineralogical raw materials in ceramic industry of China. Nanjing University Press, Nanjing
- Guo Yanyi (1984) Raw material for porcelains and porcelain ware of north and south China in the ancient times. *J Jingdezhen Ceram Inst* 5(1):55–68

- Guo Yanyi, Wang Shonying, Chen yaocheng (1980) A study on the northern and southern celadon of ancient Chinese dynasties. *J Chinese Ceram Soc* 8(3):232–243
- Li Jiazhi (1998) *Zhongguo ke xue ji shu shi: Tao ci juan* [The history of science and technology in China: Ceramics]. Science press, Beijing, pp 110–111
- Ren Cuiping (1986) A new material with high silicon for ceramic industry. *J Zhenzhou Univ* 9 (1):103–106
- Tao Weiping (1984) *China Kaolin mineral deposit geology*. Shanghai scientific and technological Literature, Shanghai, pp 31–48
- Wang Ling (1986) Approach to the ceramic material terms: porcelain clay, porcelain stone, ware clay and ware stone. *J Sichuan Inst Build Mater* 1(4):89–96

Part II
Stone, Plaster and Pigments (Technology
and Provenance)

Palaeolithic Paintings at Riparo Dalmeri, a Northern Italian Rock Shelter: Materials, Technologies, Techniques

R. Belli, G. Dalmeri, A. Frongia, S. Gialanella, M. Mattarelli, M. Montagna, and L. Toniutti

1 Introduction

Riparo Dalmeri, a rock shelter located in the north-eastern part of Italy (Trentino) and dated back to 13,000 BP, has provided a wide assemblage of archaeological finds, including animal bones, fireplace remains and, particularly, painted limestone rocks. Some of the coatings and “paintworks” present on stone fragments were determined to be natural, while others were clearly man-made artefacts.

The main aspects of the present research address: the origin and, where applicable, the provenance of the materials used for the paintings; the technologies employed for manufacturing some of these materials; the application techniques; the paleoclimatic implications (Belli et al. 2007). An interesting aspect that emerged from the research is the indication that the painters who operated at Riparo Dalmeri were able to master a variety of different materials, including moonmilk, goethite, and hematite, from which ochre and white colours with different shades were obtained. With regards to the red coloured pigment materials, it is worth mentioning that around the prehistoric shelter a geological survey has evinced that only goethite nodules are present, while in the prehistoric layer several small red ochre nodules were found. This would suggest that hematite might have been produced by a thermal induced transformation of goethite, which occurs at about 300°C. In this work, we present the results of X-ray diffraction, transmission

R. Belli, M. Mattarelli, M. Montagna, and L. Toniutti (✉)
Dipartimento di Fisica, Università di Trento, Via Sommarive 14, 38050 Povo (TN), Italy
e-mail: toniutti@science.unitn.it

G. Dalmeri
Museo Tridentino di Scienze Naturali, via Calepina 14, 38100 Trento, Italy

A. Frongia and S. Gialanella
Dipartimento di Ingegneria dei Materiali e T.I, Università di Trento, Via Mesiano 77, 38050 Povo (TN), Italy

electron microscopy and Raman spectroscopy for the purpose of studying the possibility of recognizing the natural or man-made origin of the red ochre remains.

2 Experimental

In order to address the origin of the red ochre, the transformation of goethite into hematite was studied by heating in air a commercial goethite powder (Sigma-Aldrich, Goethite – CAS No. 20344-49-4: ca. 35 wt% Fe; note that for pure goethite Fe would be 63 wt%), at temperatures ranging from 200 to 1,000°C, temperatures selected on the basis of the results of thermal analyses (see Table 1). The different thermally treated powders and some archaeological samples (43 Mb, 42 Mf, 42 Mb, 44 Lf, 51 Mh, and 43 Gc) were microstructurally characterised. The structural evolution and phase transformation of goethite and hematite were characterised using X-ray diffraction (XRD) on an IPD 3000 diffractometer (Debye-Sherrer in reflection geometry) with Cu K α radiation ($\lambda = 0.15408$ nm). Each pattern was processed with the MAUD software (Lutterotti and Gialanella 1998), a specialised programme able to extract quantitative crystallographic and microstructural information (Lonardelli et al. 2005) using a Rietveld code. In this study, quantitative phase analysis (QPA) and line profile analysis (LPA) were performed using the entire diffraction pattern.

Selected powder samples were prepared for transmission electron microscopy (TEM) observations by suspending them into ethanol using an ultrasonic bath to eliminate agglomeration. A drop of this suspension was deposited onto a carbon coated copper grid. Microstructural imaging and relevant selected area electron diffraction (SAED) patterns were acquired using an analytical electron microscope, operated at 120 KeV and equipped with an energy dispersive X-ray spectrometer (EDXS).

Raman spectra upon 632.8 nm excitation were collected by means of a Jobin Yvon HR800 LabRam microRaman single grating spectrometer. The polarization of the collected spectra was not defined. The measurements were performed with low power of excitation (about 0.02 mW, on a 5 μm^2 region) in order to avoid a significant heating of the samples induced by the laser absorption. The resolution, as obtained from the measure of the Rayleigh line, was 2 cm^{-1} .

Table 1 Crystallite sizes along $\langle 104 \rangle$ and $\langle 110 \rangle$ directions obtained from XRD data through Rietveld analysis for synthetic (*left side* of the table) and archaeological (*right side*) hematite samples. The error on the size is 5%

Label	Heat treatment	(104) Å	(110) Å	Label	(104) Å	(110) Å
SA300	1 h at 300°C	380	120	43Mb	880	1,100
SA400	1 h at 400°C	400	130	42Mb	650	860
SA600	1 h at 600°C	420	180	42Mf	690	785
SA800	1 h at 800°C	730	400	43Gc	200	420
SA1000	1 h at 1,000°C	1,000	1,000	44Lf	310	610
GN1000	1 h at 1,000°C			51Mh	310	700

3 Results and Discussion

At a given temperature, the broadening of the Raman peaks is related to the presence of chemical impurities and microstructural defects. In Fig. 1, the full-width at half maximum (FWHM) of the peak at 226 cm^{-1} is displayed as a function of the $I(660)/I(610)$ ratio. The 660 cm^{-1} peak in the Raman hematite spectrum is not Raman active in a pure infinite crystal of hematite; its presence is due to the contribution of the chemical impurities and of the surface, for which the cell symmetry breaks (Bersani et al. 1999). This feature is particularly evident in the trend of the thermally treated synthetic hematite, which indeed occupies the upper right region of the plot. The decreasing trend of these data with increasing temperature, up to 800°C , is induced by the loss of OH groups, which, abandoning the material, reduce the effective number of impurities. On the other hand, at $1,000^\circ\text{C}$ we can observe a sudden increase of the line-width, while the intensity of the defect-peaks is scarcely affected. We ascribe this behaviour to the re-crystallization and sintering of the material at this temperature. As observed in the TEM images, at $1,000^\circ\text{C}$ sintering takes place. This leads to a sudden drop of the surface contribution to the defect-peaks. On the other hand, a fraction of the impurities from the surrounding “earths” become embedded into the hematite grains. The net effect on the Raman spectra is an increase of the line-widths, while the higher contribution to

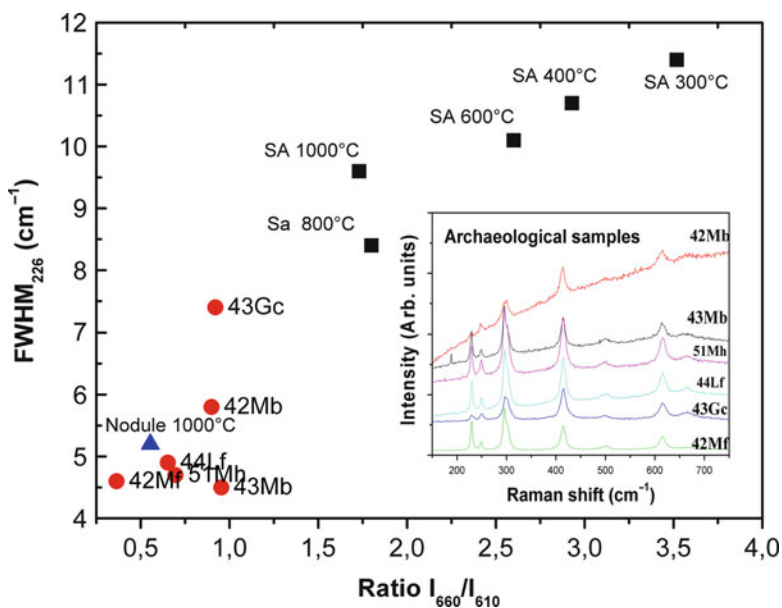


Fig. 1 FWHM of the 226 cm^{-1} peak as a function of the intensity ratio of the 660 and 610 cm^{-1} peaks of the archaeological and synthetic hematite samples. *Inset:* Raman spectra upon 632.8 nm excitation of archaeological ochre fragments found at Riparo Dalmeri

the intensity of the 660 cm^{-1} peak is balanced by the decrease of the surface one. Similar trends are observed when examining the other Raman peaks. The spectra reported in the inset confirm that hematite is actually present in the archaeological samples, which for this reason appear red in colour. Moreover, in view of the location that the experimental points occupy in the graph (Fig. 1), it can be assumed that the archaeological samples are quite pure.

The distribution of points for archaeological samples, where for a given I_{660}/I_{610} ratio several line-widths are observed, indicates that other mechanisms, apart from the defects concentration, contribute to the broadening of the Raman peaks. A known source for such broadening is related to the phonon confinement induced by the nanometric size of the crystalline domains. As their size decreases, the exchanged wave-vector q in the Raman process is no longer next to zero as in an infinite crystal, and more and more q vectors contribute to the process. Because of the optical mode dispersion, the exchanged energy has higher variability and this causes a broadening of the peaks.

In order to validate these considerations, we made a comparison with the results obtained by XRD measurements performed on the annealed goethite powders and on the archaeological ochres (Belli et al. 2008). In the annealed samples, at temperatures between 200 and 300°C, goethite begins to transform into hematite. By a detailed analysis of the line shapes of the diffraction peaks, it is possible to follow the evolution of crystallite size and shape with reference to hematite, which gradually becomes the predominant phase. Figure 2 shows the evolution of the shape of synthetic hematite crystals as a function of the annealing temperature. Goethite features prismatic, highly asymmetric crystallites. Once goethite is transformed into hematite, the crystallites progressively lose their initial asymmetry, related to the shape of the original goethite grains, and become more and more equiaxed with temperature. TEM observations (insets of Fig. 2) that were conducted in order to validate the results of the microstructural characterisation, revealed that the shape of the original material was retained up to 800°C. After 1 h at 1,000°C, a complete recrystallisation of the prismatic domains occurs. Coherently with this picture, partially sintered clusters of equiaxed grains now become visible.

As for the archaeological nodules, the crystallographic domains of hematite present a significant variability in size and shape. The values of the grain size in the $\langle 110 \rangle$ and $\langle 104 \rangle$ directions are reported in Table 1. Whether this variability is related to an effective difference in the formation of the hematite is still under study. A working hypothesis is that archaeological hematite, which appears asymmetric and with small domains, might be obtained through thermal treatments of goethite materials; whereas the archaeological hematite which shows a rather equiaxed scattering of the domains might be either natural hematite or synthetic hematite formed by long term heating.

Comparing this data with the Raman results, it is apparent that for the same I_{660}/I_{610} ratio, the broadening is indeed related to the domain size, the samples with larger peaks (43 Gc, 42 Mb) presenting smaller grains than 43 Mb. Finally, it is worth noting that we measured the Raman spectra of the goethite nodules found

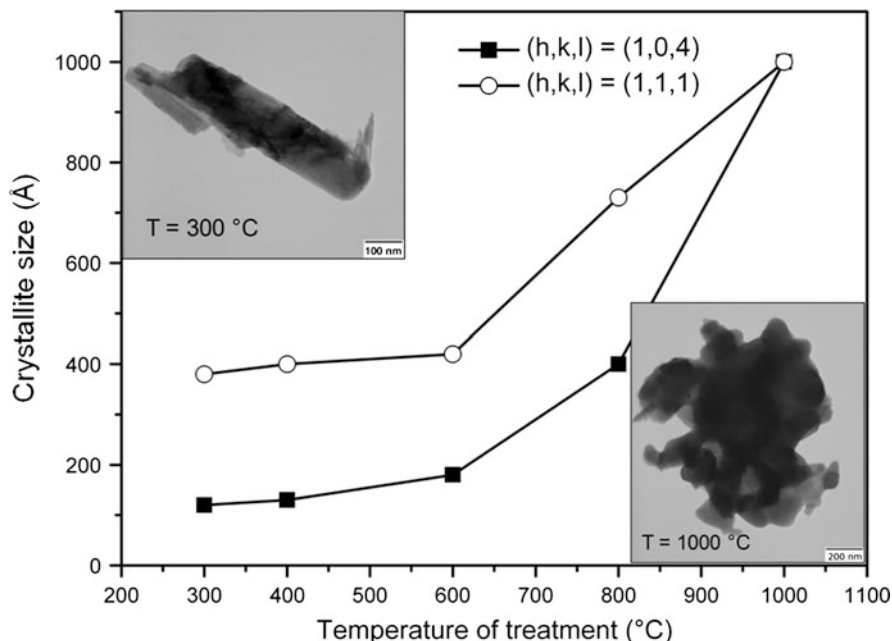


Fig. 2 Evolution of the size of synthetic hematite crystallite along the $\langle 104 \rangle$ and $\langle 110 \rangle$ directions with annealing temperature. *Insets:* TEM images of the goethite powder heat treated at 300 °C (*upper left*) and 1,000 °C (*lower right*)

near Riparo Dalmeri. After heat treatment at 1,000 °C for 1 h, the features of the spectra resemble those of the archaeological samples (see Fig. 1). A temperature of 1,000 °C is probably unattainable by a wood fire, but it is plausible that prolonged heat treatment at a lower temperature may induce similar effects.

4 Conclusion

Microstructural analyses of synthetic hematite, obtained by annealing commercial goethite, show an evolution of the shape of the crystal upon heating the starting goethite powder. This evolution might be used to verify if the palette of several ochre fragments originating from Riparo Dalmeri is natural, or if it is due to contact with a heating source. The XRD results show that almost all of the archaeological hematite specimens have asymmetric grain shapes similar to the asymmetric grain shape of the synthetic hematite obtained by heat treatment of a goethite powder. The significant correlation with the Raman results indicates that the size effect plays a significant role in the Raman spectra of the archaeological ochres. This aspect can open the way to less invasive analyses of the microstructure of valuable specimens.

Acknowledgements The authors acknowledge the financial support of Provincia Autonoma of Trento through the MATIS project, and of the “Museo Tridentino di Scienze Naturali” of Trento.

References

- Belli R, Frisia S, Gialanella S, Dalmeri G, Benedetti L, Zadra M, Armellini C (2007) Red painted stones from Riparo Dalmeri: a methodological approach to palaeoclimatic reconstruction. *Proceeding of AIAR Pisa 2006*. Patron Editore, Bologna, pp 15–24
- Belli R, Lonardelli I, Quaranta A, Girardi F, Cusinato A, Dalmeri G (2008) A methodological approach to discriminate between natural and synthetic haematite used as prehistoric pigments: preliminary results (Riparo Dalmeri – Trentino, Italy). *Proceedings of AIAR Firenze 2007*
- Bersani D, Lottici PP, Montenero A (1999) Micro-Raman investigation of iron oxide films and powders produced by sol–gel syntheses. *J Raman Spectrosc* 30:355–360
- Lonardelli I, Wenk HR, Lutterotti L, Goodwin M (2005) Texture analysis from diffraction images with the Rietveld method: dinosaur tendon and salmon scale. *J Synchrotron Radiat* 12:354–360
- Lutterotti L, Gialanella S (1998) X-ray diffraction characterization of heavily deformed metallic specimens. *Acta Materialia* 46:101–110

“Ramses II in Majesty”: A Minero-Petrographic and Provenance Rock Study

A. Borghi, E. D’Amicone, M. Serra, G. Vaggelli, and L. Vigna

1 Introduction

Egyptian stones are of primary importance among all the natural stones used for monumental works in various historical epochs, from the Ancient Egyptians through the Romans and until today. Recently, a straightforward project aimed at investigating the stony handcrafts preserved in the Egyptian Museum of Turin, Italy, has been undertaken, with the specific purpose of obtaining a systematic petrographic classification of these objects and determining their possible geological source.

The purpose of the present paper is the minero-chemical investigation of rock fragments collected from the statue of “Ramses II in Majesty”, a symbol of the Egyptian Museum of Turin and universally considered as one of the most important masterpieces of the Egyptian civilisation. This statue was found in 1818 by Drovetti and his collaborator Jean-Jacques Rifaud in the God Amon temple of Karnak, Thebes. Although this statue has been extensively studied by archaeologists, the geological classification of the source material is poorly known. In fact, the Ramses II statue is made of a dark-coloured and fine-grained stone that, until recently, was believed to be a basalt or a gabbro.

The recent cleaning and conservation work carried out with the purpose of restyling the statuary rooms of the museum and promoting the “Riflessi di Pietra” exhibition provided the opportunity to examine the nature of the stone in this statue and to investigate the provenance of the source rock. Indeed, a detailed minero-chemical investigation of the stony material in the “Ramses II in Majesty” has been

A. Borghi (✉) and M. Serra

Dipartimento di Scienze Mineralogiche e Petrologiche, Via V. Caluso, 35, 10125 Torino, Italy
e-mail: alessandro.borghi@unito.it

E. D’Amicone and L. Vigna

Soprintendenza Archeologica per il Piemonte e del Museo Antichità Egizie, Via Accademia delle Scienze, 6, 10123 Torino, Italy

G. Vaggelli

CNR – Istituto di Geoscienze e Georisorse, Via V. Caluso, 35, 10125 Torino, Italy

performed in order to determine the rock type and to discover the provenance of the original rock for restoration purposes.

A preliminary geological/bibliographic study permitted the identification of strong macroscopic analogies between the ancient stony handcraft and the so-called “Black Granites” outcrop in the southern part of Egypt, near Aswan (Klemm and Klemm 2001). According to archaeological evidence, the hypothesis that the stone in the Ramses II statue may have been exploited in the famous quarry district of Aswan was thus formulated. The collection of several stony fragments from the still active Aswan quarry sites was carried out following the criterion of macroscopic analogy with the stone samples taken from the statue.

The Aswan quarry district has been active since the fourth millennium BC and is very well-known as the primary mining district for the so-called “Red Granite” and “Black Granites”: intrusive rocks, from granite to granodiorite and tonalite, whose formation is attributed to the late Precambrian Age (Ragab et al. 1979). Red granite represents the main magmatic body outcropping in the Aswan area, east of the Nile River. Its peculiarity derives from the occurrence of reddish large K-feldspar porphyrocrystals, which confer an unmistakable and unique aspect to the stone. Black granites include granodiorite and tonalite varieties (Klemm and Klemm 2001) outcropping on the east side of the River Nile, between Aswan and El-Shellal, as well as on fluvial islets near these areas.

2 Results

Two small fragments were removed from the back of the Ramses II statue and were prepared as polished thin sections. Petrographic examination was undertaken using a polarizing microscope; a scanning electron microscope (SEM; Cambridge Stereoscan S360), equipped with an energy-dispersive spectrometer (EDS; Oxford Instruments), was used for the minero-chemical analysis. For provenance purposes, geological samples collected from the Aswan quarry district were analysed in the same analytical condition in order to determine if any of them presented a match and could perhaps constitute a potential source of the rock used for the statue. Therefore, both the main granodiorite body and the more mafic and finer-grained tonalite intrusions from “Black Granites”, outcropping in the Gebel Ibrahim Pasha area, as well as the common “Red Granite” variety from Marmonil quarry, were sampled.

2.1 Petrography

The stone in the statue of Ramses II consists of a dark grey-coloured and medium/fine-grained igneous rock. It has a holocrystalline texture and is composed of plagioclase (ca. 35 wt%), quartz (ca. 20 wt%) and a high (ca. 40 wt%) content of

femic minerals (green amphibole and dark biotite). Plagioclase is mainly euhedral and perthitic, containing most accessory minerals. Quartz is less abundant than plagioclase and occurs as anhedral grains with sutured or interlocking boundaries. Some grains show undulose extinction, indicating strain during crystallisation or the subsequent geological history. Green amphibole, most likely hornblende, has a higher modal abundance than biotite. Strongly pleochroic, from dark green to yellow, amphibole generally occurs in subhedral prismatic crystals. Biotite shows strong pleochroism, from yellow-brown to dark brown, locally with irregular resorption shapes. The main accessory minerals are apatite, ilmenite and magnetite. Apatite (ca. 1 wt%) is present as euhedral grains, with hexagonal prismatic to acicular shapes, often present in silic minerals. Zircon, monazite, allanite, barite and pyrite also occur as small and minor accessory phases. Despite the high colour index due to the occurrence of high amounts of biotite and amphibole, the modal abundance of quartz with respect to the other silic minerals is >20% in volume, and, therefore, the stone in the Ramses II statue is a “granite rock-type”. Finally, considering the relative modal contents of silic constituents, it may be classified as a tonalite according to the QAPF diagram of Le Bas and Streckeisen (1991).

The geological samples collected in the Aswan quarry district to determine a potential source of the rock used for the “Ramses II in Majesty” were identified as granodiorite and tonalite magmatic rock sources. Granodiorite samples have a holocrystalline texture, tending to porphyritic, and a medium/large grain size. The mineralogical assemblage is represented by quartz, plagioclase, reddish K-feldspar, biotite and green amphibole. The colour index is around 30%. Plagioclase is dominant with respect to quartz and K-feldspar. It is generally anhedral or tabular, and sporadically forms myrmekitic or antiperthitic textures. K-feldspar occurs as microcline, is idiomorphic and micropertthitic. Quartz forms interstitial aggregates. Biotite is dark and more abundant than green amphibole, but both minerals are rich in accessory minerals, such as apatite, titanite, Fe–Ti oxides and zircon. The presence of silic mineral aggregates, partially iso-oriented, is a typical and widespread occurrence (Middleton and Klemm 2003). These aggregates are constituted by perthitic plagioclase and subordinate quartz in the core, and by reddish K-feldspar as the border rim. Microscopic veinlets of pink granite, due to the occurrence of reddish K-feldspar along the vein border, sometimes traverse the main granodiorite assemblage.

Tonalite samples are medium/fine-grained, have a holocrystalline texture, tending to omeo-granular, and a colour index comparable to granodiorite, even if the macroscopic appearance of the rock is much darker (dark grey) than that of granodiorite. The rock is composed of biotite, green amphibole, plagioclase, quartz and much more subordinate K-feldspar (<5%). Amphibole is slightly more abundant than biotite, even if both femic minerals tend to occur as aggregates. Plagioclase and quartz occur in comparable amounts, but plagioclase is euhedral, partially sericitic, and sporadically occurs as phenocryst, while quartz is mostly interstitial and sometime with undulose extinction. Apatite is widespread and present in larger amounts with respect to granodiorite samples. Other accessory minerals are titanite, Fe–Ti oxides, zircon, epidote (allanite) and pyrite.

2.2 Mineral Chemistry

Electron microprobe analyses of mineral phases were performed on both fragments from the Ramses II statue and on rock samples from Aswan. The chemical composition of biotite from the stone in the Ramses II statue corresponds to a Fe-biotite. Green amphibole occurs as Fe-hornblende or rarely as Fe-edenitic hornblende. Plagioclase is a slightly normal-zoned oligoclase, with low contents of anorthite (ca. 27% in the core and 21% in the outer rim). Apatite is the main accessory mineral and is widespread, abundant (about 1 wt%), idiomorphic and occasionally zoned. The main characteristics of apatite are the partial substitution of P by Si (about 0.2%) in the core of the crystals and the occurrence of significant amounts of fluorine (about 1 wt%).

Figure 1, which displays the chemical distribution field for granodiorite, tonalite (“Black Granites”) and granite (“Red Granite”) amphiboles from the Aswan quarry district, shows that Ramses II amphibole overlaps with the tonalite chemical field. The same situation is visible in Fig. 2, which shows the chemical distribution of biotite for granodiorite, tonalite and granite, in comparison with the stone from the “Ramses II in Majesty”. With regards to plagioclase, it is worth noting that all rock samples coming from Aswan have in common a relatively low content of anorthite ($Ab/An < 30\%$) and a slight compositional zoning, more evident in granite than in granodiorite and tonalite samples. Moreover, they are all characterised by a high modal content of apatite, increasing in amount from granite to tonalite through granodiorite.

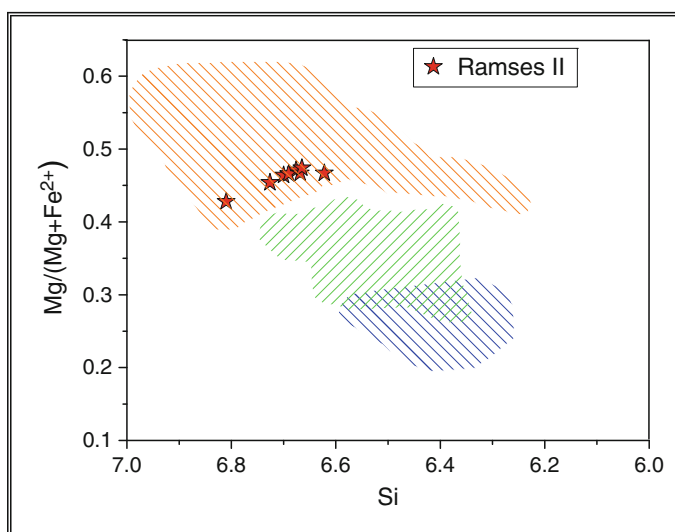


Fig. 1 Variation in the chemical composition of amphibole expressed as $Mg/(Mg+Fe^{2+})$ versus Si atoms per formula unit. Red field = amphibole chemical distribution for tonalite samples. Green Field = amphibole chemical distribution for granodiorite samples. The amphibole chemical distribution of “Red Granite” samples collected from the Marmonil quarry district is also reported (blue field)

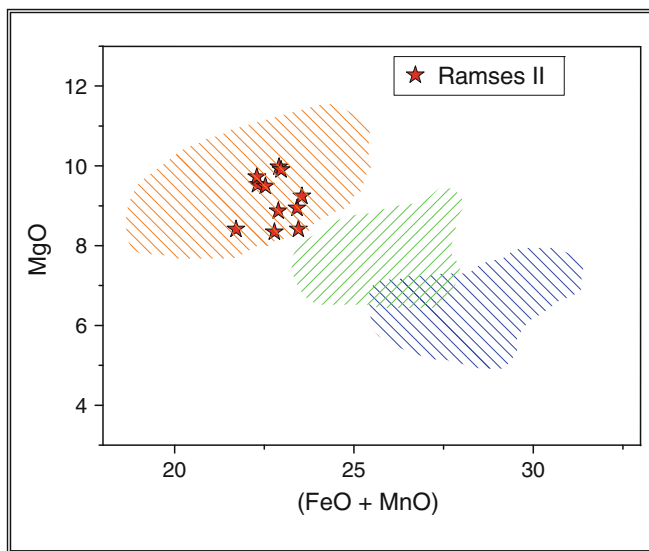


Fig. 2 Variation in the chemical composition of biotite expressed as (FeO + MnO) versus MnO (wt%). Red field = biotite chemical distribution for tonalite samples. Green Field = biotite chemical distribution for granodiorite samples. The biotite chemical distribution of “Red Granite” samples collected from the Marmonil quarry district is also reported (blue field)

3 Conclusions

The petrographic and minero-chemical study has shown that the stone material used for the construction of the Ramses II statue can be classified as a melanocratic tonalite. The provenance hypothesis, based on the archaeological and geological literature, has been confirmed by the close similarities between the stone in the Ramses II statue and the rock samples collected in the Aswan quarry district. In particular, a good compatibility with the so-called “Black Granites” of Aswan has been recognized, including granodiorite and tonalite rock. The first piece of evidence is represented by the identical macroscopic aspect of Aswan tonalites and the stone in the “Ramses II in Majesty”. Both rocks are fine grained and dark coloured. Indeed, according to microscopic observations, the colour index has been valued at approximately 40% in volume. It is important to emphasize that all Aswan rocks are characterised by a high colour index, ranging from about 10% in granites to 40% in tonalites. The petrographic study also revealed a comparable microscopic holocrystalline texture with a common mineralogical assemblage of “granite” type, with the exception of K-feldspar, absent in small fragments from the Ramses II, seldom and subordinate in the tonalite variety, and much more significant and widespread in the granodiorite samples. Plagioclase compositional zoning, both in the Aswan samples and in the stone from the Ramses II, shows a low content of anorthite,

while quartz is always an interstitial phase, often present in aggregates with undulose extinction.

The constant coexistence of green amphibole and biotite, often concentrated in aggregates, is also remarkable. Compositional data clearly indicate that the stone in the Ramses II statue overlaps with the tonalite field, both in the biotite and in the amphibole diagrams (Figs. 1 and 2). With regards to the accessory minerals, a remarkable feature, common to all studied samples, is the relative abundance of apatite, about 1% in the stone from the Ramses II, and with an amount that increases from Aswan granites to granodiorites and tonalites. Moreover, both in the stone from the Ramses II statue and in Aswan samples, apatite is characterised by a partial substitution of P by Si in the crystal core. The constant occurrence of allanite, titanite and zircon, together with the coexistence of ilmenite and magnetite, finally confirm the provenance of the stone in the “Ramses II in Majesty” to the tonalite rock belonging to the well-known “Black Granite” quarried in the area of Aswan.

References

- Klemm R, Klemm DD (2001) The building stones of ancient Egypt – a gift of its geology. *J Afr Earth Sci* 33:631–642
- Le Bas MJ, Streckeisen AL (1991) The IUGS systematics of igneous rocks. *J Geol Soc* 148(5): 825–833
- Middleton A, Klemm D (2003) The geology of the Rosetta stone. *J Egypt Archaeol* 89:207–216
- Ragab AL, Meneisy MY, Taher RM (1979) Contributions to the petrography, petrochemistry and classification of Aswan granitic rocks. *Chemie der Erde* 38:121–135

Using Non-destructive X-Ray Fluorescence Analysis to Investigate the Prehistoric Use and Distribution of Hornfels in Southern Quebec

A.L. Burke and G. Gauthier

1 Introduction

In the middle St. Lawrence Valley of southern Quebec, Canada, there is a lack of suitable raw material for making chipped stone tools. Throughout prehistory, aboriginal groups used different strategies to compensate for this deficiency such as regional movement of groups during seasonal subsistence cycles to visit quarries (Paleoindian period, 11,500–9,500 BP), long distance trade (Late Archaic and Early Woodland periods, 6,000–2,000 BP), or substituting stone with other materials like bone to make tools (Late Woodland period, 1,000–400 BP). Aboriginal people could also use local materials that were of lesser quality (e.g., quartz, shale, and hornfels). In southern Quebec, Cretaceous igneous intrusions created the Monteregian hills and through contact metamorphism converted the overlying Utica shale to hornfels. In 1993, archaeologists discovered a prehistoric hornfels workshop site on the northern flank of Mont Royal in the heart of Montreal (Ethnoscop 1998). This site is an extensive workshop for the bifacial reduction and transformation of hornfels associated directly with bedrock outcrops further up the hillside. Hornfels is found on at least 21 other prehistoric habitation sites in southern Quebec spanning 5,000 years from the Late Archaic to the Late Woodland period (Table 1). For this study we characterized samples from six of these sites.

A.L. Burke (✉)

Département d'Anthropologie, Université de Montréal, C.P. 6128, succursale Centre-ville
Montréal, Montreal, QC, Canada H3C 3J7
e-mail: adrian.burke@umontreal.ca

G. Gauthier

Département de Chimie, Université de Montréal, Montreal, QC, Canada

Table 1 Archaeological sites containing hornfels, and periods of occupation, analyzed as part of this study

Archaeological site	Late Archaic	Early Woodland	Middle Woodland	Late Woodland
Place-Royale				X
Île Ste-Hélène				X
Petit Séminaire St-Sulpice				X
Place Jacques-Cartier			X	X
LeMoyne-LeBer			X	X
N.-Dame-de-Bon-Secours			X	X
Nivard			X	X
MacFarlane			X	X
Île du Large			X	X
Bilodeau		X	X	X
Pointe-du-Gouvernement	X		X	X
Pointe-du-Buisson	X	X	X	X
Île Beaujeu	X	X	X	X
Oka	X	X	X	X
Baie Martin		X		
Île Ste-Thérèse		X		
Lac Leamy 7	X		X	
Île Morrison	X			
Île aux Allumettes	X			
Brouillet	X			
Jacques	X			

2 Research Objectives

The archaeometric research problem can be divided into three inter-related steps:

- (a) Geochemical characterization of the Mont Royal hornfels quarry (BjFj-97) in order to measure the intra-source variability of the hornfels from Mont Royal and decipher its geochemical signature.
- (b) Compare the geochemical signature of Mont Royal hornfels to that of hornfels artifacts found in the greater Montreal area in order to see if they originate from this quarry.
- (c) Assess the effects of weathering of archaeological hornfels on the precision and accuracy of the geochemical characterization and our ability to assign the artifacts to a specific quarry source.

3 Sample Preparation

Geological samples from the quarry source on Mont Royal were cut on a rock saw, polished and then cleaned in alcohol using an ultrasound. The resulting flat (relief-free) surface reduces absorption and fluorescence effects and ensures uniform, within sample X-ray path lengths. Flakes and tool fragments were cleaned in alcohol using an ultrasound.

4 Methods

A PANalytical Epsilon 5 energy dispersive X-ray fluorescence spectrometer with polarizing optics equipped with a 100 kV generator, a side window Gd tube, a liquid nitrogen cooled Ge detector and 15 secondary targets was used to analyze geologic and archaeological samples. Major and trace elements were determined using calibration curves established with up to 20 geologic certified reference materials (USGS, GSJ, IGGE, CANMET, NIST). The analytical parameters of the analyses are available from the authors upon request. Additional ongoing analyses include thin section petrography, neutron activation analysis, and scanning electron microscopy.

5 Geochemical Characterization

Major and trace element concentrations were determined by EDXRF on 9 geological samples, and 24 flakes and tool fragments from 6 archaeological sites. Geochemical characterization was performed using a modified spider diagram. EDXRF data were normalized to Upper Continental Crust values of Taylor and McLennan (1985) and McLennan (2001). Spider diagrams were chosen to highlight chemical distinctiveness and facilitate sample comparison. Major element and trace element box plots were constructed using geological data. Concentration data for individual weathered artifacts were then overlaid on the former to evaluate the goodness of fit.

6 Results and Discussion

Do the hornfels artifacts found on prehistoric sites in southern Québec come from the Mont Royal quarry? Some of the artifacts are a perfect match for the Mont Royal source (Fig. 1). Other artifacts do not match the Mont Royal quarry very well which strongly suggests that there are undiscovered prehistoric quarries on some of the other Monteregian hills of southern Quebec.

As archaeologists we must be fully aware of the geochemical impacts of artifact weathering (e.g., during burial) as it can seriously compromise provenance sourcing. At the Université de Montréal we are developing the non-destructive analytical capabilities of EDXRF which precludes the removal of artifact surface alteration. We have looked at various weathered and unweathered hornfels samples to try and evaluate the reliability of most major and trace elements. Figure 2 presents the box plot values for a heavily weathered hornfels flake which, based on the major elements, appears to not match well with the Mont Royal quarry. As expected, the more mobile major elements (Fig. 2) are significantly affected by the weathering of the samples. On the other hand, some of the heavier or higher energy elements such as the lanthanides and the high field strength elements (Fig. 3) seem unaffected by the surface weathering judging from the overall fit of the values of the weathered hornfels flake with the box plot values for the cut and polished quarry hornfels. As

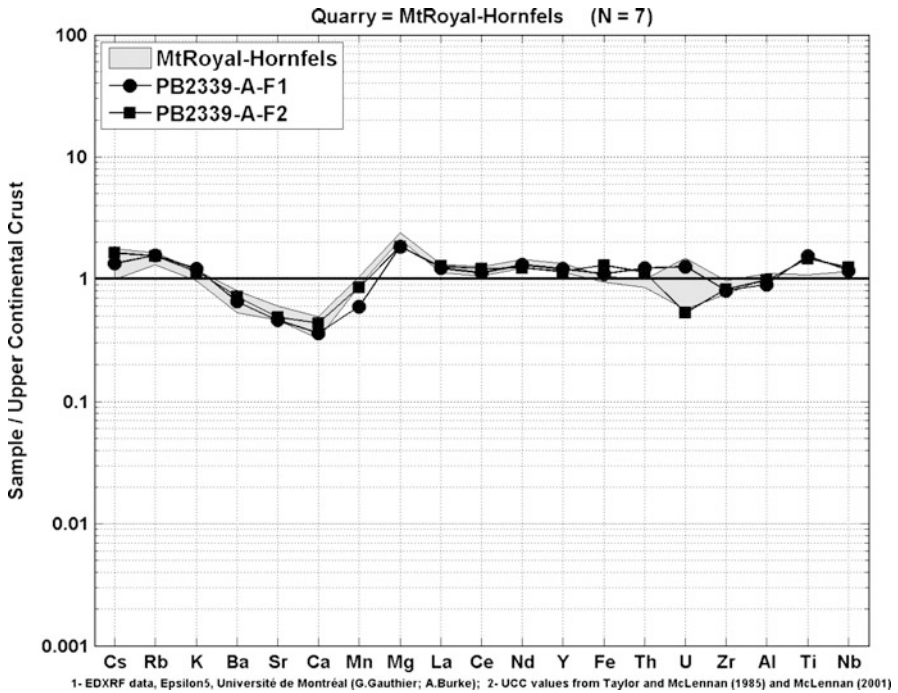


Fig. 1 Spidergram of EDXRF concentrations for a hornfels flake from the Pointe du Buisson archaeological site showing a strong affinity with the Mont Royal hornfels quarry (grey area). Both faces (F1, F2) of the artifact were analyzed showing very good reproducibility for a weathered sample

the analysis depth varies greatly with the energy of the X-ray radiation (roughly 8 μm for Mg, 110 μm for Cr, and 0.9 cm for Sn), not all elements will thus reflect the average composition of the artifact. Figures 2 and 3 (increasing analysis depth from left to right, x axis) clearly show the impact of the variable depth of X-ray penetration as the major elements (2, small analysis depth) are essentially sampling the altered surface while most trace elements (3, greater analysis depth) show greater compatibility with the Mont Royal quarry chemical composition determined from an unweathered surface.

7 Conclusion

The non-destructive EDXRF analysis of geologic and archaeological samples of hornfels has proven quite successful to date, and we have been able to achieve our three research goals.

- (a) We were successful in deciphering the geochemical signature (spidergram pattern) of the hornfels coming from the Mont Royal prehistoric quarry and

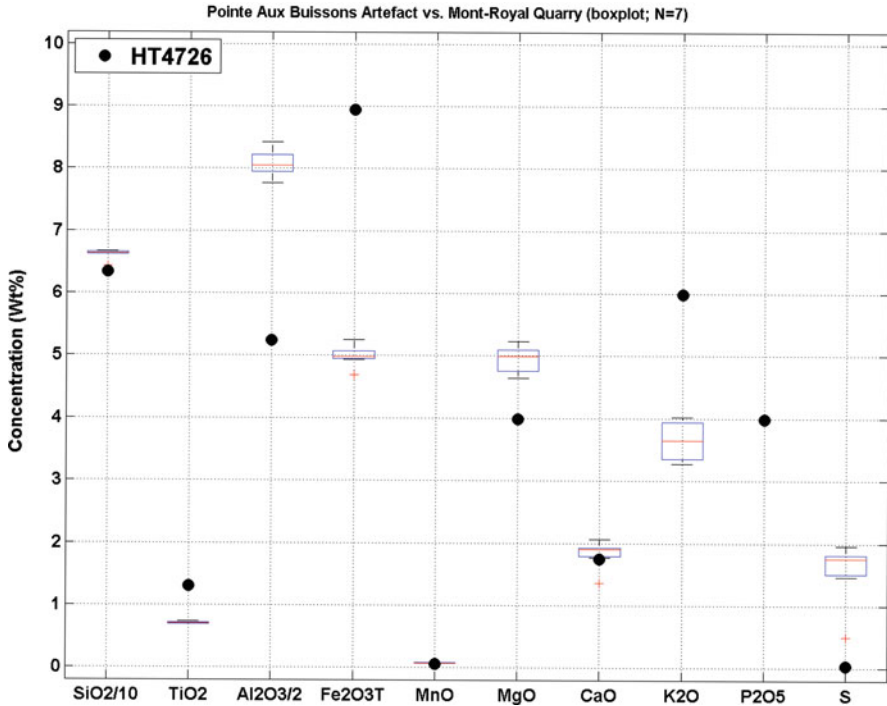


Fig. 2 Box plot of EDXRF major element values for a heavily weathered hornfels flake (dots) compared to the values for the Mont Royal hornfels quarry (boxes)

workshops. The intra-source variability appears to be measurable and manageable and we now have the baseline data we need to compare many more artifacts from various sites in the region and test if they come from the Mont Royal quarry. Our initial results also clearly suggest that there are other prehistoric quarries of hornfels that were exploited, most likely on the other Monteregian hills of southern Quebec. The sampling of these hornfels outcrops is part of the next phase of our study of prehistoric hornfels use in southern Quebec.

- (b) We have confirmed that several sites in southern Quebec contain hornfels artifacts that come from the Mont Royal quarry in Montreal. Some sites also produced hornfels artifacts from other sources. To locate these prehistoric quarries will require further geoarchaeological fieldwork. We plan to continue the EDXRF analysis of a number of archaeological sites in order to increase the number of archaeological artifacts analyzed. This will help us to better understand the use of this local and somewhat mediocre lithic resource throughout prehistory and track the changes in its distribution throughout southern Quebec and adjacent states and provinces.
- (c) We were able to assess the effects of surface weathering on the geochemical signature of archaeological hornfels. It appears that the major elements are especially affected by weathering and are therefore not very reliable for

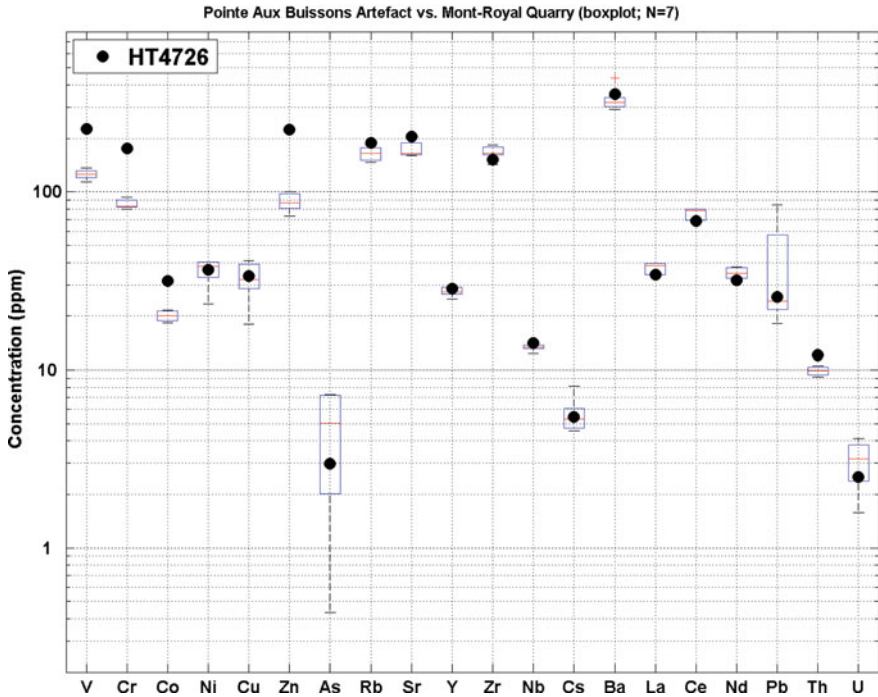


Fig. 3 Box plot of EDXRF trace element values for a heavily weathered hornfels flake (*dots*) compared to the values for the Mont Royal hornfels quarry (*boxes*)

assigning artifacts to a quarry source. On the other hand, this research has also demonstrated that we may be able to use the lanthanides, high field strength elements, and other higher energy elements to characterize weathered artifacts reliably. Clearly this will require further testing and we are now proceeding with *before and after* type analyses of altered artifacts by polishing one side to analyze a fresh surface and compare the results.

Acknowledgements Thank you to Dr. Christian Gates St-Pierre, archaeologist, Ville de Montréal, for supporting this research and providing access to the archaeological materials.

References

- Ethnoscop Inc. (1998) Parc du Mont-Royal, Montréal. Inventaire archéologique du site préhistorique BjFj-97. Report submitted to the Ministère de la culture, Québec
- McLennan SM (2001) Relationships between the trace element composition of sedimentary rocks and upper continental crust. *Geochem Geophys Geosyst* 2:doi 2000GC000109
- Taylor SR, McLennan SM (1985) The continental crust: its composition and evolution. An examination of the geochemical record preserved in sedimentary rocks. Blackwell, London

Clinical Test Strips for Rapid Identification of Binder Materials in Rock Paintings

D. Fraser and R.A. Armitage

1 Introduction

Clinical test strips were developed by the Bayer Corporation in the 1960s for rapid and simple analysis of urine samples. The test strips consist of a waterproof plastic strip with reagent-impregnated pads that undergo color changes to indicate pH or the presence of protein, glucose, or blood. The blood diagnostic is based on the fact that the heme iron complex catalyzes the reaction between diisopropylbenzene dihydroperoxide with 3,3',5,5'-tetramethylbenzidine to give a green or blue color. Bayer (2003) specifies that optimal results require the use of fresh, well-mixed, uncentrifuged urine.

Such colorimetric presumptive tests for blood are commonly employed in forensic applications. Starting in the early 1980s, these test strips were further utilized to detect blood residues on lithic materials (Loy 1983; Loy and Hardy 1992; Loy and Dixon 1998), though concerns about cross-reactivity with substances in the burial environment from which most tools were recovered have remained (Custer et al. 1988; Gurfinkel and Franklin 1988; Smith and Wilson 1992; Manning 1994; Downs and Lowenstein 1995). From this application, it was a small step to applying the strips to identifying blood as a binder in rock art (Williamson 2000). Either water or a buffered solution of EDTA was used to “extract” some of the hemoglobin from the paint while still on the wall, and the resulting solution was then placed on the reagent strip. A green result was interpreted as proof that blood was present in the paint. Cross-reactivity with other peroxidases from bacteria and plants could conceivably cause false positive results. Use of EDTA was proposed to reduce such likelihood by supposedly chelating the magnesium in the porphyrin structure of chlorophyll.

D. Fraser (✉)

Chemistry Department, Lourdes College, 6832 Convent Blvd, Sylvania, OH 43560, USA
e-mail: dfraser@lourdes.edu

R.A. Armitage

Department of Chemistry, Eastern Michigan University, Ypsilanti, MI 48197, USA

On-site testing of rock art would be useful for screening paintings prior to sampling for dating; however, few tests have adequately investigated the reliability of applying presumptive colorimetric tests to rock art. We have here undertaken detailed analysis of both known and unknown rock painting binders to determine if the Hemastix analysis is truly a useful technique for identifying blood under these conditions. Further evaluation of the biochemical and inorganic reactions at work is certainly warranted, considering the many reports on cross-reactivity that exist in the archaeological science literature.

2 Experimental

2.1 *Materials*

Several modern binder materials were studied. These included: defibrinated dried beef blood reconstituted in pH 7.4 phosphate-buffered saline solution (PBS); hemoglobin suspended in pH 7.4 PBS; bone marrow from beef long bones; egg (whole, yolk, and white); plant carbohydrates (aloe, prickly pear, yucca root); saliva; animal fat (whole and rendered). Controls were deionized water and pH 7.4 PBS. The study took place in three phases: a short term outdoor phase (I), a short term temperature-dependent phase (II), and a long term room temperature phase (III).

A selection of authentic rock painting samples from Texas, Idaho, North Dakota, Montana, and Guatemala were also subjected to the Hemastix procedure. Red and black paints and unpainted substrate were tested for comparison. The Idaho sample had small patches of lichen present on the substrate sample.

2.2 *Preparation*

Each binder was prepared both with and without pigment to evaluate how the presence of a pigment affects the Hemastix test. For Phases I and II, the binder alone and the paint (binder plus pigment) was applied in duplicate to sterile microscope slides which were then mounted on two plexiglass sheets. For Phase I, one sheet was placed vertically at a height of ~2.5 m above the ground and exposed to the elements to simulate rock paintings in an outdoor environment. For Phase II, the other sheet was placed vertically at a height of ~2 m in an enclosed dirt-floored structure to simulate an enclosed cave environment, where temperature was the only variable. The paints in Phases I and II consisted of the binders listed with several different pigments: iron oxide (Fe_2O_3 , red), limonite (FeOOH , yellow), manganese dioxide (MnO_2 , black), and calcium carbonate (CaCO_3 , white). For Phase III, the binder alone or the paint (binder + Fe_2O_3 pigment) was applied to sterile microscope slides as well as on either cut limestone slabs or limestone chunks. These samples were stored in the laboratory over 6 years.

2.3 Methods

Extractions were performed by the procedure described by Williamson (2000). A 10 μL aliquot of ultrapure water (distilled deionized, 18 $\text{M}\Omega$) was applied to the surface of the paint with a sterile micropipet tip, scraping the paint with the tip. The resulting solution was usually drawn up with the same pipet time; however, as fat and bone marrow typically clogged the tip, a new one was needed to remove the solution. The solution was then applied to the yellow hemoglobin-detecting tab on Hemastix or Combistix reagent strips. To evaluate the Na-EDTA solution proposed by Loy for reducing false positives, we applied the same method of extraction, using a 0.5 M pH 8 Na-EDTA solution. The intensity of the color developed on the reagent pad was classified on a scale of 0 (no reaction) to 6 (instantaneous complete color change to dark green-blue).

3 Results and Discussion

The response of the reagent pads to hemoglobin decreased markedly in less than 6 years, even under laboratory conditions. None of the authentic rock art samples gave a positive result for the presence of hemoglobin. The observed trends in reactivity between blood and the Hemastix reagents over time are shown in Fig. 1. Figure 1a shows how blood alone loses all reactivity quickly when exposed to the weather (Phase I) and naturally-fluctuating temperatures (Phase II); Fig. 1b shows the effect of Fe_2O_3 pigment. Whether the pigment accelerates the aging process or protects the proteins is not yet clear from this study.

The assessment and validation of any analytical technique should be based on such performance characteristics as sensitivity, lower limit of detection, selectivity, rate of false positives and negatives, and use of appropriate blanks. Consider Hemastix and Combistix for screening rock painting samples for blood. The sensitivity, defined as the amount of change in color of the test pad with small changes in hemoglobin concentration, is considered to be good, though this project was not sufficiently quantitative to determine a numerical sensitivity. The lower limit of detection, which should not be confused with the sensitivity, for the strips was determined by Bayer to be very low at 0.15 $\text{pg}/\mu\text{L}$. The selectivity of the method is poor, however, as the tetramethylbenzidine (TMB) reagent in the strip pad reacts non-selectively with most peroxidases and other redox-active species.

Lack of selectivity can lead to a high rate of false positives, an indication that hemoglobin is present when it is in fact not. In this study, there were no false positives obtained. None of the binder materials that did not contain blood or hemoglobin yielded a positive hemoglobin test. This should not be taken to mean that false positives cannot occur. Over the timescale of the experiment, lichen colonies (bearing chlorophyll in some cases, which also reacts with TMB to yield a blue-green product) and bacteria did not develop on the paint samples. The black lichen on the Idaho rock painting sample did not yield a false positive result either.

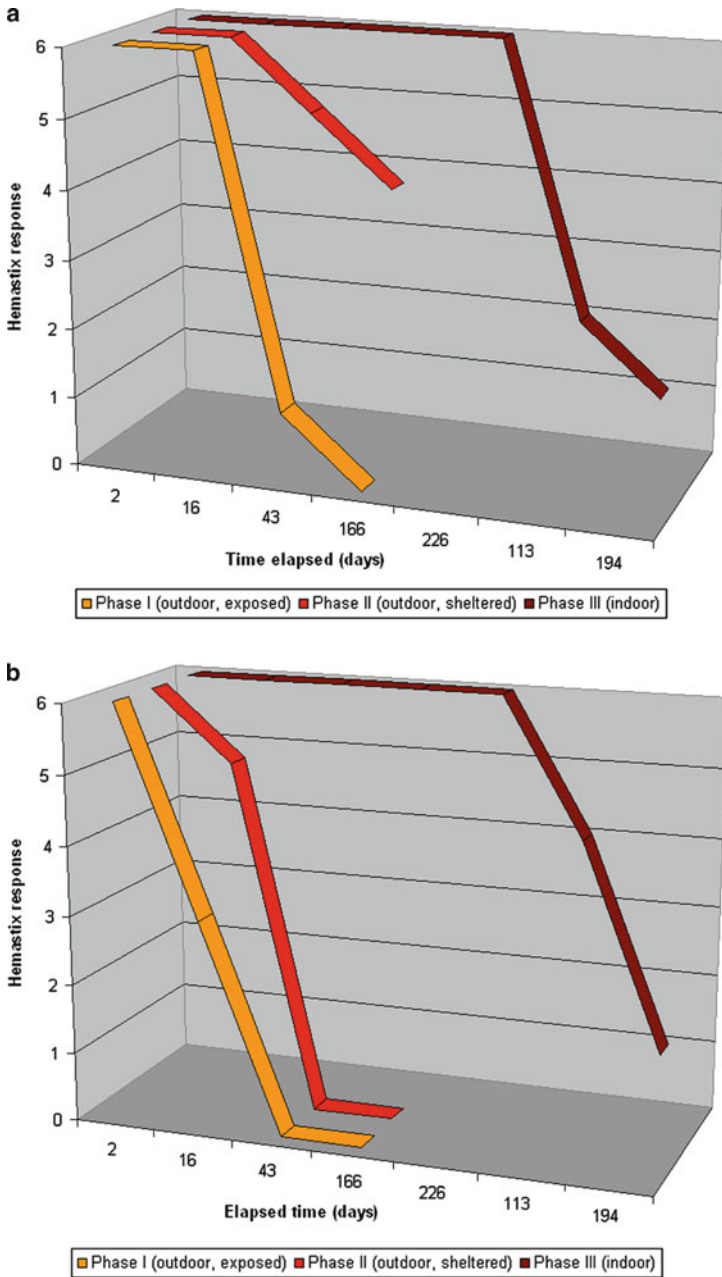


Fig. 1 Plots of change in Hemastix response to blood over time: (a) blood only; (b) blood plus iron oxide pigment

False negatives occur when a paint sample containing the heme Fe failed to give a positive result with the test strip. After 5.5 years, blood stored at room temperature still gave a positive result. Blood binders stored outdoors stopped giving positive results after just over 1 month in the presence of iron oxide pigment, and after 110 days without pigment. As the heme Fe complex decomposes due to exposure to the elements and bacterial action, weaker reactions were observed, indicating that the rate of false negatives will likely increase over time. This means that even paints that did at one time contain blood would be extremely unlikely to yield a positive result with the Hemastix test after any archaeologically-relevant passage of time.

One of the most important aspects of any analytical procedure is the use of appropriate controls. Three types of controls were used in this study. When either deionized water or pH 7.4 PBS is applied to the test strip pad as a negative control, no reaction occurs. Either solution containing fresh hemoglobin, the positive control, yields a fast, strong color change in the strip. The buffered Na-EDTA solution proposed by Loy as a scavenger for interferences merely suppresses the reaction between the TMB and the heme Fe complex: positive controls with Na-EDTA yield less of a color change than was observed for deionized water or PBS. EDTA is only a quantitative chelating agent for Mg^{2+} and Mn^{2+} over specific pH ranges (9.5–11.8 and 5.2–7.8 respectively, (Ueno 1965)), so at a pH of 8 (necessary to make Na-EDTA dissolve) the EDTA would not remove those contaminants prior to testing.

Hemastix and other hemoglobin-sensitive test strip methods are valid for their intended use in urinalysis. Based on the results of this project, the Hemastix procedure for identifying blood in rock painting samples is not a valid method.

4 Conclusions

Clinical test strips do not yield useful information about rock painting binders over even short nonarchaeological timescales. The reactivity of the test strips to blood decreases quickly – within a few years at most – as the heme breaks down. Exposure of the paints to fluctuating temperatures, weathering, and UV light speeds the breakdown of the heme iron complex. Clinical test strips, such as Hemastix, are inappropriate for screening rock paintings for the presence of blood.

References

- Bayer HealthCare (2003) Hemastix reagent strips for urinalysis. Bayer HealthCare, Elkhart, IN
- Custer JF, Ilgenfritz J, Doms KR (1988) A cautionary note on the use of Chemstrips for detection of blood residues on prehistoric stone tools. *J Archaeol Sci* 15:343–345
- Downs EF, Lowenstein JM (1995) Identification of archaeological blood proteins: a cautionary note. *J Archaeol Sci* 22:11–16
- Gurfinkel DM, Franklin UM (1988) A study of the feasibility of detecting blood residue on artifacts. *J Archaeol Sci* 15:83–97

- Loy TH (1983) Prehistoric blood residues: detection on tool surfaces and identification of species of origin. *Science* 220:1269–1271
- Loy TH, Dixon EJ (1998) Blood residues on fluted points from eastern Beringia. *Am Antiq* 63:21–46
- Loy TH, Hardy BL (1992) Blood residue analysis of 90,000-year-old stone tools from Tabun Cave. *Isr Antiq* 66:24–35
- Manning AP (1994) A cautionary note on the use of Hemastix and dot-blot assays for the detection and confirmation of archaeological blood residues. *J Archaeol Sci* 21:159–162
- Smith PR, Wilson MT (1992) Blood residues on ancient tool surfaces: a cautionary note. *J Archaeol Sci* 19:237–241
- Ueno K (1965) Guide for selecting conditions of EDTA titrations. *J Chem Edu* 42(8):432–433
- Williamson BS (2000) Direct testing of rock painting pigments for traces of haemoglobin at Rose Cottage Cave, South Africa. *J Archaeol Sci* 27(9):755

Archaeometric Processing of Polished Stone Artefacts from the Ebenhöch Collection (Hungarian National Museum, Budapest, Hungary)

O. Friedel, B. Bradák, G. Szakmány, V. Szilágyi, and K.T. Biró

1 Introduction

The petrological processing of archaeological polished stone artefacts from the Carpathian Basin has started to develop only in the last decades. This work benefited much from the systematic elaboration of historical collections from the nineteenth century. One of the most significant collections of this type was donated to the Hungarian National Museum by Ferencz Ebenhöch, abbot-prebend in Győr. The collection is extremely rich in polished stone artefacts, and unique not only because of its quantity (nearly 700 pieces), but also due to the beauty of the tools. To date, only a preliminary macroscopic petrographic identification had been carried out on the items. The aim of the present investigations was to identify and describe the raw material of the artefacts, and, if possible, determine their provenance.

2 Methods

A detailed macroscopic study of the complete set of artefacts was performed. Polarising microscope investigations were carried out on 30 samples, selected from each macroscopic group. Additionally, for more specific determinations, all samples were measured by the *magnetic susceptibility method* (MS). The bulk chemical composition of 41 samples was determined by non-destructive *prompt*

O. Friedel (✉) and G. Szakmány
Department of Petrology and Geochemistry, Eötvös Loránd University, Budapest, Hungary
e-mail: tolleetege@gmail.com

B. Bradák
Department of Physical Geography, Eötvös Loránd University, Budapest, Hungary

V. Szilágyi
Institute of Isotopes HAS, Budapest, Hungary

K.T. Biró
Hungarian National Museum, Budapest, Hungary

gamma activation analysis (PGAA). In seven samples, spot chemical analyses of mineralogical phases were obtained by *Scanning Electron Microscopy with Energy Dispersive X-ray Spectroscopy* (SEM–EDS).

2.1 General Overview of the Raw Material Types

The dominant raw material types of the polished stones are different types of greenschist-metabasites (three types at least), volcanites (mainly basalt and rarely andesite, trachyte, latite), metagabbro, serpentinite and nephrite. Rarer raw material types include hornfels, dyke and metadyke rocks, HP metamorphic rocks (eclogite, jadeite bearing rocks), sandstone, limestone and marl (Fig. 1).

3 Results

3.1 Petrography

“*Greenschist*” types (greenish, schistose metamorphic rocks, i.e. greenschist, amphibolite, amphibolite schist) contain fine- or very fine-grained massive rocks. On the basis of a macroscopic view, three different types were distinguished.

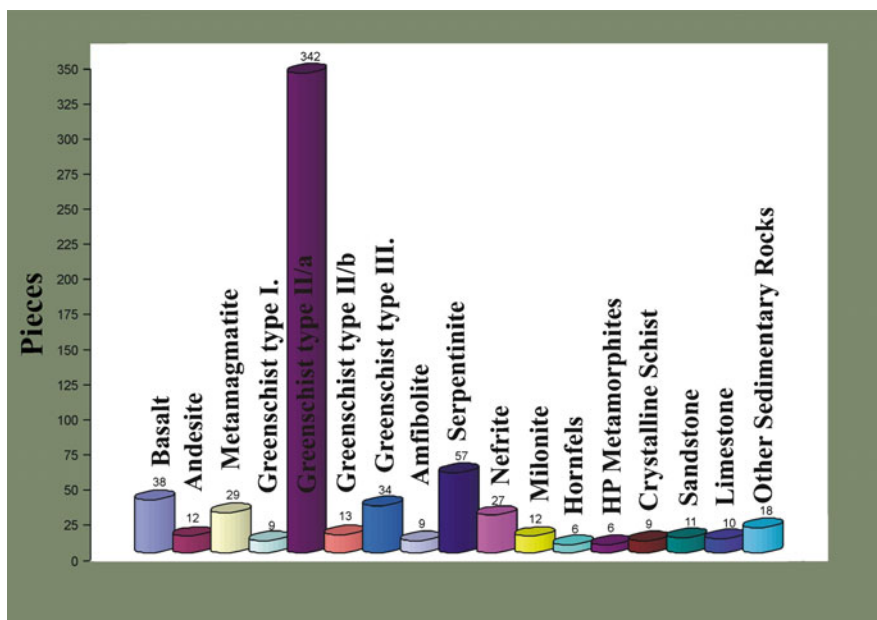


Fig. 1 The distribution of the rock types in the polished stone artefacts from the Ebenhöch Collection

Type I rocks have medium green colour, well foliated structure, and contain white, large (up to 1 cm length), lens-shaped feldspar aggregates. The average size of these tools is 3–10 cm. The typical mineral components of the greenschists are fine-grained amphibole (tremolite–actinolite), fine grained plagioclase (albite), opaque minerals, and sometimes chlorite, zoisite–epidote.

Type II rocks are characterized by dark green colour, slaty texture, almost perfectly foliated, and very fine-grained structure. The foliation consists of deep green and black bands, less than 1 mm thick, and sharply separated. The size of these stone tools varies from a few centimetres up to 40 cm.

According to the differences observed by scanning electron microscopy (SEM–EDS) among very similar greenschists of this group, two subtypes were established, namely II/a and II/b. Greenschists of type II/a have two kinds of amphibole, one of them is magnesium-rich hornblende, the other either anthophyllite or cummingtonite. The dominant feldspar is basic plagioclase; albite appears only in small quantities. We could recognise one opaque phase, i.e. ilmenite with a small Mn content, and small-sized apatite.

In the greenschist type II/b, the inhomogeneous plagioclases were mainly basic, and less frequently, acidic. The anthophyllite or the cummingtonite also appeared in this type of rock. Two kinds of opaque minerals (pyrite and ilmenite) were successfully determined. We also found a small amount of apatite and quartz in these rocks. Actually, the only difference between the two subtypes is represented by the presence of hornblende.

Type III rocks are greenschist-metabasites with dark green colour. They are less markedly foliated and contain large white feldspar aggregates. These rocks differ in macroscopic appearance from the samples of the above mentioned two groups. The length of the stone tools was between 4 and 13 cm. There are only complete specimens of this rock type; therefore, we could not obtain thin sections from them.

The *serpentinites* are fine- or very fine-grained rocks. Their colour is various: green, greenish yellow, or sometimes reddish yellow (due to alteration). The typical mineralogical phases are antigorite, chrysotile, opaque minerals, and occasionally pyroxene relics. Newly formed amphibole may also occur.

The *basalts* are macroscopically black or dark grey, fine- or very fine-grained rocks. The minerals present are olivine and clinopyroxene phenocrysts in fine-grained, partly glassy matrix.

3.2 Magnetic Susceptibility (κ) Measurements

Magnetic susceptibility is defined according to the equation proposed by Rochette et al. (1992). This rapid, cheap, and non-destructive method was discovered in archaeometry following a research in the 1990s (Thorpe and Thorpe 1993). This

geophysical method helps to distinguish special stone types, thus integrating other mineralogical, petrological and geochemical methods.

About 700 measurements were elaborated with a Kappameter-KT5 field magnetic susceptibility meter to classify the groups of stone artefacts, to complement the other methods employed, and possibly to determine the source region of the raw material. The results of the measurements were corrected according to the Thorpe thickness correction factor (Thorpe et al. 2000). The corrected κ was depicted on a cumulative curve.

Macroscopically, three characteristic types were identified within the *greenschist* group. The MS method yielded only two groups within this rock type, one group with low ($0.1\text{--}2.5 \times 10^{-3}$ SI) and the other with very high κ value ($4\text{--}60 \times 10^{-3}$ SI). Low MS values were characteristic for the macroscopic greenschist types I and III, and for part of the samples belonging to type II. The high MS values were measured among the other samples of the macroscopically distinguished type II. Thus, on the basis of the MS data, we can divide the macroscopically determined greenschist type II into two subgroups, II/a and II/b, a classification which is in agreement with the SEM–EDS results.

Two main subgroups of *basalt* artefacts were identified on the cumulative curve: one group with $0.35\text{--}12 \times 10^{-3}$ SI, and another group with $15\text{--}33 \times 10^{-3}$ SI.

The magnetic susceptibility of the serpentinite tools varies between 0.1 and 86×10^{-3} SI, possibly due to the inhomogeneous distribution of magnetic minerals.

3.3 Prompt Gamma Activation Analysis (PGAA)

Prompt gamma activation analysis (PGAA) was selected as a geochemical fingerprinting method, because of its non-destructive character and high sensitivity for certain elements. In addition, we have previous experience in utilising this method successfully on polished stone tools and their raw materials (Szakmány and Kasztovszky 2004).

PGAA is a multi-elemental nuclear method used to determine major (SiO_2 , TiO_2 , Al_2O_3 , Fe_2O_3 , MnO , MgO , CaO , Na_2O , K_2O , H_2O) and some trace (Sc, V, Co, Ni, Cr, B, Cl, Nd, Sm, Eu, Gd) elements (Anderson and Kasztovszky 2004).

The present data (Table 1), compared with the data of Szakmány and Kasztovszky (2004), confirm that the *greenschist* type I can be correlated with the tools from Felsőcsatár, and the *greenschist* type II with the tools from the Bohemian Massif.

The results show that most of the *basalt* raw material originated from the Balaton Highland – Little Hungarian Plain, and that a smaller number of basalt artefacts are from other source areas (Füri et al. 2004).

Table 1 Chemical composition of archaeological samples (major elements in oxides and in wt%, trace elements in ppm)

Inventory no.	1871.285.II.18	1871.285.III.100	1871.285.III.113	1876.300.50	1876.300.63	1876.300.84	1876.300.99
Greenschist types	Type II. b	Type II. a	Type II. b	Type II. a	Type II. a	Type I	Type I
Chemical composition	C% ox/ox	C% ox/ox	C% ox/ox	C% ox/ox	C% ox/ox	C% ox/ox	C% ox/ox
Major (oxide wt%)							
SiO ₂	40	49	57	55	50	50	48
TiO ₂	<DL	3.380	2.466	3.556	4.197	1.319	1.293
Al ₂ O ₃	0.95	10.98	11.26	9.73	11.45	13.77	15.20
Fe ₂ O ₃ ^t	7.34	14.00	11.85	12.51	14.20	8.94	8.97
MnO	0.103	0.209	0.160	0.140	0.205	0.149	0.200
MgO	38.573	8.81	6.57	6.61	6.92	8.72	9.47
CaO	0.11	10.41	6.48	10.08	10.18	11.40	8.60
Na ₂ O	<DL	1.32	3.15	0.94	1.75	2.63	4.11
K ₂ O	<DL	0.20	0.107	0.25	0.07	2.838	<DL
H ₂ O	11.845	1.382	1.220	1.319	1.333	2.838	3.785
Trace (ppm)							
B	20.2	1.7	<DL	2.5	<DL	<DL	<DL
S	<DL	<DL	<DL	<DL	<DL	<DL	<DL
Cl	41	<DL	239	<DL	87	140	83
Sc	<DL	39	39	32	40	50	33
V	<DL	368	285	339	371	319	298
Cr	2,630	393	<DL	285	<DL	673	<DL
Co	72	215	<DL	<DL	284	107	<DL
Ni	1,596	<DL	<DL	<DL	<DL	<DL	<DL
Nd	<DL	<DL	<DL	43.9	<DL	22.5	<DL
Sm	<DL	5.33	5.10	5.35	7.29	2.22	2.19
Gd	<DL	7.00	6.70	6.89	8.39	1.95	3.72

(continued)

Table 1 (continued)

Inventory no.	1871.285.II.18	1871.285.III.100	1871.285.III.113	1876.300.50	1876.300.63	1876.300.84	1876.300.99
Greenschist types	Type II. b	Type II. a	Type II. b	Type II. a	Type II. a	Type I	Type I
Chemical composition	C% ox/ox	C% ox/ox	C% ox/ox	C% ox/ox	C% ox/ox	C% ox/ox	C% ox/ox
Major (oxide wt%)							
SiO ₂	56	49	49	47	49	46	44
TiO ₂	3.391	2.344	1.892	0.935	1.932	2.958	0.924
Al ₂ O ₃	10.40	8.83	7.41	15.90	7.70	11.26	20.03
Fe ₂ O ₃ t	12.85	14.29	13.33	7.78	15.60	13.47	8.06
MnO	0.182	0.240	0.204	0.139	0.228	0.161	0.150
MgO	5.56	16.93	15.15	9.31	15.81	11.79	7.89
CaO	8.91	1.60	8.82	10.88	5.38	8.99	12.74
Na ₂ O	1.12	0.46	0.79	3.70	0.32	1.46	2.66
K ₂ O	0.196	1.64	0.61	0.24	0.802	<DL	0.44
H ₂ O	0.919	3.544	2.429	3.471	3.254	3.387	2.945
Trace (ppm)							
B	1.0	58.2	12.3	4.0	21.6	0.9	13.9
S	1,826	3,847	2,585	<DL	1,001	1,541	<DL
Cl	80	105	154	113	179	149	<DL
Sc	<DL	30	12	27	34	<DL	27
V	298	258	208	254	284	<DL	<DL
Cr	<DL	267	<DL	693	269	<DL	447
Co	<DL	98	70	<DL	128	60	164
Ni	<DL	283	<DL	<DL	<DL	<DL	<DL
Nd	<DL	<DL	<DL	17.7	29.4	47.6	<DL
Sm	7.33	3.62	2.86	1.11	2.70	5.51	1.77
Gd	7.49	5.04	3.49	<DL	4.08	5.85	3.08
DL detection limit							

4 Discussion and Conclusions

On the basis of our analyses, the following raw materials of the Ebenhöch Collection were identified. *Greenschist* represents the largest group, with nearly 400 pieces. The greenschist group was divided into three main types and two subtypes, as following: I, II/a, II/b, and III type. Based on petrographic and chemical data, type I showed similarity to Felsőcsatár greenschist, and type II to the Bohemian Massif greenschists. The two subgroups within type II can be successfully differentiated by MS: there is low MS for the rock type characteristic of the northern part of the Bohemian Massif (Železný Brod, Jizerské Hory Mountains), and high MS for type II/b, (Želešice type) from the southern part of the Bohemian Massif (Szakmány and Kasztovszky 2004). The two greenschist types of Bohemian origin were separable, apart from SEM–EDS, only by the MS analytical method. A third type can also be distinguished, representing a highly variable group, for which we cannot yet define the provenance of the raw material.

Apart from the greenschist, two other raw material types appear in larger quantity: *serpentinite* (57 pieces) and *basalt* (38 pieces) (Fig. 1). On the basis of their mineralogical and geochemical composition, we may suppose that *basalts* originate from Kisalföld, or the Balaton Highlands region, in Western Hungary (Füri et al. 2004). On the basis of the petrographic results and archaeometric data (Skoczylas et al. 2000), the source area of the *serpentinite* could not be identified with certainty. Possible sources are the Penninic Unit of the Eastern Alps, and/or the Gogołów-Jordanów Mountains.

The stone tools that have *hornfels* as raw material appear in the entire Carpathian Basin, in increasing amounts in the South – South-East direction. The provenance of these rocks is not clear, yet there is a high probability that they might derive from the contact zone of the Banatite Belt (Starnini and Szakmány 1998; Starnini et al. 2007). At the same time, their mineral composition (diopside, Ca-rich plagioclase) indicates a contact metamorphism zone with high temperature.

We assume that the provenance of the raw material *nephrite* is the Gogołów-Jordanów mountain range, in Southern Poland (Skoczylas et al. 2000). We also hypothesize that the provenance of the raw material *serpentinite* could be the Penninic Unit of the Eastern Alps and/or the Gogołów-Jordanów mountain range.

There are several possibilities for the provenance of *metagabbroic rocks* in the Carpathian Basin. The exact identification of the raw material's source locality is not possible at the moment.

Polished stone tools made of *andesite* are generally rare, and they were mainly used for making other stone utensils. Only few andesite tools appear in the Ebenhöch Collection. On the basis of their mineralogy and textural features, stone axes made from this raw material contain Tertiary andesites probably originating from the Slovak Volcanic Area or the Börzsöny Mountains (Fig. 2).

High-pressure metamorphites are widespread as a raw material for stone artefacts, from the Western Alps to the Po River plain and beyond. The chemical composition of the pieces found in the Ebenhöch Collection is similar to that of the



Fig. 2 Hypothetic areas of origin of the rocks

implements found in these areas, and probably originate from there (D'Amico and Starnini 2003).

Acknowledgements The authors are grateful for the PGAA measurement facilities at the Budapest Neutron Centre on the frame of project No. K 62874 of the Hungarian Scientific Research Fund (OTKA). We would also like to thank Zsolt Kasztovszky, Sándor Józsa, the staff of the Department of Petrology and Geochemistry of ELTE, and the staff of the Ebenhöch Collection at the HNM.

References

- Anderson DL, Kasztovszky ZS (2004) Application of PGAA with neutron beam. In: Molnár GL (ed) Handbook of prompt gamma activation analysis with neutron beams. Kluwer, Dordrecht, pp 148–152
- D'Amico C, Starnini E (2003) Eclogites, jades and other HP-metaphiolites employed for prehistoric polished stone implements in Italy and Europe. *Periodico di Mineralogia* 73:17–42
- Füri J, Gy S, Zs K, Biró TK (2004) The origin of the raw material of basalt polished stone tools in Hungary. *Slovak Geol Mag* 10(1–2):97–104
- Rochette P, Jackson M, Aubourg C (1992) Rock magnetism and interpretation of anisotropy of magnetic susceptibility. *Rev Geophys* 30(3):209–226

- Skoczylas J, Jochemczyk L, Foltyn E, Foltyn E (2000) Neolithic serpentinite tools of West-central Poland and Upper Silesia. *Krystalinikum* 26:157–166
- Starnini E, Szakmány GY (1998) The lithic industry of Neolithic sites of Szarvas and Endrőd (southern-eastern Hungary): typological and archaeometrical aspect. *Acta Archaeologica Academiae Scientiarum Hungaricae* 50:279–342
- Starnini E, Szakmány GY, Whittle A (2007) Polished, ground and other stone artefacts. In: Whittle A (ed) *The Early Neolithic on the Great Hungarian Plain. Investigation of the Körös culture site of Ecsegfalva 23, County Békés, vol XXI. Varia Archaeologica Hungarica*, Budapest, pp 667–676
- Szakmány GY, Kasztovszky ZS (2004) Prompt Gamma Activation Analysis, a new method in the archaeological study of polished stone tools and their raw materials. *Eur J Mineral* 16:285–295
- Thorpe WO, Thorpe RS (1993) Magnetic susceptibility used in non-destructive provenancing of Roman granite columns. *Archaeometry* 35(2):185–195
- Thorpe WO, Jones MC, Webb PC, Rigby IJ (2000) Magnetic susceptibility thickness corrections for Based on the latter analysis the following raw materials of the Ebenhöch collection were identified. The main small artefacts and comments on the effects of ‘background’ materials. *Archaeometry* 42(1):101–108

The Colour of the Façades in Siena's Historical Centre: Calcium Oxalate Films on Brickwork of the Fifteenth to Sixteenth Century Palaces

M. Giamello, F. Droghini, F. Gabbrielli, G. Guasparri, S. Mugnaini, G. Sabatini, and A. Scala

1 Introduction

For the last 10 years, we have carried out numerous detailed studies on entire façades of palaces from Siena's historical centre as scientific support for restoration works. The studies of entire brick façades of thirteenth and fourteenth century palaces in Siena have revealed traces of ancient treatments of the surfaces for aesthetic purposes (Droghini et al. 2005; Nardelli 2005). It was also possible to date these treatments, today appearing as calcium oxalate films, to the time when the façades were built (Giamello et al. 2005).

In order to determine if the application of such treatments according to similar techniques was protracted in time, we studied palaces built during the fifteenth and sixteenth centuries. In the present paper, our focus is on the *Binducci* and *Calusi-Giannini* Palaces, since they are particularly appropriate examples, but reference will also be made to other façades of the same period. It must be emphasized that collaboration with the architectural historian in our group was decisive both for the selection of façades with suitable characteristics and, above all, for the assessment of the originality of the considered architectonic elements, a crucial element for the correct interpretation of the data and for the subsequent conclusions.

M. Giamello (✉), F. Droghini, G. Guasparri, S. Mugnaini, G. Sabatini, and A. Scala
Dipartimento di Scienze Ambientali, U.R. Conservazione del Patrimonio Culturale Lapideo,
Università degli Studi di Siena, Via Laterina 8, 53100 Siena, Italy
e-mail: giamello@unisi.it

F. Gabbrielli
Dipartimento di Archeologia e Storia delle Arti, Università degli Studi di Siena, Via Roma 56,
53100 Siena, Italy

2 Sampling and Methods

The sampling entailed an accurate and detailed observation of the surfaces of all existing architectonic elements. Macroscopic recognition of Ca-oxalate film relics is not always easy, since the alteration that generally affects them (albeit to a variable degree) makes them look like anonymous whitish-greyish patches which can be easily mistaken for other surface features so frequent on bricks. Along these lines, we refer particularly to the simplest type of film made of Ca-oxalate alone, which is the most diffuse one on our brick façades. Apart from the erosive effects of meteoric water, the degradation and progressive destruction of Ca-oxalate films mainly derive from sulphation phenomena. When sulphation becomes sufficiently intense, it leads to a disconnection of the optical contact between the film and the substratum, so that the film loses its original transparency and becomes an opaque coating.

Having overcome this difficulty, the sampling was carried out so as to acquire a significant number of samples from both the wall surface and from all the architectonic and ornamental elements of the façades. The micro samples were studied by polarized light microscopy in thin and ultrathin sections cut perpendicularly to the brick surface. Ultrathin section observation, in particular, represents a fundamental technique for characterizing Ca-oxalate films, since it allows recognizing the mineral species inside the film and observing their textural relationships. This makes a detailed reconstruction of the microstratigraphy easier, even when we are dealing with more than one overlapping film, or with further complications induced by alteration processes.

As a standard procedure, XRD (or FT-IR) analyses were also performed on each sample, both directly on its surface and on powder gently scraped from it. Moreover, SEM-EDS analyses were used when a particular component remained problematic or uncertain after the aforementioned tests. A sufficiently detailed characterization of the film can result only by combining together all these analytical data obtained with different methods.

3 Fifteenth and Sixteenth Century Palaces

In the following, we will present a concise and essential report of the analytical results obtained during the study of the façades of numerous palaces (of high and medium prestige) from Siena's historical centre. We will distinguish the results obtained by analysing the wall surface from those pertaining to the architectonic and ornamental elements.

3.1 *Binducci Palace*

This building presents two adjacent façades from the fifteenth and sixteenth centuries. Remains of valuable architectonic and ornamental elements (ogival arches of

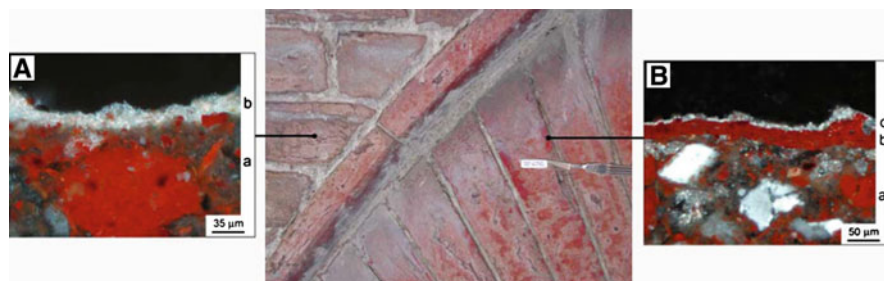


Fig. 1 *Binducci* palace. (A) Microstratigraphy of a sample from the wall surface: brick (a); simple whewellite film (b). (B) Microstratigraphy of a sample from the voussoir of the arch: brick (a); film with very dense red ochres with weddellite (b); simple whewellite film (c). These microstratigraphies are in transmitted light with two polars

the portals and twin lancet windows, multi-lobed arches of the crowning underlying the loggia) are only present on the older façade.

Wall surface: the microscopic and diffractometric analyses of various samples taken from the wall surface of this façade revealed the presence of a simple whewellite film (Fig. 1A). The brick surfaces of the adjacent sixteenth century façade also contain traces of a simple whewellite film identical to the one found on the fifteenth century façade.

Architectonic and ornamental elements: all these elements (present, as mentioned above, only on the fifteenth century façade) show relics of a film characterized by an abundant filler of red ochres with weddellite as binder. This film is always overlaid by a thin simple whewellite film (Fig. 1B).

3.2 *Calusi-Giannini Palace*

The façade of this building is composed of three floors. The ground floor and the first floor, both attributed to the 1470s, display various architectonic and ornamental elements (pilasters, arches, cornices of windows, etc.), whereas the second floor, subsequently added, lacks any decorations.

Wall surface: the analyses of various samples taken from the surfaces of the walls of the two coeval lower floors revealed the presence of a simple whewellite film. Instead, the wall surface of the upper floor presents a film consisting of very fine *cocciopesto* with weddellite, overlaid by a thin simple whewellite film. This characteristic, different from those of the lower floors, confirms the construction of the upper floor in a second phase (as already inferred on historical-architectural grounds).

Architectonic and ornamental elements: the pilasters, arches and cornices of the windows of the two lower floors contain traces of a film characterized by very dense red ochres with weddellite and an overlying thin simple whewellite film.

3.3 Other Fifteenth and Sixteenth Century Palaces

Wall surface: traces of simple whewellite films have always been found on the brick façades of other fifteenth and sixteenth century Sienese palaces, for example in the sector of the *Bargagli* Palace in via S. Pietro, dating to the early sixteenth century, in front of the Baptistery, attributed to the second half of the fifteenth century, and in the *Celsi Pollini Neri* Palace, dating to the early sixteenth century.

Architectonic and ornamental elements: in contrast, on these elements of the aforementioned palaces, relics of films characterized by an abundant filler of red ochres and/or more or less fine-grained *cocciopesto* with weddellite are always present.

4 Comparison with Thirteenth to Fourteenth Century Palaces

The types of Ca-oxalate films and their distribution in the façades of the fifteenth and sixteenth century palaces correspond to the ones found on the façades of important thirteenth and fourteenth century buildings from Siena's historical centre. We are referring in particular to the detailed studies of the *Rettore* and *Rinnovati* palaces (Nardelli 2005) and the Town Hall (Giamello et al. 2005). The most important examples are from the Town Hall, since a fortunate circumstance allowed us to reliably date the films to the fourteenth century. This refers to the part of the Town Hall façade covered in 1470 by the raising of the *Piazza del Campo* Chapel; we were able to take samples from this sector during a recent restoration which allowed access to it from the attic of the Chapel. This sector includes an entire triple lancet window and part of the wall surface of the first floor of the façade, consisting of polished and herringbone hatched bricks similar to the ones visible in the exposed part of the same floor of the building. In such an important palace, such decorations, typical of that era (Gabbrielli 2005), were used to emphasize the wall surface of the main floor with respect to the undecorated upper floors.

The characteristics of the films present on all the architectonic and ornamental elements of the covered sector seem to be in agreement with this particular refinement. For example, if we compare the microstratigraphy of Fig. 2B, referring to the voussoirs of the arch of the triple lancet window, with that of Fig. 2C, sampled from the trefoil arches, it is evident that the shade of red of the two films (note the presence of black carbon in the second) must have been macroscopically different. This led to the highlighting and differentiation of the various elements of the window, enriching the overall visual effect with various shades of red which can still be appreciated in Fig. 2A.

However, despite this greater refinement of detail, likely related to the importance of the building, the types and association of the films are very similar to those of the surfaces of the corresponding architectonic and ornamental elements of the fifteenth and sixteenth century buildings. The same can be said of the normal wall

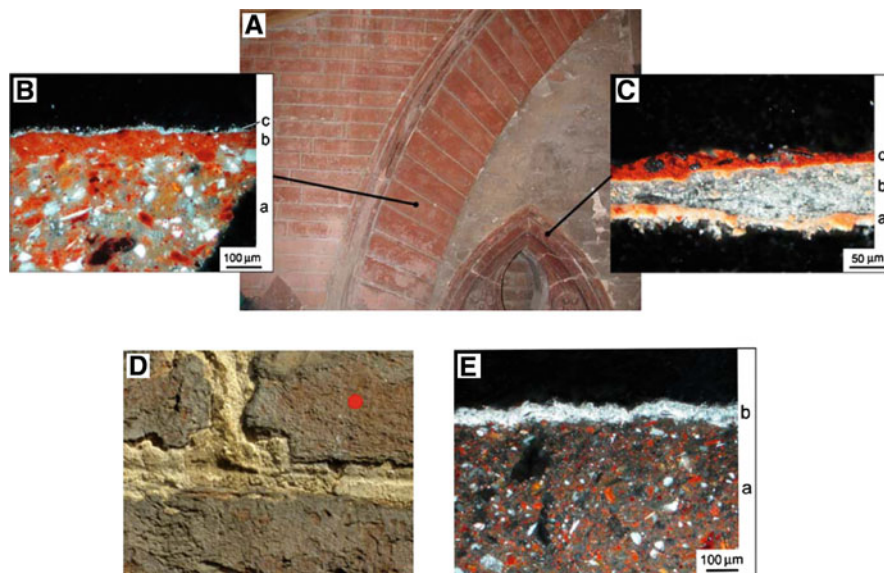


Fig. 2 Town hall. (A) Different shades of red in the various architectonic and ornamental elements of the “hidden” triple lancet window. (B) Microstratigraphy of a sample from the vousoir of the arch: brick (a); film of fine *cocciopesto* with weddellite (b); simple whewellite film (c). Transmitted light with two polars. (C) Microstratigraphy of a sample from the trefoil arch: brick (a); very thin plaster layer of a joint partially overlying the brick (b); film of red ochres and black carbon with weddellite (c). Dark field reflected light. (D and E) Traces of the Ca-oxalate film on the fourteenth century wall surface of the second floor and relative microstratigraphy: brick (a); simple whewellite film (b). Transmitted light with two polars

surfaces. In fact, the wall surfaces of the upper fourteenth century floors of the Town Hall also present a simple whewellite film (Fig. 2D and E), similar to the one observed in the more recent palaces.

5 Concluding Remarks

Numerous case studies dealing with the brick façades of Siena's historical palaces have revealed an ancient, peculiar and prolonged use of treatments on these surfaces. Two main types of Ca-oxalate films have been identified. The characteristics of the first type (generally present only on the architectonic and ornamental elements), i.e. the nature of the fillers, the colour, the homogeneity and uniqueness (on a given façade) of the filler–matrix mixture, as well as the constant presence on the homologous architectonic elements of a single façade, leave no doubts that it represents an aesthetic finish. The second type, made of simple whewellite, is not only always present on the wall surface, but it also always overlays the first type of film and even the brick joints. In other words, this type of film appears as

a continuous thin coating of the entire façade. We believe that its role was also essentially aesthetic, and that it likely derives from an original transparent treatment with linseed oil. In fact, this film is quite similar to the one found on the serpentinite of the Town Hall and of the Dome façade, for which archival data explicitly mention the use of this substance (Droghini et al. 2009).

These results are very important from the historical-architectural point of view, since they allowed us to identify two aspects of medieval and Renaissance building practices that are difficult to ascertain using only historical sources:

- The diffusion of variably treated facing brickwork in high and medium prestige buildings.
- The use of chromatic enhancement, via transparent or coloured treatments, on the wall surface and on the architectonic and ornamental elements, appropriately distinguished.

This scientific approach can also provide important information for the reconstruction of the original appearance and eventual transformations of the façades. Finally, these investigations can play an obvious role in the restoration of the façades, providing information about aspects that are little known from the historical perspective and often completely unknown from the practical perspective.

References

- Droghini F, Giamello M, Guasparri G, Mugnaini S, Nardelli MG, Sabatini S, Scala A (2005) Ancient treatments on the Sansedoni Palace façade. In: Gabbrielli F (ed) *The Sansedoni palace*. Protagon, Siena, Italy, pp 349–368
- Droghini F, Giamello M, Guasparri G, Sabatini G, Scala A (2009) The colour of the façades in Siena's historical centre. (I) – Glazings (calcium oxalate films s.s.) and other finishes on the stone materials of the Cathedral's main facade. *Archaeol Anthropol Sci* 1(2):123–136
- Gabbrielli F (2005) Finishing techniques for exposed brickwork in 12th to 15th century Tuscan architecture. In: Cramer J, Sack D (eds) *Proceedings of the congress "Technik des Backsteinbaus im Europades Mittelalters"*. Technische Universität, Berlin, 13–15 November, 2003, Petersberg, Michael Imhof Verlag, pp 50–56
- Giamello M, Guasparri G, Mugnaini S, Sabatini G, Scala A (2005) I colori della facciata del Palazzo Pubblico di Siena nell'età medievale. Un tentativo di ricostruzione tramite le pellicole ad ossalati di calcio. In: Tolaini F (ed) *Proceedings of the congress "Il colore delle facciate: Siena e l'Europa nel Medioevo"*, Siena. 2–3 Mar 2001 *Quaderni CERR*, Pacini, Pisa, Italy, pp 35–51
- Nardelli MG (2005) *I materiali lapidei della facciata del Santa Maria della Scala (Siena): stato di conservazione, diagnosi del degrado e studio delle tracce di trattamenti antichi*. PhD Thesis on the science and technology of industrial minerals and stones, vol XVII. University of Sassari, Italy

Stone Beads from Late Bronze Age and Early Iron Age Settlements from South-Western Portugal: Analyses by X-Ray Diffraction

A.P. Gonçalves, A.M. Monge Soares, A.C. Silva, and L. Berrocal-Rangel

1 Introduction

The use of non-destructive techniques is very important in the field of archaeology, as frequently the specimens are unique and often small, and damaging them may be very problematic. X-ray diffraction can be used in a non-destructive way, and provides important information not only on the crystal structure but also on the composition of the specimens. It can be used in the characterisation of small and big specimens, and it is also possible to scan their surfaces in order to detect and identify inhomogeneities.

In the present study, a set of 19 stone beads (Fig. 1) discovered during archaeological excavations or surveys at three proto-historic settlements from south-west Portugal, namely Castro dos Ratinhos, Álamo and Salsa 3, were analysed using X-ray diffraction in order to identify the rocks or minerals used for their manufacture.

Castro dos Ratinhos is a fortified settlement with Late Bronze Age and Early Iron Age occupations (Silva and Berrocal-Rangel 2005; Berrocal-Rangel and Silva 2007). Fourteen stone beads ascribed to these two occupations and a small black glass bead, this one pointing out to an Oriental connexion, were retrieved during archaeological excavations that took place during the last 4 years. Salsa 3 was the object of archaeological investigations during 2006 and 2007; Late Bronze Age and Early Iron Age occupations were also identified at this archaeological site. Two beads were selected from this site. Álamo is a fortified settlement, apparently with only one occupation, of Late Bronze Age chronology. The three beads analysed were recovered during an archaeological survey. All these proto-historic settlements are

A.P. Gonçalves (✉) and A.M.M. Soares
Instituto Tecnológico e Nuclear, Estrada Nacional 10, 2686-953 Sacavém, Portugal
e-mail: apg@itn.pt

A.C. Silva
Direcção Regional de Cultura do Alentejo, R. de Burgos, 5, 7000-863 Évora, Portugal

L. Berrocal-Rangel
Universidad Autónoma de Madrid, Ciudad Universitaria de Cantoblanco, 28049 Madrid, Spain

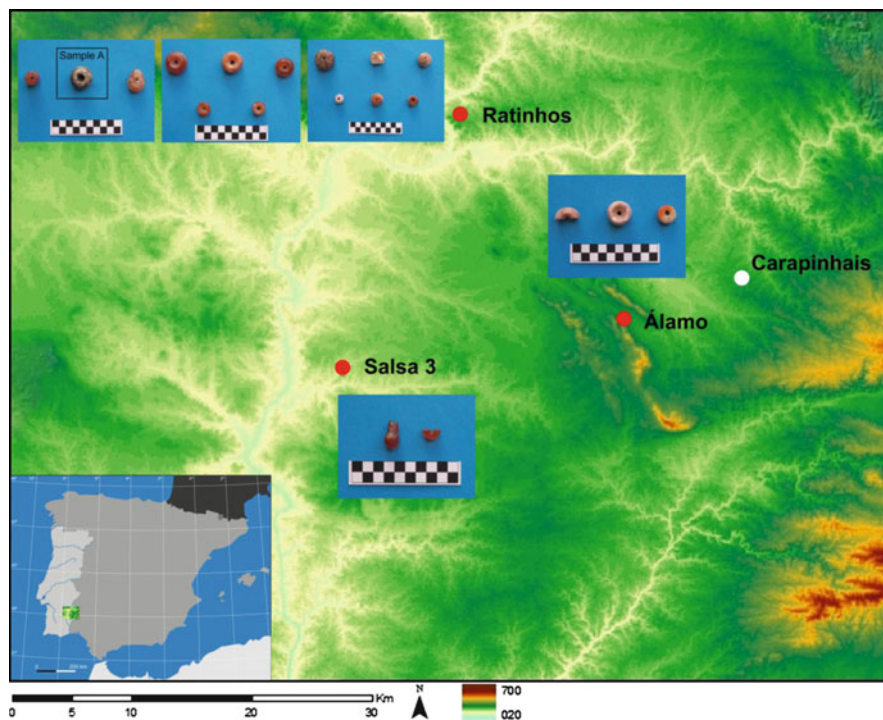


Fig. 1 Stone beads and location of the archaeological sites where the beads were discovered

located in the Guadiana Valley, close to the Portuguese–Spanish border, with distances between them smaller than 40 km (Fig. 1).

To the best of our knowledge, this work represents the first study of a set of proto-historic stone beads from Portuguese archaeological sites. Green stone beads from the Neolithic and Chalcolithic periods have been previously subject to analyses using powder X-Ray diffraction, which, due to the destructive nature of the method, were only carried out on broken beads (Canêlhas 1973; Gonçalves 1979). More recently, a bead from a burial necklace with 17 stone beads found in a cist of the south-western Middle Bronze Age necropolis of Carapinhais (see Fig. 1) was analysed by SEM, revealing a mineral belonging to the chlorite group (Gonçalves 2007). Using the same technique that we use in our study, supplemented by an Energy Dispersive X-ray Fluorescence (EDXRF) analysis, a bead of talc from a south-western Bronze Age burial was also previously analysed (Gonçalves et al. 2005).

2 Experimental

X-ray diffraction was used to identify the rocks and/or minerals that constitute the stone beads. A particular sample holder was developed in order to hold and place the entire collection of stone beads in the proper positions required to perform the

X-ray diffraction experiments. The X-ray diffraction system consisted of an X'Pert Panalytical diffractometer with a Bragg-Brentano assembly. The scans were performed at room temperature, in a reflection mode, using monochromatic $\text{CuK}\alpha$ radiation (1.54056 \AA) and under set conditions of 45 kV and 40 mA. The data were measured with a 2θ step size of 0.02° in a 2θ -range of 5° – 65° and a counting time of 3 s per step, in order to obtain good statistical data. Phase identification was derived from the X-ray diffraction data using the PowderCell programme (Nolze and Krauss 2000).

3 Results and Discussion

A first observation of the X-ray diffraction data of all samples immediately shows that most of the stone beads are composed of the same rock or mineral (Fig. 2). Only one bead, sample A, collected at Castro dos Ratinhos, shows a significantly different X-ray diffraction spectrum, pointing to a dissimilar composition. This is in agreement with the macroscopic observation of the stone beads, where only sample A appeared different and was made of a soft green stone, in contrast with the other beads, which were made of hard brown-red stones.

The spectra obtained for the majority of the samples have the most intense peak at $2\theta \sim 26.65^\circ$, followed by intense peaks at $\sim 20.87^\circ$, $\sim 39.44^\circ$, $\sim 50.14^\circ$, and $\sim 59.97^\circ$. This clearly indicates that the material used for all of the stone beads, with the exception of sample A, is quartz. The quartz used in the manufacture of these beads is of the carnelian variety. This aspect is also rendered in some identical elemental and X-ray diffraction patterns, pointing out to a similar mineralogical composition and suggesting the same lithological origin for the carnelian beads.

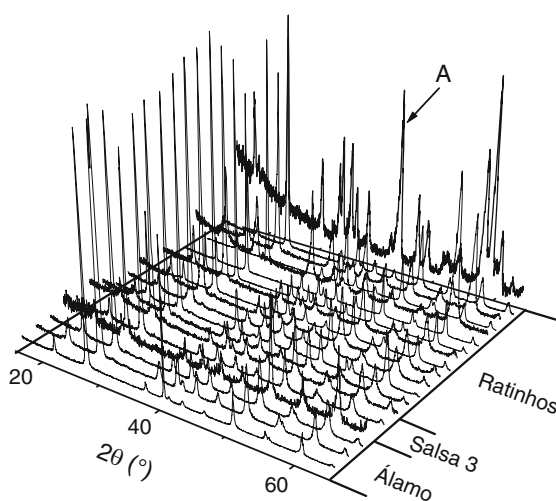


Fig. 2 X-ray diffraction patterns of the stone beads

The diffractogram obtained for sample A has a much larger number of peaks, the most intense ones being at $2\theta \sim 12.47^\circ$, $\sim 18.76^\circ$, $\sim 19.70^\circ$, $\sim 20.98^\circ$, $\sim 23.08^\circ$, $\sim 25.10^\circ$, $\sim 35.43^\circ$, $\sim 36.95^\circ$, $\sim 45.37^\circ$, $\sim 60.18^\circ$, and $\sim 67.19^\circ$. This indicates that: (1) either the constituent stone is composed of several different minerals or (2) it is composed of a mineral with low structural symmetry. The analysis of the position and intensity of the peaks allowed us to conclude that stone bead A is mainly composed of only one mineral, belonging to the chlorite group, most probably clinocllore.

The clinocllore constitution of sample A has parallels with the aforementioned necklace with 17 similar beads found in the SW Bronze Age necropolis of Carapinhais, not far (approximately 30 km) from Castro dos Ratinhos (Fig. 1).

The uniformity of the material used for the manufacture of the beads found in Castro dos Ratinhos, Álamo and Salsa 3 contrasts with the general variety of stones used in earlier times (in Neolithic or Chalcolithic times, for instance) for producing this type of artefacts. Beads in carnelian seem to be common in SW Iberian proto-historic settlements (Gibson et al. 1998). However, due to the lack of geological studies concerning this type of rock, it is not possible to identify the lithological origin of the carnelian beads found in the south-west of the Iberian Peninsula.

4 Conclusion

In conclusion, the analysis of the samples by X-ray diffraction, a non-destructive technique, allowed us to identify the raw material of all the beads as quartz, with the exception of one (Sample A) made of a soft dark green stone, belonging to the chlorite group, most probably clinocllore, with parallels in a necklace with stone beads found in the SW Bronze Age necropolis of Carapinhais, not far from Castro dos Ratinhos. Moreover, the quartz used in the manufacture of most of the beads is of the carnelian variety. Identical elemental and X-ray diffraction patterns point toward a similar mineralogical composition, suggesting the same lithological origin for the carnelian beads, an origin which, however, was impossible to determine. This uniformity of the material used for the manufacture of the beads contrasts with the variety of stones used in earlier times (Neolithic or Chalcolithic) in the making of this type of artefacts.

References

- Berrocal-Rangel L, Silva ACS (2007) O Castro dos Ratinhos (Moura-Alqueva, Portugal): Um complexo defensivo no Bronze Final do Sudoeste peninsular. In: Moret P, Berrocal-Rangel L (eds) Paisajes Fortificados de la Edad del Hierro. Las Murallas Prehistóricas de la Meseta y de la Vertiente Atlántica en su contexto europeo. Real Academia de la Historia/Casa de Velazquez, Madrid, pp 169–190
- Canêlhas MGS (1973) Estudo radiográfico de “calaítes” portuguesas. *Revista de Guimarães* 83(1/4):125–145

- Gibson C, Correia VH, Burgess CB, Boardmann S (1998) Alto do Castelinho da Serra (Montemor-o-Novo, Évora, Portugal). A Preliminary Report on the excavations at the Late Bronze Age to Medieval Site, 1990–1993. *J Iberian Archaeol* 0:189–244
- Gonçalves AAHB (1979) Elementos de adorno de cor verde provenientes de estações arqueológicas portuguesas. Importância do seu estudo mineralógico. In: *Actas da 1ª Mesa-Redonda sobre o Neolítico e o Calcolítico em Portugal* (Porto, Abril de 1978), pp 209–225
- Gonçalves AAHB (2007) Identificação mineralógica de uma conta da Necrópole dos Carapinhais (Sobral da Adiça, Moura). *Vipasca*. 2ª Série, vol 2. pp 191–193
- Gonçalves AP, Valério P, Soares AMM, Araújo MF (2005) A stone bead from a SW Bronze Age burial: analysis by EDXRF and X-ray diffraction, *O Arqueólogo Português*, Série IV, vol 23. pp 257–264
- Nolze G, Krauss W (2000) PowderCell 2.3 Program. BAM, Berlin
- Silva AC, Berrocal-Rangel L (2005) O Castro dos Ratinhos (Moura), povoado do Bronze Final do Guadiana: 1ª campanha de escavações (2004). *Revista Portuguesa de Arqueologia* 8(2): 129–176

Integrated Research on Sixteenth to Early Nineteenth Century Panel Paintings: Chromatographic and Spectroscopic Characterisation of Paint Layers

E. Kouloumpi, G. Lawson, and V. Pavlidis

1 Introduction

The term “Post-Byzantine art” refers to an artistic movement that appeared in the mid-fifteenth century and lasted until the early nineteenth century (Clogg 2002). The movement started immediately after the fall of the Byzantine Empire in 1453 and it marked the beginning of one of the most important periods in Greek art history. The Post-Byzantine era represented a transitional period when the art of panel painting changed style, from religious to secular, due to significant exchanges with the western world. At the same time, the artists’ technique evolved; the painters changed their method from egg tempera on wooden panel to oil painting on canvas. Cultural influences also brought changes in the iconographic types: the artists exempted themselves from the strict Byzantine rules of depiction, in order to allow themselves free expression.

Even though this period is associated with a very important change in the Greek art of the time, no extensive scientific research has yet been carried out on the physico-chemical characteristics of the respective paintings.

The basic structure of a panel painting (Cennini d’Andrea 1954) comprises the substrate, the gesso ground, the paint layers, and the varnish. The paint layers consist of inorganic or organic pigments and the binding medium. The most important binders used in Post-Byzantine panel painting were egg yolk and egg yolk with the addition of a drying oil.

E. Kouloumpi (✉)

Laboratory of Physicochemical Research, National Gallery – Alexandros Soutzos Museum, 1 Michalacopoulou Street, 11601 Athens, Greece
e-mail: elenikouloumpi@nationalgallery.gr

G. Lawson

Faculty of Health and Life Sciences, De Montfort University, Hawthorn Building, Leicester 1 9BH, UK

V. Pavlidis

Allied Health Sciences, De Montfort University, Hawthorn Building, Leicester 1 9BH, UK

The present research focused on the investigation of the paint layers, and especially of the binding medium. The characterisation of the organic binding media of paintings by using analytical methods contributes not only to the understanding of the artists' technique, but also to the discernment of the evolution of painting styles. Panel paintings have been the subject of very limited research, especially with regards to the analysis of the binding media. However, while the analysis of the organic binders is quite complicated (Casoli et al. 1998), it is from these analyses that the differences in the painting techniques employed across the centuries can be understood.

The aim of this research was to provide detailed information on the nature of the materials used in the panel paintings from the island of Crete and the islands of Ionian in a period ranging from the sixteenth to the nineteenth century, and to examine whether the post-Byzantine artists adopted western features in their painting techniques, similar to the changes they adopted in their iconographic types.

2 Physico-chemical Research

2.1 *Experimental Procedure*

The techniques and materials used by artists are directly related to the period in which they live and create, and to the influences originating from a variety of interactions. Physico-chemical methods are able to characterise the materials present in a painting and hence provide information on the respective technique used.

While the analysis of the inorganic components of a work of art has acquired a nearly routine character, the identification of the organic media still faces severe difficulties. Furthermore, the sampling of paintings is a problematic procedure, since the quantity of the sample that can be obtained without affecting the object is very small and should be limited to the paint layer, taking the form of powder. Therefore, a special methodology had to be set up in order to ensure that as much information as possible would be obtained from each unique paint sample.

Hence, a decision was made to begin the analysis by using non-destructive methods, in order to collect as much information as possible before proceeding to a destructive method such as gas chromatography (GC), necessary for the positive characterisation of the binding media. Taking these factors into consideration, the following analytical methods were selected (Fig. 1):

1. Scanning electron microscopy and energy dispersive X-ray analysis (SEM/EDX) for the detection and rough identification of the pigments present.
2. Fourier Transform Infrared microscopy (μ FT-IR) for pigment identification and detection of the amide functions for egg yolk, and of the long-chain carboxyl

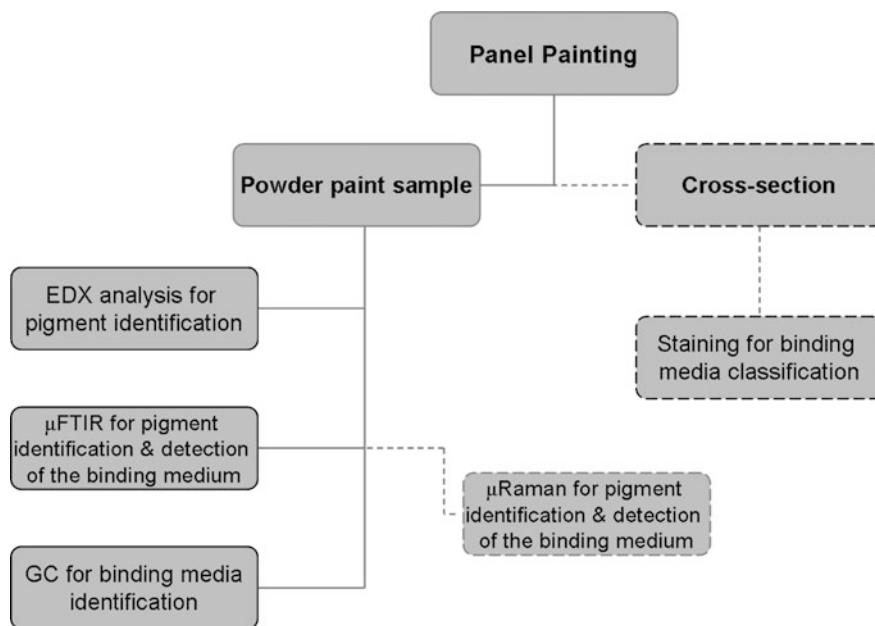


Fig. 1 The experimental procedure followed

groups for the drying oils. Also, whenever necessary, Raman analysis was carried out in order to acquire complementary information.

3. Micro-chemical tests on cross-sections, whenever the collection of cross-sections was possible, for the study of the stratigraphy and detection of the organic classes present.
4. Gas chromatographic analysis of ethyl chloroformate derivatives (GC-ECF) for medium identification and verification of the results obtained by the molecular techniques through identification of the composition of amino and fatty acids.

For reference purposes, artificial standards were created and artificially aged (Kouloumpi et al. 2006) by following the traditional recipes of both Byzantine and Western-European techniques.

2.2 *Sample Collection*

A series of 121 panel paintings, representative samples of this period (late fifteenth century – early nineteenth century) from the Cretan School and the School of Ionion, were studied. In order to find evidence related to time and location for changes in practice between Constantinople, Greece and Venice, 201 additional

samples were collected from several parts of Greece. The aim was to provide sets of data pertaining to time/location concerning the creation of the artwork.

3 Results and Discussion

The present investigation allowed us to identify the nature of the materials used by the artists. Pure binding media, as well as emulsions, were detected, while the nature of the selected pigments was also identified. The artistic changes that took place in painting during the Post-Byzantine period were also recorded. As mentioned above, the choice of the analytical techniques was based on the principle of collecting as much information as possible with non-destructive methods before proceeding to gas chromatography.

Initially, the determination of the inorganic materials was carried out. SEM–EDX offered valuable information concerning the elemental composition of the samples, but also regarding the choice of materials used by the artist.

The characterisation of pigments was also performed by means of μ FTIR and μ Raman spectroscopy. These techniques also provided valuable information concerning the presence of secondary products associated with the production of the pigments. Molecular spectroscopy also provided information regarding the organic materials found in the samples. Unfortunately though, without the additional use of gas chromatography, these techniques alone cannot provide a valid determination of the binder. This is due to the fact that the amount of organic matter in a sample is minute as compared to the pigment present, leading to the masking of important absorption bands that characterise an organic substance. In the case of emulsions, there is a significant overlapping between the bands originating from the oils and the ones of the proteins.

The characterisation of the organic binders was made possible mainly by gas chromatography. The use of the method of ethyl chloroformate derivatives allowed the simultaneous determination of both amino and fatty acids, thus characterising both single and mixed organic binding media.

Finally, in cases where the removal of powder samples was not possible, cross-sections were collected and micro-chemical techniques were applied. This procedure proved quite useful, since the staining of cross-sections indicated the class of the binding media, such as protein and oils.

Chart 1 illustrates the overall progress of changes in the binding medium during the Post-Byzantine era. It appears evident that during the fifteenth century, egg yolk was used as a binder in 70% of cases, while at the beginning of the Post-Byzantine period, the use of egg yolk/oil emulsion and drying oil was introduced. In the sixteenth century, there seems to be a significant increase in the use of drying oils. According to some artists' manuals (Cennini d'Andrea 1954; Ek Fourni 1906).

An oily layer was also employed in the production of the painting. This argument is reinforced by the fact that in many of the analysed panel paintings both egg yolk and drying oil were detected. From the seventeenth century onward, an

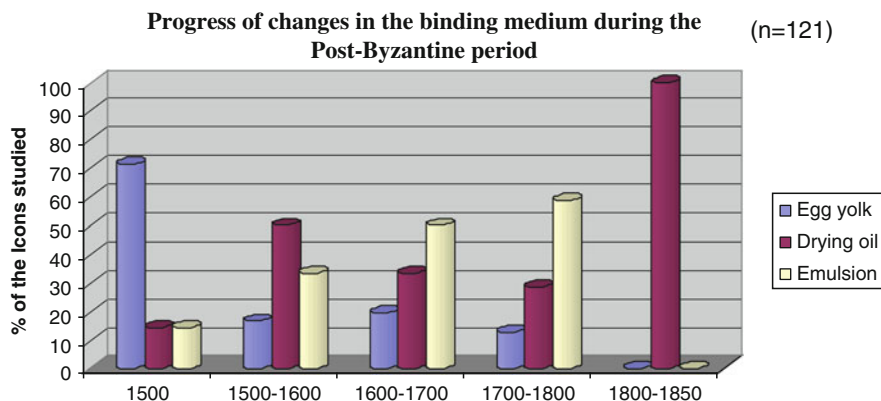


Chart 1 The overall progress of binding media in the Post-Byzantine period

increase in the use of emulsions can be observed, lasting until the eighteenth century, when the use of drying oils prevailed.

4 Conclusion

An approach integrating multiple methods of analysis was employed in order to characterise the materials used by artists in the Post-Byzantine period. The analytical methods used for the present investigation were: Energy Dispersive X-ray Analysis, Fourier Transform Infrared Microscopy, and Gas Chromatography. Additionally, two other techniques were used to obtain complementary information whenever necessary: Raman spectroscopy and staining of cross-sections.

The scientific analyses provided important information concerning the changes in the paint binding media, confirming the technological background of the artists from this period, which was so far available only from artists' manuals. The artistic changes that took place in Post-Byzantine painting were also reflected in the range of available techniques, proving that the artists moved on from egg tempera to oil painting, passing through an emulsion phase.

The results of this research led to one major conclusion: the cultural exchanges between Western Europe and Post-Byzantine space profoundly affected the art of panel painting. These interactions provided Post-Byzantine painters with the examples and the materials allowing them to "free themselves" and adhere to more contemporary styles.

Acknowledgments This work was carried out at De Montfort University, United Kingdom, and at the National Gallery of Greece. Our gratitude is extended to Dr M. Doulgeridis (NGA), Panagiotis Asimakopoulos (Perkin Elmer) for GC support, Peter Vandenaabeele (University of Ghent) for carrying out the Raman spectroscopy, and finally Agni Terlixi (NGA) for the analysis of the cross-sections.

References

- Casoli A, Palla G, Tavlaridis J (1998) Gas-chromatography/mass spectrometry of works of art: characterisation of binding media in post-Byzantine icons. *Stud Conserv* 43:150–158
- Cennini d'Andrea C 1437 (1954) *Il libro dell'arte o trattato della pittura*. English edition: *The book of art, a treatise of painting*. (Trans Thompson DV Jr), Dover, New York
- Clogg R (2002) *A concise history of Greece*, 2nd edn. Cambridge University Press, Cambridge
- Ek Fourna D (1906) *Η ερμηνεία της ζωγραφικής τέχνης*. English edition: *The interpretation of the art of painting*. Papadopoulou-Kerameos (ed) B Kirschbaum, Petroupoli
- Kouloumpi E, Lawson G, Pavlidis V (2006) The contribution of gas chromatography to the resynthesis of the Post-Byzantine artist's technique. *Anal Bioanal Chem* 387(3):803–812

A Diptych by Marcellus Coffermans Analysed by Portable XRF

A. Križnar, M.V. Muñoz, F. de La Paz, M.A. Respaldiza, and M. Vega

1 Introduction

Marcellus Coffermans is a painter who worked in Ambers from 1549. His creations reveal a strong influence of Flemish painting from the last third of the fifteenth and the first third of the sixteenth century, represented by artists such as Rogier van der Weyden. Coffermans is known by his direct imitations of those masters, often repeating the same subjects.

The Fine Arts Museum of Seville has three of his panels in its collections. The largest one (180 × 103 cm) is *The Virgin and Child* (sixteenth century), representing the coronation of the Virgin. The other two, *The Annunciation* and *The Visitation* (around 1570), are smaller in size (51 × 33 cm) and displayed together in a diptych (Fig. 1). They are painted on a wooden support, and were donated to the museum in 1928. However, they were attributed to Coffermans not earlier than two decades ago (Bermejo 1985). Both panels show Coffermans' typical tendency to recreate the sacred scenes already executed by older painters. The *Visitation* setting, for example, is practically the same as the one by Rogier Van der Weyden found in the Art Museum of Leipzig, while *The Annunciation* recalls the painting in the Wellington Museum in London (Valdivieso González 1993).

2 Objectives and Experimental Procedures

The principal objective of the present research was the identification of the pigments applied by the master in this work. The unusual colour palette was revealing possible changes of colour and, consequently, pigment alterations, which had to be

A. Križnar (✉) and M.A. Respaldiza
Centro Nacional de Aceleradores (CNA), University of Seville, Avda. Thomas A. Edison 7,
Parque tecnológico Cartuja '93, 41092 Seville, Spain
e-mail: akrižnar@us.es

M.V. Muñoz, F. de La Paz, and M. Vega
Museo de Bellas Artes, Plaza del Museo 9, 41001 Seville, Spain

Fig. 1 Marcellus
Coffermans: *Diptych of
The Annunciation and
The Visitation*, about 1570



confirmed by scientific evidence. The existence of a preparation layer, the sequence of the colour layers, and the formation of lights and shadows were also of interest. The paintings are not currently undergoing a restoration process, so it was not considered convenient to extract any micro-samples. Furthermore, it was impossible to move the paintings from the museum.

For these reasons, the non-destructive X-ray fluorescence (XRF) technique has been used for the analysis of the pigments (Gómez 2000; Seccaroni and Moiola 2002). This technique, based on elemental results, is very useful in the non-destructive study of materials, especially when applied to artworks. It provides a first examination of the artwork, identification of inorganic pigments, and is helpful for discovering possible later interventions. XRF is based on elemental results, revealing the chemical elements present at an irradiated spot. By this technique, it is not possible to identify either molecular compositions or organic pigments, because common XRF systems do not detect elements with Z lower than 13 or 14.

The equipment used is a portable device, with an X-ray generator RX38 from EIS.S.r.l. with W Anode, while the detector is a silicon drift one (SDD) with energy resolution of 140 eV. An Al filter of 1 mm was coupled to the tube to suppress the W peaks from the spectra obtained during the radiation. The analyses were carried out in situ during the days when the museum is closed to the public (Fig. 2). In each panel, more than 100 points were analysed in order to obtain reliable results about the pigments applied in this artwork. All measurements were carried out under the same fixed conditions: 80 μ A of cathode current, 29.5 kV of applied high voltage and 300 s of preset live time. This permitted a comparison of the spectra among

Fig. 2 In situ analysis by portable XRF



them and also supported semi-quantitative results. As mentioned above, the pigments were identified according to the characteristic energy (keV) of the X-ray peaks in each obtained spectrum, which correspond to specific chemical elements (Seccaroni and Moiola 2002; Matteini and Moles 2003). The spectra were also compared with a pigment database that was elaborated at Centro Nacional de Aceleradores (CNA) in Seville by analysing commercial pure pigments from old traditional recipes. In addition, the wide bibliography on pigments was also consulted, in order to be able to make attributions of different pigments.

3 Results and Discussion

The results show that the pigments applied in both paintings are the same and belong to the commonly used historic pigments (Feller et al. 1986–2007; Knoepfli et al. 1990; Serchi 1999; Bazzi 1993; Montagna 1993; Schram and Herling 1995; Calvo 1997; Gómez 2000). No modern materials have been detected and therefore no restoration intervention was confirmed. The basic pigments were applied either pure or mixed with others to obtain the desired tonality. Lead white was added to lighten the colour, while darker pigments such as ochre, umbra and some organic black were added for the shadows and to obtain darker tonalities.

3.1 Lead Compounds

In all analysed spots, a considerable quantity of Pb was detected, according to the relatively high count numbers of Pb. In most spectra, the L peaks of Pb are the

highest and the predominant ones, as compared with the K or L of other important chemical elements in each examined point. Nevertheless, the count numbers vary greatly, from 77.3 count numbers (cps) up to 612 cps, depending on the peak. The highest count rates can be found in white or light areas of the painting, while the lowest ones in the darker areas. This presence of lead in every spot analysed shows the important role of some lead compound or another in both panels. With XRF it is not possible to distinguish between different lead compounds: lead white (basic lead carbonate), yellow litharge (lead oxide) or orange-red minium (lead oxide) (Feller et al. 1986–2007 (Vol 2, 1993); Seccaroni and Moiola 2002; Dornheim and San Andrés Moya 2004). We can only assume, taking into account the fact that the highest count rates have been found in white areas, that mainly lead white was used, probably for different purposes: (a) as pigment; (b) as constitutional part of the preparation layer, mixed with calcite or gypsum; and (c) as an imprimation. A lead compound could have also been used as a dryer.

3.2 Pigments

Marcellus Coffermans' palette was composed of pigments commonly applied by the masters of that period of time.

The white pigment is most likely lead white, revealed by the high count numbers of Pb in the spectra obtained from the irradiation of white areas. These are found in the angel's tunic, the Holy Spirit dove, and the vase with white flowers in *The Annunciation*, as well as in Saint Elisabeth's wimple and border of her sleeve in *The Visitation*. The count numbers of Pb are highest in all these points, especially in the angel's white tunic (612 cps).

Lead white was also used for the carnations. The painter mixed it with cinnabar (revealed by the presence of Hg peaks) and some smaller amount of yellow or red ochre (Fe). The shadows were obtained with natural or burned umbra (Mn, Fe). Red cinnabar was also used in painting the lips of all figures. Cinnabar was added to the basic brown pigment for the hair of The Virgin Mary, and used also in the architecture in the background of *The Visitation* scene, where it is mixed with yellow and red ochre.

On the other hand, cinnabar served as the main pigment for some of the red vestments, as it can be observed in the dark red angel's coat (*Annunciation*) and in the red tunic of Saint Elisabeth (*Visitation*). In both cases it was mixed with red ochre (Fe), especially in darker areas. It is also possible that, for the shadows, the red ochre was also applied on top of the cinnabar layer, an aspect which cannot be determined by XRF. The other important red pigment applied in this painting is of an organic origin. The spectra of the red sheet on the bed (*Annunciation*) and of the red coat of Saint Elisabeth (*Visitation*) show no characteristic chemical elements for any inorganic red pigments. The painter probably used carmine (Fig. 3). At first sight, these red areas do not show important chromatic differences, so the discovery of two different red pigments is very significant.

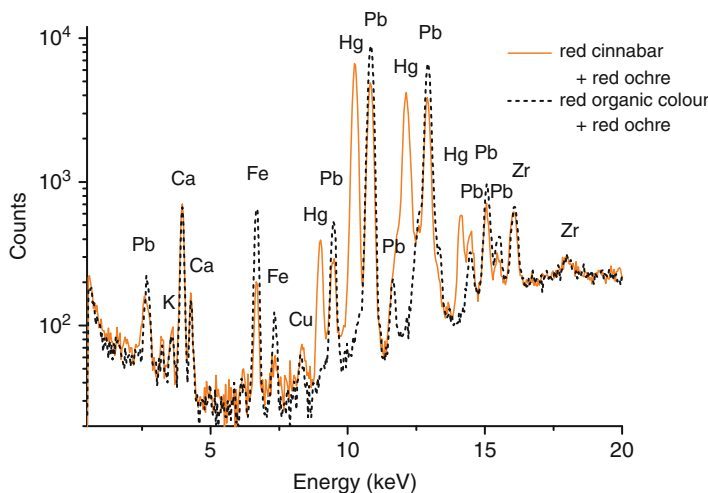


Fig. 3 Comparison of two XRF spectra showing the use of cinnabar red (*straight line*) and an organic red (*dotted line*), both mixed with some red ochre (Fe)

The warm yellow colour for the aureole around the Angel of the Annunciation is yellow ochre, as confirmed by the XRF results, showing the important role of Fe. Count numbers of Pb are low and must probably be attributed to the preparation/imprimation layer. The aureole of The Virgin Mary was painted with golden rays, as confirmed by Au peaks.

A darker tonality of yellow ochre was applied for the architecture in *The Visitation* and for the floor in *The Annunciation*, where it was combined with red ochre when painting the red squares. The spectra of dark brown colour in the floor belong in part to burned yellow ochre (Fe), but the darker areas were painted in umbra, revealed by the common presence of Mn and Fe. This pigment was also used for painting the dark hair of the protagonists, as well as for their brown eyes.

The green background in *The Visitation* was painted with some copper-based green pigment, as revealed by high Cu peaks. With XRF, it is not possible to distinguish whether the painter used malachite, verdigris, or some copper resinate (Seccaroni and Moioli 2002). The pigment was also mixed with the brown colour of the floor in the front part of the same scene. The same pigment was also used also for the green wall beyond the bed in the *Annunciation* scene. There, the Cu concentration is much higher; the count numbers reach 364.8 cps, while in the grass, where the green pigment was lightened with lead white, the counts of Cu peaks are only 117 cps.

A dark blue colour can be seen only in the roofs and windows (*Visitation*). The analyses of these spots show high peaks of Cu, which is a characteristic element for azurite. Azurite appears to have been mixed with some smalt, as revealed by the characteristic chemical elements, described below.

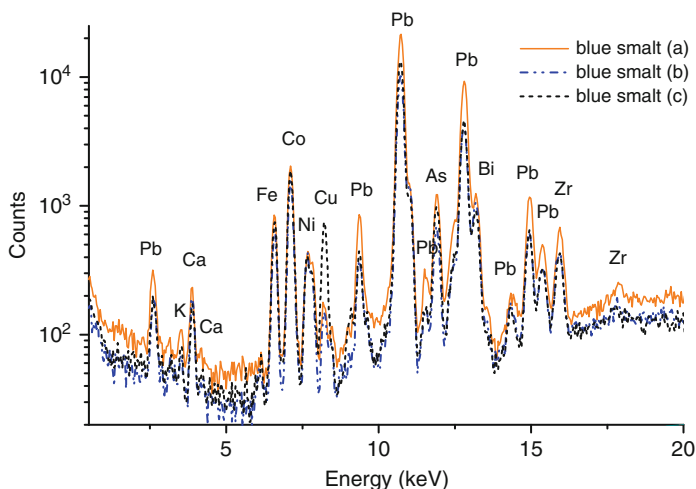


Fig. 4 Comparison of three XRF spectra, showing different tonalities of the blue pigment smalt (Co, Ni, As, Bi), applied for the Virgin's vestments

The results obtained by the analysis of the vestments of The Virgin Mary were surprising, showing high peaks of Co, Ni, As and Bi, the elements that are characteristic for the blue pigment smalt (Fig. 4). Smalt has an intense blue colour, but, due to chemical changes especially in oil medium, it tends to lose its strength and can become totally transparent or can turn brownish (Feller et al. 1986–2007 (Vol 2, 1993); Knoepfli et al. 1990; Conti 1996). This is the case of both panels in question, where the vestments of The Virgin Mary look brownish rather than blue, as would be normal in this iconographic context. Smalt appears to have lost its blue colour and can be observed only in some areas, as greyish-greenish remains. The brown colour that is seen today could be (a) the altered smalt, or (b) the under-layer, made of burned yellow or red ochre (Fe). With XRF, this cannot be determined with precision. Smalt was also used for the sky in the *Visitation* panel. Different tonalities of brownish-greyish colour correspond to higher or lower amounts of smalt in a mixture with lead white. In darker areas, there is more smalt and less lead white, while the opposite is true for clearer areas (Fig. 4). Also, the shadows on the white angel's tunic were originally blue, as demonstrated by Co, Ni, As and Bi peaks in the spectra taken from various areas of the vestment, but are today of greyish-brownish colour.

The black pigment, observed in the red coat of the Angel of the Annunciation and in some other dark areas or shadows, is of an organic origin. There are no elements characteristic for any inorganic black pigment, except Ca, that reveals a possible use of bone or ivory black.

Acknowledgements We acknowledge the financial support from the Project of Excellence 205/HUM-493 of Junta de Andalucía.

References

- Bazzi M (1993) *Abecedario pittorico*. Neri Pozza, Vicenza
- Bermejo E (1985) *Varias obras de Coffermans y una de Van der Stock en Madrid*. Archivo Español de Arte, Madrid
- Calvo A (1997) *Conservación y Restauración, Materiales, técnicas y procedimientos, de la A a la Z*. Edición del Serbal, Barcelona
- Conti A (1996) *Manuale di restauro*. Biblioteca Einaudi, Torino
- Dornheim SD, San Andrés Moya M (2004) Litargirio y masicote. Terminología, propiedades y usos. Reproducción a escala de laboratorio de algunos de sus procesos de obtención. In: XV Congreso de conservación y restauración de bienes culturales, Actas, Vol I, pp 533–546
- Feller R, Roy A, West Fitzhugh E, Berry BH (eds) (1986–2007) *Artists' pigments. A Handbook of their history and characterisation*. National Gallery of Art/Oxford University Press, Washington/ NY, Oxford
- Gómez ML (2000) *Exámen científico aplicado a la conservación de obras de arte*, Cátedra. Instituto del patrimonio histórico español, Madrid
- Knoepfli A, Emmenegger O, Koller M, Meyer A (eds) (1990) *Reclams Handbuch der künstlerischen Techniken*, vol 1–3. Philipp Reclam jun, Stuttgart
- Matteini M, Moles A (2003) *La chimica nel restauro: I materiali dell'arte pittorica*. Nardini editore, Firenze
- Montagna G (1993) *I pigmenti*. Prontuario per l'arte e il restauro. Nardini editore, Firenze
- Schram HP, Herling B (1995) *Historische Malmaterialien und ihre Identifizierung*. Ravensburg Buchverlag, Stuttgart
- Seccaroni C, Moioli P (2002) *Fluorescenza X: Prontuario per l'analisi XRF portatile applicata a superfici policrome*. Nardini editore, Firenze
- Serchi M (ed) (1999) *Cennino Cennini: Il Libro dell'Arte*. Felice Le Monnier, Firenze
- Valdivieso GE (1993) *La pintura en el Museo de Bellas Artes de Sevilla*. Edición Galve, Sevilla

The Analysis of “San He Tu” from the Haizi and Weizi Emplacements at the Tianjin Dagu Site

N. Li, Z. Guo, Z. Zhang, and D. Wang

1 Introduction

“San He Tu” was traditionally used as building material in China. It usually contains sand, lime and clay, making the material solid and hard to destroy, similar to concrete today. Ancient Chinese people used “San He Tu” to build city walls, fortresses and tombs.

The Dagu Emplacements site is located to the south-east of Tanggu District, Tianjin City. This site occupied an area of 16.08 km², and contained the Weizi Emplacement, Zhenzi Emplacement, Haizi Emplacement and Changzi Emplacement on the southern coast. These emplacements were distributed along both sides of the river bank, with their distinctive characteristics of coastal fortresses.

The Weizi Emplacement is a circular emplacement that is 13.8 m high. The perimeter of the emplacement’s base is about 200 m, and its diameter is about 63.5 m. The surface is not flat, due to weathering.

The Zhenzi Emplacement site is a square emplacement, with a perimeter of the base of about 190 m. The entire building was constructed with “San He Tu”. After hundreds of years of history, the emplacement’s surface was damaged heavily.

The remains of the Haizi Emplacement are about 9.53 m high, and the relative height of the base is 7 m. The surface is also not flat because of the weathering (Zhou 1999) (Fig. 1).

The present research was mainly focused on the determination of the composition of “San He Tu” samples from the Haizi and Weizi emplacements. The purpose of the study was to identify the ratios of the elements present in the building

N. Li (✉) and Z. Zhang

Chinese Academy of Cultural Heritage, Beijing 100029, People’s Republic of China

e-mail: lineas@mail.ustc.edu.cn

Z. Guo

Department of Scientific History and Archaeometry, Graduate University of Chinese Academy of Sciences, Beijing 100049, People’s Republic of China

D. Wang

Tianjin Dagu Emplacement Site Managing Institute, Tianjin 300000, People’s Republic of China

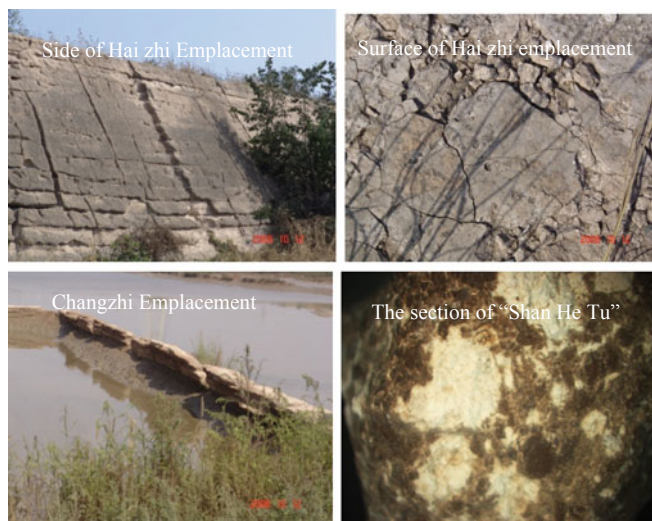


Fig. 1 The base of Da gu Emplacement made of “Shan He Tu”

material, and subsequently to try to produce an alternative material with similar properties to “San He Tu” in order to protect and consolidate the emplacement site.

2 Samples and Analysis

2.1 Samples and Sample Preparation

“San He Tu” samples were collected from the surfaces of the Haizi and Weizi Emplacements’ base (Fig. 1). Samples from the Weizi Emplacement are less dense than those from the Haizi Emplacement, and black soil and lime can be clearly observed in the cross section of samples.

Samples were taken from non-contaminated “San He Tu” parts and cut into small pieces for optical microscope observation and scanning electron microscopy (SEM) analysis. Some pieces were ground into powder for XRF and XRD analysis.

2.2 Analytical Methods and Results

2.2.1 Scanning Electron Microscopy Analysis

The SEM analysis was performed with a Japanese Hitachi S-3600N, with a voltage of 20 kV. The EDX analysis was carried out on an American Genesis 2000XMS X-ray EDS.

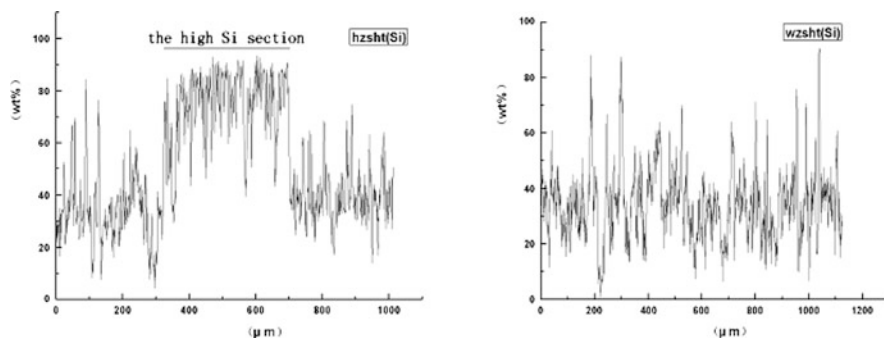


Fig. 2 The line scan of Si, Ca and Al of Hai zhi (*left*) and Weizhi (*right*) emplacement

The SEM study can be divided in two separate stages. The first stage consisted of running line-scanning and surface-scanning of Si, Ca and Al elements from sample cross sections. The second step involved calculating the composition of “San He Tu” by using the average values of Si, Ca and Al in clay, lime, sand, and the entire “San He Tu”.

Lime, clay and sand in the “San He Tu” contain certain amounts of Si, Ca and Al. It is impossible to completely separate them, because they appear as a mixture. Thus, we assumed that, when the line-scanning was performed on the cross section, the positions which contain higher levels of Si, Ca and Al could be expected to represent the distribution of sand, lime and clay (Zhang et al. 1995) taken separately. The average values of Si, Ca and Al in sand, lime and clay were calculated based on this assumption. At the same time, the average values for Si, Ca and Al in the scanned area were obtained, so that we could calculate the contents of lime, clay and sand in the “San He Tu”. A SEM image of Haizi samples is shown on the left side of Fig. 2.

According to the line-scanning results, the average values of Si, Ca and Al in sand, lime and clay can be calculated separately. Table 1 shows the contents of the Si, Ca and Al elements in Haizi “San He Tu”.

The surface-scanning was carried out on several parts of the cross sections of Haizi “San He Tu” (hzshtm₁₋₃). The average values of Si, Ca and Al in the “San He Tu” material taken as a whole can be seen in Table 2. According to the result data of line-scanning and surface-scanning, the ratio of clay, lime and sand in “San He Tu” can be calculated. If there is no sand in the sample, the line-scanning image shows slight fluctuations of the Si, Ca, and Al elements, such as those in the SEM image of the samples from the Weizi Emplacement (*right* side of Fig. 2).

2.2.2 XRF and XRD Analysis

XRF spectra were obtained on a Japanese SHIMADZU EDX-800HS-energy X-ray scattering large cavity fluorescence analyzer. The samples were measured with a

Table 1 The contents and average values of Si, Ca and Al elements in a section with high level of silicon from Haizi “San He Tu” (wt%)

Distance(μm)	Na	Mg	Al	Si	S	Cl	K	Ca	Fe
432.94	0.46	0.78	1.51	89.07	3.07	0.79	1.66	2.65	0
472.83	0.92	1.18	0.77	92.88	0.8	0.8	0.85	1.8	0
481.04	0	3.17	2.4	89.32	1.61	0.81	0.86	1.83	0
482.22	1.02	2.21	2.19	90.73	0.89	0	0.94	2.01	0
488.08	0	1.33	2.6	91.15	0	0	1.89	3.03	0
490.43	0.86	2.97	1.11	88.76	2.2	0	1.57	2.52	0
497.47	0.51	1.29	0.83	88.78	0.83	4.18	0	0.95	2.64
510.37	0.93	0.39	1.5	88.46	3	0.77	0	2.57	2.39
511.55	1.61	1.87	0	90.7	2.77	0.94	0	2.1	0
546.75	1.57	1.81	0.44	90.51	0.89	0	4.77	0	0
547.92	1.19	1.54	2.02	91.83	0	0	1.09	2.33	0
549.09	0	0.92	2.24	89.13	0	0.9	0.95	3.04	2.83
556.13	0.48	2	0.39	89.16	0	1.52	0.81	0.86	4.78
560.83	0	1.96	1.55	91.44	1.59	0	2.55	0.91	0
598.37	1.87	2.45	1.62	90.55	0	0.82	0.86	1.84	0
603.06	1.53	0.44	1.71	93.37	0	0	0.94	2	0
611.28	0.47	1.6	1.97	92.53	0.82	0.82	0.87	0.92	0
615.97	1.97	0.86	0.41	90.51	0.84	1.69	1.8	1.92	0
651.17	1.16	0.99	0.96	90.49	0.98	0	2.08	3.34	0
693.41	1.44	0	0.79	89.97	0.8	1.63	2.59	2.77	0
694.58	0.99	2.11	0.83	90.87	0	1.66	0	0.93	2.6
Average value			1.33	90.49				1.92	

Table 2 The content of Haizi “San He Tu” (wt%)

Elements	Samples			
	Hzshtm ₁	Hzshtm ₂	Hzshtm ₃	Hzshtm average value
Na	1.09	1.02	1.59	1.23
Mg	4.06	3.76	4.19	4.00
Al	8.18	8.81	9.78	8.92
Si	33.81	41.56	33.67	36.35
S	1.21	1.27	1.11	1.2
Cl	1.33	1.32	1.89	1.51
K	1.77	2.12	2.20	2.03
Ca	44.89	36.92	40.93	40.91
Fe	3.66	3.22	4.62	3.83

voltage of 50 kV and each spectrum was acquired for 100 s. The XRD analysis was performed on a Rigaku D/max 2200 X-ray diffraction analyzer, with a voltage of 20 kV and a current of 40 mA. The results of the XRF analysis are shown in Table 3.

According to the composition results for Si, Ca and Al elements in “San He Tu” from the Weizi Emplacement, there is no sand in the samples. Because there is no sand in the samples of Weizi “San He Tu”, we can easily obtain the ratio of clay and lime. Based on the XRF analysis, the contents of Ca, Si and Al in lime and clay were obtained, as it was possible to select them. At the same time, the contents of

Table 3 The content of Weizi "San He Tu" (wt%)

Samples	Remark	Ca	Fe	Si	K	Al	Ti	S	Cl	Mg	Br	Mn	V	Ba
Wzsht ₁	San He Tu from the	47.922	19.960	17.289	4.162	4.627	1.467	1.745		0.519	0.425	0.4		
Wzsht ₂	Weizi Emplacement	48.894	19.679	17.830	4.279	4.583	1.302	1.646		0.602	0.341	0.415	0.057	0.898
Wzsht ₃		47.757	20.098	18.099	4.247	4.811	1.441	1.815		0.684	0.455	0.407	0.062	
Wzsht ₄		43.849	22.824	18.462	4.740	5.070	1.649	1.494		0.667	0.482	0.466		
Wzshtz _{bh}	The lime in Weizi San He Tu	86.765	1.488	7.886	0.410	1.452		1.294						
Wzshtzy ₁	The clay in Weizi	39.039	18.354	25.640	5.901	6.638	1.707	1.587		0.703	0.1	0.330		
Wzshtzy ₂	San He Tu	35.451	16.957	19.518	6.610	4.576	1.409	1.011	14.058		0.126	0.285		
Wzshtzy ₃		30.900	14.072	28.988	5.932	3.464	1.169	1.365			0.100			
Wzshtzy ₄		30.528	13.955	29.890	5.887	3.418	1.162	1.294	13.535					

Ca, Si and Al were easily got by XRF; thus, it became possible to eventually obtain the ratio of lime and clay. However, if there were any sand in the “San He Tu”, it would not have been possible to separate it from the clay, and thus the XRF analysis would have been pointless. This is the reason why we only used XRF analysis for the Weizi “San He Tu” samples. Under microscope observation, white lime and soil can be clearly observed in the cross sections of Weizi “San He Tu”.

The samples above, including those from the Haizi Emplacement, have also been tested by XRD analysis. Samples from the Weizi emplacement were identified as a mixture of “Sanhe Tu” (Wzsht₁₋₄), lime (Wzshtz_{bh}), and black soil (Wzshtzty₁₋₄). The X-ray diffraction analysis shows that CaCO₃ was the main component of lime (Wzshtz_{bh}) from the Weizi Emplacement, and that α -SiO₂ and CaCO₃ are the main phases of the other samples.

3 Discussion

3.1 The Manufacture Craft of “San He Tu”

Generally speaking, as a Chinese traditional building material with good mechanical performance, “San He Tu” was made of black soil, white lime and sand, combined in a certain ratio. Based on the data from microphotographs of Haizi and Weizi Emplacement samples, the main compositions were confirmed to consist of clay and white minerals. The SEM–EDX analysis shows that the average content of Ca in these samples is about 80%, and the XRD analysis shows that the white mineral is CaCO₃. Therefore, the initial adhesive material was probably Ca(OH)₂.

3.2 Ratios of “San He Tu”

From the line-scanning images of Si, Ca and Al elements from Haizi Emplacement samples, it is easy to note that the distribution of the three elements shows significant fluctuations. The quantity of Si element is higher in the 350–700 μm part than in other sections. In this section, the quantity of Si, Ca and Al elements should be very close to the content of the three elements in the sand. Meanwhile, based on the data in the line-scanning image of the Ca and Al elements, the content of Si, Ca and Al in lime and clay can be also calculated. Based on these results, the overall average content of Si, Ca and Al in sand, lime and clay can be calculated (Table 4).

By using the data from the line-scanning and surface-scanning of Haizi “San He Tu”, the average values of Si, Ca and Al can be calculated. The highest level of Si should indicate the distribution of sand, the highest level of Ca should indicate the distribution of lime, and the highest level of Al should indicate the distribution of

Table 4 The average content of Si, Ca, Al in sand, lime and clay from Haizi “San He Tu”

Components	Elements		
	Si	Ca	Al
Sand	90.48	1.92	1.32
Lime	10	73.32	3.48
Clay	43.24	13.09	26.43

clay. The average values of Si, Ca and Al in sand, lime and clay were calculated based on this assumption. At the same time, the average values for Si, Ca and Al in the scanned area were obtained, so that we could calculate the contents of lime, clay and sand in the “San He Tu”.

If the ratio of sand, lime and clay in the “San He Tu” is defined as X:Y:Z, then, according to the contents of Si, Ca and Al, an equation can be set up as follows:

$$\text{Si: } X90.48\% + Y10\% + Z43.24\% = (X + Y + Z)36.3\%$$

$$\text{Ca: } X1.92\% + Y73.32\% + Z13.09\% = (X + Y + Z)40.91\%$$

$$\text{Al: } X1.32\% + Y3.48\% + Z26.43\% = (X + Y + Z)8.92\%.$$

The resulting ratio is X:Y:Z = 1:1.74:0.92, indicating that the ratio of clay, lime and sand in “San He Tu” from the Haizi emplacement is approximately 1:2:1.

The ratio of Weizi Emplacement “San He Tu” can be calculated according to a similar procedure, and was found to be 3:1. The material is composed of clay and lime, but contains no sand.

4 Conclusions

Through microscope observation, XRD, XRF and SEM–EDX tests, the analysis of samples from the Weizi and Haizi Emplacements showed that “San He Tu” was a building material consisting of a mixture of clay, lime and sand. The original adhesive material in “San He Tu” was probably white lime. We also calculated the ratio of clay, lime and sand in the material from the Haizi Emplacement, found to be approximately 1:2:1, while the samples from the Weizi Emplacement only contain clay and lime, in a ratio of 3:1. This research program provides an appropriate framework for the analysis of these types of materials.

Acknowledgements We are truly thankful for having received a grant for this project from the Innovative Project of State Administration of Cultural Heritage (2009023-11/03). Furthermore, the authors would also like to thank Mr. Ma Qinglin, Dr. Chen Qing, Dr. Song Yan and Dr. Shen Dawo for their generous help.

References

- Zhang Deng-ming, Xue Yong-ming, Sha Ai-ming (1995) Experimental research on early strength of Lime and Flyash stabilized soil. *Fly Ash Compr Util* 1(1):17
- Zhou Bao-fa (1999) The thought of exploitation and protection on the Emplacement Dagu Site. *J Tianjin Adult High Learn* 1(1):12

Neolithic Obsidian Economy Around the Monte Arci Source (Sardinia, Italy): The Importance of Integrated Provenance/Technology Analyses

C. Lugliè, F.X. Le Bourdonnec, and G. Poupeau

1 Methods and Aims

With few exceptions linked to locally available options, obsidian is almost the unique lithic resource used for the production of chipped stone industries in the Neolithic sites of central-southern Sardinia. However the local economy of this raw material, an important clue to support hypotheses on the dynamics of interregional interactions, had in the past been largely neglected. In order to fill this gap we initiated (Lugliè et al. 2007) a programme of “integrated” studies of Sardinian Neolithic obsidians involving the exhaustive study of reduction techniques, obsidian tools use and provenance of selected Early and Middle Neolithic assemblages. We also reached a better level of knowledge of the field occurrences and geochemical variations of the Monte Arci obsidians. The archaeological obsidian sourcing was realized by a non-destructive association of visual and geochemical characterizations. We discuss here the present status of this approach from the Sardinian Early Neolithic (EN) sites of Su Carroppu (Lugliè et al. 2007), Rio Saboccu (Lugliè et al. 2008) and Sa Punta cases.

C. Lugliè (✉)

Dipartimento di Scienze Archeologiche e Storico-Artistiche, Università di Cagliari, Piazza Arsenale 1, 09124 Cagliari, Italy
e-mail: luglie@unica.it

F.X. Le Bourdonnec

Institut de Recherche sur les Archéomatériaux, UMR 5060, CNRS, Université Bordeaux-3, Maison de l'Archéologie, esplanade des Antilles, 33607 Pessac, France
e-mail: françois.lebourdonnec@etu.u-bordeaux3.fr

G. Poupeau

Institut de Recherche sur les Archéomatériaux, UMR 5060, CNRS, Université Bordeaux-3, Maison de l'Archéologie, esplanade des Antilles, 33607 Pessac, France
and

Département de Préhistoire, UMR 5198, CNRS, Muséum national d'histoire naturelle, Musée de l'Homme, 17 place du Trocadéro, 75016 Paris, France
e-mail: gpoupeau@u-bordeaux3.fr

2 The Monte Arci Obsidians

Although it was known since long that the Pliocenic (about 3 Ma old) Monte Arci obsidians had circulated from Sardinia to the northern Tyrrhenian region of western Mediterranean during the Neolithic, a complete view of its multiplicity of types differing (notably) by their chemical composition and sources was established only recently. From an archaeological point of view however, only four obsidian types, SA, SB1, SB2 and SC are significant (Tykot 1996, 2002). Monte Arci obsidians blocks and cobbles were naturally transported in the plains surroundings this volcanic massif, offering opportunities to Neolithic men to gather also their raw materials in these secondary sources.

Since 7 years we carried out a topographic survey of the Monte Arci volcanic complex and of its nearby plains in order to precisely assess the distribution of each obsidian type. The obsidian deposits mapping covered an about 200 km² area and was recorded in a GIS environment. In the primary sources and their relative sub-primary deposits, obsidians blocks are angular in shape and may have weights of several kilograms. Although their size and morphology change progressively, on the average, with distance from the primary sources, workable fist-size nodules of up to 0.5 kg can still be found at a distance of up to 35 km from their original outcrops. The present status of the primary and workable secondary Monte Arci sources mapping appears in Fig. 1 (for a preliminary version of this map, see Lugliè et al. 2006). In secondary deposits the cobbles present more or less rounded shapes and exhibit deeply crenulated cortical surface. Their roundness, surface crenulation and cortex thickness and maturation increase with distance to the primary sources. As a consequence they are good qualitative index of transportation distances.

It results from these observations about the size/shape/surface evolution following transportation/residence time in soils of obsidian in secondary source that the characterization of pre-knapping surface remnants on artefacts (when preserved) becomes now an important criteria in sourcing studies (Lugliè 2006). This in turn has also a quite positive influence in *chaîne opératoire* analyses (see below).

3 Sourcing: Techniques, Results

The obsidian assemblages were sourced mainly from visual criteria (see f.i. Tykot 1996; Lugliè et al. 2007). Only 34% (Rio Saboccu) to 15% (Su Carroppu) of the obsidians could not be determined in this way. The elemental composition of the remaining 153 obsidians were characterized by particle induced X-ray emission (PIXE). These ion beam analyses were performed in France either with the AGLAE external beam facility (*Centre de Recherche et de Restauration des Musées de France*, Paris) or the nuclear probe line of the AIFIRA facility (*Centre d'Etude Nucléaire de Bordeaux-Gradignan*) (Fig. 2). The overall, visual/instrumental sourcing, shows that (1) all obsidians are of a Sardinian origin, (2) SB1 are virtually

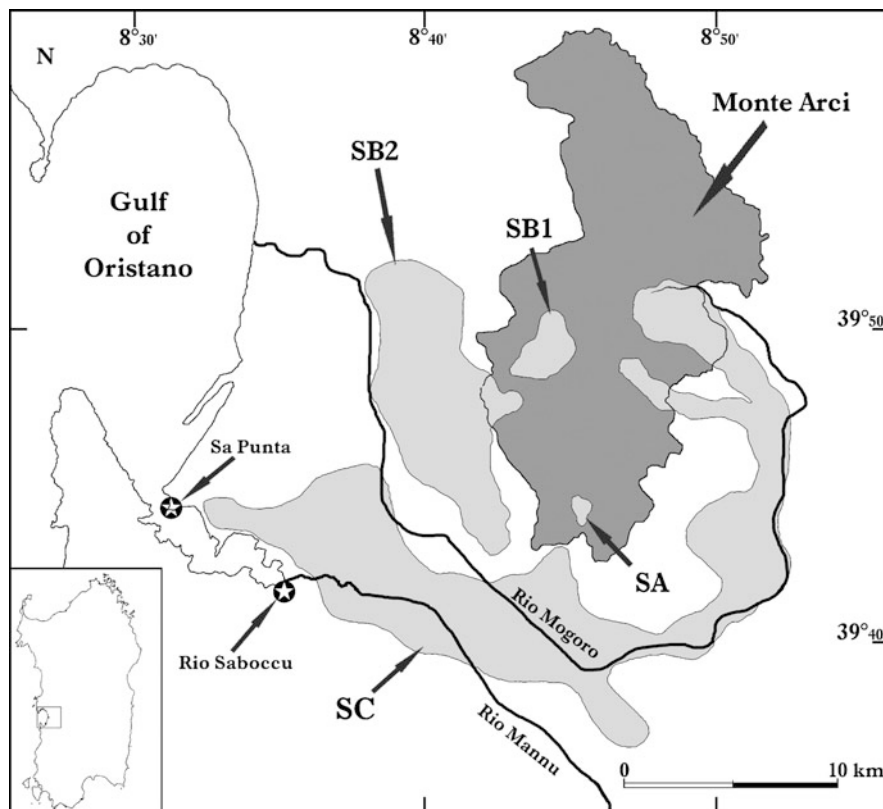


Fig. 1 Schematic map of the Monte Arci region (Sardinia) showing the extension of the SA, SB1, SB2 and SC obsidian sources (adapted from Lugliè et al. 2006). The secondary obsidian sources are distributed in the light-gray areas outside the Monte Arci massif (dark-grey area). Star symbols refer to the localisation of the Rio Saboccu and Sa Punta Early Neolithic sites

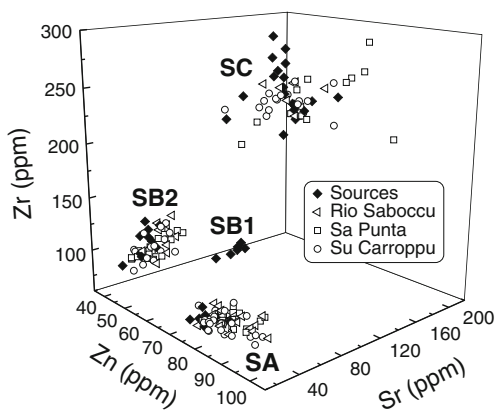


Fig. 2 Three-dimensional diagram comparing the contents of Zn, Sr and Zr in 153 obsidian artifacts and in 44 Monte Arci geological samples as determined by PIXE

absent from these assemblages. Obsidian types SA, SB2 and SC are all well represented, with a net advantage for the SA type.

4 A Three Cases Study

Among the three EN obsidian assemblages studied so far according to our integrated characterization/typo-technological approach, two come from newly discovered sites, the Rio Saboccu and Sa Punta open air settlements. Both, located in the alluvial plain some 10 km west from the Monte Arci massif (Lugliè et al. 2008) are radiocarbon-dated to the last three centuries of the sixth millennium BC. Given their distance from the primary sources and their position in close proximity with the secondary deposits of the alluvial plain, these sites offer a good opportunity to study the EN obsidian economy inside what can be considered as a raw material direct procurement area (Fig. 1). In a different situation, the slightly older (by about two centuries) Su Carroppu rockshelter is located in a restricted hilly region 65 km south-west of the Monte Arci (Lugliè et al. 2007). This site, localized in the “contact zone”, relatively to the Monte Arci obsidian sources, should provide us with informations on a different (possibly indirect way) of raw material procurement.

Nonetheless, the obsidian distribution model is almost the same in the three sites. In fact SA, SB2 and SC obsidian types are always well represented, the former being clearly dominant. Besides, SB1 obsidians which are by far scarcely used at Rio Saboccu and Sa Punta, are totally absent at Su Carroppu. With regard to the types of deposit exploited, SC obsidians in the sites of the direct procurement zone come almost exclusively from the local secondary deposits, which is not the case at Su Carroppu.

In these three sites obsidian were introduced as unworked pebbles and blocks and the reduction process was entirely performed in situ. Given the lower incidence of SC obsidians from secondary deposits in the sites of the direct procurement area, it is evident that the raw material procurement was not ruled by a least-effort law. The technological analysis of the lithic assemblages shows that the acquisition strategies were exclusively oriented toward small size pieces, even if in the exploited primary and sub-primary SA and SB2 deposits much larger blocks were generally available. Since the more disposable raw material of the secondary deposits are disregarded by the Early Neolithic people of the direct procurement zone, we are led to induce that in the second half of the sixth millennium technological imperatives in the first place influenced raw material selection and any opportunistic behaviour was working in reference either to the quality either to the size.

The visual determination for each assemblage led us on the one hand to determine the minimum number of pieces introduced in the sites for each obsidian quality and, on the other hand, to prove that two main reduction sequences were operating. The first one, less frequent, was oriented to blade(let)s production by

direct percussion technique, preferentially using SA and SB2 types. Afterwards these more technologically invested blanks were employed for the production of standardised tools like geometrics and double-backed points, always by far the minor component of the toolkits. Less specialized flakes are the most common product of the second reduction sequence.

5 Monte Arci Obsidian Across the Sea: Chronological Trends of Distribution

If one considers the available information on Monte Arci obsidians distribution in the contemporary sites of the Tyrrhenian region, similar trends can be observed with a dominant presence of the three SA, SB2 and SC types and the quasi absence of the SB1 type. Yet, out of Sardinia an appreciable increased frequency of SB2 obsidians is generalized as well as a lack of evidence of SC obsidians coming from long-distance secondary sources. Given the large number of EN sites in the obsidian direct procurement area, this observation can be interpreted as the consequence of a controlled access to the lithic resource by the local communities and of particular exchange modalities like the possible more or less deliberate selection of specific obsidian types to be exchanged.

With the Middle Neolithic (MN) a new mode and intensity of obsidian use appears clearly, with the progressive emergency of craft products and an important increase in the rate of blades and bladelets production. These changes are particularly evident during the second half of the fifth millennium BC, the MN-B phase, when a sharper shift can be noted both in the rates and modes of production in Sardinia as well as in the relative frequencies of obsidian types distribution inside and outside the island. During this period the first stages of obsidian reduction is partly displaced in close proximity to the primary sources of SA and mainly of SC obsidians, where the raw materials are more abundant and offer a wider range of variability in shapes and sizes. By then large obsidian workshops were situated close to the SA and SC source essentially for the shaping out of polyhedral cores to be introduced into the newly structured exchange networks. Whilst in the direct procurement zone a partly opportunistic behavior led to some exploitation of SB2 obsidians, this type is rare or absent among the obsidian collections outside Sardinia. Thus the overall increase of Monte Arci obsidians in MN collections of Corsica, Italian mainland and southern France is very essentially based on SA and SC obsidians.

The cultural affinities of the EN groups of the central-northern Tyrrhenian Sea can be accounted for by the intensity of interregional interactions, as documented by the diffusion of Sardinian obsidians. Yet, the following rise of more effective obsidian production systems and exchange networks during the MN deserves to be better evaluated in the frame of a more detailed understanding of the process of cultural variability and regionalization in the Tyrrhenian region during the fifth

millennium BC. Integrated provenance and typo/technological analyses proved their efficiency in the analysis of complete obsidian assemblages. There is no doubt that this approach will benefit to future studies of the west Mediterranean Neolithic.

References

- Lugliè C (2006) Les modalités d'acquisition et de diffusion de l'obsidienne du Monte Arci (Sardaigne) pendant le Néolithique: une révision critique à la lumière de nouvelles données. In: Bergès L, Pelletier M (eds) *Voyages en Méditerranée. Relations, échanges et coopération en Méditerranée. Actes du 128e Congrès national des sociétés historiques et scientifiques (Bastia, 14–21 avril 2003)*, CTHS, pp 123–131
- Lugliè C, Le Bourdonnec F-X, Poupeau G, Bohn M, Meloni S, Oddone M, Tanda G (2006) A map of the Monte Arci (Sardinia Island, Western Mediterranean) obsidian primary to secondary sources. Implications for Neolithic provenance studies. *C R Palevol* 5(8):995–1003
- Lugliè C, Le Bourdonnec F-X, Poupeau G, Atzeni E, Dubernet S, Moretto P, Serani L (2007) Early Neolithic obsidians in Sardinia (Western Mediterranean): the Su Carroppu case. *J Archaeol Sci* 34:428–439
- Lugliè C, Le Bourdonnec F-X, Poupeau G, Congia C, Moretto P, Calligaro T, Sanna I, Dubernet S (2008) Obsidians in the Rio Saboccu (Sardinia, Italy) campsite: Provenance, reduction and relations with the wider Early Neolithic Tyrrhenian area. *C R Palevol* 7:249–258
- Tykot RH (1996) Obsidian procurement and distribution in the Central and Western Mediterranean. *J Mediterr Archaeol* 9(1):39–82
- Tykot RH (2002) Chemical fingerprinting and source tracing of Obsidian: The Central Mediterranean trade in Black Gold. *Accounts Chem Res* 35:618–627

Mineralogical Characterization of the Weathering Crusts Covering the Ancient Wall Paintings of the Festival Temple of Thutmosis III, Karnak Temple Complex, Upper Egypt

H.H.M. Mahmoud, N.A. Kantiranis, and J.A. Stratis

1 Introduction

The Karnak temple complex is located on the east bank of the River Nile, about 2.5 km north of Luxor, Upper Egypt. The main building materials used in its construction are sandstones, the so-called “Nubian Sandstone”, collected from the Gebel el-Silsila area in south-western Egypt (Fitzner et al. 2003). A number of weathering crusts with different colours and thicknesses have been observed, covering the decorated walls of the temple. The present study is a preliminary examination of the physico-chemical properties of some weathering crusts covering the wall paintings of the festival temple of Thutmosis III (c.1504–1450 BC, the 18th Dynasty) at Karnak temple complex, Upper Egypt.

2 Materials and Methods

The microstratigraphy and microanalysis of some weathering crusts were carried out using a JEOL JSM-840A scanning electron microscope in backscattered electron mode, equipped with an energy dispersive X-ray (EDS) Oxford ISIS 300 microanalytical system. The structure of the crusts was also investigated by optical microscopy on polished cross-sections. Powder X-ray diffraction analysis (PXRD) was

H.H.M. Mahmoud

Department of Conservation, Faculty of Archaeology, Cairo University, Giza 12613, Egypt
and

Laboratory of Analytical Chemistry, Aristotle University, 54124 Thessaloniki, Greece

N.A. Kantiranis

Department of Mineralogy-Petrology-Economic Geology, Aristotle University, 54124 Thessaloniki, Greece

J.A. Stratis (✉)

Laboratory of Analytical Chemistry, Aristotle University, 54124 Thessaloniki, Greece
e-mail: jstratis@chem.auth.gr

used to identify the mineralogical composition of the studied samples with a Phillips (PW1710) diffractometer. The samples were scanned over the $3\text{--}63^\circ 2\theta$ interval at a scanning speed of $1.2^\circ/\text{min}$. Quantitative estimates of the abundance of mineral phases were derived from the PXRD data, using the intensity of a certain reflection, the density, and the mass absorption coefficient for $\text{CuK}\alpha$ radiation for the minerals present. Corrections were made using external standards, while the detection limit was $\pm 2\%$ w/w.

3 Results and Discussion

3.1 Optical Microscopy

The black crusts (Fig. 1a) appear in the form of an irregular layer mixed with salts, quartz and several fly ash particles embedded in the layer. These crusts are friable and their thickness ranges from 100 to 250 μm . The source of fly ash particles is probably the open waste burning in the studied area. These particles mainly deposited in the unsheltered areas of the walls. The brown crusts (Fig. 1b) appear in the form of a laminar layer with thickness reaching 150 μm , adhere well to the stone surface and cover the orange-red painted layer.

3.2 Backscattered Electron Microscopy (BSE)

Scanning electron microscopy in the backscattered electron mode (BSE) is useful when working with crusts and patinas and helps to distinguish the layers by microstratigraphy analysis of elemental distribution in the different layers. The study by BSE of cross-sections of the examined samples showed that the black

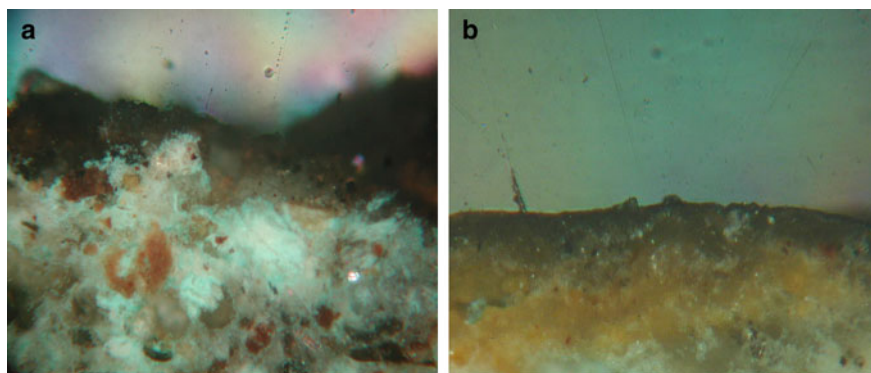


Fig. 1 Cross-sections of weathering products of: (a) black layer, (b) brown layer

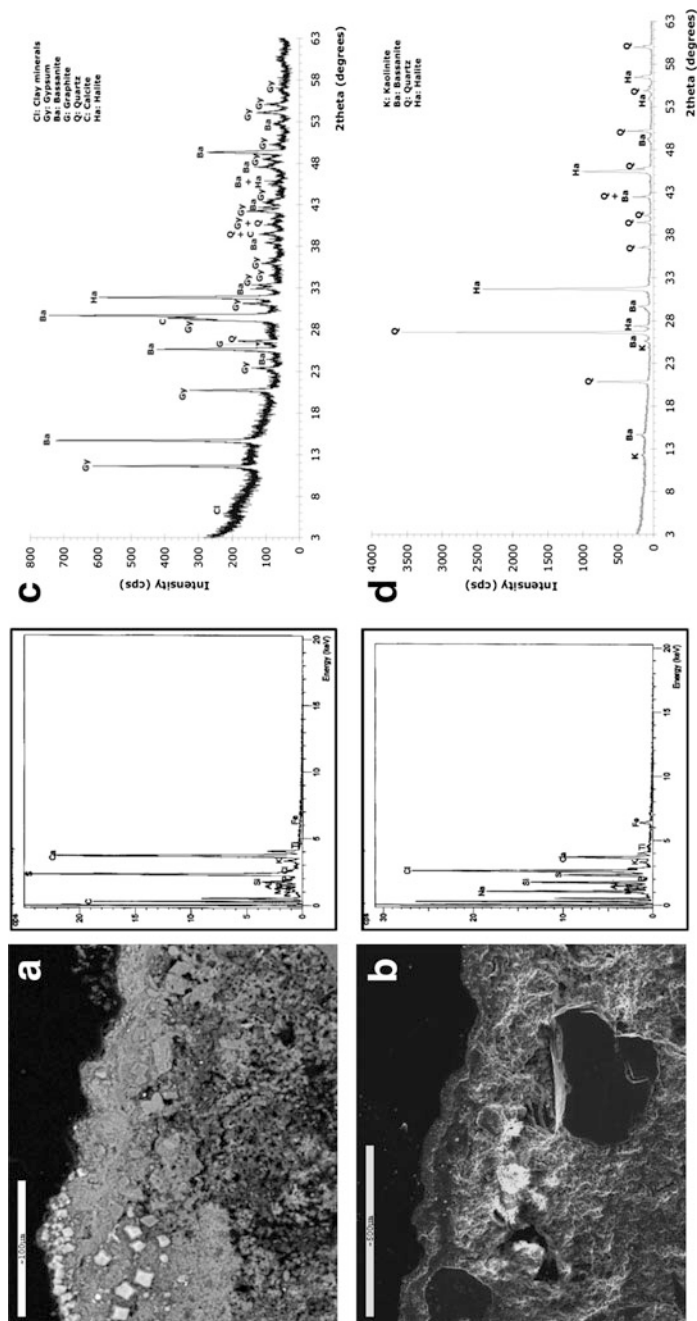


Fig. 2 *Left:* BSE micrographs and microanalysis of weathering products of: (a) black crust and salt encrustations, (b) brown layer covering the painted surfaces. *Right:* XRD patterns of: (c) black crust, (d) brown crust

crusts (Fig. 2a) appear in the form of an irregular layer with heterogeneous thickness and composed mainly of gypsum crystals scattered in the layers and embedded in clayey clusters with crystals of sodium chloride. Brown crusts appear in different consecutive layers (Fig. 2b), and they are rich in crystals of gypsum and halite with grains of quartz. The microanalysis of the black layer showed quite high concentrations of Ca and S, and low concentrations of Si, K, Mg, Cl, Na, Al, Ti and Fe. The microanalysis of the salt crust showed that Cl and Na are the major components, while Ca, Si, and S are the secondary elements. Traces of K, Al, Mg, Fe and Ti were also measured. Quartz grains were detected in all the investigated samples.

3.3 Mineralogical Characterization

Black crusts (Fig. 2c) consist mainly of gypsum ($\text{CaSO}_4 \cdot 2\text{H}_2\text{O}$, 38%), bassanite ($\text{CaSO}_4 \cdot \frac{1}{2}\text{H}_2\text{O}$, 36%), halite (NaCl, 9%) and calcite (CaCO_3 , 9%). Minor amounts of quartz (4%), graphite (2%) and clay minerals (2%) were also detected. The brown crusts (Fig. 2d) consist mainly of halite (57%) and quartz (38%), while minor amounts of bassanite (3%) and kaolinite (2%) were also detected.

3.4 Formation Mechanisms of the Degradation Products

Gypsum has low solubility and crystallizes at high levels of humidity; moreover, the continuous supply of groundwater at the studied site enhanced gypsum re-crystallization and led to the development of larger crystals. The chemical weathering of carbonatic stones is mainly attributed to the phenomenon of sulphation. In the case of non-calcareous stones, sulphates probably formed due to the chemical attack of mortars. The gypsum detected in our case has two possible sources: first, the new mortars used for conservation purposes in the temple contain limestone types from the Thebes Mountains, used as binders and aggregates in the new mortars. These stones contain two varieties of sulphates, anhydrite and gypsum, in addition to sodium chloride (halite). The environmental impact of the area enhances the crystallization and re-crystallization of these salts. The reaction between the old mortars used for restoration purposes and the groundwater, penetrating from the ancient sacred lake found at the site or from the water seepage from cultivated lands close to the site (Martinet et al. 1992; Ismail et al. 2005), results in different weathering products. Second, the plaster layers in the structure of wall paintings also provide another source of gypsum in addition to calcium carbonates, which can undergo changes due to the chemical attacks, forming calcium sulphates. On the other hand, according to Del Monte and Sabbioni (1984), the fly ash particles emitted by coal-fuelled power plants can provide another source of sulphate ions beside calcium ions, which in the presence of water precipitated as gypsum. For a long time it was believed that gypsum was the main phase found on buildings and monuments since bassanite forms only under very specific conditions. The dehydration of gypsum to

hemihydrate bassanite requires a lower relative humidity than the dehydration of gypsum to anhydrite (Charola et al. 2007), and bassanite is formed at 42°C. However, the dehydration of gypsum is extremely slow below 42°C and is affected by the nature of the other materials present in the system, as would be the case in monuments (Charola and Centeno 2002).

4 Conclusions

The damage to the decorated walls in the festival temple of Thutmosis III at Karnak temple complex, Upper Egypt, is strongly related to:

1. The dramatic rise of the water table, and not directly linked to the post-Aswan high dam rise in groundwater. Rising close to the ground surface, the water table had an adverse impact upon the stone structure of the temple. Studies have revealed that the main reasons for the water table rise are seepage from land reclamation areas in the east and leakages from poor sanitary drainage conditions in the increasingly expanding housing areas (Tortajada 2007), in addition to the penetration of the groundwater from the sacred lake situated inside the temple complex. The study confirms some of the finds provided by other authors (Saleh et al. 1992; Martinet et al. 1992; Fitzner et al. 2003) in their study of the weathering mechanisms at the Karnak temples.
2. The crusts caused several aesthetic damages to the decorations; these weathering products show the serious condition of the deterioration of the murals. The black crusts consist mainly of gypsum, bassanite, halite, calcite, clay minerals, quartz and aerosols of organic carbon (graphite). Quartz and halite are the main components of the brown crusts, with minor amounts of bassanite and kaolinite. The dehydration of gypsum to form bassanite is related to the climatic conditions of the studied region.

The understanding of the formation mechanisms of weathering products will be of great importance in the design of conservation procedures for the protection of the Egyptian cultural heritage.

Acknowledgements Mr H.M. Mahmoud especially thanks the State Scholarships Foundation (I.K.Y.) of Greece for the financial support of his PhD thesis.

References

- Charola AE, Centeno SA (2002) Analysis of gypsum-containing lime mortars: possible errors due to the use of different drying conditions. *J Am Inst Conserv* 41:269–278
- Charola AE, Pühringer J, Steiger M (2007) Gypsum: a review of its role in the deterioration of building Materials. *Environ Geol* 52:339–352

- Del Monte M, Sabbioni C (1984) Gypsum crust and fly-ash particles on carbonatic outcrops. *Arch Met Geoph Biocl Ser-B* 35:105–111
- Fitzner B, Heinrichs K, La Bouchardiere D (2003) Weathering damage on Pharaonic sandstone monuments in Luxor-Egypt. *Build Environ* 38(9–10):1089–1103
- Ismail A, Anderson NL, David RJ (2005) Hydro geophysical investigation at Luxor, Southern Egypt. *J Environ Eng Geophys* 10(1):35–49
- Martinet G, Deioye FX, Le Roux A (1992) Nature and weathering of the mortars used in the restoration of the Temple of Amon at Karnak. *Bull Liaison Lab Pouts Chaussées* 182:21–26
- Saleh SA, Helmi FM, Kamal MM, El Banna AE (1992) Study and consolidation of sandstone: Temple of Karnak. *Stud Conserv* 37:93–104
- Tortajada C (2007) International workshop on hydrogeology and impacts of the Aswan High Dam. Conference Report, ministry of water resources and irrigation of Egypt Cairo

Scientific Characterization of Roman Age Over-Paintings at Luxor Temple, Upper Egypt: Preliminary Results

H.H.M. Mahmoud, N.A. Kantiranis, E. Pavlidou, and J.A. Stratis

1 Introduction

The Roman paintings of Luxor temple in Upper Egypt, dated back to the reign of Emperor Diocletian (late third century AD), are considered one of the most important examples of the use of over-painting techniques in the world. Different plaster layers were applied and painted with scenes of Roman officials over the decorated pharaonic walls from the period of Amenophis III (eighteenth Dynasty, c.1402–1364 BC). In this study, different analytical methods were applied to identify the painting materials that were used for the construction of the over-paintings.

2 Materials and Methods

Samples of blue, yellow and red pigments, in addition to fragments of the plaster layers, were studied. The morphology, structure and microanalysis of painting layers were carried out in (SE) and (BSE) modes using a JEOL JSM-840A scanning electron microscope equipped with an energy dispersive system (EDS) Oxford ISIS 300 microanalytical system. The structure of the painting layers was investigated on

H.H.M. Mahmoud

Department of Conservation, Faculty of Archaeology, Cairo University, Giza 12613, Egypt
and

Laboratory of Analytical Chemistry, Aristotle University, 54124 Thessaloniki, Greece

N.A. Kantiranis

Department of Mineralogy-Petrology-Economic Geology, Aristotle University, 54124 Thessaloniki, Greece

E. Pavlidou

Department of Physics, Aristotle University, 54124 Thessaloniki, Greece

J.A. Stratis (✉)

Laboratory of Analytical Chemistry, Aristotle University, 54124 Thessaloniki, Greece
e-mail: jstratis@chem.auth.gr

polished cross-sections, while the transmittance FTIR spectra were obtained with a Perkin-Elmer Spectrum One Spectrometer on KBr pellets, in order to identify the colouring materials and detect any organic material in the paintings. Powder X-ray diffraction analysis was used to identify the mineralogical composition of the studied samples with a Phillips (PW1710) diffractometer. The samples were scanned over the $3\text{--}63^\circ$ 2θ interval at a scanning speed of $1.2^\circ/\text{min}$. Quantitative estimates of the abundance of mineral phases were derived from the PXRD data, using the intensity of a certain reflection, the density, and the mass absorption coefficient for CuK_α radiation for the minerals present. Corrections were made using external standards, while the detection limit was $\pm 2\%$ w/w.

3 Results and Discussion

3.1 Optical and Scanning Electron Microscopy

The stratigraphy of some of the painted plasters is illustrated in Fig. 1; from the optical investigation of the cross-sections we can clearly identify two main plaster layers: from the bottom to the top, the coarse plaster of the *arriccio*, and the second layer of finer, smoother plaster of the *intonaco*, based mainly on calcium carbonates. The coarse plaster differs throughout the walls in terms of the amount of quartz and in thickness.

The investigation of the blue pigment layer shows that the pigment is applied on a plaster layer based mainly on calcium carbonates with traces of gypsum. The loss of the dark blue colour in some areas is clearly noticed (Fig. 1a). The backscattered electron (BSE) image of a blue crystal discloses the existence of skeletal crystals, probably of cuprorivaite (Egyptian blue). The peaks of Si, Ca and Cu are present, and their atomic percentage ratios, determined by EDS microanalysis, are in agreement with the chemical formula of cuprorivaite ($\text{CuCaSi}_4\text{O}_{10}$) (Fig. 2a). Cuprorivaite, which gives the dark blue colour – in this variety, a few percent of an alkali flux such as soda or potash mixed with the other ingredients was used to produce the pigment – has a fine structure, with coarse crystals and heterogeneous (Tite et al. 1984;

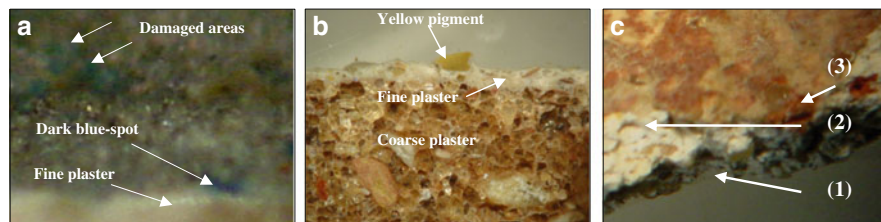


Fig. 1 Stereomicroscopic images of painted layers with: (a) blue pigment, (b) yellow pigment, (c) red pigment

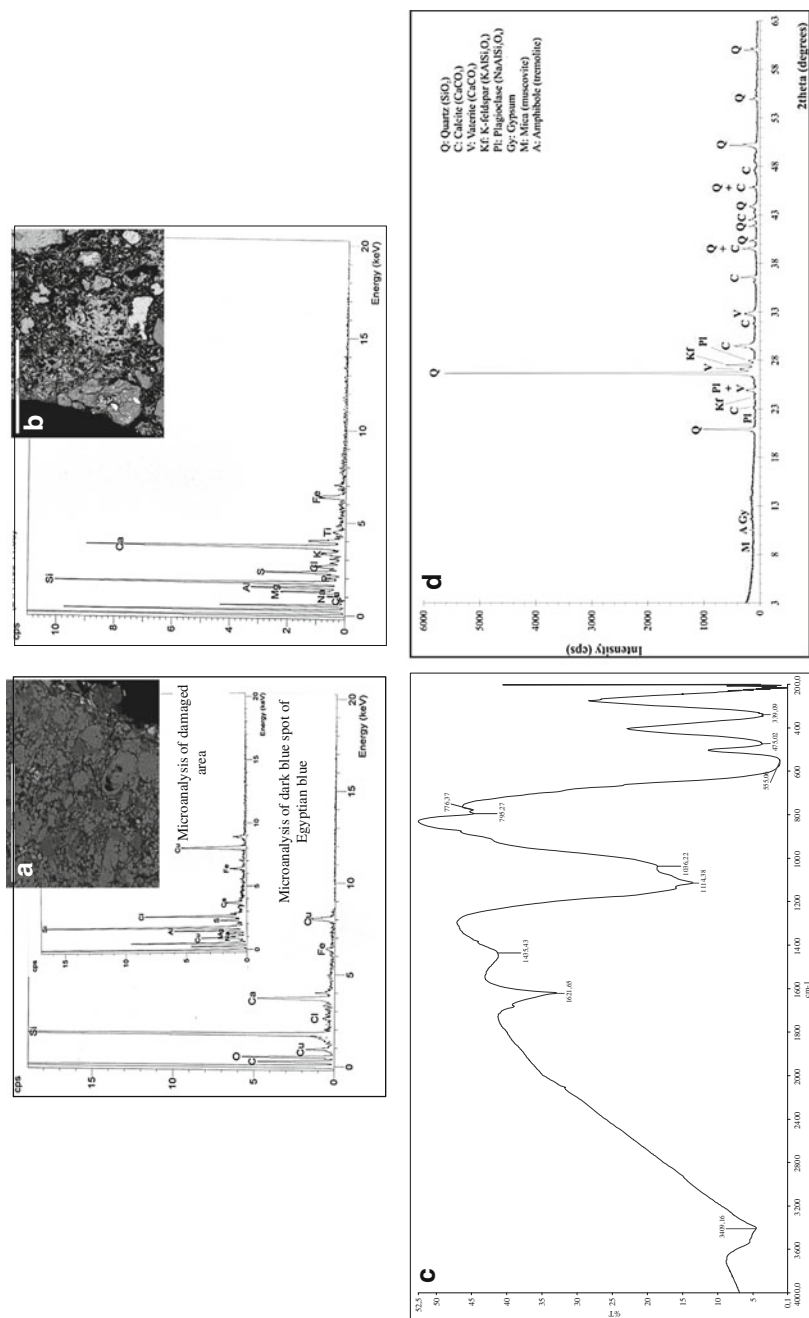


Fig. 2 (a) BSE micrograph and EDS spectra of painting layer with Egyptian blue and damaged bluish-green layer, (b) BSE micrograph and EDS spectrum of painting layer with yellow pigment, (c) FTIR spectrum of red pigment, (d) PXRD pattern of coarse plaster

Lee and Quirke 2001). The optical investigation of the damaged area indicates the presence of pale blue-greenish spots, while the microanalysis showed Si, Cu and Cl as the major ions contained in this layer. Probably, this deterioration process starts with the devitrification of the glass phase – the formation of a glass phase is basically controlled by the ingredients used to produce the pigment, especially the flux material, in addition to the firing temperature and cooling rates – in the Egyptian blue, followed by decomposition of the residual material. Migration of chlorine-bearing solutions leads to reactions with copper in the residual glass. The copper- and chlorine-bearing solutions will then react with calcite – in the plaster layers – and precipitate basic copper chlorides (Schiegl et al. 1989). The yellow pigment layer (Fig. 1b) is a thin layer partially separated from the substrate and applied on a thick lime-based coat; underneath it, a coarse plaster layer rich in calcite and quartz grains can be noticed. The BSE image of the yellow pigment shows fibrous and massive particles of the pigment within a matrix of granular aggregates of calcite (Fig. 2b). The EDS microanalysis of the sample (Fig. 2b) shows that the peak of Fe is present, a feature confirmed by the presence of iron oxides (mainly goethite) in the PXRD and FTIR analyses. The red pigment (Fig. 1c) sample shows a thin layer of tiny particles of red ochre applied on a white lime-based plaster, while the coarse plaster can also be noticed. The EDS spectrum of the red pigment shows that the peak of Fe (19.54%) is present, indicating the existence of iron oxide as the possible material producing the red colour. In addition, a strong contribution of Al and Si indicated the existence of an aluminosilicate material, probably from the clay minerals associated with ochres.

3.2 Infrared Spectroscopy and X-Ray Powder Diffraction Analysis

The representative FTIR spectrum of the red painted layer and PXRD pattern of the coarse plaster are shown in Fig. 2. The FTIR spectrum of the blue pigment presents characteristic peaks lying mainly between 1,280 and 1,000 cm^{-1} , which are attributed to Si–O–Si stretching vibrations, the intense bands at 977.76, 1,023.94 and 1,076.72 cm^{-1} , and the medium intensity band at 1,155.89 cm^{-1} , respectively, which are all characteristics of the Egyptian blue. In the case of the red pigment, the presence of a strong band at 555 cm^{-1} indicates the presence of iron oxide (hematite) (Fig. 2c), the band at 1,435.43 cm^{-1} is attributed to calcium carbonates and mainly assigned to calcite, and the band at 1,621.65 cm^{-1} is attributed to gypsum. The bands at 1,036.22, 1,114.38, 795.27 and 776.37 cm^{-1} are attributed to (Si–O) stretching. An interesting feature of the FTIR spectra is the region of 1,200–850 cm^{-1} , resulting from several overlapping bands of silicates or aluminosilicate materials. The most important of these bands are those attributed to the TO_4 silicate groups (T = Si, Al) of silicates and clays, as well as to the SO_4^{2-} group. The precise assignment of the vibration modes of this band is not easy, because of the aforementioned overlapping. Asymmetric internal T–O stretching vibrations of

the TO_4 primary building units give rise to strong absorption bands in the range $1,250\text{--}850\text{ cm}^{-1}$. The bands at 797 and 902 cm^{-1} collected on the yellow pigment are assigned to the vibrational modes of goethite. The bands at $\sim 400\text{--}475\text{ cm}^{-1}$ indicate the presence of amorphous silicates (glass), probably originating in the ceramic fragments contained in the mortar. According to Velosa et al. (2007), crushed ceramic particles were employed in Roman mortars for the purpose of creating pozzolanic reactions between the finer particles and lime. FTIR spectra for the plaster layers *arriccio* and *intonaco* are very similar, and both show the calcite spectrum and components of quartz and aluminosilicate materials. To confirm these results, powder X-ray diffraction measurements were performed on some samples. The mineralogical composition of the coarse plaster layer indicated the presence of the following crystalline phases: quartz (65%) as the main component; among the minor components, there are K-feldspar (11%), calcite (rhombohedral CaCO_3 , 10%), vaterite (7%, a rare hexagonal polymorph of CaCO_3 , which has been described as a carbonation product of aged mortars incorporating hydraulic components – McConnell, 1960), plagioclase (2%), gypsum (2%), amphibole (tremolite, 2%) and mica (muscovite, 1%) (Fig. 2d).

4 Conclusions

The present work illustrates the first results obtained from the combined study of some painted plasters from Roman age over-paintings at the Luxor temple, Upper Egypt. The blue pigment is an artificial pigment, the so-called “Egyptian blue” (cuprorivaite, $\text{CaCuSi}_4\text{O}_{10}$), with colour transformation to greenish hues. Red colour was mainly obtained from red ochre (hematite, $\alpha\text{-Fe}_2\text{O}_3$), while yellow colour was obtained mainly from yellow ochre (goethite, $\alpha\text{-FeOOH}$). The fine plaster consists mainly of calcite with traces of gypsum, while the coarse plaster consists of quartz, calcium carbonate phases, feldspars, gypsum, tremolite and mica (muscovite). We did not clearly identify organic binders in the studied samples, and the microanalysis revealed the occurrence of Ca both in the painting and plaster layers. On the other hand, the constant presence of calcium carbonates, detected by FTIR and PXRD analyses in all the examined samples, suggests the use of fresco techniques. The presence of gypsum in the studied samples could be attributed to the use of powders of local limestone, which contains two varieties of sulphates. On the one hand, the sulphation phenomenon of calcium carbonates was probably produced due to restoration attempts. On the other hand, the optical investigation of the painting layers and the presence of gypsum in the samples allow us to infer that *secco fresco* rather than *buon fresco* was used, and that the pigments were applied on a dry plaster mainly based on calcium carbonates and containing variable amounts of gypsum. Further identification of organic binders in the samples is still under progress and will be clearer with the use of different analytical techniques. The investigation of additional samples would allow us to understand

the composition of the original materials and to identify the modern paints recently applied on the murals for retouching purposes.

Acknowledgements Mr H.M. Mahmoud especially thanks the State Scholarships Foundation (I.K.Y) of Greece for the financial support of his PhD thesis.

References

- Lee L, Quirke S (2001) Painting materials. In: Nicholson PT, Shaw I (eds) *Ancient Egyptian materials and technology*, 1st edn. Cambridge University Press, London, pp 104–120
- McConnell JDC (1960) Vaterite from Ballycraigy, Larne, Northern Ireland. *Miner Mag* 32:535–545
- Schiegl S, Weiner K, El Goresy A (1989) Discovery of copper chloride cancer in ancient Egyptian polychromic wall paintings and faience: a developing archaeological disaster. *Naturwissenschaften* 76:393–400
- Tite MS, Bimson M, Cowell MR (1984) Technological examination of Egyptian blue. In: Lambert BJ (ed) *Archaeological chemistry III*. American Chemical Society, Washington, pp 215–242
- Velosa LA, Coroado J, Veiga RM, Rocha F (2007) Characterisation of Roman mortars from Conímbriga with respect to their repair. *Mater Characterization* 58(11–12):1208–1216

Gilding Techniques in Mural Paintings: Three Examples from the Romanesque Period in France

A. Mounier, F. Daniel, and F. Bechtel

1 Introduction

Since paleo-Christian times, gold maintains a close relationship with colour within the church. However, more than just colour, gold is also matter and light. It is heat, weight and density. The use of the precious metal has an artistic, aesthetic, political and liturgical function: it is a sign, mark, and symbol of power and authority.

In Romanesque mural paintings, to the most part only traces of gildings remain today. These metallic decorations were applied on frescoes with a “dry” technique, using an organic binder. Because of their alteration in time, very often we can only see today the coloured sub-layer (“bole”), where the binders which allow the adhesion of the metal leaf over the support are located. These organic compounds are often UV fluorescent. Their examination makes possible the identification of traces of the metallic decorations (Fig. 1). That is the reason why, in our technological study of gilding techniques from Romanesque mural paintings, particular importance is given to in situ examination by UV fluorescence.

Numerous ancient treatises evoke gilding techniques. From antiquity to the eighteenth century AD, the materials and methods did not undergo significant modifications. In the present work we only consider two of the types of gilding techniques employed in mediaeval times. For the adhesion of the metallic leaf, the first method requires pigments ground in water and mixed with an organic binder (glue or Arabic gum). The second technique requires a different type of organic binder, the so-called ‘mordant’ (a fixing agent, such as linseed oil), mixed with litharge (PbO) acting as a dryer.

Not only gold, but also silver and tin have been used for the metallic decorations on mural paintings. The tin leaf could be applied as such, or covered with gold. It is plausible that gilders used tin leaves rather than silver for outdoor paintings,

A. Mounier, F. Daniel (✉), and F. Bechtel

Institut de Recherche sur les Archéomatériaux (IRAMAT), Centre de Recherche en Physique Appliquée à l'Archéologie, UMR 5060-IRAMAT, Université de Bordeaux/CNRS, 33607 Pessac Cedex, France

e-mail: fdaniel@u-bordeaux3.fr

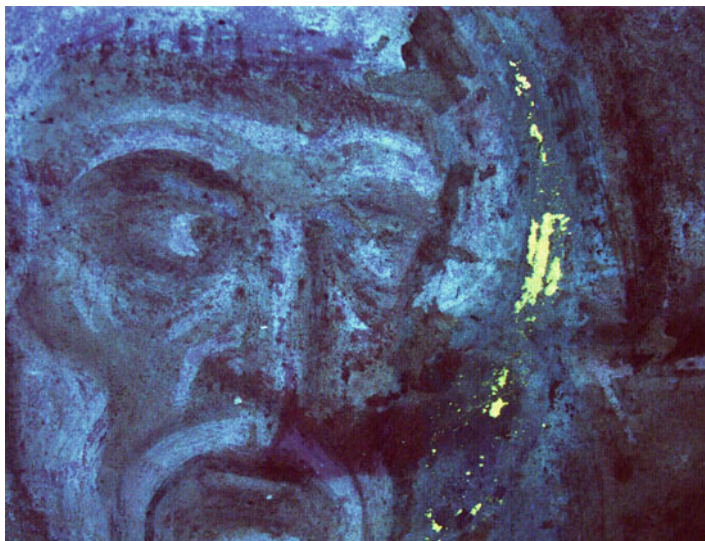


Fig. 1 UV fluorescence of a figure on the vault of the chapel in Moissac. This yellow fluorescence corresponds to the presence of a lipidic binder, such as linseed oil. Similar yellow fluorescences are observed in all tetramorphous aureoles

submitted to bad weather, knowing that the latter metal, which has a tendency to tarnish and blacken, has worse conservation properties.

Two examples of application of gold on a tin leaf have been found on paintings of the twelfth century in Angers and Poitiers (Verret and Steyert 2002). Both leaves are stuck together without any mordant. This method allowed the use of smaller amounts of gold, maintained the prestige linked to gold decoration, and conferred more relief to the gilding by the use of a thicker tin leaf. The effect of these metallic decorations was a silver plated aspect. Tin was also used to obtain a pseudo-gold colour, by the use of a tin leaf coated with a yellow varnish in order to imitate gold, a method referred to as “false gilding” in this paper. We have found analytical information on mediaeval gilding techniques in the bibliography pertaining to 25 sites (42 samples). At the same site, different techniques may have been used. Most of these gildings are composed of gold sheets or gold on tin. Only one sample of gold on silver is described, and another one of mercury gilt. Four samples, however, are made only with a silver leaf, in spite of the bad conservation properties of this metal.

UV fluorescence is observed on sites where gilding was used. Each type of gilding, depending on the metal and the organic binding employed, has a different fluorescence. Generally, a yellow (or a pale yellow) fluorescence is visible if the binder is of a lipidic type (Fig. 1). A pale blue fluorescence indicates the presence of a proteinic binder. Often, this fluorescence appears in the layer which ensures the adhesion of the metal leaf.

In this study, three examples of mural paintings located in the south of France have been chosen: in the St. Nicolas church in Nogaro (eleventh century, Gers), on the vault of the old abbey home in Moissac (twelfth century, Tarn-et-Garonne), and on the occidental portal of the Cahors cathedral (thirteenth century, Lot). A total of 12 samples have been taken from the mural paintings at the three sites.

2 Sites and Materials

The Saint Nicolas church of Nogaro was built in 1060. In the nineteenth century, the primitive architecture underwent significant modifications. The wall paintings, dated back to the end of the eleventh century, are located in the apsidal chapels. The iconographic theme represented is a “Christ in Majesty”, sitting enthroned in a *mandorla*, a book in his hand.

Chapel of the ancient abbey home in Moissac. An iconographic and stylistic study of the murals paintings of the vault of the ancient abbey home in Moissac was carried out. Due to bad microclimate conditions of conservation, only the northern part of the vault maintained its decoration. The iconographic theme (Jesse Tree) was very popular in the twelfth century.

The occidental portal of the Cahors cathedral. The edification of the Romanesque Saint Etienne cathedral is dated between 1109 and 1140. The portal shows traces of polychromy. Two painted figures on a blue background are located on the tympanum at the end of a series of blind arcades. The decorations are very lacunar and the pictorial layer is very faded. Originally, the tympanum was positioned on a straight lintel. These decorations were occulted in the seventeenth century by another architectural element, which has protected the mediaeval decoration. These masonries, still in place, have ensured the preservation of the original decoration of the Gothic lintel: red flowers, covered in places by a grey layer, painted on the thirteenth century lintel, and black fleur-de-lys on a blue background. Gilding was also discovered near the lintel.

3 Methods

Micro samples have been taken in UV fluorescent zones. Their examination was carried out with an optical microscope and with a low-vacuum scanning electron microscope (SEM-LV) JEOL JSM 6460LV, coupled to an energy dispersive X-ray spectrometer (EDXS) Oxford INCA 300. UV images have been obtained using the ARTIST multispectral imaging system (Art Innovation). For the identification of pigments, we used a Raman micro spectrometer Renishaw RM 2000. The analyses of the binders have been carried out by infra-red spectroscopy (IRTF Nicolet Nexus), in attenuated total reflectance (ATR) mode.

4 Results and Discussion

4.1 *Gildings in Saint Nicholas Church (Nogaro, France)*

Gilt was found on the murals of the north absidiole, on the mantle of the Christ and on little gold stars (probably added in the eighteenth century) strewing the blue background of the vault. The support consisted of two layers of mortars (*arriccio* and *intonaco*), a layer of red ochre, another of azurite, and then the last layer consisting of lead white (hydrocerussite) mixed with a lipidic binder. A very thin leaf of gold was applied on a thicker tin leaf. This technique is known from medieval texts (Theophilus, twelfth century; Cennini, fourteenth century). Traces of gilt were also found on the mantle of the Christ. The infrared spectra show bands attributed to drying oils. An intense band due to the absorption of carbonate stretching is attributed to white chalk.

We were also able to note here the desire of the artist to emphasize the figure of the Christ by using expensive materials. Only one gold leaf was used, and red ochre was mixed with cinnabar, identified by Raman spectroscopy. Associated with these gilds, numerous pigments (identified by Raman spectroscopy) were also employed: ochre, lapis lazuli, aerinite, azurite and cinnabar. We could observe a hierarchical organization of the blue pigments: lapis lazuli is reserved for the Christ, whereas the less expensive aerinite (Daniel et al. 2008) is employed for the tetramorphous figures.

4.2 “False Gildings” in Moissac

On the frescoes of the vault of the ancient abbey home of Moissac, “false gilding” was identified by UV imagery (Fig. 1) and confirmed by analytical methods. These metallic decorations are located on the aureoles of the “Christ in Majesty” and on one of the four symbols of the evangelists. EDS and Raman μ -spectrometry showed a superposition of layers (yellow ochre and/or red ochre; lead white; phosphorus and tin traces; gypsum, attributed to an alteration process by reaction with environmental contaminants of the calcite of the frescoes).

The interpretation of the FTIR spectra confirms the use of a lipidic binder. The use of linseed oil is the most plausible assumption, corresponding to the results obtained by FTIR and previous observations under UV light, where the aureoles had a yellow fluorescence, due to the presence of linseed oil (Fiorin and Vigato 2007).

The results obtained by the various analyses carried out are in agreement with the “false gilding” techniques known from medieval treatises (Theophilus, twelfth century; Cennini, fourteenth century). The effect of these metallic decorations was a silver plated aspect. Tin was used to imitate silver or to give a gilded aspect, using a varnish, yellow pigment or maceration in old wine. Because of this, we have chosen to refer to this technique as “false gilding”.

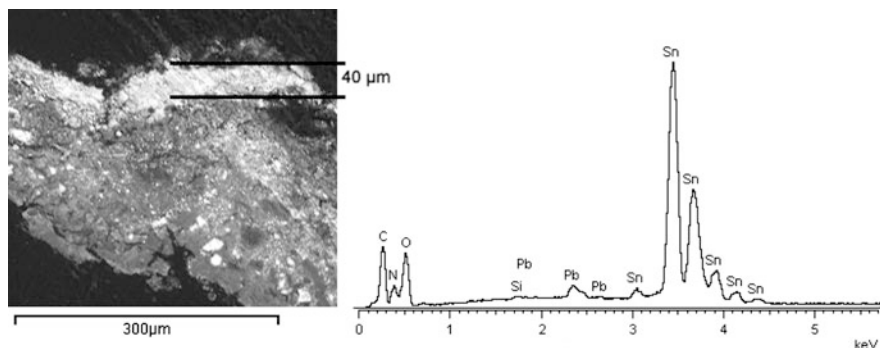


Fig. 2 Cross section of a sample taken from a fleur-de-lys on the occidental portal of the cathedral of Cahors. EDS analysis shows the presence of a tin leaf (40 μm). Other analyses show that this leaf is onto a blue layer of azurite and on a preparatory layer containing red lead and ochre

4.3 *Metallic Decorations on the Occidental Portal of the Cathedral of Cahors*

A sample was taken from a black fleur-de-lys from the lintel. SEM/EDS analysis showed that the black layer is a tin leaf (Fig. 2) applied onto a blue layer of azurite. The preparatory layer contains red lead oxide (minium) and ochre. On the painted figures, gildings are present: a gold sheet (1–2 μm) is applied on a preparation layer of yellow ochre (30 μm) and of an adhesive or resin, the entire layer resting on another preparation layer based on lead white.

“False gildings” were employed on the arch and the lintel. In the case of gilding imitations, the sheets of tin (40 μm) were certainly coloured to give them a gold aspect. Real gildings can be noted on the painted figure on the portal of the cathedral in Cahors, particularly on the aureole of a character which holds a musical instrument.

Gilded hexalobe flowers decorated the white curves. They act, in this case, as “false gildings”, obtained by certainly coloured tin leaves. On the lintel, we could observe a similar imitation of gilding by means of painted tin leaves. The flowers were applied on a preparatory layer of cinnabar (red). The fleur-de-lys is also made of tin, certainly gilded. The infrared spectra show broad bands attributed to drying oils.

5 Conclusions

In the St. Nicolas church in Nogaro, gold is present on the mantle of the Christ. In the coloured layer, on the mortar, cinnabar mixed with red ochre is used as a pigment. The gold leaf covers a preparatory layer composed of lead white, an

organic binder and yellow ochre. In Moissac, UV imagery revealed the characteristic fluorescence of a lipidic binder on the aureoles of the Christ and on one of the four evangelists. As the tin leaf was analysed, we can advance the hypothesis of a “false gilding”, in accordance with the old treatises which talk about this technique. In the case of such imitations of gilding, the tin sheets (40 μm), posed on a layer of azurite, were certainly coloured in yellow using a varnish. In the painted decoration on the occidental portal of the Saint Etienne cathedral in Cahors, similar results were obtained: on the painted figures, a gold leaf (1–2 μm) was deposited on a surface composed of yellow ochre (30 μm) and an adhesive or resin, the entire layer resting on a preparation layer containing lead white. “False gildings” were employed on the curves and the lintel. In these paintings, a fine layer of white or red lead mixed with lime or ochre is directly applied to the stone. The pigments are then applied on a white preparatory layer of lead white and calcite.

These various gildings are in agreement with the recipes described in ancient treatises. The use of gildings was associated with expensive pigments (lapis lazuli, cinnabar). Their localization, according to the iconography, is governed by their symbolic value. For example, in Moissac, lapis lazuli and tin gilding are used for the representation of the Christ; in Nogaro, gold sheet is used for the figure of Christ, also associated with lapis lazuli and cinnabar. Considering the technical aspects, the gilding was carried out according to a mixed technique, on a fresco. Thin sections of the samples show that the stratigraphy is composed of three or four layers: two of mortar, followed by one or two layers of pigments.

If a metallic decoration is believed to be present on a mural painting, UV fluorescence can be an efficient tool for clarifying such a hypothesis, because the colour of the fluorescence depends of the organic binder used and also on the technique used. This was confirmed on the samples analysed in this study, and the procedure holds significant potential for the quick identification of possible metallic decorations in Romanesque mural paintings.

Acknowledgements This study is part of a project supported by the Aquitaine region.

References

- Cennini C (1991) *Il libro dell'arte*. Berger-Levrault, Paris, pp 188–313
- Daniel F, Mounier A, Laborde B (2008) Pigment aerinite as a sign of artist circulation through Pyreneas in the mediaeval period, V Congresso Nazionale di Archeometria “Scienza e Beni Culturali”, Syracuse. 26–29 Feb 2008
- Fiorin E, Vigato PA (2007) Teodelinda's tales at Monza Cathedral: A physico-chemical diagnosis of the pictorial cycle. *J Cult Herit* 8:13–25
- Theophilus (Moine), (12th century, re-ed. Laget 1996) *Essais sur divers arts*. Cte Charles de l'Escalopier, Nogent Le Roi, pp 39–44
- Verret D, Steyert D (2002) La couleur et la Pierre. Polychromie des portails gothiques. Actes du colloque Amiens, 12–14 Oct 2000. Picard, Paris, p 299

The Basalts of the Independent State of Samoa

L.A. Pavlish, R.G.V. Hancock, and A.C. D'Andrea

1 Introduction

There is now a long history in the study of the movement of stone tools, especially those made of basalt, around Oceania (e.g. Shotton 1971; Binns and McBryde 1972; Sheppard et al. 1997). Both petrography and geochemistry have been used to sort basalts from different Pacific islands and from sources within specific island groups (e.g. Best et al. 1992). Many basaltic samples from Tutuila (American Samoa) have been analyzed. Such studies can be critical in the study of trade and socio-economic interactions in the Pacific Islands. (e.g. Best et al. 1992; Clark et al. 1997; Davidson 1977; James et al. 2007; Kaeppler 1978). This paper adds new information on the geochemical variability of basalts from the two large islands of Savai'i (latitude: 13° 34' 60 S, longitude: 172° 25' 0 W) and Upolu (latitude: 13° 55' 0 S, longitude: 171° 45' 0 W) in The Independent State of Samoa that lies just to the east of the international data line. Given the apparent absence of quarry sites in Samoa (Green 1947; Clark et al. 1997) these chemical data provide archaeologists with another avenue to pursue the sourcing tools made from basaltic rock.

2 Sample Collection

The two islands of Upolu and Savai'i in Samoa are divided into 41 geographical regions – 1–22 on Upolu and 23–41 on Savai'i (bolded numbers in Fig. 1, and bolded in Tables 1 and 2). A collection of basalt samples was conducted in 1989 by

L.A. Pavlish

Department of Physics, University of Toronto, Toronto, ON, Canada M5S 1A7

R.G.V. Hancock (✉)

Department of Medical Physics and Applied Radiation Sciences and department of Anthropology, McMaster University, Hamilton, ON, Canada L8S 4K1

e-mail: ronhancock@ca.inter.net

A.C. D'Andrea

Department of Archaeology, Simon Fraser University, Burnaby, BC, Canada V5A 1S6

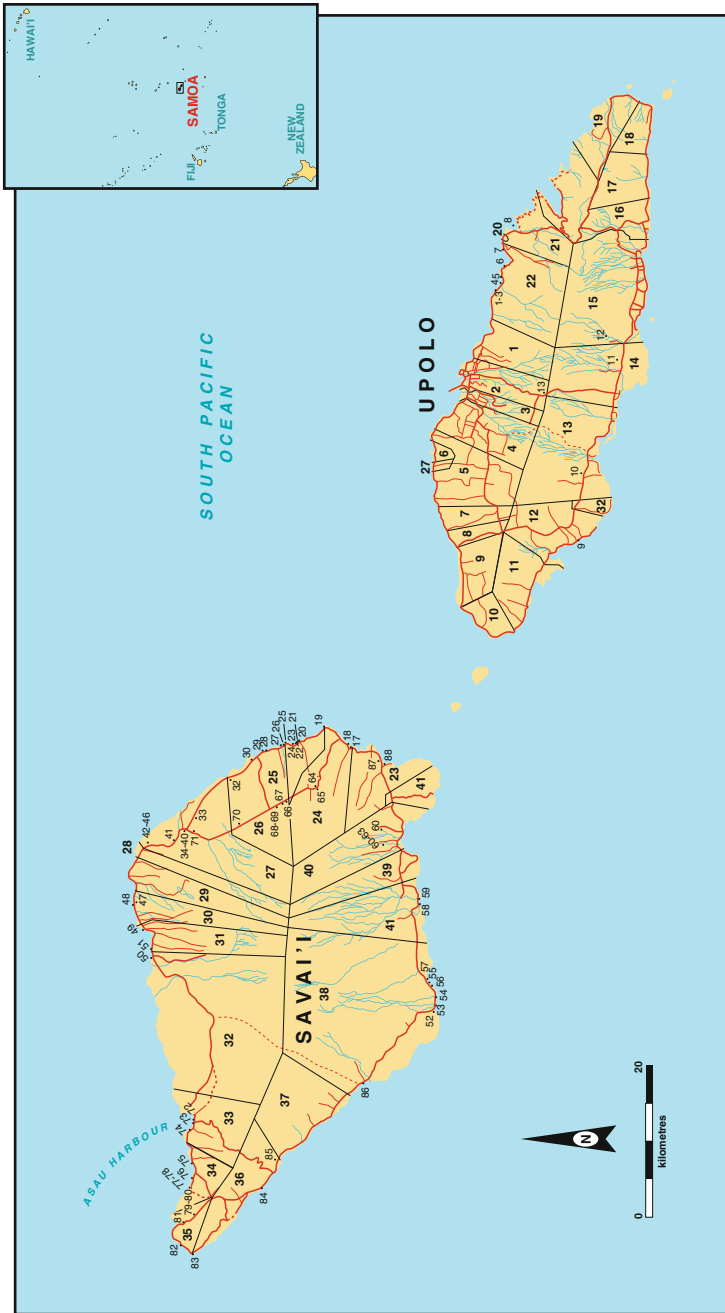


Fig. 1 The geographical regions (*in bold*) of The Independent State of Samoa and sample collection locations (*not in bold*)

Table 1 Sources of the basalt samples

Island	Region	Location	Name(s)	Number of samples
Upolu	2, 21, 22 12–15	North side	Vimauga East, Anoamaa	11
		South side	Lefaga, Safata, Siumu, Falealili	8
Savai'i	23–26 27 30, 31 33, 34 35, 36 38, 40	East	Faasaleleaga	15
		Northeast	Gagaemauga	6
		North	Gagaifomauga	19
		Northwest	Vaisigano	7
		West	Falealupo, Alataua East	7
		South	Palauli	15

L.A.P. and A.C.D. This collection resulted in the retrieval of 88 outcrop and boulder samples of basalts (19 from Upolu and 69 from Savai' – non-bolded, smaller numbers in Fig. 1) from many of the geographic regions, as may be seen in Table 1.

3 Analysis

The samples were investigated using instrumental neutron activation analysis at SLOWPOKE-Toronto, following procedures adopted for ceramic analyses. Chunks of basalt of up to 1 g were weighed into 1 mL plastic vials. Elements that produce short-lived radioisotopes, such as U, Dy, Ba, Ti, Mg, Na, V, Al, Mn, Ca, and Cl, were detected in the samples that were irradiated serially for 1 min at a neutron flux of 1.0×10^{11} n cm⁻² s⁻¹). After about 19 min, and the decay of ²⁸Al to acceptable limits, each sample was assayed using five minute counts with on-site gamma ray spectrometers. The samples were recounted for 5 min the next day for Eu, Ga, Na, and K. All samples were later batch irradiated for 16 h at a neutron flux of 2.5×10^{11} n cm⁻² s⁻¹. After 7 to 8 days, the concentrations of Sm, U, Yb, La, As, Sb, Br, Sc, Fe, and Na were determined, using 10 min countings of each sample. Sodium was used to cross-check the first and second analyses. After 2 weeks, the samples were recounted and the concentrations of Nd, Ce, Lu, Ba, Th, Cr, Hf, Sr, Cs, Ni, Th, Sc, Rb, Fe, Co, Ta, and Eu were determined using $\geq 6,000$ second counts. Again, Fe and Sc were used as cross-checks with the third phase of the analysis. Multielemental calibrations were confirmed using international rock standards. Before analyzing the data, the Mg concentrations were corrected for the (n,p) interference from Al, and the Na concentrations were corrected for NaCl, based on measurable Cl concentrations.

4 Results and Discussion

The analytical data were sorted by chemistry and location. Group means and standard deviations were calculated and are presented in Table 2, with major element concentrations in percent. The first point to note is that some groupings have few samples. The second point is that the standard deviations in each group are large relative to the means, much like those produced by coarse-ware ceramics, making simple separations impossible.

Table 2 Group means and standard deviations for the different chemical groups. Trace elements are in ppm

Region	Savai'i Island							western							Upoto Island							Eastern			
	33	34	nw	35	36	west	38	40	south	23	26	east	27	ne	30	31	nor	13	15	south	2	21	22	north	
Samples	7	7	7	7	7	7	15	15	15	15	6	6	6	19	19	8	8	8	11	11	11	11	11	11	11
Al%	6.55	0.67	7.22	0.68	6.61	0.71	6.38	0.40	6.54	0.41	6.74	0.36	6.39	0.26	6.72	1.80									
Ca%	6.20	0.53	6.21	0.78	6.19	0.66	6.71	0.49	7.28	1.33	6.62	0.56	7.28	0.46	5.11	1.84									
Fe%	9.64	0.88	9.05	0.32	9.94	0.92	10.24	0.73	9.29	0.43	9.66	0.53	11.01	0.79	11.86	1.54									
Mg%	6.4	1.0	6.2	1.3	6.9	1.5	7.6	0.9	6.7	0.6	6.6	0.8	6.2	0.9	4.5	3.1									
Na%	1.67	0.35	1.81	0.43	1.73	0.39	1.21	0.44	1.68	0.57	1.71	0.34	1.70	0.82	1.46	0.62									
Ti%	1.76	0.34	1.46	0.21	1.63	0.28	1.86	0.22	1.56	0.18	1.54	0.20	2.08	0.25	2.38	0.44									
Ba	579	151	550	219	508	142	594	164	598	137	479	156	885	228	604	194									
Co	59.9	8.3	55	6	66.1	11.7	68.8	5.5	60.2	3.3	65.2	10.5	67.8	7.3	63.3	24.1									
Cr	610	246	493	127	601	158	640	78	560	62	585	90	397	76	464	673									
Hf	5.80	0.42	5.36	1.61	5.34	1.15	5.90	0.64	4.89	0.45	4.76	1.00	6.18	0.91	7.57	2.23									
Mn	1229	100	1296	77	1302	102	1338	74	1248	95	1309	36	1412	109	1545	285									
Rb	67	21	62	23	73	28	53	36	42	32	55	31	44	29	42	37									
Sc	21.6	3.3	20.6	3.4	22.2	3.4	23.0	1.8	22.2	0.9	22.7	1.5	21.8	2.3	24.5	5.3									
Sr	543	98	532	101	473	135	525	105	744	490	479	99	754	219	389	345									
Ta	4.24	0.55	3.96	1.54	3.73	0.98	4.44	0.59	3.52	0.33	3.32	0.87	4.42	0.74	3.78	0.49									
Th	3.59	1.05	3.27	1.30	3.35	2.53	3.16	1.00	3.44	0.68	2.48	0.31	6.58	1.01	3.55	1.98									
V	273	55	235	43	275	46	296	30	258	44	268	21	285	29	331	68									
La	30.4	9.3	27.9	9.4	24.0	8.8	26.8	7.8	31.6	5.5	22.8	2.0	58.7	9.3	37.4	9.7									
Ce	61.7	15.5	57	18	50.6	16.6	58.4	14.7	66.0	12.1	47.0	5.8	109.6	14.1	86.1	23.0									
Nd	29	5	26	7	25	6	29	8	28	7	22	3	48	7	41	14									
Sm	6.88	0.98	6.24	1.40	6.07	1.18	6.76	1.07	7.10	1.06	5.68	0.50	10.36	1.55	9.93	2.58									
Eu	2.27	0.30	2.03	0.36	2.01	0.32	2.26	0.32	2.47	0.50	1.89	0.12	3.28	0.47	3.30	0.91									
Tb	0.97	0.16	0.89	0.09	0.88	0.13	0.83	0.27	0.73	0.54	0.76	0.44	1.16	0.18	1.35	0.40									
Yb	1.81	0.31	1.86	0.18	1.89	0.50	1.66	0.22	1.72	0.24	1.84	0.38	2.13	0.22	2.73	0.89									
Lu	0.24	0.03	0.24	0.02	0.21	0.03	0.23	0.07	0.24	0.03	0.24	0.04	0.31	0.04	0.38	0.14									

Eight different chemical groups were established, six from Savai'i and two from Upolo. Their group means and standard deviations were calculated and are presented in Table 2. Elements for which detection limits were regularly obtained, or that were measured with poor analytical precisions, such as As, Br, Cl, Cs, Dy, K, Ni, Sb and U, were not included in this data set. Higher average concentrations are presented in *bold* and lower average concentrations are listed in *italicized bold*.

From these data, there is a clear separation between the basalts of Savai'i and Upolo. The basalts of Upolo contain, on average, more Fe, Ti, Mn, and REEs, and less Cr and Rb, than do the basalts of Savai'i.

Within Upolo, the basalts from the north are separable from the basalts from the south based on their Mg, Ba, Sr, and Th contents.

The Savai'i basalt picture is more complex, with six chemical sub-groupings. Here the divisions appear to be west, northwest, north, northeast, east, and south (see Table 1). Basalts from the northwest (regions 33 and 34) appear to have average concentrations with no extreme highs or lows relative to the other samples. The western basalts (regions 35 and 36) are higher in Al, and lower in V and Ti. The southern basalts (regions 38 and 40) are similar to the northwestern basalts in that they have no characteristic highs and lows, but they do exhibit average concentrations that are often slightly lower than those in the western basalts (e.g. Sr, Ta, and light REEs) and are a little higher in their average Co, Mn, and Rb contents. The eastern basalts (regions 23–26) give the highest Mg and V contents on Savai'i and the lowest Na contents. The northeastern basalts (region 27) tend to be high in Sr and low in Eu, Ta and Hf. The northern basalts (regions 30 and 31) are the most distinct of all of the Savai'i basalts. In relative terms, they are low in Ba, Hf, Ta, Th, La, Ce, Nd, Sm, Eu, and Tb.

5 Rare Earth Element Concentration Interpretations

Stimmel et al. (1984) studying sediments at the Yagi site in southeastern Hokkaido in Japan, found that older sediments displayed lower chondrite-normalized rare earth element (REE) patterns, while ever younger sediments had sequentially greater REE contents, especially in the LREEs (light rare earth elements). If this chronological REE fractionation scheme is applied to the islands of Savai'i and Upolo, it would appear from the REE concentrations presented in Table 1 that the basalts of Savai'i are formed from older magmas than those that formed Upolo. We would also interpret the northern basalts as coming from the oldest magma associated with Savai'i. This proposal is supported by the finding by Koppers et al. (2008) that the volcanic construction of Savai'i began as early as 5.0 Ma ago.

The basalts of Upolo follow the REE concentration progression found by Stimell et al. (1984). Stearns (1944) found older Pliocene formations in the northeast and younger Quaternary basalts in the south and we present 11 samples from Regions 2, 21, and 22 in the northeast that have lower REE concentrations than do the eight samples from Regions 13–15 in the south.

The REEs of Savai'i do not follow this pattern. The 19 samples that were collected from Regions 30 and 31 in northern Savai'i contain the lowest REE contents of all samples analyzed from The Independent State of Samoa, while the other basalts of Savai'i display REE contents that are lower than their basaltic relatives on Upolo.

6 Conclusions

It appears to be possible by elemental analyses to source archaeological basaltic tools found in Samoa and other islands in Oceania, not just to The Independent State of Samoa but to specific regions of each of the two major islands of Savai'i and Upolo.

Acknowledgements We are grateful to Shannon Wood (Simon Fraser University) for completing the maps, and to Katharine Hancock for designing the poster.

References

- Best S, Sheppard P, Green RC, Parker R (1992) Necromancing the stone: archaeologists and adzes in Samoa. *J Polynesian Soc* 101:45–85
- Binns RA, McBryde I (1972) A petrological analysis of ground-edged artefacts from northern New South Wales. *Australian aboriginal studies* 47; Australian Institute for Aboriginal Studies, Canberra
- Clark J, Wright E, Herdrich DJ (1997) Interactions within and beyond the Samoan archipelago: evidence from basaltic rock geochemistry, In: Weisler MI (ed) *Prehistoric long-distance interaction in Oceania: an interdisciplinary approach*. New Zealand Archaeological Association, Monograph 21, pp 68–84
- Davidson JM (1977) Western Polynesia and Fiji: prehistoric contact, diffusion and differentiation in adjacent archipelagos. *World Archaeol* 9:82–94
- Green R (1947) Excavations of the prehistoric occupations of SU-Sa-3. In: Green RC, Davidson JM (eds) *Archaeology in Western Samoa*, vol 1, Auckland Institute and Museum Bulletin 7., pp 108–154
- James WD, Raulerson MR, Johnson PR (2007) *Archaeometry at Texas A & M University*. *Archaeometry* 49(2):395–402
- Kaeppler AL (1978) Exchange patterns in goods and spouses: Fiji. *Tonga and Samoa*, *Mankind* 11: 246–252
- Koppers AAJ, Russell JA, Jackson MG, Konter J, Staudigel H, Hart SR (2008) Samoa reinstated as a primary hotspot trail. *Geology* 36(6):435–438
- Sheppard PJ, Walter R, Parker RJ (1997) Basaltic sourcing and the development of Cook Island exchange systems. In: Weisler MI (ed) *Prehistoric long-distance interaction in Oceania: an interdisciplinary approach*. New Zealand Archaeological Association, Monograph 21, pp 85–110
- Shotton FW (1971) Petrological enamination. In: Brothwell D, Higgs E (eds) *Science and archaeology*. Thames and Hudson, London, pp 571–577
- Sterns HT (1944) Geology of the Samoan Islands. *Geol Soc Am Bull* 55:1279–1332
- Stimmell CA, Hancock RGV, Davis AM (1984) Chemical analysis of archaeological soils from Yagi site, Japan. In: Lambert JB (ed) *Archaeological chemistry III*, *Advances in chemistry series* 205. American Chemical Society, Washington, DC, pp 79–96

Petrographic and Geochemical Investigation of Sarmatian Grinding Stones from the Üllő 5 Site, North Hungary

B. Péterdi, G. Szakmány, K. Judik, G. Dobosi, Z. Kasztovszky, and V. Szilágyi

1 Aim of the Study

The present study reports some preliminary results of petrographic and geochemical analyses carried out on Sarmatian age grinding stones from the archaeological site Üllő 5 (Pest County, Hungary). The purpose of the study was to define the provenance of raw materials through a petrographic and geochemical description of the finds.

2 Archaeological Background

Between 2001 and 2005, archaeological rescue excavations were carried out at a location situated on the planned route of the M0 motorway. Üllő 5 is the largest Sarmatian site excavated to date: 8,794 objects were found in an area of 380,000 m². The findings (ceramics and coins, mainly of Roman import) ascribe the settlement to the third to fourth century AD. A total of 3,800 finds (all made of stone) were macroscopically surveyed, among them the 888 grinding stones, fragments of grinding stones and grinders reported in the present paper.

B. Péterdi (✉)

Geological Institute of Hungary, Geological Museum of Hungary, Stefánia u. 14, 1143 Budapest, Hungary

e-mail: peterdi@mafi.hu

G. Szakmány

Department of Petrology and Geochemistry, Eötvös Loránd University (ELTE), Budapest, Hungary

K. Judik and G. Dobosi

Hungarian Academy of Sciences, Institute of Geochemical Research, Budapest, Hungary

Z. Kasztovszky, and V. Szilágyi

Hungarian Academy of Sciences, Institute of Isotopes, Budapest, Hungary

3 Methods

All the finds were surveyed macroscopically; they were grouped, and characteristic samples were investigated further in thin section by polarisation microscopy. Additional chemical analyses have been carried out. Bulk chemical analyses of five samples (made of andesite and acidic volcanic tuff) were performed with ICP-ES and ICP-MS. The same five samples were analysed with Electron Probe Micro Analysis (EPMA). Bulk chemical analyses of three samples (from the former five ones) were performed with Prompt Gamma Activation Analysis (PGAA).

In order to obtain more information about the provenance of the archaeological finds, we collected and studied andesite samples from natural outcrops of the neighbouring volcanic mountains (Börzsöny, Cserhát, Mátra and Karancs Mountains) (Fig. 1). The resulting data were compared with data of analyses found in the literature consulted.

4 Raw Materials in General

Most of the investigated finds are made of almost fresh or weakly altered andesite, and two major groups can be distinguished among them. In the studied set, strongly

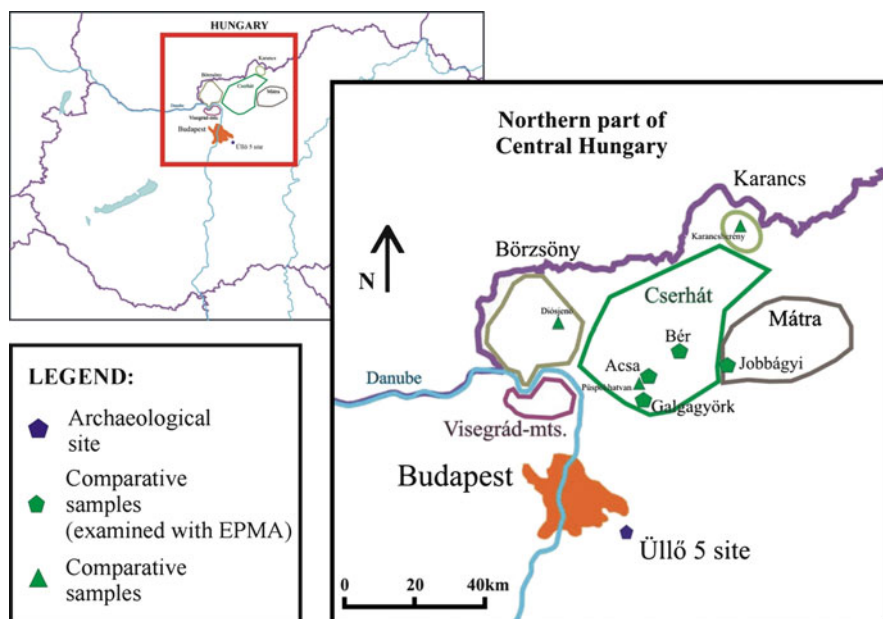


Fig. 1 Map of the northern part of Central Hungary with the archaeological site and the sampling localities of the comparative (geological) samples

altered (silicified) andesites, andesitic tuffs, acidic volcanites and pyroclasts can also be found (116 pieces, i.e. 13% of the total). The limited space available for this paper does not permit us to dwell on the results we obtained on these other raw materials.

5 Group 1 Andesites (462 Pieces, i.e. 52% of the Total)

Macroscopically, these samples appear as dark grey or black very fine-grained andesites without or with only a very small amount of phenocrysts – large plagioclases (3–5 mm average size). Most of them contain many amygdales and/or vesicles (with an average size smaller than 2 cm; examples with larger size (3–6 cm) are also frequent). Due to weathering, they show dark brown, brown, or dark red colour.

6 Group 2 Andesites (310 Pieces, i.e. 35% of the Total)

Macroscopically, these samples appear as grey, dark grey, or black coarse-grained andesites, with large phenocrysts – plagioclases (1–3 mm average size) and pyroxenes (1–4 mm average size), without discernible amygdales or vesicles. Due to weathering, they show dark red, red, or purplish-grey colour.

6.1 Microscopic Features

The microscopic features of the two andesite types are almost the same. They are andesites with porphyritic, pilotaxitic, trachytic texture and with amygdales and vesicles (in the second group only small microscopic amygdales).

6.1.1 Phenocrysts

- Idiomorphic-hypidiomorphic, millimetre-sized plagioclase crystals with tabular or lath-shaped habit and with a number of inclusions. Polysynthetic twinning and zoning (and, for the samples of Group 2, intergrowth) often occur.
- Hypidiomorphic, thick-set columnar, some-hundred micrometer-sized pyroxene crystals (ortho- and clinopyroxenes). The pyroxenes of Group 2 are larger, and some of them contain inclusions. In Group 2, zoning, overgrowth and twinning (also polysynthetic twinning of the clinopyroxenes) occur.

In Group 1, the quantity of pyroxenes is smaller than the quantity of plagioclases. There is a larger quantity of phenocrysts in Group 2 than in Group 1. Plagioclase, pyroxene and plagioclase–pyroxene glomeroporphyritic clusters also occur.

In the groundmass, plagioclase, pyroxene and opaque minerals (titanomagnetites) occur and the quantity of glass is less than 10%; the glass is dark, brown and shows a uniform distribution and iso-oriented arrangement.

The amygdales and vesicles in the section are millimetre-sized (or smaller). In Group 1, on the edges of the amygdales/vesicles, a reddish limonite–hematite coating is visible. In some places, a glassy groundmass with opaque minerals occurs in this reddish coating (without plagioclase and pyroxene). Amygdales in Group 2 are smaller than those in Group 1, and some of them are filled with secondary carbonates.

7 Comparative Samples

We collected andesite samples from outcrops of the neighbouring volcanic mountains. Macroscopically, they are all similar to the raw material of the grinding stones. Among them, four samples appear to be most similar to the aforementioned raw material under microscopic examination (sample AV-25, from Acsa; sample AV-28, from Jobbágyi; sample AV-39, from Bér; sample G-1, from Galgagyörk) (Fig. 1).

7.1 Microscopic Features

Texture: porphyritic, hyalopilitic texture (AV-25, AV-28), porphyritic, pilotaxitic texture (AV-39, G-1), with amygdales and vesicles (AV-25, AV-28, G-1).

7.1.1 Phenocrysts

- Idiomorphic-hypidiomorphic, millimetre-sized plagioclase crystals with tabular or lath-shaped habit and with a number of inclusions. Polysynthetic twinning and zoning often occur. Their size can reach 5 mm (AV-25, AV-28, AV-39).
- Hypidiomorphic, thick-set columnar pyroxene crystals (ortho- and clinopyroxenes). They are some-hundred micrometer-sized in samples AV-25, AV-39 and G-1, and millimetre-sized in sample AV-28. Twinning and zoning also occur. In sample G-1, the clinopyroxenes show also polysynthetic twinning. In sample AV-39, only a few pyroxene phenocrysts exist and twinning does not occur. In sample G-1, on the edges of some pyroxene-phenocrysts, 10–100 μm -sized

diverse composite pyroxene crystals occur. In sample AV-25, clinopyroxene overgrowth occur on some orthopyroxene phenocryst.

Plagioclase, pyroxene and plagioclase-pyroxene glomeroporphyritic clusters also occur in all samples.

In the groundmass: plagioclase, pyroxene and opaque minerals (titanomagnetites) occur, and the quantity of glass is 10–20% (AV-25, AV-28), 10% (AV-39), or less than 10% (G-1); the glass is dark, brown (AV-25, AV-28, G-1) or reddish-brown (AV-39), and shows uniform distribution.

In samples AV-39 and G-1, some hundred micrometer-sized (in the groundmass, 10–100 μm -sized) limonite-hematite aggregates can be seen. Their shape shows that these aggregates are pseudomorphs after olivine.

The amygdales and vesicles in samples AV-25, AV-28 and G-1 are millimetre-sized (or smaller). In samples AV-25 and G-1, on the edges of the amygdales/vesicles, a reddish limonite–hematite coating occurs. In sample AV-28, on the edges of the amygdales/vesicles, a brownish green or reddish limonite-hematite coating occurs, and some of them are filled with glassy material.

8 Electron Probe Microanalyses (EPMA)

In addition to the examination of the grinding stones, we had the opportunity to use EPMA for the study of the four comparative samples. Our primary interest was to investigate the composition of plagioclase feldspars and of pyroxenes that are visible in the form of phenocrysts and glomeroporphyritic clusters, and also of plagioclase feldspars, pyroxenes, opaque minerals and glass in the groundmass. The composition of independent phenocrysts and the composition of phenocrysts that are found in glomeroporphyritic clusters are not significantly different. The composition of plagioclases and of pyroxenes that appear in the groundmass differs from that of the phenocrysts. This may well be explained by the earlier concretion of the phenocrysts.

The composition of the plagioclase phenocrysts is labradoritic–bytownitic in samples of Group 1, Group 2, AV-39 and G-1, labradoritic in sample AV-25, and bytownitic in sample AV-28 (Table 1).

The composition of the plagioclase crystals in the groundmass is more acidic: labradoritic in samples of Group 1, Group 2, AV-28, AV-39 and G-1; andesitic–labradoritic in sample AV-25 (Table 1).

Ortho- and clinopyroxene phenocrysts show compositional zoning (except sample AV-28). Most pyroxene phenocrysts have a rim (corona) of small clinopyroxene-crystals compositionally similar to the clinopyroxenes in the groundmass. These small clinopyroxenes are richer in Ca than the orthopyroxene phenocrysts, but poorer than the clinopyroxene phenocrysts (Table 1).

On the basis of the Fe quantity of the zones, there are two types of pyroxene phenocrysts. In the first type, the amount of Fe is decreasing from the core to the

Table 1 Selected results of the EPMA-measurements

Sample	Plagioclase phenocrysts				Plagioclases in the groundmass			
	Anorthite%		Albite%		Anorthite%		Albite%	
	Core	Outer zone	Rim	Orthoclase%	Core	Outer zone	Rim	Orthoclase%
Group 1	63–84	15–35	0–2	56–75	24–39	1–3		
Group 2	60–85	15–37	0–2	57–60	38–40	3–4		
AV-25	58–71	27–39	2–4	40–71	28–53	2–8		
AV-28	73–84	16–26	0–1	54–60	38–44	2		
AV-39	60–83	17–38	0–1	55–60	38–42	2–3		
G-1	65–80	20–33	1–3	54–70	29–42	1–8		
Sample	Orthopyroxene phenocrysts				Clinopyroxene phenocrysts			
	Core	Outer zone	Rim	Core	Outer zone	Rim	Core	Outer zone
Gr.1: FeO%	18.5–19.2	17.6–18.3	–	11.0–11.6	10.5–10.8	10.3	11.0–11.6	10.5–10.8
Gr.1: CaO%	1.8–2.0	1.8–2.1	–	18.7–18.8	19.1–19.5	15.6	18.7–18.8	19.1–19.5
Gr.2/1: FeO%	23.5–24.4	7.3	–	–	–	–	–	–
Gr.2/1: CaO%	1.7–1.8	17.6	–	–	–	–	–	–
Gr.2/2: FeO%	22.1–24.9	14.5–19.0	22.0–25.0	4.7–5.2	–	10.8	20.7–21.0	–
Gr.2/2: CaO%	0.8–1.9	1.9–2.0	1.9–6.7	9.2–11.2	–	19.2	9.2–11.2	–
AV-25: FeO%	13.6–18.2	13.9–15.4	20.1	16.4–17.4	8.1–9.1	10.7–12.1	16.4–17.4	17.4–19.0
AV-25: CaO%	2.1–2.4	2.2–2.4	2.1	10.7–11.1	–	17.0–17.9	10.7–11.1	–
AV-28: FeO%	16.9–18.1	–	–	17.9–18.7	–	–	17.9–18.7	–
AV-28: CaO%	1.8–1.9	–	–	–	–	–	–	–
AV-39: FeO%	21.7–22.6	16.2–16.4	20.0–20.3	–	–	–	–	–
AV-39: CaO%	1.8	2.2	2.2–2.3	–	–	–	–	–
G-1: FeO%	14.4–16.2	–	–	10.8–11.0	7.4–8.9	8.7–9.1	10.8–11.0	7.4–8.9
G-1: CaO%	2.3–2.5	–	–	16.7–16.9	18.1–19.6	17.4–18.6	16.7–16.9	18.1–19.6

Ground-mass + corona

outer zones. In the second type, the Fe quantity is also decreasing from the core to the outer zones, and there is a rim with a higher amount of Fe than that of the outer zone (Table 1). In Group 1, only the first type of pyroxene phenocrysts can be found, while both types are present in Group 2. In the comparative samples AV-25, AV-39 and G-1, the second type of phenocrysts can be found. In sample AV-28, the pyroxene phenocrysts do not show compositional zoning. Most of the opaque minerals are titanomagnetites in every sample.

On the basis of the composition of the plagioclase and zoned pyroxene crystals, the raw material of the grinding stones appears most similar to the one of samples AV-39 (Bér, Cserhát Mountains) and G-1 (Galgagyörk, Cserhát Mountains) and is also close to the one of sample AV-25 (Acsa, Cserhát Mountains).

9 Bulk Chemistry (ICP-ES, ICP-MS and PGAA) and Discussion

The results of the analyses (major elements) performed with ICP-ES and PGAA show no significant difference. Analyses carried out with PGAA (a non-destructive method) can therefore be performed more extensively in future examinations.

The results of the ICP-ES-analyses were plotted on a TAS (total alkali silica) diagram including the grinding stones and comparative samples we collected and data from the existing literature concerning the Börzsöny, Visegrád and Cserhát Mountains (Korpás 1998; Póka et al. 2004; Karátson et al. 2000, 2007) (Fig. 2).

From this diagram, it appears clear that basaltic andesite also occurs among the volcanic rocks of the Börzsöny and the Visegrád Mountains, but that samples originating from these locations may also show some amphibole (Karátson 2007),

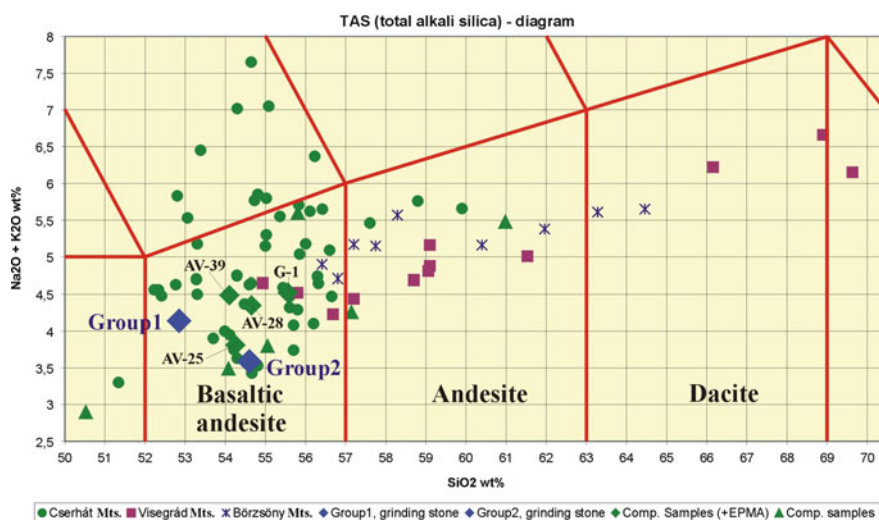


Fig. 2 TAS (Total Alkali-Silica)-diagram

contrary to the grinding stones and the samples we collected from the Cserhát Mountains. Nevertheless, further examinations are necessary to exclude them from the category of possible source rocks.

10 Conclusion

The present study reports preliminary results of petrographic and geochemical analyses on Sarmatian age (third to fourth century AD) grinding stones from the archaeological site Üllő 5 (Pest County, Hungary). A total of 888 grinding stones and fragments of grinding stones were macroscopically surveyed; two main groups were established among them, and characteristic samples were investigated further in thin section by polarisation microscopy.

Most of the investigated grinding stones are made of andesite. Among them, two major macroscopic groups could be established. The microscopic features of the two andesite types are almost the same. Subsequently, additional chemical analyses have been performed (ICP-ES, ICP-MS, PGAA and EPMA) on selected samples.

On the basis of the analyses of the archaeological finds and the comparative samples we collected (i.e. macroscopic, microscopic and chemical examinations), we can put forth the hypothesis that the basaltic andesite raw materials originated from the Cserhát Mountains. Further investigations are needed for excluding with certainty a provenance of the basaltic andesites in the Visegrád and the Mátra Mountains.

Acknowledgements The authors wish to thank the archaeologists who worked at the Üllő 5 site: Edit Tari, Valéria Kulcsár, Róbert Patay and Dóra Mérai; and also express their gratitude for the financial help of the Hungarian Scientific Research Fund, OTKA Grant No. K 62874.

References

- Karátson D (2007) A Börzsönytől a Hargitáig. Vulkanológia, felszínfejlődés, ősföldrajz. Typotex, Budapest
- Karátson D, Márton E, Sz H, Józsa S, Balogh K, Pécskay Z, Kovácsvölgyi S, Gy S, Dulai A (2000) Volcanic evolution and stratigraphy of the miocene Börzsöny mountains, Hungary: an integrated study. *Geologica Carpathica* 51:325–343
- Karátson D, Oláh I, Pécskay Z, Márton E, Sz H, Dulai A, Zelenka T, Sz K (2007) Miocene volcanism in the Visegrád Mountains (Hungary): an integrated approach to regional volcanic stratigraphy. *Geologica Carpathica* 58:541–563
- Korpás L (ed)(1998) Magyarázó a Börzsöny és a Visegrádi-hegység földtani térképéhez 1:50000. Geological Institute of Hungary, Budapest
- Póka T, Zelenka T, Seghedi I, Pécskay Z, Márton E (2004) Miocene volcanism of the Cserhát Mts (N Hungary): integrated volcano-tectonic, geochronologic and petrochemical study. *Acta Geol Hung* 47:221–246

Brick-Lime Mortars and Plasters of a Sixteenth Century Ottoman Bath from Budapest, Hungary

F. Pintér, J. Weber, B. Bajnóczi, and M. Tóth

I have explained how plastering is executed in dry situations; now I shall give directions for it, that it may be durable in those that are damp. [. . .] The wall is then to be plastered with the potsherd mortar, made smooth, and then polished with the last coat.

Vitruvius (Ten books on architecture)

1 Introduction

There are two ways to obtain mortar and plaster binders that can harden under water. Both procedures lead to similar products, i.e. compounds of Ca with Si, Al and Fe, capable of binding water molecules in their solid structure.

1.1 The Pozzolanic Principle

The admixture of reactive siliceous compounds such as volcanic tuff or crushed bricks, the so-called “pozzolanas”, to slaked lime produces hydrate compounds.

F. Pintér (✉)

Scientific Laboratory – Federal Bureau for Monument Protection, Arsenal Objekt 15, Tor 4, 1030 Vienna, Austria

e-mail: farkas.pinter@bda.at

J. Weber

Institute of Art and Technology – Conservation Sciences, University of Applied Arts Vienna, Salzgries 14/1, 1010 Vienna, Austria

B. Bajnóczi and M. Tóth

Hungarian Academy of Sciences, Institute for Geochemical Research, Budaörsi út 45, 1112 Budapest, Hungary

Such mortars can not only be set under water, but are also water-resistant and develop higher mechanical strength than air-hardened lime mortars. The ancient Greeks and especially the Romans developed this technique to a high level, which enabled them to construct aqueducts, bridges and bath buildings, and even to cast large elements in a manner similar to the modern concrete technology. The use of crushed or finely ground bricks, called *Horasan* in present day Turkey, or *cocciopesto* in the Roman Empire, continued in Byzantine times, and survived during the Ottoman Empire in the construction of several buildings, among which thermal baths.

1.2 The Hydraulic Principle

At the end of the eighteenth century, a major change occurred in producing binders with hydraulic properties. The calcination of limestone contaminated with clay (natural hydraulic lime), or of marlstones (natural cements), produces Ca-silicate and Ca-aluminate phases that can react with water, producing mortars with increased mechanical strength and durability. From the second half of the nineteenth century onward, the development of this technology made possible the production of modern Portland cements burned at high temperatures.

When impure limestone or marlstone containing silica and clay are burned at temperatures between 800 and 900°C, the clay decomposes and reacts with the lime, forming calcium silicates and aluminates. The maximum burning temperatures for natural hydraulic limes and Roman cement is 1,250°C. Modern Portland cement is produced from mixtures of limestone and clay burned in the range of 1,400°C, a temperature at which sintering occurs and a clinker is formed.

Between 1526 and 1686, part of the Hungarian Kingdom was occupied by the Ottoman Empire. During this period, several buildings, among which thermal baths, were constructed. One of the largest Ottoman baths in Budapest, the Császár (Emperor) Bath (Fig. 1a) was built in 1574 by Sokollu Mustafa and rebuilt several times during the last centuries. In recent years, a modern renovation of the structure has begun, including aspects of art historical research aimed at reconstructing the original Ottoman colouring of the interior of the building. The archaeometric study of plasters and mortars represents part of this interdisciplinary cooperation. Ottoman brick-lime plasters and mortars of different colours (white, pink, and red) were identified in the interior of the Bath (Fig. 1b). The determination of their physical, mineralogical and microstructural characteristics and the assessment of their pozzolanic and hydraulic properties are essential for understanding the motives for using brick-lime mixtures as plasters and mortars in this building. In this study we present some preliminary results of material characterization carried out by polarizing and scanning electron microscopy, as well as X-ray diffractometry (XRD).

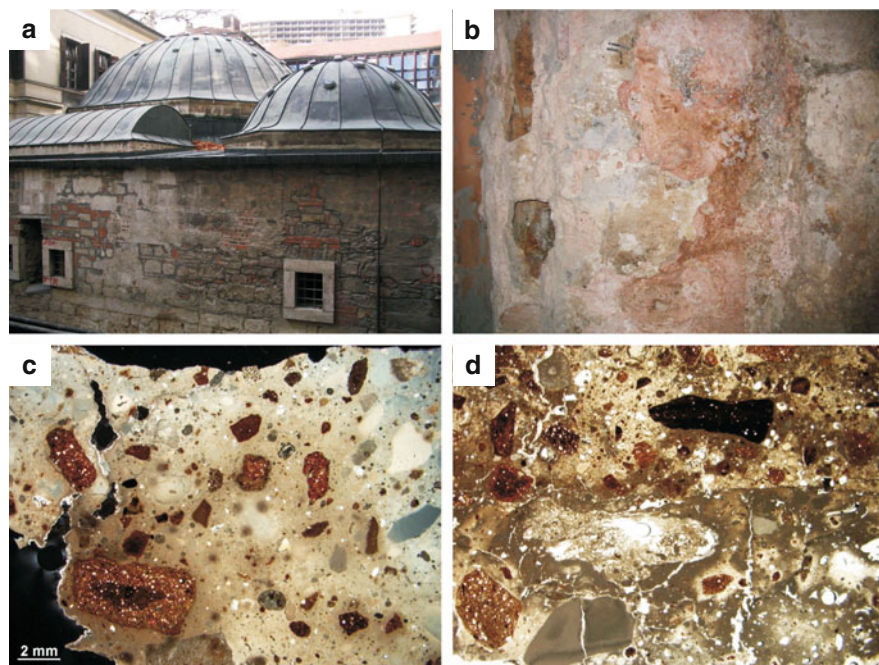


Fig. 1 (a) The Császár Bath in Budapest, Hungary. (b) Ottoman brick-lime plaster fragments in the Császár Bath. (c) Microscopic image of white brick-lime mortar (+N). (d) Microscopic image of pink (*bottom*) and red (*upper part*) brick-lime plaster (1N, width of image: 8 mm)

2 Results

2.1 Polarizing Microscopy

Microscopic analyses showed that in all three colour types the binder seems to be microcrystalline calcite; however, with an atypical low birefringence, cloudy structures, and dense texture around the brick fragments (Fig. 1c, d). The amount of inert aggregates, i.e. sand, is very low; only some small quantities of quartz and feldspar clasts were observed. Very fine-grained brick dust, together with larger brick fragments up to 3–4 mm in diameter, represents the pozzolanic additive in the samples. The admixed brick fragments are red to reddish brown in colour, with identifiable mica, quartz, and feldspar grains. Some larger brick fragments exhibit darker or lighter reaction rims (Fig. 1c, d). Partly zoned, fine-grained, binder-related particles, the so-called “lime lumps” (Hughes et al. 2001), with irregularly low birefringence were also observed in all samples. The reddish type plasters are cracked perpendicularly to the surface, and cracks and pores are often filled with secondary sparitic calcite (Fig. 1c, d).

2.2 X-Ray Diffractometry

Calcite, quartz, K-feldspar, plagioclase and phyllosilicates (sericite–illite, chlorite, sometimes kaolinite) are the main phases of the plaster and mortar samples. Hematite was mainly identified in pink and red material. Some samples contained additional components, such as diopside, gypsum, aragonite and vaterite. After dissolving the carbonate content of the samples with dilute hydrochloric acid, the relative amount of silicates has increased, and the presence of an amorphous phase can be assumed due to the elevated baseline of the XRD profile, between 15° and $30^\circ 2\theta$.

2.3 Scanning Electron Microscopy

The average chemical composition of the “limy” matrix (Fig. 2a) measured by SEM–EDX is ca. 70–80% CaO and 20–30% SiO₂. Most of the brick pebbles exhibited Ca-enrichment in their outer zones. Around them, at the brick–lime interface, compact zones of up to 0.1 mm thickness were observed, predominantly

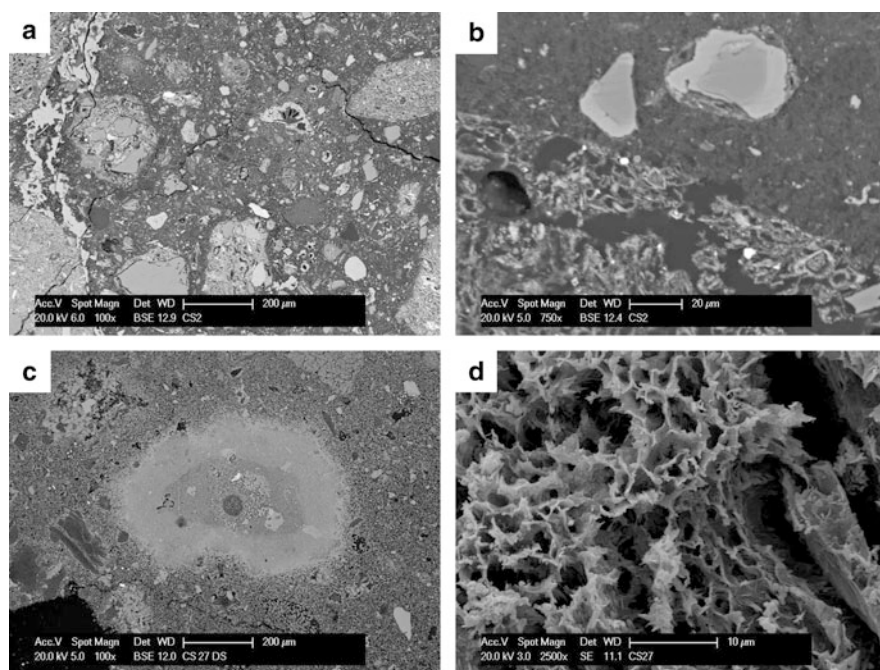


Fig. 2 SEM–BSE images of a red plaster. (a) Brick fragments and Si-rich matrix. (b) Quartz grains with clear Ca diffusion rims. (c) “Lime lump” with Si-rich core. (d) Ca- and Si-rich card-house structure of the matrix

composed of Ca with a slight amount of Si and Al. Monocrystalline quartz and feldspar grains with typical Ca diffusion margins were also detected in the matrix (Fig. 2b). Several “lime lumps” showed a typical zoned appearance: their outer rim was rich in Ca, while their inner zones were rich in Si (Fig. 2c).

The SEM-SE observations carried out on broken surface samples showed that the microstructure of the matrix consists of 1–5 μm long needles and plates; sometimes, a so-called “card-house network” of probably amorphous calcium-silicate-hydrate (CSH) phases could be observed (Fig. 2d).

3 Discussion and Conclusions

Based on the macroscopic and microscopic observations, the white and pinkish-reddish plaster and mortar samples from the Ottoman Császár Bath in Budapest seem to be brick-lime mixtures commonly used during Ottoman times for several water-resistant building constructions (Baronia et al. 1997; Böke et al. 2006). Especially in the pinkish-reddish samples, high amounts of brick fragments and dust can be found as pozzolanic additives. The Ca (i.e. calcium-carbonate) enrichment of the matrix in the immediate surrounding of brick pebbles found in several cases does not, however, clearly refer to the presence of abundant calcium-silicate-hydrate (CSH) phases at the brick-matrix interfaces, which are typical for brick-lime mortars (Baronia et al. 1997; Böke et al. 2006; Moropoulou et al. 2002, etc.).

However, the microscopic appearance of the “micritic” groundmass suggests that the binder was probably not composed exclusively of pure CaCO_3 . This optical microscopic observation is supported by scanning electron microscopy analyses showing relatively high (20–30%) and generally homogeneously distributed Si content in the CaCO_3 matrix, which may suggest a relatively good hydraulicity of the materials. The large amount of amorphous material detected by XRD can be derived from the brick aggregates (Böke et al. 2006), but may also refer to the presence of amorphous CSH phases in the matrix. The latter hypothesis can also be supported by the card-house and irregular needle-like structure of the binding material; these structures seem to be unusual for brick-lime plasters and mortars, but were found in nineteenth century natural (Roman) cements (Weber 2007).

Quartz and K-feldspar grains with a Ca-rich rim show inward diffusion of calcium; this phenomenon was also identified in natural cements (Weber et al. 2007), and may refer to the presence of silicate impurities that react with the calcite in the raw material during the lime burning process. The presence of zoned “lime lumps” that contain a certain amount of Si (plus minor quantities of Al and Mg) in their cores also suggests a lime with hydraulic properties, most probably originating from the calcination of impure limestone (Elsen et al. 2004; Zamba et al. 2007).

Preliminary results suggest that the Ottoman mortars and plasters of the Császár Bath may have received their good hydraulic properties not only due to the partly pozzolanic brick additives, but additionally through the formation of new phases with hydraulic properties during the firing of the impure carbonate raw material.

Such potential raw materials (i.e. clayey limestones and marlstones) are widespread on the Buda Hills in the vicinity of the Császár Bath (Wein 1977). Similar brick-lime mortars made from marly limestones or limestone–clay mixtures were found by Moropoulou et al. (2002) in Hagia Sophia (Istanbul).

The precipitation of secondary coarse calcite in cracks and voids, as well as the presence of aragonite in the mortars and plasters, can be explained by the flow of thermal water containing a high amount of dissolved carbonates (Leél-Óssy 1995). Further studies are planned, with the purpose of delineating the effects of thermal waters on the brick-lime materials of the Bath.

Acknowledgements The authors would like to express their gratitude to Judit G. Lászay (Field Service for Cultural Heritage, Budapest), Adrienn Papp (Budapest History Museum), and Gizella T. Makoldi for the samples and for discussions about the historical background of the Bath.

References

- Baronia G, Binda L, Lombardini N (1997) The role of brick pebbles and dust in conglomerates based on hydrated lime and crushed bricks. *Construct Build Mater* 11:33–40
- Böke H, Akkurt S, İpekoğlu B, Uğurlu E (2006) Characteristics of brick used as aggregate in historic brick-lime mortars and plasters. *Cem Concr Res* 36:1115–1122
- Elsen J, Brutsaert A, Deckers M, Brulet R (2004) Microscopical study of ancient mortars from Tournai (Belgium). *Mater Charact* 53:289–294
- Hughes JJ, Leslie A, Callebaut K (2001) The petrography of lime inclusions in historic lime based mortars. *Proceedings of the 8th Euroseminar on microscopy applied to building materials. Athens*, pp 359–364
- Leél-Óssy SZ (1995) A budai Rózsadomb és környékének különleges barlangjai (Special caves of Rózsadomb on Buda and its environment). *Földt Közl (Bull Hung Geol Soc)* 125:363–432
- Moropoulou A, Cakmak AS, Biscontin G, Bakolas A, Zendri E (2002) Advanced Byzantine cement based composites resisting earthquake stresses: the crushed brick/lime mortars of Justinian's Hagia Sophia. *Construct Build Mater* 16:543–552
- Weber J (2007) Romanzemente als Fassadenbaustoffe der Gründerzeit. In: Gänßmantel J, Hecht C (eds) *Bauinstandsetzen und Bauphysik. WTA-Almanach 2007*, Wien, pp 539–562
- Weber J, Gadermayr N, Kozłowski R, Mucha D, Hughes D, Jaglin D, Schwarz W (2007) Microstructure and mineral composition of Roman cement produced at defined calcination conditions. *Mater Charact* 58:1217–1228
- Wein GY (1977) A Budai-hegység tektonikája (Tectonics of the Buda Mountains). Special publication of the Geological Institute of Hungary. p 76
- Zamba IC, Stamatakis MG, Cooper FA, Themelis PG, Zambas CG (2007) Characterization of mortars used for the construction of Saithidai Heroon Podium (1st century AD) in ancient Messene, Peloponnesus, Greece. *Mater Charact* 58:1229–1239

Manufacturing Analysis and Non Destructive Characterisation of Green Stone Objects from the Tenochtitlan Templo Mayor Museum, Mexico

J.L. Ruvalcaba, E. Melgar, and Th. Calligaro

1 Introduction

In the archaeological excavations carried out at the Great Temple of Tenochtitlan, the Aztecs' main ceremonial building, archaeologists have recovered hundreds of objects representing rich offerings corresponding to the foundation of the pre-Hispanic city until the Spanish conquest (1325–1521 AD). Among the recovered objects, a significant number of green stone artefacts, which were particularly appreciated by pre-Hispanic cultures, were found. They were produced using raw materials from the Mexico Basin and other Mesoamerican areas. Various green minerals (jadeites, antigorite, lizardite, diopside) and rocks (serpentinites and even green marble) may have been used in the production of these artefacts. Jadeite sources are located far away, in the Motagua river basin in Guatemala, and, as a result, we may expect that a limited number of jadeite objects arrived to Central Mexico through trade (Taube et al. 2004). Nevertheless, the identity and provenance of most of the different green stones employed as raw materials for producing beads, pendants, plaques, earplugs, and pectorals is still unknown. Because of that, the aim of this study is to identify the green minerals and/or rocks used for producing the artefacts and to establish a relationship between raw materials and their sources with the manufacturing techniques employed for the Aztec offerings. Some preliminary results on manufacturing trends and materials characterisation for some green stone objects are presented in this paper.

J.L. Ruvalcaba (✉)

Instituto de Física, Universidad Nacional Autónoma de México (UNAM), Mexico City, Mexico
e-mail: sil@fisica.unam.mx

E. Melgar

Museo del Templo Mayor, INAH, Mexico City, Mexico

Th. Calligaro

Centre de Recherche et de Restauration des Musées de France, UMR 171 du CNRS, Paris, France

2 Manufacturing Analysis

Unfortunately, due to the destruction of the Tenochca's capital by the Spanish conquerors in 1521 and to subsequent urban modifications during the time of the colonial city and afterwards of the modern Mexico City, there is no data on the primary production contexts of these items, such as the original workshops, for example. Because of this aspect, recent analyses carried out by E. Melgar et al. during the last 5 years in the context of the project "The lapidary objects of the Great Temple: styles and technological traditions" (Melgar and Bautista 2006) have identified the tools and techniques employed in the artefacts' production, using experimental archaeology and characterisation of the tool traces visible in the manufactured objects. In this project, all the modifications to the objects were reproduced by cutting, abrading, drilling, incising, polishing and brightening, with tools and processes that were mentioned in the historical sources, or are found and inferred from archaeological contexts. Parallel to the development of these experiments, systematic comparisons have been carried out between the manufacture traces of replicas and the archaeological objects' tools traces, using optical microscopy and Scanning Electron Microscopy (SEM). SEM offered the best results and precision for distinguishing the different tools and manufacture traces.

3 Analytical Methodology

Our analytical approach consisted of two separate stages. The first one was an in situ analysis using light reflection and colorimetric measurements by an Ocean Optics fibre optic VIS-NIR USB2000 spectrometer (350–900 nm) and a halogen light source with a white colour reference, as well as portable X-ray fluorescence (XRF) on the full set of objects using our SANDRA XRF system. This setup is composed of a 75 W Mo X-ray tube and a Si-Pin detector. Afterwards, portable Raman was performed on selected pieces. A Delta-Nu Inspector equipment with a 785 nm laser was used for this purpose. Elemental and mineral compositions could be determined according to this procedure.

Subsequently, a limited set of representative and unique objects was selected for transportation to the laboratory, in order to complete the characterisation using an external beam setup with a 3 MeV proton beam and a combined analysis by Particle Induced X-ray and Gamma spectrometry (PIXE–PIGE) in the Pelletron Accelerator of the IF-UNAM. PIXE provides most of the elemental data (major and trace elements), while from the PIGE spectra reliable measurements of Na contents can be obtained. Reference minerals, as well as standard reference material from NIST (SRM 2704, 2711 and 1412), were used for both in situ and laboratory measurements. This combination of techniques has proved to be suitable for the analysis of jade and other green stones (Ruvalcaba Sil et al. 2008; Cheng HS et al. 2004, Cheng TH et al. 2004).

4 Results

The results of the manufacture study showed two distinct patterns. Thus, there is a high heterogeneity in the tools employed in the production of lapidary objects during the earlier stages of Tenochtitlan (1325–1426 AD), when the Aztecs were tributaries of the Tecpaneca people at Azcapotzalco. The identified processes used in the production of the artefacts from this period are: abrading with basalt, basalt and sand, or andesite; cutting with obsidian or chert flakes; drilling with chert burins or sand and reed; and polishing with chert nodules. In contrast, we found a significant technological standardisation in the production of the lapidary objects during the later stages (1427–1521 AD) of the period under consideration, when the Aztecs defeated the populations of their ruling city of Azcapotzalco, became an Empire, and commanded the Triple Alliance. At this time, the manufacturing was reduced to abrading with basalt, cutting and drilling with chert flakes, and polishing with chert nodules. This second pattern allowed us to consider the concentration and centralisation of the productive areas and artisans, perhaps under the strict control of the Aztec elite. The manufacturers of these objects could be the specialised craftsmen that lived and worked inside the palace of the Mexican Tlatoanis (main rulers), as they appear in the historical sources.

Our portable Raman system was tested in the Templo Mayor Museum. Unfortunately, it was not possible to obtain positive identifications of the green minerals due to the polished surface of the pieces. The quality of the Raman spectra was very bad, due to reflection of the laser beam. Nevertheless, other pieces with a non-polished surface are good candidates for Raman measurements.

On the other hand, *in situ* XRF measurements of the green stone artefacts mainly provide data for Si, Cl, K, Ca, Fe, Cr, Mn, Cu and Sr elements. X-ray intensities were used for the screening of the items, and Si, Ca, Fe, Cu and Cr appeared to be the most prevalent elements. According to the XRF data, a limited number of green stone objects were chosen for PIXE and PIGE analysis in the Pelletron laboratory of the IF-UNAM (Fig. 1). During the irradiation, the high intensity green luminescence induced by the proton beam on jadeite was observed only for few items (Ruvalcaba Sil et al. 2008). Thus, it was not expected to identify many jadeite pieces among the selected objects. A comparison of the elemental contents of the Templo Mayor objects and of the jadeite reference data from the Motagua area showed differences in terms of Na, Ca, Cr, Ni, Br and Sr contents.

PIXE–PIGE elemental composition data were calculated using the GUPIX code. A statistical analysis was applied on the logarithm of the concentrations. Cluster analysis considering Euclidian distances and weighted pair group average, and factor analysis considering a Varimax rotation gave the same results. Serpentine and several jadeite references from Motagua region were included in the analysis. Figure 2 shows the corresponding dendrogram of the factor analysis considering three main factors for the analysed regions on various artefacts.

From the compositions of the archaeological objects and the mineral references, it is clear that only few items (35, 38, 40-9, 45, 26-94) might contain jadeite



Fig. 1 Some of the green stone objects from the Templo Mayor offerings

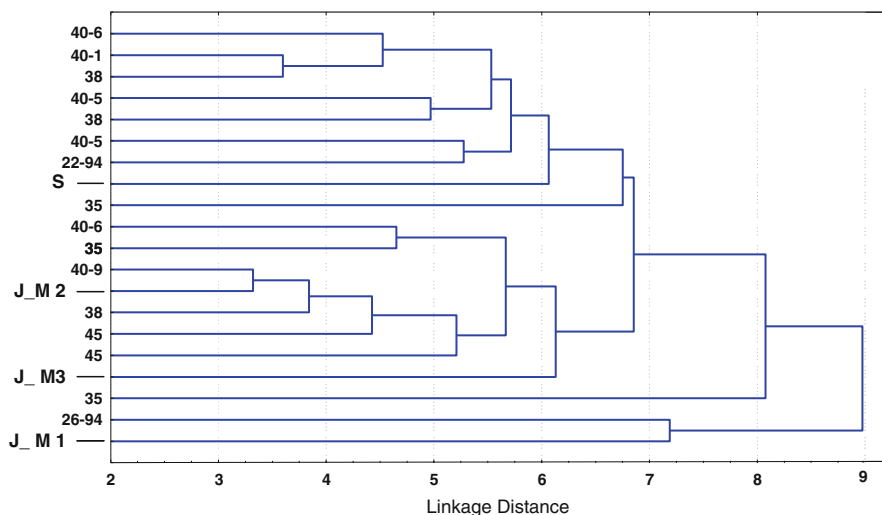


Fig. 2 Dendrogram of factor analysis from PIXE-PIGE elemental composition data. S: Serpentine reference; J: Jadeite references M1, M2 and M3

(J_M1, J_M2, J_M3) in their composition. Most of the pieces could be related to serpentine (from the Guerrero region) and other green minerals. One sample is not included in any cluster (26-94), but it fits the composition of the jadeite reference M1 from the Motagua basin. Nevertheless, it can be observed that for some samples, their composition varies significantly and a single piece may be very inhomogeneous (e.g., 35 and 38). For this reason, its measured composition changes depending on the analysed region and it may cluster several groups.

This means that it is necessary to carry out several measurements on a given sample in order to determine a mean elemental composition; however, the mineralogical information is essential for completing its characterisation. The elemental composition alone is not sufficient for identifying the mineral, due to the similarities in the composition of the green minerals and the natural heterogeneity of this type of materials. Also, more comparisons with known sources of green stone minerals in the Central Highlands of Mexico are required.

5 Conclusions

The studied green stone artefacts fit the pattern of manufacture traces observed for other lithic materials discovered among the offerings from the Templo Mayor of Tenochtitlan. Yet, more experimental archaeology on jadeite, one of the hardest available materials, is required. Local manufacturing was determined for all samples, but a more standardised production was observed for samples dating from a later period, prior to the Spanish conquest.

In situ XRF data showed good agreement with PIXE measurements. Few objects fit the compositional profile of jadeite from the Motagua region, but most of the pieces may correspond to other green stone minerals. The similarities in the composition of green minerals, as well as the natural heterogeneity of these materials are the main difficulties for their characterisation, if carried out only on the basis of elemental composition. Thus, mineralogical analyses of the samples appear necessary. Even if Raman spectroscopy is appropriate for this purpose, due to the polished surface of the items it was very difficult to obtain suitable Raman spectra. Further analyses, probably by in situ Mid-FTIR, are required in order to complete the characterisation of the green stone minerals.

More measurements on the green stone objects discovered among the offerings from various constructive stages of the Templo Mayor and from different periods may provide more data in order to contrast the manufacturing profile observed from the tool traces in the artefacts with their elemental composition, as well as their probable provenance. This information is very important for understanding the exchange and tribute patterns of raw materials in the Aztec Empire.

Acknowledgements The authors would like to thank archaeologist Fernando Carrizosa Montfot, curator of the Museo del Templo Mayor, INAH, for providing the facilities used to carry out this research, as well as Karim López and Francisco Jaimes for the accelerator measurements. This study has been supported by the Mexico CONACyT grand U49839-R.

References

- Cheng HS, Zhang ZQ, Zhang B, Yang FJ (2004) Non-destructive analysis and identification of jade by PIXE. *Nucl Instrum Methods B* 219–220:30–34
- Cheng TH, Calligaro T, Pagès-Camagna S, Menu M (2004) Investigation of Chinese archaic jade by PIXE and μ Raman spectrometry. *Appl Phys A* 79:177–180

- Melgar E, Bautista P (2006) Análisis de mosaicos de piedra verde incrustados en dos cráneos humanos a través de sus huellas de manufactura. In: Mendoza D, Arenas J, Rodríguez V, Ruvalcaba JL (eds) *La Ciencia de Materiales y su Impacto en Arqueología*, Vol III. Academia Mexicana de Ciencia de Materiales AC, pp 161–176
- Ruvalcaba Sil JL, Manzanilla L, Melgar E, Lozano Santa Cruz R (2008) PIXE and Ionoluminescence for Mesoamerican Jadeite Characterization. *X Ray Spectrom* 37:96–99
- Taube K, Hruby Z, Romero L (2004) Jadeite sources and ancient workshops: archaeological reconnaissance in the Upper Río El Tambor, Guatemala, FAMSI reports. <http://www.famsi.org/reports/03023/index.html>

Traces of Ancient Treatments on the Stone Materials of the Main Façade of the Siena Cathedral: Glazings (Calcium Oxalate Films *s.s.*) and Other Finishes

G. Sabatini, F. Droghini, M. Giamello, G. Guasparri, S. Mugnaini, and A. Scala

1 Introduction

The results of previous works have shown that a decisive contribution to an appropriate resolution of the long-debated topic of so-called “calcium oxalate films” can derive primarily from very detailed studies of extensive and architecturally varied surfaces, such as entire monumental façades. This approach, already successfully utilized for Sienese palaces made mainly of bricks (Giamello et al. 2005; Droghini et al. 2009), is applied here to the façade of the main cathedral in Siena, entirely made with natural stone materials.

This façade (Fig. 1) contains in fact the three most typical local stones used in historical Sienese buildings: marble from the Montagnola Senese, red ammonitic limestone from Gerfalco, and serpentinite from the Vallerano quarries. The construction of the cathedral took place between 1284 and 1317, but numerous interventions have been performed since then, so that only a small proportion of the surfaces is original, as shown in the mapping performed by Haas and von Winterfeld (Haas and Winterfeld 1999). Such substitutions, historically well documented, have provided very useful data for reconstructing the chronology of the different films.

2 Sampling and Methods

The samples were taken from all places where evident or even uncertain traces of films were identified, in an attempt to include all of the different architectural surfaces. A total of approximately 400 micro samples were collected. First, these were examined under the stereomicroscope. Subsequently, thin and ultrathin sections (at least two per sample, taken perpendicular to the external surface) were analysed

G. Sabatini, F. Droghini, M. Giamello (✉), G. Guasparri, S. Mugnaini, and A. Scala
Dipartimento di Scienze Ambientali, U.R. Conservazione del Patrimonio Culturale Lapideo,
Università degli Studi di Siena, Via Laterina 8, 53100 Siena, Italy
e-mail: giamello@unisi.it



Fig. 1 Different types of Ca-oxalate films on the natural stone materials of the main façade of the Siena Cathedral: (a) and (b) on marble; (c) on red ammonitic limestone; (d) on serpentinite

under a polarized light microscope in both transmitted and reflected light. The study of ultrathin sections represents a particularly fundamental technique for characterizing this type of films, especially if opportunely coupled with XRD (or FT-IR) and SEM–EDS analyses. Indeed, such a procedure permits a very detailed observation of the microstratigraphy, but also allows the determination of the mineral species present inside the film and the observation of their textural relationships.

3 Results

For the sake of brevity we will limit here the description of the films to the bare essentials, reserving the observations relevant to their relative chronology for a further study. In the following presentation, we will use the term “calcium oxalate film” to refer to films in which the binder consists exclusively or at least prevalently of calcium oxalate, adding “s.s.” (*sensu stricto*) to those films in which the binder is greatly predominant over the filler.

3.1 *Films on Marble*

In terms of diffusion, there are two main types of Ca-oxalate films on the marble surfaces of the façade. The first type (G1) appears macroscopically in the form of patches, usually of limited extension and with a more or less intense brownish-orange colour (Fig. 1a). Traces of G1 were found on both the lower and upper half

of the façade, and equally on smooth wall surfaces and on the various ornamental elements. Moreover, G1 traces have only been found in the original elements of the façade (Haas and Winterfeld 1999). In thin section, the G1 films consist of a filler of very fine yellow-orange ochres and rare black carbon within a Ca-oxalate binder (whewellite). They have a mean overall thickness of 20–40 μm . The filler–binder ratio is strongly in favour of the binder. XRD analyses confirmed and completed the mineralogical composition of this film and revealed the presence of a subordinate quantity of silicate minerals. SEM–EDS analyses indicated that the ochreous material is the carrier of these silicates. A layer of microcrystalline calcite, rarely discontinuous and 20–25 μm thick on average, always underlies G1 (Fig. 2A).

The second type of Ca-oxalate film (G2) was found exclusively in the lower half of the façade, in much larger patches as compared to the G1 film. Macroscopically, its colour varies from yellowish-brown to light brown (Fig. 1b). Under microscopic observation, this film (Fig. 2B) appears much thicker than the G1 film (70–100 μm) and has a coarser filler, also consisting of yellow-orange ochres and black carbon, in a greatly prevalent oxalate binder (whewellite). XRD and SEM–EDS results appear very similar to the ones obtained for the G1 type.

For both types of film (G1 and G2), strong homogeneity of the filler–binder mixture can be observed in all the samples. According to the qualifications established above, these films must be considered Ca-oxalate films *s.s.* In several cases, the thin sections show superimposition of the G2 film on the G1. The overlapping of the two films can be observed even macroscopically in an area of the right portal.

3.2 Films on Red Ammonitic Limestone

The area of the right portal is the only one with frequent traces of these films, perhaps also because it was not subjected to excessive cleaning in recent restorations.

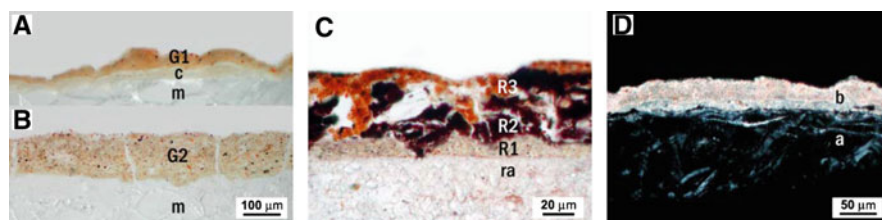


Fig. 2 (A) and (B) Ca-oxalate films, G1 and G2 respectively, on marble (m). A layer of microcrystalline calcite (c) always underlies the G1 film. These microstratigraphies are in dark-field reflected light, with a white paper under the thin section; (C) Overlapping of three different Ca-oxalate films (R1, R2 and R3) on red ammonitic limestone (ra). Transmitted light, one polar; (D) Ca-oxalate film (b) on serpentinite (a). The film sulphation, visible in its lower part with minor birefringence, produces the optical disconnection with the substratum. Transmitted light, two polars

The spiral mouldings of the arch of this portal are particularly interesting since they are considered to be original, leading us to concentrate our study on them. Traces of colouring treatments on these mouldings, in the form of dark red patches with orange striations, are sometimes evident at the macroscopic level (Fig. 1c).

Microscopically, the samples show a succession of three distinct films (Fig. 2C). The first (R1), sometimes discontinuous and generally thin (20 μm), consists of a whewellite binder with a scarce yellow-orange ochre filler. The second (R2) is composed of a dense filler of very coarse red ochres and rare black carbon in a cement consisting of microcrystalline calcite (50 μm). In many samples, the calcite of the cement has almost disappeared, sometimes replaced by gypsum or even leaving voids. The third film (R3) is much more homogeneous, with a filler of fine yellow-orange ochres in a whewellite binder. This mixture often penetrates into the voids in the R2 film. XRD and SEM–EDS analyses indicate a composition qualitatively similar to G1 and G2 for R1, and a notably higher Fe/silicates ratio for R3. As per the previous definition, R1 and R3 are classified as Ca-oxalate films *s.s.*, whereas R2 cannot be considered a Ca-oxalate film since it has a predominantly calcite binder.

3.3 *Films on Serpentinite*

Relics of Ca-oxalate films on serpentinite are rare and concentrated in small sectors. Macroscopic identification of traces of Ca-oxalate films on serpentinite elements is not easy, because the decay that usually affects such films often renders them as anonymous dirty white or pale yellow patches indistinguishable from other surface stains present for various reasons on this stone material. Figure 1d shows the macroscopic appearance of these films (in an area of the structure believed to be original) in a case where small islands characterized by a greenish colour, with borders highlighted by yellowish-white halos, are visible.

In thin section (Fig. 2D), these films appear to be constituted by a consist of Ca-oxalate (whewellite) alone, sometimes with small quantities of very fine black carbon. No other component is revealed by XRD and SEM–EDS analyses. An accurate study of many thin sections has revealed that the greenish islands correspond to zones devoid of sulphation phenomena, so that the film is transparent and the typical colour of the stone is visible. In contrast, in the halos, sulphation is ubiquitous and progressive. This produces a disconnection of optical contact between the film and the substratum, and the film becomes an opaque coating. This type of film, usually rather thin (10–20 μm) is the only one present on serpentinite.

4 Discussion and Conclusions

The three lithotypes that are present in the façade include different types of Ca-oxalate films, each of which is never found on the other types of stone. Moreover, all the types of films have a constant thickness and a constant homogeneity of the internal distribution of filler and oxalate phases. The combination of these characteristics is a further confirmation of the anthropic origin of these films.

It is also true that the current appearance of the films cannot correspond to their original appearance. On the other hand, the transformations of the binder into oxalate, but mostly the sulphation processes, have profoundly changed their original look. All the preceding observations and descriptions bring us then to conclude that these films were originally mixtures of an organic substance that acted as binder, coupled with a filler now recognized as the pigment component (Fe-ochres \pm black carbon).

Experimental trials (under way, and conducted in collaboration with the “Opificio delle Pietre Dure”) with mixtures of linseed oil and a filler that is qualitatively and quantitatively identical to those present in films found on the marble of Jacopo della Quercia’s Gaia Fountain (very similar to G1 and G2 films) have revealed what must have been the original appearance of these treatments: a soft ivory-coloured glazing that allows the marble to be seen but at the same time gives it a brighter tonality and a more valuable appearance. An example of unequivocal evidence regarding this aspect is provided by several invoices related to the fourteenth century building works of the Siena Cathedral, found in the OPA archives by Giorgi and Moscadelli (2005). The purchase description reads:

“oglio di semelino che si comprò per tignare marmi neri” (2 soldi e 6 denari)

(linseed oil bought to stain black marbles)

“nero ad olio per ognate marmi neri” (18 soldi)

(black with oil to anoint black marbles)

This archival evidence not only attests to the normal practice, in those times, of treating stone materials, but even confirms the use of linseed oil and thus the origin of the Ca-oxalate films. The role of these treatments was essentially aesthetic, aimed at enhancing the natural colour of the stone by rendering it homogeneous, highlighting it and preserving it in time, as well as creating a better chromatic harmonization of the entire façade.

As mentioned above, we could not report the data relevant for a reconstruction of the chronology of the different treatments identified in this summarized version of our work. We thus limit ourselves to pointing out that, by combining the information pertaining to the distribution of the different films with the aspects regarding the substitution of façade elements over time, deduced from archival data, it was possible to reconstruct a chronology of the treatments from the fourteenth to the nineteenth century.

References

- Droghini F, Gabrielli F, Giamello M, Guasparri G, Mugnaini S, Sabatini G, Scala A (2009) the colour of the façades in Siena's historical centre. (II) – calcium oxalate films on brickwork of XV – XVI century palaces. *Archaeological and Anthropological Sciences*, 1 (2):123–136
- Giamello M, Guasparri G, Mugnaini S, Sabatini G, Scala A (2005) I colori della facciata del Palazzo Pubblico di Siena nell'età medievale. Un tentativo di ricostruzione tramite le pellicole ad ossalati di calcio. In: Tolaini F (ed) *Proceedings of the Congress "Il colore delle facciate: Siena e l'Europa nel Medioevo"*, Siena, 2–3 Mar 2001. Quaderni CERR, Pacini, Pisa, Italy, pp 35–51
- Giorgi A, Moscadelli S (2005) Costruire una cattedrale. L'Opera di Santa Maria di Siena tra XII e XIV secolo. In: *Die Kirchen von Siena*, hg. v. Peter Anselm Riedl und Max Seidel. Beiheft 3, Deutscher Kunstverlag, München, Germany
- Haas W, Winterfeld Dv (1999) Der Dom S. Maria Assunta. Architektur. Planband. In: *Die Kirchen von Siena*, hg. v. Peter Anselm Riedl und Max Seidel. Band 3.1.3, München, Germany

Investigating Trade and Exchange Patterns in Prehistory: Preliminary Results of the Archaeometric Analyses of Stone Artefacts from Tell Gorzsa (South-East Hungary)

Gy. Szakmány, E. Starnini, F. Horváth, and B. Bradák

1 Introduction and Archaeological Framework

The purpose of this paper is to provide a preliminary report on the analyses of the polished and ground stone assemblage from the site of Hódmezővásárhely-Gorzsa, a Tisza Culture tell site which lies at the confluence of the Tisza and Maros rivers in the Great Hungarian Plain (Fig. 1). During the excavations, 1,000 m² of the tell settlement were investigated (Horváth 2005). The layers of the settlement contained remains dating from the Late Neolithic to the Sarmatian period. The thickest layer discovered was a Late Neolithic one, dating to the periods II–V of the Tisza Culture, which are considered contemporary to the Proto-Lengyel and Lengyel I–IIIa Culture (Horváth 2005). In terms of absolute chronology, ¹⁴C calibrated dates place the occupation of the tell to a period between 4970 and 4380 BC (Horváth 2005).

A multidisciplinary study of the stone tool assemblage is in progress, involving a traditional typological classification of instruments combined with functional (Starnini et al. 2007a) and archaeometric analyses of raw material. The present study is a brief outline of the state of research concerning the ground (representing the larger part of the assemblage) and polished stone assemblage, whose study is in progress.

Gy. Szakmány (✉)

Department of Petrology and Geochemistry, Eötvös Loránd University, Pázmány P. sétány 1/c,
1117 Budapest, Hungary
e-mail: gyorgy.szakmany@geology.elte.hu

E. Starnini

Department of Archaeology and Classical Philology, University of Genova, Via Balbi 4, 16126
Genova, Italy

F. Horváth

Móra Ferenc Museum, Roosevelt tér 1-3, 6720 Szeged, Hungary

B. Bradák

Department of Physical Geography, Eötvös Loránd University, Pázmány P. sétány 1/c, 1117
Budapest, Hungary

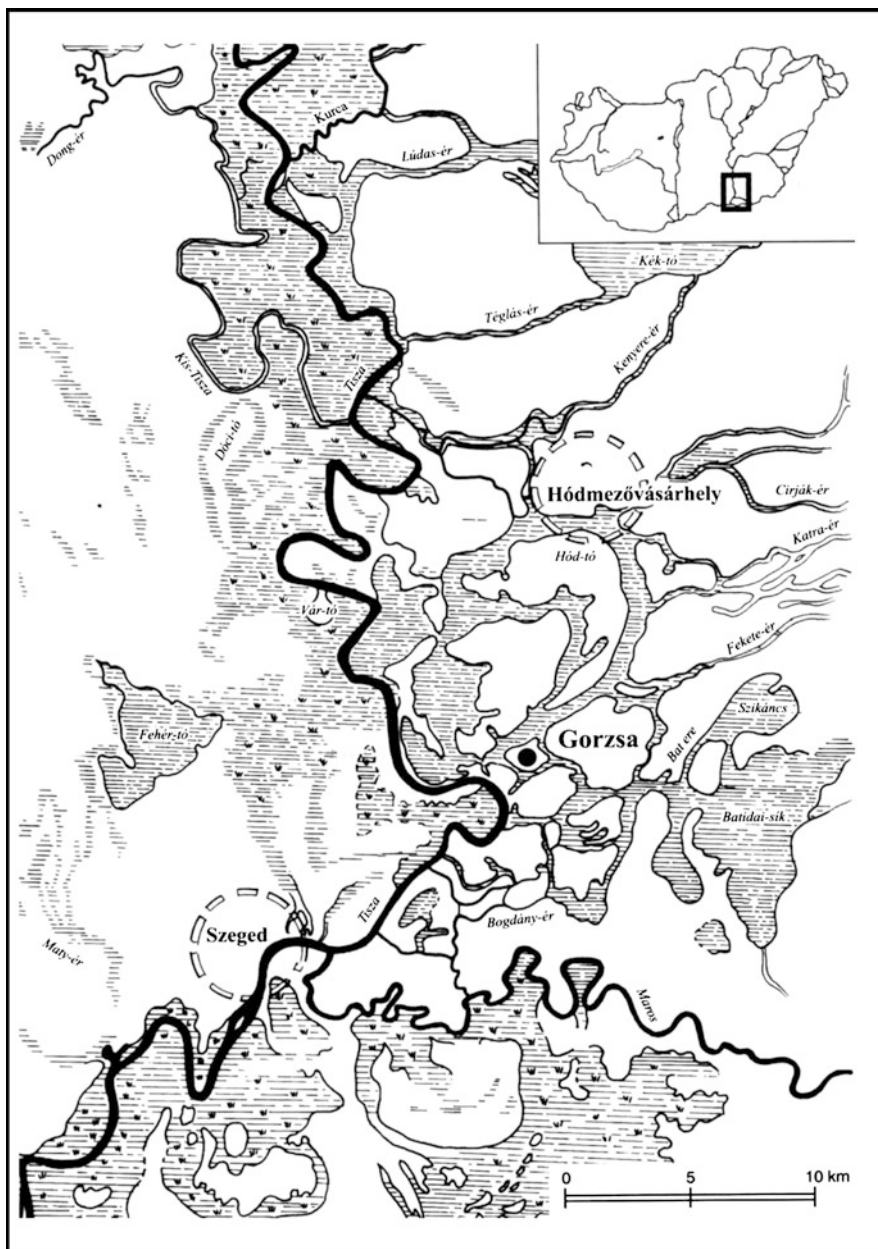


Fig. 1 Location of the site

2 Analytical Methods

After macroscopic description, 150 samples out of 679 stone artefacts were studied by Optical Microscopy (OM) in thin section. The Magnetic Susceptibility (MS) was measured for all the implements.

2.1 Magnetic Susceptibility (MS)

The measurement of volume MS is at present a rapid, cheap and non-destructive method of analysis for stone materials (Williams-Thorpe and Thorpe 1993). In spite of this, it has not yet been used to a significant extent for the basic discrimination of stone artefacts. The instrument used in the present work is a Kappameter KT-5 handheld meter (Kappameter n.d.).

The main problem encountered in the archaeometric application of this method is that usually the results of measuring are influenced by the intrinsic characteristics of the stone artefacts, such as heterogeneity of the rock, uneven dispersion of magnetic mineral in the rock, weathered surface, surface irregularity, etc. Other problems are related to the shape of analysed implements – sometimes the active face of the Kappameter does not fit the measured surface (Williams-Thorpe and Thorpe 1993; Williams-Thorpe et al. 2000). Thus, we elaborated other test experiments in order to solve both the problem of the elongated shape of the artefacts (1) and of the generally small size of those artefacts which do not cover the sensor surface of the instrument (2).

1. Elongated experimental test specimens ($12 \times 3 \times 3$ cm) were made of basalt from the Medves Plateau (North Hungary).

In the first stage of the experiment, we studied the decrease of the κ value in relation to the decrease of the length of the sample. The starting length (12 cm) was decreased step by step, by 0.5 cm on average, until the length of the experimental axe was 6 cm. The κ values decreased significantly under an 8 cm length of the test specimen (Fig. 2). This aspect indicated that an overlap correction is necessary when the artefact is under 8 cm in length.

2a. If size correction factors have to be applied on the measured κ values, the diameter of the surface of the stone artefact needs to be measured as well (Kappameter n.d.). The shape of the stone tools infrequently forms a circle. In order to address the problem of the shape of the measured surface, we created two ellipsoid based prism model samples (EBPM) (a: $12 \times 3 \times 3$ cm; b: $8 \times 4.5 \times 3$ cm). The κ values for these samples were a = 8.01×10^{-3} SI and b = 10.00×10^{-3} SI, respectively.

2b. The range of the two ellipsoids with the decreased length was counted (see the results of stage (1) of the experiment). A 7 cm length was used in the calculation because the entire surface of the sample can be measured with certainty according to this value.

2c. Our assumption was that the κ value of this EBPM and the κ value of a “theoretical circle” based prism (circle with the same range as a calculated ellipsoid range) are consistent:

$$\kappa_{EBPM(\text{model artefact})} \approx \kappa_{\text{theoretical circle based prism}}$$

2d. To confirm this hypothesis, two circle based prisms with a similar range to the calculated range of the EBPM were created. To determine the diameter of the “theoretical circle”, the following equations were used:

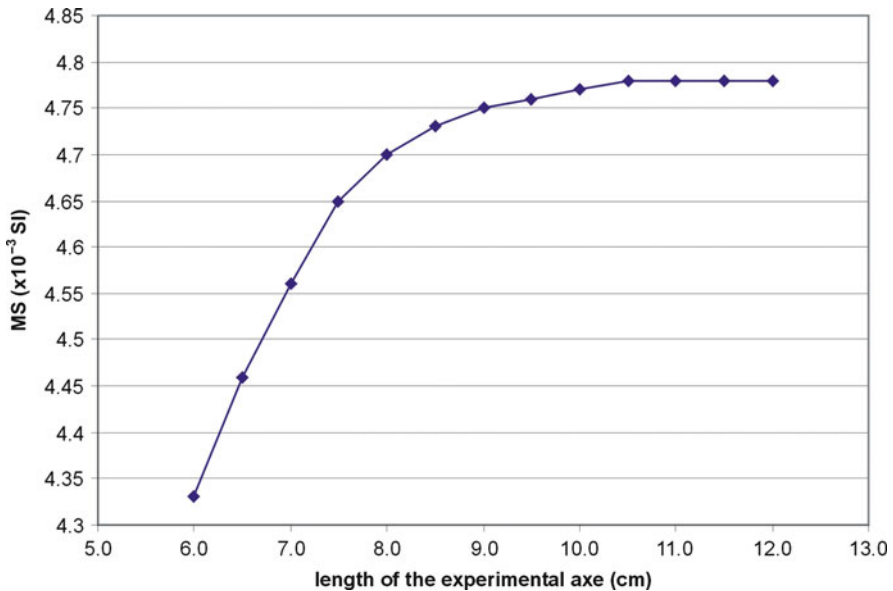


Fig. 2 The decrease of the κ value during the decrease of the length of the experimental axe

$$\text{range}_{\text{ellipsoid}} = \text{range}_{\text{circle}} \quad (\text{a})$$

$$\pi(\text{width}/2)(\text{length}/2) = r^2\pi \quad (\text{b})$$

$$d = 2\sqrt{(\text{width}/2)(\text{length}/2)} \quad (\text{c})$$

The measured κ value of the two circle based samples was very similar to the κ value of the EBPM sample (8.01×10^{-3} SI and 9.94×10^{-3} , respectively; see results 2a).

Based on the results of the model experiments, if the length (width) of the elongated stone artefacts is smaller than 8 cm, the equation mentioned above (c) can be used to determine the diameter of the sample for the correction factor counted according to the data in the Instruction Manual of the Kappameter instrument:

$$\text{correction factor} = 4.3792 \times \text{diameter of sample}^{-0.3215} \quad (\text{d})$$

Real MS values are obtained after the correction is carried out according to the above-mentioned parameters, in order to eliminate any bias from the measurements.

3 Results

3.1 Polished Stone Tools (Table 1)

Several types of rocks were used for the manufacture of polished stone tools at Gorzsa. However, only a few of these were commonly employed, while others occurred only sporadically.

Table 1 The dominant raw material types present in the stone tools and their identified constituents

Raw material types	Petrographically identified constituents
Polished stone tools (axes, adzes, perforated hammer-axes, chisels)	
Hornfels	cpx (di), fp, op ± bi
Dolerite–metadolerite–metagabbro	pla (saussuritized, ±ab), cpx (altered to amph), ilm (altered to tit), ±ap, ±chl, ±zeo, ±preh
Basalt	Phenocryst: ol (rare); Matrix: ol, cpx, pl, op, glass
Alkaline dolerite–tephrite–phonolite	pl, kfp, cpx, alk amp, bi, op, ap, ±ol, ±anal+cc, ±neph, ±alk px
Greenschist–amphibole schist–chlorite schist	amp (tre-act or hbl), pl, op, ±epi-zoi, ±chl, ±tit, ±cc, ±cpx, ±tour
Acidic-intermediate volcanites–metavolcanites–dyke rocks	kfp, ±pl, ±Q, ±bi, ±op, ±ap, ±ru, ±epi
White stone	microcrystalline Quartz, ±mag, ±cc,
Meta-ultrabasite	serp, chl, op (secondary mt), ±Cr-spi
Ground stone tools (millstones, grinding stones, hand-stones, pestles, whetstones, abraders)	
Well sorted grey sandstone (a)	mQ, pQ, pl > kfp, mus, (tour, metasedimentary rocks)
Poorly sorted grey sandstone (b)	mQ, pQ, Q-muscovite schist, phyllite, shale, mus, kfp, (± pl, chert, volcanite, gt, st)
Red-lilac sandstone (c)	mQ > pQ, kfp ≫ pl, acidic volcanites, mus, chloritized bi, (tour, zir, gt, op)
White metasandstone (d)	mQ, pQ, kfp, (shale, metasilstone–metasandstone, chert, op, ru, tour,)
Sandstone with sparite cement (e)	mQ, pQ, kfp ≫ pl, mus, bi, gt, volcanite, siltstone, chert, ±hbl, ±px, ±zoi;
Wacke (f)	mQ > pQ, (mus, op)
Andesite (a)	Pl, cpx, opx, op, ap, endogenous inclusion, glass, ±hbl, ±bio
Andesite (b)	pl, bio, op, ap, glass
Andesite (c)	pl, op, glass, vesicles
Andesite–dacite (d)	pl, opacitized bio, gt, op, ap zir, ru, glass
Andesite (e)	pl, hbl, bi, op, ap, zir
Granite (a)	kfp ≥ pl, Q, bi, mus-ser, op, zir, ap
Tonalite (b)	pl ≥ kfp, Q, bio, mus gt (2 generations), op, ap, zir
Quartz monzonite (c)	K-feldspar ≈ pl, Q (few), hbl, bi, op, ap
Granite aplite (d)	kfp > pl1, pl2 (new), Q, bio (few), epi, tit, op
Metagranite1 (e)	kfp, pl1, pl2 (new), wmic, limonite–chlorite aggregates, op, tour
Metagranite2 (f)	Q, kfp, mus-ser, op, zir

ab albite, *alk* alkaline, *amp* amphibole, *anal* analcite, *ap* apatite, *bi* biotite, *cc* calcite, *chl* chlorite, *cpx* clinopyroxene, *di* diopside, *epi* epidote, *fp* feldspar *gt* garnet, *hbl* hornblende, *ilm* ilmenite, *kfp* K-feldspar, *mag* magnesite, *mt* magnetite, *mQ* monocrystalline quartz, *mus* muscovite, *neph* nepheline, *ol* olivine, *op* opaque minerals, *opx* orthopyroxene, *pl* plagioclase, *pQ* polycrystalline quartz, *Q* quartz, *preh* prehnite, *ru* rutile, *ser* sericite, *serp* serpentine minerals, *spi* spinel, *st* staurolite, *tit* titanite, *tour* tourmaline, *tre-act* tremolite–actinolite, *wmic* white mica, *zeo* zeolite, *zir* zircon, *zoi* zoisite–clinozoisite

1. The most common raw material is hornfels, which is a pale green-greyish, very fine grained, massive hard, tenacious rock. Usually flat axes/axe blades and shoe last chisels were produced with this raw material. Mineral components are predominantly diopside and feldspar. Real MS values are low and within a strict range ($0.2\text{--}0.4 \times 10^{-3}$ SI).
2. Dolerite–metadolerite–metagabbro polished stone tools are also common. They are fine/medium grained, hard, massive rocks. The original mineral composition consisted of plagioclase, pyroxene, ilmenite and a small amount of apatite. Hornblende, actinolite, saussurite, albite, titanite and occasionally chlorite formed during the metamorphism. Real MS values show two different groups: one with high MS values ($20\text{--}45 \times 10^{-3}$ SI), and another with low ones (generally <1 , maximum 2.5×10^{-3} SI).
3. Basalt also occurs as raw material. It is fine grained, has fluidal texture and there are only few olivine phenocrysts. The matrix consists of plagioclase, clinopyroxene, altered olivine, opaque minerals and glass. MS values are generally high ($7\text{--}27 \times 10^{-3}$ SI).
4. Alkaline gabbro–alkaline dolerite–tephrite–phonolites are represented in the assemblage. Their mineral components are plagioclase, clinopyroxene, alkaline amphibole, biotite, relict olivine and apatite. Occasionally, a few analcime and calcite minerals occur together. Sanidine and nepheline with alkaline pyroxene occur only in phonolite. MS values are generally high ($11\text{--}15 \times 10^{-3}$ SI).
5. Greenschist, amphibolite, chlorite schists are represented in small quantities. Their mineral composition, texture and secondary alteration are highly variable. MS values are very different ($0.1\text{--}40 \times 10^{-3}$ SI).
6. Acidic-intermediate volcanites, metavolcanites and dyke rocks are represented sporadically. MS is highly variable, but does not reach high values ($0.5\text{--}6 \times 10^{-3}$ SI).
7. There are several chisel blades or shoe last axes made of very fine grained white rocks; part of them turned out to be hornfels, but there are also aleurolites or limy silicified mudstones. The MS values are very low (maximum 0.2×10^{-3} SI).
8. Only few perforated hammer-axes are made from meta-ultrabasite rock. MS values are highly variable ($4\text{--}57 \times 10^{-3}$ SI).

3.2 *Ground Stone Tools (Table 1)*

1. Several types of sandstones occur among the grinding stones, in terms of colour variability, grain size, and composition of clasts:
 - (a) Well sorted dark grey sandstones
 - (b) Polimict, poorly sorted dark grey sandstones
 - (c) Red or lilac sandstones
 - (d) White silicified meta-sandstones
 - (e) Well sorted, grey sandstones with well-rounded clasts, and coarse calcite cement

- (f) Wacke.
MS values show differences among these types
2. Different types of andesite could be distinguished:
- (a) The most common type has plagioclase, clinopyroxene, opaque minerals as phenocrysts, and endogenous inclusions. Rare orthopyroxene, brown hornblende and biotite also occur. There is glass in the matrix.
Less common types are:
- (b) Biotite andesite with an almost completely glassy groundmass
(c) Andesite lacking mafic minerals with large vesicles
(d) Garnet-bearing andesite–dacite
(e) Hornblende andesite with few opacitized biotite and recrystallized groundmass.
Real MS values have two different ranges, $2\text{--}8 \times 10^{-3}$ SI and $13\text{--}17 \times 10^{-3}$ SI, respectively
3. The granitoid–metagranitoid types are:
- (a) Pink coloured granite consisting of perthitic K-feldspar and sericitized plagioclase. Quartz is abundant, biotite occurs generally in aggregates.
(b) The components of reddish coarse-grained granite are quite large biotite aggregates, feldspar with many very fine-grained amphibole needle inclusions, quartz and two generations of garnets.
(c) Quartz monzonite has coarse grained microcline, finer grained plagioclase, some quartz, hornblende and biotite.
(d) Fine grained granite aplite.
(e) Metagranite(1) consists of fresh K-feldspar, sericitized and newly formed plagioclase, completely altered biotite and tourmaline.
(f) Metagranite(2) consists of quartz (dominantly), sericitized K-feldspar, sericite–muscovite and limonite.
MS values are generally low (<2.5 , maximum 5×10^{-3} SI)

4 Origin and Provenance, Preliminary Results

Despite the fact that research is still in a preliminary stage, it is possible to provide some indications regarding the geological sources of the lithotypes of the stone tools found at Gorzsa.

On the basis of their geology and petrological similarities to the raw materials of the stone tools, the Sava-Vardar Zone and the Apuseni Mountains, together with the Maros Valley, can be indicated as the possible sources of some andesite and other volcanites and dyke rocks, sandstones, granitoid–metagranitoid, dolerite–metadolerite–metagabbro, greenschist, amphibolite, chlorite schists and meta-ultrabasites.

The Banatite belt or other contact areas could be the source of hornfels; however, according to the archaeological distribution of the finds in Hungary and Serbia (Antonović 2006; Starnini et al. 2007b), we might be able to limit this area to the SE part of the Carpathian Basin. The Mecsek Mountains could be the source of lilac sandstone, basalt, alkaline magmatites, and acidic-intermediate dyke. The provenance of some andesite types might be the Börzsöny Mountains and the

Sub-Carpathian Volcanic Area. Szarvaskő (Eastern Bükk Mountains) is the possible provenance of dolerite–metadolerite–metagabbro. Finally, the Bohemian Massif can be indicated as the possible source of some of the greenschist.

5 Conclusions

Scientific investigations, aimed at determining the provenance of the Gorzsa polished and ground stone assemblage, were undertaken using petrographic and MS measuring techniques.

Studies of ceramics and chipped stone assemblages have shown that the people of Gorzsa had extensive cultural and economic interactions with neighbouring sites and archaeological cultures (Horváth 2005; Starnini et al. 2007a). The chipped stone assemblages demonstrate ongoing contacts with medium and long distance regions. Preliminary results from the studies of the polished and ground stone assemblage have suggested similar results. The identified

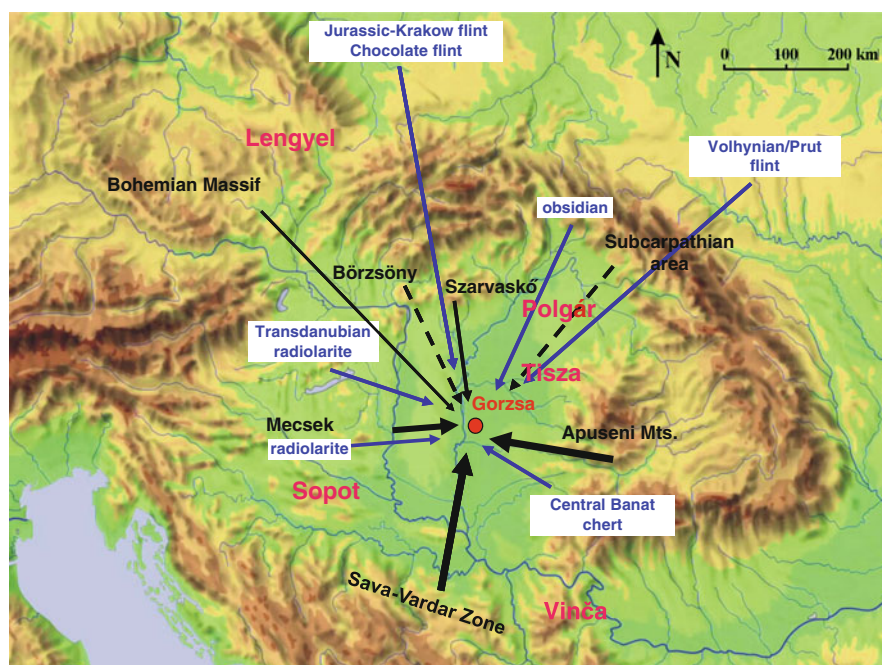


Fig. 3 Possible provenance of the raw materials (in black) of the polished stone tools: the thickness of the arrows is related to the major/minor occurrences of the rocks at Gorzsa. Possible raw material sources (in blue) of the chipped stone tools (Starnini et al. 2007a) and distribution of Late Neolithic cultures (in red)

possible provenance areas for most of the polished and ground stone artefacts are the Sava-Vardar Zone, the Apuseni and Mecsek Mountains; occasionally, raw materials or artefacts were imported from northern areas, such as the Börzsöny Mountains, Sub-Carpathian Area, Szarvaskő and Bohemian Massif (Fig. 3).

Acknowledgements Thanks are due to Sándor Józsa and Orsolya Friedel for their technical support. This research is conducted within the framework of the Intergovernmental Bilateral S&T Cooperation Program 2008–2010 between Hungary and Italy, and with the OTKA K62874 grant.

References

- Antonović D (2006) On importance of study of the Neolithic ground stone industry in the territory of Southeast Europe. *Analele Banatului, S.N., Arheologie – Istorie*, XIV(1):53–61
- Horváth F (2005) Gorzsa. Előzetes eredmények az újkőkori tell 1978 és 1996 közötti feltárásából. In: Bende L, Lőrinczy G (eds) *Hétköznapi Vénuszai*. Tornyai János Múzeum, Hódmezővásárhely, pp 51–83
- Kappameter (n.d.). *Field Rock Magnetic Susceptibility Meter, Kappameter KT-5, Instruction Manual*, Geofizika a.s., Brno, Czech Republic
- Starnini E, Voytek BA, Horváth F (2007a) Preliminary results of the multidisciplinary study of the chipped stone assemblage from the Tisza Culture site of Tell Gorzsa (Hungary). In: Kozłowski JK, Raczky P (eds) *The Lengyel, Polgár and related cultures in the Middle/Late Neolithic in Central Europe*. Polish Academy of Arts and Sciences, Krakow, pp 257–268
- Starnini E, Gy S, Whittle A (2007b) Polished, ground and other stone artefacts. In: Whittle A, Kovács G (eds) *The Early Neolithic on the Great Hungarian Plain: investigations of the Körös culture site of Ecsegfalva 23, Co Békés, vol XXI, Varia Archaeologica Hungarica*. Institute of Archaeology, Hungarian Academy of Sciences, Budapest, pp 667–676
- Williams-Thorpe O, Thorpe RS (1993) Magnetic susceptibility used in non-destructive provenancing of Roman granite columns. *Archaeometry* 35:185–195
- Williams-Thorpe O, Jones MC, Webb PC, Rigby IJ (2000) Magnetic susceptibility thickness corrections for small artefacts and comments on the effects of ‘Background Materials’. *Archaeometry* 42:101–108

Intra-site Obsidian Subsource Patterns at Contraguda, Sardinia (Italy)

R.H. Tykot, L. Lai, and C. Tozzi

1 Introduction

Obsidian sourcing studies have been done in the Mediterranean for more than 40 years, while in the last decade the importance of attributing artifacts to specific subsources has been demonstrated, as it reveals geographic and chronological patterns of obsidian usage. In particular, changes in the usage of the Monte Arci (Sardinia) subsources have raised questions about quality, quantity, access, and socioeconomic factors involved in the acquisition, production, trade, and use of obsidian during the Early, Middle, and Late Neolithic periods (ca. 6000–3000 BC).

In this study, nearly 250 obsidian artifacts from the Late Neolithic site of Contraguda in northern Sardinia were chemically analyzed by LA-ICP-MS and pXRF and attributed to specific Monte Arci subsources. This large number of analyses, at present the most done for a single site in Sardinia or Corsica, allows testing for subsource usage patterns from different contexts within the site, and provides some interpretations about obsidian selection and use.

2 Contraguda

The open-air site of Contraguda sits on a hill in the Coghinas Valley of northern Sardinia (Fig. 1). Used during the Late Neolithic, or the Ozieri period, this site extends over several hectares and is the largest Ozieri settlement known on Sardinia. Not only is the site one of the largest open-air sites from this time, but it is also one of the only open-air sites with obsidian artifacts.

This site was identified in 1980 during an archaeological survey that was conducted to identify and catalog archaeological features in the region. In 1992,

R.H. Tykot (✉) and L. Lai

Department of Anthropology, University of South Florida, Tampa, FL 33620, USA
e-mail: rtykot@cas.usf.edu

C. Tozzi

Dipartimento di Scienze Archeologiche, Università di Pisa, 56126 Pisa, Italy

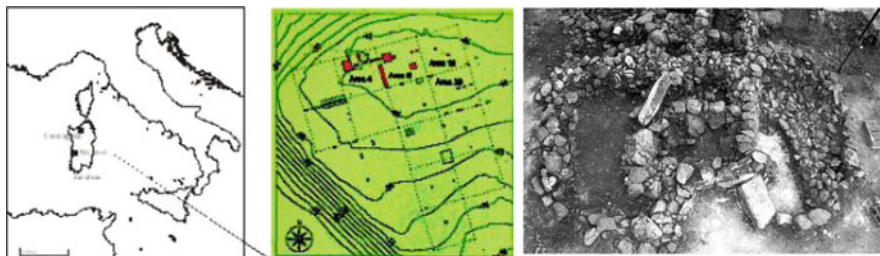


Fig. 1 Regional map showing location of Contraguda in northern Sardinia (*left*); detailed grid map showing the open-air archaeological site and the areas with obsidian artifacts tested (*center*); and a photograph of Structure A–B (*right*)

Boschian et al. (2000–2001) conducted a systematic investigation of Contraguda, with radiocarbon dates placing it in the fourth millennium BC, ca. 4050–3770 BC. The context of the obsidian tools are mainly later in the Ozieri period. Much of the obsidian was found outside of a feature, called Structure A–B, composed of a series of small, interrelated walls, which are of unknown function.

3 Monte Arci Obsidian

Previous work has identified many obsidian subsources on Monte Arci, with differences in their quantity, quality, and accessibility, while these subsources may be chemically distinguished using a variety of analytical methods (Tykot 1997; 2002). Chronological changes in the usage of the respective subsources has also been demonstrated for many sites in Sardinia and Corsica (Tykot 1996; 2004).

The main subsources are identified as SA, SB1, SB2, and SC, while SB1 and SC may be further subdivided into further subgroups. The SA and SB2 subsources, located on the southwest and west side of Monte Arci, respectively, have the glassiest, most transparent obsidian; the SC subsource is located on the northeast side of Monte Arci, is opaque and less brittle than the SA and SB2 obsidian, and appears to have been the major subsurface used in the Late Neolithic. Type SB1 obsidian, from the west-central part of Monte Arci, was rarely used in any time period, most likely because it exists only in modest quantities and in small blocks. Besides primary source localities, it is also important to note that unworked raw material may be found in secondary natural deposits, especially SC obsidian to the south of Monte Arci (Lugliè et al. 2006).

4 Analytical Methods and Results

For the Contraguda project, samples were initially categorized based on visual examination and density testing. This was followed by trace element analyses on a mostly random selection of 93 artifacts using laser ablation inductively coupled

Table 1 Portable XRF data for Contraguda obsidian artifacts tested, with assigned Monte Arci subsources. All elemental data are in ppm

USF#	Source	Fe	Rb	Sr	Y	Zr	Nb	USF#	Source	Fe	Rb	Sr	Y	Zr	Nb	USF#	Source	Fe	Rb	Sr	Y	Zr	Nb
2944	SA	8,006	190	25	29	77	33	3007	SA	8,690	201	24	29	78	35	3082	SA	8,653	198	25	29	82	37
2945	SC	10,225	124	99	19	190	20	3008	SC	11,904	134	111	21	192	20	3083	SC	12,467	142	133	18	214	20
2946	SA	7,707	185	24	24	71	31	3010	SC	11,487	142	115	21	213	24	3084	SC	11,791	138	116	20	211	23
2947	SC	10,808	139	106	21	204	19	3011	SC	11,716	142	121	22	219	23	3085	SC	12,132	144	124	21	217	24
2948	SA	7,425	176	24	29	76	35	3013	SC	11,599	139	110	22	216	21	3086	SC	12,366	152	121	20	220	24
2949	SC	11,573	137	116	20	201	21	3015	SA	8,801	201	24	27	81	35	3087	SC	11,556	144	116	22	218	25
2950	SA	9,099	210	25	27	84	37	3017	SC	10,783	130	111	20	198	22	3088	SC	11,505	149	113	22	213	23
2951	SC	11,649	142	109	18	207	22	3018	SA	8,043	191	26	24	77	32	3090	SC	13,562	144	118	18	200	20
2952	SC	10,796	134	109	20	196	21	3020	SA	9,064	214	26	28	81	36	3091	SC	12,139	143	113	20	204	20
2953	SA	8,440	200	27	27	86	34	3022	SC	11,557	148	114	17	206	23	3092	SC	11,328	139	116	22	209	24
2954	SC	11,365	140	110	19	203	21	3024	SA	9,781	218	28	29	80	34	3093	SC	10,834	136	103	19	196	20
2955	SA	9,147	210	27	30	84	37	3026	SC	11,485	138	112	21	206	22	3095	SC	12,223	146	115	19	223	22
2956	SC	11,372	131	113	21	198	20	3027	SC	10,907	134	108	20	199	21	3096	SC	11,669	140	120	21	214	21
2957	SC	11,494	137	112	21	204	23	3029	SB2	8,565	181	40	18	103	20	3097	SC	11,537	142	109	21	203	22
2958	SA	9,708	212	28	27	83	36	3030	SC	13,197	157	124	20	214	22	3098	SA	10,005	226	26	26	81	35
2959	SC	12,165	144	119	23	212	22	3032	SB2	8,168	189	39	16	119	20	3100	SC	11,747	143	118	21	222	22
2960	SC	11,265	137	111	22	208	25	3033	SC	12,273	140	117	20	203	19	3101	SC	13,846	167	123	19	213	20
2961	SA	8,681	200	25	27	83	35	3034	SC	11,489	140	108	21	193	22	3103	SA	8,196	215	27	29	78	36
2962	SC	8,669	114	92	17	160	17	3035	SB2	6,551	155	25	14	77	18	3104	SC	13,236	156	121	20	213	22
2963	SC	11,942	136	125	21	203	21	3036	SC	12,178	144	111	22	209	23	3105	SC	12,039	143	116	21	211	22
2964	SC	11,557	141	116	22	209	22	3037	SC	10,012	124	102	20	197	20	3107	SC	11,069	139	108	19	194	22
2965	SA	7,868	188	23	28	73	33	3038	SC	10,453	126	97	21	184	21	3108	SA	9,491	211	28	29	86	36
2966	SA	7,824	185	23	26	80	36	3039	SC	11,759	144	117	21	207	23	3109	SA	12,840	256	28	26	89	35
2967	SC	10,841	126	105	18	188	19	3040	SC	12,219	153	113	19	201	22	3110	SC	11,087	140	117	19	212	21
2968	SC	11,206	135	110	22	198	22	3041	SC	10,937	136	108	20	205	21	3112	SC	12,118	145	118	19	201	22
2969	SC	11,687	132	116	21	200	22	3043	SC	11,094	134	107	19	203	22	3113	SA	8,740	203	25	26	80	33
2970	SA	8,487	201	27	31	85	35	3044	SA	9,165	215	27	28	83	37	3114	SA	10,043	224	30	28	79	37
2971	SC	11,148	135	105	21	196	22	3046	SC	11,933	140	117	21	195	20	3115	SC	10,913	136	110	20	200	19
2972	SA	8,225	195	23	24	76	34	3048	SB2	7,691	174	26	15	78	18	3116	SC	10,996	131	108	22	194	22
2973	SC	12,274	145	121	21	219	23	3049	SA	8,344	201	25	27	77	34	3118	SC	11,454	132	118	21	198	19

(continued)

plasma mass spectrometry (LA-ICP-MS), at the University of Missouri Research Reactor (Lai et al. 2006; Speakman et al. 2007).

In this study, an additional 155 artifacts were tested using a Bruker Tracer III–V portable X-ray fluorescence spectrometer. This instrument, which is entirely non-destructive, was previously tested on geological samples to demonstrate that it could differentiate all of the Mediterranean sources and subsources. A specific “obsidian” filter (12 mil Al + 1 mil Ti + 6 mil Cu) was used to enhance results for certain elements known to be useful for sourcing obsidian, while the analysis settings chosen were 40.00 kV, 10.00 μ A, and 300 s. The results were calibrated against known obsidian samples used in multiple laboratories, including the Missouri University Research Reactor and the Smithsonian Institution (Table 1). Geological samples from all of the Monte Arci subsources were also tested with the exact same instrument.

It is fairly straightforward to distinguish chemically between the Monte Arci subsources, by LA-ICP-MS and pXRF, using simple X–Y plots of a few elements (Fig. 2).

The results clearly indicate that type SC obsidian is the most represented, while type SB2 is barely present (seven samples), and thus match with studies done for other Late Neolithic sites in Sardinia and Corsica (Fig. 3).

5 Discussion

The study of such a large collection of obsidian artifacts at the open-air Late Neolithic site of Contraguda is significant both for the methodological approaches used, which are non-destructive and of modest cost, and for the archaeological

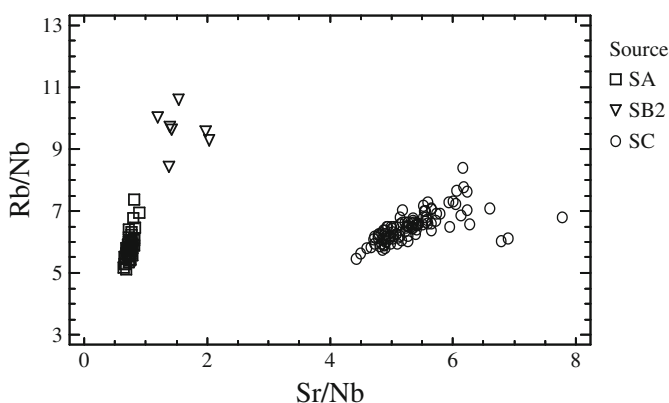


Fig. 2 Simple X–Y plot of rubidium/niobium (Rb/Nb) vs. strontium/niobium (Sr/Nb) for all of the Contraguda obsidian artifacts tested by pXRF, distinguishing between the three Monte Arci obsidian subsources (SA, SB2, SC)

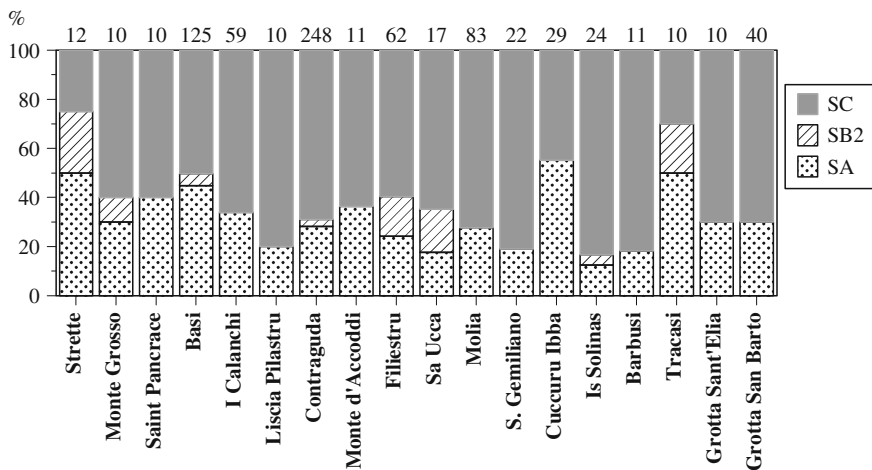


Fig. 3 Monte Arci subsources frequency at Late Neolithic sites in Corsica and Sardinia with ten or more chemical analyses done (number of samples on top of each bar)

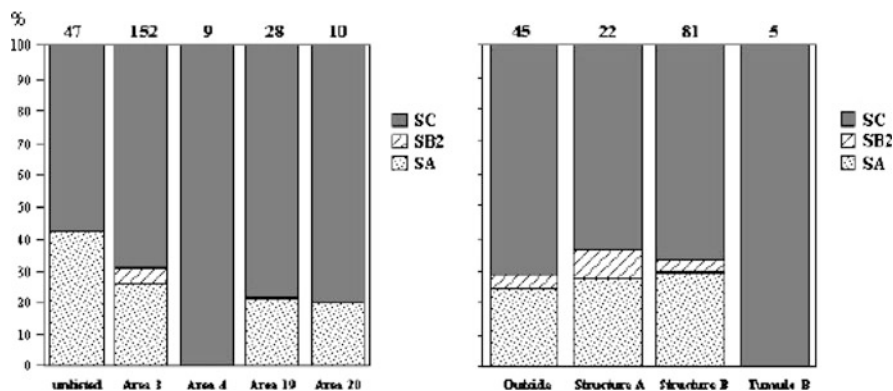


Fig. 4 Comparison of obsidian subsources present in different areas of the Contraguda site (left), and within Area 3 (right). The number of samples tested is at the top of each bar

significance of the findings. First, it is clear that a statistically significant number of samples should always be tested in order to reveal any patterns in obsidian acquisition, use, and discard. Use-wear studies on many of the obsidian samples tested already suggest that type SC obsidian was used for processing more hard inorganic materials than type SA, while SA was used to process more medium hard inorganic materials (Setzer et al. 2004). It has also been shown that density measurements and visual examination by experienced individuals can potentially provide a reasonable overview of Monte Arci obsidian subsources usage, especially the percentages of the SA and SC subsources. More significantly, the analysis of obsidian artifacts from different areas of the Contraguda site show some variation in subsources usage (Fig. 4). While the 47 general finds (from

localities outside Areas 3, 4, 19 and 20) from the site are approximately 42% SA and 58% SC, the four excavated Areas have much greater percentages of SC, especially Area 4 (albeit only nine artifacts tested).

The importance of selecting samples from specific site features is quite clear when we focus on Area 3, where there is the one structure found at Contraguda. Within Area 3, at the tumulus, there is a modest cluster (five pieces) of entirely type SC obsidian, comparable to the similar cluster in Area 4, while found within the other parts of Area 3 were all of the SB2 obsidian artifacts. The proportions of SA and SC are quite similar between all parts of Area 3 except for the tumulus, and have more SA represented than in Areas 19 and 20.

6 Conclusion

The analyses of such a large number of artifacts from specific contexts at a single site provide statistically significant data about obsidian subsource selection and use, which may be combined with lithic technology, use-wear studies, and other contextual information to reconstruct the chaîne opératoire for this important period in Sardinian prehistory. This type of detailed sourcing study, using non-destructive portable XRF analysis, may also make major contributions in other areas of Italy and beyond.

References

- Boschian G, Brilli P, Falchi P, Fenu P, Martini F, Pitzalis G, Sarti L, Tozzi C (2000–2001) Prime ricerche nell'abitato neolitico di Contraguda (Perfugas, Sassari). *Rivista di Scienze Preistoriche* 51:235–287
- Lai L, Tykot RH, Tozzi C (2006) Nuovi risultati sulla provenienza dell'ossidiana del sito neolitico recente di Contraguda (Sardegna). *Atti del XXXIX Riunione Scientifica dell'Istituto Italiano di Preistoria e Protostoria: Materie prime e scambi nella preistoria italiana*, Firenze, 25–27 Nov 2004, pp 598–602
- Lugliè C, Le Bourdonnec F-X, Poupeau G, Bohn M, Meloni S, Oddone M, Tanda G (2006) A Map of the Monte Arci (Sardinia Island, Western Mediterranean) Obsidian Primary to Secondary Sources. Implications for Neolithic Provenance Studies. *C R Palevol* 5:995–1003
- Setzer TJ, Tykot RH, Tozzi C (2004) Combining Obsidian Provenance and Use-wear Studies: an analysis of artifacts from the Late Neolithic Site of Contraguda, Sardinia. 34th international symposium on Archaeometry. Zaragoza, Spain, May 3–7
- Speakman RJ, Glascock MD, Tykot RH, Descantes C, Thatcher JJ, Skinner CE, Lienhop KM (2007) Selected applications of Laser Ablation Inductively Coupled Plasma-Mass Spectrometry Archaeological Research. In: Glascock MD, Speakman RJ, Popelka-Filcoff RS (eds) *Archaeological chemistry: analytical techniques and archaeological interpretation*, American chemical society symposium series. 968, Washington, DC, pp 275–296
- Tykot RH (1996) Obsidian procurement and distribution in the Central and Western Mediterranean. *J Mediterranean Archaeol* 9(1):39–82

- Tykot RH (1997) Characterization of the Monte Arci (Sardinia) Obsidian Sources. *J Archaeol Sci* 24:467–479
- Tykot RH (2002) Chemical fingerprinting and source-tracing of Obsidian: the Central Mediterranean trade in Black Gold. *Acc Chem Res* 35:618–627
- Tykot RH (2004) L'esatta provenienza dell'ossidiana e i modelli di diffusione nel Mediterraneo centrale durante il Neolitico. In: Castelli P, Cauli B, Di Gregorio F, Lugliè C, Tanda G, Usai C (eds) *L'ossidiana del Monte Arci nel Mediterraneo: recupero dei valori di un territorio*. Tipografia Ghilarzese, Ghilarza, pp 118–132

The Characterisation of Lime Plasters from Lamanai, Belize: A Diachronic Approach to the Study of Architectural Practices

I. Villasenor, E. Graham, R. Siddall, and C.A. Price

1 Introduction

This paper presents the micromorphological and compositional characteristics of architectural plasters from Lamanai dating from ca. 100 BC to the sixteenth century AD, as well as non-archaeological local raw materials. The study made use of petrography and X-ray fluorescence (XRF) for the analyses of 45 samples.

1.1 *Lamanai*

The site of Lamanai is located in the Orange Walk District of northern Belize, along the western bank of the New River Lagoon. Archaeological investigations are currently directed by Elizabeth Graham, University College London, and Scott Simmons, University of North Carolina Wilmington.

Lamanai was first inhabited perhaps as far back as 1500 BC. In contrast to sites in the central Petén, Lamanai was not abandoned at the end of the Terminal Classic period (AD 770-950/1000) but continued as a vibrant centre with its inhabitants carrying out important architectural programs and expanding the scope of long-distance trade and exchange (Pendergast 1990; Graham 2004, 2006, 2007). The site remained inhabited after the Spanish conquest, with some parts of the site occupied until the nineteenth century (Graham 2008; Pendergast 1985).

1.2 *Lime Production in the Maya Area*

Lime has been used in the Maya area since ca. 1100 BC (Hammond and Gerhardt 1990) and continues to be widely used until the present day. Lime plasters were

I. Villasenor (✉), E. Graham, R. Siddall, and C. Price
University College, London, UK
e-mail: m.villasenor@ucl.ac.uk

used abundantly in pre-Hispanic masonry architecture and most of the Maya Lowlands benefited from the availability of limestones in the Yucatan Peninsula.

Ethnohistorical accounts from the seventeenth century (Ruiz de Alarcón 1629), as well as recent ethnographic research (Schreiner 2002, 2003; Russell and Dahlin 2007), describe how lime production in Maya culture is associated with birth and fertility and lime itself is conceived as a young fertile woman. These studies also inform on the labour and material demands of this industry.

2 Characterisation of the Plasters

2.1 *Early Plasters*

The earliest lime plasters found at Lamanai date from the Late Preclassic, when the tallest structure, N10-43, was built. The bulk composition of these plasters, as obtained by XRF, proved to be highly calcareous, with more than 92% CaCO_3 in all cases, which corresponds to the composition of local limestones. The microscopic observation of samples from this period showed a calcareous non-hydraulic matrix with subrounded and angular particles of micritic calcite as the main aggregate material.

The subrounded aggregates correspond without any doubt to sascab, a calcareous sediment that comprises a range of particle sizes, from clays to boulders, which is formed by in situ weathering of limestones and which is abundant in the karstic terrain of the Maya lowlands. The microscopic examination of non-archaeological sascab collected from a quarry close to Lamanai showed the characteristic micritic nature of the sediments and their rounded edges. The same characteristics can be observed in the aggregates of the Lamanai plasters. The use of sascab as aggregate material in Maya plasters was also documented in the sixteenth century chronicles of Fray Diego de Landa (Pagden 1975).

The angular aggregates of micritic calcite observed in Late Preclassic plasters are probably fragments of crushed limestone that was incorporated in the plasters in order to obtain an interlocking effect, providing the plasters with better mechanical properties. Micritic limestones are found as raw materials in the site in the upper strata of the bedrock and date from the Upper Neogene or Lower Quaternary (McDonald 1978) (see Fig. 1).

Sascab continued to be used as the main aggregate material during the Early and Late Classic plasters, as can be seen by petrography. In addition to sascab, microscopic observations showed the clear presence of fragments of a previously painted plaster or stucco recycled as aggregate material in a Late Classic floor, sampled between Structures N10-78 and N10-79, both of which were part of Plaza Group N10[3]. The recycled fragments showed a red layer overlain by a blue/green layer, probably composed of Maya blue. Similar fragments of painted plasters have also been reported in fill material from the Terminal Classic and were originally part of a Late Classic stucco frieze that adorned Str. N10-28, which faced Str. N10-77 across the plaza (see Graham 2004).

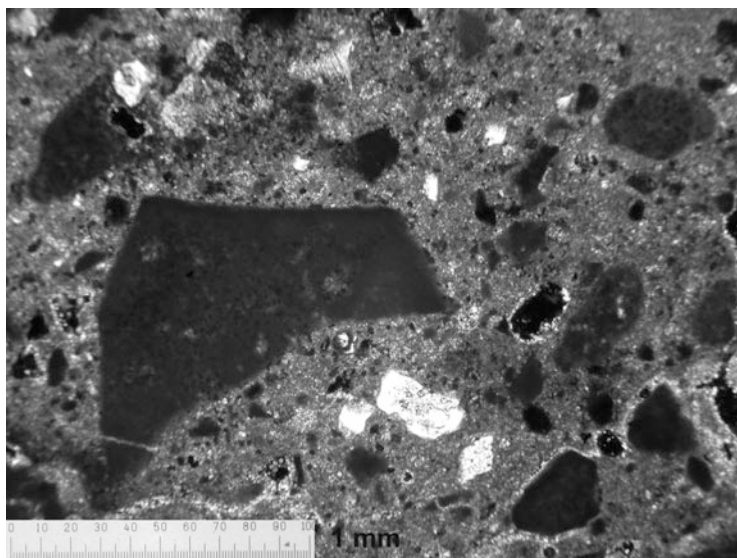


Fig. 1 Late Preclassic plaster showing small rounded aggregates of micritic calcite (sascab) to the *right*, and larger angular fragment (crushed limestone) at the *left*. Crossed polarised light, scale bar: 1 mm

2.2 The Terminal Classic Period: Quarrying Activities

In contrast to earlier periods, considerably larger aggregates made up of crystalline calcite prevailed over micritic calcite in the plasters from the Terminal Classic period onwards, as observed with microscopic examinations. These crystalline aggregates are probably related to the quarrying activities that took place during this period for the infilling of Plaza Group N10[3], which exploited hard crystalline limestones from the Cretaceous period, and which have been reported by Pendergast (1985) and Graham (2004). The numerous fragments of crystalline calcite, therefore, probably represent quarrying waste from these building works.

Considerable amounts of quartz are also visible in the plasters from the Terminal Classic period onwards, indicating a change in the procurement of raw materials in comparison to earlier plasters; quartz is however a common constituent of many types of stones and is therefore not diagnostic of any particular geology.

2.3 Postclassic and Spanish Colonial Periods

From the Late Postclassic period onwards, plasters show a higher content in silicon and aluminium in their bulk composition (up to 12% of SiO_2 and 6% in Al_2O_3), as shown by XRF analyses. This characteristic may indicate the deliberate exploitation

of siliceous materials in order to obtain moderate hydraulicity in the lime mixtures. Hydraulicity is the formation of calcium silicate and aluminate hydrates in the plasters, which result in increased mechanical properties, reduced porosity, and the ability of the plasters to set under water (see Moropoulou et al. 2000).

The deliberate production of moderately hydraulic plasters is also suggested by the observation of isotropic phases and angular fragments of devitrified glass, as well as a higher hardness in comparison to earlier plasters. The likely incorporation of volcanic materials to the plasters bespeaks an empirical knowledge of materials, while the exploitation of these deposits may have been favoured by the increased trade during the Late Postclassic period.

Principal component analyses of XRF data show that Late Postclassic and Early Spanish Colonial samples are dissimilar to the plasters of earlier periods and are located away from the local raw materials, which is most probably related to the incorporation of non-local raw materials in the plaster mixtures.

2.4 The Use of Tamped Sascab

In addition to the use of sascab as aggregate materials in the plasters, the silt and clay-size fractions of sascab were also used as tamped powder for the laying of floors during the Preclassic, Early and Late Classic periods at Lamanai. The characterisation of non-burnt tamped sascab is based on the microscopic examination of

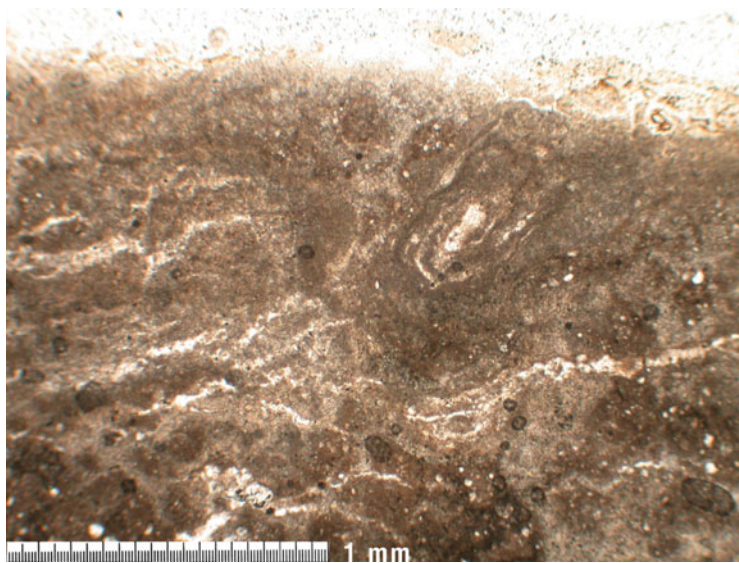


Fig. 2 Late Classic floor characterised as tamped sascab (unburnt calcareous sediments). Plane polarised light, scale bar: 1 mm

the samples, which showed masses of micritic calcite with cracks running parallel to the surface of the floors, and without the clear presence of aggregates or lime lumps (see Fig. 2). The construction of non-burnt sascab floors was apparently carried out without the use of burnt lime, and hardness was probably obtained solely by tamping the fine calcareous sediments when wet, as is still practiced today in the region for the construction of sascab roads.

The use of tamped sascab was observed only in floors, most likely because this material provides adequate performance characteristics for floors but not for wall renders or sculptures. The use of sascab represented a less energy-intensive construction technique for floors in comparison to lime plasters. Tamped sascab has also been reported by Brown (1986).

3 Conclusions

Lime plasters were used in Lamanai since the Late Preclassic period. During early periods, plasters were characterised by the use of local raw materials, such as sascab and crushed limestone.

From the Late and Terminal Classic periods, there is an increase in the size of aggregates and in the prevalence of crystalline calcite, which is probably related to the quarrying activities that were taking place at that time.

During the Late Postclassic and Spanish Colonial periods, volcanic materials seem to have been exploited deliberately, probably to obtain hydraulic properties in the plasters.

Compacted sascab (unburnt calcareous sediments) was also used as an alternative to lime plasters for the laying of floors, which was observed in many chronological periods.

Acknowledgments We thank Kevin Reeves and Philip Connolly, Archaeological Science Laboratories, UCL, for the assistance provided for the analysis of plasters. We are also grateful to Dr. Linda Howie, University of Western Ontario, Dr. Scott Simmons, University of North Carolina Wilmington, Dr. James Aimers, State University of New York at Geneseo, as well as Dr. David Pendergast, for their assistance with the sampling and the interpretation of the data. We also thank the Institute of Archaeology, NICH, Belize, for providing sampling and export permits of archaeological material. We finally thank CONACYT – Consejo Nacional de Ciencia y Tecnología, Mexico – and the Institute of Archaeology and Graduate School, UCL, for the funding provided.

References

- Brown GE (1986) Report on the examination of mortars from Lamanai. Unpublished report submitted to the Archaeological Project of Lamanai, Belize
- Graham E (2004) Lamanai reloaded: alive and well in the Early Postclassic. In: Awe J, Morris J, Jones S (eds) Paper presented at Archaeological investigations in the Eastern Maya Lowlands: Papers of the 2003 Belize Archaeology Symposium

- Graham E (2006) An ethnicity to know. In: Sachse F (ed) *Maya ethnicity: the construction of ethnic identity from Preclassic to modern times*, Acta Mesoamerica, vol 19. Verlag Anton Saurwein, Markt Schwaben, pp 109–124
- Graham E (2007) Lamanai, Belize from collapse to conquest: radiocarbon dates from Lamanai. 106th Meeting of the AAA. 28 November to 2 December, Washington, D.C
- Graham E (2008) Lamanai historic monuments conservation project: recording and consolidation of New Church architectural features at Lamanai, Belize. Report submitted to FAMSI, Foundation for the Advancement of Mesoamerica. Available at: <http://www.famsi.org/reports/06110C/06110CGraham01.pdf>. Accessed on Sep 2009
- Hammond N, Gerhardt JC (1990) Early Maya architectural innovation at Cuello, Belize. *World Archaeol* 21(3):461–481
- McDonald R (1978) Preliminary report on the physical geography of Northern Belize. In: Cuello Project 1978 Interim Report. Archaeological Research Program, Douglass College, Rutgers University, New Brunswick, pp 79–87
- Moropoulou A, Bakolas A, Bisbikous K (2000) Investigation of the technology of historic mortars. *J Cult Herit* 1(1):45–58
- Pagden AR (1975) *The Maya*. Diego de Landa's account of the affairs of Yucatán. J. Philip O'Hara, Chicago
- Pendergast DM (1985) Stability through Change: Lamanai, Belize, from the ninth to the seventeenth century. In: Sabloff JA, Andrews EW (eds) *Late lowland Maya civilization, Classic to Postclassic*, A School of American Research Book. University of New Mexico Press, Albuquerque
- Pendergast DM (1990) Up from the dust: the central lowlands Postclassic as seen from Lamanai and Marco Gonzalez, Belize. In: Clancy FS, Harrison PD (eds) *Vision and revision in maya studies*. University of New Mexico Press, Albuquerque, pp 169–177
- Ruiz de Alarcón H (1629) *Treatise on the heathen superstitions that today live among the indians native to this New Spain, 1629*. (Trans and ed Andrews JR and Hassig R). The civilization of the American Indian series. University of Oklahoma Press, Norman
- Russell BW, Dahlin BH (2007) Traditional burnt-lime production at Mayapán, Mexico. *J Field Archaeol* 32:407–423
- Schreiner T (2002) *Traditional Maya lime production: environmental and cultural implications of a native American technology*. PhD thesis. Department of Architecture, University of California, Berkeley
- Schreiner T (2003) Aspectos rituales de la producción de cal en Mesoamérica: evidencias y perspectivas de las tierras bajas mayas. paper presented at Simposio de Investigaciones Arqueológicas en Guatemala, 2002. pp 480–487

Provenance Studies of Midwestern Pipestones Using a Portable Infrared Spectrometer

S.U. Wisseman, T.E. Emerson, R.E. Hughes, and K.B. Farnsworth

1 Introduction

Affordable, portable, and non-destructive instruments that work equally well in the field and in the lab are rare. For several years, our team of archaeologists and geologists at the University of Illinois has been using a Portable Infrared Mineral Analyzer (PIMA) along with X-ray diffraction and selected chemical techniques to determine the types and origins of pipestones used to make prehistoric North American figurines and pipes (Emerson and Hughes 2000).

The PIMA is an instrument first used by Australian geologists to locate precious metals, assess ore quality, study the degree of crystallinity of minerals, and to map zones of alteration in rocks changed by hydrothermal processes. This shoebox-sized, non-destructive instrument can be operated in the field or in a museum setting. PIMA spectroscopy is an excellent precursor to standard laboratory analyses by the complementary technique of X-ray diffraction or more costly elemental techniques such as neutron activation analysis.

The PIMA requires no sample preparation if a small, preferably flat, surface of the sample can be brought up to the 1-cm diameter window of the instrument. The PIMA uses the short wavelength infrared part of the electromagnetic spectrum (from 1,300 to 2,500 nm) and measures the reflected radiation from the surface of

S.U. Wisseman (✉)

Illinois Transportation Archaeological Research Program, University of Illinois, Urbana-Champaign, IL, USA

and

Program on Ancient Technologies and Archaeological Materials, University of Illinois, Urbana-Champaign, IL, USA

e-mail: wisarc@illinois.edu

T.E. Emerson and K.B. Farnsworth

Illinois Transportation Archaeological Research Program, University of Illinois, Urbana-Champaign, IL, USA

R.E. Hughes

Illinois State Geological Survey, University of Illinois, Urbana-Champaign, IL, USA

a sample, part of which is absorbed by the sample. These absorption features reveal the inter-atomic bond energies characteristic of specific minerals, particularly those with hydroxyl, carbonate, or phosphate bonds. Some examples are clay minerals (e.g. kaolinite), carbonates (e.g. calcite), and phosphates (e.g. apatite). Archaeologically, this means stone and low-fired clay artifacts, corrosion products, bone, and restoration materials such as plaster and shellac (Wisseman et al. 2002, 2004).

The PIMA instrument can be held either horizontally or vertically and has exposure settings that compensate for small sample areas and dark samples. A reading takes only 30–60 s, allowing the rapid collection of many analyses. Measurements can be made on whole or partial artifacts, sherds, rock chips, thin sections, powders, soil and sediments, and cores.

Pipestone is a generic term for fine-grained, carvable metamorphic rocks such as argillite, flint clay, and catlinite. Flint clay is a tough, smooth, nonplastic usually kaolinitic claystone, while catlinite is characterized by a dominance of pyrophyllite and muscovite, sometimes with kaolinite and often with traces of diaspore.

Usually red, such pipestones were employed by several different native cultures in the American Midwest to manufacture high-status, often sacred items such as effigy pipes and “red goddess” figurines. Until recently, the best known pipestone sources were quarries in Ohio and Minnesota (Fig. 1).

In traditional procurement and exchange models, people seek “exotic” materials from distant sources to make high prestige items and reserve local materials for the manufacture of utilitarian objects. In examining several cases studies of pipe manufacture and distribution in Pre-Columbian eastern North America, we find these theories fall short of explaining actual quarry use and the complexity of the production and consumption revealed in the archaeological record (Emerson et al. 2003, 2005).

1.1 Hopewellian Pipes

One case study focused on Hopewellian pipes dating to the Middle Woodland period (ca. 50 BC–AD 250). During that period, Ohio was supposedly the center for a pipe exchange system that covered most groups east of the Mississippi River. We began with XRD studies of whole pipes and pipe fragments and raw materials from Ohio and also a previously unknown source near Sterling, Illinois. Once the raw materials were characterized and the constituent minerals quantified, we took high-quality PIMA spectra from the same samples. The result is a reference library of typical Midwestern pipestone types (Figs. 2 and 3).

Our combined analyses demonstrate that, contrary to popular belief, Hopewellian craftsmen working at Tremper Mound, Ohio, did not produce all of their pipes from the nearby Feurt Hill pipestone quarries. In fact, only about 15% of the pipes were made from local rock; 85% of the pipes were produced from northwestern Illinois and Minnesota pipestones.

On the other hand, 97% of the pipes found at nearby Mound City National Monument were made from local rock. The Ohio pipestone quarries, only a mile

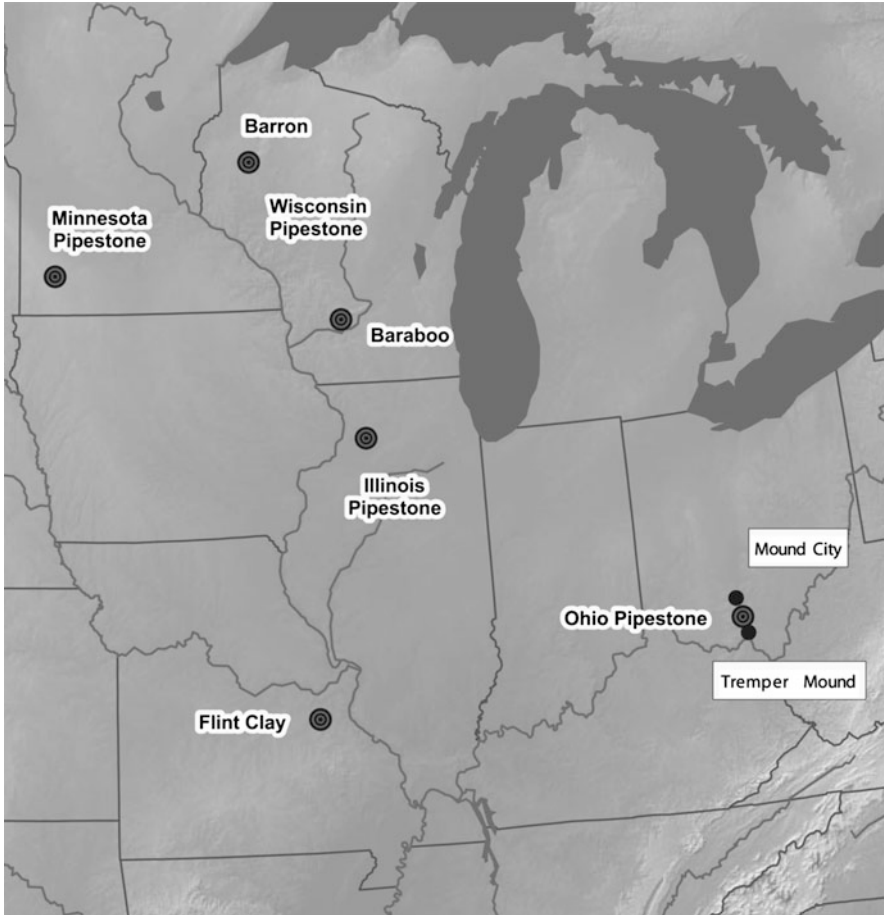


Fig. 1 Map of Midwestern pipestone sources

or two from Tremper, saw minimal use during the Middle Woodland period but were used sporadically 1,000 years later during Fort Ancient times. The same quarries have been used to make fake Hopewell pipes in modern times.

1.2 *Catlinite*

In the past, many red pipestones were labeled “catlinite,” but our results confirm that true catlinite came from a single source: the quarries at Pipestone National Monument (PNM) near the town of Pipestone in southwestern Minnesota.

The Minnesota quarries, considered a sacred site by many Native Americans, were not used continuously over time. Historical and archaeological evidence

Fig. 2 Typical PIMA spectra for Midwestern pipestones (“Barron Co.” and “Baraboo” pipestones are from Wisconsin; “catlinite” is from Minnesota)

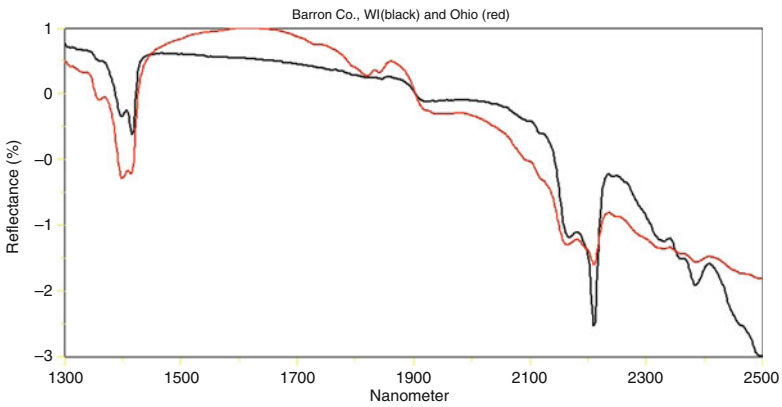
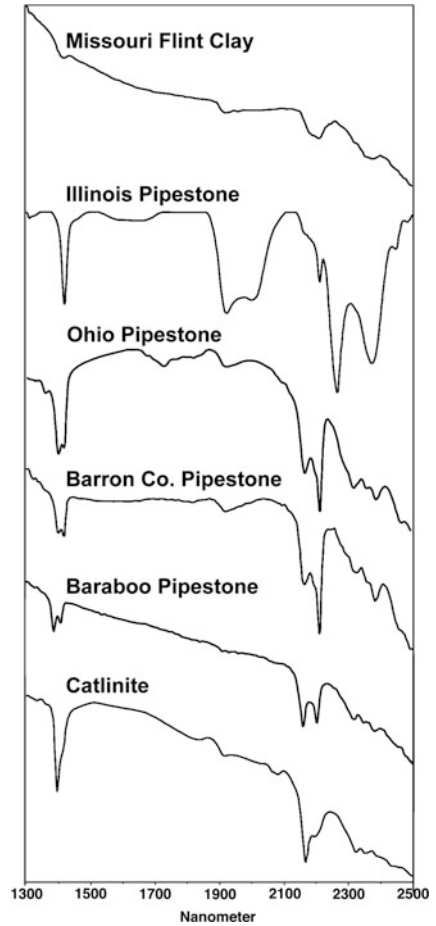


Fig. 3 Overlay of PIMA spectra for Barron Co., Wisconsin (*black*) and Ohio (*red*) pipestones. Note the differences in absorption features at 1,400, 1,818, and 2,200 nm

shows that they were used briefly during the Middle Woodland period, were virtually abandoned during Mississippian times, and heavily used after ca. AD 1300. Most of the historic period “red peace pipes” that commonly appear in early travelers’ accounts and in modern museums were made from catlinite.

Our PIMA work at Tremper Mound revealed two variants of catlinite: “A” with subequal pyrophyllite and muscovite, and “B” with two or three times as much pyrophyllite as muscovite. Both variants are distinctly different from Ohio pipestone (Fig. 2).

We have now taken PIMA readings from numerous rock samples from different parts of Pipestone National Monument, originally collected by J.N. Gundersen and now housed at the National Park Service center in Nebraska.

Preliminary analyses of Gundersen’s samples show more within-quarry variation than expected. For example, in Quarry 15, which is in the lower unit of the southern quarry, PIMA sample 5178a shows a catlinite B spectrum on the “light side” and a catlinite A spectrum on the “diagonal fracture” of the same piece. Mineralogically, the difference is that the fracture zone contains more muscovite than the “light side.”

There are many other examples from the quarries at Pipestone National Monument that show similar variation. However, sometimes different colors or observed weathering on two sides of the same rock sample do *not* produce different PIMA spectra (for example, the “red” and “cream” faces of a sample in quarry 34 both produce good catlinite B spectra).

The A and B variations of catlinite are a result of either (1) the original potassium content in the paleosol, and/or (2) the penetration by potassium-rich hot fluids during metamorphism. Some of the catlinite layers at PNM are quite thin, presumably with quartzite deposits in between. We notice that archaeological samples, catlinite pipes, are often thin in one dimension. Further analyses of these pipes may show how differences between the top and bottom of specific beds are reflected in the artifacts.

1.3 Mississippian Figurines

Another case study focused on the large “red goddess” stone figurines crafted by twelfth century AD Mississippian peoples at the site of Cahokia, near St. Louis, Missouri (Fig. 4).

These are some of the most spectacular prehistoric works of art in North America. Examples of these figurines and effigy pipes have been found in archaeological sites within an area stretching from Wisconsin to Mississippi and from Oklahoma to Alabama. Representing both mythological and real individuals, these artifacts are a rich source for understanding Mississippian symbolism, iconography, lifestyles, and sources and distribution of raw materials.

X-ray diffraction and PIMA analyses show that the pipestone used by Cahokia artisans matches flint clay from a quarry near St. Louis. This pipestone has a distinctive

Fig. 4 Keller figurine, Cahokia site, twelfth century A.D. (courtesy of ITARP)



combination of lithium bearing chlorite, abundant boehmite (an aluminum oxyhydroxide) and a heavy-metal phosphate mineral suite.

First, we tested all the figurines recovered from the site of Cahokia. In 17 out of 24 instances, PIMA and XRD confirmed that the source was Missouri flint clay. We observed some slight differences in the spectra taken from burnt versus unburnt artifacts.

Then, we tested Cahokia-style figurines found at sites in the Arkansas River Valley of Oklahoma, the Red River valley of Louisiana, and other sites in Arkansas, Mississippi, Alabama, and Tennessee. Over 175 PIMA spectra were taken from 12 figurines, drilled figurines, and figure pipes; 156 of these spectra confirm that all but one figurine was made from Missouri flint clay.

Our conclusion is that many Cahokia figurines previously thought to have been made from Arkansas or Minnesota pipestones were in fact made from Missouri flint clay. Furthermore, unlike other pipestone quarries, the Missouri quarry was apparently used only for a single 100-year period in the twelfth century.

1.4 Other Pipestone Sources

In addition to the Ohio, Northern Illinois, and Minnesota sources, we have also characterized sources in Wisconsin (Barron and Baraboo counties) and one in

Kansas. Although some spectra initially look similar, careful comparison shows crucial differences. For example, if the spectra for Ohio and Wisconsin pipestones are stacked together (Fig. 3), we observe differences in depth and symmetry of the absorption features near 1,400 and 2,200 nm. These kaolinite-rich pipestones have completely different geological origins, which give rise to subtle structural and crystal size differences that are revealed in the spectra.

1.5 Museum Applications of PIMA

As we tested figurines across the Eastern U.S., we discovered another PIMA application: distinguishing between original material and gypsum plaster restorations.

One of the most intricate and unique Cahokia figurines is the Conquering Warrior pipe recovered by commercial looters of the Spiro site in eastern Oklahoma, now in the Smithsonian Institution in Washington, D.C. The main figure represents a standing man wearing a thick headband, a knee length kilt, heavy arm and leg bands, and armor on his chest and back. He is bending over and appears to be in the midst of “decapitating” a smaller figure crouched between his feet. The heavily fragmented piece was restored and colored, making it impossible to distinguish between original fabric and added materials.

Thirteen PIMA spectra verified the originality of portions of the base and of the primary warrior’s arm, forehead and headdress, left shoulder, right elbow, and hairstyle. Three distinctive plaster spectra suggested that features of the warrior’s kilt, the victim’s back, and the base were reconstructions.

2 Conclusions

PIMA spectroscopy is a valuable technique for mineralogical characterization, especially when combined with X-ray diffraction. Our analytical approach has allowed us to locate and characterize previously unknown sources of North American pipestone, and to define variation both between sources and within individual quarries such as Pipestone National Monument. Now that a solid reference database of pipestones is established, PIMA can be used as a stand-alone technique to match museum artifacts that cannot be destructively sampled with raw material sources.

References

- Emerson TE, Hughes RE (2000) Figurines, flint clay, the Ozark Highlands, and Cahokian acquisition. *Am Antiq* 65(1):79–101
- Emerson TE, Hughes RE, Hynes M, Wisseman SU (2003) The interpretation and sourcing of Cahokian Figurines in the Trans-Mississippi South and Southeast. *Am Antiq* 68(2):287–313

- Emerson TE, Hughes RE, Farnsworth KB, Wisseman SU, Hynes M (2005) Tremper mound, Hopewell Catlinite, and PIMA technology. *MidCont J Archaeol* 30(2):189–216
- Wisseman SU, Moore DM, Hughes RE, Hynes M, Emerson TE (2002) Mineralogical approaches to sourcing Pipes and Figurines from the Eastern Woodlands, USA. *Geoarchaeology* 17(7): 689–715
- Wisseman SU, Emerson TE, Hynes M, Hughes RE (2004) Using a portable spectrometer to source archaeological materials and to detect restorations in museum objects. *J Am Inst Conserv* 43(2):129–138

Application of Micro-CT: 3D Reconstruction of Tool Marks on an Ancient Stone Bead and its Implication for Jade Drilling Techniques

Y. Yang, M. Yang, Y. Xie, and C. Wang

1 Introduction

China has a long and splendid history of working jade; thus, the presence of a jade culture is one of the main features distinguishing the ancient Chinese culture from other ancient civilizations. In Chinese language, the definition of jade has both a broad and a narrow sense, the broad sense meaning “beautiful stones”, and the narrow sense referring to nephrite and jadeite.

The carving techniques of jade show the integration of ancient mechanical processing technologies in China. Of these, the perforations on jade and the related drilling technology from the Neolithic Age are especially mysterious and charming.

As compared to ancient Chinese ceramics, glass and metallurgy, involving chemical processes, much less is known about the mechanical process of jade carving. In general, the main carving procedures include: sawing, drilling, riffling, filing, grinding, cutting and polishing.

Drilling and grinding technology in China can be traced back to the later period of the Paleolithic Age. In the Zhoukoudian Site (Beijing, about 27,000 BP) of Shandingdong Culture, perforated or polished animal bone artifacts had been excavated (Li 1987; Pei 2002). In the early period of the Neolithic Age, after jade was separated from stone artifacts, different types of perforations were needed, due to the specific requirements associated with the jade’s shape and related decoration, thus promoting the development of drilling technology. A large number of jade objects with diverse shapes and perforations were excavated from many

Y. Yang (✉) and C. Wang

Department of Scientific History and Archaeometry, Graduate University of Chinese Academy of Sciences, Beijing, China

e-mail: yiminyang@gucas.ac.cn

M. Yang

School of Mechanical Engineering and Automation, Beijing University of Aeronautics and Astronautics, Beijing, China

Y. Xie

Institute of Archaeology of Shanxi Province, Shanxi Province, China

archaeological sites. According to the general opinion of scientists, there existed at least three drilling methods in the Neolithic Age: awl drilling without the aid of a machine, solid and tubular drilling, depending on the mechanical rotation (Kong 2007).

Because records or discoveries of ancient drilling tools are rare, research on drilling technology depends mainly on understanding tool marks found on the inner walls of perforations. Until now, there are two methods employed for the study of these marks. One method entails examining the perforation directly under the optical microscope or SEM with oblique view, while the other consists of making negative silicone rubber casts of perforations, which are subsequently examined (Gorelick and Gwinnett 1983; Stocks 1993; Sax and Meeks 1995). For big perforations, there is no difficulty in inspecting them directly; however, for small perforations, only partial areas of the inner wall near the opening can be examined directly, and it is also difficult to obtain the corresponding negative cast. The difficulty of observation prevented further analysis on drilling techniques employed for small perforations; this aspect thus calls for a new methodology to be developed in order to disclose drilling marks.

When detailed information is needed on the internal structure of objects in non-destructive mode, Computed Tomography (CT) scanning with three-dimensional reconstruction can often provide a solution. Recently, this method was successfully applied in archaeology (Ryan and Milner 2006; Coppa et al. 2006; Wang and Yang 2007). However, for clinical or common industrial CT, the spatial resolution ranges from tens to hundreds of microns, which is insufficient for disclosing tool marks. In recent years, Micro-CT (μ CT) scanning with higher resolution ($<10\ \mu\text{m}$) has become accessible, and some work using this technology has been carried out in archaeology. These studies provided us with the inspiration to use μ CT for reconstructing small perforations, in order to clearly display drilling tool marks. The present work demonstrates the validity of this initiative.

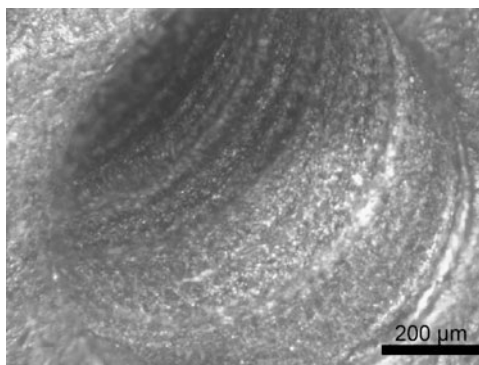
2 Sample

The sample originated from one tomb of the graveyard of the “Peng” Nation, Western Zhou Dynasty (1046–771 BC). A black perforated bead with a length of 3 mm, outer diameter of 2.5 mm, and perforation diameter of 1.6 mm was selected and confirmed as talc by XRD and XRF.

3 Experimental Methodology

Before carrying out any experiments, the bead was cleaned in a supersonic water bath, in order to wipe off any traces of attached soil.

Fig. 1 Oblique view of the perforation opening under a digital microscope



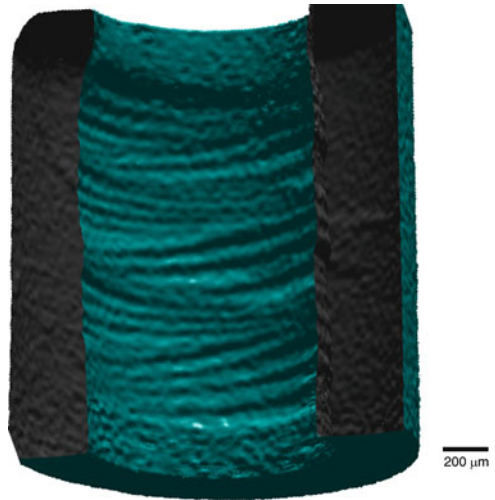
A digital microscope (VHX-500K, Keyence, Japan) was used to observe this stone artifact. The perforation is perfectly circular (the roundness is 1.02, computed in Image Pro Plus 6.0), indicating that the craftsman could not have directly held an awl in order to drill. Instead, this perforation must have been drilled by rotation, and solid drilling appears more likely because of the small diameter. By an extension of field technology, the digital microscope has a large depth of field with increased magnification, having a similar effect to an SEM. In oblique view, circular grooves on the inner wall just near the opening (Fig. 1) could be clearly seen. It is clearly difficult to describe the direction and distribution of the circular grooves, and it is also difficult to obtain a negative cast due to the small diameter of the perforation. Thus, as the information regarding the drilling was not clear, this sample was chosen for μ CT scanning.

This bead was scanned by μ CT at the Chinese Academy of Engineering Physics, Mianyang City, Sichuan Province. A cone beam of X-rays was directed at the object with source energy settings of 160 kV, and 551 cross-sectional images were obtained, with magnification levels up to $50\times$. The actual spatial resolution was $3.971\ \mu\text{m}$. The scanning data were imaged and analyzed using the Mimics 10 software (Materialise, Belgium). The reconstructed virtual 3D model can be adjusted to any angle, which made it convenient to find the most suitable observation angle.

4 Results and Discussion

Comparing the virtual model with the optical photo, the image of the microwear appears to be the same, and so the model does indeed present real details of the bead. When the model was sectioned in half, the inner wall was exposed, and this allowed the best possible view (see Fig. 2). In this image, the tool marks were displayed clearly – left and right circular grooves distributed alternately, with angles that change dramatically. Each direction included four or five rotations,

Fig. 2 The half-sectioned virtual model



each of which advanced further with approximately 100 μm . The alternate spiral direction demonstrated that the drill changed its rotary direction regularly in the drilling procedure, indicating a conversion of linear motion into rotary motion. Furthermore, the rotation axis was unstable. These phenomena were more similar to those associated with hand-held drills turned between the palms rather than to those related to a bow drill.

Not only was μCT successfully applied on a soft stone, as described in the present paper, but it could also be used in analyzing hard stones, according to physical theory. In fact, one agate and one jadeite, drilled by supersonic drilling or electric drilling, were also successfully scanned and visualized. However, because the selected agate and jadeite had bigger size, the resolution decreased into 25 μm and 12 μm respectively. Evidently, a higher resolution will guarantee a better quality of the reconstruction. In the future, we firstly choose smaller perforated hard stones to analyze; then we plan to develop a new algorithm for bigger samples, only scanning a chosen Region of Interest, and carrying out a local reconstruction of perforations. This procedure will allow maintaining a higher resolution.

5 Conclusion

In conclusion, drilling technology represents one of the most complex jade carving techniques. For small and long perforations, made with the more advanced technology available in the Neolithic, it is nearly impossible to observe drilling marks by using the microscope. Thus, 3D reconstruction of a drilled area using μCT could be an exclusively effective method for clearly exposing drilling marks, making

possible the advancement of our understanding of ancient drilling technology in the future.

Acknowledgements We would like to thank Janet G. Douglas, Freer Gallery of Art/Arthur M. Sackler Gallery, Smithsonian Institution, Washington DC, for her helpful comments. This work was supported by the Chinese Academy of Sciences, Grant KJCX3.SYW.N12, and the Talent Fund of the Graduate University of CAS.

References

- Coppa A, Bondioli L, Cucina A et al (2006) Early Neolithic tradition of dentistry: Flint tips were surprisingly effective for drilling tooth enamel in a prehistoric population. *Nature* 440:755–756
- Fu'an Kong (2007) The study of technology of Chinese ancient Jade producing. Doctoral Dissertation, Shanxi University, China
- GenPan Li (1987) The economy of primal society in China. China Social Sciences Press, 190
- Gorelick L, Gwinnett AJ (1983) Ancient Egyptian stone drilling. *Expedition* 25:40–47
- Pei W (2002) The culture of Shandingdong in Zhoukoudian site (Chinese abridgment). *Stories Relics* 2:1–7
- Ryan TM, Milner GR (2006) Osteological applications of high-resolution computed tomography: a prehistoric arrow injury. *J Archaeol Sci* 33(6):871–879
- Sax M, Meeks ND (1995) Methods of engraving Mesopotamian quartz cylinder seals. *Archaeometry* 37:25–36
- Stocks DA (1993) Making stone vessels in Ancient Mesopotamia and Egypt. *Antiquity* 67:596–603
- Wang Changsui, Yang Yimin, Yaowu, (2007) Current status and expectation for the study of Chinese ancient materials. *Scientific Research of Culture Relics*. vol 5

Non Destructive In Situ Study of Mexican Codices: Methodology and First Results of Materials Analysis for the Colombino and Azoyu Codices

S. Zetina, J.L. Ruvalcaba, M. Lopez Cáceres, T. Falcón, E. Hernández, C. González, and E. Arroyo

1 Introduction

Little is known about manuscript writing and painting practices in pre-Hispanic Mesoamerica. Around the world, only 16 codices from pre-Hispanic Mexico survived the Spanish conquest, most of them preserved in European collections. Even though the manufacture of codices was widespread during the post-Classical period (1325–1521 AD), the features of the surviving pre-Hispanic and Early Colonial documents show some technical differences that can be related to local traditions. The only pre-Hispanic codex held at a Mexican Collection is the Colombino Codex from the Mixtec coast in the south of Mexico. Nevertheless, many manuscripts produced in New Spain preserved the indigenous codices traditions and practices. These manuscripts are an outstanding information source in terms of the materials used in the writing and colouring traditions. Usually, organic colours obtained from local plants and carbon inks on calcium-rich preparation layers were employed. However, there are few studies of original manuscripts, carried out on a limited number of samples (Gonzalez Tirado 1998), and scarce information has been made available on this subject to date.

In the present research, a specific non-destructive methodology has been developed for carrying out a first in situ general examination of the codices and an analysis of the inks, dyes and pigments used. In particular, this work represents a comparative study between the pre-Hispanic codex Colombino and the colonial codex Azoyu I. Previously, the colonial codex de la Cruz-Badiano has been studied using the same methodology (Zetina et al. 2008). The Colombino codex (circa

S. Zetina, T. Falcón, E. Hernández, and E. Arroyo
Instituto de Investigaciones Estéticas UNAM, Mexico City, Mexico

J.L. Ruvalcaba (✉)
Instituto de Física, Universidad Nacional Autónoma de México (UNAM), Mexico City, Mexico
e-mail: sil@fisica.unam.mx

M. Lopez Cáceres and C. González
Biblioteca Nacional de Antropología e Historia, INAH, Mexico City, Mexico

twelfth century AD) tells the history of the Mixtec lord Eight Deer Jaguar Claw (Carrasco 2001). The support is animal skin, sewn with an agave thread. One side of it was prepared for painting with a thick polished white ground. Colours were applied mainly saturated and flat on sharply defined areas. The proportion and regularity of the figures is constant. The colour palette is reduced: blue, green, red and yellow, which are used saturated and diluted, a bright orange, which has almost completely disappeared, found only in few details; and black, in transparencies, and more opaque for the contour lines.

On the other hand, the Azoyu I codex was produced during the sixteenth century AD. The front section presents a historical account of the Guerrero region during the reign of Tlachinollan Caltitlan between 1300 and 1565 AD according to the pictographic tradition. In the Tlapa region, Nahuatl, Mixtec and Tlachinollan people coexisted as they do today. In 38 pages, the document describes the conquest of about 20 places located in eastern Guerrero. One folio shows words written in the Latin alphabet (23r). The support is an amate paper (made from an indigenous bark) screen folded in 28 pages. The historical section, the most antique, covers the obverse. A calendaric frame delimits each page; the squares at the centre contain historical pictographs, and were prepared with a slight wash applied over the surface of the paper before painting. Pink, red, orange, brown, yellow, black and grey, blue–green and green, were found, in pale shades. Over the reverse, a genealogical section is depicted in 11 pages, and due to its style it is considered more recent than the other section. The painting technique is quite similar in this second section. Finally, there is a third later addition, a cartographic and economic section with iron-gallic ink notes.

2 Methodology

First, all the documents were digitally photographed after light calibration. We used fluorescent illumination and an EyeOne X-Treme spectrophotometer from X-Rite in order to measure colour temperature at 5,700 K. All the photographs were taken with a digital camera Nikon D2× having a 50 mm objective. Limited UV examinations were carried out with a low power 8 W UV lamp with long and short waves (365 and 254 nm, respectively). All the images were recorded by digital photography. Also, IR reflectography was performed with a lead sulphide vidicon tube (Hamamatsu C2741), with a sensibility range from 400 to 1,800 nm and led array lighting (at 940 nm). IR images were obtained by a digital shot directly to the monitor.

In order to interpret the IR and UV images of the codex, a comparison with material references of pigments, dyes, inks and other materials commonly used in manuscripts and illuminations was fundamental. Reference standards were prepared on 100% cotton paper with carboxymethyl-cellulose used as binder. Under IR illumination, gypsum has a brilliant appearance, but iron-gall inks have a medium absorbance, and iron oxides – earth pigments – appear very opaque.

In contrast, different dyes prepared as lakes or fixed into clays look transparent to different degrees. Under UV lighting, gypsum had a bright violet fluorescence, while the lakes, cochineal and achiote plant colours showed some type of bright fluorescence. Iron oxides and iron gall inks (even mixed with cochineal) appeared opaque under UV. After proceeding with imaging techniques, the manuscripts were analysed using our SANDRA XRF portable system. This device has a 75 W Mo X-ray tube. Two sets of measurements were carried out by CZT and Si-PIN X-ray detectors. The CZT detector is more suitable for pigment analysis and medium and heavy elements, while the Si-PIN detector may detect lighter elements. The measuring time was 90 s at 40 kV and 30 mA, with an X-ray spot of 1 mm diameter. Only qualitative measurements were carried out.

3 Results and Discussion

Figure 1 shows the colour calibrated digital photography of one folio of the Colombino codex, as well as the corresponding UV and IR images. The examination of the complete document showed similar behaviours for the entire codex. The homogeneity of the materials and depictions suggests a single writing period. The UV red colour fluorescence is quite similar to the cochineal dye, but the yellow colorant presents a bright fluorescence and its identity is unknown (Fig. 1). Under IR illumination, the green and blue colours present a light grey tone, similar to the features of the organic materials in the prepared references.

Considering the results of the imaging techniques and the IR and UV fluorescence observations, XRF measurements focused on eight folios in order to obtain representative data pertaining to the document. The XRF results for the Colombino

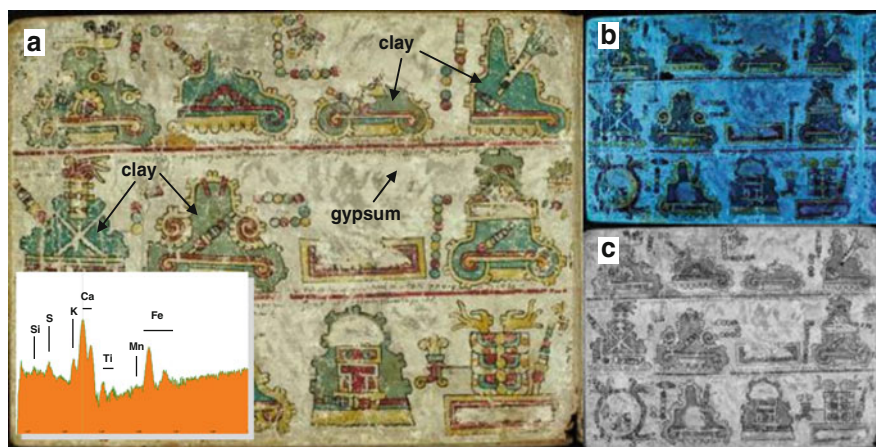


Fig. 1 (a) The Colombino codex, folio 7; (b) UV imaging at 365 nm; (c) IR reflectography using 940 nm led illumination. Typical XRF spectrum from green and blue region is shown

codex indicate the presence of S, K, Ca, Mn, Fe, Cu, Zn, Sr and Pb in the leather. However, in the white areas and the exposed zones of preparation layer, only S, Ca, K, Fe and Sr were detected. The S/Ca X-ray measured ratio matched the gypsum reference ratio. On the other hand, the black and red colours did not show any significant difference as compared to the X-ray ratios of the preparation layer. This indicates that the black colour may be carbon and that the red paint is a dye. The yellow colour presents a similar behaviour, but with an increase in the K content by a factor of 7. From historical records, there are at least two plants (Zacatlaxcalli and Cempaxochilt) that may have been used to produce the yellow dye. We believe that K may be an elemental tracer for the yellow organic colour, and may be of help in identifying the plant used. In addition to the elements detected in the ground, the green and blue colour spectra show Al, Si, Mn, Ti and an increase of Fe (Fig. 1). Pre-Hispanic iron pigments do not fit the observed IR imaging behaviour of green and blue colours, and also Fe is not related to the colours. In XRF spectra, the intensities of light elements are low, due to a high decrease in the X-ray fluorescence production cross sections. Thus, the Si X-ray signal can be observed only when the light elements content in the material is significant. Imaging and XRF results suggest the use of clays to fix these colours, like in the Maya blue preparation. A blue or green dye may have been fixed to the clay, and green may also have been produced by mixing the yellow and blue dyes.

The calibrated colour image, as well as the UV and IR imaging for the first part of the Azoyu codex are shown in Fig. 2. Several differences have been observed between the epochs when the document was written, but each section seems homogeneous. For instance, in the first part, the internal frame presents the observed gypsum fluorescence. Several corrections may be detected from UV images. The red colour has a fluorescence similar to that of the cochineal one, while the blue colour may correspond to indigo. No preparation layer has been observed for the outer calendaric frame. Under IR lighting, most of the colours showed light grey opacities typical of dyes.



Fig. 2 (a) The Azoyu I codex, folio 18, first epoch; (b) UV imaging at 365 nm; (c) IR imaging

Table 1 Identification of the colours and inks used in the Azoyu codex in the three epochs

Colour	First epoch	Second epoch	Third epoch
Red	Organic	Organic	Minium (Pb)
Pink	Organic	Organic	Minium and lead white
Yellow	Organic	Organic	Limonite (Fe oxides)
Green	Organic	Organic	Dark.: organic Light: limonite + indigo
Blue	Organic (indigo)	organic (indigo)	Organic (indigo)
White	Gypsum	Gypsum	Lead white
Black	Carbon	Carbon	Carbon
Inks	Carbon+iron-gall inks	Carbon+iron-gall inks	Iron-gall inks

The main XRF results for the Azoyu codex are shown in Table 1. Carbon and iron-gall inks were used in the three sections. Dyes were used for the first and second parts, but European pigments and mixtures with dyes (mainly for green colours) appear only in the third section. This aspect suggests that the last section was written very late, perhaps during the second part of the seventeenth century, when the Spanish influence reached remote regions of New Spain. Despite the European influences, we may consider that the earlier sections of the Azoyu codex were written and painted following the pre-Hispanic traditions of preparation of colour materials.

4 Conclusions

From our UV-IR imaging and XRF measurements, we may conclude that the composition of the Colombino codex is very homogeneous. Dyes were applied on a gypsum preparation layer, and carbon inks were used. Blue and green colours were prepared by fixing a dye to clays; also, the green colour may have been made from a combination of blue and yellow.

In the Azoyu codex, although it was written during the Colonial period, dyes are used in the first and second parts (corresponding to the respective epochs), while only in the last section organic colours are replaced by European pigments. These results suggest that the pre-Hispanic traditions and the employment of organic colours were still used in the first colonial codices written during the second half of the sixteenth century.

Our methodology is suitable for a first study of this type of documents, since it allows us to contrast the use of pigments and dyes. UV-IR imaging works perfectly for a general examination of the document; subsequently, XRF may be applied on representative areas. Finally, further analyses using Raman and FTIR spectroscopy for the characterisation of organic compounds appear necessary.

Acknowledgements This research has been supported by the Mexico CONACyT grant U49839-R.

References

- Carrasco D (2001) Colombino-Becker codex in *The Oxford Encyclopedia of Mesoamerican Cultures*, vol 1. Oxford University Press, Oxford, pp 231–232
- Gonzalez Tirado C (1998) *Análisis de pigmentos en ocho códices mexicanos sobre piel*. M.Sc. thesis, The Monfort University, Leicester
- Zetina S, Ruvalcaba JL, Falcón T, Hernández E, González C, Arroyo E, López Cáceres M (2008) Painting syncretism: a non destructive analysis of the Badiano codex, ART2008. <http://www.ndt.net/search/docs.php3?MainSource=65>

MissMarble, an Interdisciplinary Data Base of Marble for Archaeometric, Art History and Restoration Use

J. Zöldföldi, P. Hegedüs, and B. Székely

1 Introduction

Archaeological research projects result in various types of data: sample descriptions, analytical data, photographs, measured values. After the completion of the project, these partly structured data remain typically unpublished. Although these data would be, in principle, ready for dissemination for any scientific purposes upon request, only the author possesses the information regarding the storage and code system of the data. The verification of the conclusions of the publications is often difficult in light of the gathered data. Their transfer to interested third research parties is blocked by their unstructured or undocumented formats. Consequently, sometimes work is unnecessarily repeated: the resources employed by the applied research equipment are used needlessly. Moreover, although researchers are expected to publish their data together with the scientific contributions, the publication of voluminous raw data is discouraged. Some journals provide data repository functions, but even if such a repository is provided, the storage must be organised in such a manner that the structure and format are comprehensible for any specialist. Furthermore, the data must be stored in reliable data centres, where they are archived for a long time and remain available even if the information technology (IT) solutions change.

J. Zöldföldi (✉)

Institute of Geoscience, University of Tübingen, Wilhelmstrasse 56, 72074 Tübingen, Germany
e-mail: zoeldfoeldi@yahoo.de

P. Hegedüs

Arany János út 1, 7754 Bóly, Hungary

B. Székely

Institute of Photogrammetry and Remote Sensing, Vienna University of Technology, Vienna, Austria

There is general agreement in the scientific community that the availability of research data fosters interdisciplinary studies and helps international efforts. Via the availability of research results, clearly attributed to the originating researchers, the raw data also gain importance and become valuable.

The aim of our project was to develop a scientifically and technologically interdisciplinary and accessible data management system with user-friendly interfaces for data entry, quality control, storage, dissemination, and exchange. Such a database required innovative, efficient and practical ways of processing, archiving, and disseminating the appropriately structured data. Furthermore, the system also needs to provide practical hints for understanding the techniques applied on various samples and link them to literature data.

2 The Demand for Data Integration in Marble Provenance Studies

Determining the source area of marbles used in antiquity for sculptures and buildings is an important issue in archaeology and art history. Deciphering the source of an artefact requires a multidisciplinary–multi-method approach: from stylistic characteristics, archaeology and art history supply the most likely time frame and place of fabrication, together with data pertaining to the known quarries in use during the respective time period. Physical, chemical, mineralogical and petrographical analytical techniques help identify the marble used for producing the artefact based on individual properties. Reliable determinations are usually based on a multi-method approach in order to reach a high confidence level (Zöldföldi et al. 2004). Moreover, almost all techniques available to date are destructive for the artefact, i.e., they consume material. Thus, the extractable size of samples obtained from an archaeological artefact sets limits on the quantitative use of certain techniques. Therefore, it is important to apply those techniques that cover the entire set of characteristics of the extracted material, i.e., not only the bulk chemical fingerprint, but also chemical, mineralogical and petrological heterogeneities. Cathodoluminescence, texture, fabric analysis, and especially stable isotope ratios are low-cost methods that are suitable for the characterisation of material (e.g., Attanasio et al. 2006).

Uncertainties regarding the assignment to a source are due to the following aspects: (1) not all ancient quarries are known, while certain quarries used in antiquity were reopened later or are still in use, keeping the exact location of the ancient quarry unclear; (2) often only small, randomly oriented chips from ancient waste disposal sites are available, which are not necessarily representative for the quarry if the marble is heterogeneous. Thus, the knowledge at quarry level is limited and depends on the sampling method employed. Any substantial improvement in the determination of the provenance of white marble used for an artefact

requires detailed studies of the 3D variability at each ancient quarry site. Furthermore, still unknown sites also need to be located.

3 Conceptual Elements and General Properties of the System

The new, internet-based IT tools make it possible to integrate the already existing analyses and results pertaining to marble occurrences, archaeological objects and architectural elements into an appropriate information system (Fig. 1). Conceptually, we intend to manage the results of the analyses of both types of material together, in order to handle the data in the same manner (Zöldföldi et al. 2004, 2008). This feature emphasises the existing overlaps and outlines the gaps in the analytical results, thus defining the further analyses to be carried out. The integration facilitates spare expensive and time-consuming measurements on material with the same provenance.

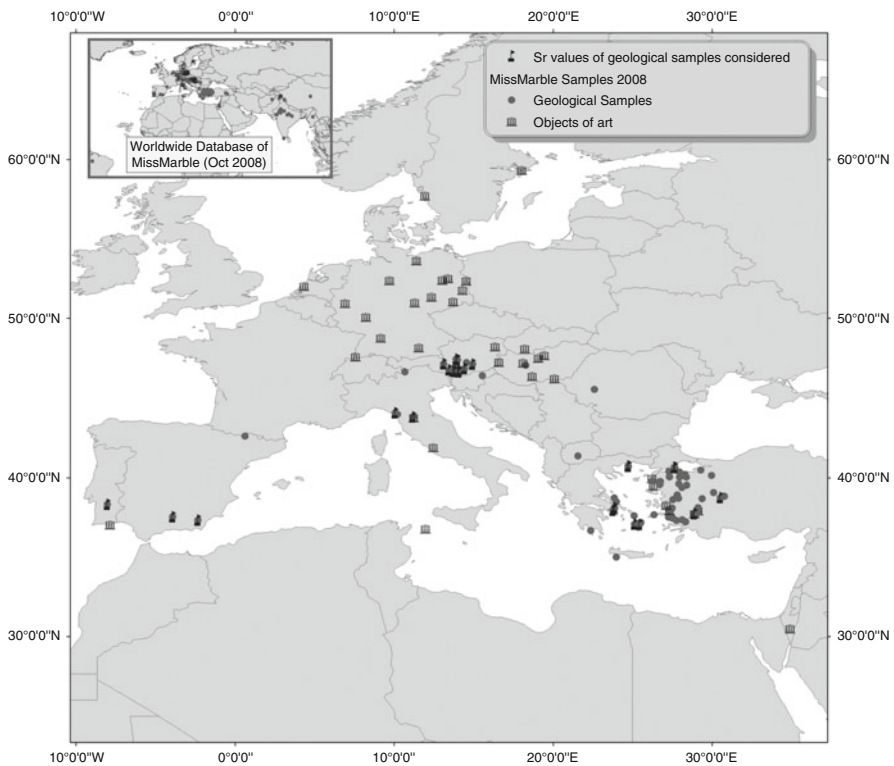


Fig. 1 Map of European and Middle East localities of marble occurrences and archaeological objects currently stored in *MissMarble* (see inset for worldwide coverage, status October 2008)

3.1 *General Properties*

As any such IT solution, the system should fulfil three criteria: user friendliness, scalability and data security. Our system, named *MissMarble*, provides a user-friendly interface for specialists familiar with the principles of marble sampling and investigations. The structure of the menu follows the logic of sample identification, processing and measurements, rendering it self-explanatory. The system is designed to be extendable to include new methods that are being developed. From the server side, the database can include new fields for each record. The client-side application can be easily updated by the user with a single mouse click when upgrades are implemented by the system administration. This solution ascertains that the entire community possesses the same interface and no outdated access tools exist. The system is designed to perform user defined filtering operations practically on any combination of logical “AND” criteria, i.e., restricting the selection set by multiple criteria.

3.2 *Conceptual Issues*

The aim of the system is to provide help for data comparison, provenance analyses, and to reveal missing analytical results. It integrates data on raw material (*geological samples*) and results on material from archaeological, art historical and/or architectural objects (*objects of art*). The system manages both types of data according to the same concept, using mostly the same data entries for both object types, with some differences related to the nature of the sample type.

All records may contain the following entries: sample identification; colour and fabric; mineralogical composition; textural properties; chemical composition; isotope geochemical data; electron paramagnetic resonance; engineering physical properties. The aspects dependent on the type of sample are the following: in the case of *geological samples*: geological classification (age, facies); in the case of *objects of art*: archaeological description of the objects; art historian description; probable provenance if determined; conservational and restoration experience.

The system is designed in such a manner that further updates are possible as user demand requires. Its functionalities, data structure and data content are regularly revised according to the needs of the users and data providers. However, the amendments are carried out so that the changes do not hamper the comparisons with the previous data and applied methods.

3.3 *Implementation*

The implementation is based on client/server architecture. The server-side engine is based on platform/independent freeware PostgreSQL-technique, while the client software is Windows-based. The client software connects to the server via a standard internet connection layer, so the user does not need to install any additional software.

3.4 Examples of Applications

The system is conceptually intended for provenance analyses of historical monuments and marble masterpieces. In addition to provenance determination, possible applications include verifying the authenticity of “antique” marble objects, fit together the different pieces of objects of art, and preliminary investigations in restoration projects.

3.5 Provenancing Powder Samples of White Marbles

The optimal first steps in sourcing a lithic artefact should be the macroscopic and thin section study with the petrographic microscope. Unfortunately, it is often the case that it is not allowed to take a sample which is suitable for thin section preparation from precious artefacts. Instead, a common procedure is to analyse powder samples in various ways. The system most widely used today is that of stable $\delta^{13}\text{C}$ and $\delta^{18}\text{O}$ isotopic signatures (e.g., Attanasio et al. 2006). However, the signatures of many quarry fields overlap. Because of the already proven advantages of isotopic ratio analysis, principally the need of only small samples and homogeneity over large areas, another isotopic ratio, the $^{87}\text{Sr}/^{86}\text{Sr}$ system could be of help in provenancing white marbles. In order to benefit from the combination of these techniques, more than 2400 data pairs of $\delta^{13}\text{C}$ and $\delta^{18}\text{O}$ isotopic system and 433 data of $^{87}\text{Sr}/^{86}\text{Sr}$ ratios (Fig. 2) are included in the *MissMarble* database (as of October 2008). Although the ranges of the Greek and Anatolian quarry areas are notably overlapping, there are differences between the East Mediterranean and

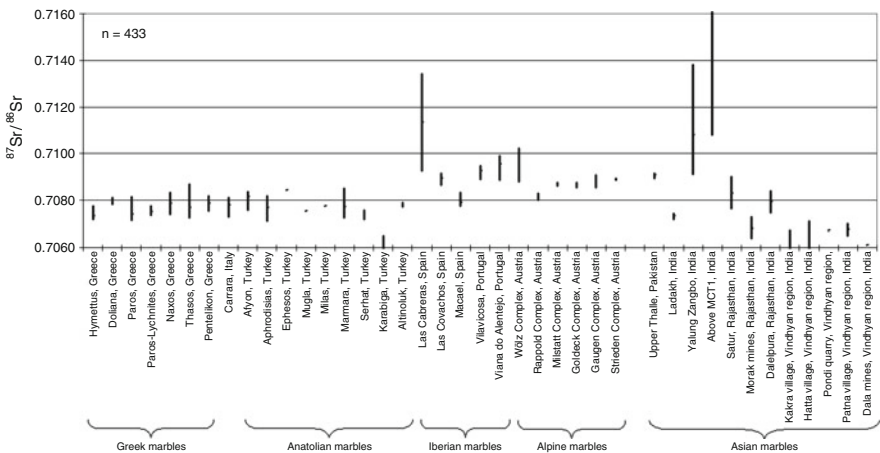


Fig. 2 Summarising diagram of the $^{87}\text{Sr}/^{86}\text{Sr}$ ratios published in archaeological and geological literature and unpublished data that are presented in the *MissMarble* database (Kumar et al. 2002; Pentia et al. 2003; Zöldföldi and Satir 2003; Brilli et al. 2005; Schuster et al. 2005; Liu et al. 2006; Morbidelli et al. 2007)

West Mediterranean marble quarries, and the quarries of Asia. Therefore, in some special cases the adoption of the Sr-ratio for distinguishing the quarry locations used for architectural and sculptural artefacts could be of help in assigning the provenance.

4 Conclusions

A data management system has been developed for storage and manipulation of various properties of marble rock samples and artefacts. The system applies a client-server architecture, allowing multiuser access. A novel conceptual approach, entailing the handling of geological samples similarly to archaeological artefacts, has been found advantageous for managing the data records and for making provenance decisions using various filtering criteria. The system is able to manage the samples at any spatial resolution, including the within-quarry identification if the appropriate spatial data (coordinates) of the samples are available.

Acknowledgements JZ has initiated this project while at the University of Tübingen, in the Graduate College 442 of the Deutsche Forschungsgemeinschaft (“*Anatolien und seine Nachbarn*”). The German-Hungarian DAAD-MÖB project *Archaeometrical study of Roman and Medieval Marbles from Hungarian Monuments* also contributed to its development. BS was supported by the University of Tübingen and Békésy György Postdoctoral Fellowship.

References

- Attanasio D, Brilli M, Ogle N (2006) The isotopic signature of classical marbles. *L’Erma di Bretschneider*, Roma, 297
- Brilli M, Cavazzini G, Turi B (2005) New data of $^{87}\text{Sr}/^{86}\text{Sr}$ ratio in classical marble: an initial database for marble provenance determination. *J Archaeol Sci* 32:1543–1551
- Kumar B, Das SS, Sreenivas B, Dayal AM, Rao MN, Dubey N, Chawla BR (2002) Carbon, oxygen and strontium isotope geochemistry of Proterozoic carbonate rocks of the Vindhyan Basin, central India. *Precambrian Res* 113:43–63
- Liu Y, Zs B, Massone H-J, Zhong D (2006) Carbonatite-like dykes from the eastern Himalayan syntaxis: geochemical, isotopic, and petrogenetic evidence for melting of metasedimentary carbonate rocks within the orogenic crust. *J Asian Earth Sci* 26:105–120
- Morbidelli P, Tucci P, Imperatori C, Polvorinos A, Martinez MP, Azzaro E, Hernandez MJ (2007) Roman quarries of “Anasol” and “Anasol”-type marbles. *Eur J Mineral* 19:125–135
- Pentia M, Herz N, Turi B (2003) Provenance determination of classical marbles: a statistical test based on $^{87}\text{Sr}/^{86}\text{Sr}$, $^{18}\text{O}/^{16}\text{O}$ and $^{13}\text{C}/^{12}\text{C}$ isotopic ratios. In: Lazzarini L (ed) *Interdisciplinary studies on ancient stones*. Bottega D’Erasmus, Padova, pp 219–226
- Schuster R, Moshhammer B, Abart R (2005) Tectonic and stratigraphic information on Greenschist to Eclogite facies metamorphic Austroalpine units by a Sr–C–O isotope study on marbles. In: Tomljenovic B, Balen D, Vlahovic I (eds) *7th Workshop on Alpine Geological Studies*, Abstract book. Croatian Geological Society, Opatija, pp 87–88

- Zöldföldi J, Satir M (2003) Provenance of white marble building stones in the monuments of the ancient Troia. In: Wagner GA, Pernicka E, Uerpmann HP (eds) Troia and the troad. Springer, Berlin, pp 203–223
- Zöldföldi J, Székely B, Franzen Ch (2004) Interdisciplinary data base of historically relevant marble material for archaeometric, art historian and restoration use. In: Grassegger-Schön G, Patitz G (eds) Natursteinsanierung Stuttgart 2004, Neue Natursteinsanierungsergebnisse und messtechnische Erfassungen. Siegl, München, pp 79–86
- Zöldföldi J, Hegedüs P, Székely B (2008) Interdisciplinary data base of marble for archaeometric, art historian and restoration use. In: Yalcin Ü, Özbal H, Pasamehmetoglu G (eds) Ancient mining in turkey and the Eastern Mediterranean. Atilim University, Ankara, pp 225–251

Part III
Micro-nano Diagnostic and Ancient
Technology

Look Into the Objects: Why? Cultural Heritage Motivations of Neutron-Based Imaging Techniques

K.T. Biró, É. Durkovic, S. Farkas-Szóke, and The Ancient Charm Collaboration

1 Introduction

One of the basic concepts of archaeometry involves knowing more about the objects with the help of scientific methods concerning visual, structural, as well as chemical aspects. Obtaining a combination of these types of information on the micro- and nano-diagnostic level is made possible by the use of analytical techniques using neutrons (Gorini 2007). The advance of physical techniques in archaeometry made this question topical and the “Ancient Charm” project made it feasible.

The possibility to look inside, by the assessment of physical qualities, and visualise the contents of archaeological sites is manifested in different prospection techniques, which are now applied as routine methods in archaeological geophysics: magnetometer surveys, electromagnetic measurements, ground penetrating radar, resistivity measurements, etc. (Herz and Garrison 1998). Archaeological excavations, especially large surface projects, have become today either not feasible, or at least tediously long and ineffective, without the application of these methods. By extrapolating, the question we are addressing here is whether there is a similar need for “looking inside” on the level of the object.

2 The Ancient Charm Project

“Ancient Charm” (Analysis by Neutron Resonant Capture Imaging and other Emerging Neutron Techniques: New Cultural Heritage and Archaeological Research Methods) is an ADVENTURE project, an action line of NEST (New

K.T. Biró (✉) and S. Farkas-Szóke
Hungarian National Museum, Budapest, Hungary
e-mail: tbk@ace.hu

É. Durkovic
Department of Archaeology, ELTE University, Budapest, Hungary

and Emerging Science and Technology) in the Sixth Framework Programme (FP6) of the European Union. Its aim is to develop methods of neutron imaging techniques able to penetrate solid and non-transparent inorganic objects, and test their applicability in the field of cultural heritage. Detailed information on the project can be found at the project's website (<http://ancient-charm.neutron-eu.net/ach>). The initiative has been reported on in a number of meetings and scientific communications (Festa et al. 2006; Kasztovszky and Belgya 2006a, b; Kudejova et al. 2007), practical examples being also presented at the Archaeometry Conference in Siena by various authors.

In parallel with the methodological development, we are interested in the possible use of these techniques: will they be in demand? Is there a justification, on the “consumer side”, for the obviously large input of work and development entailed by this project?

The techniques covered by Ancient Charm include elemental analysis techniques based on nuclear reactions, by capturing or scattering neutrons: prompt gamma activation; neutron resonance capture analysis and imaging; neutron radiography and tomography; and time-of-flight neutron diffraction studies. An overview of these techniques was provided in Kockelmann and Kirfel (2006), especially Table 1.

These techniques may provide different images of the interior, normally invisible parts of objects: 3D contrast images, structural information on the (mineral) phases included, and elemental distribution. The application of these methods individually may provide important new information concerning the objects; their joint application offers a unique composite view. Theoretically, all aspects of the objects can be studied according to these techniques; practically, we have yet to verify if the results justify the efforts.

3 Looking Into the Objects: Possible Reasons on Behalf of Neutron Physics

3.1 Testing Methodology

The study of archaeological and other (historical, artistic) objects belonging to the cultural heritage domain (=CH objects) can be considered an ideal area for testing the potential of new advances in the field of applied sciences. Leading edge technologies are preferentially “tested” on CH objects; however, they will not typically become part of the routine applications of archaeological/art historical methodology, and have little or no impact on mainstream research in the humanities. To be considered essential for art history, extensive programmes of examinations are needed, involving fast and possibly cheap methodologies.

3.2 *Publications*

The main purpose of having CH objects analysed by neutron physicists is doubtlessly having quality publications in high-impact factor journals. To that purpose, objects of high artistic quality and great historical importance would be preferred by the analysts. The problem with such objects is that they are more difficult to move, from a certain collection and even more so across boundaries, as they are considered to have exceptional cultural value. A significant effort is needed in order to convince curators and museum managements of the benefits of the analysis, and, in any case, the objects must be highly insured.

4 Looking Into the Objects: Possible Reasons on Behalf of CH

4.1 *Conservation*

The most compelling need for looking inside objects emerges prior to their conservation/restoration. The conservator and the curator would like to know what is inside the artefact, in case the object deserves special treatment. Some chemicals used for fixing metal parts may be harmful for organic components, for example, and vice versa, and any chemical interference (necessary for preservation) can unfavourably influence the possibilities for later analysis. It would thus be ideal to verify “suspect” objects (that is, objects of possible high complexity and aesthetic/historical value) as soon as they are found and stabilised. The problem with this approach is, partly, methodological: in routine archaeological practice, there is no time to “play with” the individual objects, and there are also too many candidates for detailed “look inside” studies with uncertain outcomes.

For the time being, we can see little chance of applying neutron imaging techniques as a routine methodology for masses of archaeological objects coming “fresh” from excavation contexts. However, this can represent a future prospect if the availability of the method and the suitable equipment become widely accessible.

The most important routine application of neutron imaging techniques could be the fast and effective study of “fresh” archaeological finds to optimise treatment. X-ray radiography, in fact, has for a long time been applied for purposes of conservation science and can be regarded as a routine methodology for assessing different (hidden or not visible) qualities of the object. Considering the large number of “fresh” archaeological finds, the biggest problem here is selecting the really appropriate pieces and getting them in a stable enough state to undergo the analytical process without doing damage to the objects, their possible further conservation treatment, and the analytical equipment itself¹.

¹Excavation-fresh materials, especially unconsolidated, might be harmful: they have to be stabilised, desinfectionalised first.

4.2 *Presentations*

The most successful applications in terms of visualising the interiors of CH objects is typically that of digital presentations in the context of an exhibition or another event benefiting from the attention of a wide range of public media. Such applications can add up to the understanding and visualisation of the archaeological objects in a modern context that is required by the current audience. Exhibits are supposed to be not only “beautiful”, “valuable” and “meaningful” in a historical sense, but also attractive in the modern IT world. This appeals most to the young generation, whose visual (and non-visual) culture develops in the context of sophisticated (e.g., 3D) imaging techniques where most of the information is derived from the image, much less the text.

4.3 *Technology Studies*

Neutron imaging techniques can support the scientific study of objects in the field of humanities. The most plausible field for their application is that of ancient technology, its recognition and analysis. Differentiating authentic pieces from fakes might also represent one of the marketable benefits of such a methodology. With a library of ancient technological fingerprints, modern fakes could be easily recognised. Such procedures could also support experimental archaeology studies in reviving and reconstructing former technological knowledge.

5 **Suggestions for a “Best Practice”**

In order to explore the potentials of neutron imaging techniques for art history and archaeology, we have constructed a database on known instances of applications carried out with the aim of mapping the interior contents of an object. On the basis of the collected evidence and consultations with experts on both sides, we are suggesting the following guidelines for the investigation of CH materials by 3D neutron imaging techniques:

Excavation-fresh material

- Careful documentation
- Preliminary conservation in view of possible later needs for analytical treatment (minimal interference)
- Assessment of composition/complexity
- Measurement of weight, specific gravity (dimensions in this state may be misleading)
- Fast and high resolution imaging techniques (radiography, maybe tomography)
- Decisions on further steps

Conserved/complete objects from museum collections

- Attempt to trace the history of the object: recovery, conservation, previous treatment and/or analyses
- Simple tests: measurements of dimensions, weight, specific gravity
- Is there a question concerning interiors? (hollow objects, complex objects, technology)
- Information on bulk chemical composition
- Assessment of significance
- Of the object (in respect of possible publication/presentation)
- Of the question, in view of the historical/artistic added value to the already known information
- Planning a possibly optimal sequence of analysis
- Assessment of difficulties
- Transport of objects including administration and insurance
- Analytical requirements and limitations
- Activation/cooling time
- Sample size – analytical equipment sample holders and individual support

6 Conclusions

Neutron imaging techniques can be widely applicable in the 3D mapping of archaeological and other CH objects. These methods can be applied individually or as a package, providing visual information on the exact locations of high/low contrast parts (NR/NT), phase composition of hidden “inclusions” and different phases inside the object (TOF-ND, SANS), or pinpointing parts of different chemical composition inside the objects (=PGAA/PGAI, NRCA/NRCI).

Knowing simple physical parameters like dimensions, weight and specific gravity, archaeologists/conservators may find it necessary to investigate the internal parts of an object. Depending on the actual circumstances pertaining to the find, investigations can be carried out both on “excavation fresh” or on “gem of collection” pieces, typically in order to define:

- (a) The best available treatment
- (b) Visualisation (for presentations)
- (c) Improved scientific information available on the object

It is suggested to begin with the visualisation techniques, which are fast and offer high resolution. They might be adequate for deciding if further neutron-imaging techniques for the determination of phase compositions (=minerals) or elemental compositions might be necessary, and, if so, on which parts of the objects. The next step consists of an assessment of the bulk chemical composition (to be able to predict the behaviour of the object during the further steps of analysis). The continuation of the process may turn towards the identification of the spatial

ordering of atoms (crystalline structure, orientation) and suspected different elemental compositions of hidden parts. It is important to note that the resolution of neutron radiography/tomography is in the order of 100 μm , whereas the resolution of neutron diffraction and elemental analysis is of a minimum of 1 mm, and thus the visualisation potentials of these methods are significantly different.

All observations should be carefully recorded in an unambiguously defined 3D coordinate system within the object. The interpretation of the data should involve both analysts and experts from the CH field. It is necessary to construct reference libraries for typical ancient techniques, even on simple objects.

The most likely candidates for in-depth analysis will be composite objects that are the products of elaborate skill, typically made, at least partly, of metal(s). Organic composite objects will probably result in a poor contrast for elemental mapping, as hydrogen is a strong neutron-scatterer.

References

- Festa G, Andreani C, Filabozzi A, Malfitana D, Poblome J (2006) Neutron techniques in cultural heritage. *Archeometriai Műhely* 2:32–36
- Gorini G, Ancient Charm collaboration (2007) Ancient charm: a research project for neutron-based investigation of cultural heritage objects. *Il Nuovo Cimento C* 1:1–12
- Herz N, Garrison EG (1998) *Geological methods for archaeology*. Oxford University Press, New York
- Kasztovszky Z, Belgya T (2006a) Non-destructive investigations of cultural heritage objects with guided neutrons: the ancient charm collaboration. *Archeometriai Műhely* 1:12–17
- Kasztovszky Z, Belgya T (2006b) From PGAA to PGAI: from bulk analysis to elemental mapping. *Archeometriai Műhely* 2:16–21
- Kockelmann W, Kirfel A (2006) Neutron diffraction imaging of cultural heritage objects. *Archeometriai Műhely* 2:1–15
- Kudejova P, Cizek J, Schulze R, Jolie J, Schillinger B, Lorenz K, Musshlbauer M, Masschaele B, Dierick M, Vlassenbroeck J (2007) A marker-free 3D image registration for the Ancient Charm Project. Case study with neutron and X-ray tomography datasets. *Notiziario Neutroni e Luce di Sincrotrone* 12(2):6–13

Internet Resources

- Ancient Charm central homepage: <http://ancient-charm.neutron-eu.net/ach>
- Ancient Charm-WP1 homepage: <http://www.ace.hu/acharm/>
- Geophysical methods homepage: http://www.geosphereinc.com/main_geo-methods.html
- Archeometriai Műhely/Archaeometry Workshop (<http://www.ace.hu/am>)

Nano-Scale Investigation of Some Dichroic/Opalescent Archaeological Materials

D. Dungworth and S. Paynter

1 Introduction

This paper explores the origin of dichroism and/or opalescence in vitreous waste materials from some glassworking sites. Similar properties have been noted and investigated in some other archaeological materials, such as Chinese glazes and the Lycurgus Cup, but the dichroism/opalescence of the materials reported here appears to have occurred accidentally. The production of dichroism/opalescence in common bottle glass was already noted in the eighteenth-century. Bosc D'Antic, writing in 1765, said that glass turning opalescent with a blue or green colour was particularly a problem in making bottle glass (Cable 2003), and suggests that such opalescence was the result of high levels of lime in the glass (Cable 2003). William Lewis (1763) describes how in the course of an experiment to distil soot the glass apparatus (made from common bottle glass) was transformed into a dichroic material; pale blue in reflected light but yellowish in transmitted light.

2 Dichroic/Opalescent Glassworking Waste

The investigation of vitreous materials from several post-medieval glassworking sites has identified amorphous lumps, cream to blue in colour and often highly vesicular (Dungworth and Cromwell 2006). Examples of failed blown vessels (wasters) displaying similar characteristics have also been noted (Fig. 1). A careful examination of this waste shows that it is dichroic or opalescent: it is usually pale blue in reflected light but yellow, brown or green in transmitted light. This dichroic/opalescent waste is mainly recovered from sites engaged in the manufacture of wine bottles and similar wares made from high-lime low-alkali (HLLA) glass and it usually has the same (or similar) chemical composition as the HLLA glass manufactured

D. Dungworth (✉) and S. Paynter
English Heritage, Portsmouth PO4 9LD, UK
e-mail: david.dungworth@english-heritage.org.uk



Fig. 1 Opalescent glassworking waste. Eighteenth-century wine bottle waster from Limekiln Lane, Bristol, UK (sample 4)

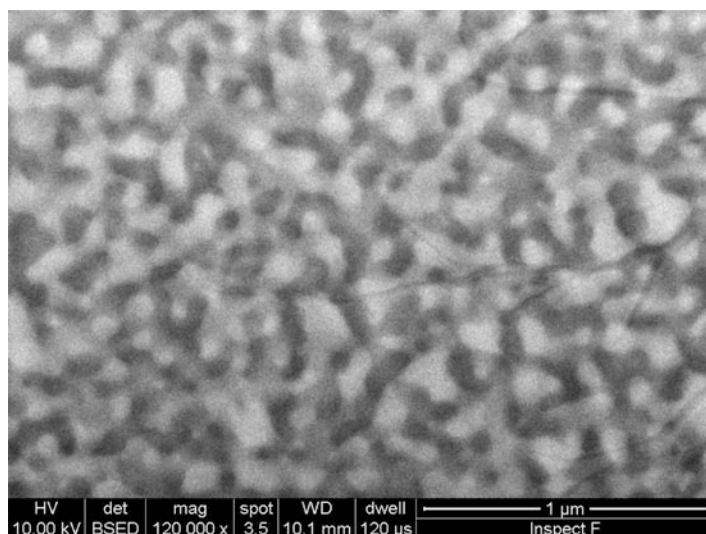
on that site. The initial examination of samples of dichroic/opalescent waste from several glassworking sites showed that it was completely vitreous – we could not detect any signs of devitrification (crystalline phases).

3 FEG-SEM Examination of Dichroic/Opalescent Materials

Several samples of dichroic/opalescent glass waste (Table 1) have been examined using a Field Emission Gun Scanning Electron Microscope (FEG-SEM). The samples were mounted in epoxy resin and polished to a $\frac{1}{4}$ -micron finish (diamond abrasive). The polished samples were carbon coated and examined using a FEI Inspect-F FEG-SEM – images were obtained using a solid-state back scattered electron detector. Most samples were vitreous, although a few contained some regions with crystalline phases (usually wollastonite). All samples showed the presence of small (<250 nm diameter) chemically distinct droplets (Fig. 2). These droplets resemble those identified in a wide range of dichroic/opalescent vitreous materials (Kingery et al. 1983; Li et al. 2003; Strnad 1986; Vogel 1985). The use of energy dispersive X-ray detectors attached to the FEG-SEM could not shed light on the nature of the chemical differences between the droplets and the matrix as the droplets are substantially smaller than the X-ray interaction volume. The average size of the droplets varied from 50–250 μm : samples with barely perceptible dichroism/opalescence had the smallest droplets (<100 μm) but the droplets tended to be larger in the more strongly dichroic/opalescent samples (up to 250 μm).

Table 1 Origins of samples examined

Sample	Provenance	Date	Description	Droplet size
1	Bristol (Bedminster)	Eighteenth century	Bottle fragment	76 nm
2	Silkstone	Late seventeenth century	Amorphous lump	80 nm
3	Bristol (Avon Street)	Nineteenth century	Amorphous lump	107 nm
4	Bristol (Limekiln Lane)	Eighteenth century	Bottle fragment	65 nm

**Fig. 2** FEG-SEM back scattered electron image of nineteenth-century opalescent waste from Avon Street, Bristol, UK (sample 3)

4 Discussion

The dichroic/opalescent glassworking waste reported here, as well as opalescent wood-ash glazes on some Chinese ceramics, share similar compositions; they are silica-rich with high concentrations of lime and low concentrations of alkalis (Table 2).

In addition they all have similar colour and opacity properties, and in the case of the Chinese glazes it has already been demonstrated that these properties are the result of liquid-liquid micro-phase separation (Kingery et al. 1983; Li et al. 2003). At high temperatures many silicate systems exhibit immiscibility – they tend to form two immiscible liquids which can be preserved after the glass has solidified (Shelby 2005; Strnad 1986; Vogel 1985). The two components of such a micro-structure are still both glasses but of different chemical compositions. The morphology of micro-phase separated glass may consist of either droplets within a matrix or as a connected morphology (spinodal). Micro-phased separated glass with

Table 2 Chemical composition (SEM-EDS) of samples examined

Sample	Na ₂ O	MgO	Al ₂ O ₃	SiO ₂	P ₂ O ₅	K ₂ O	CaO	TiO ₂	MnO	FeO	BaO
1	1.4	4.3	5.0	57.6	<0.2	2.1	25.6	0.2	0.3	1.8	0.7
2	1.6	4.8	3.6	57.2	2.0	3.9	23.8	0.2	0.5	1.9	<0.2
3	0.6	0.6	7.8	59.0	<0.2	3.9	23.9	0.4	0.1	3.9	<0.2
4	2.2	4.3	5.5	56.7	1.7	2.7	23.2	0.3	0.3	2.5	<0.2

a droplet morphology will often be dichroic or opalescent – the precise optical properties will depend on the size of the droplets and any differences between the refractive indices of the droplets and the matrix (see Mishchenko et al. 2002, for further details).

Kingery et al. (1983) investigated the Na₂O–K₂O–Al₂O₃–CaO–SiO₂ system to determine the conditions under which liquid-liquid immiscibility and phase separation would occur. They showed that glasses with low alkali and high lime content were most likely to produce liquid-liquid immiscibility and phase separation. Most divalent oxide-silica phase systems show extensive high temperature immiscibility regions (Levin et al. 1956). Therefore, it is the high lime and low alkali content of HLLA glass that gives rise to the formation of the distinctive colour effects of opalescent/dichroic glassworking waste. Most dichroic/opalescent glassworking waste shares the same composition as the green HLLA glass from the same site (e.g. Blakelock 2007). In a few cases the waste contains elevated levels of aluminium, titanium, and iron compared to HLLA glass from the same site (e.g. Dungworth and Cromwell 2006). It is likely that the increase in the concentration of these oxides is due to reactions with crucibles and/or coal ash (Dungworth 2008).

5 Conclusions

The examination of dichroic/opalescent HLLA glass waste demonstrates that they have undergone micro-phase separation due to liquid-liquid immiscibility. Unlike the Lycurgus cup (Barber and Freestone 1990) or some Chinese glazes (Kingery et al. 1983; Li et al. 2003) where dichroism/opalescence was deliberately produced, the materials examined here all acquired their optical properties by accident. The experiments by Lewis in the 18th century suggest that normal HLLA glass can be transformed into dichroic/opalescent waste by holding at red heat or above for hours to days. Thus we conclude that the dichroism/opalescence of glassworking waste has arisen because it was held at a high temperature for too long.

Micro-phase separation may also be present in glasses which display no changes in colour properties (due to the small size of the droplets) but it may significantly affect physical properties such as viscosity (Shelby 2005; Vogel 1985). Where the chemical composition of the droplets differs significantly from the matrix, a phase separated glass will have different viscosity properties compared to one which is not phase separated. Further research into historic vitreous materials could provide

more detail on the nature of phase separation. The preparation of thin specimens for STEM imaging coupled with the use of a FEG-SEM and energy dispersive X-ray detectors may allow the droplets and matrix to be characterised in terms of their chemical composition (cf. Anderhalt 2007). This information would shed light on the effects of phase separation on a range of the properties such as viscosity.

Acknowledgements Permission to report the investigation of the Avon Street, Bristol sample (Fig. 2) ahead of publication of the excavation was granted by Ian Miller of Oxford Archaeology North. We would like to thank Jeremy Rees and David Beamer for their assistance. We would like to thank Ian Freestone for advice and inspiration.

References

- Anderhalt R (2007) X-ray microanalysis in nanomaterials. In: Zhou W, Wang ZL (eds) Scanning electron microscopy for nanotechnology. Springer, New York, pp 76–100
- Barber DJ, Freestone IC (1990) An investigation of the origin of the colour of the Lycurgus Cup by analytical transmission electron microscopy. *Archaeometry* 32:33–45
- Blakelock E (2007) Bedminster Glue factory, Bristol: examination and analysis of glass and glassworking debris, Research Department Report 11/2007. English Heritage, Portsmouth
- Cable M (ed) (2003) *Bosc D'Antic on glass making*. Society of Glass Technology, Sheffield
- Dungworth D (2008) Glass-ceramic reactions in some post-medieval crucibles: an instrumental analysis study of archaeological samples. *Glass Technol* 49:157–167
- Dungworth D, Cromwell T (2006) Glass and pottery manufacture at Silkstone, Yorkshire. *Post-Medieval Archaeol* 40:160–190
- Kingery WD, Vandiver PB, Huang IW, Chiang YM (1983) Liquid-liquid immiscibility and phase separation in the quaternary systems $K_2O-Al_2O_3-CaO-SiO_2$ and $Na_2O-Al_2O_3-CaO-SiO_2$. *J Non-Crystalline Solids* 54:163–171
- Levin EM, McMurdie HF, Hall FP (1956) Phase diagrams for ceramists. American Ceramic Society, Columbus
- Lewis W (1763) *Commercium philosophico-technicum, or the philosophical commerce of arts*. Willock, London
- Li W, Li J, Wu J, Guo J (2003) Study on the phase-separated opaque glaze in ancient China from Qionglai kiln. *Ceram Int* 29:933–937
- Mishchenko MI, Travis LD, Lacin AA (2002) Scattering, absorption, and emission of light by small particles. Cambridge University Press, Cambridge
- Shelby JE (2005) Introduction to glass science and technology, 2nd edn. Royal Society of Chemistry, London
- Strnad Z (1986) *Glass-ceramic materials*. Elsevier, Amsterdam
- Vogel W (1985) *Chemistry of glass*. Translated and edited by N Kreidl, American Ceramic Society, Westerville

Sienee “Archaic” Majolica: Characterisation of Enamels and Glazes by Analytical-Transmission Electron Microscopy (AEM–TEM)

G. Giorgetti, C. Fortina, I. Turbanti Memmi, and A. Santagostino Barbone

1 Introduction

The Sienee “archaic” majolica coated with enamels and glazes was produced in many workshops within the city from the thirteenth to the end of the sixteenth century AD. This type of ceramics has been the subject of few, but detailed archaeometric studies (Grassi et al. 2003; Fortina et al. 2005). Fortina et al. (2005) reconstructed the production technology of ceramics recovered from the Convent of the Carmine (Siena) according to petrographic and mineralogical evidence. Optical microscopy, X-ray diffraction (XRD), X-ray fluorescence (XRF), scanning electron microscopy (SEM), and Raman spectroscopy helped reveal the texture and the mineralogical compositions of the ceramic bodies and the coatings, both glaze and enamel. However, it was not possible to properly characterise very fine-grained, newly-formed phases with these micron-scale techniques. Nanometric-size mineral phases grown in artefacts can be recognised by high-resolution techniques, such as analytical-electron, transmission-electron microscopy (AEM–TEM), as it has been done in few recent studies. The characterisation of reaction processes and mineral phases at a nanometric scale led to the determination of technological processes (Mata et al. 2002), mineralogy of coatings in Renaissance pottery (Viti et al. 2003) and of Tuscan black glosses (Giorgetti et al. 2004).

In the present study, the glazes and enamels coating three different types of “archaic” majolica (Fortina et al. 2005) have been investigated by AEM–TEM in order to better characterise the newly-formed mineral phases and, consequently, to obtain better constraints regarding the firing processes.

G. Giorgetti (✉) and I. Turbanti Memmi
Dipartimento di Scienze della Terra, Università di Siena, Siena, Italy
e-mail: giorgettig@unisi.it

C. Fortina
Dipartimento di Scienze della Terra, Università di Pavia, Pavia, Italy

A.S. Barbone
Opificio delle Pietre Dure, Firenze, Italy

2 Materials and Techniques

The coated artefacts from the Convent of the Carmine have been divided into three groups by Fortina et al. (2005): (1) post-firing wastes are fragments with good glazes and enamels; (2) wastes of uncertain classification show faded enamels and were produced by a finer and lead-richer initial mixture; (3) technological wastes have coatings with high-temperature mineral phases, indicating that they were accidentally fired at a higher temperature. The studied samples are reported in Table 1, where the mineralogy, as determined by the previously applied techniques (Fortina et al. 2005) and by the methods used in the present study, is also reported.

Sticky-wax polished thin sections cut perpendicular to the coated surfaces were prepared for TEM investigations. Samples of glazes and enamels obtained from one sample from each group were ion-milled using a Gatan Dual Ion Mill 600. The AEM-TEM study was performed using a Jeol 2010 microscope operated at 200 kV and equipped with a Link ISIS EDX system.

3 Results and Discussion

Glazes and enamels on artefacts belonging to the three groups of samples show similar textural characteristics at nanometric scale. They all consist of a glassy matrix, where detrital and newly-formed phases are embedded (Fig. 1). The newly-formed minerals have euhedral shape and an almost constant size of a few hundreds of nanometres; they are unevenly distributed in the matrix. The coupling of structural data obtained by electron diffraction and analytical data provided by the AEM analyses led us to determine a single mineral phase (Table 1).

Newly-formed minerals in glazes found on post-firing wastes and on wastes of uncertain classification (groups 1 and 2) are Ca-Mg pyroxene (previously defined as Ca-Mg silicates by Fortina et al. 2005), wollastonite, Fe oxides, and K-Pb feldspar (Table 2; analyses 1, 2, 4) (Fig. 1a-b). Ca-plagioclase and Ca-richer

Table 1 Mineralogical composition of glazes and enamels in the three studied samples, as a result of the SEM-Raman study by Fortina et al. (2005) and of TEM analyses performed in the present study

	Post-firing wastes		Wastes of uncertain classification		Technological wastes	
	SEM-Raman	TEM	SEM-Raman	TEM	SEM-Raman	TEM
Glazes	Ca-Mg silicate, woll, K-Pb fs	Ca-Mg px, woll, K-Pb fs, Fe-ox	Ca-Mg silicate, woll, K-Pb fs	Ca-Mg px, woll, K-Pb fs, Fe-ox	Ca-plag, Ca-px	Ca-plag, Ca-px
Enamels	Ca-Mg silicate, woll, K-Pb fs, cass	Ca-Mg px, woll, Kfs, plag, cass	Ca-Mg silicate, woll, K-Pb fs, cass	Ca-Mg px, woll, Kfs, plag, cass	Ca-Mg silicate, crist, cass	Ca-Mg px, crist, cass

woll wollastonite, K-Pb fs KPb feldspar, Ca-Mg px Ca-Mg pyroxene, Fe-ox Fe oxides, cass cassiterite; Kfs K-feldspar, plag plagioclase; crist cristobalite

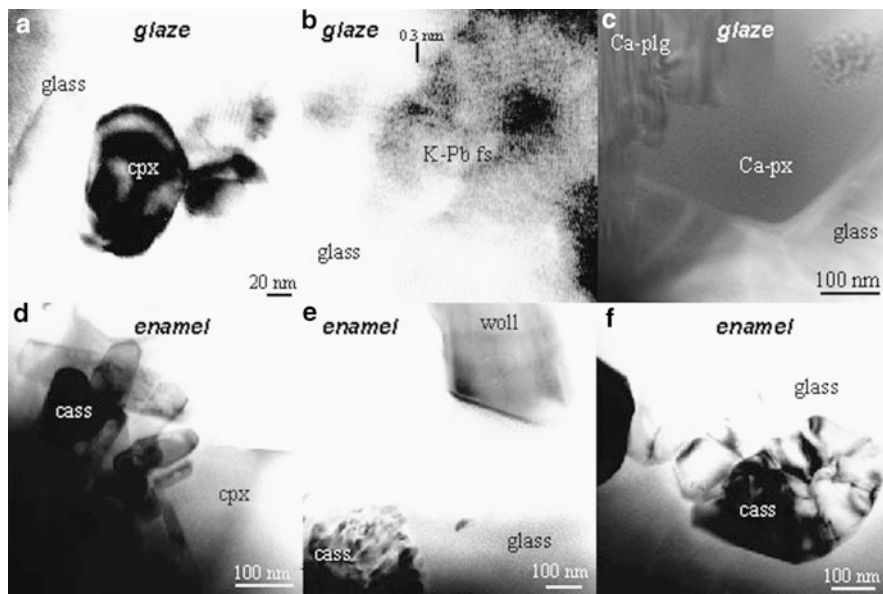


Fig. 1 TEM images of glazes and enamels. (a) newly-formed Ca–Mg pyroxene (cpx) and glass in post-firing wastes glaze; (b) high resolution TEM image of a K–Pb feldspar (K–Pb fs) in post-firing wastes glaze; (c) Ca-rich plagioclase (Ca-plg) and Ca-rich pyroxene (Ca-px) in technological waste glaze; (d) cassiterite (cass) and pyroxene in enamel from waste of uncertain classification; (e) wollastonite (woll) and cassiterite from post-firing waste enamel; (f) cassiterite in technological waste enamel

Table 2 Representative, semi-quantitative chemical compositions of newly-formed minerals as a result of AEM–TEM analyses

	(1) cpx	(2) woll	(3) Kfs	(4) K–Pb fs	(5) Ca-plag	(6) cpx
Si	1.94	2.09	3	2.33	2.57	1.84
Al	0.21	0	0.99	1.53	1.23	0.27
Fe	0.17	0.03	0	0.1	0.18	0.41
Mg	0.88	0.07	0	0.05	0.06	0.43
Ca	0.7	1.78	0.03	0.15	0.57	1.03
Na	0.04	0.09	0.23	0.24	0.24	0.02
K	0	0	0.71	0.19	0.07	0

cpx clinopyroxenes; *Ca-plag* plagioclase; other abbreviations as in Table 1

pyroxene (Table 2; analyses 5, 6) have been recognised in glazes found on technological wastes (group 3; Fig. 1c).

Newly-formed minerals in group 1 and 2 enamels are Ca–Mg pyroxene, wollastonite, K-feldspar, plagioclase and cassiterite (Fig. 1d–e). Ca–Mg pyroxene, cassiterite, and cristobalite occur in group 3 enamels (Fig. 1f). At a nanometric scale, no K–Pb feldspar has been recognised in group 1 and 2 enamels, rather only K-feldspar has been identified. Chemical analyses performed at micron scale on feldspar show a high Pb content as a result of contamination by high-lead bearing glass.

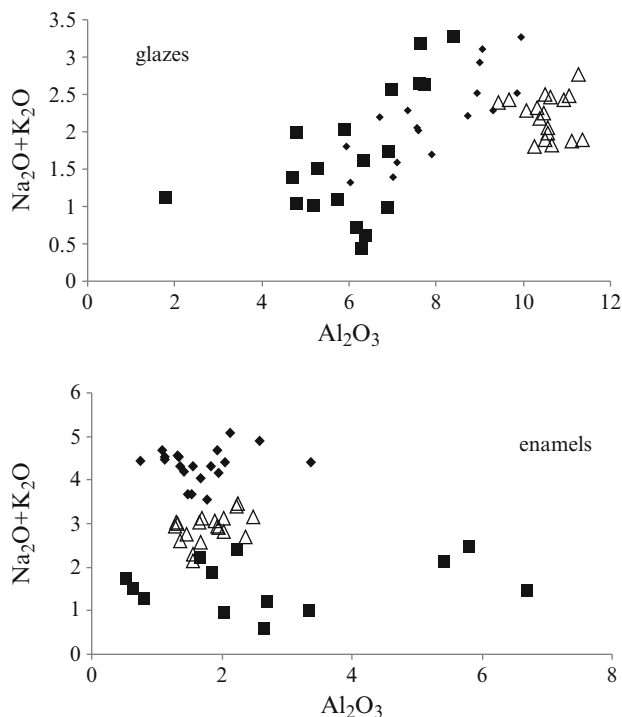


Fig. 2 Alkali (Na_2O+K_2O) vs. Al_2O_3 (expressed in wt%; analyses on glass from Fortina et al. 2005) in *glazes* and *enamels* from the three groups of samples. *Solid diamonds*: post-firing wastes; *solid squares*: wastes of uncertain classification; *empty triangles*: technological wastes

TEM–AEM analyses allowed a better characterisation of the newly-formed phases in the majolica coatings. The occurrence of pyroxenes has been recognised in all the coatings; K–Pb feldspar only occurs in glazes of groups 1 and 2, but not in the enamels. Although all the coatings show a high Pb content (Fortina et al. 2005), the formation of K–Pb feldspar is probably due to the higher Al_2O_3 /alkali ratio in groups 1 and two glazes as compared to the same ratio in groups 1 and 2 enamels, where only K-feldspar is present (Fig. 2).

High-temperature, Ca-rich phases appear in group 3 coatings, confirming that technological wastes result from a flawed, too high firing temperature, which Fortina et al. (2005) suggested to be higher than 1,050°C.

References

- Fortina C, Santagostino Barbone A, Turbanti MI (2005) Sienese “archaic” majolica: a technological study of ceramic bodies and coatings. *Archaeometry* 47:535–555
- Giorgetti G, Gliozzo E, Memmi I (2004) Tuscan black glosses: a mineralogical characterization by high resolution techniques. *Eur J Miner* 16:493–503

- Grassi F, Fortina C, Santagostino Barbone A, Turbanti Memmi I (2003) La maiolica arcaica senese: studio del ciclo produttivo. In: III Congresso Nazionale di Archeologia Medievale. All'insegna del Giglio, 665–670
- Mata MP, Peacor DR, Gallart-Martí MD (2002) Transmission electron microscopy (TEM) applied to ancient pottery. *Archaeometry* 44:155–176
- Viti C, Borgia I, Brunetti B, Sgamellotti A, Mellini M (2003) Microtexture and microchemistry of glaze and pigments in Italian Renaissance pottery from Gubbio and Deruta. *J Cult Herit* 4: 199–210

From Micro- to Nano-Arrangement: Alteration Products in Archaeological Glass from Marine and Land-Based Environments

A. Silvestri, C. Viti, G. Molin, and G. Salviulo

1 Introduction

The alteration of archaeological glass in natural environments is a very complex process affected by many factors, including glass characteristics and external conditions, such as climate, temperature, time, pH, and composition of aqueous solution (Newton and Davison 1996). The present study was carried out on the alteration products of glasses from various archaeological sites, both marine and land-based, in order to understand the relationships between optical features and micro/nano-structural arrangements, and the possible role played by chemico-physical conditions on the morphology and composition of the alteration products.

The materials analysed here are glass fragments originating from the cargo of the Roman ship *Iulia Felix*, discovered at a depth of about 15 m off Grado, in the northernmost part of the Adriatic Sea (Italy). These fragments, exposed to the marine environment for about 1,800 years, were buried in carbonatic sand and subsequently cemented by calcite. All the samples show an exceptional degree of alteration and represent an elective case for the study of alteration processes in glasses, because the geochemical parameters of the conservation environment are known. The results are subsequently compared with those from alteration products of buried Roman and Medieval glass found in sites in the Italian area, e.g., Vicenza, Grado, and Pozzuoli. Some samples show signs of decay due to their prolonged contact with soil and groundwater.

A. Silvestri (✉), G. Molin, and G. Salviulo
Dipartimento di Geoscienze, University of Padova, Padova, Italy
e-mail: alberta.silvestri@unipd.it

C. Viti
Dipartimento di Scienze della Terra, University of Siena, Siena, Italy

2 Materials and Methods

Macroscopically, the “marine” samples show two textural morphologies of the alteration crusts. The coloured glass samples are coated with many iridescent lamellae, imparting a rainbow-like effect. In contrast, the surfaces of colourless glass samples are coated with an opaque white crust, extending more and more deeply into the bulk of the glass. In the case of land-based samples, the alteration products of both coloured and colourless glass are only represented by iridescent lamellae (Silvestri et al. 2005).

The analytical techniques employed in this study are (a) scanning electron microscopy (SEM, CamScan MX2500, operating at 20 kV, 160 μ A and 35 mm working distance; both back scattered electron – BSE – and secondary electron – SE – images), for micro-textural morphologic inspection of alteration layers; (b) electron microprobe (EMPA, CAMECA-CAMEBAX equipped with four WDS spectrometers working at 15 kV, 10 nA and 10 s counting time) for chemical analyses of both pristine and altered portions; (c) transmission electron microscopy (TEM, Jeol 2010, working at 200 kV with 1.9 Å resolution), to define nano-structural details of the alteration crusts.

3 Results and Discussion

4 Micro-Arrangements

In the case of marine samples, SEM observations showed three distinct regions, variable in thickness: (1) a central layer of pristine glass (PG), varying in thickness from 200 to 1,500 μ m; (2) a gel layer (GL) formed on the outside of the original glass fragments (thickness: 10 \div 100 μ m); (3) an alteration crust (AC) over the original glass surface (thickness: 150 \div 1,000 μ m) (Fig. 1a).

The iridescent lamellae of marine samples consist of consecutive multiple layers, each a few micrometers thick, with different morphologies (Fig. 1a–b), according to the morphological types described by Cox and Ford (1993).

The white opaque crusts are characterised in SEM-SE images by a spongy, distorted, ramified texture. This structure is initiated at locally distinct spots on the surface, giving rise to pitting. Pitting develops as the surface channels increase their depth of penetration with time (Fig. 1c–d).

In addition, as also visible in Fig. 5 of Silvestri et al. (2005), SEM-BSE images of the opaque white crusts show dissolution of the gel layer, resulting in an irregular network of thin walls consisting of minute globules, interconnected as straight, curved or circular chains. The dissolution of the gel layer caused the formation of layers 1 m thick, which constitute the advancing corrosion front. In contrast, alteration of glasses from land-based environments reveals only iridescent lamellae, with textural morphologies similar to those of marine samples.

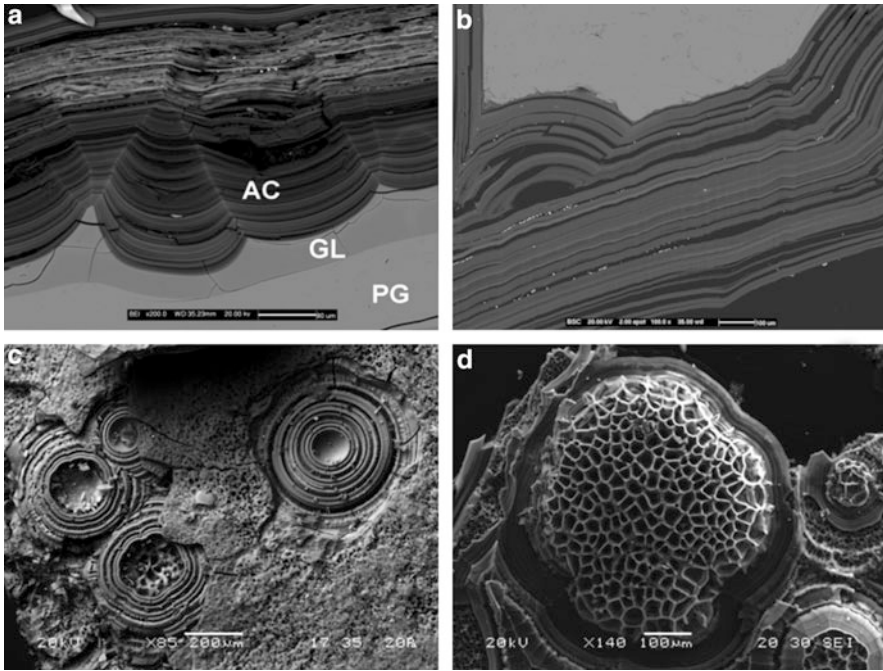


Fig. 1 SEM images of marine glasses showing different shapes of iridescent lamellae and opaque white crusts. (a) Hemispheric layers (SEM-BSE); (b) Parallel layers (SEM-BSE); (c) Opaque white crusts where distinct spots on the surface give rise to pitting (SEM-SE); (d) Spongy structure of single pit in opaque white crust (SEM-SE)

EMPA analyses show that, regardless of the site of alteration and the sample considered, when compared with pristine glass, alteration products are poorer in Na_2O and CaO , and relatively enriched in SiO_2 and Al_2O_3 . The total percentage of oxides constituting the alteration crust is about 60%, due to the presence of water. Apart from possible differences in the chemical composition of pristine glass and extent of alteration lamellae, the alteration products are mainly composed of a hydrated ‘silica gel’ in both submerged and buried glasses (Silvestri et al. 2005).

4.1 Nano-Arrangements

TEM observations show that the alteration products from both marine and land-based environments consist of a lamellar nanostructure, slightly changing from sample to sample. In some cases, the nano-lamellae have a constant size, typically 150–200 nm in width, and are arranged in regular sequences, resulting in a perfectly periodic nanostructure (Fig. 2a–b).

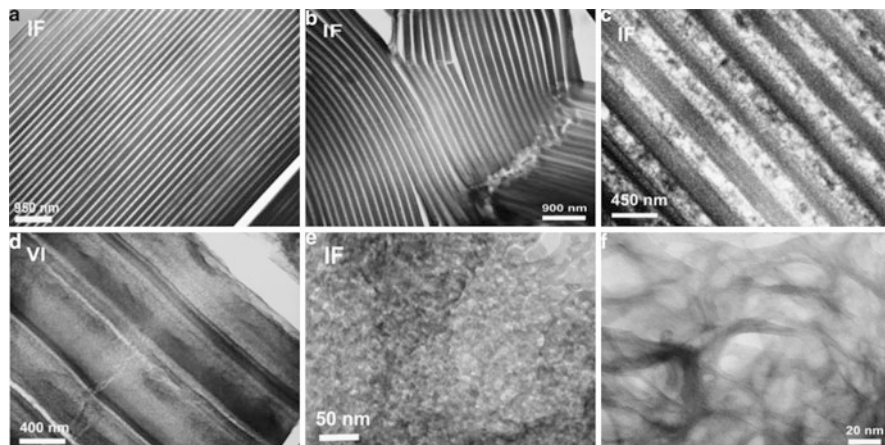


Fig. 2 TEM images showing lamellar and periodic nanostructure of alteration crusts of glass from marine (IF) and land-based (VI) environments (**a,b,c,d**), the grainy and porous texture of marine and buried glass (**e**), and the smectite-like inter-lamellar material (**f**)

In other cases, associated nano-lamellae may display variable width, ill-defined boundaries and inner contrast heterogeneities, giving rise to a less regular structure (Fig. 2c–d).

In both ordered and irregular sequences, the nano-lamellae are completely amorphous, as attested by the corresponding electron diffraction patterns; high-magnification images reveal that this amorphous material, in both marine and land-based environments, has a grainy, porous texture, recalling a sponge-like material (Fig. 2e).

The inter-lamellar space (typically 20–30 nm wide) is often filled by poorly crystalline material, with diffuse, ring-shaped diffraction effects and ill-defined, bent lattice fringes; overall TEM observations suggest a smectite-like material (Fig. 2f).

As regards TEM/EDS results, the nano-lamellae show complex inter- and intra-sample variability, with Si and Al ranging from 70 to 85 and from 7 to 13 wt%, respectively; the Fe, Mg, Ca, and K contents depend on the bulk composition of the pristine glass. The chemical composition of the inter-lamellar space is also variable, but it is always Si-depleted with respect to the associated nano-lamellae (showing variable enrichments in Fe, Mg, K and Na).

5 Conclusions

The similarity of micro- and nano-arrangements in archaeological glass alteration products from marine and land-based environments suggests that the alteration process is similar, independent of the conservation environment.

The formation of alteration products is probably due to the dissolution of glass, with subsequent precipitation of an amorphous material characterised by porous texture. This amorphous material reorganises into extremely regular nano-lamellar structures. The alteration products for both submerged and buried glass are mainly composed of hydrated “silica gel”.

The observed compositional variability shown by TEM/EDS among nano-lamellae and inter-lamellar spaces is ascribed to differing features, including (a) pristine glass bulk chemistry; and (b) the nano-structural evolution of the alteration crusts (i.e., ordered, “mature” vs. irregular, less-evolved sequences).

The ordered periodic nano-lamellar structure explains the typical iridescence of the alteration crusts. The nano-lamellae spacings are in the range of the visible-light wavelength, giving rise to selective diffraction processes. This optical process is similar to the one occurring in opal-based material, although in this case it is produced by silica amorphous nano-lamellae rather than by silica amorphous spheres.

References

- Cox GA, Ford BA (1993) The long-term corrosion of glass by ground-water. *J Mater Sci* 28:5637–5647
- Newton RG, Davison S (1996) Conservation of glass. Butterworth Heinemann, Oxford, pp 135–164
- Silvestri A, Molin G, Salviulo G (2005) Archaeological glass alteration products in marine and land-based environments: morphological, chemical and microtextural characterisation. *J Non-Cryst Solids* 351:1338–1349

An Investigation of the Sulfur–Iron Chemistry in Timbers of the Sixteenth Century Warship, the *Mary Rose*, by Synchrotron Micro-X-Ray Spectroscopy

A.D. Smith, M. Jones, A. Berko, A.V. Chadwick, R.J. Newport, T. Skinner, M. Salomé, J. Frederick, and W. Mosselmans

1 Introduction

The problem of sulfur oxidation in archaeological marine timbers and the risk this poses to historically important wood built ships was first discovered in 2000 by conservators of the *Vasa* in Stockholm. They identified outbreaks of sulfur salts on the ship in their care, which were prevalent under raised humidity levels in the display environment and had the potential to produce sulfuric acid, with obviously damaging consequences to the timber. The original source of sulfur is due to concentration of sulfur dissolved in sea water during the time of the vessel's burial in the marine environment and the occurrence of these sulfur salts is enhanced by the presence of iron corrosion products within the timber (Sandström et al. 2002, 2005). The issue of sulfur contamination and subsequent oxidation has come to be known simply as “the sulfur problem”.

The flagship of the British Tudor King, Henry VIII, is of particular national importance. Since being alerted to the risks posed by the sulfur problem, our research team have been working to determine the extent of the sulfur oxidation process within the *Mary Rose*, understand the sulfur/iron interaction in the ship's

A.D. Smith (✉)
STFC, Daresbury Laboratory, Warrington WA4 4AD, UK
e-mail: andrew.d.smith@stfc.ac.uk

M. Jones
The Mary Rose Trust, Portsmouth PO1 3LX, UK

A. Berko, A.V. Chadwick and R.J. Newport
University of Kent, Canterbury CT2 7NH, UK

T. Skinner
The National Museums of Scotland, Edinburgh EH1 1JF, UK

M. Salomé
ESRF, BP 220, 38043 Grenoble CEDEX 9, Grenoble, France

J. Frederick and W. Mosselmans
Diamond Light Source, Didcot OX11 0DE, UK

timbers and develop new conservation techniques. To this end, a variety of laboratory experiments are underway with particular emphasis being given to techniques employing synchrotron radiation.

One of the primary questions raised by the sulfur problem is the chemical speciation of the sulfur and iron compounds and their relationship to each other in the ship's timbers. X-ray absorption spectroscopy (XAS) is a powerful SR tool that allows local chemical information to be determined for elements of choice within a sample. In previous studies we have utilised both X-ray absorption near edge structure (XANES) and extended X-ray absorption fine structure (EXAFS) to determine sulfur and iron speciation in timber samples taken from the hull of the *Mary Rose* (Skinner et al. 2004; Wetherall et al. 2008). The two main XAS techniques are complementary. XANES gives detailed information on the electronic structure of the target atom and is a strong indicator of oxidation state. (Koningsberger and Prins 1988). The extended range EXAFS measurement yields information on the local structure, specifically the number, type and distances of the neighbouring atomic structure (Rehr and Albers 2000). These previous measurements have used relatively large beam dimensions of approx 1 mm, which provides an average over many thousands of wood cells.

The advent of high brightness, third generation SR sources such as the European Synchrotron Radiation Facility (ESRF) in Grenoble, France and Diamond in the UK, have enabled the focussing of X-rays to very small dimensions and the use of these techniques at microscopic levels (Attwood 1999). In this paper we compare the information gained from two complementary X-ray microprobe instruments at the ESRF and Diamond synchrotrons to reveal chemical information on the iron-sulfur relationship at and below the scale of the wood cell structure.

The X-ray microscope (ID21) at ESRF uses Fresnel zone plate optics to provide a focal beam of a few hundreds of nanometres (Susini et al. 2002). This is considerably smaller than the size of a typical wood cell (~10 μm), so provides high spatial imaging of the cell structure including the cell wall structure and connecting mid-lamella regions. Fresnel zone plates are however highly chromatic devices whose focal length changes with energy, requiring the need to vary the optic sample distance whilst scanning the selected photon energy. The difficulties of doing this limits the energy scan range to XANES type measurements. By comparison, the microprobe XAS beamline (I18) at Diamond uses Kirkpatrick-Baez (KB) optics to produce a beam of 3–5 μm . This obscures the finer cellular structures, although it still enables the larger vessels in the wood to still be imaged. An advantage over the zone plate microscope however is that KB optics are non-chromatic and so can be used for the wider energy ranges needed for EXAFS measurements. The two instruments therefore offer complimentary capabilities.

We demonstrated the ability of the X-ray microscope of beamline ID21 at ESRF to record the spatial distributions of both sulfur and iron chemical species within the wood cell structure in an earlier paper (Wetherall et al. 2008). Due to space constraints we will refer the reader to that paper for more details, and in this paper will concentrate on the complementarity offered by microprobe EXAFS.

The high spatial resolution available on ID21 allows imaging at the sub-cellular level and allowed us to identify individual grains of iron sulfide. Additionally we revealed the presence of iron oxides in the cell walls for samples extracted from the proximity of iron artefacts. These areas were not observed to contain any sulfur, although organic-sulfur species were seen in neighbouring mid-lamella regions. The high spatial resolution of the X-ray microscope constrained us to the study of small sample areas and we did not locate any areas containing sulfate. Therefore the origin of the sulfate remained unclear.

2 Experimental Method

For the X-ray microprobe techniques, the sample needs ideally to be very thin. The X-rays can penetrate some tens of micron into the sample, depending upon the photon energy selected and the density of the sample. This can make interpreting images from materials with small scale heterogeneity in 3 dimensions, difficult. For wood cells it is relatively straightforward to slice samples a few micron thick (*i.e.* less than a wood cell dimension) by careful application of a flexible razor blade. These slices can then be sandwiched between two thin polymer sheets such as Ultralene. This method was utilised for both instruments.

2.1 Microprobe EXAFS

The X-ray microprobe of I18 at Diamond has a lower spatial resolution than the ID21 microscope; this is convenient for the examination of larger areas of timber samples. Additionally, it has been designed for extended range XAS studies, allowing more detailed atomic structures to be determined. Figure 1 shows a series of X-ray images, combined with an optical microscope image of a vessel in a sample of oak timber recently raised (2004) from the *Mary Rose*. In the optical micrograph, iron mineralisation can be seen in the interior walls of the vessel, and in neighbouring cells and has a characteristic orange colour. Although the spatial resolution offered by I18 is not high enough to probe individual cells, iron and sulfur concentrations and speciations can be identified over broader regions. Exploiting the technique of imaging at specific energies, characteristic of individual oxidation states ($\text{Fe}^{2+}/\text{Fe}^{3+}$ and sulfur/sulfate), it can be seen that the iron is clustered in the orange coloured areas observed in the optical micrograph and is of Fe(III) valency. The sulfur valency maps show that in the region of iron mineralisation the sulfur is principally sulfate, whereas in the iron free areas it is reduced sulfur. This is the first time that the co-location of iron minerals and sulfate has been confirmed in waterlogged archaeological wood.

Analysis of the Fe K-edge EXAFS data of the iron in the mineralised region can be fitted to a goethite like structure ($\alpha\text{-Fe}^{3+}\text{O(OH)}$). Data from locations A and B

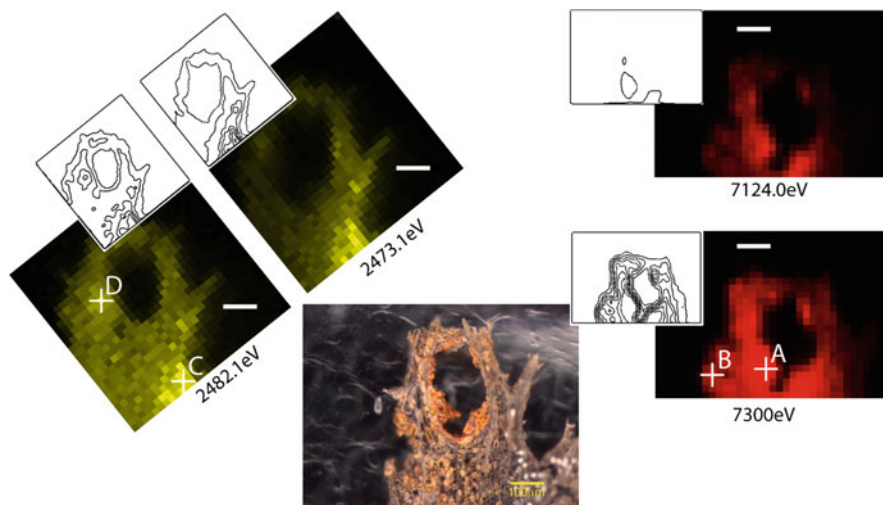


Fig. 1 Optical and X-ray images of a sample of oak from the *Mary Rose* (MRT04). (Left) X-ray maps from I18 of the elemental sulfur (2,473.1 eV) and sulfate (2,482.1 eV); (centre) an optical micrograph of the area neighbouring a vessel and exhibiting extensive iron mineralisation; (right) the same area imaged by X-rays on I18 showing Fe^{2+} (7,124 eV) and combined Fe^{2+} and Fe^{3+} (7,300 eV). Inset are contour plots of the XRF maps. The intensities in the X-ray images have been autoscaled. Scale bars are 100 μm

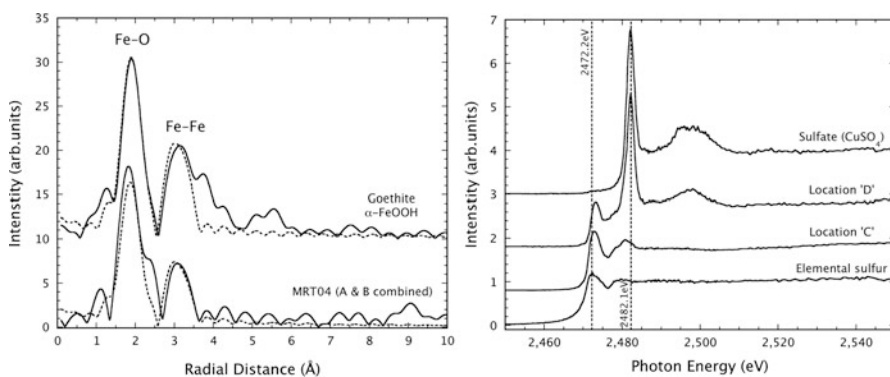


Fig. 2 (Left) Fe EXAFS, combined from locations A & B illustrated in Fig. 1, compared to reference data from goethite ($\alpha\text{-FeO}(\text{OH})$); (Right) Sulfur XANES from locations C & D marked in Fig. 1, compared with reference sulfate and elemental sulfur spectra, showing the prevalence of sulfate in the vicinity of the iron – at location D

were combined and compared with model compound data collected from beamline 16.5 at the SRS and the predicted theory for goethite. The results of this are summarised in Fig. 2 and Table 1 and show a good fit.

Table 1 Fe EXAFS analysis of mineralised iron growth seen in optical micrograph of Fig. 1. Comparison made with goethite model and measurement of goethite standard. R and χ^2 factors are measures of goodness of fit of theoretical models to the experimental data

	Mary Rose MRT04 (A+B)	Goethite standard	Goethite model
Theoretical fits	3O @ 1.927 ± 0.016 Å	3O @ 1.951 ± 0.012 Å	3O @ 1.956 Å
to experimental data	3O @ 2.089 ± 0.021 Å	3O @ 2.095 ± 0.019 Å	3O @ 2.106 Å
	2Fe @ 3.017 ± 0.024 Å	2Fe @ 3.022 ± 0.015 Å	2Fe @ 3.018 Å
	–	1O @ 3.671 ± 0.229 Å	1O @ 3.209 Å
	1.3 ± 0.7Fe @ 3.390 ± 0.042 Å	2Fe @ 3.273 ± 0.094 Å	2Fe @ 3.311 Å
	–	4Fe @ 3.427 ± 0.040 Å	4Fe @ 3.438 Å
R	34.20%	32.03%	–
χ^2	9.06	2.22	–

The inability to fit the oxygen expected at 3.209 Å arises from the limited scattering expected from this single atom. Analysis of the *Mary Rose* sample also shows a noticeable reduction in the number of iron atoms at radial distances of ~ 3.3 Å and beyond. This could reflect a lack of longer range organisation in the iron oxidation that has developed in the wood vessel: similar effects have been reported elsewhere in the literature for iron hydroxide growths (*e.g.* Kaneko et al. 1989).

The nature of the sulfate compound in this region has still to be identified, although ferric sulfate, possibly highly amorphous, is a very likely candidate. We plan future studies using these instruments to better understand the nature of the oxidation of sulfur in marine archaeological timbers, and thus develop potential treatments.

3 Conclusions

In developing an understanding of the underlying chemistry responsible for the “sulfur problem” affecting archaeological marine timbers, we have found it necessary to conduct studies at a range of spatial scales. The use of high spatial resolution X-ray microscopy at the ID21 beamline at ESRF has given unique insights into the interaction between iron and sulfur chemistries within the wood cell structure. The only places where both iron and sulfur are found to co-exist are as iron sulfide grains. Elsewhere they are essentially separate, with iron corrosion products residing in the cell walls with organic sulfur compounds in the mid-lamella regions. X-ray microprobe analysis using I18 at diamond has allowed us to extend this study over a broader region, comparing regions with a heavy iron mineral content with nearby regions which are largely iron free. This has shown the occurrence of sulfates in proximity to the iron, strengthening the supposition that iron is responsible for the oxidation of the sulfur content in archaeological marine timbers.

References

- Attwood D (1999) Soft X-ray microscopy with diffractive optics. In *Soft X-rays and extreme ultraviolet radiation*. Cambridge University Press, Cambridge, pp 337–394. ISBN 0-521-65214-6
- Kaneko K, Kosugi N, Kuroda H (1989) Characterisation of iron oxide-dispersed activated carbon fibres with Fe K-edge XANES and EXAFS and with water absorption. *J Chem Soc, Faraday Trans I* 85(4):869–881
- Koningsberger DC, Prins R (Eds) (1988) *X-ray absorption: principles, applications, techniques of EXAFS, SEXAFS and XANES*. Chemical Analysis. vol 92 Wiley, New York. ISBN:0-471-87547-3
- Rehr JJ, Albers RC (2000) Theoretical approaches to x-ray absorption fine structure. *Rev Mod Phys* 72(3):621–654
- Sandström M, Jalilehvand F, Persseon I, Gellus U, Frank P, Hall-Roth I (2002) Deterioration of the seventeenth-century warship *Vasa* by internal formation of sulphuric acid. *Nature* 415: 893–897
- Sandström M, Jalilehvand F, Damian E, Fors Y, Gelius U, Jones AM, Salomé M (2005) Sulfur accumulation in the timbers of King Henry VIII's warship *Mary Rose*: A pathway in the sulfur cycle of conservation concern. *PNAS* 102:14165–14170
- Skinner T, Erpenbeck S, McConnachie G, Jones AM, Smith AD (2004) XANES spectroscopic study of changes in sulfur speciation in waterlogged archaeological wood in to high RH. In: *Proceedings of the 9th ICOM-CC WOAM conference*. Copenhagen
- Susini J, Salomé M, Fayard B, Ortega R, Kaulich B (2002) The scanning X-ray microprobe at the ESRF 'X-ray microscopy' beamline. *Surf Rev Lett* 9:203–211
- Wetherall KM, Moss RM, Jones AM, Smith AD, Skinner T, Pickup DM, Goatham SW, Chadwick AV, Newport RJ (2008) Sulfur and iron speciation in recently recovered timbers of the *Mary Rose* revealed via X-ray absorption spectroscopy. *J Arch Sci* 35:1317–1328

The Role of TOF-SIMS in the Characterisation of Inorganic and Organic Components in Paint Samples

A. Tognazzi, F. Benetti, R. Lapucci, and C. Rossi

1 Introduction: Aim of the Research and Description of the Painting

The conservation of cultural heritage requires a profound knowledge of the materials and technologies used for its production. In particular, the analysis of the surface of an object of art is of primary importance, considering that it constitutes a basic tool for the understanding of the history of the object and of its ageing processes. In fact, the surface is not only the visible part of the artwork, but it also represents the interface between the object and the environment, where the interactions with physical, biological and chemical agents occur. In order to provide chemical information regarding the surface of the artwork under study and to understand its interactions with the environment, the employment of ToF-SIMS (Time-of-Flight Secondary Ion Mass Spectrometry) appears of fundamental importance. ToF-SIMS provides elemental data and a certain degree of molecular information, while also allowing depth profiling, mapping or imaging to be carried out (Spoto 2000). As a result, this procedure was successfully applied for the characterisation of inorganic and organic components of a wide range of cultural heritage objects (Keune and Boon 2004; Adriaens and Dowsett 2006; Mazel et al. 2006).

The aim of the present paper is to characterise inorganic and organic components in paint samples from “*The Martyrdom of St. Catherine*” (Fig. 1), conserved in the parish Church of St. Catherine in Zejtun (Malta), by the application of ToF-SIMS. This work of art represents Saint Catherine’s, one of the great Christian martyrs of

A. Tognazzi (✉), F. Benetti, and C. Rossi

Department of Chemical and Biosystem Sciences, University of Siena, Via A. Moro 2, Siena, Italy and

Inter-University Center of Colloid and Surface Science - CSGI, Via della Lastruccia 3, Sesto Fiorentino, Florence, Italy

e-mail: tognazzi@unisi.it

R. Lapucci

Studio Art Centers International - SACI, Via Sant’Antonino 11, Florence, Italy



Fig. 1 “*The Martyrdom of Saint Catherine*”, oil on canvas, 268 × 204 cm, seventeenth century, attributed to Francesco Cassarino, conserved in the church of Saint Catherine, Zejtun (Malta)

the fourth century AD, execution at the hands of a Turkish executioner with his curved scimitar (Lapucci 2008)

2 Experimental Method

In 2007, during the diagnostic campaign, 14 micro-fragments (mostly smaller than 1 mm) were collected from different areas of the painting, according to the principle of minimum invasiveness, i.e. the minimum number of collected samples required to obtain the maximum amount of information.

As mentioned above, the analysis of the inorganic and organic components and their spatial distribution within the paint samples were carried out by ToF-SIMS. The employed instrumentation consisted of a TRIFT III (PHI – Physical Electronics, USA) device, equipped with a single Au LMIS (FEI Beam Technology, France), with a slope of 45° with respect to the sample surface, a triple Electrostatic Analyzer and Dual Multi Channel Plate Detector, combined with a Phosphoscreen. The sample is introduced in a vertical position into a pre-chamber.

The micro-fragments were attached to an aluminum foil by bi-adhesive tape and inserted into the SIMS sample holder. This was kept in the intro-chamber at a pressure of 10^{-6} torr for 36 h, to avoid degassing in the main chamber of the instrument during the analysis. All samples were analysed in static mode (primary ion dose $<10^{12}$ ions/cm²) on an area of $200 \times 200 \mu\text{m}^2$, in a mass range of 0–2,000 m/z.

3 Results and Discussion

For each micro-fragment, both secondary ion spectra, positive and negative, and the images of the distribution of some of the detected ions (elements and molecular fragments) on the analysed surface were collected. Examples of secondary ion spectra, positive and negative, with chemical images of the spatial distribution of inorganic and organic compounds are reported in Figs. 2a, b and 3a, b.

Figure 2a shows the positive mass spectra in the mass range of 10–610 m/z. The presence of silicon (probably originating from the matrix of the bi-adhesive tape) and traces of aluminum, potassium and calcium were primarily detected, as confirmed by the signals at 27, 28, 29, 39, 40, and 41 m/z. The region of the spectrum close to 200 m/z shows the presence of characteristic signals of the three isotopes belonging to lead, at 206, 207, and 208 m/z, respectively; in addition, one of the three isotopes of PbH is evident at 209 m/z. The intense peaks at 355 and 399 m/z are attributable to residues of the bi-adhesive tape, whereas the signals at 323, 325, and 339 m/z are typical of walnut oil, as confirmed by the comparison with spectra of thin films of drying oils used as reference materials (not reported). In addition, the peaks at 339 and 603 m/z, indicated by asterisks, are associated with the fragmentation of the triolein, and the peak at 603 m/z is characteristic of diolein. The region of the spectrum over 400 m/z shows peaks characteristic of a natural compound with high molecular weight, not identified, probably a polymerised natural resin.

In Fig. 2b, the negative ion mass spectrum in the mass range of 10–1,500 m/z is reported. The signals of chlorine and sulphur are clearly observable at 32, 35 and 37 m/z. In addition, the presence of characteristic signals of fatty acids can be observed in the region between 250 and 300 m/z. In particular, the more intense signals at 255, 281 and 283 m/z are respectively attributed to palmitate, oleate and stearate ions. The signals of an organic substance with high molecular weight, probably a polymerised natural resin, are also present in the negative spectra.

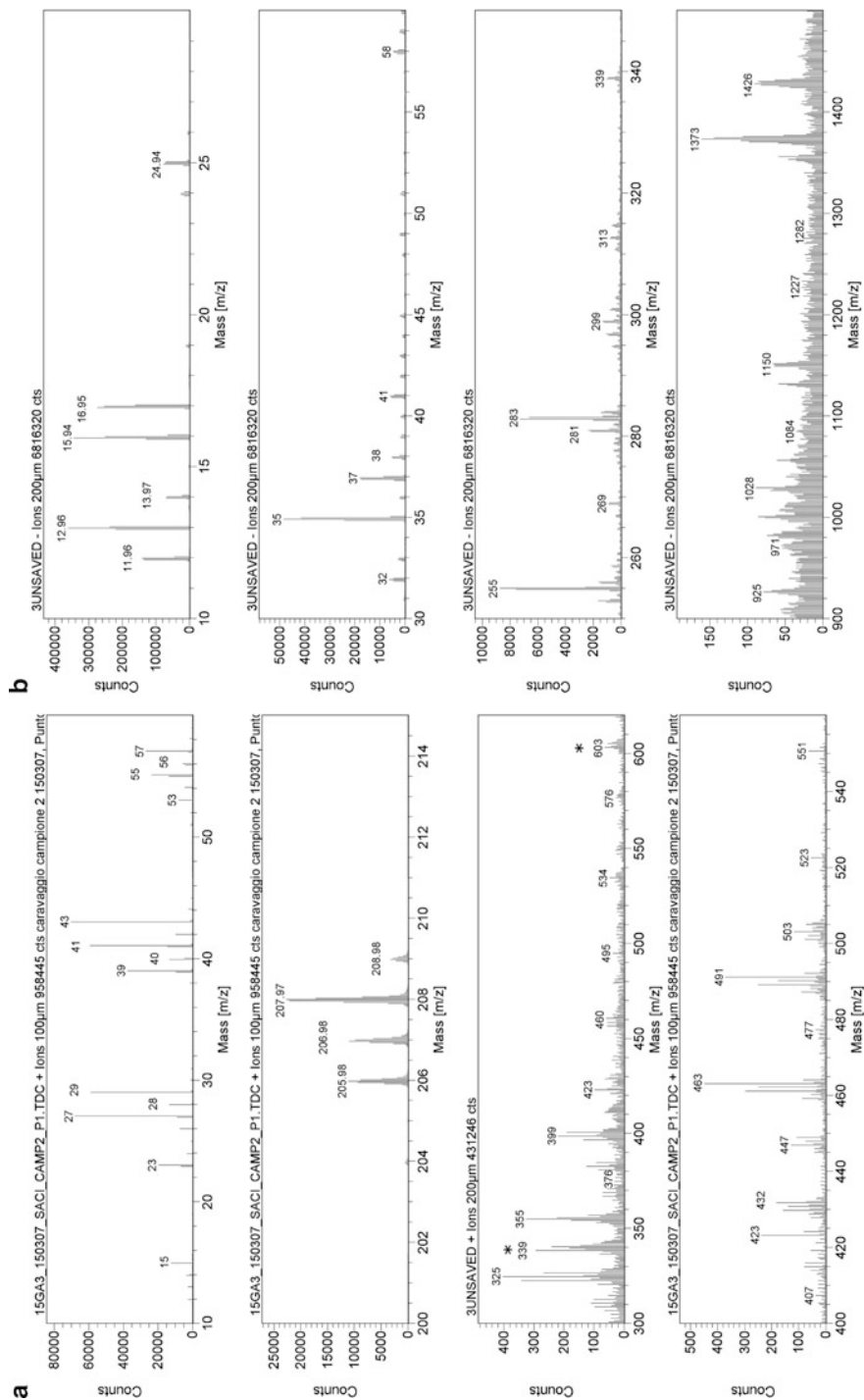


Fig. 2 (a) positive secondary ion spectrum in the region of 10–610 m/z; (b) negative secondary ion spectrum in the region of 10–1,500 m/z

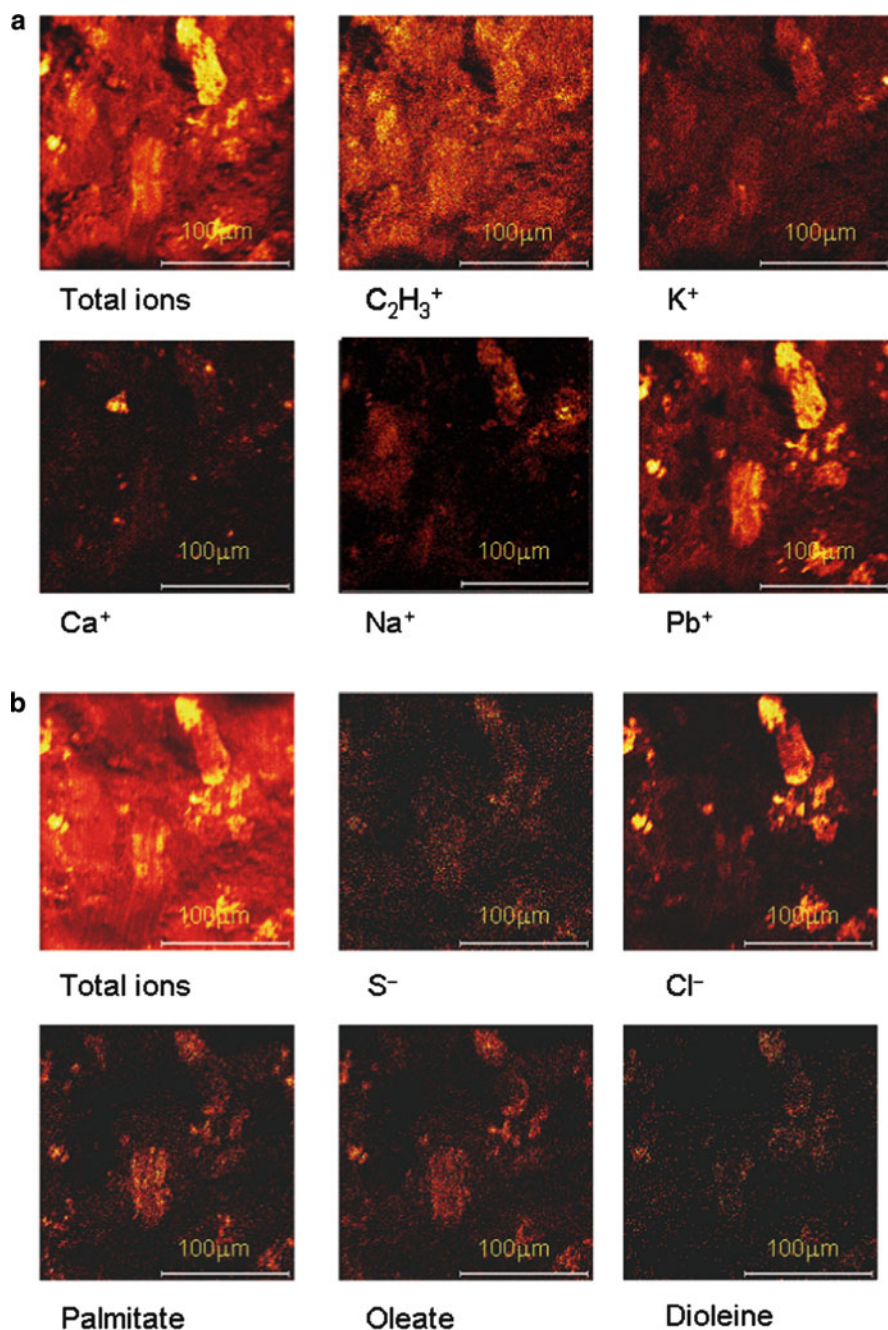


Fig. 3 ToF-SIMS images: (a) positive ion images on a $200 \times 200 \mu m^2$ area show the distributions of total positive ion signals, $C_2H_3^+$, K^+ , Ca^+ , Fe^+ , Pb^+ ; (b) negative ion images on a $200 \times 200 \mu m^2$ area show the distributions of total negative ion signals, S^- , Cl^- , palmitate, oleate and dioleine

In Fig. 3a, the ToF-SIMS images of a $200 \times 200 \mu\text{m}^2$ area show the distribution of the total positive ion signals (i.e. the sum of all signals in the interval 0–2,000 m/z) of Pb^+ , Na^+ , Ca^+ , K^+ , and an organic fragment with mass 27 (associated to C_2H_3^+ , one of the most common fragments originating from organic molecules, representative of the distribution of organic matter).

In Fig. 3b, on the right, the ToF-SIMS images of the distribution of the total negative ion signals and some negative ions (S^- and Cl^-) in the analysed area are reported. In the lower part of the same figure, the distributions of 253, 281 and 339 m/z ions are reported, related to the presence of palmitic acid, oleic acid and diolein (or another diglyceride with the same weight as the linoleic stearic mixed diglyceride), typical components of drying oil binders.

4 Conclusions

Fourteen micro-fragments were collected from different areas of the painting “*The Martyrdom of St. Catherine*” and analysed by ToF-SIMS. This analytical technique represents an innovative approach for the characterisation of organic and inorganic materials in paintings. More specifically, ToF-SIMS analyses are able to identify both the pigments and binders used in paintings and show their distribution, by means of chemical images, on a micro-fragment or a micro-stratigraphy.

In particular, in the present study of “*The Martyrdom of Saint Catherine*”, aluminum, potassium, calcium and lead signals were detected. This information, in addition to the Raman, FORS-VIS, SEM-EDS, FTIR and Optical Microscopy results of a previous study (Lapucci 2008), ascertains the presence of Lead White, Green Earth, and Red and Yellow Ochre pigments. Additionally, a drying oil is also present as a pictorial binder, namely walnut oil. Moreover, the presence of chlorine could be associated with marine spray, compatible with coastal areas such as the Maltese one. Finally, in positive and negative ion mass spectra, the presence of a natural compound with high molecular weight (perhaps a polymerised natural resin) was identified.

Acknowledgements We want to thank the Caravaggio Foundation of Malta, Studio Art Centers International, CTS Srl, in the person of Dr. L. Borgioli, and Dr. S. Ristori of Florence University, for the support given during this study.

References

- Adriaens A, Dowsett MG (2006) Applications of SIMS to cultural heritage studies. *Appl Surf Sci* 252:7096–7101
- Keune K, Boon JJ (2004) Imaging secondary ion mass spectrometry of a paint cross section taken from an early Netherlandish painting by Rogier van der Weyden. *Anal Chem* 76:1374–1385

- Lapucci R (2008) *The Zejtun painting: shades of caravaggio*. Edifir – Edizioni Firenze, Florence
- Mazel V, Richardin P, Touboul D, Brunelle A, Walter P, Lapr evote O (2006) Chemical imaging techniques for the analysis of complex mixtures: New application to the characterization of ritual matters on African wooden statuettes. *Anal Chim Acta* 570:34–40
- Spoto G (2000) Secondary ion mass spectrometry in art and archaeology. *Thermochim Acta* 365:157–166

Part IV
Bioarchaeology

Provenance Study of Wood Found in Archaeological and Architectural Objects

S. Fossati, G.L.A. Pesce, and A. Decri

In this paper we would like to address the study of the provenance of wood used for artistic objects (e.g., statues, panels), architectural structures (e.g., rafters, beams) and archaeological findings, (e.g., foundation piles) through the analysis of its growing curves. The comparison of these curves (sample curves) with different standard curves that originated from different places can in fact be used for discovering the provenance of the wood used in the respective objects. The method that we emphasize here is based on the analysis of two values: the “correlation coefficient” value and the “coincidence rate” value, developed by Eckstein (2007) in a study of a few statues and panels of the Lübeck Cathedral. However, our study is also based on a graphic comparison of the trend curves of samples with the trend curves of the references. In fact, by following this methodology, it has been possible to study the provenance of a large number of samples gathered by the Dendrochronological Laboratory of the Institute for the History of Material Culture (ISCUM – Genoa, Italy) during the past years.

1 Materials and Methods

ISCUM’s archive contains more than 335 dendrochronological curves of samples coming from locations throughout the Ligurian region and about 400 curves coming from all other Italian regions. These samples have been collected both from archaeological excavations and from studies of “building archaeology”. They represent many different types of objects, like foundation piles, rafters, frames of windows, etc., made between the fourteenth and the nineteenth century. The 335 curves originating from Liguria can be divided in conifers (268 curves), chestnut (27 curves), elm (28 curves) and oak (12 curves).

S. Fossati (✉), G.L.A. Pesce, and A. Decri
Institute of the History of Material Culture (ISCUM), c/o Museum of St. Agostino, Piazza Sarzano,
35r 16128 Genoa, Italy
e-mail: dendrolab@iscum.it

Table 1 List of reference curves used in the study

N°	Curve	Species	First year	Last year	Author	Source (cfr. Bibliography)
1	Kostomuksha (Karelia – Russia)	<i>Pinus Sylvestris L.</i>	1578	1992	Schweingruber	International Tree-Ring Data Bank
2	Pyhan Hakin National Park (Finland)	<i>Pinus Sylvestris L.</i>	1643	1978	Schweingruber	International Tree-Ring Data Bank
3	Gotland (Sweden)	<i>Pinus Sylvestris L.</i>	1127	1987	Schweingruber	International Tree-Ring Data Bank
4	Dannensterm House (Riga – Lithuania)	<i>Pinus Sylvestris L.</i>	1445	1739	Zunde	International Tree-Ring Data Bank
5	Col de Sorba Mount Renose (Corsica – France)	<i>Pinus Nigra</i>	1518	1980	Schweingruber	International Tree-Ring Data Bank
6	Ceppo Bosco of Mortense (Abruzzo – Italy)	<i>Abies Alba.</i>	1654	1980	Schweingruber	International Tree-Ring Data Bank
7	Pratomagno-Bibbiana – Apennines Mountain (Toscana – Italy)	<i>Abies Spp. Mill.</i>	1540	1973	Becker	International Tree-Ring Data Bank
8	Mount Ventoux (France)	<i>Abies Alba Mill.</i>	1653	1975	Serre-Bachet	Serre-Bachet (1986)
9	Ardennes (Liege - Belgium)	<i>Quercus Spp. L.</i>	1118	1986	Hoffsummer	International Tree-Ring Data Bank
10	Munich (Bavaria – Germany)	<i>Quercus Spp. L.</i>	960	1961	unknown	N.A. (1970)
11	Germany (west bank of Rhine)	<i>Quercus Spp. L.</i>	822	1964	Hollstein	Le Roy Ladurie (1982)
12	French Jura (France)	<i>Quercus Spp. L.</i>	1360	1984	André Billamboz	Billamboz (1990)

Reference curves used for the comparisons with the above mentioned sample curves are published both in the scientific literature and on the Internet sites of some dendrochronological laboratories. In particular, we found that the curves listed in Table 1 were very useful for the examples presented below.

The evaluation of the best fitting of sample curves with the reference curves has been based on three elements: (a) calculation of the so called “correlation coefficient” between two parts of the curves (the sample curve and the reference curve); (b) calculation of the so called “coincidence rate” between the same parts of the curves; (c) graphic comparison of curves in the years emphasized by the statistical analysis. All calculations are based on the “*t* test” and are obtained by

a software specifically developed inside the Dendrochronological Laboratory of ISCUM, which summarises the different data inside two tables and is very simple to use. By using this software, we can recognize the parts of the reference curves that present the best possible fit to the sample curves, and we can plot these parts of the curves for a graphic evaluation (a very important step of the analysis because sometimes the statistical comparisons are deceptive) in a very short time.

2 Results

As previously mentioned, we studied almost all of the curves of our database according to this methodology. Some examples are very useful for understanding the method and the results we achieved. The first example is the case of sample n° 595: a table of Pine Sylvester from the eighteenth century, stored in the Royal Palace of Genoa. The comparison of the growing curve of this sample with different standard curves gave some very different results for the correlation coefficient and the coincidence rate that highlight a specific reference curve. In fact, the comparison of the sample curve with the curve from Karelia (see Table 1) gave a value of 7.05 for the correlation coefficient and a value of 53 for the coincidence rate, whereas the comparison of the same sample with the curve from central Finland gave a correlation value of 4.65 and a coincidence value of 40. The same sample, when compared with the reference curve from Sweden, gave a value of 3.86 for the correlation coefficient and a value of 40 for the coincidence rate; the comparison with the reference curve from Lithuania gave a correlation value of 3.32 and a coincidence value of 42. The last comparison with the curve from Corsica gave a correlation value of -2.55 and a coincidence value of 36. By the analysis of these data and the graphic comparison of curves (see Fig. 1), it is possible to note that the curve from Karelia fits better than the others when compared to the growing curve of the sample. From a historic point of view, it is well-known that Genoa, since the fifteenth century, has had extensive commercial relations with the north-west regions of Russia, and probably also with the region of Karelia. On these bases, we can advance the hypothesis that the wood of sample n° 595 came from an area of the Russian Empire located between the White Sea and the Gulf of Finland.

Curve n° 39 of the archive is another very useful case for understanding this method. This sample is from a fir tree originating from a floor in a building of the *Salita del Prione* street of Genoa, dated to 1808. In this case, the growing curve of the sample, as compared with the curve from Abruzzo, gave a correlation value of 3.76 and a coincidence value of 57, whereas the comparison with the curves of Pratomagno (near Florence, Italy), Corsica and Ventoux Mountain (France) gave the following results, respectively (the first one indicates the correlation and the second one the coincidence): 2.16/45; 1.30/53; 0.46/43. In this case, according to the statistical and graphic comparisons, it is possible to advance the hypothesis

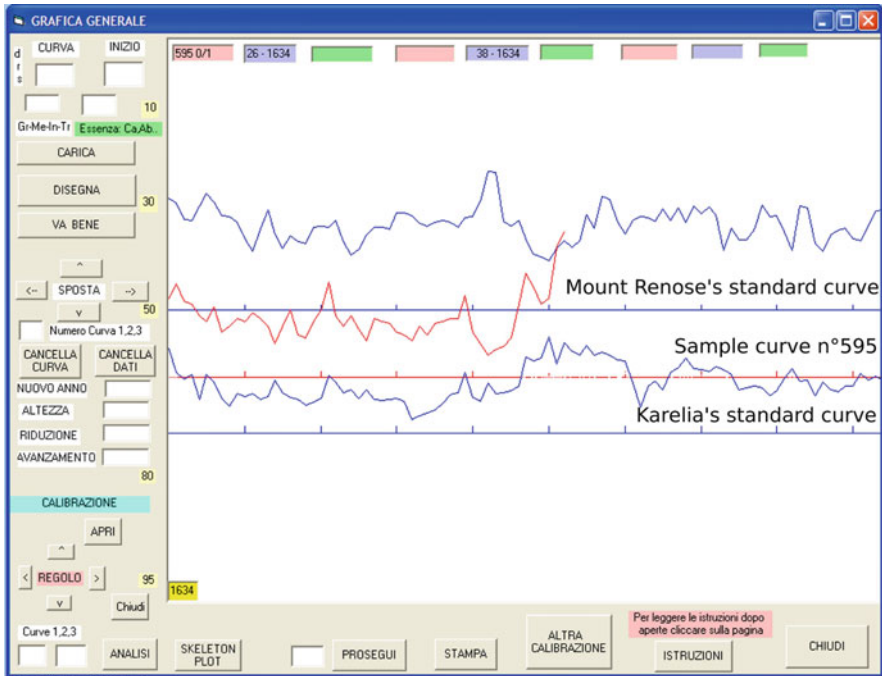


Fig. 1 Graphic comparison of sample curve n° 595 with standard curve from Kostumuksha (Karelia) and Col de Sorba Mount Renose (Corsica – France)

that the sample comes from a central area of Italy, and it is well known that Genoa, during the nineteenth century, had imported timber from that area.

Another object of our study is an oak rafter coming from the *Palazzo Ducale* in Genoa (sample n° 314), dated to the sixteenth century. The comparison between the growing curve of this sample and the reference curve from the Ardennes gave a value of 5.06 for the correlation and a value of 62 for the coincidence, while the comparison with the reference curve from Bavaria gave a correlation value of 3.62 and a coincidence value of 41. The same analysis, carried out in comparison with the reference curves coming from the west bank of the River Rhine and from the Jura Mountains, gave the values of, respectively, 3.28/46 and $-0.14/52$ for the correlation and the coincidence rate. In this manner, after the graphic comparisons of curves, it was possible to advance the hypothesis that the wood of the rafter was imported from the area of Flanders. From the studies of historical documents, it is well-known that Genoa had extensive commercial relations with Flanders in the Middle Ages and in the Modern Age, but it is also well known that the few oaks imported from that region were considered of too poor quality for being used in the boatyards (the main destination of oaks imported in Genoa). It is probably for this reason that we found an oak rafter inside a building and not a boatyard.

3 Discussion

If we try to summarise the results obtained according to this methodology, it is possible to underline that it thus becomes feasible to identify the area of provenance of the wood used in archaeological and architectural objects by means of comparison of the growing curve of samples with different reference curves. In fact, it is always possible to find a reference curve that fits better than others when compared to the growing curve of samples and, at the same time, it is always probable that some curves will give unacceptable results for the correlation (like in the case of sample n° 595, in which the correlation values vary between 7.05 and -2.55).

The value of the “coincidence rate” must be considered only in relation with the results of the “correlation” test; in fact, in the case of sample n° 314, the comparison with the curve from the Jura Mountains gave a value of coincidence higher than the value obtained with the curve from Munich, for which we obtained a value of correlation higher than for the curve from the Jura Mountains (3.62 instead of -0.14). However, in this case the graphic comparison has clearly shown that the curve from Munich fits better than the curve from the Jura Mountains when compared to the sample growing curve. As already mentioned above, the graphic study of the sample and the reference curves completes the analysis, as it allows a verification of the statistical analysis, which in some cases can give very skewed results.

As a general observation, it has to be noted that, for this type of analysis, the choice of the reference curves is fundamental, as it can heavily condition the final result. For this reason, it will be necessary to obtain a larger number of reference curves from different areas of the world. At the same time, it is also necessary to emphasize that, regardless of the availability of reference curves, it is possible to identify the provenance area with high precision only in the case of conifers, because, as it is known, the curves of two conifer trees grown in areas located at a distance of even only 200–250 km away from each other can have very different curves. On the other hand, the identification of the provenance of broad-leaved trees (such as, for example, the chestnut oak) that do not change their curves so much as a function of the different place of origin, does not allow for high precision.

References

- Billamboz A (1990) Etude Dendrochronologique et approche historique d'un village du Jura comtois. *Dendrochronologia* 8:99–117
- Eckstein D (2007) Human time in tree rings. *Dendrochronologia* 24(2–3):53–60
- International Tree-Ring Data Bank. Da: <http://www.ncdc.noaa.gov/paleo/treering.html>, last consultation: November 2008
- Le Roy Ladurie E (1982) Tempo di festa, tempo di carestia. Storia del clima dall'anno mille. Giulio Einaudi Editore s.p.a, Torino, pp 411–414
- Serre-Bachet F (1986) Une chronologie maîtresse du Sapin du Mont Ventoux (France). *Dendrochronologia* 4:87–96
- NA (1970) *Dendrochronologia*. La Starcia 1:w.p.

Hormone Mass Fingerprinting: Novel Molecular Sex Determination of Ancient Human Skeletal Remains

L. Mark, Z. Patonai, A. Vaczy, N. Kajsza, and A. Marcsik

1 Introduction

The identification of an unknown individual consists of many different steps, similar to a complex puzzle, and one of the most significant of these is the determination of the individual's sex. Currently, the morphological investigation of the sex of excavated skeletal remains is widely accepted in anthropological science. The methods used in this field have been primarily focused on the morphology of the pelvis, where the sexual dimorphism is best visible, of the skull and the long bones, where the size and morphology are varied and best represented (Acsádi and Nemeskéri 1970). However, the sex determination of fragmented and infantile bones is impossible with these classic methods. Sexual hormones and other steroids are essential biomolecules in human and animal organisms, with pronounced biological activities at low concentrations. It is a well known fact that the manifestation of the sexual dimorphism is regulated by steroid hormones after the initial foetal period (Hughes et al. 1999). They regulate maturation and reproduction, and are involved in bone metabolism, affecting osteogenesis and bone mineral density. Their etiologic importance is also acknowledged, as these substances play an important role in several frequent chronic diseases, like breast and prostate cancer, or osteoporosis (Leder 2007; Thomas et al. 2008; Wells 2007).

L. Mark (✉), A. Vaczy and N. Kajsza
Institute of Biochemistry and Medical Chemistry, University of Pécs, Szigeti str.12, 7624 Pécs,
Hungary
e-mail: laszlo.mark@aok.pte.hu

Z. Patonai
Institute of Biochemistry and Medical Chemistry, University of Pécs, Szigeti str.12, 7624 Pécs,
Hungary
and
Institute of Forensic Medicine, University of Pécs, Szigeti str.12, 7624 Pécs, Hungary

A. Marcsik
Department of Anthropology, University of Szeged, Egyetem str. 2, 6722 Szeged, Hungary

In this study, a rapid, high-throughput, sensitive matrix-assisted laser desorption/ionization time-of-flight mass spectrometric (MALDI TOF MS) technique has been developed for the analysis of steroids in human tissues. The method was used for molecular sex determination of ancient human skeletal remains, and it was thoroughly tested with well-known clinical and forensic human bone samples.

2 Materials and Methods

Estrone (E1; 1,3,5(10)-estratrien-3-ol-17-one), β -estradiol (E2; 3,17 β -dihydroxy-1,3,5(10)-estratrien), estriol (E3; 1,3,5(10)-estratrien-3,16 α ,17 β -triol), progesterone (4-pregnene-3,20-dione) and testosterone (17 β -Hydroxy-3-oxo-4-androstene) (Sigma–Aldrich Kft., Budapest, Hungary) were used as analytical steroid standards. The reference solutions were prepared by dissolving 0.1 mg of the steroid hormones in 10.00 cm³ of dichloromethane (LiChrosolv, Merck KGaA, Darmstadt, Germany). Following complete dissolution, the 100 μ l of the reference solutions were diluted up to 1.00 cm³. The C₇₀ fullerene (Gold grade) was purchased from Hoechst AG (Frankfurt, Germany).

In this study, various forensic bone samples and paleoanthropological remains have been analysed. The measured bone samples are presented in Table 1. All of the archaeological bones (1–8) and the clinical samples (15–18), as well as the forensic remains in the majority of cases (9–13), were well preserved and the morphological

Table 1 The analysed skeletal remains and identified steroid hormones

No.	Location	Grave	Anatomy	Age	Period	Identified steroid hormones				Sex
						E1	E2	E3	T	
1	Gorzsa	5	Thoracic vertebra	Adult	4850–4550 B.C.	+		+		Female
2	Gorzsa	10	Thoracic vertebra	Adult	4850–4550 B.C.	+	+	+		Female
3	Gorzsa	12	Thoracic vertebra	Adult	4850–4550 B.C.			+	+	Male
4	Gorzsa	18	Thoracic vertebra	Adult	4850–4550 B.C.				+	Male
5	Szegvar	424	Thoracic vertebra	Adult	900–1000 A.D.				+	Male
6	Szegvar	435	Thoracic vertebra	Adult	900–1000 A.D.				+	Male
7	Szegvar	511	Thoracic vertebra	Adult	900–1000 A.D.	+	+	+		Female
8	Szegvar	597	Thoracic vertebra	Adult	900–1000 A.D.			+		Female
9	Bataszek 1		Thoracic vertebra	Adult	1980 A.D.				+	Male
10	Bataszek 2		Thoracic vertebra	Adult	1980 A.D.				+	Male
11	Kalocsa		Thoracic vertebra	Adult	1980 A.D.				+	Male
12	Pecs		Thoracic vertebra	Adult	1980 A.D.	+	+	+		Female
13	Bonyhad		Thoracic vertebra	Adult	1980 A.D.	+	+	+		Female
14	Harta		Thoracic vertebra	Adult	1980 A.D.			+	+	Male
15	Clinical 1		Thoracic vertebra	Adult	2007 A.D.	+	+	+		Female
16	Clinical 2		Thoracic vertebra	Adult	2007 A.D.	+	+	+		Female
17	Clinical 3		Thoracic vertebra	Adult	2007 A.D.				+	Male
18	Clinical 4		Thoracic vertebra	Adult	2007 A.D.	+	+	+		Female

E1: estrone, E2: estradiol, E3: estriol, T: testosterone

sex had been previously determined using classic anthropological methods. Archaeological bone samples were collected from the Late Neolithic site of Hodmezovasarhely-Gorzsa-Czukortanya (Hungary). The settlement and the cemetery are radiocarbon dated to a period around 4850–4550 BC (2σ , 95% confidence) (Hertelendi et al. 1998). The forensic sample n. 14 was an extremely disintegrated human torso, recently found in the Danube River. The human skeletal remains were provided by the Department of Anthropology, University of Szeged, and the Institute of Forensic Medicine, University of Pecs.

2.1 Steroid Extraction

Estrogens and testosterone were detected after a straightforward extraction procedure. The bone fragments were trimmed free of soft tissues and washed with phosphate buffer saline (PBS) and distilled water to remove contaminants. The bone powder was ground by hand with an agate mortar; the particle size was ca. 0.2 mm. In brief, steroid hormones were extracted from pulverized bone samples as follows: 100 mg of calcified bone powder (Thoracic vertebra) was homogenized with 10.00 cm³ of dichloromethane (LiChrosolv, Merck KGaA, Darmstadt, Germany) in an ultrasonic bath for 15 min. The extract was centrifuged and the supernatant was collected. The supernatants were then evaporated to dryness at room temperature, and the solid residues were re-dissolved in 10 μ L of dichloromethane/methanol/water (7:2:1, v/v).

2.2 MALDI TOF Mass Spectrometry

1 μ L of the standard solutions and the bone extracts were loaded onto the target plate (MTP 384 target plate, ground steel TF, Bruker Daltonics, Bremen, Germany) by mixing with the same volume of a saturated matrix solution, prepared by dissolving C₇₀ fullerene in toluene. The mass spectrometer used in this work was an Autoflex II TOF/TOF (Bruker Daltonics, Bremen, Germany) operated in reflector mode. The ions were accelerated under delayed extraction conditions (80 ns) in positive and negative ion mode with an acceleration voltage of 20.00 kV. The instrument uses a 337 nm pulsed (50 Hz) nitrogen laser, model MNL-205MC (LTB Lasertechnik Berlin GmbH., Berlin, Germany). External calibration was performed in each case by using saturated α -cyano-4-hydroxycinnamic acid solution in acetonitrile/0.1% TFA (1/2, v/v) and Bruker Peptide Calibration Standard (#206195 Peptide Calibration Standard, Bruker Daltonics, Bremen, Germany). Hormone masses were acquired in a range of 50–1,000 m/z. Each spectrum was produced by accumulating data from 500 consecutive laser shots. The Bruker FlexControl 2.4 software was used for control of the instrument and the Bruker FlexAnalysis 2.4 software for spectra evaluation (Bruker Daltonics, Bremen, Germany).

3 Results and Discussion

Non-derivatised, neutral steroids are difficult to analyse by MALDI TOF mass spectrometry using common matrix materials (α -cyano-4-hydroxycinnamic acid, sinapinic acid, 2,5-dihydroxybenzoic acid). Nevertheless, the ionization of estrogens and androgens was more effective when using C₇₀ fullerene as matrix (Mernyák et al. 2008). We can distinguish significant differences between the female and male sexual hormones by using the positive ionization mode (Fig. 1). The presence of testosterone and estrogens (E1, E2, E3) was used for sex identification. The protonated quasimolecular ion of the testosterone (m/z 289.3) was identified from the male samples, while in the case of the female skeletal remains the peak of testosterone was undetectable. The peaks of estrone (m/z 271.2) and estradiol (m/z 272.4) were detected in the female bone samples; however, the peak of estriol (m/z 288.4) could be identified in two male samples (an archaeological case from Gorzsa grave 12 and a forensic bone sample from Harta) as well. Sample 14 showed the applicability of the method in forensic work. This sample was an extremely disintegrated human torso recently found in the Danube River. In this case, the morphological sex determination was inefficient, while hormone mass fingerprinting (HMF) proved successful in determining the sex; furthermore, this steroid result was confirmed by DNA analysis. In order to verify the applicability of

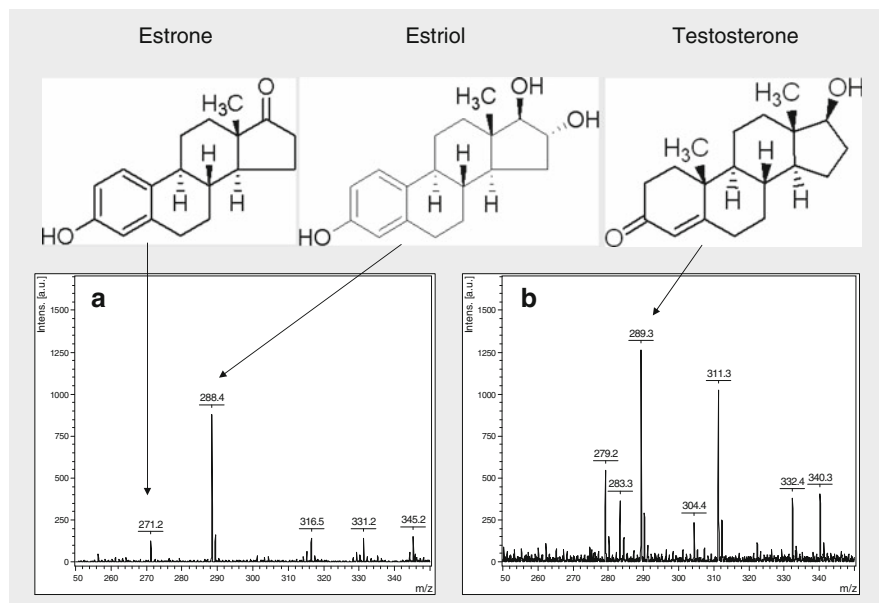


Fig. 1 Positive ion MALDI TOF spectra of 7,000-year-old archaeological bones. (a) Steroid profile of a female anthropological sample; it shows the protonated quasimolecular ion of estrone at m/z 271.2 and the positively charged molecular ion of estriol at m/z 288.4. (b) Steroid profile of a male bone sample; the positively charged molecular ion of testosterone appears at m/z 289.3

our novel sex determination technique, several well-known clinical human bone tissues (samples 15–18) were analyzed using HMF. The results of the morphological and the HMF sex determination techniques correlated significantly.

4 Conclusion

Establishing the identity of unknown individuals from human skeletal remains is of vital importance in the fields of physical anthropology, bioarchaeology, forensic osteology and military exhumation. In the present paper, we developed, for the first time, a high-throughput molecular sex determination technique for ancient and forensic skeletal remains using MALDI TOF MS. In our study, 6,800-year-old steroid hormones were extracted and identified, and the results of female and male steroidal profiles correlated with the morphological and the genetic sex determination of human remains. Based on our preliminary results, hormone mass fingerprinting (HMF) is a potentially useful method for the anthropological analysis of ancient and forensic skeletal remains. Further studies are required to determine the steroid hormone profile of infantile skeletal remains. In our opinion, the sex of fragmented archaeological bone samples, as well as of forensic remains found in an advanced state of disintegration, can be determined using the novel HMF technique. However, the method requires further investigations to verify the real potential of its applicability in paleoanthropological research.

References

- Acsádi G, Nemeskéri J (1970) History of the human life span and mortality. Academic, Budapest
- Hertelendi E, Svingor E, Raczky P, Horvath F, Futo I, Bartosiewicz L (1998) Duration of tell settlements at four prehistoric sites in Hungary. *Radiocarbon* 40:659–669
- Hughes IA, Coleman N, Ahmed SF, Ng KL, Cheng A, Lim HM, Hawkins JR (1999) Sexual dimorphism in the neonatal gonad. *Acta Paediatr Suppl* 88:23–30
- Leder B (2007) Gonadal steroids and bone metabolism in men. *Curr Opin Endocrinol Diabetes Obes* 14:241–6
- Mernyák E, Zs B, Hazai E, Márk L, Gy S, Wölfling J (2008) Steroidal δ -alkenyl oximes as ambident nucleophiles: Electrophile-induced formation of oxazepane derivatives in the bis-estrone series. *Lett Org Chem* 5:17–21
- Thomas W, Caiazza F, Harvey BJ (2008) Estrogen, phospholipase A and breast cancer. *Front Biosci* 13:2604–13
- Wells JC (2007) Sexual dimorphism of body composition. *Best Pract Res Clin Endocrinol Metab* 21:415–30

Hair: An Untapped Forensic Resource

N.C. McCreesh, A.P. Gize, and A.R. David

1 Introduction

Hair is one of the least studied aspects of forensic Egyptology and archaeology as a whole. A wealth of information, however, may be gained from even a single strand. Hair is extremely stable and resistant to decomposition and enzymatic digestion (Wilson 2005). Therefore, hair is often the least degraded part of human and animal remains. With the scarcity of archaeological remains, taking a sample of hair is much less intrusive or destructive than more frequently studied samples such as skin and bone.

The objective of this communication is to show the wealth of information, both social and pathological, available from non-destructive studies of hair. The research aim is to utilise hair as an archaeological resource, using predominantly non-destructive techniques, focusing on ancient Egyptian contexts.

2 Materials and Methods

The study comprised human scalp and facial hair. These were taken from contemporary and ancient Egyptian remains. The non-destructive techniques used were light and electron microscopy coupled with energy dispersive spectroscopy. The study aimed to prioritise use of non-destructive techniques to preserve as much of the sample in its original condition.

N.C. McCreesh (✉) and A.R. David
The KNH Centre for Biomedical Egyptology, F Floor The Mill, The University of Manchester,
PO Box 88, Manchester M60 1QD, UK
e-mail: natalie.mccreesh@postgrad.manchester.ac.uk

A.P. Gize
School Earth Atmospheric Environmental Sciences, University of Manchester, Manchester M13
9PL, UK

3 Results

The information was gained from twenty ancient Egyptian hair samples. Results here are from one case study, with general observations discussed in the following section.

3.1 *Cyfarthfa Castle Museum Mummified Head*

The subject was an ancient Egyptian detached male head. It had been mummified and was still partially wrapped. The head dated from the late New Kingdom (1550–1069 BC) or early Late Period (747–332 BC), (Nicholson and Stevenson 1998). The head is relatively well preserved, with areas still concealed within bandages. The majority of the hair is exposed on the back of the head. The hair is short approx 10 mm long, and is orange-red. Intriguingly, the hair exposed on the left side of the head is a pale blond-orange, whilst the hair on the lower back of the head towards the nape of the neck is a much darker orange-red. Samples from both areas of the head were taken for comparison.

The hair from the back of the head showed fungal hyphae and spores spanning the entire surface. The fungi are unidentified at present. Below the fungal layer is a coating of a hard material. It is likely that this coating was applied to the hair as part of the embalming process during mummification. Below this coating the hair shaft was revealed in a perfectly preserved condition. The cuticle was highly visible. The scales lie flat, are smooth around the edges, indicating the hair was healthy (Fig. 1.).

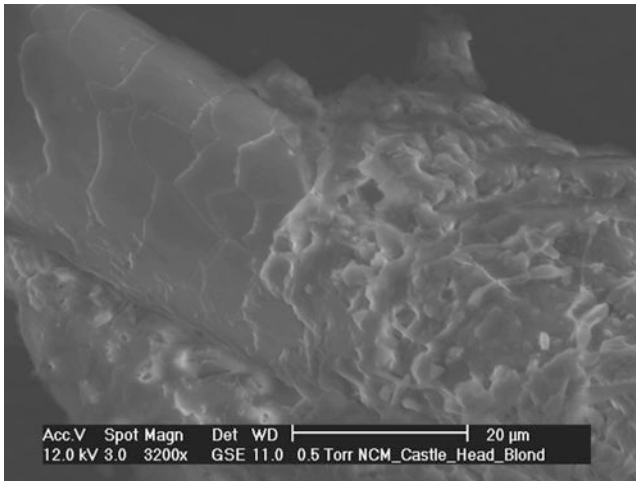


Fig. 1 ESEM image. The cuticle is indicative of a healthy hair. The image shows a sequence of events, with a late coating of debris and fungal matter, below which is a resinous coating over the hair shaft

Where the hard coating has separated from the underlying hair, the reverse side had perfectly preserved a negative cast of the hair. There were pieces of debris in the cast which indicate that the hair was not entirely clean prior to embalming. This may imply that the hair was not washed as part of the embalming process. The coating showed conchoidal fractures, characteristic of materials which do not have natural planes of separation (e.g. cleavage: Watts 1868). This observation indicates the hair coating was likely to be a resin or bitumen based application.

In contrast, the hair from the side of the head was either without the hard coating or with the coating applied much more thinly. The hair showed cuticle lifting and peeling where uncoated (Fig. 2).

As the hair was in a healthy state when mummified, this damage occurred post-mortem.

Light microscopy shows the uncoated hair to be colourless or “white”. This may be an effect of degradation, rather than an indication of the deceased natural hair colour at the time of death. The colour of the embalming coating varied with location on the head. On the back of the head, the coating colour is a vibrant red. On the side of the head, the coating is a paler orange-yellow, almost clear in some places. The colour of the coating intensified due to thickness of application. It is speculated that the coating was applied unevenly; perhaps because the coating may have been semi-liquid and pooled down to the lowest altitude i.e. the back of the head, rather than the sides of the head. It is thought that the body was placed lying on the back whilst the embalming was carried out.

Examining the tips of hair can indicate if the hair has or has not been recently cut. In this instance the ends of the hair were cut to a diagonal tip, this indicates that the hair was cut with a razor or blade as opposed to scissors. Hair grows at a rate of approximately 10 mm per month (Wilson 2005). As the hair is 10 mm long, the hair would have been shaved close to the scalp approximately a month prior to death.

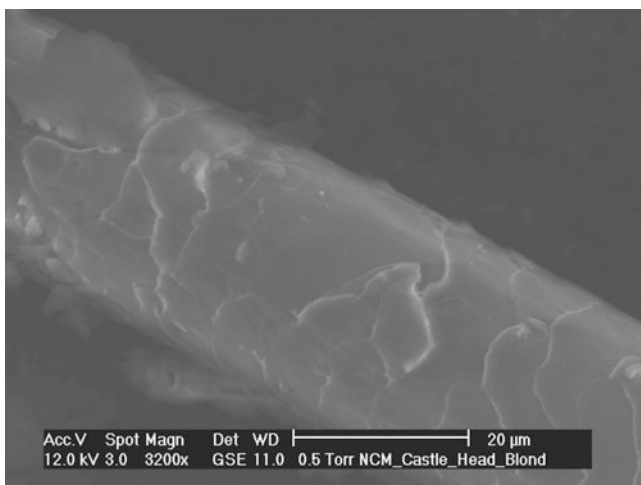


Fig. 2 ESEM image of the hair shaft showing damage by peeling and lifting of the cuticle scales

4 Discussion

Ancient Egyptian hair samples are either coated or uncoated. For uncoated hair, cuticle diagnostics can be used to develop medical diagnoses; indicating hair or scalp diseases and other diseases affecting the hair, and states of nutrition and climate. Original traits such as hair colour and race are also possible to detect.

Scalp hair is frequently treated, typically post-mortem. Such treatments include application of oils and unguents used to anoint the hair and body during funerary rituals, and application of preservatives as part of the embalming process. Cuticle diagnostics can also indicate the treatment of hair by brushing and washing.

Social standing is reflected in the quality of the burials. Mummy scalp hair from Noble (high social status) ancient Egyptians does not show fungal infections to a great extent, whereas mummy scalp hair from poorer burials show extensive mildew. This probably reflects the effectiveness of the preservatives used when embalming the body. Trends in the treatment of the hair by cutting and colouring give further information regarding status and socio-political treatment. For example, a female noble woman and a male priest, having different social identities, may have had different treatments to the hair in life and in death. For the Cyfarthfa Castle head we know that his hair had been shaved only a few weeks prior to his death. Unfortunately, the head was detached in antiquity and the body has not been identified. Consequently the cause of death and any other information which may have been gained from his coffin or tomb is unknown. In ancient Egypt there are two possible causes as to why the hair would be shaved. It has been suggested that the hair was shaved on most ancient Egyptians to keep lice at bay. As a post-pubescent male, however, it is not thought he would have been affected by lice (Grey and Dawber 1999; Dawber 1997). The other possibility is that he was a member of the priesthood, who were believed to be totally shaven to ensure ritual purity.

From a single case study it can be seen that hair can be utilized to a great extent. Very small samples can be taken from scarce archaeological remains, yet providing major results. From a few strands of hair taken from a detached mummified head an extraordinary insight has been gained into the life of an ancient Egyptian, proving that hair is an extremely valuable forensic tool and archaeological resource.

References

- Dawber R (1997) *Diseases of the hair and scalp*. Blackwell, London, p 434
- Grey J, Dawber R (1999) *A pocketbook of hair and scalp disorders*. Blackwell, London, p 97
- Nicholson P, Stevenson S (1998) The Egyptian collection at Cyfarthfa Castle, Methyr Tydfil. *Egyptian Archaeol* 12:11–13
- Watts H (1868) *A dictionary of chemistry and the allied branches of other science*. Green, Longman and Roberts, London, p 199
- Wilson AS (2005) Hair as a bioresource in archaeological study. In: Tobin DJ (ed) *Hair in toxicology: an important bio-monitor*. RSC, Cambridge, pp 321–345

Archaeobotany as an *In-Site/Off-Site* Tool for Paleoenvironmental Research at Pulo di Molfetta (Puglia, South-Eastern Italy)

M. Primavera and G. Fiorentino

1 Introduction

Archaeobotanical investigations of the Early Neolithic settlement of *Fondo Azzollini* (Molfetta, SE Italy) have been carried out since 1999 in order to reconstruct the environmental changes that occurred in the Murgia region (Puglia) during the main occupation phases of the site. The archaeological site is located on a calcareous plateau sloping down to a sinkhole called “the *Pulo*”. The rock surfaces of the sinkhole are marked by several caves, inhabited also during the Bronze Age. The heavy erosion processes active in the settlement area and the distinctive morphology of the plateau have caused eroded sediments to flow into the adjacent natural basin. This study compares archaeobotanical remains from the archaeological site (*in-site data*) and plant remains from the S1-bis core drilled in the *Pulo* (*off-site data*). AMS radiocarbon dating indicated that the lowest part of the S1-bis core had the same age as the Neolithic settlement, whereas the upper part of the core corresponded to the Bronze Age habitation of the caves. The *off-site* plant remains found in the core enriched the rather scarce archaeobotanical data from the archaeological site itself and enabled us to identify changes in plant resources and cultivation practices.

2 The Concept Of *In-Site/Off-Site* Archaeobotany

We postulate that in *archaeobotanical analysis*, the *ecofact* (Butzer 1971) can be used as a “basic unit” for paleoenvironmental reconstruction, just as the *artefact* has been used in *settlement archaeology* as the “basic unit” of landscapes. The notion of *off-site archaeology* was defined by Foley (1981) and concerns the concept of “*site*”

M. Primavera and G. Fiorentino (✉)

Laboratory of Archaeobotany and Paleoecology, Department of Cultural Heritage, Salento University, Via D. Birago, 64 - 73100 Lecce, Italy
e-mail: charcoal@unile.it

in *settlement archaeology* (Isaac 1989); for a long time, archaeologists focused on the *site* as the central element of regional analysis. Foley's hypothesis, widely accepted, is that human activity is not restricted to the site: the pattern of archaeological remains can be described in terms of variable densities of *artefacts* across landscapes. Since the concept of *off-site archaeology* (or *non-site survey*) posits the artefact as the basic item, there was a shift in attention from the site to the landscapes around it.

In this study we have extended these concepts to archaeobotanical analysis and *ecofacts*, especially plant remains: seeds/fruits and charcoal from *in-site* layers, assumed to have been transported by erosion processes into the Pulo, were gathered by the S1-bis sediment core; despite being found in *off-site* sediment strata, these remains can be considered *ecofacts*, by virtue of being by-products of human activity. This integrated study carried out at Pulo di Molfetta enables us to evaluate changes in human/environment relationships during the mid-Holocene; our findings provide information about the exploitation of wood and the use of land.

3 Study Area

The prehistoric settlement of *Fondo Azzollini* is one of the most ancient Neolithic settlements in the Puglia region and its importance is strongly connected to the spread of the Neolithic from the Near East towards the western Mediterranean basin (Guilaine 1998). The site is located at 47 m above sea level, on a calcareous plateau which slopes down to the Adriatic Sea, 2 km away. The first archaeological investigation, which took place at the beginning of the twentieth century (Mosso 1910), showed that the entire area was densely settled from the Early to the Late Neolithic period; moreover, the abundant finds (pottery, lithic tools, etc.) recovered in the surrounding area and the caves inside the oval-shaped depression suggested that the area was also settled during the Bronze Age. The Pulo, 30 m high and 600 m wide, was originally formed by the collapse of the roof of an underground cavity formed by the erosive action of water on the calcareous Mesozoic rocks (Maggiore 2007). Systematic archaeological research carried out in 1997 on the east side of the plateau revealed an Early Neolithic settlement (dated to 7134 ± 60 BP) enclosed by a thick drystone wall (Radina 2007). The function of this structure is believed to be connected to the morphological features of the plateau: it was probably built to prevent the erosion of the sediment and its flowing into the adjacent sinkhole.

4 Materials and Methods

The *in-site* analysed archaeological sediments were collected from each stratigraphic layer; the soil was floated using a drum equipped with two sieves (4 mm and 0.5 mm). The resulting fractions were dried and the plant remains (seeds/fruits and charcoal) were picked out using a stereo-microscope.

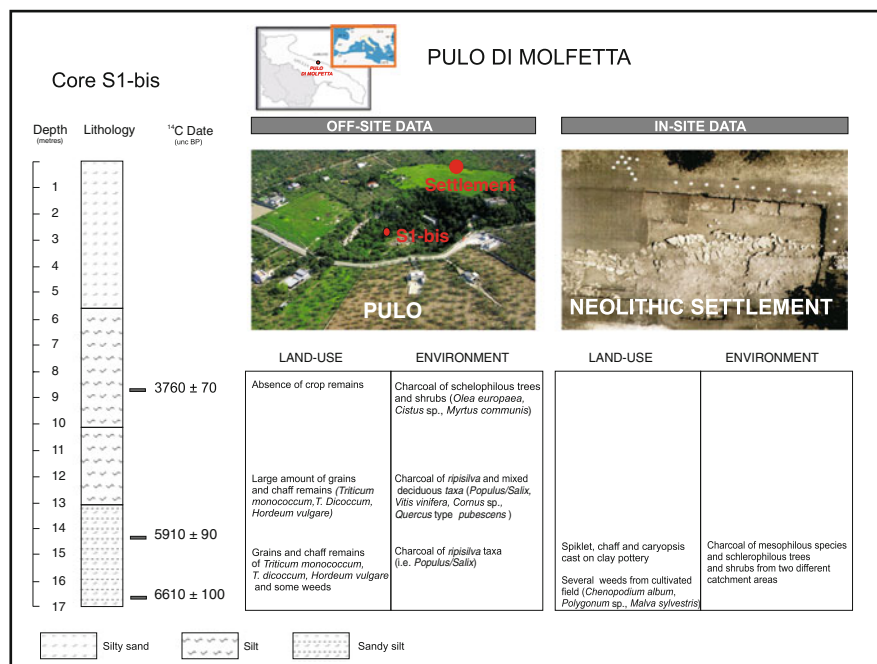


Fig. 1 Paleoenvironment and landscape reconstruction from *off-site* and *in-site* archaeobotanical analyses: on the left, data from core S1-bis; on the right, data from the Early Neolithic settlement of *Fondo Azzollini*

In terms of the *off-site* sediments, the S1-bis sediment core was drilled in 2000 on the bottom of the Pulo. The core was 17 m high and 10 cm in diameter, with alternate layers of silt and sand, in some cases with abundant calcareous clasts. The layers at the base of the core (grey to black silty sand) contained a large amount of Neolithic pottery fragments and charred plant remains (Fig. 1).

AMS radiocarbon dating performed by Geochron Laboratories showed that the core layers from -17 m to -9 m corresponded chronologically to the Early Neolithic settlement and Bronze Age caves. The relevant sediment samples from these layers were then collected from S1-bis and washed through sieves of different sizes (500, 250, and 60 μ m). Plant macrofossils were selected and identified.

The *in-site* and *off-site* archaeobotanical materials were recognized by reference to the anatomical and morphological characteristics of the plant remains, using the key atlas and modern day analogous samples.

5 Results

Despite floating all the sediment from each layer, the archaeobotanical record from the Early Neolithic settlement was rather limited, due to erosion. The findings included just 54 charcoal fragments and 36 charred seed/fruit remains.

The charcoals gathered contained ten taxa, identified to varying taxonomical levels: *Carpinus betulus* L., *Cistus* sp., *Corylys avellana* L., *Erica* sp., *Hedera helix* L., *Olea europaea* L., *Pistacia lentiscus* L., Pomoideae, Prunoideae, and *Vitis vinifera* L. The seed/fruit remains were made up of one charred cereal fragment (caryopsis of *Hordeum vulgare* L.), cereals cast on pottery, and a few weeds, such as *Chenopodium album* L., *Galium aparine* L., *Polygonum* sp., *Malva sylvestris* L. and *Silene alba* (Miller) Krause.

Given the relative lack of *in-site* archaeobotanical data, the paleoenvironmental investigation was extended to those sediment samples from S1-bis that were chronologically associated with the main archaeological phases of the site. Anthracological analysis identified the following taxa: *Acer* sp., *Cistus* sp., *Cornus* sp., *Erica* sp., *Euphorbia* sp., *Fraxinus ornus* L., Gramineae, Leguminosae, *Myrtus communis* L., *Olea europaea* L., *Pistacia* sp., *Populus/Salix*, *Quercus* type *ilex*, *Quercus* type *pubescens* and *Quercus* sp. The *off-site* sediments also contained a large amount of seed/fruit remains, particularly cereal grains and chaff (Gramineae, *Hordeum vulgare* L., *Triticum dicoccum* Schrank, *Triticum* type “hulled”, *Triticum monococcum* L., Leguminosae, *Capparis spinosa* L., cfr. *Dianthus*, *Heliotropium europaeum* L., *Medicago* sp, Moraceae, *Rubus fruticosus* L. and *Stellaria media* (L) Vill (Primavera *et al.* 2007).

6 Discussion and Conclusion: Paleoenvironments and Landscapes

Given the close interrelationship between human beings and their environment, paleoenvironmental studies in archaeological contexts can shed light on past landscapes and environmental dynamics (Dincauze 2000); it was to this end that we compared *in-site* and *off-site* archaeobotanical data from Pulo di Molfetta (Fig. 1). As already pointed out, soil erosion processes had transported *ecofacts* from *in-site* layers to *off-site* natural deposits. The gathering of these *ecofacts* in both contexts enabled us to investigate relationships between human beings and their environment in a wider spatial and chronological perspective. What type of environment did the Neolithic farmers of *Fondo Azzollini* live and work in? What did these early agricultural communities cultivate? What was the role of the Pulo at that time? How did the exploitation of the area change through the different phases of occupation of the site, from the Early Neolithic to the Bronze Age? Our results concern the catchment area for wood exploitation and land use practices on the plateau.

All the *in-site* charcoals analysed date back to the Early Neolithic; since they were mainly related to domestic use, they are assumed to have originated from the surrounding area. Anthracological analysis of these finds confirmed that the wood was gathered in two distinct catchment areas, as revealed by differences in the eco-pedological features of the recognized taxa. The first area was one of mixed deciduous wood and mesophyllous species (hornbeam, hazel, ivy and grape); the second one was associated

with sclerophyllous trees and shrubs of *maquis* or *garigue* formations (evergreen oaks, *Erica* sp., olive, lentisc, rock rose, etc.). Despite the low frequency of cereals in the seed/fruit remains, the occurrence of several weeds such as pigweed, mallow, polygonum – and above all the presence of spikelet, chaff and caryopsis casts on clay pottery (Fiorentino 2002) – can be considered as indirect traces of agricultural activities.

On the other hand, the anthracological record of the *off-site* data, consisting of *ripisilva* and mixed deciduous taxa (poplar/willow, deciduous oak, cornel), suggests wet conditions during the Early Neolithic period, and thus more abundant water resources for the ancient farmers. The large amount of cereal grains (einkorn and emmer) and chaff preserved (Fig. 2) confirms that the plateau was intensively cultivated by the farmers of the *Fondo Azzollini* settlement from 6610 ± 100 BP to 5910 ± 90 BP. The record suggests that changes in vegetation and agricultural practices took place between 5910 ± 90 BP and the Bronze Age: the greater abundance of olive charcoals (Fig. 2) around 3760 ± 70 BP confirms the drier conditions prevalent during this period. The absence of cereal remains in the respective layer coincides with the abandonment of the settlement and the ritual use of the Pulo caves.

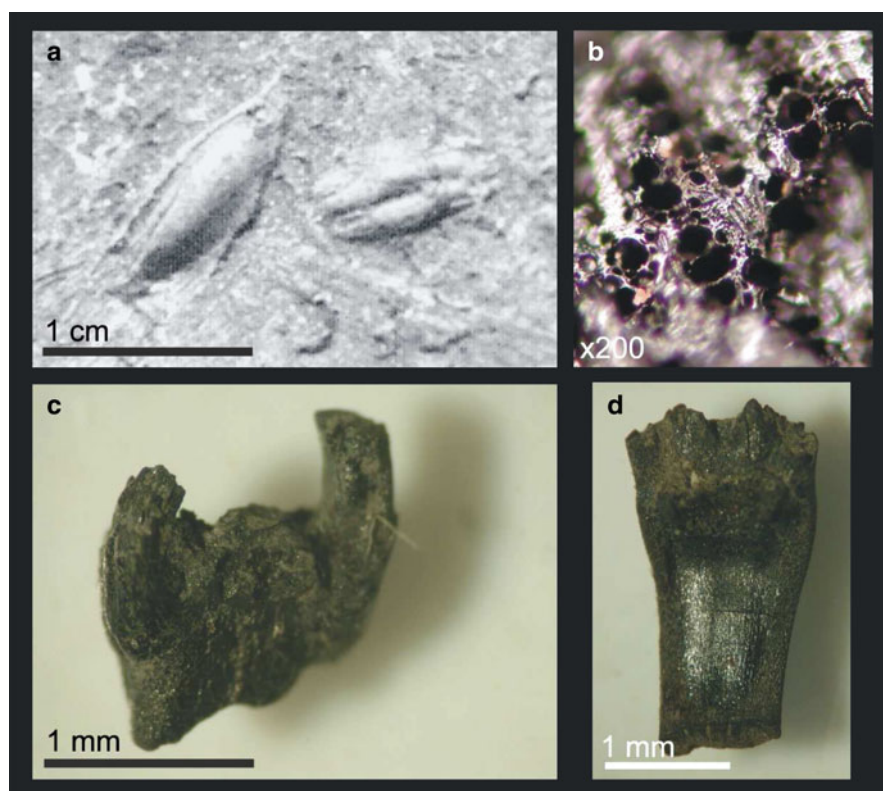


Fig. 2 Plant remains: (a) spikelet, chaff and caryopsis casts on clay pottery; (b) transversal section of charred wood of olive; (c) fork of einkorn; (d) rachis fragment of barley

In conclusion, the archaeobotanical investigation at Pulo di Molfetta, aimed at reconstructing the environmental changes which occurred in the Murgia region (Puglia) during the main phases of occupation of the site, entailed a comparison of *in-site* and *off-site ecofacts*. This approach proved to be a helpful tool which can be transferred to other situations characterised by comparable geomorphological dynamics (erosion vs. deposition); in particular, it enabled us to evaluate the changes in the relationships between human beings and their environment, and to identify changes in plant resources and cultivation practices in the area, pointing to changes in the landscape and human occupation patterns.

References

- Butzer K (1971) Environment and archaeology: an ecological approach to prehistory. Aldine-Atherton, Chicago
- Dincauze DF (2000) Environmental archaeology: principles and practice. Cambridge University Press, Cambridge
- Fiorentino G (2002) I più antichi agricoltori ed i processi di sfruttamento delle risorse vegetali. In: Radina F (ed) Paesaggi, uomini e tradizioni di 8.000 anni fa. Mario Adda Editore, Bari, pp 221–225
- Foley R (1981) Off-site archaeology: an alternative approach for the short-sited. In: Isaac G, Hodder I, Hammond N (eds) Pattern of the past. Cambridge University Press, Cambridge, pp 157–183
- Guilaine J (1998) Atlas du Neolithique Europeen. L'Europe occidentale. Eraul 46, Liege
- Isaac G (1989) Stone age visiting cards: approaches to the study of early land-use patterns. In: Isaac B (ed) The archaeology of human origins. Cambridge University Press, Cambridge
- Maggiore M (2007) Geologia del Pulo di Molfetta. In: Radina F (ed) Natura, archeologia e storia del Pulo di Molfetta. Mario Adda Editore, Bari, pp 45–56
- Mosso A (1910) La Necropoli Neolitica del Pulo di Molfetta. Mon Ant XX:238–351
- Primavera M, Radina F, Maggiore M, Caldara M, Fiorentino G (2007) The exploitation of environmental resources during the Neolithic period at Pulo di Molfetta (Italy) by *in-site* and *off-site* archaeobotanical investigations. Quat Int 167–168(suppl 1):332
- Radina F (2007) L'insediamento preistorico al Pulo di Molfetta. In: Radina F (ed) Natura, archeologia e storia del Pulo di Molfetta. Mario Adda Editore, Bari, pp 89–107

Analysis of Archaeological Bones for the Purpose of Reconstructing the Paleodiet of Medieval Inhabitants

V. Rudovica, A. Viksna, G. Zarina, and I. Melne

1 Introduction

Bone is one of the few materials that are consistently recovered from archaeological and paleontological sites; its chemical composition has the potential to provide valuable information about ancient human and faunal diet and health status. Diet is one aspect of the development of human culture; changes in dietary regimes occurred together with changes in the manner of food procurement. Gathering, hunting and, after domestication, cattle breeding, and finally agriculture, each stage of development of the dietary process also brought social stratification, which in turn led to a preferred diet for certain individuals (Smrčka 2005). The most frequently examined elements for the reconstruction of a paleodiet are Zn, Cu, Mg, Mn and Sr (Gilbert 1985). According to Gilbert (1985), Zn and Cu should be related to the supply of animal protein, while Sr, Ba, Mg and Mn could indicate the supply of vegetal food. Other elements, such as Cd and Pb, should give information about anthropogenic activities and environmental pollution.

Thus, the aim of the present paper is to determine several major and trace elements in archaeological bones by Inductively Coupled Plasma Mass Spectrometry (ICP-MS), in order to be able to reconstruct the paleodiet of the medieval inhabitants of Veselava, in modern Latvia.

V. Rudovica and A. Viksna (✉)

Department of Analytical Chemistry, University of Latvia, Riga, Latvia
e-mail: arturs.viksna@lu.lv

G. Zarina

Institute of the History of Latvia, University of Latvia, Riga, Latvia

I. Melne

National History Museum of Latvia, Riga, Latvia

2 The Study Site

The medieval cemetery of Veselava was located in the Veselava Parish of Cēsis District in modern Latvia (Fig. 1). This cemetery was used over a period of 500 years, during the thirteenth to seventeenth centuries. Between the fourteenth and the eighteenth century AD, the area of present-day Latvia was partitioned several times among major neighbouring powers. Most important in terms of their consequences were the partition following the Livonian War (1558–1583) and especially the partition that followed the 1629 Peace of Altmärk, which ended the Polish-Swedish War (1600–1629). The Latgale region came under the rule of Catholic Poland, the Vidzeme region (in the central part of which Veselava is located) was acquired by Protestant Sweden, while in the regions of Kurzeme, Zemgale and Augšzeme, the Duchy of Courland and Semigallia was established, under strong Polish and German influence. This fragmentation brought about significant economic differences between the different regions in the area of present-day Latvia (Cimermanis 1999).

Diet in medieval Veselava chiefly consisted of cereals (bread, porridges), with a small addition of milk products. Use of meat was seasonal, mainly in the autumn.



Fig. 1 The geographical location of the medieval cemetery of Veselava (*square*)



Fig. 2 Excavated burials at the cemetery of Veselava

The major part of this excavation site was covered with road surfacing; the first burial layer was destroyed as a result of road construction. 1,244 m² of the cemetery were excavated from 2004 till 2007 and 941 interments were uncovered. In 524 burials (56% of the total), the deceased persons had been buried along with various medieval artefacts. Among the objects found there were bead necklaces, brooches, finger-rings, pendants, knives, belt buckles and coins (Melne 2008).

The osteological material recovered in the course of the excavation (Fig. 2) provided an insight into the paleodemography, paleopathology, physical development and paleodiet of the inhabitants of Veselava.

Demographic indices, estimated using conventional methodology (Ferembach et al. 1980, Buikstra and Ubelaker 1994, Scheuer and Black 2004, Acsádi and Nemeskéri 1970), show that the population was characterized by high mortality rates among juveniles aged 15–20, and among women aged 15–35. Among males, the highest mortality rate was observed at the age of 30–40, remaining high in the age range of 40–50. As a result, adult life expectancy, e^{0}_{20} , is 5.1 years shorter for females than for males.

3 Material and Methods

3.1 Samples and Sample Preparation

The material used in the present study consisted of 40 human bone samples. In addition to these, 20 soil samples from the respective burials were also analysed.

The bones were rinsed with deionised water. Samples were taken from the proximal end of the tibia using a drill. The samples were dried in an oven at

105°C for 2 h. For chemical analysis, 0.3 g of dried bone powder (with precision of 0.0001 g) was weighed. The samples were placed in a PTFE pressure vessel and a mixture of 4 ml HNO₃ (Merck, suprapur) and 2 ml H₂O₂ (Merck, suprapur) was added. The closed vessels were placed in the microwave oven (Anton Paar 300) with an assisted sample digestion system and heated for 40 min (maximum temperature: T = 125°C, maximum pressure: 35–40 bar). After cooling, the digested samples were diluted to 25.0 ml with deionised water. The resulting solutions were diluted 10 and 50 times with deionised water before being analysed with a Perkin Elmer ELAN DRC-e ICP-MS instrument.

Quality control and method validation were performed by analysis of the NIST-SRM 1486 (animal meal) standard reference material.

Twenty soil samples were dried in an oven with a fan at 50°C until constant weight was reached, after which they were sieved through a 1 mm mesh. 10.00 g of the dried soil was transferred into a 50 ml beaker, and 50 ml of deionised water was added. The pH was measured after 16 h of equilibration.

20.00 g of dried soil was transferred into an Erlenmeyer flask and 100 ml of 0.5 M HNO₃ was added. The extract was shaken for 30 min with a shaker rotation speed of 200 rpm and later filtered into a polyethylene flask (Ranst et al. 1999). After extraction, the metal content (Al, Cr, Mn, Fe, Ni, Cu, Zn, Cd and Pb) in the soil samples was determined by Inductively Coupled Plasma Atomic Emission Spectrometry, ICP-AES (Varian Vista-MPX).

4 Results and Discussion

Soil acidification, the presence of soot and soluble salts, and the medium-grained sandy soil seem to be the main factors accelerating deterioration. The stability and mobility of trace elements and their compounds in the soil control their bioavailability, which depends from soil properties, such as pH and texture. The soil type at the excavation site was mainly sandy. At the site as a whole, the soil is alkaline, with pH values ranging from 7.1 to 8.1. Table 1 presents the element content of the

Table 1 The mean concentration values ($\mu\text{g g}^{-1}$) of elements present in the soil solution of the analysed soil samples with standard deviation (SD) (soil extracted in 0.5 M HNO₃ solution); n = 20

Element	Mean value	SD
Al	1,186	335
Cr	0.55	0.14
Mn	34	12
Fe	706	284
Ni	0.33	0.18
Cu	2.4	1.7
Zn	4.4	1.9
Cd	0.03	0.01
Pb	1.2	0.8

extracted soil solution. Al, Fe and Mn are relatively abundant elements in sandy soil, but are highly insoluble in an oxidized state, at “normal” pH and eH conditions. Cation exchange capacity is very low. The sandy soil is also characterized by low content of organic matter.

The small percentage of each element present in the soil solution indicates that it would have had little influence on the archaeological bone mineral composition, and can be considered as a background level.

The high content of Ca and P might produce spectral interferences and cause limitations and problems in the determination of trace elements in bones using ICP-MS. The sample preparation and analysis methods by ICP-MS were validated by applying them to the standard reference material NIST-SRM-1486 (animal bone). Successful recoveries (>90%) of Cu, Zn, Sr, Cd, Pb were achieved; the results are presented in Table 2.

The element content was analysed in archaeological human bone samples mainly in order to find differences between the sexes in terms of elemental content (Fig. 3).

Table 2 ICP-MS analysis results of the bone powder standard reference material (NIST SRM-1486) after acid microwave digestion; n = 6

Element	Mass concentration $\mu\text{g g}^{-1}$	
	Analysed value	Certified value
Mn	1.16 ± 0.03	1
Cu	0.72 ± 0.11	0.8
Zn	138 ± 16	147 ± 16
Sr	266 ± 7	264 ± 7
Cd	0.0029 ± 0.0004	0.003
Pb	1.34 ± 0.14	1.34 ± 0.01

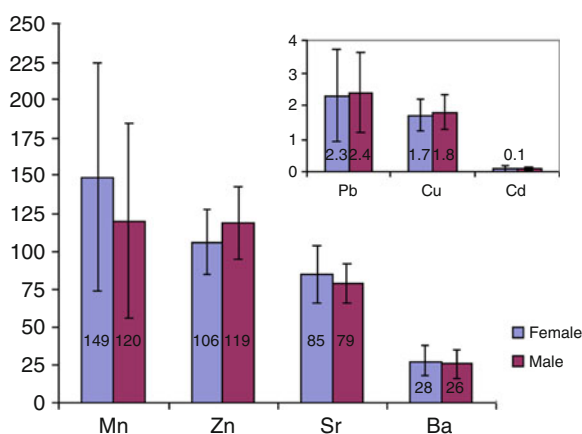


Fig. 3 The content of elements in archaeological bone samples analysed by ICP-MS ($\mu\text{g g}^{-1}$); female n = 28 and male n = 12

Higher strontium levels reflect a higher proportion of vegetal food in the diet. Mean bone Sr levels reported in regional studies of Middle Age materials in Poland, Bulgaria and England generally lay in the range of 109–250 $\mu\text{g g}^{-1}$ (Smrčka 2005; Mays 2003), but showing large variations from region to region and among individuals. Obtained results are comparable with literature data (Smrčka 2005; Mays 2003), especially with the polish results. The lower concentrations of Sr suggest that the plant food consumed was not wholesome.

Ba and Mn contents also characterise the quantity of plant foods in a diet. The present data showed that fruits and vegetables were consumed daily more often by females. According to our data, strontium, barium and manganese contents were slightly higher in female than male bones, but a significant variation was not found.

The Zn content of bones does not change so rapidly over time, and it is not affected by the soil solution. Thus, Zn and Sr can serve as approximate indicators of the proportional presence of vegetal and animal albumens in the diet. Carnivores have more Zn (170–250 ppm) in their bones than herbivores (90–150 ppm), but less Sr (100–300 ppm) than herbivores (400–500 ppm). A slightly higher mean level of zinc was found in male bones. In the Polish and Bulgarian regions, the determined mean content of Zn in the bones was in the range of 150–173 $\mu\text{g g}^{-1}$, but also with high variations among analysed samples (Smrčka 2005).

There is more Cu in the bones of carnivores than in those of herbivores. The analysis of Cu contents showed an increased level in male bone samples.

The main source of Pb pollution in man during Late Medieval times comes from lead glazed artefacts and dishes. They were used for acid food or drink, and acids may have leached out Pb from the glazing. The mean lead content in bone samples was five to ten times lower in the current study as compared to our previous studies from the Riga city excavation. This indicates that the inhabitants of this region mostly used unglazed clay vessels for cooking. In the studied area, the Pb and Cd contents were found to be at background levels.

Summarizing the current study, the obtained level of analysed elements in the bone samples of Veselava inhabitants are not as high as would be expected if compared with data published by other authors. This can be explained by the geographic location (wet and cool weather conditions, poor fertility of soil), famine during hostilities, and a low level of social stratification.

5 Conclusions

The contents of Sr, Mn, Ba, Cu, Zn, Pb and Cd in archaeological bones from the cemetery of Veselava were investigated using Inductively Coupled Plasma Mass Spectrometry (ICP-MS), and evaluated in order to reconstruct the medieval inhabitants' paleodiet. The method used for preparing archaeological bone samples allowed an accurate determination of the studied elements. Digestion with a small amount of HNO_3 acid decreased the possibility of spectral overlap, and the added H_2O_2 completely destroyed organic matter.

The 40 archaeological human bone samples that were analysed did not show significant differences between the sexes in terms of elemental content, although strontium, barium and manganese contents were slightly higher in female than male bones.

It is thus possible that the inhabitants of Veselava between the thirteenth and the seventeenth century AD often had a rather poor diet.

Acknowledgements V. Rudovica is grateful for financial support from the European Social Fund (ESF).

References

- Acsádi G, Nemeskéri J (1970) History of human life span and mortality. Akademiai Kiado, Budapest, 256
- Buikstra JE, Ubelaker DH (1994) Standards for data collection from human skeletal remains. Arkansas Archeological Survey Research Series No.44, Arkansa
- Cimermanis S (1999) Par Latvijas vēsturiski etnogrāfiskajiem apgabaliem. In: Caune A (ed) Latvijas zemju robežas 1000 gados. Rīga, pp 34–53
- Ferembach D, Schwidetzky I, Stloukal M (1980) Recommendations for age and sex diagnoses of skeletons. *J Hum Evol* 9:517–549
- Gilbert RI (1985) Stress, paleonutrition and trace elements. In: Gilbert RI, Milke JH (eds) The analysis of prehistoric diets. Academic, Orlando, pp 339–357
- Mays S (2003) Bone strontium: calcium ratios and duration of breastfeeding in a Mediaeval skeletal population. *J Archaeol Sci* 30:731–741
- Melne I (2008) Archaeological excavations in the medieval cemetery of Veselava, In *Archaeological Investigations in Latvia 2006–2007*. Zinatne, Rīga, pp 164–170
- Ranst EV, Verloo M, Demeyer A, Pauwels JM (1999) Manual for the soil chemistry and fertility laboratory. Faculty agricultural and applied biological sciences. Ghent University, Belgium, 231
- Scheuer L, Black S (2004) The juvenile skeleton. Elsevier Academic, Amsterdam
- Smrčka V (2005) Trace elements in bone tissue. The Karolinum Press, Charles University in Prague, Prague, 213

Integrating Stable Isotopes to the Study of the Origin of Management Strategies for Domestic Animals: $\delta^{13}\text{C}$ and $\delta^{18}\text{O}$ Results from Bioapatite Enamel of Cattle from the Tell Halula Site, Syria (7800–7000 BC)

C. Tornero and M. Saña

1 Introduction

The Near East is one of the first geographical areas where the domestication of cattle during the Neolithic Revolution took place (Higgs and Jarman 1969; Ucko and Dimbleby 1969). Animal domestication engendered changes in social organization and social relationships between human groups and also caused changes on the ethological and biological patterns in the passage from wild to domestic animals (Saña 2005). One of the most important factors that could be evaluated in these changes is the control of animal reproduction. The modification of natural reproduction patterns are one of the key aspects in the understanding of the dynamics of animal domestication.

In particular, in the case of bovines, data from natural populations show a stable pattern of reproduction with births taking place during the season with the maximum natural resources available. Changes of the natural season of birth become possible only when sufficient capacity to obtain artificial resources in less favourable seasons exists (Balasse and Tresset 2007); this could have implied an important work input for the first Neolithic communities, especially in those areas where changes in environmental conditions during the complete seasonal cycle were more significant. The middle Euphrates Valley was presumed to have been characterized during this time, and up to the present, by a marked bimodal seasonal dynamic of climatic and environmental conditions (Besançon et al. 2000; Helmer et al. 1998; Hillman 1996).

Following these considerations, this work aims to evaluate the birth season of bovines during the first stages of their domestication. For this purpose, different remains of cattle from the Tell Halula site have been selected for stable isotope

C. Tornero (✉) and M. Saña

Laboratory of Archaeozoology, Prehistory Department, Universitat Autònoma de Barcelona, Edifici B – Campus UAB, 08193 Bellaterra, Barcelona, Spain
e-mail: carlos.tornero@uab.cat

analysis. As already shown in previous works, the analysis of stable isotopes on faunal remains is a way of effectively approximating the management strategies of domestic animals in archaeology (Balasse et al. 2001, 2003; Makarewicz and Tuross 2006)

1.1 *The Neolithic Tell Halula Site*

Tell Halula is an archaeological site located in the middle of the Euphrates Valley (Department of Rakka, Republic of Syria). It was occupied between the eighth and sixth millennia BC. PPNB (*Pre-Pottery Neolithic – B*) levels are related to an approximate absolute chronology between 7800 and 7000 BC (Molist 1996; Molist and Saña 2003). Data from archaeozoological analyses carried out until now (morphological and biometric analyses, skeletal representations, butchering and slaughtering patterns, etc.) show significant changes in the bovine management strategies during this period, some of which could be related to the process of animal domestication (Saña 1999, 2001).

2 Materials and Methodology

$\delta^{13}\text{C}$ and $\delta^{18}\text{O}$ values were recounted from *Bos sp.* remains related to the PPNB sequence (7800–7000 BC) of the Tell Halula site. Samples were recounted from the enamel of tooth remains. Enamel is not remodelled once it has formed (Steele and Bramblett 1988), and isotopic values are only representative of the formation period tissue (Lee-Thorp and van der Merwe 1987).

All samples were taken from third lower molars. Third molars, especially in the case of hypsodont dental formations, are formed during longer periods of time. The enamel formation time proposed for third molars on cattle is around 1 year and half (Brown et al. 1960; Andrew 1982). Results were recounted in a sequential order on enamel from neck to occlusive superficies from similar teeth of different individuals. The main objective of following this strategy was to represent sequential values in relation to the individual's life. Between 5 and 6 bands were analysed in cattle teeth from four individuals. Remains were selected related to levels with (*Bos_01*, *Bos_04* and *Bos_05*) and without (*Bos_02*) domestic forms from PPNB sequence.

Samples were chemically treated following protocols originally proposed by Lee-Thorp & van der Merwe (1987), and recently modified by Koch et al. (1997), and Balasse et al. (2002). Organic matter was removed with 2% NaClO (0.1 mg/ml) for 24 h. The samples were then rinsed five times in distilled water (pH 5–8) and oven dried at 60°C for 24 h. Then, samples were reacted by 0.1 M acetic acid (0.1 mg/ml) for 4 h, and rinsed and oven dried again. During treatment, samples lost a mean of 45% of their weight, as had already been observed in others work

(Balasse et al. 2002). Finally, samples were recounted by means of the *Europa Scientific 20-20 IRMS* at the *Iso-Analytical Laboratory* (Crewe, UK), according to the original McCrea (1950) method, adapted to enamel by Kolodny and Kaplan (1970) and Coplen et al. (1983). Results are expressed in delta values (δ) and ‰, in agreement with the corrections from standard V-PDB (*Viena – Pee Dee Belemite*) for carbon values and V-SMOW (*Viena – Standard Mean Ocean Water*) for oxygen values, following the established equation $\delta = [(R_{\text{sample}}/R_{\text{standard}})-1] \times 1000$.

3 Results

The first diagram (Fig. 1) displays the $\delta^{13}\text{C}$ (x-axis) and $\delta^{18}\text{O}$ (y-axis) values measured on cattle remains. Low variability is observed on $\delta^{18}\text{O}$ values between individuals. However, $\delta^{13}\text{C}$ values present important differences between individuals related to middle-PPNB phases (7800–7600 BC) and individuals related to late-PPNB phases (7600–7000 BC). *Bos_01*, *Bos_04* and *Bos_05* show $\delta^{13}\text{C}$ values between -6.7‰ and -10.4‰ , while *Bos_02* show $\delta^{13}\text{C}$ values between -11.9‰ and -13‰ .

The second diagram (Fig. 2) shows $\delta^{18}\text{O}$ values from tooth enamel crown in sequential order. Sequences indicate similar dynamics for all individuals, related to seasonal variations: higher $\delta^{18}\text{O}$ values are located at the same distance from the neck (mm) for each individual.

The periods of enamel formation point toward the same seasonal sequence for all individuals, an aspect which indicates a similar (or identical) season of birth for all individuals analysed.

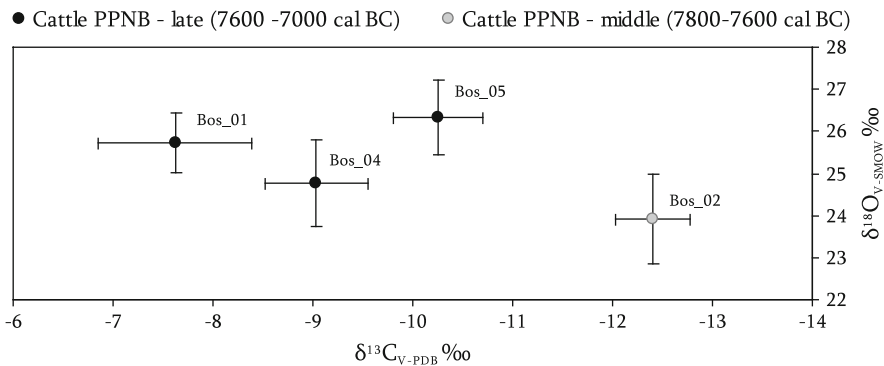


Fig. 1 $\delta^{13}\text{C}$ (x-axis) and $\delta^{18}\text{O}$ (y-axis) values measured on cattle remains related to middle-PPNB levels (7800–7600 BC) (black dots) and remains related to late-PPNB levels (7600–7000 BC) (gray dots)

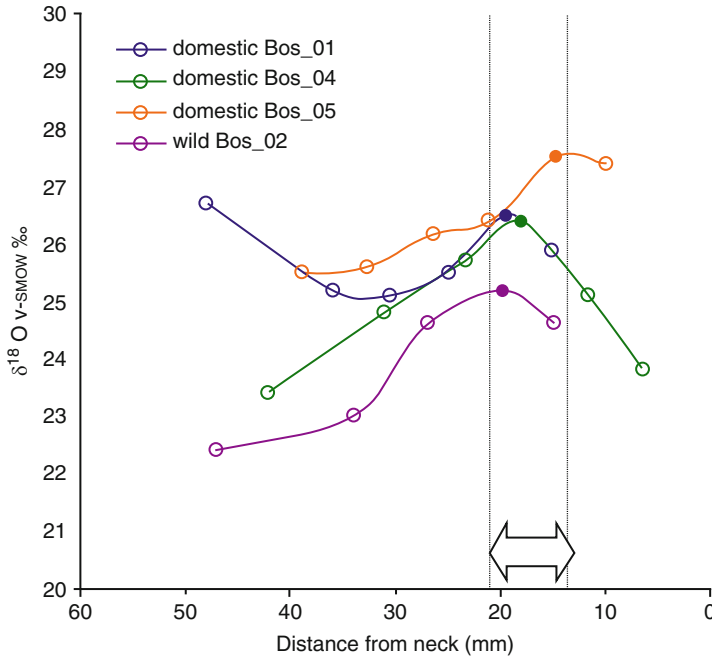


Fig. 2 $\delta^{18}\text{O}$ values from tooth enamel crown in sequential order. *White arrow* indicates the interval where higher $\delta^{18}\text{O}$ values for each individual are located at the same distance from the neck (mm)

4 Conclusions

These results allow us to propose an interesting hypothesis pertaining to the management of *Bos taurus* populations from the first Neolithic societies in the Near East. In this sense, the measured values represent isotopic differences between wild and domestic animals. The domestic population group shows more positive $\delta^{13}\text{C}$ values than the wild one. This difference has already been documented in previous works. Balasse and co-authors found similar differences in $\delta^{13}\text{C}$ values in cattle remains recovered from Neolithic sites (Bercy, fourth millennium BC, France) (Balasse et al. 2000) and Noe-Nygaard and co-authors found identical trends analysing cattle remains from Mesolithic and Neolithic sites in eastern Denmark and southern Sweden (Noe-Nygaard et al. 2005). This trend has usually been explained as a result of the *canopy effect* on wild populations, although more research on this aspect is still required.

Secondly, results show that although differences from $\delta^{13}\text{C}$ values are observed between aurochs and the first herds of domestic cattle, all individuals share the same season of birth. Consequently, changes in the season of birth probably did not occur during the first stages of the process of domestication. This data helps us understand the initial rhythm and dynamic of the process of domestication and indicates that cattle domestication could have been more complex than previously assumed.

Finally, this work emphasises the potential for archaeozoology to integrate stable isotope analyses as a methodological approach capable of bringing a valid contribution to the study of herding strategies and changes due to animal domestication, not focussing exclusively on the morphological and biometric characteristics of faunal remains.

Acknowledgements This work has been carried out as part of different archaeological research projects: Project (HUM200766237-/HIST), directed by Dr. Miquel Molist, and Projects (EME2006-17) and (HUM2007-65016/HIST), directed by Dr. Maria Saña. In the frame of research teams from the UAB: SAPPO: *Seminari d'Arqueologia del Pròxim Orient* (2005 GR 00241) and GRLA: *Grup de Recerca del Laboratori d'Arqueozoologia* (code1792). Finally, Carles Tornero is a FPI – PreDoctoral student benefiting from a grant accorded by the *Ministerio de Educación y Ciencia* (Spain), (BES-2005-8158).

References

- Andrews A (1982) The use of dentition to age young cattle. In: Wilson B, Grigson C, Payne S (eds) *Ageing and sexing animal bones from archaeological sites*. BAR British Series Oxford 109: 141–153
- Balasse M, Tresset A (2007) Environmental constraints on reproductive activity of domestic sheep and cattle: what latitude for the herder? *Anthropozoologica* 42(2):71–88
- Balasse M, Tresset A, Bocherens H, Mariotti A, Vigne J-D (2000) Un abattage “post-lactation” sur des bovins domestiques néolithiques. Etude isotopique des restes osseux du site de Bercy (Paris, France). In: Bassano G, Giacobini G, Peracino V (eds) *La gestion démographique des animaux à travers le temps – Animal management and demography through the ages (VI^e Colloque international de l’association “L’Homme et l’Animal. Société de Recherche Interdisciplinaire”*. Turin, Italie. 16–18 September). *Anthropozoologica* 31:39–48
- Balasse M, Bocherens H, Mariotti A, Ambrose S (2001) Detection of dietary changes by intra-tooth carbon and nitrogen isotopic analysis: an experimental study of dentin collagen of cattle (*Bos taurus*). *J Archaeol Sci* 28:235–245
- Balasse M, Ambrose SH, Smith AB, Price TD (2002) The seasonal mobility model for prehistoric herders in the South-western Cape of south assessed by isotopic analysis of sheep tooth enamel. *J Archaeol Sci* 29:917–932
- Balasse M, Smith AB, Ambrose SH, Leigh SR (2003) Determining sheep birth seasonality by analysis of tooth enamel oxygen isotope ratios: the late stone age site of Kasteelberg (South Africa). *J Archaeol Sci* 30:205–215
- Besançon J, Moulins D, Willcox G (2000) Cadre naturel, végétation actuelle et agriculture contemporaine dans la région d’El Kown. In: Stordeur D (ed) *El Kown 2, Une ile dans le désert. La fin du Néolithique précéramique dans la steppe syrienne*. CNRS Editions, Paris, pp 15–20
- Brown WAB, Christofferson DVM, Massler M, Weiss MB (1960) Postnatal tooth development in cattle. *Am J Vet Res* XXI 80:7–34
- Coplen TB, Kendall C, Hopple J (1983) Comparison of stable isotope references samples. *Nature* 302:236–238
- Helmer D, Roitel V, Saña M, Willcox G (1998) Interprétations environnementales des données archéozoologiques et archéobotaniques en Syrie du Nord de 16000BP à 7000BP, et les débuts de la domestication de plantes et des animaux. In: Fortin M, Aurenche O (eds.) *Espace naturel, espace habité en Syrie du Nord (10^e–2^e millénaires av. J-C)*, Actes du colloque tenu à

- l'Université Laval (Québec) du 5 au 7 mai 1997. Lyon: Travaux de la Maison de l'Orient 28:9–33
- Higgs ES, Jarman MR (1969) The origins of agriculture: a reconsideration. *Antiquity* 43:31–41
- Hillman G (1996) Late Pleistocene changes in wild plant-foods available to hunter-gatherers of the northern Fertile Crescent: possible preludes to cereal cultivation. In: Harris DR (ed) *The origins and spread of agriculture and pastoralism in Eurasia*. University College, London, pp 159–203
- Koch P, Tuross N, Fogel ML (1997) The effects of samples treatment and diagenesis on the isotopic integrity of carbonate in biogenic hydroxylapatite. *J Archaeol Sci* 24:417–429
- Kolodny Y, Kaplan IR (1970) Carbon and oxygen isotopes in apatite CO_2 and co-existing calcite from sedimentary phosphorite. *J Sediment Petrol* 40:954–959
- Lee-Thorp JA, van der Merwe N (1987) Carbon isotope analysis of fossil bone apatite. *South African J Sci* 83:712–715
- Makarewicz C, Tuross N (2006) Foddering by Mongolian pastoralists is recorded in the stable carbon and nitrogen isotopes of caprine dentinal collagen. *J Archaeol Sci* 33:862–870
- McCrea JM (1950) On the isotopic chemistry of carbonates and a paleotemperature scale. *J Chem Phys* 18:849–857
- Molist M (1996) Tell Halula (Siria). Un yacimiento neolítico del valle medio del Eufrates. Campañas de 1991 a 1992., Ministerio de Educacion y Cultura, Madrid
- Molist M, Saña M (2003) Tell Halula, en los orígenes de las sociedades campesinas en el Valle del Eufrates. *Jornadas Temáticas Andaluzas de Arqueología*, 211–249
- Noe-Nygaard N, Price T, Hede S (2005) Diet of aurochs and early cattle in southern Scandinavia: evidence from ^{15}N and ^{13}C stable isotopes. *J Archaeol Sci* 32:855–871
- Saña M (1999) Arqueología de la domesticación animal. La gestión de los recursos animales en Tell Halula (Valle del Eufrates-Siria) del 8800 al 7000 BP., *Treballs d'Arqueologia del Pròxim Orient*, 1., Universitat Autònoma de Barcelona, Barcelona
- Saña M (2001) Dynamique de processus de domestication animale d'après le site neolithique de tell Halula (Vallée de l'Euphrate, Syrie). *IV^e ASWAD*, Paris, 1998. Univ, Paris I.
- Saña M (2005) Animal domestication: subject of study and subject of historical knowledge. *Revue de Paleobiologie*, Geneve 10:149–154
- Steele DG, Bramblett CA (1988) *The anatomy and biology of the human skeleton*. Texas A&M University Press, College Station, TX
- Ucko PJ, Dimbleby GW (1969) *The domestication and exploitation of plants and animals*. London

Chemical Analysis of Hair Segments and Short-Term Dietary Variation: Results for the Ancient Site of Chongos (Peru)

R.H. Tykot, A. Metroka, M. Dietz, and R.A. Bergfield

1 Introduction

One of the major questions about pre-Inca societies in Peru and other areas of South America is the spread and importance of maize agriculture and its relationship with the development of complex societies. While archaeological studies to answer dietary questions have long been done on faunal and floral remains, chemical analysis of human remains has provided quantitative data on the importance of particular foods for individuals, and thus potential variation in dietary patterns based on sex, age, status, etc. The majority of such studies have been done on human bone, due to preservation issues, with the results referring to average diets over at least the last several years of the individual's life.

In this study, preserved hair samples from seven individuals at the Early Horizon – Early Intermediate Period site of Chongos (Pisco River Valley, Peru) were tested in segments in order to look at short term dietary variation. The stable carbon and nitrogen isotope analysis data demonstrate significant short-term dietary variation in the consumption of both seafood and C4 plants such as maize, as well as variation among individuals.

2 Chongos (Peru) Archaeological Site

Chongos is located in the Pisco river valley on the outskirts of Pisco, north of Paracas (Fig. 1). The site is approximately 1 km south of the Pisco river, and about 12 km from the Pacific coast. It was excavated by a team of Peruvian and U.S. archaeologists in the mid to late 1980s as a salvage operation sponsored by the National Institute of Culture in Peru (Peters 1987/1988; 1997). The Chongos site

R.H. Tykot (✉) and A. Metroka
Department of Anthropology, University of South Florida, Tampa, FL 33620, USA
e-mail: rtykot@cas.usf.edu

M. Dietz and R.A. Bergfield
Department of Anthropology, University of Missouri-Columbia, Columbia, MO 65211, USA

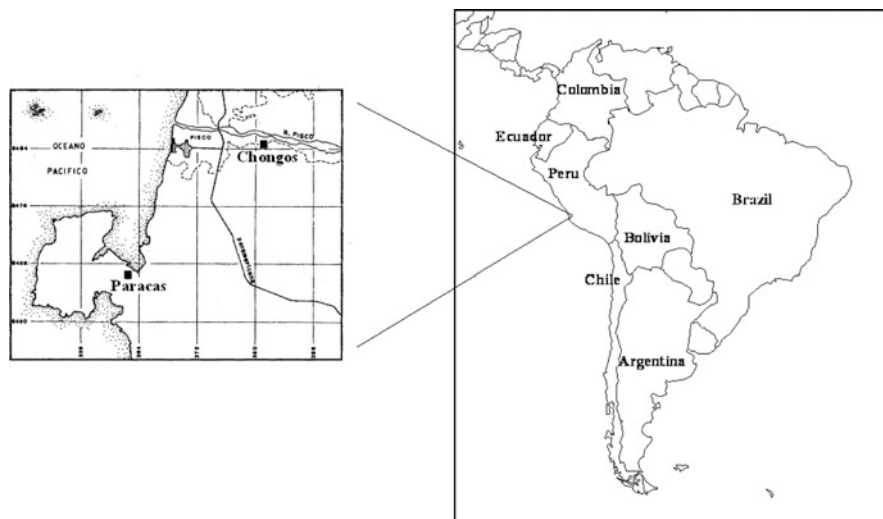


Fig. 1 Map showing location of the site of Chongos, near the Pisco River, north of Paracas on the coast of Peru

contains components that correspond to both the Paracas and Topará traditions during the Early Horizon/Early Intermediate Period (ca. 2300–1700 BP), meaning that the site was perhaps occupied at different times by people from different cultures over a relatively short period of time.

Chongos was likely an agricultural village, with an adjacent cemetery. The burials recovered at Chongos may or may not reflect a social community, with individuals from one place. So while they came from a similar time period, the cemetery may have included individuals associated with both the Paracas and Topará traditions, coming from different sites and different communities.

By the Horizon Period in Peru, formal agriculture and animal husbandry was well organized, so a broad menu including freshwater and marine fish and shellfish would have been available (e.g. Tykot and Staller 2002). Plant food items actually recovered at Chongos include peanuts, maize, sweet potato and manioc.

Human remains excavated at Chongos range from fully mummified to completely skeletonized individuals (Fig. 2). While full osteological investigation was not possible for those with soft tissues preserved, it was clear that Chongos people had a very high caries rate, a high rate of systemic infection, and a high rate of cribra orbitalia, but no external auditory exostoses (Dietz, forthcoming).

3 Hair Sample Preparation and Stable Isotope Analysis

The preservation of hair samples at Chongos specifically allowed us to do stable isotope analysis on individuals without being destructive to the skeletal remains, and at the same time investigate short-term, i.e. monthly, dietary variation



Fig. 2 Examples of skulls found at Chongos. Above *left*: adult male with braided hair, and cranial deformation typical of Paracas. Above *center*: adult female from Chongos, location BW 1500, burial 4. Above *right*: skull of a child age 5–6, location BP 1820, burial 7, with braided hair and Paracas style cranial deformation

(see Tykot 2004, 2006 for principles and history of stable isotope analysis). Hair samples had already been studied separately, using elemental analysis (Bergfield 2007). Because the hairs were in many cases still attached to the cranium, it was possible to obtain several adjacent hairs for each individual and maintain their alignment. After cleaning to remove any contaminants, samples were then cut in one-centimeter segments, with enough mass (1 mg) to provide both C and N isotope results. The comparison of 1 cm segments were expected to show monthly dietary variation.

The 1-cm length hair segment samples were weighed into tin cups, and analyzed on a Finnigan MAT Delta Plus XL stable isotope mass spectrometer in the Paleolab at the University of South Florida, using a Costech CHN multi-sampler. C and N gas yields as well as C:N ratios were used to determine the reliability of the results. The precision of the analyses were 0.1‰ for C and 0.2‰ for N, and the isotope values reported are relative to the VPDB and AIR standards, respectively. The isotope data for the hair segments is provided in Table 1.

4 Discussion

The range and overall average isotope values ($\delta^{13}\text{C} = -15.1 \text{ } \forall \text{ } 2.5\text{‰}$; $\delta^{15}\text{N} = 12.2 \text{ } \forall \text{ } 3.3\text{‰}$) for the seven individuals tested overlap with those obtained for other pre-contact period sites in Peru, e.g. highland sites including Chavín de Huantar (Burger and van der Merwe 1990), Conchopata (Finucane et al. 2006), Pacopampa (Tykot et al. 2006), and the Ayacucho Valley (Finucane 2007), and lowland/coastal sites including the Virú Valley (Ericson et al. 1989), Pacatnamu (Verano and DeNiro 1993), the Osmore Valley (Tomczak 2003), Mina Perdida and the Lurin Valley (Tykot et al. 2006), and San Geronimo, Chirabaya Alta, Chirabaya Baja, and El Yaral in the Osmore Valley (Tomczak 2003; Knudson et al. 2007). Unlike those other sites, especially for the time period represented by Chongos, there is much greater variation among these individuals, as is clear from the standard deviation values.

Table 1 Stable isotope data for hair segments from seven Chongos individuals

Ind.	Segment	USF #	$\delta^{13}\text{C}$	$\delta^{15}\text{N}$	$\delta^{13}\text{C}$ Range	$\delta^{13}\text{C}$ average/ std	$\delta^{15}\text{N}$ Range	$\delta^{15}\text{N}$ average/ std
12	1	10006	-16.7	12.6				
12	2	10007	-16.8	14.4				
12	3	10008	-17.8	14.3				
12	4	10009	-17.2	13.4	1.1	-17.1 \forall 0.4	1.7	13.7 \forall 0.7
18	1	10010	-17.4	7.0				
18	2	10011	-17.1	7.4				
18	3	10012	-16.9	8.3				
18	4	10013	-16.6	9.9				
18	5	10014	-15.8	10.9	1.6	-16.8 \forall 0.5	4.0	8.7 \forall 1.5
30	1	10015	-17.4	15.9				
30	2	10016	-17.8	15.1				
30	3	10017	-17.8	15.9				
30	4	10018	-17.2	16.1				
30	5	10019	-16.4	16.7	1.4	-17.3 \forall 0.5	1.6	15.9 \forall 0.5
40	1	10020	-11.9	16.8				
40	2	10021	-11.5	16.5				
40	3	10022	-12.0	15.2				
40	4	10023	-13.0	12.6	1.5	-12.1 \forall 0.5	4.2	15.3 \forall 1.7
47	1	10024	-12.0	13.8				
47	2	10025	-12.7	13.8				
47	3	10026	-12.8	13.9				
47	4	10027	-13.2	13.5	1.2	-12.7 \forall 0.4	0.4	13.8 \forall 0.1
51	1	10028	-16.8	8.1				
51	2	10029	-18.1	7.2				
51	3	10030	-15.4	8.2				
51	4	10031	-14.5	8.1				
51	5	10032	-15.7	7.7				
51	6	10033	-17.8	8.0				
51	7	10034	-17.5	8.2	3.6	-16.5 \forall 1.3	1.0	7.9 \forall 0.3
52	1	10035	-14.1	12.2				
52	2	10036	-11.9	13.3				
52	3	10037	-10.2	14.1				
52	4	10038	-10.1	14.7	4.1	-11.6 \forall 1.6	2.5	13.6 \forall 0.9

Like other studies of human hair in South America (Tykot et al. 2006; Shelnut 2006; Gil et al. 2006; Knudson et al. 2007), there is also clearly significant short-term variation for each of the individuals tested at Chongos (Fig. 3). One can immediately see that two individuals (18, 51) have low nitrogen isotope values, indicating a mostly terrestrial diet. But individual 18 has short-term variation in which both C and N isotope values increase, suggesting seasonal variation in seafood consumption. Individual 51, on the other hand, has short-term variation only in the carbon isotope values, most likely from seasonal maize consumption.

Individuals 12 and 30 have fairly low carbon isotope values but much higher nitrogen isotope values, clearly indicating major consumption of freshwater fish, with individual 12 appearing at times to have some maize in the diet. Individuals 40, 47, and 52 have very high carbon and nitrogen isotope values in their hair segments, clearly indicating major consumption of higher trophic level marine foods.

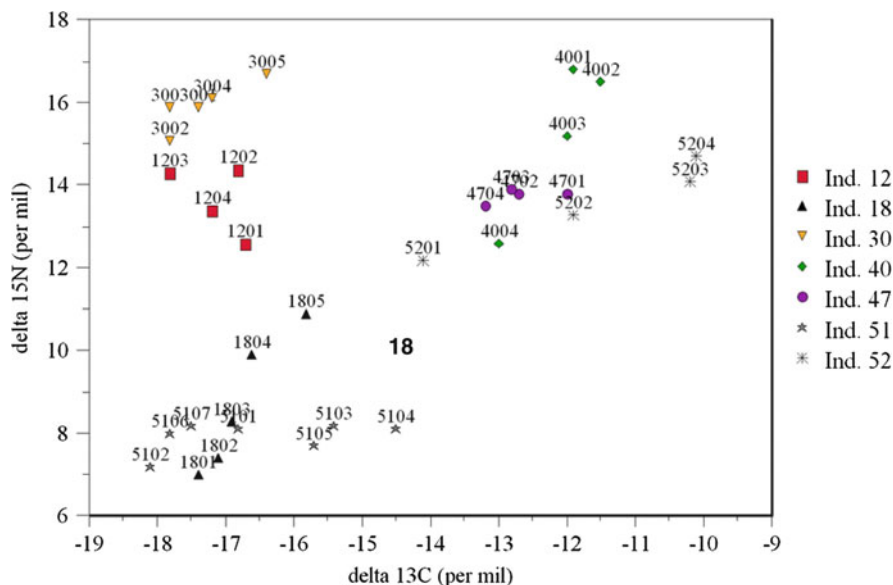


Fig. 3 Carbon vs. nitrogen stable isotope data for hair segments of seven individuals from Chongos, Peru

5 Conclusion

There clearly were major differences in diet in general, and in seasonal practices, between the seven individuals tested at Chongos. Overall, the variation in the isotope data and the diets they represent is due either to individual and/or political choice, and raises socioeconomic questions about food acquisition and production, labor organization, and exchange that developed in Peru by the Early Horizon/Early Intermediate Period. Could individual 18 be a traveler between highlands and lowlands thereby consuming plants and fish? Were individuals 30 and 40 strictly lowland dwellers that consumed mainly what was caught from a water source? In particular, this dietary variation supports our hypothesis that these burials may well represent a mixture of people at Chongos, some affiliated with Paracas, and others who are affiliated with Topará, and thus serves as a catalyst for additional research. The results obtained here will be integrated further with the archaeological, osteological and elemental analyses done, to further understand this important period in ancient Peru.

Acknowledgments This research was initiated by Prof. Robert Benfer, Department of Anthropology, University of Missouri-Columbia, and supported by a USF Honors College award to Anne Metroka for her senior honors thesis research. We also thank Dr. David Hollander and Ethan Goddard for directing the Paleolab and running these samples on the mass spectrometer.

References

- Bergfield RA (2007) Dietary analysis of archaeological hair samples from Peru. MA Thesis, University of Missouri-Columbia
- Burger RL, van der Merwe NJ (1990) Maize and the origin of highland Chavín civilization: an isotopic perspective. *Am Anthropol* 92:85–95
- Ericson JE, West M, Sullivan CH, Krueger HW (1989) The development of maize agriculture in the Viru Valley, Peru. In: Price TD (ed) *The chemistry of prehistoric human bone*. Cambridge University Press, Cambridge, pp 68–104
- Finucane BC (2007) Mummies, maize, and manure: multi-tissue stable isotope analysis of Late Prehistoric human remains from the Ayacucho valley, Peru. *J Archaeol Sci* 34:2115–2124
- Finucane B, Agurto PM, Isbell WH (2006) Human and animal diet at Conchopata, Peru: stable isotope evidence for maize agriculture and animal management practices during the Middle Horizon. *J Archaeol Sci* 33:1766–1776
- Gil A, Shelnut N, Neme G, Tykot RH, Michieli T, Teresa C (2006) Isotopos estables y dieta humana en el centro oeste: datos de muestras de San Juan. *Cazadores Recolectores Sudamericanos* 1:151–163
- Knudson KJ, Aufderheide AE, Buikstra JE (2007) Seasonality and paleodiet in the Chiribaya polity of southern Peru. *J Archaeol Sci* 34:451–462
- Peters AH (1987/1988) Chongos: sitio Paracas en el valle de Pisco. *Gaceta Arqueologica Andina* 16:30–34
- Peters AH (1997) Paracas, Topara and Early Nasca: ethnicity and society on the South Central Andean Coast. PhD dissertation, Cornell University
- Shelnut N (2006) Prehistoric subsistence patterns in Western Argentina. MA Thesis, University of South Florida
- Tomczak PD (2003) Prehistoric diet and socioeconomic relationships within the Osmore Valley of southern Peru. *J Anthropol Archaeol* 22:262–278
- Tykot RH (2004) Stable isotopes and diet: you are what you eat. In: Martini M, Milazzo M, Piacentini M (eds) *Physics methods in archaeometry, Proceedings of the international school of physics “Enrico Fermi” course CLIV*. Società Italiana di Fisica, Bologna, Italy, pp 433–444
- Tykot RH (2006) Isotope analyses and the histories of maize. In: Staller JE, Tykot RH, Benz BF (eds) *Histories of maize: multidisciplinary approaches to the prehistory, linguistics, biogeography, domestication, and evolution of maize*. Academic Press (Elsevier), Amsterdam, Netherlands, pp 131–142
- Tykot RH, Burger R, van der Merwe NJ (2006) The importance of maize in initial period and early horizon Peru. In: Staller JE, Tykot RH, Benz BF (eds) *Histories of maize: multidisciplinary approaches to the prehistory, linguistics, biogeography, domestication, and evolution of maize*. Academic Press (Elsevier), Amsterdam, Netherlands, pp 187–197
- Tykot RH, Staller JE (2002) The importance of early maize agriculture in coastal Ecuador: new data from La Emerenciana. *Curr Anthropol* 43:666–677
- Verano JW, DeNiro MJ (1993) Locals or foreigners? Morphological, biometric, and isotopic approaches to the question of group affinity in human skeletal remains recovered from unusual archaeological contexts. In: Sandford MK (ed) *Investigations of ancient human tissue: chemical analysis in anthropology*. Gordon and Breach Science Publishers, Langhorne, PA, pp 361–86

Distinguishing Between Reindeer Antler and Bone Using Raman Spectroscopy

J. Watson and C.C. Nordby

1 Introduction

Distinguishing between reindeer antler and bone can often be challenging as they are essentially the same material, with antler being morphologically similar to rapidly formed bone (O'Connor 1987). Determination can be aided by observation of function, macrostructure, texture, colour, shape, and size of an object, but only in rare cases can these factors lead to an unequivocal identification, especially on small and/or worked material, as artefacts commonly are (O'Connor 1987) (Fig. 1).

Adding to the challenge is the fact that archaeological objects have often been modified, either in the manufacture of the object, or in the burial environment, or both (O'Connor 1987). Accurate determination is important to archaeologists because it provides information about a wide range of areas including resource management, material preferences, economy, exchange and ritual behaviour.

Raman spectroscopy is a non-destructive analytical technique that has been demonstrated to be of value in distinguishing between keratinaceous material from different species (as well as identifying imitation materials) (Akhtar and Edwards 1997; Edwards et al. 1998, *inter alia*). Recent research has shown that it is possible to distinguish between human finger- and toe-nails using Raman spectroscopy, most probably as a result of the fact that fingernails grow more quickly (Widjaja and Seah 2006). If collagens behave similarly (*i.e.* if the more rapid formation of antler as compared to bone results in a difference that is reflected

J. Watson (✉)

Museum Conservation Institute, Smithsonian Institution, 4210 Silver Hill Road, Suitland, MD 20746, USA

e-mail: watsonj@si.edu

C.C. Nordby

Culture Historical Laboratory, Department of Archaeology, Tromsø Museum, University of Tromsø, N-9037 Tromsø, Norway



Fig. 1 Human figurine carved in reindeer antler or bone. From Advik, Finnmark, Northern Norway (2200–1800 BC). Photo: A. Icagic, Tromsø University Museum. This object illustrates the problem archaeologists and conservators face when dealing with artefacts made from reindeer antler and bone. Because the material looks so similar in many cases, it can be impossible to make a determination, especially when sampling is not permitted

in Raman spectra), this would offer archaeologists a non-destructive method of accurately classifying this important material regardless of the size or nature of the artefact. Here we present the results of a study testing the applicability of this approach on collagens, using vouchered samples of modern reindeer (*Rangifer tarandus tarandus*) antler and bone.

2 Methods

Using a Thermo Electron NXR FT-Raman Spectrometer with a 1,064 nm NdYVO₄ laser and a germanium detector, antler and bone samples from five individuals were analysed at 1 W for 1,024 scans (taking approximately 25 min for each analysis). Each sample was cut into several smaller samples so that analyses could be performed on different areas of sections as well as surface areas. At least five analyses were performed on each of at least three subsamples from each individual. This sampling protocol was chosen as different areas of the sample interacted differently with the laser, with some areas yielding very clear spectra and others (on the same sample, and in some cases superficially identical to the other areas) yielding highly fluorescent spectra, or spectra with a higher background, or showing signs of sample heating. Surfaces of the samples varied in colour from white to medium brown, which is an issue as the darker the sample is, the more likely it is to heat, which may cause problems including damage to the sample by the laser.

45 spectra were used to develop and test a discriminant analysis method on the TQ AnalystTM software package from Thermo Scientific. Two classes were created (one each for antler and bone) with some spectra from each class being used to calibrate the method and others being used to test it. No alterations were made to the spectra prior to statistical analysis (*e.g.* background subtraction or smoothing). The method was tested with a combination of good and poor spectra, and the best group cohesion was attained by using spectra representing the full range of quality as reference standards.

3 Results and Discussion

Careful visual examination of the spectra revealed that the ratio between the two peaks in the area between 1,054 and 1,020 cm⁻¹ clearly differed between the two types of material. In bone, the peak on the right is roughly the same height as or lower than the peak on the left, whereas in antler the peak on the right is much higher (Fig. 2). Discriminant analysis of these two classes of material using the full spectrum was successful, with all “unknowns” (including very fluorescent spectra) being correctly classified and falling well within the 95% confidence range.

The question of the persistence of these signals throughout time and as a result of diagenetic and/or anthropogenic modification is a crucial one, and will be resolved both experimentally (repeating this experiment using vouchered archaeological bone and antler samples) and by means of further research to correlate the differences in the Raman signals of these two materials to the physical structure of the tissue and to the biological processes occurring during tissue formation.

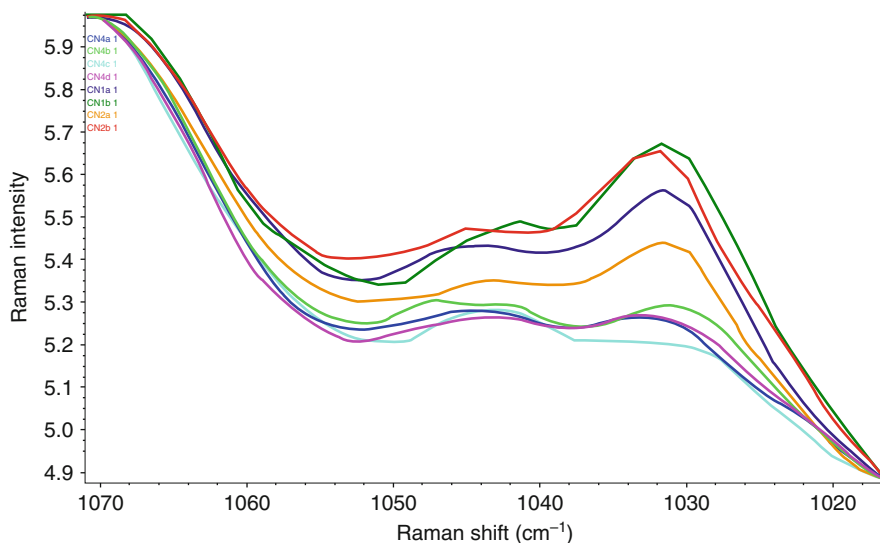


Fig. 2 Close-up of an area of the spectra. The ratio between the two peaks at around $1,042\text{ cm}^{-1}$ and $1,030\text{ cm}^{-1}$ show the clearest difference between the two materials. The spectra showing a higher peak near $1,030\text{ cm}^{-1}$ (the top four spectra) are antler; the spectra where the peak at around $1,042\text{ cm}^{-1}$ is approximately equal to or higher than the $1,030\text{ cm}^{-1}$ (the bottom four spectra) are bone

4 Conclusion

This study was the first step in developing a non-destructive method of unequivocally distinguishing between reindeer antler and bone in archaeological objects. We have demonstrated that FT-Raman spectroscopy provides a rapid, non-destructive method of securely discriminating between modern antler and bone. Further research focusses on testing the method on vouchered archaeological samples and developing an understanding of the mechanism behind the difference in the bone and antler spectra.

Acknowledgements The authors wish to thank the Smithsonian Museum Conservation Institute, specifically Dr Robert Koestler, Dr Paula DePriest, Robert J. Speakman, Nicole Little, and Odile Madden for their support.

References

- Akhtar W, Edwards HGM (1997) Fourier-transform Raman spectroscopy of mammalian and avian keratotic biopolymers. *Spectrochimica Acta Part A* 53:81–90
- Edwards HGM, Hunt DE, Sibley MG (1998) FT-Raman spectroscopic study of keratotic materials: horn, hoof, and tortoiseshell. *Spectrochimica Acta Part A* 54:745–757
- O'Connor S (1987) The identification of osseous and keratinaceous materials at York. In: Starling K, Watkinson D (eds) *Archaeological bone, antler and ivory*. UKIC Occasional Paper No. 5
- Widjaja E, Seah RKH (2006) Use of Raman spectroscopy and multivariate classification techniques for the differentiation of fingernails and toenails. *Appl Spectrosc* 60:343–345

Part V
Food Preparation and Consumption
in Antiquity

Fish-Based Subproducts in Late Antiquity. Archaeometric and Archaeological Evidence from the Fish Factories at Traducta (Algeciras, Cádiz, Spain)

S. Dominguez-Bella, and D. Bernal Casasola

1 Introduction

Recent rescue archaeological excavations carried out in San Nicolás Street (modern Algeciras, Andalusia, Spain) have brought to light a very important and well preserved industrial quarter of the Roman city of Iulia Traducta. Five buildings related to fish processing – *cetariae* – have been unearthed, dating back to a period between the first century BC and the early sixth century AD.

An interdisciplinary research program has been developed to study all biofacts found, including sediments and archaeozoological remains. At this site, a great abundance of Roman millstones that had been used for industrial purposes appeared in different deposits. More than 20,000 archaeozoological remains were also discovered, but there are almost no fish bones among them (Arévalo et al. 2004). This aspect led us to hypothesize that this high number of millstones, found together in an industrial context, could be related to the elaboration of flours of fish.

In the third century AD, Eliano's descriptions of the Roman manufacture of flours of fish in his "History of the Animals" already existed. Up to this moment there are no clear references in the literature regarding the existence of processing remains of flours of fish from the Roman period, which makes this field of study especially interesting.

The aim of this work has been to try to identify organic or inorganic remains in the active surfaces of the millstones, in order to determine what materials were crushed there, and to check the possibility that these artefacts could have been used for crushing fish bones to obtain fish flour and oil. The study and characterization of the raw materials out of which the millstones were elaborated, and their comparison with geological materials from the environment of the Strait of Gibraltar were also carried out in order to determine their origin.

S. Dominguez-Bella (✉)

Department of Geology, University of Cádiz, Cádiz, Spain
e-mail: salvador.dominguez@uca.es

D. Bernal Casasola

Department of History, Geography and Philosophy, University of Cádiz, Cádiz, Spain

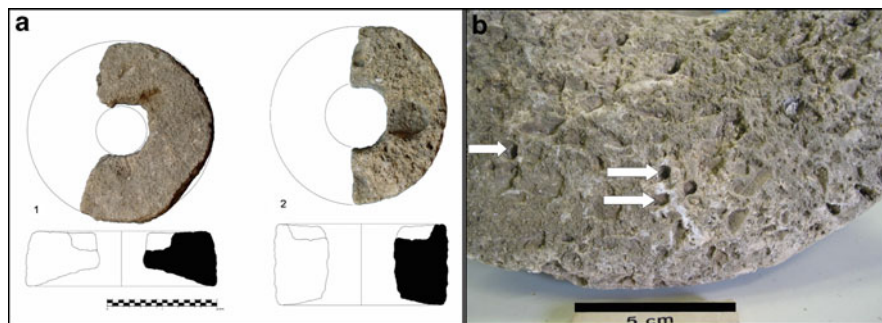


Fig. 1 (a) View of two of the studied millstones, (*meta*); (b) Close-up view of the active surface of a millstone, with a great abundance of pores and hollows filled by sediments (*white arrows*)

2 Materials

A series of 11 millstones, recovered during the 2001–2006 surveys of the salting factory of San Nicolas Street and dated back to the beginning of the sixth century AD, have been studied. The studied samples are stones that constitute the lower part of the mill (*meta*), with cylindrical plate morphology and a great central orifice (Fig. 1a). The size of the pieces of millstone analysed is around 30–35 cm in diameter and 8–12 cm in height.

Apart from the archaeological samples, many rocks' lithotypes have also been analysed. They originate from different geological outcrops of the Gibraltar Strait littoral, located at sites with vestiges of rock exploitation (at least as construction material) during Roman times. In addition, two other samples of similar Roman millstones from the Cadiz province and a sample from the Roman millstone quarry of Cape Espartel, near Tangier (Morocco), known as Hercules' Grotto, have been studied. The purpose of these comparative studies has been to determine the possible geological and geographical origins of the millstones. The sediments recovered from the hollows of the active surfaces of some of the millstones (Fig. 1b) have been studied by Optical Microscopy (OM), Scanning Electron Microscopy (SEM), X-ray Diffraction (XRD), and Energy Dispersive X-ray Spectroscopy (EDS) techniques.

3 Methods

Optical microscopy with a polarization microscope (OM) and X-ray diffraction analysis (XRD) were employed in order to characterize the mineral phases, textures or fossils present in these rocks (geological and archaeological samples). XRD has been undertaken with Cu K α radiation and phase identification by means of the

Bruker-AXS software. A detailed OM and SEM study has been carried out on the remains deposited inside the pores and hollows of the surfaces of the millstones.

The methodology employed has consisted in scraping, by means of scalpel or needle, the sediment contained in some of these irregularities of the active surface, in contact with both millstones during grinding. Indeed, clear possibilities exist that some remnants of the crushed materials have remained attached to these hollows of the rock (Fig. 1b). The extracted sediment was mixed with bi-distilled water, passed in an ultrasound bath and filtered, in order to eliminate clay minerals and salts remains. The residue was dried, deposited in a glass capsule and separated manually under a stereomicroscope. Grains or selected fragments were separated from the main body, metallised with Au, and examined under the SEM. During the SEM study, a semi-quantitative chemical analysis of grains and fragments present in the extracted residual material was carried out. EDX analyses, coupled with the XRD results, allowed us to recognize calcite bioclasts. Other organic fragments, corresponding to osseous remains, possibly of fish, were recovered in two of the millstones. Furthermore, inorganic components consisting of quartz and cinnabar grains were recovered.

4 Results and Discussion

4.1 Petrographic and Mineralogical Features of the Millstones

From the study of the thin sections, it was concluded that the millstones are constituted by bioclastic calcarenite, or conglomerate or micro-conglomerate with bioclast. Rounded grains of quartz, pebbles of quartzite and other rocks also occur. The bioclastic component mainly consists of fragmented mollusc shells, especially bivalves and oysters. Bryozoans, echinoderm spicules, coral remains and different types of foraminifers were also observed. All the components appeared to be cemented with sparitic and locally micritic calcite cement.

The fossil content of these rocks allows us to date these lithologies as biocalcarenites of the Pliocene (Gutiérrez-Más et al. 1991). It would correspond to a lithologic facies type similar to “ostionera rock”, as it is called in the Cadiz area.

References to the grinding stones appear in Book 36 of Pliny the Elder’s *Natural History*. Other papers (Williams-Thorpe 1988; Williams-Thorpe and Thorpe 1993) deal with millstone features used in the Mediterranean area from the Neolithic to the Roman period. The majority of these are made of igneous rocks, generally volcanic, such as basalts and andesites (Renzulli et al. 2002; Antonelli et al. 2005), plutonic or metamorphic ones, often used in the Roman world for the production of this type of millstones. All the described igneous or metamorphic lithologies do not exist in this area, while various types of biocalcarenites and bioclastic conglomerates are widespread, outcropping in different locations on the coast of Cadiz and Morocco, in the Strait of Gibraltar.

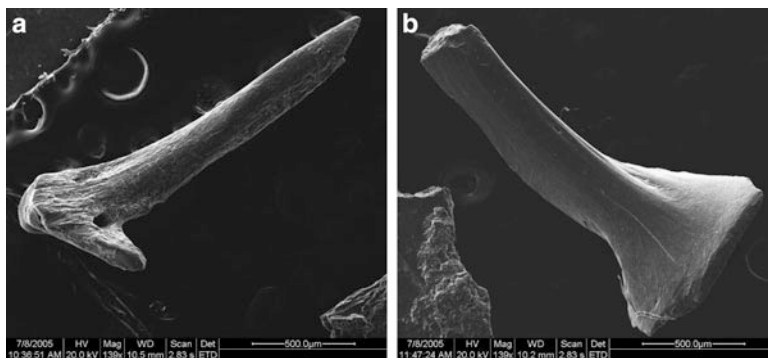


Fig. 2 (a and b) SEM views of fish bones remains recovered from the filler of the hollows of a millstone

4.2 Considerations About the Presence of Fish and Marine Animal Remains in the Millstones

During examination under the stereomicroscope, different organic remains and mineral grains have been identified. Remains of scales and vertebrae of fish were observed in several samples (Fig. 2a, b). In other millstones, spicules of sea urchin and a snail shell were present. A complete identification of these ictiofauna remains is in course. These studies provide us with significant information about the utility and use of these millstones and about the materials that were crushed. Due to the strange abundance of millstones in an industrial installation dedicated to the manufacture of marine products such as conserves and salted fish, it was of great interest to confirm the hypothesis regarding the possible use that these millstones had during the Roman period.

4.3 Considerations About the Provenance of the Cinnabar Grains

Many small grains of vermilion red colour (50–70µm in diameter) were detected in one of the millstones. Undoubtedly, these grains are of cinnabar (HgS), a completely exotic mineral in this geographical context, which cannot derive either from the millstones or from any mineral deposit of the geological environment of Algeciras Bay and the Gibraltar Strait. It will thus be necessary to determine its origin by studying the appropriate geological environments (Domínguez-Bella 2004) that probably correspond to remote source areas, located at least a few hundred kilometres from the site. Among the Spanish deposits of cinnabar, those of the Almadén area (Ciudad Real) are known to have been exploited in Roman times. The mineral was extracted and exported for the production of an expensive

vermillion pigment, the “Pompeian red”, obtained by crushing cinnabar (Pliny the Elder, *Natural History*). This pigment was used in Roman wall painting. Many examples of its use exist (Damiani et al. 2003), especially in Pompeii, but also in other sites of the Empire, such as Roman Spain; of these, some are located in the Cadiz province (Domínguez-Bella and Morata 2002; Domínguez-Bella 2004).

5 Conclusions

A further necessary direction of research regards the identification of the lithologies from the Strait of Gibraltar that represent the most probable raw materials for the manufacture of these millstones. So far, these appear to be the cemented conglomerates of the Upper Pliocene (ostionera facies) (Gutiérrez-Más et al. 1991).

It is very difficult to determine with accuracy the source area of these rocks due to the great homogeneity in the lithologic types present in these millstones. More detailed studies on the petrology and fauna of the rocks are currently in progress in order to determine their origin more accurately, even though a local or regional origin of these materials (in the Cadiz coast area) seems to be very likely.

In this study, the occurrence of organic remains inside the different manufactures associated with the fishing industry or processing of marine products is confirmed for the first time. Fish bones and other minerals have been identified in the millstones, confirming the hypothesis that flour and fish oil were produced in these fish factories on the coast of the Fretum Gaditanum in ancient times.

These processes of systematic crushing of fish and other marine animals could have been due to the systematic production of flours of fish and/or of sauces or salted fish derivative products. With the exception of the work of Bernal et al. (2002), no other bibliographical references to this type of activities and products in the Roman world exist up to date. The presence of grains of cinnabar in two of the millstones might correspond to a peculiar use of some of the millstones in the preparation of red pigments for wall painting. An alternative hypothesis would be the employment of cinnabar in some of the processes of conservation or elaboration of fish conserves, but the toxic character of the mercury compounds does not favour this idea.

This work thus opens a new and exciting direction for future research within the study of the conserves and salted fish in the “Circle of the Strait of Gibraltar” area.

References

- Antonelli F, Lazzarini L, Luni M (2005) Preliminary study on the import lavic millstones in Tripolitania and Cyrenaica (Lybia). *J Cult Herit* 6:137–145
- Arévalo A, Bernal D, Torremocha A, (eds) (2004) *Garum y salazones en el Círculo del Estrecho*. Fundación Municipal de Cultura José Luis Cano. Algeciras

- Bernal D, Jiménez R, Lorenzo L, Torremocha A, Expósito JA (2002) Las industrias de salazón de época romana en Iulia Traducta (Algeciras, Cádiz). Espectaculares novedades arqueológicas. *Revista de Arqueología* 249:49–57
- Damiani D, Gliozzo E, Turbanti Memmi I, Spangenberg J (2003) Pigments and plasters discovered in the House of Diana (Cosa, Grosseto-Italy): an integrated study between Art History, Archaeology and scientific analyses. *Archaeometry* 45:341–354
- Domínguez-Bella S, Morata D (2002) Mineralogical and chemical characterization of roman wall painting from Medina-Sidonia, Cádiz, Spain. In: Jerem E, Biró KT (eds) *Archaeometry* 98. Proceedings 31st International Symposium on Archaeometry. 1998 Budapest. BAR International Series 1043 (II): 715–722. Oxford
- Domínguez-Bella S (2004) Pinturas murales romanas en la Neápolis Gaditana (Cádiz). Análisis de pigmentos minerales y caracterización de estucos, In: Feliu MJ et al. (eds) *Avances en Arqueometría 2003*: 201–207. Servicio de Publicaciones. Universidad de Cádiz
- Gutiérrez-Más JM, Martín AA, Domínguez-Bella S, Moral Cardona JP (1991) Introducción a la geología de la provincia de Cádiz. Servicio Publicaciones, Universidad de Cádiz
- Pliny the Elder, *Natural History*, Book 36, ED. Gredos, Madrid 1998
- Renzulli A, Santi P, Nappi G, Luni M, Vitali D (2002) Provenance and trade of volcanic rock millstones from Etruscan-Celtic and Roman archaeological sites in Central Italy. *Eur J Mineral* 14:175–183
- Williams-Thorpe O (1988) Provenancing and archaeology of Roman millstones from the Mediterranean area. *J Archaeol Sci* 15:253–305
- Williams-Thorpe O, Thorpe RS (1993) Geochemistry and trade of eastern Mediterranean millstones from the Neolithic to Roman periods, *J. Archaeol Sci* 20(3):263–320

Chemical Analyses of Floors at San Genesio (San Miniato, Pisa): A Medieval Tavern

F. Inserra and A. Pecci

1 Introduction

Chemical analyses of floors are useful for identifying the organisation of the archaeological space and the distinction of daily activities (Barba 1986, 2007; Middleton 2004). They study chemical compounds that can be considered markers of human activities, and that are different from the ones commonly employed in archaeological projects.

Chemical residues are a particular archaeological indicator. They can offer a “photograph” of the “systemic context” (Schiffer 1972), as they are absorbed by the pores of the soil, or of the floors, in the position in which the activities were carried out (Barba 1986; Barba and Lazos 2000). Both the presence and the absence of residues are important archaeological indicators that allow us to understand what kind of human activities took place at a certain location (Barba 1986). The presence or absence of residues depends on: (1) the surface being analysed (which has to be porous and homogeneous); (2) the type of activity carried out and its duration; (3) the reiteration and the intensity of the activity; (4) the type of abandonment; (5) the eventual re-use of space for different functions (which brings about a very difficult interpretation of the distribution maps); and (6) the effects of modern society and the contamination of the surface during its excavation (Ortiz 1990).

The interpretation of the correlation between human activities and chemical data from archaeological contexts is usually based on ethnoarchaeological studies (Barba and Ortiz 1992). In this paper, we present the results of the analyses carried out at San Genesio (San Miniato, Pisa), in a medieval structure that can be interpreted as a tavern.

F. Inserra (✉) and A. Pecci

Archaeometric Laboratory, Department of Archaeology and History of Art, University of Siena, via Roma, 56, 53100 Siena, Italy
e-mail: fernandainserra@hotmail.it, alepecci@gmail.com

2 The Site

San Genesio (San Miniato, Pisa) was an important location on the Via Francigena, the famous medieval “road” connecting Northern and Southern Europe to the Holy Land. The site was inhabited since the beginning of the fourth century/the end of the third century BC to 1248 AD, when the inhabitants of the nearby locality of San Miniato set the entire site on fire.

During the second half of the seventh century AD, a large church dedicated to Saint Genesio was built, and the place became an important political and religious centre, in which some councils and imperial diets took place (Cantini and Fatighenti 2007).

During the fifth campaign of archaeological excavations directed by F. Cantini and M. Valenti (Medieval Archaeological Area, Department of Archaeology and History of Arts, University of Siena), a structure built during the thirteenth century AD was identified. It was affected by the 1248 fire which caused the destruction of the entire site. The structure was composed of three communicating rooms; it had earthen walls and it was covered by a roof of tiles. The floors of two rooms (room C and room B) of the structure were sampled in order to carry out chemical analyses and establish their function. The third room (room A) was excavated before the beginning of this study, and, as a result, it was not possible to sample it. This was also the case of the big fireplace present in room B.

3 Methodology

Eighty-eight samples were collected using a regular grid of 1×1 m and a smaller grid for analysing specific details. All the samples were analysed by spot tests in order to establish the presence of phosphates, fatty acids, and protein residues, and to measure the pH level of each sample, following the methodologies established by Barba et al. (1991) and Barba (2007).

The sample data and the results of the analyses were inserted in the GIS excavation database. The results of the analyses were interpolated using an Arc Map application, in order to obtain a distribution map for each compound. The analyses were carried out at the Archaeometric Laboratory of the Department of Archaeology of the University of Siena (at Grosseto). The interpretation of the use of space was carried out taking into account the concentration/absence of the different compounds and the archaeological data.

Phosphorus is present in soil, but human activities also add to its concentration, through the waste produced, such as excrements, residues of food, and fertilizers. Concentrations of phosphates suggest activities of preparation, cooking and consumption of food, slaughtering or milking activities, animal breeding, or the presence of waste disposal sites. Fatty acids are present in animal or vegetable oils and fats, blood or meat. Their presence in the floor samples suggests domestic activities connected with food preparation and consumption, or the storage of fatty foods or

liquids. Protein residues suggest the presence of animal or vegetable foods containing proteins. They can be the results of activities of preparation, cooking, and consumption of food, or of the slaughtering of animals. Ph values inform on the acidity or alkalinity of the soil. The alkalinity of the floors can be influenced by the composition of the floor and the presence of ash produced by fireplaces or fires. Food preparation and consumption areas are characterised by the presence of a high level of pH, together with concentrations of fatty acids, phosphates and protein residues (Barba and Lazos 2000; Pecci and Marazzi 2006).

4 Results and Discussion

The alkalinity of the pH level suggests the presence of ash in the entire surface, produced by the fireplaces and most likely by the fire of 1248, which burned the wooden beams (see Fig. 1).

The maps show the distribution of fatty acids, protein residues and phosphates almost all over the floor of the structure, suggesting an intense activity of storage and preparation of food. In room B of the structure, there is a greater concentration of residues, especially next to the fireplaces. The floor of room C is very rich in residues.

Ethnoarchaeological projects such as those carried out at Tlaxcala (Barba and Ortiz 1992) and Cuentepec (Lopez Varela et al. 2005) in Mexico, and archaeological projects such as the ones at Donoratico (Pecci 2004) and San Vincenzo al Volturno (Pecci and Marazzi 2006) in Italy, have shown that the areas used to prepare and consume food are characterised by the presence of fatty acids, protein residues, phosphates and high levels of pH in the soil samples. These same residues can be also produced by different activities, such as ritual activities and slaughtering of animals. The interpretation of activity areas must therefore be performed by taking into account the data related to residues together with other archaeological indicators.

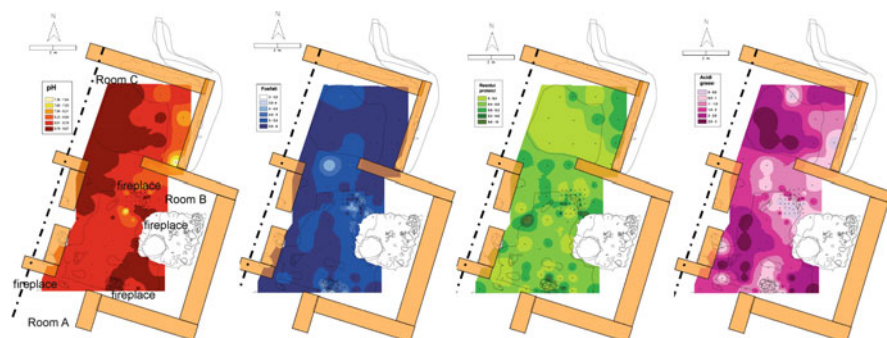


Fig. 1 Distribution maps (from *left to right*) of the pH level, protein residues, phosphates and fatty acids

The relative quantity of residues present in rooms B and C is particularly high: fatty acids, protein residues and phosphates are present almost all over the floor. Due to the presence of abundant ceramics typical of food cooking and storage in rooms B and C, we believe that the residues identified are related to food preparation and storage. In particular, in room B there are several fireplaces from the top of which cooking vessels were recovered, suggesting that this room was used for cooking food. In room C, no fireplaces are present, and the ceramics recovered are mainly associated with food storage. This aspect seems to confirm the interpretation of room C as a storeroom. Nevertheless, the huge quantity of residues on the floor of the entire room suggests that it was also probably used for the preparation of food before cooking.

The floor of room A could not be sampled, but during the excavation a fireplace was found near its northern side, and many small post holes were identified. This feature suggests that room A could be the place in which the food was consumed, and the small post holes could be due to the presence of tables and benches.

Comparing the results of the chemical analyses with the archaeological excavation data, we can put forth the hypothesis that the structure was a tavern: the analyses of the residues indicate an intense activity of food storage, preparation and consumption that is not compatible with a normal domestic life. Moreover, coins from Lucca and Pisa, three stone gaming-pieces, fragments of glasses and two bone dice were found during the excavation of the structure, suggesting the typical activities carried out in a tavern. The three rooms could have different functions: the food was prepared and stored in room C, it was prepared and cooked in room B, and consumed in room A.

Archaeozoological analyses show the consumption of different types of meats in the sampled structure: pig, goat/sheep, ox, cock, in addition to molluscs and eggs. The meat was probably consumed after boiling in the pots found on the fireplaces (Fig. 2).

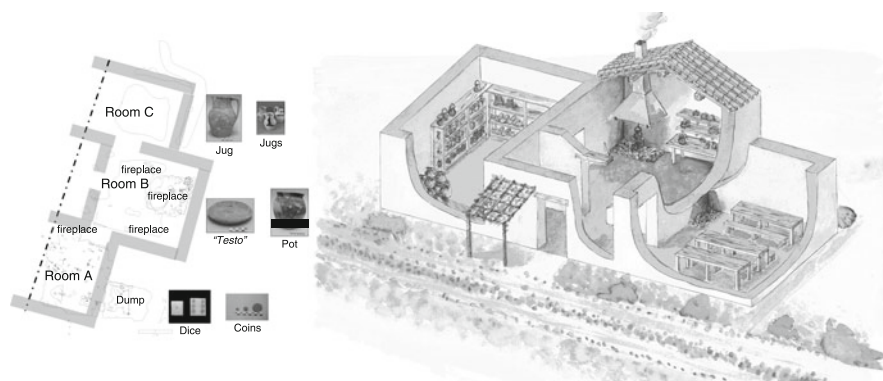


Fig. 2 Map of the structure with some of the materials found and hypothetical reconstruction of the tavern

The study of the bones of the animals suggests that also secondary products, such as cheese, were consumed (Buonincontri and Buonincontri 2007).

Chemical analyses of the residues absorbed in the pottery vessels recovered in the structure are in progress, in order to establish what was cooked in the tavern and the function of the different types of pottery.

5 Conclusion

It is useful to introduce chemical analyses of residues as part of multidisciplinary projects that include excavation, study of the archaeological materials, paleobotanical and archaeozoological data, as this integrated approach offers the possibility of a better understanding of past human activities.

Although the structure suffered an important fire, it was possible to identify the presence of chemical residues in the floors, as previous studies have also shown (Pecci and Marazzi 2006). The multidisciplinary approach adopted in the study of the structure allowed the identification of its possible function. Only by considering together the spreading of the chemical traces of food preparation, the quantity of ceramics around the fireplaces, the presence of the dice, the gaming-pieces and the coins, it was possible to interpret the structure as a tavern, an unusual building to discover at an archaeological level.

Acknowledgements The project was financed by the Fondazione Monte dei Paschi di Siena through the Progetto dei Paesaggi Medievali, and by the Comune di S. Miniato. The project is directed by F. Cantini and M. Valenti (Department of Archaeology, University of Siena). M. Buonincontri was in charge of the excavation of the area. B. Fatighenti is in charge of the GIS of the site. The ceramic typological study was carried out by B. Fatighenti and J. Bruttini. The archaeozoological study was carried out by S. Buonincontri.

References

- Barba L (1986) La química en el estudio de áreas de actividad UNAM. In Manzanilla L (ed) *Unidades habitacionales mesoamericanas y sus áreas de actividad*, Mexico. pp 21–39
- Barba L (2007) Chemical residues in lime plastered archaeological floors. *Geoarchaeology* 22 (4):439–452
- Barba L, Ortiz A (1992) Análisis químico de los pisos de ocupación: un caso etnográfico en Tlaxcala, México. *Lat Am Antiq* 3(1):63–82
- Barba L, Lazos L (2000) Chemical analyses of floors for the identification of activity areas: a review. *Anthropología y Técnica* 69:59–70
- Barba L, Rodríguez R, Córdova JL (1991) *Manual de técnicas microquímicas de campo para la arqueología*, Mexico
- Buonincontri S, Buonincontri M (2007) A tavola nel borgo. In: Cantini F (ed) *Con gli occhi del pellegrino. Il borgo di San Genesio: archeologia lungo la via Francigena*, Florence. pp32–33
- Cantini F, Fatighenti B (2007) Indagini archeologiche nel sito di S Genesio: nuovi dati delle campagne 2005–2006, *Milliarium. Periodico di informazione archeologica* 7:28–35

- López VS, Ortiz A, Pecci A (2005) Ethnoarchaeological Study of chemical Residues in a “living” household in Mexico. *Geoarchaeological and Bioarchaeological Studies*. Vrije Universiteit, Amsterdam, pp 19–22
- Middleton WD (2004) Identifying chemical activity residues on Prehistoric house floors: a methodology and rationale for multi-elemental characterization of a mild acid extract of anthropogenic sediments. *Archaeometry* 46:47–65
- Ortiz A (1990) Ozttoyahualco: Estudio químico de los pisos estucados de un conjunto residencial teotihuacano para determinar áreas de actividad. Degree thesis, ENAH, Mexico
- Pecci A (2004) Per una definizione funzionale degli spazi e delle ceramiche all’interno degli insediamenti in corso di scavo: un progetto archeometrico. unpublished PhD thesis in Archaeology, University of Siena
- Pecci A, Marazzi F (2006) Chemical residues of human activities in San Vincenzo al Volturno, Proceedings del 34th International Symposium on Archaeometry, 3–7 May 2004. Zaragoza, Spain, Zaragoza, pp 39–43
- Schiffer M (1972) Archaeological context and systemic context. *Am Antiq* 32(7):156–165

Food Habits and Social Identity During the Archaic Age: Chemical Analyses of Organic Residues Found on Pottery Vessels from the Messapian Settlement of San Vito dei Normanni (South-Eastern Italy)

F. Notarstefano, M. Lettieri, G. Semeraro, and L. Troisi

1 Introduction

Food preparation and consumption are strictly connected to everyday life, but they can be also viewed as indicators of human relations on many different levels: social, economic and political. The identification of the vessels' function is, therefore, an important source of information in the study of the practices related to eating and drinking, as well as in the investigation of the relationship between food habits, status, power and identity in the context of ancient societies (Goody 1982; Dietler 1996; Dietler and Hayden 2001; Bray 2003).

Recent developments in chemical analysis of visible and absorbed organic residues in archaeological ceramics have opened up new perspectives in the study of pottery use (Pollard and Heron 1996; Evershed et al. 1997, 2002). The chemical characterisation of the foodstuff cooked, consumed and stored in ancient vessels can be of crucial importance in determining the vessels' use, especially when the results are combined with contextual data: archaeozoological and palaeobotanical remains, shape and size of vessels, use-alteration analysis, and pottery distribution.

In the present paper, we report the results of a study on food habits during the Archaic Age in the Messapian settlement of San Vito dei Normanni (south-eastern Italy), integrating chemical analysis of organic residues by Gas Chromatography–Mass

F. Notarstefano (✉) and G. Semeraro,
Dipartimento di Beni Culturali, Università del Salento, via D. Birago 64, 73100 Lecce, Italy
e-mail: florinda.notarstefano@ateneo.unile.it

M. Lettieri
Istituto per i Beni Archeologici e Monumentali (CNR-IBAM), Complesso Ecotekne, Via
Monteroni, 73100 Lecce, Italy

L. Troisi
Dipartimento di Scienze e Tecnologie Biologiche ed Ambientali (Di.S.Te.B.A.), Laboratorio di
Chimica Organica, Università del Salento, Complesso Ecotekne, Via Monteroni, 73100 Lecce,
Italy

Spectrometry (GC–MS) and Fourier Transform Infrared Spectroscopy (FTIR) with the enquiries aimed at determining the actual use of pottery vessels from archaeological contexts. In the framework of a contextual approach, the traditional examination of the pottery was supported by a series of analytical techniques: analyses of technological, morphological and stylistic characteristics, use-alteration and residue analyses.

The indigenous settlement of San Vito dei Normanni is located on the top of a natural low hill, 20 km west of Brindisi. The excavations carried out at the site have distinguished two main phases of occupation, from the Iron Age until the end of the Archaic period, when the site was suddenly abandoned.

We discuss here the results related to the study of the use of pottery belonging to the Archaic phase of the settlement (sixth century BC), when a great habitation area, surrounded by two fencing walls, was built on the top of the hill. The east side is currently occupied by the foundations of a great building (700 m²) with rectangular rooms; the base of a stone altar – whose function seems to be strictly related to the great building – was discovered in the courtyard. Architectural features are different from those of the houses on the west side of the hill, suggesting that the building probably had a major role in the settlement (Semeraro 2003).

The excavation of structures from the Archaic phase brought to light a significant number of Greek imported ceramics, associated mainly with wine consumption: transport amphorae, Ionic cups, Corinthian and Attic vessels, among which some fragments of big black figured craters. All of these data, together with the presence of many imported cooking pots, probably indicate the introduction of new forms of food preparation and changes in food habits among the native populations of Archaic Age Messapia (Semeraro in press).

2 Chemical Analysis of Organic Residues

2.1 *Sample Selection and Analytical Techniques*

Thirty-one vessels were sampled for the analysis of organic residues. Twenty-seven samples belong to the category of cooking wares (pots and pans), displaying burn traces on the exterior surfaces. Most of the pots are imported, while the pans are locally produced. No visible residues adhering on the interior surfaces were observed on these vessels. The other samples were taken from four transport amphorae, characterised by the presence of a dark residue adhering to the interior surface of the ceramic potsherds. The amphorae belong to types A and B of Corinthian production, widely attested in the Mediterranean during the Archaic Age, and probably used for oil and wine transport (Koehler 1979).

GC–MS was applied to the samples of cooking vessels with no visible residues on the interior surfaces. Charred surface residues on the four sherds of transport amphorae were analysed both by GC–MS and FTIR.

2.2 Gas Chromatography/Mass Spectrometry

Samples of approximately 2 g of potsherd were surface cleaned with a sterile scalpel and crushed in a mortar and pestle. The powdered potsherds were solvent extracted and derivatised using established protocols (Charters et al. 1993; Dudd and Evershed 1999). Samples were analysed using an Agilent Technologies 6850 II series gas chromatograph (5% phenyl-polymethylsiloxane capillary column, 30 m, internal diameter 0.25 mm, 0.25 μm film thickness), with a split/splitless injection system used in the splitless mode and maintained at 300°C, coupled to an Agilent 5973 Network mass spectrometer operated in the EI mode (70 eV). The mass spectrometer was set to scan in the range of m/z 50–600 in a total cycle time of 1 s. The GC oven temperature was programmed from 100 to 280°C at 10°C/min, and maintained at 280°C for 15 min. Helium was used as the carrier gas at a constant flow rate of 1 ml/min.

Compounds were identified partially by their retention time within the GC, based on comparisons with analysed reference compounds, but mainly by their mass spectra. Mass spectral data were manually interpreted with the aid of the NIST Mass Spectral Library and comparison with spectra reported in literature.

2.3 Fourier Transform Infrared Spectroscopy

The FTIR spectroscopic analyses were performed using a ThermoNicolet Continuum IR microscope; the spectra were collected in μ -ATR (Attenuated Total Reflectance) mode in the range 4,000–650 cm^{-1} , with a resolution of 8 cm^{-1} and 300 scans for each measurement; a Si crystal was employed. The analyses were performed on areas, selected by means of the attached optical device, where encrusted residues were observed; only the inner side of the potsherd was taken into account. The analyses were repeated, on the same area, after the abrasion of a superficial thin layer of the deposits.

3 Results and Discussion

The higher concentration of stearic acid ($\text{C}_{18:0}$) as compared to that of palmitic ($\text{C}_{16:0}$) acid, together with the presence of cholesterol, detected by GC-MS in most of the cooking pots, show that they contained animal derived products (Fig. 1a). The presence of odd numbered, branched chain acids, as well as positional isomers of octadecenoic acid, is a good indicator of ruminant animal fats (Craig et al. 2005; Kimpe et al. 2002). Few samples of pots and pans show a relative high abundance of unsaturated fatty acids ($\text{C}_{18:1}$; $\text{C}_{18:2}$), together with the presence of β -sitosterol, indicating that products of vegetable origin were also processed in these vessels

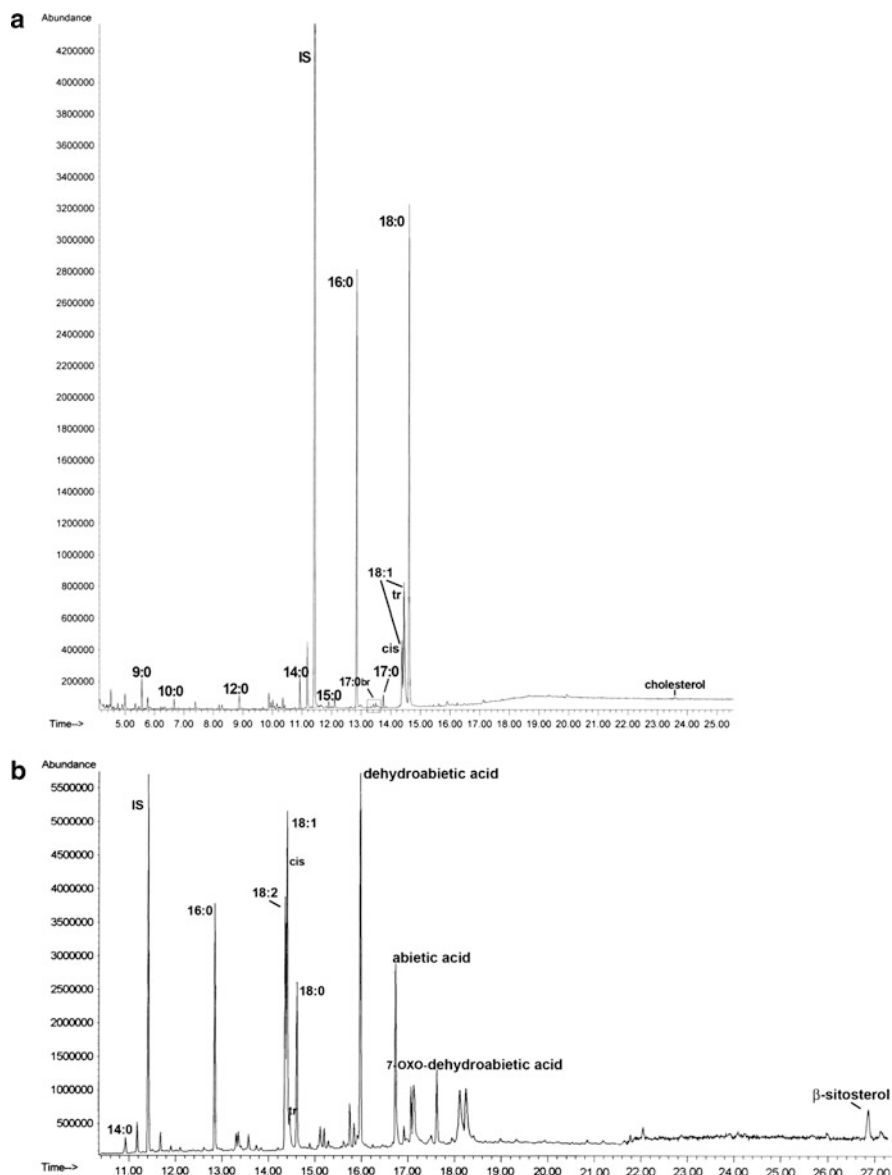


Fig. 1 GC-MS chromatograms of the lipid extracts of two samples (**a** and **b**) of cooking pots. *IS* Internal Standard (*n*-nonadecane)

(Fig. 1b). In some cases, the simultaneous presence of animal fats was detected, suggesting that meat and vegetable products have been prepared in the same pot.

In the lipid extracts from eleven samples of pots and pans, considerable amounts of diterpenoids (dehydroabiatic and 7-oxo-dehydroabiatic acids) characteristic of

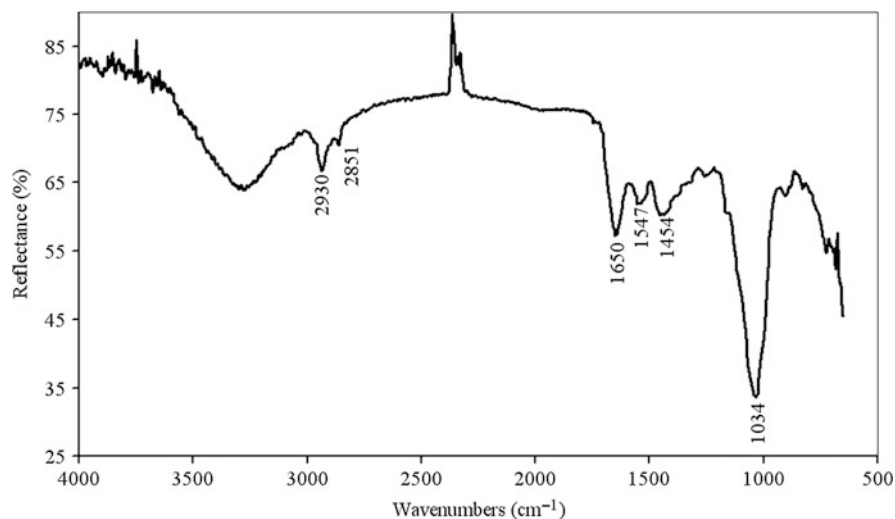


Fig. 2 FTIR spectrum of one sample of Corinthian B type amphora

pine resin (Colombini et al. 2005) were identified (Fig. 1b). The same diterpenoid compounds were detected in the dark deposits of two Corinthian B type transport amphorae, while two samples of type A contained high amounts of unsaturated fatty acids, indicating a vegetable origin of the residue, probably oil.

The μ -ATR-FTIR analysis carried out on one sample of Corinthian B type amphora revealed the presence of a covering mainly consisting of calcium carbonate (peaks at 1,410 and 872 cm^{-1}). Very weak signals at 2,932 and 1,650 cm^{-1} , that can be attributed to organic material, and a band (around 1,034 cm^{-1}), due to the Si–O stretching band, were also detected. On the other hand, the analysis performed after the removal of the superficial layer of the residue revealed the presence of proteinaceous material; the peaks at 1,650 and 1,547 cm^{-1} , along with the band at 1,454 cm^{-1} (Fig. 2), form a stair-step pattern undoubtedly related to the presence of proteins (Derrick et al. 1999). Furthermore, the signals at 2,935 and 2,851 cm^{-1} can be attributed to vegetable resins.

4 Conclusions

The GC–MS and FTIR analyses carried out on pottery vessels from the Messapian settlement of San Vito dei Normanni show that most of the imported cooking pots were used to boil meat, probably of ruminant animals. These data can be related to ritual meals and feasting activities based on animal sacrifice, as confirmed also by the significant amounts of faunal remains found in the courtyard of the great building and by the distribution of consuming and serving vessels in the rooms. Furthermore, the FTIR spectrum of one transport amphora revealed the presence of

proteins, indicating a possible re-use of the vessel as a container for meal leftovers. In contrast, most of the locally produced pans were used to boil vegetables, maybe legumes or cereals, as suggested by the botanical remains.

Some markers of pine resins were found in several pots and pans. These results could suggest that resin coatings were applied on cooking wares, probably with the aim of reducing water permeation when boiling foods. Ethnographic research shows in fact that a resin coating is the best surface treatment in terms of the performance characteristics of cooking pots, but it is rarely observed in archaeological ceramics because of biodegradation (Skibo 1997).

Two samples of Corinthian A type amphorae contained a vegetable oil, while the presence of pine resins in two B type samples could indicate that they originally transported wine. Pine resin is known in fact to have been used in the past as a coating on amphorae and for purposes of wine conservation, due to its antibacterial properties.

In conclusion, the contextual study of pottery use and chemical analysis of organic remains can contribute to understanding the food habits of past human societies, their relation to the use of space, and the “social dimension” in which ceramics were used. The quality and composition of both the foodstuffs and the pottery assemblage seem to confirm the hypothesis that the great building in San Vito dei Normanni was a palace with different functions – not only residential, but also political and ritual – where local elites used to articulate and reinforce their power using fine pottery in contexts of ritual or ritualised consumption.

References

- Bray TL (ed) (2003) *The archaeology and politics of food and feasting in early states and empires*. Kluwer Academic/Plenum, New York
- Charters S, Evershed RP, Goad LJ, Blinkhorn PW, Denham V (1993) Quantification and distribution of lipid in archaeological ceramics: implications for sampling potsherds for organic residue analysis. *Archaeometry* 35:211–223
- Colombini MP, Modugno F, Ribechini E (2005) Direct exposure electron ionization mass spectrometry and gas chromatography/mass spectrometry techniques to study organic coatings on archaeological amphorae. *J Mass Spectrom* 40:675–687
- Craig OE, Taylor G, Mulville J, Collins MJ, Parker PM (2005) The identification of prehistoric dairying activities in the Western Isles of Scotland: an integrated biomolecular approach. *J Archaeol Sci* 32:91–103
- Derrick MR, Stulik DC, Landry JM (1999) *Infrared spectroscopy in conservation science*. The Getty Conservation Institute, Los Angeles
- Dietler M (1996) Feasts and commensal politics in the political economy: food, power and status in prehistoric Europe. In: Wiessner P, Schiefenhövel W (eds) *Food and the status quest, an interdisciplinary perspective*. Berghahn, Providence, Oxford, pp 87–125
- Dietler M, Hayden B (eds) (2001) *Feasts. Archaeological and ethnographic perspectives on food, politics and power*. Smithsonian Institution Press, Washington, DC
- Dudd SN, Evershed RP (1999) Evidence for varying patterns of exploitation of animal products in different prehistoric pottery traditions based on lipids preserved in surface and absorbed residues. *J Archaeol Sci* 26:1473–1482

- Evershed RP, Mottram HR, Dudd SN, Charters S, Stott AW, Lawrence GJ (1997) New criteria for the identification of animal fats preserved in archaeological pottery. *Naturwissenschaften* 84:402–406
- Evershed RP, Dudd SN, Copely M, Berstan R, Scott A, Mottram H, Bulley S, Crossman Z (2002) Chemistry of archaeological animal fats. *Accounts Chem Res* 35(8):660–668
- Goody J (1982) *Cooking, cuisine and class: a study in comparative sociology*. Cambridge University Press, Cambridge
- Kimpe K, Jacobs PA, Waelkens MJ (2002) Mass spectrometric methods prove the use of beeswax and ruminant fat in late Roman cooking pots. *J Chromatography A* 968:151–160
- Koehler CG (1979) *Corinthian A and B transport Amphoras*. University of Michigan Press, Ann Arbor
- Pollard AM, Heron C (1996) *Archaeological chemistry*. The Royal Society of Chemistry, RSC Paperbacks, Cambridge, UK
- Semeraro G (2003) San Vito dei Normanni (Brindisi). In: Guaitoli M (ed) *Lo sguardo di Icaro*. Roma, Campisano, pp 320–322
- Semeraro G (in press) Forme e funzioni dei vasi attici in contesti culturali di età arcaica: nuovi dati dall'insediamento messapico del Castello di Alceste (S. Vito dei Normanni-BR), In *Ceramica attica da santuari della Grecia, della Ionia e dell'Italia*, Atti del Convegno Internazionale (Perugia, 14–17 marzo 2007)
- Skibo JM (1997) Ceramic surface treatment and abrasion resistance: an experimental study. *J Archaeol Sci* 24:311–317

Finding Food While Protecting Pots: A Non-Destructive Protocol for Absorbed Residue Analysis

J.M. Vanderveen

1 Introduction

The technique of absorbed residue analysis is used to extract and identify food compounds from pottery sherds in order to reconstruct diets of people in the past (Evershed et al. 1999; Malainey et al. 1999). Organic materials, like cholesterol and other fatty acids, interact with the porous walls of unglazed ceramics over the use-life of vessels. Consequently they do not readily leach out of the vessels during burial, nor are they destroyed by mild washing and long-term storage in plastic bags (Heron et al. 1991). The analytical procedure, however, involves irrevocably damaging the artifact by crushing a sample into a fine powder.

There are instances, however, in which extremely rare samples or small collections of irreplaceable pottery could provide significant detail regarding changes in cultural patterns of subsistence. A few researchers have attempted to resolve this dilemma, often by scraping ceramic material from inside a vessel with a scalpel or drill (e.g., Coyston 2002). But since the outermost surfaces should ideally be discarded to protect against contaminants, the remaining amount of powder becomes too small to extract meaningful information. In any case, the vessel is still damaged. Other studies have been able to extract residue with little damage, but the methods have been labor intensive, costly, and still subject to modern contamination (Gerhardt et al. 1990).

2 Materials

During the course of a larger project researching the selection and utilization of food resources in the Greater Antilles at the time of contact between Taíno people and European explorers, the idea of an improved non-destructive method of residue

J.M. Vanderveen

Department of Sociology and Anthropology, 1700 Mishawaka Avenue, South Bend, IN 46634-7111, USA

e-mail: jmvander@iusb.edu

extraction was investigated (VanderVeen 2006). Selected for the study were fragments of indigenous vessels collected from sites on the north coast of the Dominican Republic. The sherds, from unglazed and relatively low-fired domestic pots dating to ca. AD 1200–1500, were large enough to be broken into control and experimental samples approximately 15 g in weight. Three sets of these pairs (with the identifiers LEO 01/02, LEO 03/04, and TAM 25a/25b) were created. The sherds were already slated to be destroyed during the process of the larger research program. It was decided that a few of the ceramic fragments, those large enough to provide both a control and experimental sample, would be ideal candidates for the testing of a revised method. Since the sherds were from an archaeological context, any recovered residue would be associated with patterns of prehistoric use and signify that the method of extraction was replicable in other such vessels. The alternative of using experimental sherds impregnated with modern organic matter would not account for the problem of residue deterioration and the changes that affect molecular chains of fatty acids over time. If this pilot study proved successful in recovering absorbed residue from within the fabric of centuries-old pottery without the need for pulverization, the method could then be employed on rarer samples and even intact vessels. The only limiting factor would be the size of the equipment used in the laboratory.

3 Revised Methodology

The control sample of each pair was processed using traditional methods for extraction (e.g., Charters et al. 1995). The technique includes removing the surface layer with a drill, grinding the sherds into a fine powder with a mortar and pestle, combining the powder with a methylene chloride/methanol solution (2:1 v/v) in a glass centrifuge tube, and agitating the tubes in an ultrasonic bath.

The experimental sherd was instead dipped into the solvent for 3 s to remove any surface contaminants. Then a large beaker containing the entire sherd was placed in the ultrasonic bath. Enough solvent was poured into the beaker to cover the sherd. The beaker was draped with baked aluminum foil to prevent splashing, and the whole assembly was ultrasonicated for the same duration as the control samples.

All further processing was the same for the control and experimental samples. The solvent, now infused with residue, was decanted, filtered, collected, and then evaporated off, leaving behind the material of interest (total lipid extract). The samples were weighed, derivatized, and then injected into a gas chromatograph or gas chromatograph – mass spectrometer (GC–MS) for analysis. The specific analytical program used in this study started with one microliter sample injected with an auto-injector into a 30 m long × 0.32 mm wide inner diameter fused-silica capillary column from J&W Scientific, coated with a 0.25 mm film of (5%-Phenyl)-methylpolysiloxane. Helium was used as a carrier gas, with a flow rate of 7 ml/min. The temperature program was set to begin at 60°C

and remain at that temperature for 1 min, then ramping 4°C/min to 320°C, with a 90 min hold isothermal hold at this temperature. A complete program lasted 156 min, significantly longer than any other run time listed in the chemical archaeology literature. This program is more similar to that used by geologists, and it resulted in compounds sometimes eluting more than 2 h into the run.

4 Results

The output of compounds eluting at different times from each sample was compared to a broad library of peak signatures from fatty acids and other substances identified during this research. The types of organic material recovered from the experimental and control samples were similar in kind and amount. The non-destructive protocol actually resulted in a larger amount of total lipid extract per gram of sherd than the standard protocol in two of the three artifact pairs (see Table 1). A Student's *t*-test was used to evaluate the concentration levels of all target lipids measured in the pair of samples analyzed by GC-MS (TAM 25a/25b). The test yielded a significance level 0.55, meaning there was no statistically significant difference in their composition.

Qualitative analysis of the chromatograms of the sample pairs confirms this result (see Fig. 1). Although there is some dissimilarity between the abundance levels of the compounds, nearly all of the target lipids are present in each of the samples. In the pair analyzed by GC-MS, only three fatty acids and three alcohols varied in their presence by more than 5%. The remaining compounds in those classes showed approximately the same relative percentage of abundance. Significant levels of saturated fats, including long-chain saturated fats, were found in all samples, along with both mono- and polyunsaturated fats. Cholesterol was also present in two of the three pairs of samples (LEO 01/02 and TAM 25a/25b). Trace amounts of phthalate, a modern plasticizer, was also noted.

Each vessel was used to process different types of foods. The residues suggest Taíno cooks selected a variety of fish, greens, mammals, mollusks, and roots, most likely in a stew of many ingredients similar to the pepper pot dishes made by West Indians today.

Table 1 Descriptions of ceramic samples used in analysis

Sample	Protocol	TLE µg/Sherd g	Total peak area	Decoration style	Vessel form
LEO 01	Sonication	0.3617	1.33×10^7	Meillacan	Bowl body
LEO 02	Standard	0.1559	1.31×10^7		
LEO 03	Sonication	0.1143	1.31×10^7	Undecorated	Jar rim
LEO 04	Standard	0.0712	1.34×10^7		
TAM 25b	Sonication	0.2474	1.22×10^7	Undecorated	Bowl body
TAM 25a	Standard	0.2941	1.28×10^7		

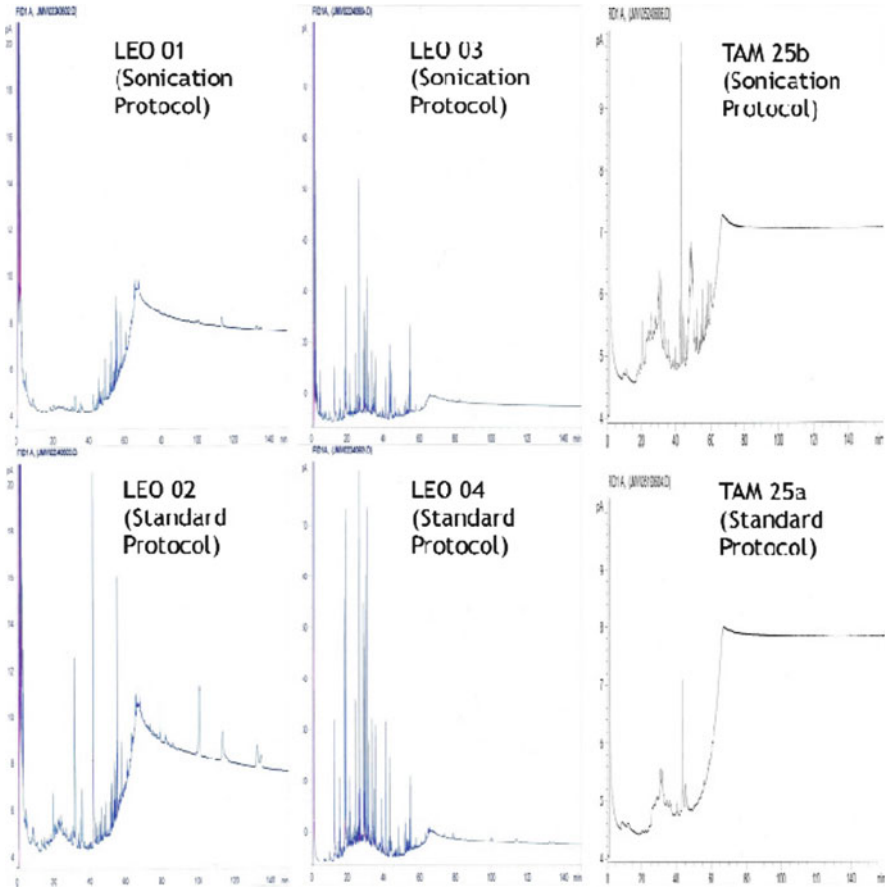


Fig. 1 Gas chromatograms of the samples investigated

5 Discussion

While the non-destructive sonication protocol has only been tested on a few samples, it shows promise as an alternative method for the absorbed residue analysis of uncommon or irreplaceable artifacts. Although the sherds in this study were broken for the purpose of creating a control, the technique may be easily applied to fragments and whole vessels without fear of injury. The only limiting factor is the size of the ultrasonication bath tank. It is unknown if the solvents cause any long-term damage to the integrity of the ceramic fabric, but they are commonly used chemicals that evaporate very quickly at low temperatures and are expected to cause little to no ill effect. Visual examination of the samples after one year's time gave no indication of any surface damage (see Fig. 2).



Fig. 2 Sherds before sonication protocol (*left* in each pair) and 1 year after

Still, any harm to the pottery can only be a fraction of that produced by drilling or deeply scraping its walls, to say nothing of the crushing that occurs in the traditional method of residue extraction. If further tests of this protocol continue to produce similar results, it is possible that exceptional artifacts, including museum-quality pieces, can be tested for organic compounds with little risk of damage.

The ability to analyze unique vessels and rare sherds broadens the scope of research into dietary reconstructions and also allows for comparable studies of organic compounds from non-food origins, such as ritual behaviors. This novel method is analogous to remote sensing of archaeological sites: it gathers useful information, and can direct further research, without destroying the source.

References

- Charters S, Evershed RP, Blinkhorn PW, Denham V (1995) Evidence for the mixing of fats and waxes in archaeological ceramics. *Archaeometry* 37:113–127
- Coyston S (2002) Noble chemists and archaeologists: chemical analyses of food residues from ancient Maya vessels. PhD dissertation, Department of Anthropology, McMaster University
- Evershed RP, Dudd SN, Charters S, Mottram H, Stott AW, Raven A, Van Bergen PF, Bland HA (1999) Lipids as carriers of anthropogenic signals from prehistory. *Phil Trans: Biol Sci* 354:19–31
- Gerhardt KO, Searles S, Biers WR (1990) Corinthian figure vases: non-destructive extraction and gas chromatography-mass spectrometry. *MASCA Research Papers in Science and Archaeology* 7:41–50
- Heron C, Evershed RP, Goad LJ (1991) Effects of migration of soil lipids on organic residues associated with buried potsherds. *J Archaeol Sci* 18:641–659
- Malainey ME, Przybylski R, Sherriff BL (1999) Identifying the former contents of late precontact period pottery vessels from Western Canada using gas chromatography. *J Archaeol Sci* 26:425–438
- VanderVeen JM (2006) Subsistence patterns as markers of cultural exchange: European and Taíno interactions in the Dominican Republic, PhD dissertation, Department of Anthropology, Indiana University

Part VI
Archaeochronometry

ESR and U/Th Dating Methodologies Applied to Carbonates from Southern Italy

J.J. Bahain, G. Burrafato, C. Falguères, A.M. Gueli, G. Stella, S.O. Troja,
and A.R. Zuccarello

1 Introduction

Since the dating of a stalactite from the Akiyoshi cave in Japan by Ikeya (1975), significant progress has been made in the utilisation of electron spin resonance spectroscopy (ESR) for the assessment of past radiation doses in the context of archaeological and geological dating (Rink 1997). The method is applicable to various materials such as speleothems, spring deposited travertines, mollusc shells and corals (Grün 1989). Discoveries of human remains in Western Europe have been proposed to indicate the sites of the earliest arrival of humans there, and have been dated to the Early Pleistocene by ESR using quartz and tooth enamel (Falguères 2003). The researches based on the dating of quartz allow the age assessment of heated ceramics, volcanic rocks, intrafault material, or windblown sediments (Grün 1989). The method is also used on archaeological artefacts made of obsidian, which are precious for archaeologists, allowing them to obtain information about cultural, social and economic relations between prehistoric populations (Duttine et al. 2003).

The present work is focused on speleothems, secondary carbonates precipitated in caves, because these deposits are often connected with archaeological sites (DeLumley and Labeyrie 1981) and their dating is important for supporting paleoclimatic studies based on the stalagmite growth rate and oxygen and carbon stable isotope variations with time (Schwarcz 1986). In particular, we carried out a campaign of dating on speleothems originating from Monello Cave, located in the Monti Climiti area, near Siracusa (Sicily, southern Italy), within the framework

J.J. Bahain and C. Falguères

Département de Préhistoire, Muséum National d'Histoire Naturelle, UMR 5198 du CNRS, 1 rue René Panhard, 75013 Paris, France

G. Burrafato, A.M. Gueli, G. Stella, S.O. Troja, and A.R. Zuccarello (✉)

LDL & BBCC, Laboratorio di Datazione tramite Luminescenza e di Metodologie Fisiche applicate ai Beni Culturali del Dipartimento di Fisica e Astronomia, Università di Catania and INFN Sezione di Catania, via Santa Sofia 64, 95123 Catania, Italy

e-mail: agnese.zuccarello@ct.infn.it

of a global project aimed at the chronological reconstruction of tectonic and climatic events in eastern Sicily, closely related to karst infilling. The Monello Cave was discovered in 1948 and declared a wildlife reserve in 1998. Since then, its management has been taken over by the *Centro Universitario per la Tutela e la Gestione degli Ambienti Naturali e degli Agroecosistemi* (CUTGAN) of the University of Catania. With a total length of approximately 540 m, this cave is a splendid example of a karst structure, with a series of rooms full of stalactites and stalagmites of various shapes and dimensions. It has a rather linear structure, with its principle axis located along an ENE-WSW fault line, and lateral branches along a system of NNW-SSE faults (Fig. 1a). The survey of the paleomorphology and of

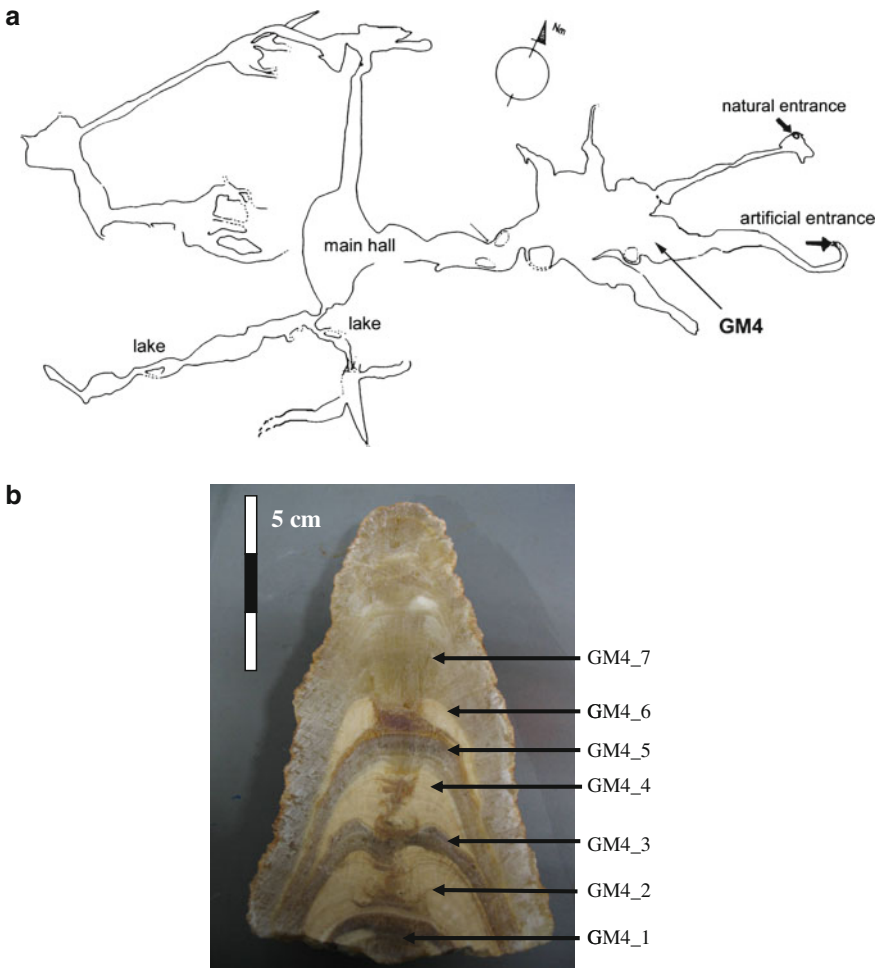


Fig. 1 Monello Cave (Siracusa, southern Italy): (a) plan with localization of the sampling site of the stalagmite designated GM4 (adapted from Caruso 1994) and (b) section of stalagmite GM4

the karstic deposits has allowed the subdivision of the cave, from a speleogenetic point of view, into three sectors, found at different depths, which, according to Ruggieri and Zocco (2000), were related to regression stages and tectonic phases during the Middle Pleistocene. The cave, in fact, underwent tectonic and climatic changes that generally affected this sector during the Pleistocene, with various transgressive-regressive cycles and intense karstification in the carbonate substrate during the formation of the Monti Climiti (Ruggieri and Zocco 2000).

The present preliminary study, currently undergoing further development, was aimed at investigating the correlation between the karst paleomorphology and the eustatic Pleistocene events by means of carbonate speleothem dating. From a methodological point of view, the results also represent a fundamental starting point for all ESR applications on carbonates extracted from samples and sites of archaeometric interest.

2 Materials and Methods

In this study, we present the experimental analysis and the results obtained from one of the stalagmites collected from the Monello Cave, designated GM4, by means of electron spin resonance (ESR) and U/Th dating methods (for details about these methods, see Grün 1989; Ivanovich and Harmon 1992). The stalagmite GM4 (see localization in Fig. 1a) has an overall height of approximately 40 cm. It was sectioned in two symmetrical parts along a vertical plane passing through the central growth axis. From one of these two parts, we extracted seven samples, designated GM4_1 to GM4_7, from the oldest to the youngest one, respectively (Fig. 1b).

The chemical and physical preparation was initiated by grinding up each sample in an agate mortar in order to select grains in the range of 100–200 μm . The selected grains were etched by 0.5% acetic acid for a few minutes in order to remove the grinding-induced ESR signal at $g = 2.0001$. The action of the acid was then interrupted by adding ethanol that also favoured the evaporation of any liquid present. The samples thus prepared underwent ESR measurements. The ESR age was determined by the following equation (Ikeya 1993):

$$\text{Age}(a) = \frac{\text{Equivalent Dose}(\text{Gy})}{\text{Annual Dose}(\text{Gy}/a)} \quad (1)$$

in which the equivalent dose (D_E) is the total amount of radiation damage accumulated by the sample from its formation or from its last “zeroing” event, while the annual dose (d) is the rate at which this dose was absorbed. The irradiation results from the disintegration of the radionuclides (U, Th and K) contained in the material to be dated and in the surrounding environment. A further contribution comes from cosmic rays.

In order to obtain D_E values, the additive dose method was used (Ikeya 1993). In this study, each sample was divided into 11 aliquots, of approximately 100 mg

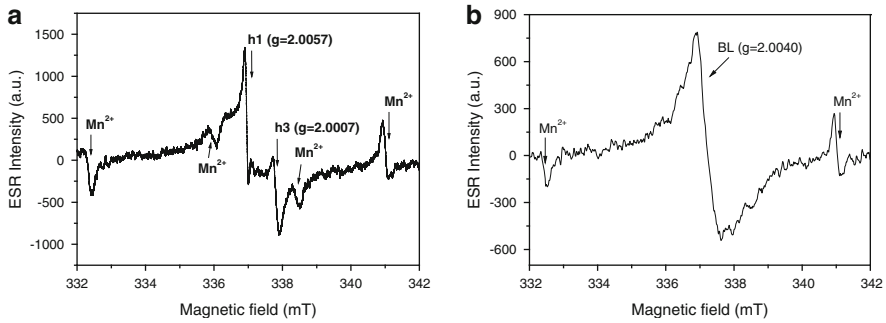


Fig. 2 ESR signals of sample GM4_7. (a) Measurement conditions: P = 10 mW, modulation width = 0.06 mT, amplitude = 1,600, time constant = 0.1 s, sweep time = 1 min. (b) Measurement conditions: P = 0.05 mW, modulation width = 0.2 mT, amplitude = 1,400, time constant = 0.1 s, sweep time = 1 min

each. Ten of these were irradiated by a ⁶⁰Co calibrated source at the *Ente per le Nuove tecnologie, l'Energia e l'Ambiente* (Casaccia, Rome). The irradiation doses were 0, 20, 63, 125, 200, 400, 630, 800, 1000, 1250 and 1500 Gy. ESR measurements were carried out at the *Dipartimento di Fisica e Astronomia* of the University of Catania, using an X band Jeol ESR spectrometer (Series JES FA-100). Acquisition parameters at room temperature are indicated in the Fig. 2 caption.

ESR intensities were normalised by the aliquots' weights. A single saturating exponential (SSE) function was fitted to the experimental data points in order to obtain the D_E value (Apers et al. 1981):

$$I(D) = I_S \left(1 - e^{-(D+D_E)/D_S} \right) \quad (2)$$

where $I(D)$ is the measured ESR signal intensity, D the laboratory added dose, I_S the ESR saturation level, and D_S the characteristic saturating dose. The D_E value was calculated from extrapolating the SSE function to the zero ordinate.

The annual dose rate is composed of two parts: the internal dose rate (d_{int}) and the external dose rate (d_{ext}). The α and β contributions to the internal dose rate were calculated from the concentrations of U, Th and K, determined by ICP-MS analysis (Table 1). The dose rate was then evaluated using the conversion factors of Adamiec and Aitken (1998) assuming secular equilibrium. For the external γ contribution, GR-200A TL dosimeters were used. The internal γ component was calculated by simulations using the Montecarlo MCNP code, taking into consideration the dimensions and the shape of the stalagmite, as well as the concentration values of the natural radioactive elements in the speleothem under investigation.

In order to get an independent age control for the ESR results, we applied the U/Th dating method on one of the extracted samples. With this method, the age is obtained by measuring the concentration of ²³⁰Th formed from the disintegration of ²³⁴U (Ivanovich and Harmon 1992). To this purpose, in parallel with the ESR

Table 1 ESR dating results obtained from the stalagmite GM4

Sample	U (ppm)	Th (ppm)	K (%)	D_E (Gy)	d_{int} (Gy/ka)	d_{ext} (Gy/ka)	d (Gy/ka)	ESR Age (ka)
GM4_1	0.26 ± 0.01	^a	0.03 ± 0.01	88.96 ± 7.10	0.11 ± 0.02	0.24 ± 0.03	0.35 ± 0.03	252 ± 31
GM4_2	0.25 ± 0.01	^a	0.02 ± 0.01	83.23 ± 2.78	0.10 ± 0.03		0.34 ± 0.04	250 ± 31
GM4_3	0.18 ± 0.01	0.11 ± 0.05	0.07 ± 0.01	83.86 ± 3.34	0.12 ± 0.04		0.36 ± 0.05	233 ± 33
GM4_4	0.17 ± 0.01	^a	^a	66.68 ± 2.88	0.05 ± 0.01		0.29 ± 0.03	229 ± 23
GM4_5	0.13 ± 0.01	^a	^a	89.16 ± 7.44	0.04 ± 0.01		0.28 ± 0.03	320 ± 40
GM4_6	0.17 ± 0.01	^a	0.02 ± 0.01	65.62 ± 2.86	0.07 ± 0.02		0.31 ± 0.03	211 ± 24
GM4_7	0.18 ± 0.01	0.12 ± 0.05	0.07 ± 0.01	75.04 ± 6.34	0.12 ± 0.04		0.36 ± 0.05	211 ± 33

^aConcentrations below the minimum detection level

studies, sample GM4_7 was analysed by classical alpha spectrometry (surface barrier detector) at the *Département de Préhistoire du Muséum National d'Histoire Naturelle* (Paris, France). These analyses were preceded by a chemical-physical preparation of the samples, similar to the one described in Bischoff et al. (1988), in order to obtain thin films.

3 Results and Discussion

The experimental measurements carried out on whole samples show the presence of typical composite ESR signals of carbonates. With 10 mW microwave power (Fig. 2a), it was possible to identify the isotropic *h1* signal (Yokoyama et al. 1981, 1985), centred at $g = 2.0057$, probably linked to the presence of SO_2^- radicals (Barabas 1992), and the isotropic *h3* signal at $g = 2.0007$ (Yokoyama et al. 1981, 1985), associated to CO_2^- radicals (Barabas et al. 1992). Overlapping these two signals there is the widest peak (Fig. 2b), detectable at 0.05 mW and centred at $g = 2.0040$, called *broad line* (*BL*), whose intensity increases with the dose (Fig. 3).

These signals were found between the third and fourth peaks of Mn^{2+} , whose characteristic hyperfine structure develops in the largest region of the magnetic field (Fig. 2b).

The *BL* signal was used for the D_E calculation and its intensity was extracted from peak-to-baseline measurements. The *h1* peak, in fact, is not sensitive to the radiations and the suggestion of using it for chronological purposes following heating (Yokoyama et al. 1981) is not accepted by the entire scientific community

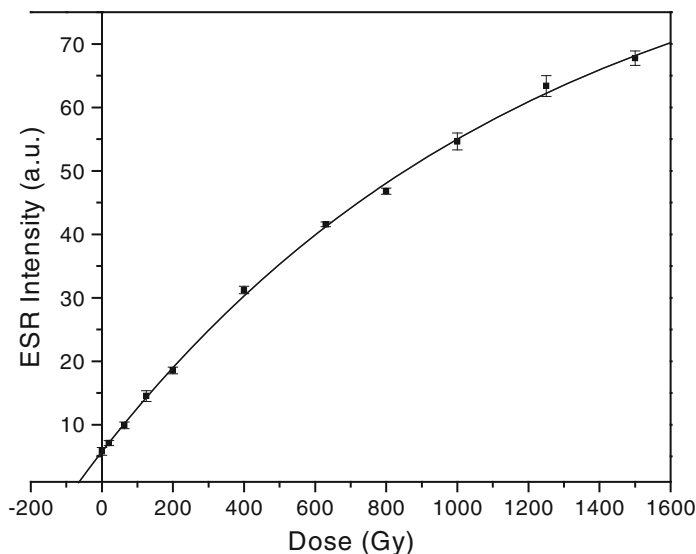


Fig. 3 Growth curve of the *BL* signal for sample GM4_7

Table 2 U/Th results obtained by α -spectrometry on sample GM4_7

Sample	U (ppm)	$^{234}\text{U}/^{238}\text{U}$	$^{230}\text{Th}/^{232}\text{Th}$	$^{230}\text{Th}/^{234}\text{U}$	U/Th Age (ka)
GM4_7	0.16 ± 0.01	1.00 ± 0.08	>100	0.801 ± 0.075	$176 + 73/-39$

working in this field, because it would lead to an overestimation of the age of the sample (Hennig and Grün 1983; Skinner 1983; Grün 1989). On the other hand, the measurement of the h^3 intensity is difficult, due to the overlapping of the grinding signal at $g = 2.0001$ in the samples that were laboratory irradiated.

Figure 3 shows the dose-response curve of the *BL* signal for the GM4_7 sample. The D_E value, obtained by fitting the exponential curve (2), is 75.04 ± 6.34 Gy. This procedure was repeated for each of the samples, and the results are shown in Table 1, together with the contents of U, Th and K, necessary for the calculation of the internal contribution of the annual dose, and thus of the age (see equation 1).

The TL measurement, carried out using dosimeters placed in various parts of the cave for the determination of the external gamma dose rate, provided results which are not significantly different. As a result, the weighted average value was considered (Table 1). The U-series results of sample GM4_7 are presented in Table 2.

4 Conclusions

The analysis provided satisfactory ESR dating results. It is, in fact, clear that the ages calculated for all samples are globally coherent considering the associated error, except for the GM4_5 sample. For this sample, the age seems overestimated, of about 100 ka, and this is probably due to the low uranium content in comparison with the other samples (Table 1).

On the other hand, the growth speed of the speleothem could not be assessed because of overlapping ESR ages. However, this is understandable if we consider the fact that the duration of the stalagmite's growth is relatively short compared to its age and the associated error. Even if it is necessary to verify the behaviour of the GM4_5 sample, we calculated the ESR average age of the stalagmite: 236 ± 11 ka. This is in agreement with the U/Th dating result of $176 + 73/-39$ ka, and places the time of the stalagmite's growth during the marine isotopic stage (MIS) 7. These values are fully compatible with the hypothesis of the geologists who attribute the principal evolutionary phases of the cave to the Middle Pleistocene (Ruggieri and Zocco 2000).

These preliminary results, that are part of a wider research project, allowed us to obtain important chronological data on the Monello Cave. The results obtained indicate good perspectives for this research, encouraging us to continue ESR dating together with U/Th analysis, in order to obtain a more precise and reliable dating of the cave and thus of the tectonic and climatic past events.

Acknowledgements The authors wish to thank CUTGAN, *Centro Universitario per la Tutela e la Gestione degli Ambienti Naturali e degli Agroecosistemi* of the University of Catania for the opportunity to carry out this study, and, in particular, Dr. Sandro Privitera for his assistance in all

the phases of the work. Special thanks are due to Ivana Faraci, undergraduate student at the department of Physics, University of Catania, and to Anta Saw for her assistance during U-series analyses.

References

- Apers DJ, Debuyst R, De Canniere P, Dejehet F, Lombard E (1981) A criticism of dating by electron paramagnetic resonance (ESR) of the stalagmitic floors of the Caune de l'Arago at Tautavel. *Proc. Absolute Dating Isotope Anal. Prehistory Meth. Limits*, 553–550
- Adamiec G, Aitken M (1998) Dose-rate conversion factors: update. *Ancient TL* 16:37–50
- Barabas M (1992) The nature of the paramagnetic centres at $g = 2.0057$ and $g = 2.0031$ in marine carbonates. *Nucl Tracks Radiat Meas* 20:453–464
- Barabas M, Bach A, Mudelsee M, Mangini A (1992) General properties of the paramagnetic centre at $g = 2.0006$ in carbonates. *Quat Sci Rev* 11:165–171
- Bischoff JL, Rosenbauer RJ, Tavoso A, de Lumley H (1988) A test of uranium-series dating of fossil tooth enamel: results from Tournal cave, France. *Appl Geochem* 3:135–141
- Caruso D (1994) La fauna della grotta Monello, *Atti e Memorie dell'Ente Fauna Siciliana*, II, pp 87–121
- DeLumley H, Labeyrie J (1981) Absolute dating and isotope analysis in prehistory – methods and limits. *Proceedings, Préhistoire*, 720
- Duttine M, Villeneuve G, Poupeau G, Rossi AM, Scorzelli RB (2003) Electron spin resonance of Fe^{3+} ion in obsidians from Mediterranean islands. Application to provenance studies. *J Non-Crystalline Solids* 323:193–199
- Falguères C (2003) ESR dating and the human evolution: contribution to the chronology of the earliest humans in Europe. *Quat Sci Rev* 22:1345–1351
- Grün R (1989) Electron spin resonance (ESR) dating. *Quat International* 1:65–109
- Hennig GJ, Grün R (1983) ESR dating in quaternary geology. *Quat Sci Rev* 2:157–238
- Ikeya M (1975) Dating a stalactite by electron paramagnetic resonance. *Nature* 255:48–50
- Ikeya M. (1993) *New applications of Electron Spin Resonance. Dating, dosimetry and microscopy*, World Scientific, Singapore
- Ivanovich M, Harmon RS (1992) *Uranium-series disequilibrium: applications to earth, marine and environmental sciences*, 2nd edn. Clarendon Press, Oxford
- Rink WJ (1997) Electron spin resonance (ESR) dating and ESR applications in Quaternary science and archaeometry. *Radiat Meas* 27:975–1025
- Ruggieri R, Zocco M (2000) Il carsismo dell'area Grotta Perciata – Chiusazza (Sicilia Sud-Orientale): morfostutture e speleogenesi, *Atti del I Seminario di Studi sul Carsismo negli Iblei e nell'Area sud Mediterranea*, 9–11 aprile 1999. *Ragusa* 8:169–185
- Schwarcz HP (1986) Geochronology and isotope geochemistry of speleothem. In: Fontes JC, Fritz S (eds) *Handbook of environmental geochemistry. The terrestrial environment*. Elsevier, Amsterdam, pp 271–303
- Skinner AR (1983) Overestimate of stalagmitic calcite ESR dates due to laboratory heating. *Nature* 304:152–154
- Yokoyama Y, Quaegebeur JP, Bibron R, Leger C, Nguyen HV, Poupeau G (1981) Electron spin resonance (ESR) dating of stalagmites of the Caune de l'Arago at Tautavel. In: DeLumley H, Labeyrie J (eds) *Absolute dating and isotope analysis in Prehistory – Methods and limits*, Préhistoire. CNRS, Paris, pp 532–537
- Yokoyama Y, Bibron R, Leger C, Quaegebeur JP (1985) ESR dating of palaeolithic calcite: fundamental studies. *Nuclear Tracks* 10:929–936

The *Mezza Spiaggia* Tower (Cagliari, Italy): The Dating of Structures by the Metrological–Chronological Analysis of Masonry and the Petro-Geochemical Stratigraphy of Building Materials

C. Giannattasio and S.M. Grillo

1 Introduction

This study is part of a more extensive research aimed at examining a number of important defence towers in and around Cagliari, Sardinia, Italy. These towers form part of Sardinia's historic coastal defence system, dating to a period between the early sixteenth and the late seventeenth century (Fois 1981; Montaldo 1992; Pillosu 1957; Russo 1992). These historically and architecturally distinctive towers were originally built for defence purposes; however, since the nineteenth century when they no longer performed this function, they have declined into disuse and abandonment.

This investigation intends to record and evaluate the traditional building techniques used for the construction of these sixteenth century masonry structures. Specifically, the three principal objectives of this study are:

1. The recording through visual observation of any particular building techniques that differentiate these structures from other constructions of this period
2. A description of the construction systems employed and a report on the degree of deterioration observed, in order to enable appropriate measures for the conservation of these historic structures in the future
3. To facilitate the dating of other contemporary edifices, especially the dating of vernacular architecture (“minor” buildings)

C. Giannattasio

Department of Architecture, University of Cagliari, Via Corte d'Appello, 87 - 09124 Cagliari, Italy
e-mail: cgiannatt@unica.it

S.M. Grillo (✉)

Department of Geo-engineering and Environmental Technologies Piazza d'Armi, University of Cagliari, 16 - 09123 Cagliari, Italy
e-mail: grillo@unica.it

2 The Methods Applied

This analysis has been carried out using the following methods:

1. Observation techniques usually applied in architectural and historical analysis
2. Evaluation of the effects of meteorological phenomena on weathering behaviour
3. Typological analysis of masonry, illustrating their structural systems and construction techniques
4. Physical and chemical laboratory-based analysis of building materials

Initial data were collected by physical measurement and photographic surveys, and recorded utilising drawing techniques that emphasize the peculiarities of these constructions and the chronological periods associated with the masonry structures analysed. This method has already been applied in several case studies. It was specifically used in the past by archaeologists studying different medieval constructions (see Brogiolo 1988; Ferrando et al. 1989; Francovich and Parenti 1988; Mannoni 1984; Mannoni and Milanese 1988). The metrological classification of elements included the specific study of stone measurement, manufacturing of the base material, basic components of mortar and of the type of finish given to masonry surfaces. The masonry samples investigated in the context of this project have also been studied by mineralogical-petrographic methods (OM, X-Ray Diffraction, EPMA), by the analysis of the components of thin film elements, and by the analysis of the components of plasters and mortars, in order to characterise the main components and their provenance.

The investigations carried out to date demonstrate that, during the sixteenth century, it was common practice for masonry work to be carried out according to the so-called “*cantiere*” technique, found throughout Sardinia. Typical of the “*cantiere*” technique was the preparation of two or three courses of rubble masonry walling, rough-hewn in the external edges and support faces. The façade resulted in an irregular coarse opus, with horizontal joints generally distanced between 30 and 60 cm. These joints were pointed with weak mortar, sometimes showing the presence of slaked lime. Very often, the regularity of the rubble wall was interrupted by haphazard rough stone groupings. The fact that these characteristics and typology were dictated to the builders by economic circumstances meant in practice that the stones available for the construction of the rubble wall were of all shapes and sizes. By accurately dressing external angles and using horizontal elements, a significant degree of structural stability was achieved without using uniformly shaped stones, in areas where transportation was difficult and where appropriate raw material and suitable quarries were not available.

3 Case Study: *Mezza Spiaggia* Tower

3.1 *The Site*

Cagliari’s *Mezza Spiaggia* tower is situated along the city’s *Poetto* beach (Rassu 2000, 2005). The geological formations of Oligocene-Miocene-Holocene sequences occurring in the Cagliari area consist of a calcareous arenaceous argillitic

series (Barroccu et al. 1979). The more important lithotypes used for building and construction purposes are usually rocks of a calcareous nature from the Miocene. The stratigraphic sequence of that area comprises, from the bottom to the top (local names in brackets): (1) soft marly arenaceous limestone (*Pietra Cantone*); (2) a more or less marly calcarenite (*Tramezzario*); (3) a hard compact organogenic limestone (*Pietra Forte*).

The arenaceous and argillitic sediments of the same series were used to produce mortar, bricks and low quality pottery. Traces of quarrying activities on the calcareous strata have been found, illustrating the use of this material in ancient times within close vicinity to the city of Cagliari. The immediate availability of these calcareous strata in the proximity of historic settlements allowed it to be used for various purposes, and also for the construction of the coastal towers near the city: the *Su Perdusemini*, *del Poetto*, *Serra Pauli* and *Mezza Spiaggia* towers.

3.2 The Building

The *Mezza Spiaggia* tower was constructed in 1578 and is part of Sardinia's historic coastal defence system. The tower is conic in shape, with a diameter at the base of 6.60 m and height of 8.60 m. It was unfortunately not possible to enter the building since the entrance has been walled up. Two different kinds of masonry construction periods can be observed, one dating back to the original building, and the other to a later period when the tower was partially reconstructed.

3.3 The Technique

The masonry construction shows a carefully designed rubble surface, with irregular use of ashlar blocks of similar size intermixed with various other materials. The façade has two or three courses that constitute a course band, “*cantieri*”, of 62 cm in height. The masonry has also been built with diverse stone sizes, hewn and dressed in different ways, i.e. rubble pieces or regular ashlar blocks, in some points simply laid on top of each other. One may also frequently find the occasional use of discarded shards, usually thrown away while dressing the stone. These were used to fill the empty spaces, supporting the structural stability of the wall. The use of these small fragments dictated the size of the joints to be pointed, eliminating the need for large quantities of mortar and thick joints (Fig. 1)

This structure is composed of regular ashlar blocks and rubble stones, approximately 9–40 cm high and 8–45 cm long. The joints, both vertical and horizontal, vary from 1 to 2 cm in width. One may also find regular holes, distanced about 1.15–1.96 m horizontally and 2.10–2.45 m vertically, employed for the erection of the form work. For obvious reasons, they occur at the upper limit of the “*cantiere*”. Between two courses, one may find small stony materials, together with a double



Fig. 1 Detail of the masonry, which highlights the “*cantiere*” technique

mortar layer, illustrating the end of one strata of the masonry wall and the commencement of the next phase. Sometimes these double mortar layers include unslaked lime modules.

3.4 The Materials

The ashlar blocks used for the construction of the *Mezza Spiaggia* tower are mostly of the Miocene carbonatic type; primarily, these are *Pietra Forte*, named after *Pietra Cantone*, some *Arenaria di Pirri*, and very few granite stones (Fig. 2). *Pietra Forte* has good mechanical properties and very low porosity and permeability. In contrast, *Pietra Cantone* is very easily affected by weathering, due to its relatively high porosity and hygroscopy (Hermann et al. 1995).

The different effects of weathering can be easily observed on the exterior part of the tower. *Pietra Forte* shows very few decay morphologies, while both the *Pietra Cantone* and the old original white mortar exhibit severe damage due to weathering, especially on the façade exposed to the sea (Elsen et al. 2004). Furthermore, it is evident that replacement works were carried out mostly on the side of the tower exposed to the sea, recognizable by the presence of very regular shaped stones of *Pietra Forte* fixed by new grey mortar.

Studies on the two types of mortars, white and grey, by optical microscopy, X-ray diffraction and other chemical tests, focused on the investigation of the aggregates and the composition of the binder. Both types of mortars show similar aggregate composition, of quartz and feldspars, and smaller amounts

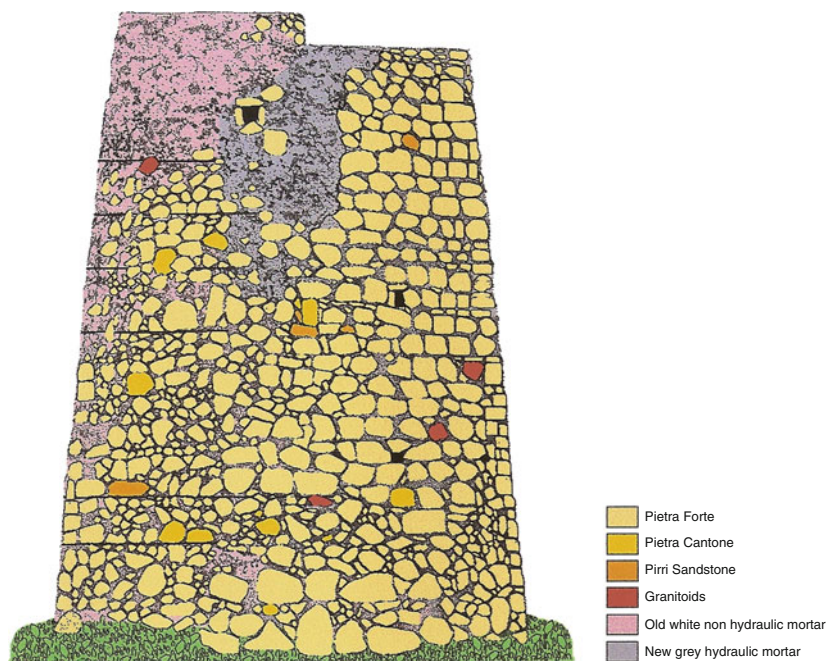


Fig. 2 Map of tower showing distribution of the different stones and mortars used for its completion (drawing by M. Porcu)

of mica. This composition, as well as the granulometric and morphometric characteristics of the aggregate grains, is similar to those of the marine beach sand of *Poetto*. The white mortar binder is ordinary calcitic aerial lime, while the new grey lime mortar is characterized by hydraulic properties.

4 Conclusions

This study, based on an interdisciplinary approach using data related to construction techniques together with a physical-chemical analysis of materials, aims to provide a chronological *datum* that can be applied to identify and date certain masonry structures, previously anonymous constructions, consisting mostly of vernacular architecture without formal architectural features. It allows us to re-evaluate our architectural heritage and to understand the wider sense of the word “monument”, which may thus also include traditional historic urban fabric. Moreover, the ultimate goal of this paper is to highlight the need for a restoration strategy that will ensure the preservation and management of such historically important structures.

References

- Barroccu G, Crespellani T, Loi A (1979) Caratteristiche geologico-tecniche dei terreni dell'area urbana di Cagliari. *Rivista Italiana di Geotecnica* XV(2):98–144
- Brogiolo GP (1988) *Archeologia dell'edilizia storica*. Como
- Elsen J, Brutsaert A, Deckers M, Brulet R (2004) Microscopical study of ancient mortars. *Mater Characterization* 53:289–295
- Ferrando I, Mannoni T, Pagella R (1989) Cronotipologia. *Archeologia Medievale* XVI:647–661
- Fois F (1981) Torri spagnole e forti piemontesi in Sardegna. Cagliari
- Francovich R, Parenti R (eds.) (1988) *Archeologia e restauro dei monumenti*. Firenze
- Hermann JJ, Herz N, Newman R (eds) (1995) *ASMOSIA 5: Interdisciplinary studies on ancient stone*
- Mannoni T (1984) Metodi di datazione dell'edilizia storica. *Archeologia Medievale* XI:396–403
- Mannoni T, Milanese M (1988) Mensiocronologia. In: Francovich R, Parenti R (eds) *Archeologia e restauro dei monumenti*. Firenze, pp 383–402
- Montaldo G (1992) *Le torri costiere della Sardegna*. Sassari
- Pillosu E (1957) *Le torri litoranee in Sardegna*. Cagliari
- Rassu M (2000) *Guida alle torri e forti costieri*. Cagliari
- Rassu M (2005) *Sentinelle del mare. Le torri della difesa costiera della Sardegna*. Cagliari
- Russo F (1992) *La difesa costiera del Regno di Sardegna dal XVI al XIX secolo*. Roma

Preliminary Results of Magnetic Archaeointensity Measurements in Brazil

G.A. Hartmann, M.C. Afonso, and R.I.F. Trindade

1 Introduction

Variations in intensity and direction of the Earth's magnetic field oscillate according to time scales ranging from seconds to millions of years. Variations in time period of 10^2 – 10^3 years are referred to as “archaeomagnetic variations” and may be used as a dating tool due to their stochastic behavior. Archaeomagnetic dating is based on the comparison of the magnetic record of archaeological material of unknown age with master-curves for the variation of the magnetic field in a given region of the planet (e.g. Le Goff et al. 2002). Hence, archaeomagnetic dating depends on the quality of a given master-curve. Accurate curves for the last 2,000 years have been developed for Europe and Western Asia. In contrast, significantly less data is available for continents in the southern hemisphere; South America contributes with less than 1% to the world geomagnetic intensity database (or “archaeointensity” database) (Genevey et al. 2008).

The possibility of providing magnetic archaeointensity data depends on the characteristics of archaeological materials. Directional and/or intensity data acquisitions are carried out in structures fired in situ, as kilns and hearths; intensities data acquisitions can be performed on displaced artefacts, as fragments of pottery, bricks and tiles. For this reason, intensity data are very common in comparison with directional data. The methodology for paleointensities measurements was developed by Thellier and Thellier (1959), with modifications proposed by Coe (1967) and Aitken et al. (1988). The natural remanent magnetization (NRM) of archaeological samples is compared with the one induced in the laboratory. These two magnetizations are acquired step by step, with progressively increasing

G.A. Hartmann (✉) and R.I.F. Trindade

Departamento de Geofísica, Instituto de Astronomia, Geofísica e Ciências Atmosféricas,
Universidade de São Paulo, São Paulo, Brazil
e-mail: gelvam@iag.usp.br; gelvam@gmail.com

M.C. Afonso

Museu de Arqueologia e Etnologia, Universidade de São Paulo, São Paulo, Brazil

temperature: the linear correlation between them allows the definition of the ancient intensity field.

In order to derive a South American archaeointensity master-curve, we have initiated a systematic paleointensity survey in well-dated (TL and/or ^{14}C methods) potsherds from south-eastern Brazil. We present here the first results on pottery collected in 21 archaeological sites with ages ranging from 1800 BP up to 100 BP, located in 11 cities of the São Paulo State (south-eastern Brazil). In general, the fragments are very distinct in morphological characteristics such as thickness, size and coloration of ceramic paste, this being probably due to original burning temperatures and production context.

2 Preliminary Results

2.1 *Magnetic Mineralogy and Thermal Stability*

On each potsherd, we carried out, in air, bulk susceptibility versus temperature measurements. Curves of low (-192 to 0°C) and high (20 – 700°C) temperatures were designed using KLY-4S Kappabridge (Agico Inc.). A good overall stability of the magnetic mineralogy was observed during the thermal treatment; this behavior is favourable for intensity experiments. Moreover, the susceptibility/temperature curves indicate that the main magnetic carrier in all pottery samples is low-Ti titanomagnetite to pure magnetite. However, for a complete discussion about magnetic characterization and domain state, the IRM (isothermal remanent magnetization) and hysteresis magnetic curves acquisitions are necessary.

2.2 *Archaeointensity Measurements*

The potsherds were analyzed using the Thellier and Thellier (1959) method, revised by Aitken et al. (1988), and monitored by pTRM's checks (partial Thermoremanent Magnetization checks). Samples were submitted in double heating step (for the same temperature): the first in an induced field of $35\ \mu\text{T}$ and the second in a zero field. For each of the two steps, we carried out a pTRM check for monitoring magnetic alteration. The success rate reaches 50% of the total sampled sites. Figure 1 shows six samples from different sites. The so-called *Arai diagrams* are plotted together with their corresponding NRM decay and orthogonal diagrams (to verify stability of components). For the majority of our selected samples, we observed a minor and low temperature magnetic component ($< 200^\circ\text{C}$) on the orthogonal diagrams. In the moderate to high temperature samples, the stable

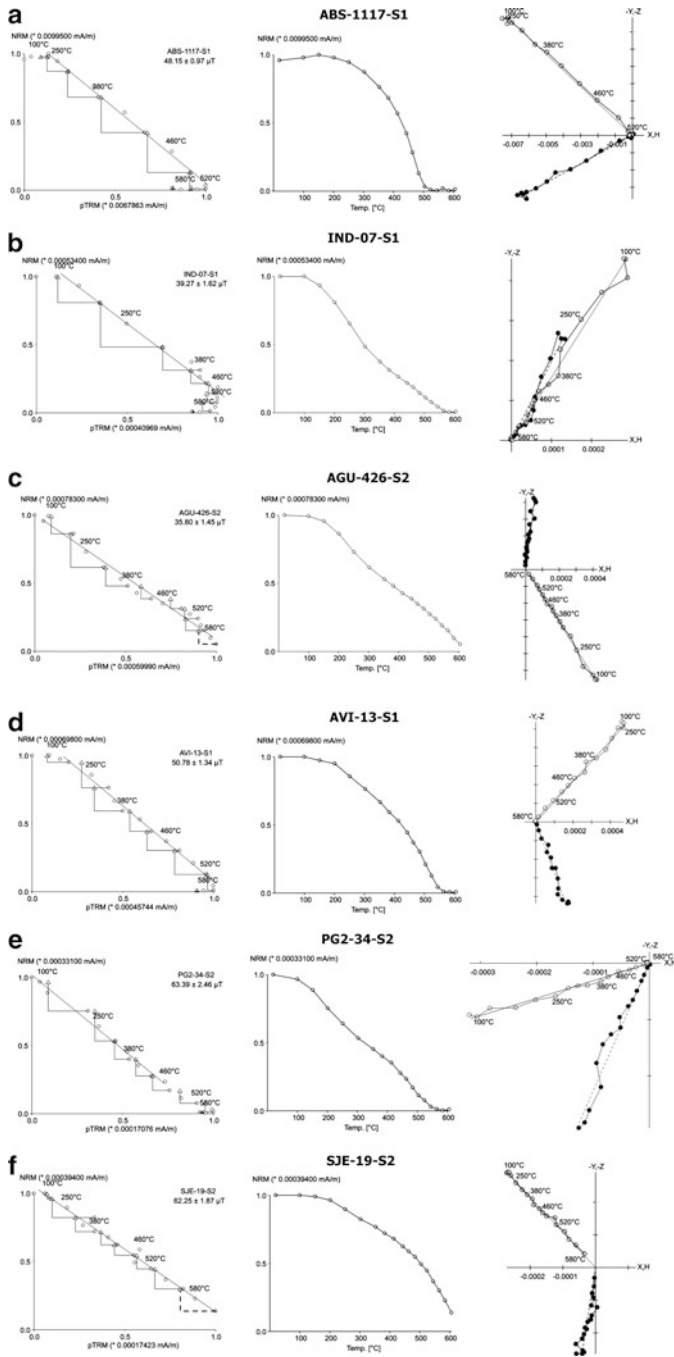


Fig. 1 NRM–TRM, NRM decay and orthogonal vector plots for six representative samples. The NRM–TRM diagram shows the correlation between the natural remanent magnetization (NRM) and the thermoremanence (TRM) acquired in the laboratory, the NRM decay curve shows the

component corresponds to the TRM acquired during the original fired ceramics. This component was used for archaeointensity estimates.

3 Discussion

The age distributions for 21 dated sites are almost evenly distributed from 1000 AD to 1900 AD, while two sites only were dated between 100 AD and 1000 AD. A new dating will be carried out for the first time interval (100 AD to 1000 AD) in other sites. Figure 2 compares the archaeointensity results obtained here with the ones computed from the Korte and Constable (2005) archaeomagnetic model (in grey). The intensities obtained in the present study were consistent within sites and between fragments of pottery of similar ages. Intensity values vary from 35 μ T (around 700 AD) up to a peak of 53 μ T around 1450 AD, and decrease continuously

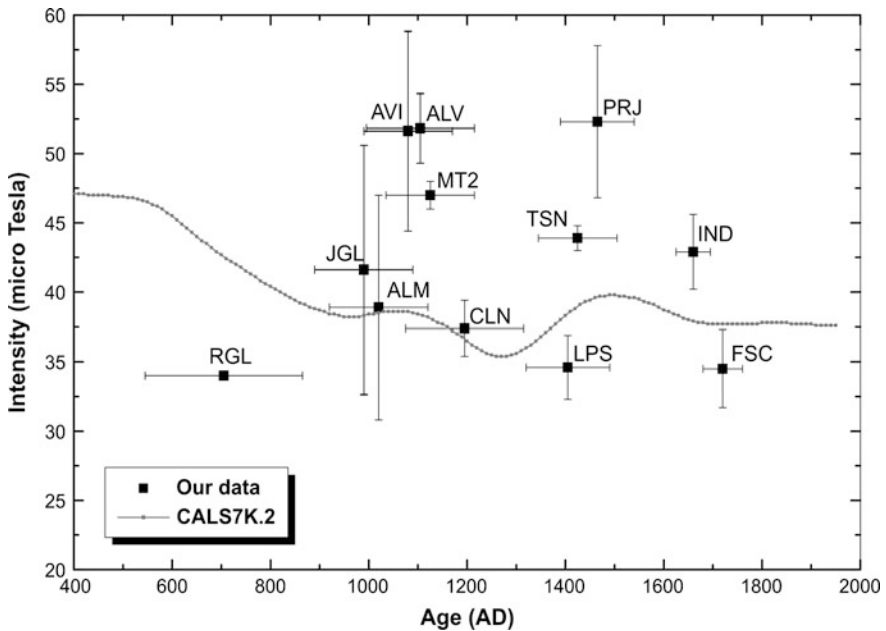


Fig. 2 Geomagnetic field intensity results for São Paulo State. All data were corrected for the latitude of São Paulo. CALS7K.2 geomagnetic field model from Korte and Constable (2005). Sites in the figure: RGL Ragil, JGL Jango Luís, ALM Almeida, AVI Alvim, ALV Alves, MT2 Pajeú, CLN Colina, LPS Lopes, TSN Terras do Sol Nascente, PRJ Piracanjuba, IND Indaiá, FSC Fonseca

Fig. 1 (continued) continuous demagnetization of the natural remanence during the archaeointensity measurement, and the orthogonal vectors show the horizontal and vertical projections of the vector of natural remanent magnetization

down to the present-day value of $\sim 30 \mu\text{T}$. These strong oscillations suggest that archaeomagnetic data may be very useful for dating pottery in South America.

However, the intensities data were not corrected for TRM anisotropy and cooling rate effects. These corrections are very important to better define archaeomagnetic variations (e.g., Chauvin et al. 2000; Genevey and Gallet 2002). Moreover, other intensities data are needed for understanding the geomagnetic field variations and, consequently, for defining the archaeomagnetic master-curve in South America.

Acknowledgments The authors thank Fondazione Monte dei Paschi di Siena, CNPq and FAPESP (grant 05/57782-4) for the financial support.

References

- Aitken MJ, Allsop AL, Bussell GD, Winter MB (1988) Determination of the intensity of the Earth's magnetic field during archaeological times: Reability of the Thellier technique. *Rev Geophys* 26:3–12
- Chauvin A, Garcia Y, Lanos PH, Laubenheimer F (2000) Paleointensity geomagnetic field recovered on archaeomagnetic sites from France. *Phys Earth Planet Int* 120:111–136
- Coe RS (1967) The determination of paleointensities of the Earth's magnetic field with emphasis on mechanisms which could cause non ideal behavior in Thellier's method. *J Geomag Geoelectric* 19:157–179
- Genevey A, Gallet Y (2002) Intensity of the geomagnetic field in western Europe over the past 2000 years: new data from ancient French pottery. *J Geophys Res* 107(B11):2285
- Genevey A, Gallet Y, Constable CG, Korte M, Hulot G (2008) Archeoint: An upgraded compilation of geomagnetic field intensity data for the past ten millennia and its application to the recovery of the past dipole moment. *Geochem Geophys Geosyst* 9(4):1–23
- Korte M, Constable CG (2005) Continuous geomagnetic field for the past 7 millennia: 2.CALS7K. *Geochem Geophys Geosyst* 6(1):1–18
- Le Goff M, Gallet Y, Genevey A, Warme N (2002) On archeomagnetic secular variation curves and archeomagnetic dating. *Phys Earth Plan Int* 134(3–4):203–211
- Thellier E, Thellier O (1959) Sur l'intensité du champ magnétique terrestre dans le passé historique et géologique. *Ann Geophys* 15:285–376

The Dating of a Sixteenth Century Settlement in the Vicinity of Quebec City (Canada) by Means of Elemental Analysis of Glass Beads Through Thermal and Fast Neutron Activation Analyses

J.F. Moreau, B. Gratuze, R.G.V. Hancock, and M. Blet Lemarquand

1 Introduction

In 2008, Quebec City celebrated the fourth centennial of its foundation by Samuel de Champlain in 1608. Quebec represented the first attempt at permanent settlement in this area to succeed, and gave way to New France.

However, previous such settlement attempts are known according to (ethno) historical records, among which the *Relations* of Jacques Cartier (Cartier 1986; Lacoursière 1984). This work describes Cartier's first two voyages, in 1534 and 1535, which eventually led him to Montreal (at the time, the Iroquoian town of Hochelaga). Some 5 years later (1541–1543), Cartier and Roberval were involved in establishing a settlement at Cap Rouge (the western vicinity of today's Quebec City). The settlement was occupied for several months and, apparently, was abandoned following tensions between Cartier and Roberval, combined with other factors (including possible Iroquoian raids), not to be intensively revisited before the late nineteenth century, when a large building was erected there. Thereafter, archaeological investigations did not result in clear artefactual evidence of the 1541–1543 settlement, until new archaeological investigations, undertaken since 2005 under the leadership of the *Commission de la Capitale Nationale*,

J.F. Moreau (✉)

Laboratoire d'Archéologie and Département des Sciences Humaines, Université du Québec à Chicoutimi, Chicoutimi, Canada
e-mail: jfmoreau@uqac.ca

B. Gratuze and M. Blet Lemarquand

Institut de Recherche sur les Archéomatériaux (IRAMAT), Centre Ernest Babelon, CNRS UMR5060, Université d'Orléans, Orléans, France
e-mail: gratuze@cnrs-orleans.fr

R.G.V. Hancock

Department of Medical Physics and Applied Radiation Sciences and Department of Anthropology, McMaster University, Hamilton, ON, Canada
e-mail: ronhancock@ca.inter.net

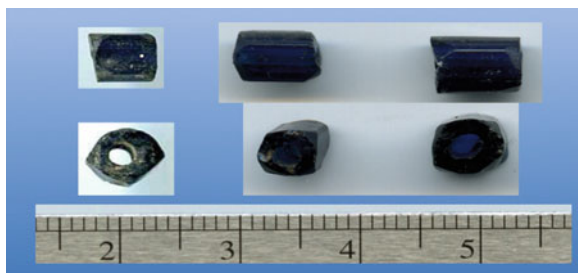


Fig. 1 The three cobalt beads from the Cartier-Roberval site

revealed a series of artefacts that are typologically assignable to the sixteenth century (see Chrétien et al. 2008 for a brief summary). Among these artefacts, three glass beads of dark blue colour (Fig. 1) were found in the 18A3 unit excavation, in which two samples of charcoal provided two ^{14}C dates (1430–1500 and 1440–1530).

The purpose of this paper is to determine whether, on the basis of their elemental composition, these beads could be assigned to the 1541–1543 date proposed by the archival material and relatively supported by the ^{14}C dating.

2 Materials and Methodology

The analyses of the three beads from the Cartier-Roberval site were carried out at the medium flux MacMaster University nuclear reactor. Beads were irradiated serially for 20 or 40 s at a neutron flux of 2×10^{12} neutrons per cm^2 per second. After a delay time of 6–10 min, each bead was assayed for 2 min for its gamma-ray activity, using a Ge detector-based, loss-free-counting, gamma-ray spectrometer to provide data for Al, Ca, Cl, Co, Cu, Mn, Na and Sn. After 18–24 h, they were recounted for 5 min (depending on the level of K) in order to obtain data for As, K, Na and Sb, with Na linking the two counts to ensure analytical credibility.

The comparisons of the three Cartier-Roberval beads are presented in two steps. First, a series of dark blue (cobalt-coloured) beads firmly dated to the French Regime of New France (1600–1750) that had already been analysed using INAA (see Hancock et al. 2000; Moreau et al. 1997; see also Table 1) was used as reference material for comparisons with the Cartier-Roberval beads. Since these series of cobalt blue beads present significant differences according to their specific time period during the French Regime, we can advance the hypothesis that the Cartier-Roberval beads should be markedly different from these series of beads dated between 1600 and 1750. Subsequently, the elemental compositions of the three Cartier-Roberval beads were compared with those

Table 1 Summary of INAA data for cobalt glass beads from the Cartier-Roberval site and seven series dated from 1600 to 1750

		Al	Ca	Cl	Co	Cu	Mn	K	Na	Sn	As	Sb
		(%)	(%)	(%)	(%)	(%)	(%)	(%)	(%)	(%)	(%)	(ppm)
Cartier-Roberval (1541–1543)	N	3	3	3	3	3	3	3	3	3	3	3
	Mean	1.76	10.7	0.10	0.10	0.03	0.59	6.93	1.01	0.13	0.08	31
	Sx	0.55	0.76	0.02	0.02	0.01	0.01	0.84	0.12	0.03	0.01	5
Amsterdam ^a (1601–1610)	N	10	10	10	10	10	10	10	10	10	10	10
	Mean	0.89	7.06	0.84	0.11	0.05	0.32	1.90	9.64	0.13	0.23	88
	Sx	0.09	0.60	0.04	0.02	0.00	0.07	0.25	0.47	0.04	0.06	30
Grimsbys ^a (1625–1636?)	N	48	48	48	48	48	48	48	48	48	48	48
	Mean	0.80	5.85	0.81	0.11	0.04	0.23	4.23	8.43	1.13	0.31	81
	Sx	0.13	0.91	0.12	0.06	0.01	0.18	1.10	0.81	1.87	0.15	34
Ossossane ^a (1636)	N	31	31	31	31	31	31	31	31	31	31	31
	Mean	0.78	6.18	1.00	0.10	0.05	0.20	2.55	10.63	1.20	0.22	99
	Sx	0.26	0.98	0.20	0.03	0.02	0.16	1.08	0.97	1.17	0.12	36
Chicoutimi ^b (1610–1663)	N	86	86	86	86	86	86	86	86	86	86	86
	Mean	0.80	5.93	0.70	0.08	0.04	0.49	3.38	9.20	0.82	0.26	1,530
	Sx	0.14	0.88	0.14	0.02	0.03	0.16	0.86	1.18	0.84	0.44	5,790
Ashuap 90 ^b (1610–1675)	N	9	9	9	9	9	9	9	9	9	9	9
	Mean	0.82	6.04	0.73	0.09	0.03	0.14	4.02	9.43	0.05	0.19	3,290
	Sx	0.17	2.00	0.23	0.03	0.02	0.16	3.12	1.55	0.03	0.10	8,950
Ashuap94Gr1 ^c (1675–1750)	N	76	76	76	76	76	76	76	76	76	76	76
	Mean	0.77	6.18	0.96	0.01	0.76	0.06	3.13	11.61	0.08	0.01	170
	Sx	0.03	0.38	0.04	0.00	0.05	0.00	0.28	0.35	0.04	0.01	173
Ashuap94Gr2 ^c (1675–1750)	N	46	46	46	46	46	46	46	46	46	46	46
	Mean	0.40	5.15	0.95	0.01	0.96	0.02	2.01	11.01	0.07	0.06	129
	Sx	0.02	0.27	0.04	0.00	0.03	0.00	0.26	0.33	0.04	0.00	31
All beads	N	309	309	309	309	309	309	309	309	309	309	309
	Mean	0.75	5.97	0.85	0.06	0.36	0.23	3.17	10.03	0.56	0.17	608
	Sx	0.22	0.98	0.18	0.05	0.40	0.22	1.20	1.70	1.04	0.27	3,457
	V (%)	29	16	21	81	111	97	38	17	185	158	568

^aSource of data : Hancock et al. (2000)^bUnpublished data^cSource of data: Moreau et al. (1997)

obtained through cyclotron-produced fast neutron analyses of cobalt-coloured glasses from France, dated to the period between 1400 and 1700 (Gratuze et al. 1992a, b).

3 Results

Through the collaboration of a group of researchers led by R.G.V. Hancock, monochrome glass bead series had been intensively examined for their elemental compositions by means of INAA (Table 1). More specifically, ten cobalt-coloured beads were found in a glass workshop in Amsterdam dated to ca. 1610 (Hancock et al. 2000). The elemental compositions of 48 beads from the 1625 to 1636 Neutral

site of Grimsby in Ontario (Canada), as well as those of 31 beads from the 1636 Ossossane Huron site, also in Ontario, were also reported in the same publication (Hancock et al. 2000). The 1610–1663 and the 1610–1675 time periods are covered respectively by a series of 86 cobalt-coloured beads from the trading post of Chicoutimi (today Saguenay, Quebec, Canada) and a series of nine cobalt blue beads from the 1990 excavation area of a small site (DhFk-7) with several cultural components, located on the shore of the head of the Ashuapmushuan River (Lac-Saint-Jean region, Quebec, Canada). The Chicoutimi and the Ashuapmushuan 1990 series of INAA data have not yet been reported. During the 1994 excavation of the DhFk-7 site, two series of glass beads (group 1 with 76 beads, and group 2 with 46 beads) were found, that are most probably dated to the 1675–1750 time period (Moreau et al. 1997; see also complementary information in Moreau et al. 2002). It should be emphasised that the Amsterdam, Grimsby, Ossossane, Chicoutimi series and the Ashuapmushuan 1990 collection of beads from DhFk-7 are coloured with cobalt in the order of 1,000 ppm, with copper variations between 250 and 500 ppm. In contrast, the two series from the 1994 excavation of DhFk-7 were coloured with copper ranging between 7,500 and 10,000 ppm, and with cobalt in the vicinity of 100 ppm. While questions could be

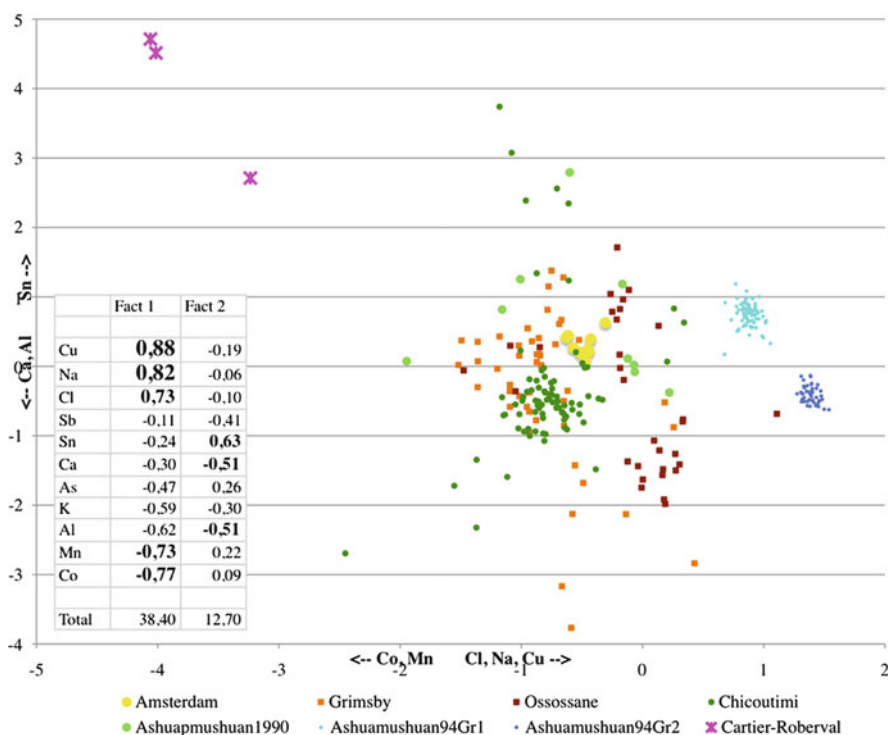


Fig. 2 The Cartier-Roberval beads vs. seven series of cobalt beads dating from 1600 to 1750

raised about the intentional addition of cobalt, it is clear that these two series of beads are clearly different in terms of colour perception (darker shade of blue) as compared to the turquoise beads well known in the first half of the seventeenth century (copper between 0.3% and 0.8% – 3,000–8,000 ppm – with less than 25 ppm of cobalt: Hancock et al. 1996).

In order to compare data from all the abovementioned series of seventeenth century beads to the data pertaining to the three beads from Cartier-Roberval, a factor analysis, using the Statistica software, was performed, taking into account the entire set of data (see Baxter 2003, for a discussion of the limitations of factor analysis). This analysis resulted in the two first factors barely accounting for 50% (38% and 12%, respectively) of the overall variation. The diagram of the two first factors (Fig. 2) shows that the beads from Cartier-Roberval are clearly not akin to any of the series of cobalt beads dated between 1600 and 1750. Moreover, this diagram shows a left to right time vector, with Cartier-Roberval at the extreme upper left, while the two most recent series of Ashuapmushuan 1994 (1700–1750) are right-oriented, with a continuous tendency to the left of slightly older bead series (from the 1600s). In these cases, however, while the 1610 beads from Amsterdam are centrally located among all the seventeenth century series, the relatively contemporaneous Grimsby and Ossossane collections are distributed left and right of the Chicoutimi and Ashuapmushuan 1990 collections. It should however be remembered that the 1610–1663 and 1610–1675 periods are time intervals attributed to these two collections with maximum extension from a typological point of view. Yet unpublished INAA data on the white beads from Chicoutimi, contemporaneous to the cobalt blue beads reported here, show that the Chicoutimi beads would be more precisely dated to a time around 1625; this aspect could thus explain why these beads are so closely clustered. Moreover, the central position of the Amsterdam beads dated to 1610 is not far from those of the ca. 1625–1635 time period for the Ossossane, Grimsby, Chicoutimi and Ashuapmushuan 1990 series, taking into account the time lag between the making of the beads in Europe and their uses in Amerindian contexts.

In brief, the hypothesis put forward at the onset of this paper, that, logically, the three Cartier-Roberval beads should be markedly different from later series of the French Regime (1600–1750) is amply verified.

Gratuze et al. (1992a) reported on the elemental composition of cobalt-coloured glasses from Europe, dated between Roman times and the 1700s, by means of fast neutron activation analysis using a cyclotron. For the present work, the experimental facilities of the laboratory CEMHTI (CNRS-Orléans) were used. The glass objects were irradiated with a fast neutron flux produced by a deuteron beam (17.5 MeV and 25 μ A) impinging on a beryllium target. The neutron spectrum has a maximum energy of 18 MeV, and the mean neutron flux energy ranges between 7 and 8 MeV for an intensity of about 10^{11} – 10^{12} neutrons/s. Two irradiations, followed by direct gamma-ray spectrometry measurements, were carried out to determine the maximum number of elements. The first one was a 30 s irradiation which allows the measurement of short half-life nuclides produced by Si, Al, Mg, K and Cl. The second one was carried out a few days later for 5–240 min,

depending on the object's weight. Three measurements of the radioactivity were performed for a period of 12–24 h after the following cooling times: 3, 5 and 60 days, respectively. Twenty-four others elements can be determined according to this methodology (Na, Ca, Sc, Ti, Mn, Fe, Ni, Cu, Zn, As, Rb, Y, Zr, Nb, Ag, In, Sn, Sb, Cs, Ba, Ce, Au, Pb and U). Sodium was used as an internal standard to take into account the geometrical shape of the objects, and the neutron flux was monitored using the ^{24}Na produced during both irradiations. Concentrations were then calculated and normalised to 100%. For more details on the methodology, see Gratuze et al. 1992b.

Essentially, all the glass fragments from this database dating between 1400 and 1700 were analysed for the same elements as those used for the cobalt-coloured glass beads presented above. Hence, 89 glass fragments were used in comparison to the Cartier-Roberval beads, including glasses from 24 different locations in France, and totalling 19, 34, 17 and 19 specimens for the years 1400, 1500, 1600 and 1700, respectively. Given that several elements exhibited very high variation coefficients, the ones with lower variation coefficients were selected for factor analysis (Ca, K, Mn, Al, Co, Cl, Na). The first two factors accounted for up to 62% of the total variation (43% for the first factor and 19% for the second one). Figure 3 reports the result of this factor analysis. The central

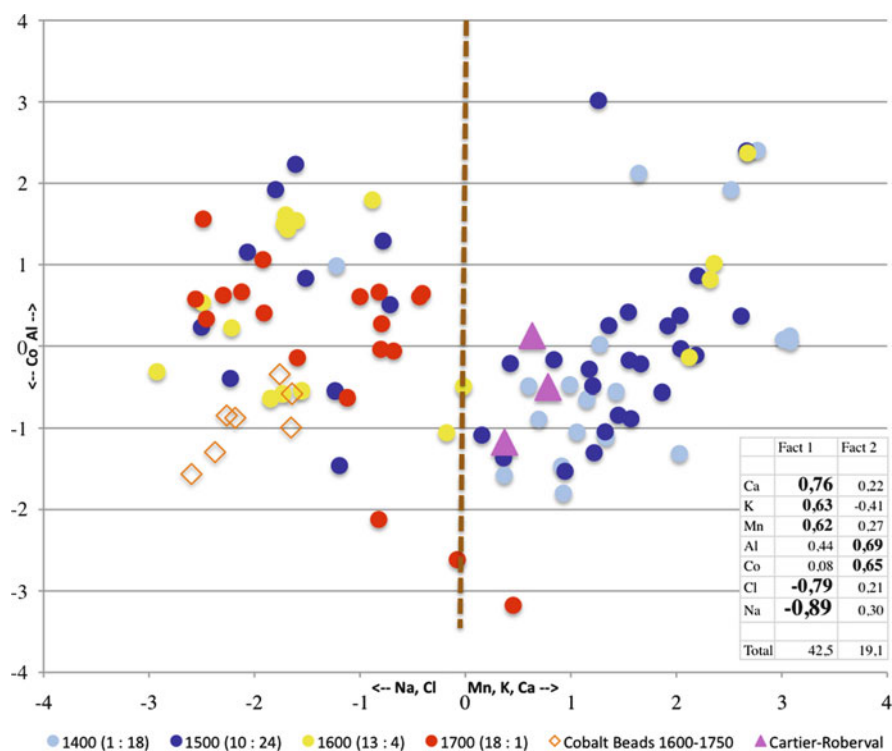


Fig. 3 The Cartier-Roberval beads vs. European series of cobalt glasses dated from 1400 to 1700

dotted line separates those glasses with Ca/K composition (rightward) from the leftward data that represent the Na-based glasses. Interestingly, the Na-based glasses include almost all of the glasses from the 1700s (18 of a total of 19) and most of the glasses from the 1600s (13 out of 17). It is relevant to note that seven beads (one each for the seven cobalt-coloured bead series for which data are reported above) cluster well in this area of the diagram. In contrast, while most of the glass fragments from the 1500s (24 out of 34) are located to the right of the dotted red line, those from the 1400s are almost all (18 out of 19) located in this area, with the three Cartier-Roberval beads clearly located in the Ca/K glass zone.

4 Discussion and Conclusion

In brief, although the glass fragments from Europe were analysed by means of a different technique (cyclotron) from the one used for the series of coloured beads (INAA), it appears that, generally speaking, the results obtained by the two methods are compatible. Thus, for example, the relative position of the 1600–1750 cobalt-coloured beads fits well with the collections of glass fragments dated to the 1600s and 1700s. In contrast, the proposed position of the three Cartier-Roberval beads in the general time frame of the 1500s is verified, although it does not exclude an earlier date (1400s), which, however, does not make much sense when taking into account the archaeological context, as well as the archival observations.

References

- Baxter M (2003) *Statistics in archaeology*. Arnold, London
- Cartier J (1986) *Relations*. Critical edition established by Michel Bideaux. Montréal, Les Presses de l'Université de Montréal
- Chrétien Y, Côté H, Fiset R, Samson G (2008) L'or des fous. In: Dionne H (dir) *Or des Amériques*, Québec, Septentrion/Musée de la Civilisation. p 129
- Gratuze B, Soulier I, Barrandon J-N, Foy D (1992a) De l'Origine du cobalt dans les verres. *Revue d'archéométrie* 16:97–108
- Gratuze B, Barrandon J-N, Dulin L, Al IK (1992b) Ancient glassy materials analyses: a new bulk non destructive method based on fast neutron activation analysis with a cyclotron. *Nucl Inst and Meth B* 71:70–80
- Hancock RGV, Aufreiter S, Moreau J-F, Kenyon I (1996) Chemical chronology of Turquoise blue glass trade beads from the Lac-Saint-Jean Region of Québec. In: Orna MV (ed) *Archaeological chemistry. Organic, inorganic, and biochemical analysis*. ACS Symposium Series n 625. Washington, American Chemical Society, pp 23–36
- Hancock RGV, McKechnie J, Aufreiter S, Karklins K, Kapches M, Sempowski M, Moreau J-F, Kenyon I (2000) Non-destructive analysis of European cobalt blue glass trade beads. *J Radioanal Nucl Chem* 244(3):567–573
- Lacoursière J (1984) La Tentative de colonisation. In: Braudel F (dir.) *Le Monde de Jacques Cartier*, Montréal, Libre-Expression and Paris, Berger-Levrault. pp 273–283

- Moreau J-F, Hancock RGV, Aufreiter S, Kenyon I (1997) Taphonomical and chronological studies of a concentration of European glass trade beads from Ashuapmushuan, Central Québec (Canada). *Iskos (Finska Fornminnesföreningen)* 11:173–181
- Moreau J-F, Hancock RGV, Aufreiter S, Kenyon I (2002) Late French (1700–1750) to Early English (1750–1800) Regime White Glass Trade Beads From A Presumed Decorated Bag Found at the Ashuapmushuan Site (Eastern Central Québec), Canada. In: Jerem E, Biro KT (dir.) *Archaeometry 98. Proceedings of the 31st Symposium*, 2 volumes, British Archaeological Research. Coll. BAR International Series n 1043. pp 613–619

Faster and More Accurate Processing of Samples for Microtephrochronology

J. Watson, C.A. Tryon, and M.C. Vicéns

1 Introduction

Microtephrochronology is a stratigraphic dating method used by archaeologists and Quaternary scientists involving the location and characterisation of volcanic glass particles present in soils and sediments in sizes and amounts invisible to the unaided eye (e.g., Alloway et al. 2007; Turney and Lowe 2001). Accurate determination of the presence or absence of volcanic glass shards in a soil or sediment sample precedes quantitative analysis. This determination is typically accomplished using optical microscopy (Fig. 1) and is one of the most time-consuming and laborious steps in the process, with great potential for misclassification or miscounting error. Here we present a novel method of identifying and counting volcanic glass particles while simultaneously providing a rough geochemical characterisation of all the particles present in the sample (glass and non-glass), using an Aspex PSEM 3025 Particle Analyzer with Automated Feature AnalysisTM (AFA) software (Fig. 2).

J. Watson (✉)

Museum Conservation Institute, Smithsonian Institution, 4210 Silver Hill Road, Suitland, MD 20746, USA
e-mail: watsonj@si.edu

C.A. Tryon,

Department of Anthropology, New York University, 25 Waverly Place, New York, NY 10003, USA
and

Human Origins Program, Department of Anthropology, National Museum of Natural History, Smithsonian Institution, Washington, DC 20013, USA
e-mail: christian.tryon@nyu.edu

M.C. Vicéns

Aspex Corporation, 175 Sheffield Drive, Delmont, PA 15626, USA
e-mail: mvicens@aspexcorp.com

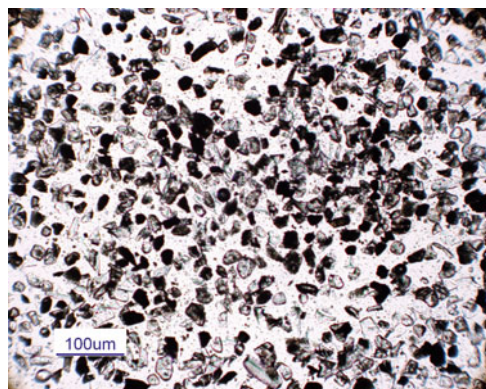


Fig. 1 An example of a sieved tuffaceous sand showing glass and non-glass grains of various morphologies from the flanks of Göllü Dağ, Turkey. Polarised light microscopy is used to identify and count shards of volcanic glass in soil and sediment samples. This is laborious and time consuming, and identification of glass shards can be highly subjective and not always secure. Counting of hundreds of shards, even when samples are spore-seeded, can be inaccurate due to the nature of the sample or operator error. (Photo by Mel Wachowiak, Museum Conservation Institute, Smithsonian Institution.)

2 Background

After extracting the fraction of soil or sediment where distal microtephra is likely to be found, samples are typically mounted on glass slides and visually “scanned” using polarised light microscopy to determine if volcanic glass shards are present (see Gehrels et al. 2008 for a recent review). If found, the shards must be counted in order to determine the number of shards per cm^3 , data which is required to estimate relative shard abundance, eruption volume, and post-depositional reworking. Shard morphologies differ within and between eruptions and/or volcanic systems, and methods for optically distinguishing between tephra and non-tephra vary in their usefulness from sample to sample. Hence there is a long training period before a worker becomes skillful in identifying tephra, and even then there is a certain amount of subjectivity involved in identifying shards, especially when seeing a new morphology (or diagenetic state) for the first time.

The Aspek Personal Scanning Electron Microscope (PSEM) is a specially designed SEM paired with an energy dispersive spectrometer (EDS) and particle recognition and statistical software. It was developed for automated imaging and analysis in industrial applications, but it has obvious applications to microtephrochronology. The PSEM analyses upwards of 1,000 particles per hour, can be programmed to distinguish between anything elementally or morphologically distinct, will not make judgment errors, and gives an absolute count of each type of particle it finds, the size of every particle, and an EDS spectrum of major and minor elements (down to about 1% by weight) of all particles, making it

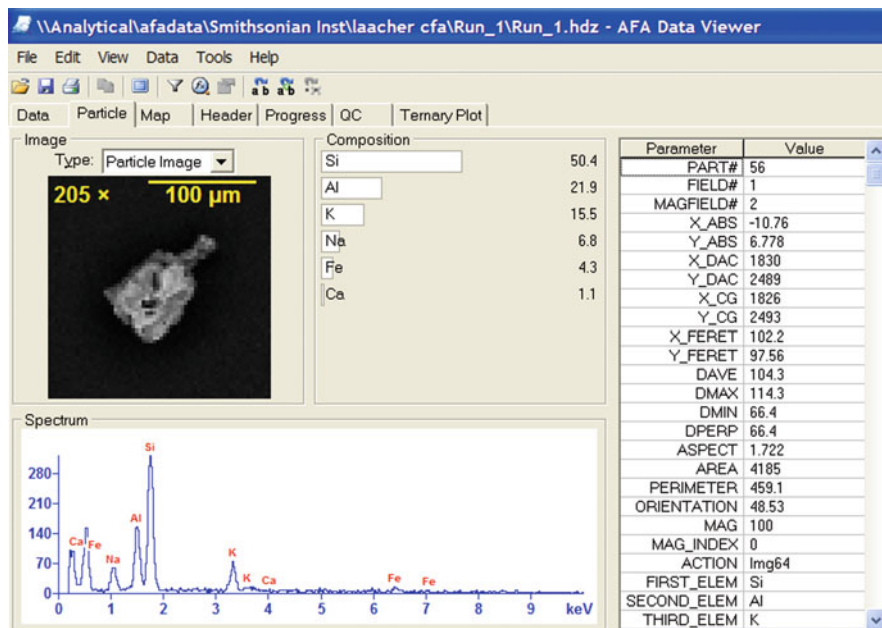


Fig. 2 Screenshot of the Automated Feature Analysis™ (AFA) Dataviewer. In this tab are displayed a low resolution image of the particle (64×64), EDS spectrum (acquisition time 2 s), histogram and quantitative results, and dimensional data. Low resolution settings were selected for quick scanning

possible to look for patterns or trends without any additional investment of time. In addition, it takes an image of each particle and records its coordinates on the SEM stub as described below (see Fig. 2), allowing rapid re-location of specific shards for further analysis (at a longer acquisition time for quantitative analysis if desired).

Identification of particles is accomplished using one of two algorithms. When a particle is identified, its image is captured, an EDS spectrum is collected, and morphological information is calculated and recorded, along with its exact position on the sample stub. The PSEM 3025 systems dynamically scan the sample. Rather than capturing a high-resolution image of the field, which is time consuming and inefficient, the PSEM 3025 instead moves the beam across this field in an array of fairly coarse steps. At each point, the brightness of the backscattered electron signal is noted. If the signal is bright enough to indicate that a particle is present at this position, the software initiates a particle-sizing sequence. There are several algorithms that can be used for this purpose, but for simple particle shapes, the rotating chord algorithm is both accurate and exceptionally fast. Once the coarse scanning identifies a particle, the center is identified and chords are drawn on the particle to define the particle's size and shape. The major reason for this improvement in speed is because the PSEM 3025 only spends time collecting detailed data where particles

are known to be present, rather than capturing and transferring vast numbers of empty pixels.

3 Methods

Three morphologically and chemically distinct tephra samples were analysed; proximal samples from Laacher See and Hekla (1947), as well as an obsidian sample from Romania (Limba) which was ground using a mortar and pestle (Watson 2006). Dry samples which had been extracted by heavy liquid flotation using sodium polytungstate and sieved to between 25 and 90 μm were dispersed onto weighing paper. Samples were transferred onto 15 mm SEM stubs bearing double sided conductive carbon adhesive discs by pressing the exposed surface of the carbon discs onto the weighing paper containing the sample. These stubs were placed (without coating) into the sample stage and introduced into the chamber. Samples were run at full vacuum at 15–25 kV. Each particle was analysed for 1–4 s. Experimental conditions for the study of highly vesicular shards were optimized to avoid double-counting, as the automated analysis is based on backscattered electron signal, and pores and voids within the shard produce a similar signal to the substrate (carbon tape).

4 Results and Discussion

The PSEM was able to identify, count, and geochemically characterise tephra shards of varying morphologies, including highly vesicular shards. Less than 4% of the total counts mistook two particles for one when particles were overlapping. This is expected to improve with experience, and there are other methods of sample dispersion which would eliminate the problem.

While the PSEM 3025 identifies all particles present in a sample by means of characterisation by EDS, a separate step is necessary for quantitative chemical analysis, as the EDS analysis for the scanning process is less than 5 s long. The separate step for quantitative analysis can be done using this same instrumentation, either specifying ahead of time that all particles matching a certain chemical profile be analysed for longer (e.g. 100 s), or by resubmitting the same stub to be analysed later, with the instrument programmed to go to specified particles for a longer acquisition time. The location of each analysis is stored so that the stage can be returned to any particle. If WDS analysis is desired, the stub could be embedded, polished, and carbon coated. In this case, analysis on a different instrument would be aided by a map of the location of volcanic glass particles which is produced by the PSEM 3025.

Further work is required to establish ideal analytical parameters for both scanning and quantitative analysis, and it is likely that these will vary somewhat with different samples.

5 Conclusion

By providing the ability to accurately distinguish between glass and non-glass at a rate of up to 3,600 particles per hour, the PSEM 3025 offers a cost-effective method of scanning soil and sediment samples for the presence of microtephra. This method is an improvement over polarised light microscopy in that it provides a total particle count broken down by material and avoids classification and counting errors.

References

- Alloway BV, Larsen G, Lowe DJ, Shane PAR, Westgate JA (2007) Tephrochronology. In: Elias SA (ed) *Encyclopedia of quaternary science*. Elsevier, Boston, pp 2869–2898
- Gehrels MJ, Newnham RM, Lowe DJ, Wynne S, Hazell ZJ, Caseldine C (2008) Towards rapid assay of cryptotephra in peat cores: Review and evaluation of various methods. *Quat Int* 178:68–84
- Turney CSM, Lowe JJ (2001) Tephrochronology. In: Last WM, Smol JP (eds) *Tracking environmental change using lake sediments. Basin analysis, coring, and chronological techniques*, vol 1. Kluwer, Dordrecht, The Netherlands, pp 451–471
- Watson JA (2006) Evaluation of extraction techniques for microtephra shards from soils and sediments. Unpublished BSc dissertation, University of Bradford

Part VII
Recent Development in Radiocarbon
Dating

The Radiocarbon Dating of Mortars from *Wielka Waga*, The Great Scales Building in The Krakow Market Square

D. Nawrocka and J. Michniewicz

1 Introduction

The subject of the present research is the age of mortars found in the walls of the Great Scales building in the Krakow Market Square (SW Poland). The first documents mentioning this building are dated to 1302 AD. There are well-preserved municipal records from the years 1390–1481 (with a few records missing) concerning municipal revenues and expenses, and providing information on municipal constructions, including the Great Scales and Small Scales buildings (Piekosiński and Szujski 1878). Its existence is mentioned and described until 1879, when the edifice was pulled down. The goal of this research was to verify the stratigraphic data obtained during the excavation works and concerning the development of the Great Scales walls in the Krakow Market Square. The research covered the period from the Middle Ages to modern times. The methods applied included comparative petrographic analysis of lime mortars and radiocarbon dating using accelerator mass spectrometry (AMS).

The mortar age can be determined by radiocarbon dating due to some specific aspects of the mortar production process (Folk and Valastro 1979; Sonninen and Jungner 2001; Michalska Nawrocka et al. 2007). In the process of limestone burning, carbon dioxide is released, and the so-called “burnt lime” (CaO) is obtained and “slaked” with water. The result of this process is slaked lime ($\text{Ca}(\text{OH})_2$). When mixed with sand and water, lime becomes harder and absorbs the existing concentration of CO_2 from the air, and calcium carbonate (CaCO_3) is once again obtained. The binder produced according to this method binds aggregate grains from the slurry. Therefore, the real age of the mortar is reflected exclusively by the age of the binder, since only the binder absorbs the existing concentration of CO_2 at the moment of hardening. In the process of radiocarbon dating of mortars, depending on the mortar composition, one can observe the effect of “rejuvenation”

D. Nawrocka (✉) and J. Michniewicz
Institute of Geology, Adam Mickiewicz University, ul. Makow Polnych 16, 61-606 Poznan,
Poland
e-mail: danutamich@go2.pl; danamich@amu.edu.pl

or the “dead carbon” effect (Folk and Valastro 1979; Lindroos et al. 2007; Michalska Nawrocka et al. 2007). The overestimation of the mortar age may be related to incompletely burnt raw material or the presence of carbonate aggregate. The rejuvenation effect may be determined by paedogenic factors and the related recrystallisation of ingredients. This attempt to verify the age of the walls of the Great Scales also covered the methodology pertaining to the radiocarbon dating of carbonate mortars.

2 Material and Methods

2.1 *Comparative Petrographic Analysis of Mortars*

The petrographic method is based on the observation of thin sections of the mortar samples. Similarities and differences in the petrographic composition between groups of mortars collected at the same site can reflect different periods of their production. However, this method is effective only if different binders, or at least different aggregates, were used in different historical periods. The present research included 55 mortar samples. It was determined that only lime mortars were used in the construction of the Great Scales walls throughout the ages. The mortar slurry was mixed with quartz sand, containing mainly quartz grains and less numerous grits of cherts, granitoids, sandstones, mudstones and feldspars. This composition is identical with the composition of sands found under the foundations of the *Sukiennice* (Cloth Hall) in Krakow. It became apparent that only the mortars from the first half of the fifteenth century were petrographically different, showing smaller fractions of highly sorted sand (Fig. 1). Most samples contained macroscopically observable white lime lumps formed as a result of mortar recrystallisation, which has a significant influence on the preparation of samples for radiocarbon dating.

2.2 *¹⁴C Dating*

The precise dating of carbonate binders can be performed after special preparation enabling the reduction of the “dead carbon” effect (connected with the presence of limestone pieces that were not fully burnt, i.e. the so-called “dead carbon”) and the “rejuvenation” effect (connected with secondary recrystallisation – see Table 1 – white lumps visible in the macrophotograph of sample KR12).

These two main error sources in the ¹⁴C dating of mortars can be eliminated or reduced primarily by using petrographic observations, and additionally by observation of the acid leaching reaction rate. The mechanical separation of those fragments is usually not sufficient, but the subsequent chemical pretreatment provides the opportunity to observe which gas fractions collected during acid leaching

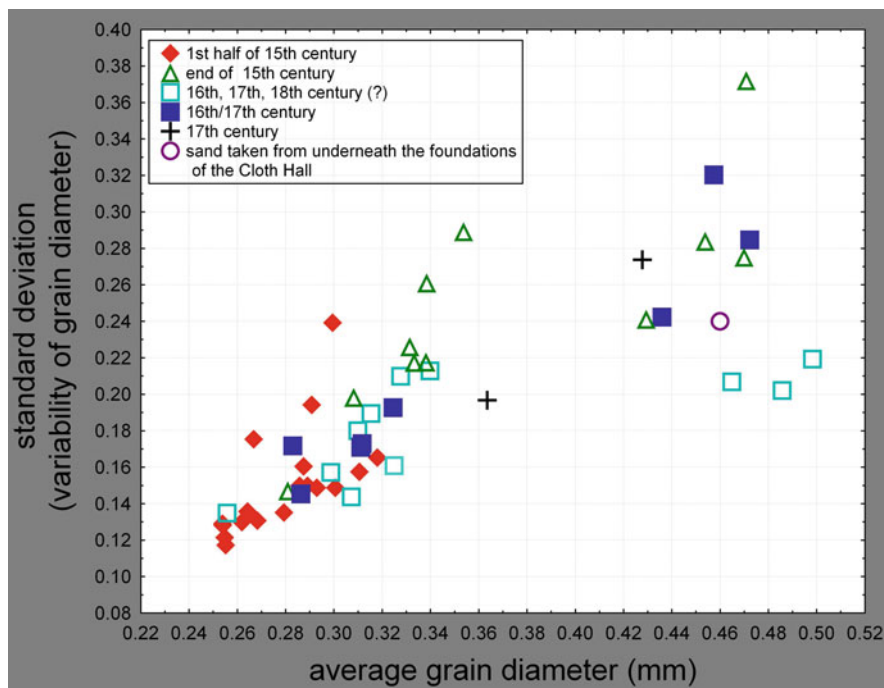


Fig. 1 Granulation of the aggregate of mortars found in the walls of the Great Scales building in Krakow. The dependence of fractions according to the sediment sorting degree (average size of sand grains in the mortar as a function of the variability of their diameter)


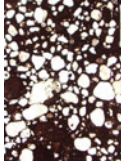
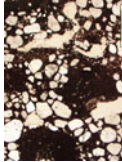
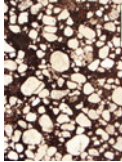
are enriched with young and old carbonate fractions, respectively. This allows choosing the most appropriate gas portion for dating, providing the largest probability for the correct interpretation of the results.

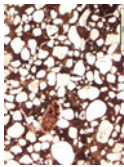
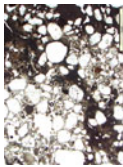
Applying the accelerator mass spectrometry (AMS) technique, the binder was dated by collecting the required amount of gas from the samples at different time intervals. Radiocarbon dating was performed in the Poznan Radiocarbon Laboratory; it was preceded by a trial leaching of mortars in orthophosphoric acid in diverse fractions and time intervals. On the basis of the monitoring of the leaching reaction and petrographic observations, those samples were selected for dating that enabled the isolation of carbonates of different genesis (Lindroos et al. 2007) and an attempt to collect them with different time intervals of gas accumulation was made (Table 1).

3 Results and Discussion

The samples of mortars collected in Krakow were dated using the accelerator mass spectrometry technique; the calibration was undertaken using OxCal v 3.10 (Bronk

Table 1 ^{14}C dating results, including the locations where the samples were collected; calibration in numerical form after using the options TAQ and TPQ; (wh- white lumps)

Sample name (dated material type)	Macro and microphotograph of mortars, (1N)	Sample origin	Sample age expected by archaeologists (relative chronology)	Lab no, ^{14}C age (BP)	Calibrated age confidence interval	confidence interval	confidence interval
KR12 (carbonates, CO_2 collected after first 10 s of leaching reaction)	 	Binder in the brick section of the southern embrasure (second from S) in the western perimeter wall of the Great Scales	Fourteenth century to the first half of the fifteenth century	Poz-13823, 625 ± 30	1300AD (21.5%) 1320AD 1350AD (46.7%) 1395AD	1300AD (95.4%) 1400AD	
KR 14 (carbonates, first 40 s of leaching reaction) KR 14 (charcoal)		Binder in the brick section of the small pillar attached to the N embrasure (second from N) in the western perimeter wall of the Great Scales	End of the fifteenth century	Poz-13370, 355 ± 50 Poz-13492, 330 ± 30 336 ± 25	1480AD (68.2%) 1505AD	1465AD (95.4%) 1505AD	
Kr14_R_combine KR 15 (carbonates, CO_2 collected after first 10 s of leaching reaction)		Binder in the stone section of the W perimeter wall of the Great Scales (facing on the W side)	Fourteenth century to the first half of the fifteenth century	Poz-13824, 605 ± 30	1300AD (58.7%) 1365AD 1385AD (9.5%) 1395AD	1300AD (95.4%) 1410AD	

KR 16 (charcoal)		Binder in the secondary brick section (in the corner of the former portal)	Sixteenth, seventeenth, eighteenth century (?)	Poz-13493, 220 ± 30	1640AD (35.1%) 1680AD 1760AD (33.1%) 1800AD 1810AD 1500AD (18.4%) 1530AD 1640AD 1550AD (49.8%) 1630AD	1640AD (42.5%) 1690AD 1730AD (52.9%) 1810AD 1490AD (95.4%) 1640AD
KR 16 (charcoal II)				Poz-14110, 355 ± 30		
KR 16 (carbonates, fraction 63–80 µm, first 45 s of leaching reaction)				Poz-14777, 960 ± 40	1020AD (22.2%) 1060AD 1080AD (46.0%) 1160AD	990AD (95.4%) 1170AD
KR 20 (carbonates, CO ₂ collected after first 10 s of leaching reaction)		Interior of the first 'stall' from N in the western part of the Great Scales; binder in the brick section of the ceiling (preserved section on the S side)	Fifteenth century	Poz-13825, 520 ± 30	1405AD (68.2%) 1435AD	1390AD (95.4%) 1445AD
KR 38 (charcoal)		Binder in the stone section of the corner (pillar?) fixed in the foundation of the longitudinal wall of the secondary interior division in the eastern part of the Great Scales building (northern division – facing on the S side)	Fifteenth century	Poz-13495, 395 ± 30	1445AD (68.2%) 1480AD	1440AD (95.4%) 1495AD

Ramsey 2005). The main problem in the ^{14}C dating of the Krakow samples was the presence of white lumps. Trial leaching reactions of mortars in orthophosphoric acid, covering samples in their natural form and samples after the extraction of the “white material”, as well as the dating results for samples collected from the Small Scales building in Krakow, enabled the conclusion that this material decreases the age obtained according to the dating process. As a result, this material was removed from the Great Scales mortar samples before dating.

Sample 14 was dated twice (carbonate fraction Poz-13370 and charcoal fragments from the same sample Poz-13492). Since the dates were obtained for the same sample, we combined them using the R_Combine option in OxCal (Fig. 2).

The combination was checked for internal consistency by a χ^2 test, which confirmed that the dates are in agreement with each other ($t = 0.2[5\% \ 3.8]$). Reliable historical sources indicate that the existence of the Great Scales was documented for the first time in 1302 AD. This information can be used for the purpose of calibrating dates using the TPQ option, i.e. no sample should be dated

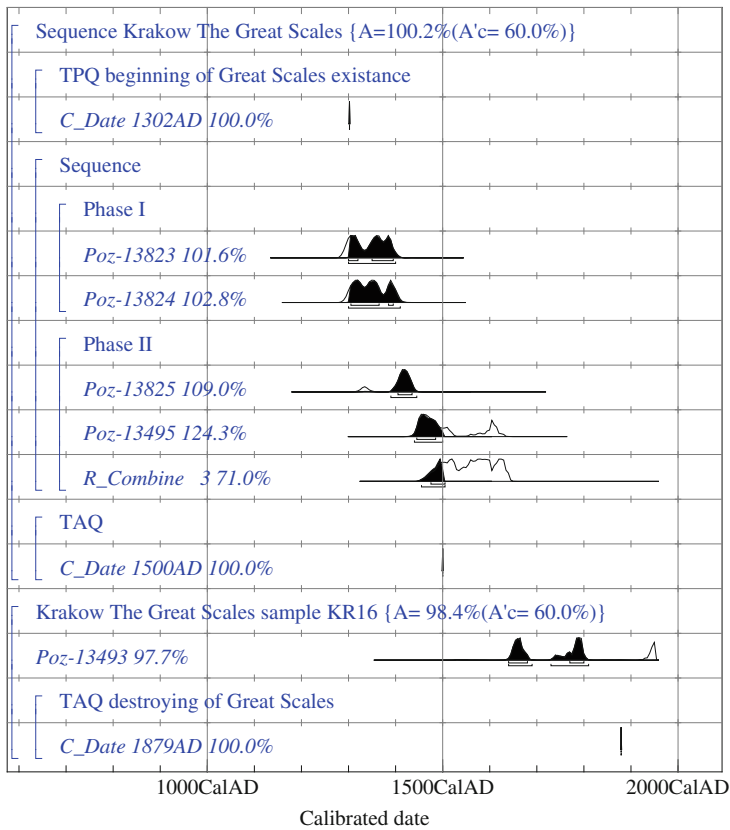


Fig. 2 Results of calibration after considering the TPQ and TAQ options in the OxCal programme (Bronk Ramsey 2005)

earlier than 1302 AD. The Great Scales edifice was pulled down in 1879, which determines a *terminus ante quem* (TAQ). The application of both the aforementioned options enabled the limitation of the calibrated age range (Fig. 2, Table 1).

The radiocarbon results of chosen samples show two general time intervals – samples from the fourteenth century (recorded by archaeologists as phase I) and samples from the second half of the fifteenth century (recorded by archaeologists as phase II). The Great Scales building historically documented in 1302 was made of wood. The first construction erected with Jurassic stone on a rectangular plan was dated by archaeologists to the second half of the fourteenth century – phase I (Buśko 2006; Sławiński et al. 2008).

The age obtained by radiocarbon dating for most of the analysed samples seems to be consistent with archaeological and historical expectations, and with premises referring to the chronology of the erection of the Great Scales. There is a discrepancy in the ^{14}C measurement of sample KR16 (Poz-13493, Poz-14110, Poz-14777). This sample was dated three times, each time prepared in a different way (charcoal and binder). Taking into consideration its composition and the manner of sample preparation (after removal of white lumps), one should conclude that the dating result for carbonates (Poz-14777), which indicates an older date than the one obtained for charcoal (Poz-13493, Poz-14110), is overestimated. In the case of charcoal radiocarbon dating, there is also a risk of overestimation in relation to the age of the building, due to the peculiarities of tree growth.

It is important whether the studied fragment originates from the outer or inner wood rings, or from young twigs (respectively conferring an over-ageing effect or reflecting the date of cutting a tree). In the case of sample KR16 (see Table 1), the radiocarbon age obtained for the charcoal (Poz-13493) seems to be more plausible than the other two results (Poz-14110, Poz-14777). However, from a methodological point of view, caution must be maintained when interpreting the results obtained for KR16, because of discrepancies in the dating of different materials from this sample. Another sample originating from the same wall should be additionally dated to verify this hypothesis.

4 Conclusion

In the present study, radiocarbon dating has been applied to the samples collected during the archaeological investigations carried out at Kraków Market Square in the year 2005. The age of the walls of Krakow's Great Scales edifice obtained by the dating of selected samples indicates a period between the fourteenth and the fifteenth century AD. This dating determined two phases (I and II) in the existence and development of the *Wielka Waga* (Great Scales) building.

The obtained results are in agreement with the established archaeological stratigraphic sequence. Since the obtained calibrated age range is very broad, as a result of the shape of the calibration curve, the radiocarbon dating obtained hitherto does not enable a precise determination of the time of erection of particular sections

of walls. Taking into account information from historic sources (TPQ and TAQ options) in the calibration programme enables a narrowing down of the obtained age range.

The present analyses allow the verification of the influence of different mortar components on the results of ^{14}C measurements (“rejuvenation” or overestimation of age). The observations of leaching reactions of mortars, together with the petrographic background, are very helpful in the selection of samples for dating and also when interpreting results.

Acknowledgements We gratefully acknowledge the “Fondazione Monte dei Paschi di Siena”.

We express our gratitude to the leader of the Krakow excavations, Dr. C. Buśko and Dr. S. Sławiński, for providing mortar samples and for content-related and practical help (relative chronology, historical sources). We sincerely thank Prof. T. Goslar and Dr. J. Czernik from the Poznań Radiocarbon Laboratory for the time devoted to this project and for fruitful discussions.

References

- Bronk Ramsey C (2005) OxCal v.3.10. <http://www.rlaha.ox.ac.uk/orau/calibration.html>
- Buśko C (2006) Wstępne wyniki badań archeologiczno-architektonicznych prowadzonych na Rynku Głównym w Krakowie w 2005–2006 roku. *Wiadomości konserwatorskie* 19:67–70 (in polish)
- Folk RL, Valastro S (1979) Dating of lime mortar by ^{14}C . In: Berger R, Suess H (eds) *Radiocarbon dating. Proceedings of the ninth international conference*. University of California Press, Los Angeles, pp 721–30
- Lindroos A, Heinemeier J, Ringbom A, Brasken M, Sveinbjornsdottir A (2007) Mortar dating using AMS ^{14}C and sequential dissolution: examples from medieval, non-hydraulic lime mortars from the Aland Islands, SW Finland. *Radiocarbon* 49(1):47–67
- Michalska Nawrocka D, Michczyńska DJ, Pazdur A, Czernik J (2007) Radiocarbon chronology of the ancient settlement on the Golan Heights. *Radiocarbon* 49(2):625–37
- Piekosiński F, Szujski J (eds) (1878) *Zestawienie rachunków miasta Krakowa z lat 1390–1393, 1395–1405*. In *Najstarsze księgi miasta Krakowa od 1300 do 1400*. t. II, Krakow (in polish)
- Sławiński S, Niewalda W, Mamica M, Rozbicka D (2008) *Badania wschodniej części Rynku Głównego w Krakowie – 2005–2007*. Wielka Waga – Architektura (typescript in polish)
- Sonninen E, Jungner H (2001) An improvement in preparation of mortar for radiocarbon dating. *Radiocarbon* 43(2A):271–3

Part VIII
Field Archaeology

Combination of Non-Destructive Methods for the Observation of the State of Subsurface Preservation of Ploughed Archaeological Sites: A Case Study from Oppidum Stradonice in Bohemia

R. Křivánek

1 Introduction

Agricultural terrains very often cover the same areas as archaeological terrains. This seems to be very often a problematic aspect, related to the adequate protection of endangered archaeological sites. In the case of many sites ploughed for a long time and also of archaeological monuments in the Czech Republic, the actual questions facing the archaeologist are: “What is the present state of subsurface preservation of archaeological sites? Can we still observe most archaeological features in situ? How deep and important could be the influence of landscape changes as a result of ploughing?” More than one method of non-destructive archaeology can today be of help in finding answers to these questions at different levels of information. This was also one particular aim of the project “Geophysical surveys in archaeologically unexcavated parts of Czech oppida” (Grant Agency of the Academy of Sciences of the Czech Republic – no. A8002301, Křivánek et al. 2003–2007, cooperation of the Institute of Archaeology in Prague, the National Museum in Prague and the Mining Museum in Příbram).

2 Archaeology of the Site

The Celtic oppidum Stradonice, with approximately 90 ha. of fortified area, is the second largest oppidum in the Czech Republic. The La Tène oppidum (destroyed in the second half of the first century BC, with a Hallstatt settlement also identified) is situated on the elevated and sloped promontory above Berounka River. The oppidum was fortified by a single rampart fortification with one known internal division, and up to now four gates were identified at the location (Drda and Rybová 1997).

R. Křivánek

Institute of Archaeology of the Academy of Sciences of the Czech Republic, Prague, v.v.i.,
Letenská 4, 118 01 Praha 1, Czech Republic
e-mail: krivanek@arup.cas.cz

Unfortunately the first long-term plundering of antiquities and devastation of site started very early, after the discovery of a large hoard of golden coins in 1877. The first regular large scale archaeological excavations were performed in 1895 and 1902 (Píř 1903). Another important excavation was then carried out in 1929 (unfortunately after the subsequent unexpected death of Stocký, a major part of the documentation was lost during World War II). The last rescue archaeological excavation (associated with the construction of a gas pipe line) inside the oppidum was undertaken in 1981 (Rybová and Drda 1994). Unfortunately, to the present day, this very important site is still an example of a ploughed out archaeological monument (approximately 75% of the inner area). The poor state of subsurface preservation of archaeological situations can be documented here as a result of a combination of aerial prospection, field surface surveys, and new geophysical surveys of the site.

3 Goals of the Project

The title of the project, “Geophysical surveys in archaeologically unexcavated parts of Czech oppida”, reflects a clear preference to apply non-destructive (mainly geophysical) techniques in the survey of Celtic sites in the Czech Republic. The main goals of the entire project were thus focused on studying subsurface situations in terrains located outside of (or next to) previous excavated areas of oppida (Křivánek 2004, 2008a). The exact spatial identification of the remains of the fortification system not visible on the surface, of the internal structure and/or of the intensity of settlement in terms of types of activities within the surveyed inner and outer areas of oppida were the main goals of the project (Křivánek 2005). Wide arable areas, as well as selected grassy or wooden terrains of oppida were chosen for the surveys. More specific questions were then aimed to the exact spatial identification of non-preserved interior structures, of interruptions or gates in the fortification system, of abandoned communications, or of specific production features or activities. In the case of surveys of many arable or otherwise degraded terrains of oppida by agricultural activities, they were also aimed at the determination of the current states of sub-surface preservation (or of the scope of later and modern surface modifications and site adjustments to the archaeological contexts). In the present paper, examples of results from the Stradonice oppidum can document how extensive, intensive and also risky could landscape changes be in the case of ploughed archaeological monuments (Křivánek 2008b).

4 Methodology of the Project

Wide area survey of inner and outer areas of oppida by caesium magnetometer (Smartmag SM-4g, Scintrex) was the main geophysical method used for this project. The other geophysical method – geoelectric resistivity survey (RM-15, Geoscan

Research) – was subsequently applied at a more detailed scale, followed by a complex survey of subsurface situations with expected stony structures. The presence of metal artefacts on intensively ploughed fields was also verified by systematic metal detector surveys. Other non-destructive methods – systematic surface artefact collection and aerial prospection of ploughed areas of oppida (including processing of old aerial photographs and maps) – then contributed to the project by providing more results that could be combined with the existing data for the interpretation of geophysical anomalies. All of these surface surveys, including visible remains of rampart fortifications of the oppidum, were then localised by parallel GPS measurements.

5 Results

Large scale magnetometric measurements in non-optimal conditions of present or previously ploughed fields helped identify more and different remains of intensive settlement inside the oppidum (for aerial photography of surveyed area see Fig. 1). However, the enclosed examples of combined non-destructive results from surveys of the oppidum proved also very poor, and, inside of the oppidum, a variable state of preservation of the original terrain was observed. This influence of prolonged ploughing is also visible on present meadows. Nevertheless, the most endangered parts, mainly inside the site, are still on arable fields, where subsurface archaeological situations are locally deeply ploughed out to bedrock. Surprisingly, beneath

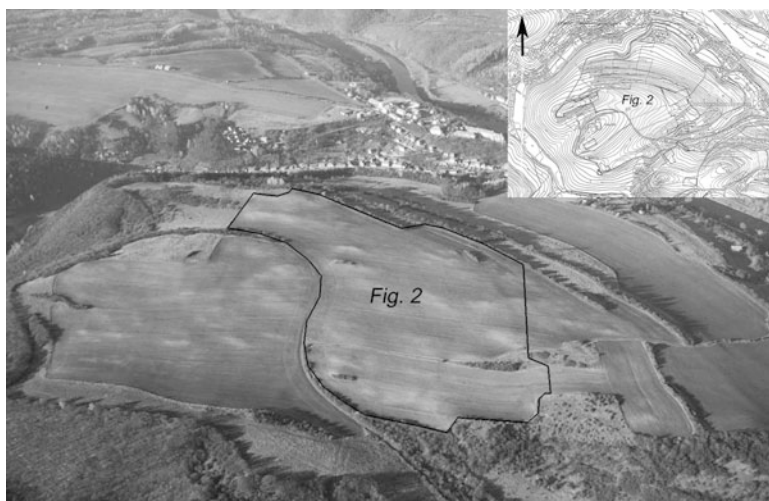


Fig. 1 Oppidum Stradonice, district of Beroun. Aerial photography (by Gojda) of ploughed inner terrain of oppidum and map of the main fortification systems with areas of geophysical surveys carried out between 2003 and 2007. Area of magnetometric survey (Fig. 2) is also indicated

some parts of the same ploughed terrains, we can still recognise the last remains of deeper sunken settlement or production features, inner ditch divisions of the area, possible places of interruptions and communications inside the oppidum, or remains of probable rectangular or stony features on flat platforms (Fig. 2).

We can explain here some of the identified magnetic anomalies (see arrows in Fig. 2). In the south-eastern area of the site, we can identify a part of a bow of ploughed out ditch (or double ditch) enclosure by means of magnetometric measurement. In the southern part of area, it is possible to recognise another single linear anomaly from a ditch enclosure which was also verified during the rescue archaeological excavation associated with the gas pipe line in 1981. In the northern area next to central acropolis of the site, due to the sensitivity of the magnetometers,

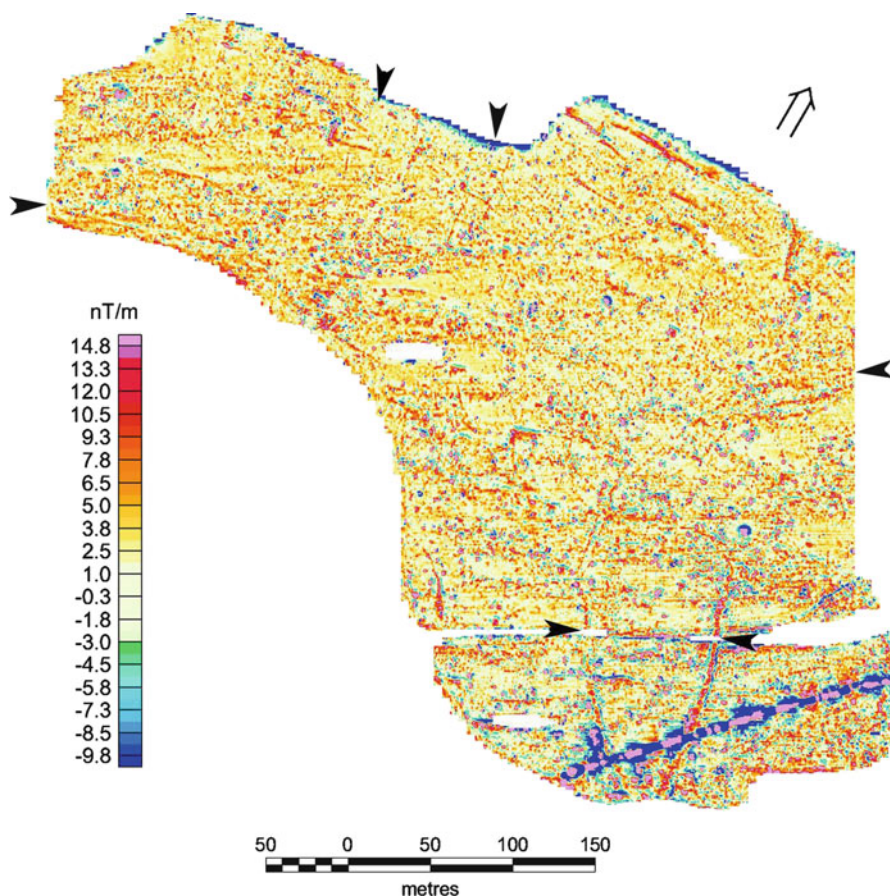


Fig. 2 Oppidum Stradonice, district of Beroun. The identification of intensive settlement, heavily ploughed out sunken production features, internal divisions, ditch enclosure remains, possible communications and also gas pipe line disturbances inside the oppidum (surveyed area approximately 13.5 ha.)

we can also recognise the last subsoil remains of a subrectangular structure of the settlement that were not ploughed out. All of these subrectangular features are situated in ploughed out terraces on sloped terrain below the acropolis. Different linear magnetic anomalies in the north-western part of the surveyed area probably indicate original inner communications from the western gate B to the central part of the oppidum.

In the case of more detailed processing of data from magnetometers, we can separate different amplitudes of various magnetic anomalies, and probable different archaeological and other sources beneath the soil. This method of processing magnetic data could be of help in identifying and separating very probable remains of other groups of production features (furnaces), different sunken features of the settled area, and also specific changes of soil layers on sloped terrains. Experience from oppidum Stradonice showed that better archaeo-geophysical interpretations of measurements could also sustain additional metal detector surveys, surface artefact collection, or surface documentation of crop marks inside the oppidum (some subsurface archaeological features are visible also from surface during vegetation time of seeded fields).

6 Conclusion

The combination of different non-destructive methods applied at larger scale for the survey of ploughed out terrains of archaeological sites is useful not only for the identification of subsurface archaeological features, but also for the observation of the real state of preservation of the archaeological terrain of sites. In the case of the ploughed La Tène oppidum Stradonice in Central Bohemia, it seems to be only a matter of time before we can observe in situ the last preserved remains of archaeological features inside the site (with evident internal structures and divisions). These results should be a sufficient argument for the more intensive future observation of other areas of the site and of other important ploughed archaeological terrains at different sites.

References

- Drda P, Rybová A (1997) Keltská oppida v centru Boiohaema – Die keltischen Oppida im Zentrum Boiohaemums. *Památky archeologické* 88:65–123
- Křivánek R (2004) Geophysical survey in the archaeologically uninvestigated parts of Czech oppida. *Antiquity – project gallery* (<http://antiquity.ac.uk/ProjGall/krivanek/index.html>)
- Křivánek R (2005) Geophysical survey in the archaeologically uninvestigated parts of Czech oppida. In: Piro S (ed) *Proceedings, extended abstracts – 6th International conference on archaeological prospection, Rome, Italy September 14–17, 2005*. Institute of Technologies Applied to Cultural Heritage (C.N.R.), Roma, pp 17–20

- Křivánek R (2008a) Geophysical survey in the archaeologically un-investigated parts of Czech oppida. In: Martin L (ed) ISAP News, the newsletter of the International Society for Archaeological Prospection, Bradford, 7–10 (<http://www.bradford.ac.uk/acad/archsci/archprospection/newsletters.php>)
- Křivánek R (2008b) Combination of non-destructive methods for observation of state of subsurface preservation of ploughed archaeological site on example of oppidum Stradonice in Bohemia. In ISA 2008, 37th International Symposium on Archaeometry, May 12th–16th, 2008, Siena, Italy – Programs and Abstracts, Siena, 347
- Píř JL (1903) Starožitnosti země České. Díl II. Čechy na úsvitě dějin. Sv. 2. Hradiště u Stradonic jako historické Marobudum. Praha
- Rybová A, Drda P (1994) Hradiště by Stradonice, rebirth of a Celtic Oppidum. Institute of Archaeology, Prague

The Different Possibilities for Collaboration Between Geophysical and Archaeological Methods in the Context of the Research Project “Neglected Archaeology” of the Department of Archaeology of the University of West Bohemia in Pilsen

R. Křivánek

1 Introduction

The Department of Archaeology of the University of West Bohemia in Pilsen obtained a grant for an extensive 6-year archaeological project in January 2005 (project no. MSM 4977751314, supported by the Ministry of Education, Youth and Sports of the Czech Republic, Gojda-Vařeka et al. 2005–2010). This project represents at the present time the leading topic of interest of the entire Department of Archaeology of the University of West Bohemia in Pilsen (Gojda 2005). Due to the intensive combination of theoretical and practical archaeological questions and methods, this project also provides wide opportunities for the education, practice and training of students in our department as archaeologists.

2 Aims of the Project

The main goals of the project were concentrated on more specific archaeological issues, to date less known and mostly neglected in Bohemian archaeology. These main goals (Křišťuf et al. 2007) were as follows:

1. Archaeological – preference given to archaeological research with respect to archaeological monuments, the starting of new programmes of theoretical

R. Křivánek

Institute of Archaeology of the Academy of Sciences of the Czech Republic, Prague, v.v.i.,
Letenská 4, 118 00 Prague 1, Czech Republic
and

Department of Archaeology, University of West Bohemia in Pilsen, Sedláčkova 15, 306 14 Pilsen,
Czech Republic
e-mail: krivanek@arup.cas.cz

archaeology in Bohemian archaeology, concentration and systematic work on less known themes of Bohemian archaeology.

2. Scientific – support of archaeological teamwork and of more theoretical and interdisciplinary work for members of the Department of Archaeology in Pilsen.
3. Institutional – establishment of archaeological bases for practical fieldwork of students without dependence on rescue archaeological excavations.
4. Pedagogical – wide cooperation between students of the Department of Archaeology in Pilsen.

3 Particular Themes of the Project Envisioning Cooperation Between Geophysical and Archaeological Methods

More practical goals of the application of geophysical methods in the current project are then connected with archaeological sub-projects, their topics and/or particular problems:

1. Archaeological survey and research on forested prehistoric and/or medieval archaeological sites.
2. Documentation and research on different types of activities at forested medieval and/or modern archaeological sites (Vařeka et al. 2006).
3. Study of lowland flood plain sediments near archaeological sites.
4. Study of sites characterised by intensive soil accumulation.
5. Surveys of hilltop sites and their slopes.
6. Survey and research on eroded and accumulated terrains below upland archaeological sites.
7. Surveys of raw material extraction and production sites.
8. Complex surveys of ploughed out archaeological terrains in chosen agricultural lowland regions.

More specific themes of sub-projects were subsequently focussed on individual problems related to particular situations, regions or sites (for example, landscape archaeology in the surroundings of the sacred hill Říp in Central Bohemia).

4 Use of Geophysical Methods

For many specific archaeological topics and questions related to the project, a wide and intensive cooperation of archaeological and other interdisciplinary methods was necessary (for example, archaeobotany, archaeogenetics, palynology, aerial prospection or GIS archaeo-application). Geophysical techniques have been applied across most of the archaeological topics of this project, both for methodological and pedagogical purposes. This paper is focussed on various specific applications

of geophysical methods at different stages of archaeological research. For the geophysical surveys of archaeological sites, the caesium magnetometer Navmag SM-5, Scintrex Ltd. of the University of West Bohemia in Pilsen (Křivánek 2007) was used, together with equipment of the Institute of Archaeology in Prague: caesium magnetometer Smartmag SM-4g, Scintrex Ltd., RM-15, Geoscan Research, U.K. for geoelectric resistivity measurement and a KT-5c kappameter, Geofyzika Brno.

5 Particular Examples of Archaeo-Geophysical Surveys

Geophysical methods were applied in the context of different topics of the project as non-destructive archaeological field methods. These were used to address at larger scale some specific archaeological questions, or studied and excavated archaeological situations. In cooperation with archaeological methods applied in the context of various sub-projects (with specific topics), geophysical measurements were applied as one from the first independent and non-destructive prospection methods during systematic field surveys and documentation. At other sites, geophysical surveys were used by archaeologists in the first stage of planned excavations or test pitting. Other detailed geophysical methods were also applied during archaeological excavations. The very different possibilities for the use of geophysical techniques in archaeology enclose thematically different examples from different archaeological regions and terrain conditions. Due to the limited space available for the present paper, only two figures and five representative examples of the combination of archaeological and geophysical methods in the context of a large project are presented.

5.1 Combination of Non-destructive Methods in the Analysis of Agricultural Terrains of Lowland Regions: Example of the Region Podřipsko, District of Litoměřice, North Bohemia

Surveys were carried out according to an efficient cooperation of field geophysical measurements and aerial prospection in a sub-project concentrated on the study of prehistoric and early medieval settlements around the legendary hill Říp (Gojda 2007). Magnetometric measurements here verified more settlements and unknown enclosures. Examples from other sites (for example Ctiněves, Černouček, Ledčice, Nížebohy, Vražkov or Straškov) document how magnetometric measurements helped verify newly discovered prehistoric and/or medieval ditch enclosures on aerial photographs (Gojda) with various shapes, dimensions or orientation, located around the sacred hill Říp.

5.2 *Revision and Research on Burial Cemeteries: Example of Burial Cemetery Dobešice, District of Písek, South Bohemia*

In the context of a sub-project aimed at the study of abandoned forested or ploughed out burial cemeteries, geophysical surveys carried out during surface surveys or geodetic documentations of sites contributed to the verification of lost archaeological features, and to estimating the real state of subsurface preservation of variably destroyed burial mounds. For example, results of magnetometric and resistivity measurements in the area of a ploughed out prehistoric (Bronze Age and Hallstatt) burial cemetery near Dobešice were used for the efficient archaeological verification (Křišťuf-Rytřř) of the site by trenches, identifying one heavily ploughed out burial mound and sunken grave pit (Fig. 1).

5.3 *Systematic Research in Flood Plain Area: Example of the Polycultural Site of Dolany, District of Plzeň-North, Western Bohemia*

Another systematic cooperation of geophysical survey, field artefact collection and subsequent archaeological excavation (Janíček 2007), including geological or environmental fieldwork, took place in the context of a sub-project focussed on

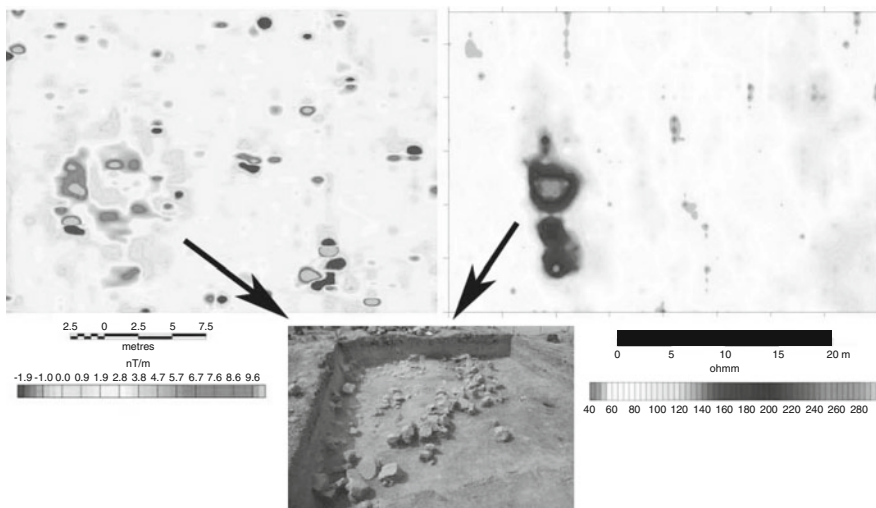


Fig. 1 Dobešice, district of Písek. The identification of ploughed out remains of burial from combined magnetometric and resistivity surveys of the prehistoric site was verified by positive archaeological excavation (detail of surveyed area, 40 × 28 m)

research pertaining to the polycultural (La Tène and medieval) site Dolany, situated on a lower flood plain terrace next to Berounka river. A combination of aerial photography (Gojda) with magnetometric and resistivity measurements helped identify more centres of settlement and the extent of different activities carried out at the site. Detailed in situ measurements of magnetic susceptibility during excavations helped differentiate the remains of sunken or burned features in flood plain sediments.

5.4 Study of Medieval Iron Production Areas: Example of a Site Near Strašice, District of Rokycany, Western Bohemia

Another combination of geophysical survey with surface surveys, and also with a study of historical written sources, in the context of a sub-project focussed on abandoned medieval or modern production areas (from the fourteenth century onwards; Nováček 2007), brought more detailed information about the intensity of specific production activities and the present extent of sites. Geophysical surveys of remodelled garden terrains of an original iron production site in Strašice confirmed very intensive and also extensive iron production (Fig. 2).

5.5 Systematic Research and Documentation on Abandoned Medieval and/or Modern Villages in Forested Regions: Example of Abandoned Village Sloupek, District of Rokycany, Western Bohemia

The site was subsequently verified by positive archaeological excavations (Nováček), which identified damaged iron production waste heaps with massive subsurface concentrations of iron slag.

The systematic study of abandoned villages in highly forested and archaeologically less known areas in different regions of Bohemia is one of the main topics of the entire project (Vařeka et al. 2006). The contribution provided by combined geophysical methods can also be demonstrated by the example of the abandoned medieval village of Sloupek. Geoelectric resistivity measurements carried out at this site contributed to a better subsequent archaeological verification of interesting situations by archaeological trenches. The results identified stony remains of settlements, and the continuation of other structures in the village (water reservoirs). Additional magnetometric measurements helped differentiate the locations

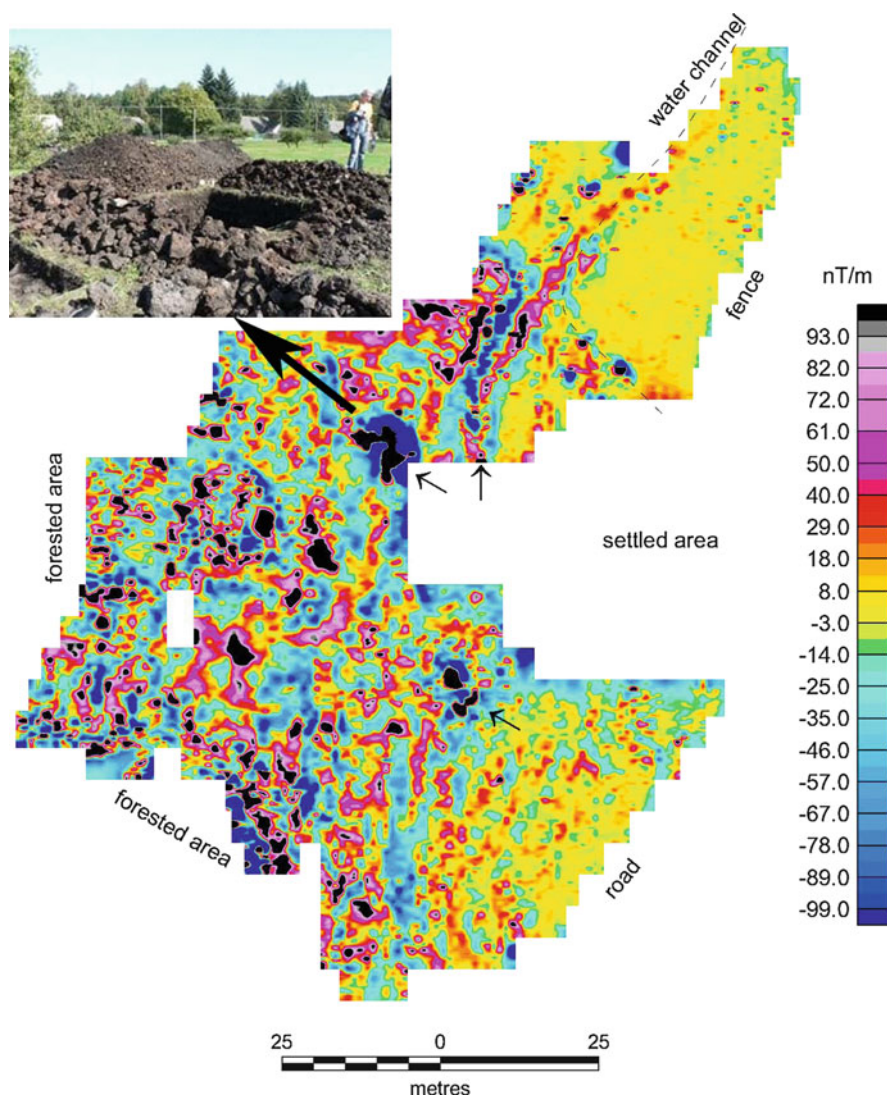


Fig. 2 Strašice, district of Rokycany. Magnetometric survey followed by subsequent archaeological excavation confirmed the presence and large extent of a medieval iron production site, where iron production waste heaps were destroyed in modern times, and the terrain remodelled to a garden (surveyed area approximately 1.1 ha.)

of furnaces and other areas of burned materials (fireplaces) before the excavation. A similar combination of detailed geodetical field documentation of the site and geophysical surveys, in combination with more methods and eventual small scale excavations, was applied at other archaeological sites of this type.

6 Conclusion

Between 40 and 50 archaeological sites (chosen situations) were surveyed by geophysical methods during the first 4 years of the project carried out by the Department of Archaeology of the University of West Bohemia in Pilsen. During the first 3 years of the research project, geophysical methods were used for archaeological studies carried out at 40–50 sites (or chosen situations). The examples discussed in this paper represent only some of the topics related to particular archaeological sub-projects (nearly 20). Other uses of geophysical methods by archaeologists are expected in future years. From an archaeo-geophysical point of view, the project offers significant potential not only for complementing archaeological data by geophysical results, but also for using non-destructive measurements for a more efficient planning of archaeological verifications of similar neglected situations in the future. An archaeo-geophysical database of the studied sites, with a comparison of the different methods applied, is planned after the end of project. The research project “Neglected Archaeology” will continue until the end of 2010.

References

- Gojda M (2005) Cíle výzkumného záměru plzeňské katedry archeologie a cesty k jejich dosažení. *Archeologické Rozhledy* 62:211–213
- Gojda M (2007) Aerial archaeology and remote sensing in the first year of the archaeology around the hill of Říp project. In: Křišťuf P, Šmejda L, Vařeka P (2007) *Opomíjená archeologie 2005–2006 – Neglected Archaeology 2005–2006*. Katedra archeologie - FF ZČU Plzeň – Department of Archaeology of University of West Bohemia in Pilsen, Elce Book Publishing, pp 19–25
- Janiček L (2007) Přehled výzkumných terénních aktivit za rok 2005 a 2006 v prostoru zaniklých Dolan, okr. Plzeň-sever – The resumption of field research activities in the area of deserted medieval village Dolany, distr. Pilsen-north, during years 2005 and 2006. Křišťuf, P.- Šmejda, L. – Vařeka, P. 2007: *Opomíjená archeologie 2005 – 2006 - Neglected Archaeology 2005 – 2006*. Katedra archeologie - FF ZČU Plzeň – Department of Archaeology of University of West Bohemia in Pilsen, Elce Book Publishing, pp 54–75
- Křišťuf P, Šmejda L, Vařeka P (2007) *Opomíjená archeologie 2005–2006 - Neglected Archaeology 2005–2006*. Katedra archeologie - FF ZČU Plzeň – Department of Archaeology of University of West Bohemia in Pilsen, Elce Book Publishing
- Křivánek R (2007) První zkušenosti s aplikací cesiového magnetometru KAR ZČU Plzeň (Navmag) na archeologických lokalitách v roce 2006 – The first practical application of the new Navmag caesium magnetometer from the Department of archaeology of the University of West Bohemia in Pilsen on archaeological sites in the year 2006. In: Křišťuf P, Šmejda L, Vařeka P (2007) *Opomíjená archeologie 2005–2006 - Neglected Archaeology 2005–2006*. Katedra archeologie - FF ZČU Plzeň – Department of Archaeology of University of West Bohemia in Pilsen, Elce Book Publishing, pp 209–218
- Nováček K (2007) První sezóna průzkumu středověkého výrobního mikroregionu Strašicko – The first season of research into the medieval proto-industrial mikro-region Strašicko. In: Křišťuf P, Šmejda L, Vařeka P (2007) *Opomíjená archeologie 2005–2006 - Neglected Archaeology 2005–2006*. Katedra archeologie - FF ZČU Plzeň – Department of Archaeology of University of West Bohemia in Pilsen. Elce Book Publishing, pp 163–173
- Vařeka P et al (2006) *Archeologie zaniklých středověkých vesnic na Rokycansku I – Archaeology of deserted medieval villages in the Rokycany – region (West Bohemia) I*. KAR FF ZČU, Plzeň

Comparative Archaeometric Analysis by 3D Laser, Short Range Photogrammetry, and Hyperspectral Remote Sensing Applied to the Celtiberian City-State of Segeda

J.G. Rejas, M. Farjas, F. Burillo, R. López, M.A. Cano, M.E. Sáiz, T. Mostaza, and J.J. Zancajo

1 Introduction

The work presented in this study took place in the archaeological area of Segeda (Mara-Belmonte de Gracián, Zaragoza), corresponding to the homonymous Celtiberian city. It is located in the north-eastern part of the Iberian Peninsula, next to the Perejiles River, an affluent of the River Jalón, covering an area of 40 ha. The extension, peculiarity and heterogeneity of the layers present at the archaeological site of Segeda are special features prompting the use of prior research into the different technologies which help facilitate the detection and recording of buried or unearthed archaeological structures in the different excavation areas.

In terms of remote sensing, one of the characteristics which make the Celtiberian site of Segeda (Burillo Mozota 2006) particularly interesting regards the sequential and meticulous state of excavation there, enabling the application of imaging methodologies which can be contrasted and improved as results are confirmed or rejected by strictly archaeological research investigations. In this type of research, where the aim is to find evidence of buried structures and man-made formations, the response of the surfaces in appropriate wavelengths from the reflective (VIS, SWIR)

J.G. Rejas (✉)

National Institute of Aeronautics and Space Technology (INTA), Madrid, Spain
e-mail: rejasaj@inta.es

M. Farjas

E.T.S.I. in Topography, Geodesy, and Cartography, Polytechnic University of Madrid (UPM), Madrid, Spain

F. Burillo, R. López, M.A. Cano, and M.E. Sáiz

Faculty of Humanities and Social Sciences of Teruel, University of Zaragoza (UZ), Zaragoza, Spain

T. Mostaza and J.J. Zancajo

Higher Polytechnic School of Ávila, University of Salamanca (USAM), Salamanca, Spain

and emissive (TIR) spectra could provide relevant information (Goovaerts et al. 2004) and support for archaeological exploration.

Following this approach, research has been undertaken since 2005 with the purpose of applying active and passive remote sensing techniques at Segeda. An acquisition campaign followed by hyperspectral data processing was consequently carried out in the summer of 2005, and another one in 2006, with an airborne SAR (Synthetic Aperture Radar) sensor.

The work presented here is therefore part of a continuing project concerning the approximation of new methods for completing a geospatial study of the Celtiberian city of Segeda and offering support to new campaigns of archaeological excavation (Farjas et al. 2003). In 2007, one specific objective was to extend the acquisition of data (thermal, short range and 3D laser photogrammetry) over the Segeda I area 4 and its environs. The aim of this endeavour was to spectrally record, identify and characterise ideal areas and materials for the continuation of excavation operations and to validate the results obtained to that date. This article seeks to present the characteristics of the data acquisition campaigns which took place in 2007, the pre-processing of images, and the initial results obtained.

2 Close Range Acquisition

The hyperspectral remote sensing techniques developed at Segeda required contrasting and validation by complementary ground levelling methods. During the summer of 2007, data were taken from different areas of the Segeda site for this purpose, with a short range photogrammetry camera, a thermal ThermaCAM sensor, and a 3D laser sweeper.

The close object photogrammetry and remote sensing campaign consisted of acquiring images in the thermal spectrum and 20% sequentially overlapping photographs over a ground platform (crane), at heights of 10 and 15 m, in such manner as to cover the 2007 excavation in Area 4 of Segeda. Moreover, another set of thermal images, corresponding to the Poyo de Mara and the surrounding areas of Segeda I, was also acquired, without following a specific spatial pattern.

2.1 3D Laser Scanner

Field data was acquired using a Trimble GX 3D Laser Scanner (Trimble Company). For scanning distances under 50 m, it guarantees a standard deviation of 1.4 mm, increasing to 2.5 mm for an approximate distance of 100 m. Five different stations were used to cover the area under study. From each station, images of the different objects to be measured were taken, scanning the nine magnetized spheres, which were located around the entire excavation.

2.2 Thermal Images

ThermaCAM is a passive sensor which records the radiation emitted by surfaces in wavelengths from 7.5 to 134 μm . The thermal sensitivity of this camera allows the recording of data in a temperature range between 0.08°C and 30°C, in a maximum image sequence of 50 per second. Under these conditions, it is possible to acquire array type images of 320 \times 240 pixels, codifying the radiation in the thermal infrared in 14 bit with a measurement precision of $\pm 2^\circ\text{C}$. One of the features which make this sensor particularly interesting for close range remote sensing is that calculations of the emissivities of the measured surfaces can be carried out due to its three internal calibration bodies. To this purpose, 3 cm diameter candles have been used as a thermal reference and as points of control for geo-referencing the images.

2.3 Short Range Photogrammetry

Photographic images were acquired using a calibrated Nikon D70 digital camera. The Nikon D70 camera is able to obtain images of 3008 columns by 2000 rows. The area was previously marked out to allow for posterior orthorectification of the images; 3 cm diameter bull's-eyes designed to this effect were used for this. Thus, photograms of 0.5 cm and 0.7 cm were obtained with a spatial resolution corresponding to the heights of the 10 and 15 m platforms, respectively.

3 Pre-processing of the Data

The main function of the different processes applied to the acquired data is to produce a single perfectly co-recorded multi-sourced file. This is useful in a subsequent analysis aimed at spatially correlating the elements of archaeological interest (walls, surfaces, structures, remains of organic origin, etc.) with the superficial temperature at which they were recorded.

The 3D laser data were processed at resolutions ranging from 2 mm for spheres, given their importance for combining the different takes, to 50 mm in less critical areas. Relevant objects, such as the bakery or the forge, were measured with a spatial resolution of 5 mm in horizontal and vertical orientations, and the rest of the objects every 9 mm, thus processing an approximate number of 2,500,000 points.

The photographic images were orthorectified using the *OrthoEngine* module of Geomatic. An internal model of the camera was made based on the calibrated internal parameters of orientation, and a mosaic of orthoimages was made following a block adjustment.

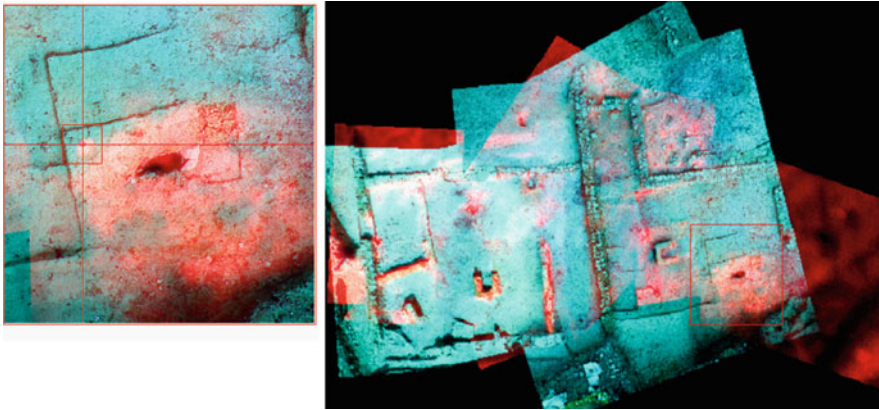


Fig. 1 Candle (thermal reference) and Celtiberian forge in a multi-source file

The thermal images were processed using the ThermoCAM Researcher programme, transforming them into an image format compatible with the orthorectification module used. Ten thermal references (candles) were used as points of control, as well as the other 47 GCPs (Ground Control Points) extracted from the orthoimage generated by short range photography (see Fig. 1). A polynomic first order adjustment was applied, allowing us to obtain a 2.7 pixel RMS, elevated, but sufficient, bearing in mind the difficult visual recognition implicit in the infrared images.

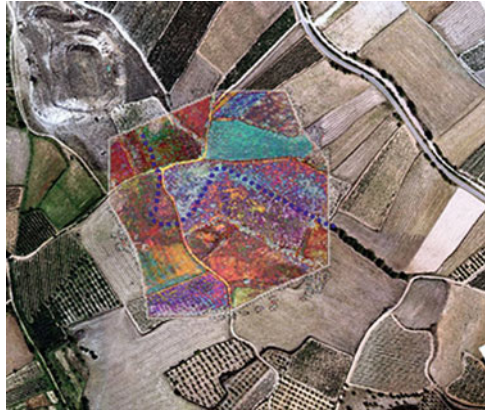
In addition to these geometric tasks, the thermographs were exported to Matlab for calculation by this array treatment programme of material emissivities and correcting them for possible patterns of thermal distortion. Candles, considered as thermal reference bodies, were used for this purpose, and the measurements of environmental temperatures were acquired by thermocouple sensors.

One last step in the pre-processing of the data has been the fusion of data, carried out according to two procedures. The thermographic mosaic has been combined with the short range photographic mosaic, in order to allow the layers from area 4 (excavated in 2007) to display the same spatial resolution in the visible spectrum and in the emissive spectrum. Furthermore, the hyperspectral images of the AHS (Airborne Hyperspectral Scanner) sensor, acquired in 2005 and converted into reflectance values (Rejas et al. 2006) have been fused with aerial photography.

4 First Analysis

Using the file with layers of short range photographic and thermographic information, diverse radiometric profiles were made in order to detect spectral variability and establish spatial correlations between the characteristic elements resulting from the excavation. We can observe how the hottest structures correspond to the adobe walls, a building material used by the Celtiberians. This type of wall may be

Fig. 2 Thermal hyperspectral PCA and aerial photographic image. Buried stone structure in the shape of an “elbow” that could possibly indicate the remains of a wall



thermally distinguished from the walls constructed with rocky materials. Similar structures, walls or archaeological remains, can be easily separated according to their thermal responses, due to different chemical composition or physical state.

The refractory materials used by the Celtiberians of Segeda were identified in the residences of the excavation area 4, presenting a very low thermographic response, while the materials located next to the forge are the hottest. These foreseeable responses are of use for the identification of houses or different buildings that could be detected in future areas of excavation.

Furthermore, an analysis of the principal components (PCA) was carried out, focusing exclusively on the thermal channels of the AHS sensor fused with aerial photography. Previous studies (Traviglia 2006) have provided satisfactory results in terms of the application of this technique on hyperspectral data for the detection of buried archaeological remains. PCA is a technique which allows for analysis of the total variability, simplifying the original data by eliminating all the information which is redundant. According to this method, we reduced the dimensionality of the original data by enhancing the contrast, thermal in surface area in this case. The first four main components (PC1, 2, 3 and 4) have enabled the detection and extraction of an obvious alignment (blue dotted line in Fig. 2), which is not visible in the original images or in the optic images, and which, in turn, presents a sharp turn in the shape of an “elbow”.

This alignment and the sharp turn experienced in the SW direction initiate exactly in a point of inflexion in the elevation of the terrain, and could correspond to any type of buried structure, fortification wall or other.

5 Conclusions

A multi-resource file of area 4 of Segeda, including visible and thermal data, was created. A precise spatial co-register addressing the different layers of information is critical for subsequent data analysis. The analysis of the main components used in

the hyperspectral image fused with aerial photography has enabled the verification of the results obtained in 2005 on the surrounding terrain of area 4. The classification by spectral angle calculated in 2006 was thus validated, from which an alignment indicative in turn of possible buried archaeological remains was extracted. The integration of these results with digital models of elevation has led to the establishment of relations between the points of inflexion of the terrain and the thermal variability extracted from the main components calculated.

This study has led to the confirmation of how diverse low cost technologies may enable the recording and updating of high precision spatial and spectral data. Finally, the present work is part of the remote sensing line of research applied at Segeda, the general aim of which is the proposal of this type of methodologies as a support for future explorations.

Acknowledgements We wish to thank INTA, the Ministry of Education and Science and Hiberus, the Premium Research group in Humanities of the Government of Aragon, for facilitating the necessary data and funds to complete this work.

References

- Burillo Mozota F (2006) Segeda and Rome. The historical development of a Celtiberian city-state. In: Abad L, Ramallo S, Keay S (eds.) *Early Roman Town in Hispania Tarraconensis*. *J Roman Archaeol. Supplementary Series* Number 62, Portsmouth Rhode Island, pp 159–170
- Farjas M, Rejas JG, Gómez JA, De Miguel E, Fernández-Renau A, (2003) Airborne multispectral remote sensing application in archaeological areas, CAA 2003. The E-way into the four Dimensions of Cultural Heritage, Viena, Austria, April 2003
- Goovaerts P, Jacquez G, Warner A, Crabtree B (2004) Detection of local anomalies in high resolution hyperspectral imagery using geostatistical filtering and local spatial statistics, *IEEE Trans Geosci Remote Sens*, 0-7803-8350—8/04/\$20.00(c).
- Rejas JG, Burillo F, López R, Farjas M (2006) Hyperspectral remote sensing application in the celtiberian city of Segeda, From Space to Place. 2nd International Conference on Remote Sensing Archaeology, Rome (Italy) 4–7 December 2006. *BAR International Series* 1568, BAR S1568 2006
- Traviglia A (2006) MIVIS Hyperspectral sensor for detection of subsoil archaeological sites and interpretation support GIS: an Italian case study. CAA 2006, Fargo, ND-USA

Part IX
Human–Environment Interaction

Shell Mounds in Brazilian Coast: Integrating Archaeological and Environmental Studies

M.C. Afonso and M.C. Tenório

1 Introduction

This paper addresses past fisher-hunter-gatherer settlements from a landscape based perspective and a contextual approach based on integration of archaeological and environmental analyses.

A project is being held at Brazilian southeastern coast, applying a landscape approach through multi-disciplinary researches. Geoarchaeology as well as bioarchaeology can contribute to an understanding of the dynamic relationship between prehistoric human societies and the environment.

In tropical regions, like Brazil, shell mounds (*sambaquis*) represent deposits of different sizes and shapes, including one over 30 m high located at the southern coast. They contain thousands of cubic meters of shells, sediments with animal remains, including fish bones, cultural remains like artefacts, hearths and burials. Huge shell mounds, acting as landmarks, occur near smaller ones, other types of coastal sites and even sites with deposits containing small amounts of shells and black earth, displaying a very complex settlement pattern.

Recent archaeological researches indicate long-term populations, specialized in exploitation of sea resources (fish and shellfish), using shells as a constructive material to build shell mounds with different sizes, deposits, geographical distribution and site functions. Shell mounds are distributed along 2,800 km in Brazilian coast, concentrated at intersections of different types of ecosystems.

We consider the landscape from interrelated perspectives, including different kinds of resources, the distribution of sites over the landscape and the symbolic significance of shell mounds. At Arraial do Cabo (Rio de Janeiro State, Southeast Brazil) an investigation into prehistoric coastlines, coastal settlement and shell mounds is under way, with formation processes indicating different site functions,

M.C. Afonso (✉)

Museu de Arqueologia e Etnologia, Universidade de São Paulo, São Paulo, Brazil
e-mail: marisa.afonso@usp.br

M.C. Tenório

Museu Nacional, Universidade Federal do Rio de Janeiro, Rio de Janeiro, Brazil

including ceremonial sites with burials, hearths and postholes. We will explore field data and models of site formation and settlement pattern considering geological, biological and cultural factors. We will also compare field data from this area with others in Brazil, noticing similarities and differences in shell mounds and other associated coastal sites.

2 Shell Mounds

Geoarchaeological studies in Brazil started at the beginning of the 1980's, carried out by archaeologists with an academic training in geology and/or geography, although, before this decade, there were researches in Brazil that can be considered "geoarchaeological". Some of these works were about shell mounds, as Leonardos (1938) with a discussion about the origin, natural or anthropogenic, of Brazilian shell mounds (*sambaquis*).

Water has an important role on the archaeological record and on the landscape as a geomorphological agent responsible for many processes as erosion, transportation and deposition of sediments. In coastal areas, water has an important role in the changes of landscape and it is necessary to identify these modifications through time to understand the spatial strategies used by the prehistoric groups.

Brazilian coastline was extensively occupied by prehistoric fisher-collector-hunters groups, with these occupations being adapted to environmental changes during the Quaternary, in a dynamic landscape.

In 1993, 958 shell mounds were recorded in Brazilian coast (Gaspar 1998). They were built from 8,000 years BP to 800 years BP and when the first Europeans arrived there were no more *sambaqui* moundbuilders (*sambaqui* is the local name for shell mounds).

Shell mounds are located normally in the intersection areas of different environments and contain mollusks and fish found in the rocky areas, estuaries, channels, mangrove and lagoons. Rodents and birds were consumed too, as well as crabs from mangrove. Animals like monkeys, armadillos and jaguars were hunted in the forested areas (*Mata Atlântica* – Atlantic Forest).

Location of the sites and associated materials indicate that preferential settlement places were areas characterized by concentration of many ecosystems. These choices strongly support the inference of sedentarism, representing an intention opposed to cyclic movement and high mobility across the landscape (Tenório 1991). The continuous occupation of the same funerary *loci* for hundreds of years, as observed in sites located at the Brazilian southern coast, also indicate a sedentary settlement pattern (De Blasis et al. 2007). However, discussions continue in order to settle the question whether sites occupied permanently were unifunctional or multifunctional, based on the activities identified by associated materials.

In almost every shell mound there are evidences of fishing, collecting and small game hunting, consumption and domestication of plants (Tenório 1991), besides evidences of stages associated to the elaboration of lithic and bone artefacts. In sites

related to funerary rituals (De Blasis et al. 1998, De Blasis et al. 2007), as the remains were associated to funerary rituals, sites are classified as ritual (unifunctional) site.

Lithic sites are also considered as unifunctional and can be represented by flaked materials associated to coastal exploitation as well as areas with fixed sharpener-polishers for making polished-stone axe-blades (Tenório et al. 2008)

3 The Study Area: Rio De Janeiro State (Southeastern Brazil)

Two different areas have been studied (Tenório et al. 2008) in the framework of long-term research projects concerning the coastal area of Rio de Janeiro State (Southeastern Brazil): Ilha Grande (an island) and Arraial do Cabo (with prehistoric sites in islands and in continental areas as well).

Arraial do Cabo presents the morphology of a little peninsula (Fig. 1) and is surrounded by 30 km of sandy beaches, with a rock complex named *Morro do Atalaia*. It also presents lacustrine formations, like Lagoa de Araruama, with the predominance of eolian dunes and typical vegetation, named *restinga*.



Fig. 1 Aerial view of the study area Arraial do Cabo (continent) and Ilha do Cabo Frio (island), State of Rio de Janeiro, Southeast Brazil. Each *arrow* on the map represents shell mounds

In the region, an archaeological assemblage, impressive by its concentration in space and by the diversity of places chosen for settlements, show 20 sites (Tenório et al. 2008), two of them in an island – Ilha do Cabo Frio e Usiminas sites (Fig. 2). There are also two groups of fixed sharpener-polishers, that are sets of marks on rocks resulting from production of polished objects; their distribution and association with surrounding sites show association to preceramic groups along the coast (Tenório 2003).

The age of the sites vary from 4,200 to 1,200 years BP (Tenório et al. 2008). Comparing settlement patterns in Ilha Grande (a big island, also located at Rio de Janeiro coastal part and systematically studied by Tenório 2003) and in Arraial do Cabo, there are some similarities and differences. In both areas, sites are located at hills and small mountains associated to sites on eolic dunes, sites near lagoons and open sea. These sites show that the most important subsistence activity was fishing, with a later introduction of mollusk harvesting and intense exploitation of malacological specimens, collected as a second choice.

In Arraial do Cabo's sites, there is a predominance of *Pinctata sp* and *Astraea sp.*, bivalve and gastropod collected on the coastal rift and with little meat, followed

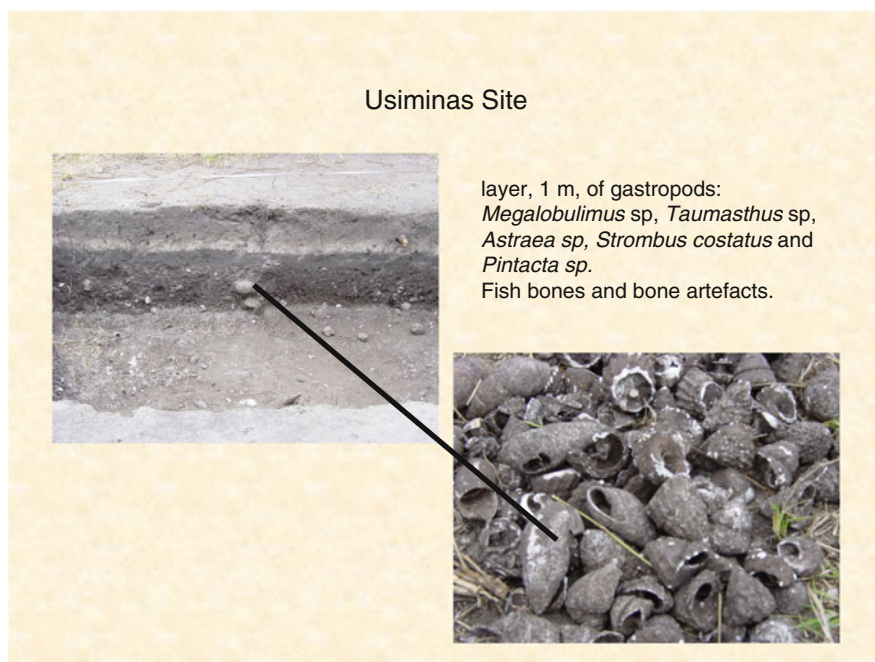


Fig. 2 Section of the Usiminas site, located at the Ilha do Cabo Frio, in a flat area, on an eolian dune 53 m above sea level. Notice the easily distinguishable layers; one layer dominated by gastropods, with fish bones and bone artefacts

by *Taumasthus sp* and *Megalobulimus sp*, terrestrial gastropods, not usually present in coastal sites with thick malacological layers.

There are also similarities in the occupations of Ilha Grande and Arraial do Cabo, such as: presence of burials associated to big rocks, diversity of positions and orientations where human remains were buried; presence of many kinds of funerary implements and hearths with food around the human remains.

There are also differences between settlement patterns of the two different areas: in Ilha Grande, occupations are more concentrated, while in Arraial do Cabo they are displayed around the area; in Ilha Grande, the occupation on the hill is more intense than on the dunes; in Arraial do Cabo, the opposite happens; Arraial do Cabo presents sites in high areas, above 50 m, quite different from Ilha Grande. Arraial do Cabo presents a dry weather with low annual precipitation while in Ilha Grande there is a high pluviometric level. In the island, there are many fixed sharpener-polishers (42), opposite to Arraial do Cabo, where there are only two, although the morphologies are similar.

The presence in one site at Arraial do Cabo (site Ponta da Cabeça) of two artefacts elaborated from *Haemulidae*, that represents 99% of the bone artefacts found at Ilha Grande, is remarkable, as well as the identification that around $2,830 \pm 50$ years BP, predominant malacological species in the Ponta da Cabeça site, such as *Olivancilaria auricalia* and *Astrea sp.*, begin to appear again in small amounts at Ilhote do Leste site (located at Ilha Grande). Data indicate an interaction between the occupants of Ilha Grande and Arraial do Cabo during the prehistoric settlement.

Based on these results, Tenório (2004) argues that sites located in Brazilian coast were constructed by people sharing a “shell mound culture” (“*cultura sambaqui-ana*”), characterized by a long-term knowledge of the techniques required to sea exploitation.

According to Tenório (2004), new habits brought by groups coming from the interior to the coast, probably along big rivers, were constantly being incorporated into this culture. Despite this intense contact and assimilation of new habits, sea culture didn't lose its supremacy till the arrival of ceramist groups, owing to technological knowledge to explore marine resources and also due to a well-structured cosmology, constantly reaffirmed in rituals involving concentration of people.

When Europeans arrived in Brazil in the sixteenth century, there were no more populations constructing shell mounds. The high density population identified in sites at Arraial do Cabo around 1,800 years BP and lack of sites with evidence of epidemics, scarcity of food or violence, may indicate that shell mound builders were forced to move by inland ceramic groups, provoking a concentration of people that could not be sustained by their traditional economic structure, causing the replacement of maritime economy by another one, based on plant domestication.

Acknowledgments The authors thank Brazilian agencies CNPq and FAPERJ for grants and financial support.

References

- De Blasis P, Fish P, Gaspar MD, Fish S (1998) Some references for the discussion of complexity among the sambaqui moundbuilders from the Southern shores of Brazil. *Revista de Arqueología Americana* 15:75–105
- De Blasis P, Kneip A, Scheel-Ybert R, Giannini PC, Gaspar MD (2007) Sambaquis e paisagem: Dinâmica natural e arqueologia regional no litoral do sul do Brasil. *Arqueología Suramericana* 3:29–61
- Gaspar MD (1998) Considerations about the sambaquis of Brazilian coast. *Antiquity* 72, n. 227:592–615
- Leonardos OH (1938) Concheiros naturais e sambaquis, Avulsos, Rio de Janeiro. *Serviço de Fomento da Produção Mineral* 37:1–109
- Tenório MC (1991) A importância da coleta de vegetais no advento da agricultura. *Dissertação de Mestrado*. Universidade Federal do Rio de Janeiro, Brasil
- Tenório MC (2003) O Lugar dos Aventureiros: identidade, dinâmica de ocupação e sistema de trocas no litoral do Rio de Janeiro há 3500 anos antes do presente. *Tese de doutoramento*. Brasil, Pontifícia Universidade Católica do Rio Grande do Sul
- Tenório MC (2004) Identidade cultural e origem dos sambaquis. *Revista do Museu de Arqueologia e Etnologia* 14:169–178
- Tenório MC, Pinto DC, Afonso MC (2008) Dinâmica de ocupação, contatos e trocas do litoral do Rio de Janeiro no período de 4000 a 2000 anos antes do Presente. *Arquivos do Museu Nacional, Rio de Janeiro* 66(2):311–321

Hydraulic Systems in the Po Plain (Northern Italy) During the Bronze Age: Archaeology and Geoarchaeology

M. Cremaschi and C. Pizzi

1 Introduction

During the Middle Bronze Age, north-western Europe and the western Mediterranean (Richard and Gautier 2007) appeared as a countryside landscape, spotted with small rural villages and cleared areas in a context of expanding woodland. The *Terramare* civilisation, characterised by large moated sites, surrounded by earth ramparts, developed during a period between 1600 and 1150 BC in the Po plain (Pearce 1998). Notwithstanding the firm cultural links between northern Italy and Europe during Late Prehistory (Barfield 1994), the *Terramare* culture promoted an extraordinary experiment in land management, based upon irrigative agriculture and sustained by an accurate exploitation of water resources.

2 *Terramare* and Water Courses

The *Terramare* are typical sites of the alluvial plain of the Po River; their strict connection with water courses had already been observed, but not fully understood, by nineteenth century scholars (Chierici 1871). More recent investigations, aimed at the study of the geomorphological context by means of remote sensing, have proven that most of the *Terramare* were systematically surrounded by moats supplied by springs or water courses (Cremaschi 1997; Ferri 1996; Balista 1997; Balista 2002).

Water management was not limited to the capture and adaptation of natural streams, but also encompassed the construction of artificial ditches and channels for irrigation. In the case of the Castello del Tartaro – Grandi Valli Veronesi – and in

M. Cremaschi (✉)

Dipartimento di Scienze della Terra “A. Desio”, Università degli Studi di Milano, Milano, Italy
e-mail: mauro.cremaschi@unimi.it

C. Pizzi

Dipartimento di Archeologia, Università degli Studi di Padova, Padova, Italy

several other examples (Balista and De Guio 1997; Cremaschi 1997), the irrigation channels were conducted outward from the moat of the site to distribute the water to cultivated fields.

The existence of a network of irrigation ditches originating from the moats demonstrates that the *Terramare* represented key locations in a man-made landscape, and that the moats surrounding the sites, aside from defensive purposes, were mostly planned for the collection and channelling of water, and for its redistribution to irrigate the fields (Balista and De Guio 1990–1991; Balista and De Guio 1997). This aspect was properly illustrated by a recent rescue excavation in the alluvial plain of Parma, at Cortile San Martino, which has unearthed, at shallow depth, a soil which was in use during the Middle and Early Bronze Age (Bernabò Brea et al. in press). On the surface of the soil, root casts have been found, surrounded by a concentration of charcoal, associated to very rare corroded small fragments of pottery, charcoals, and occasional faunal remains, probably related to soil manuring.

In spite of the scarce content of archaeological material, several archaeological features were discovered at the base of the soil, consisting of a network of artificial ditches associated with some wells reaching the local water table at a depth of about 3 m (Fig. 1). The ditches and related wells can be interpreted as a hydrological system meant to extract water from the subsoil, and to distribute it in the surrounding fields, demonstrating the emergence at this time of a practice of cultivating fields on the long term, as opposed to the short-term cultivations associated with the

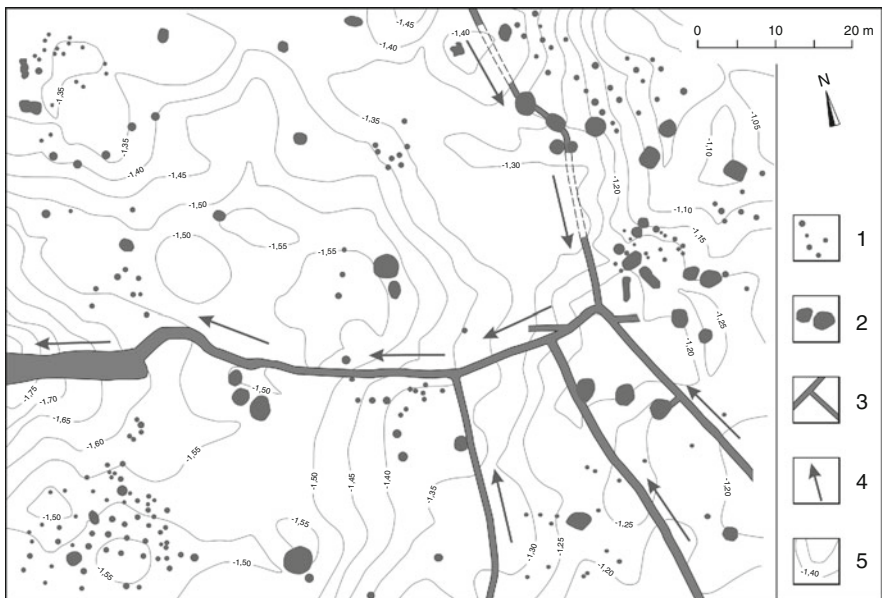


Fig. 1 Cortile San Martino (PR); the irrigation/drainage ditches on the early Middle Bronze Age soil: (1) post holes, (2) wells, (3) channels, (4) drainage, (5) contour lines; the elevation is recorded below the present ground level

slash and burn practices which were in use during previous periods. Aside from the hydrological structures, some post-hole concentrations have also been found at the location, which may be interpreted as small isolated buildings, possibly storage huts, while the rare sherds associated with this evidence are to be referred to the Middle Bronze Age, which represents the early period of the *Terramare* civilisation (Bernabò Brea et al. in press).

3 The Hydraulic Systems in the *Terramara* of Santa Rosa

The Villaggio Grande of the *terramara* Santa Rosa of Poviglio was built in the late Middle Bronze Age, according to a carefully organised urban plan (Bernabò Brea and Cremaschi 2004). The quarter of rectangular houses – as attested by the post holes – is delimited by a fence, outside of which there is a moat containing a rather complex system of hydraulic structures, all of which indicate particular care in processing the water source (Cremaschi et al. 2006) (Fig. 2). These structures changed their

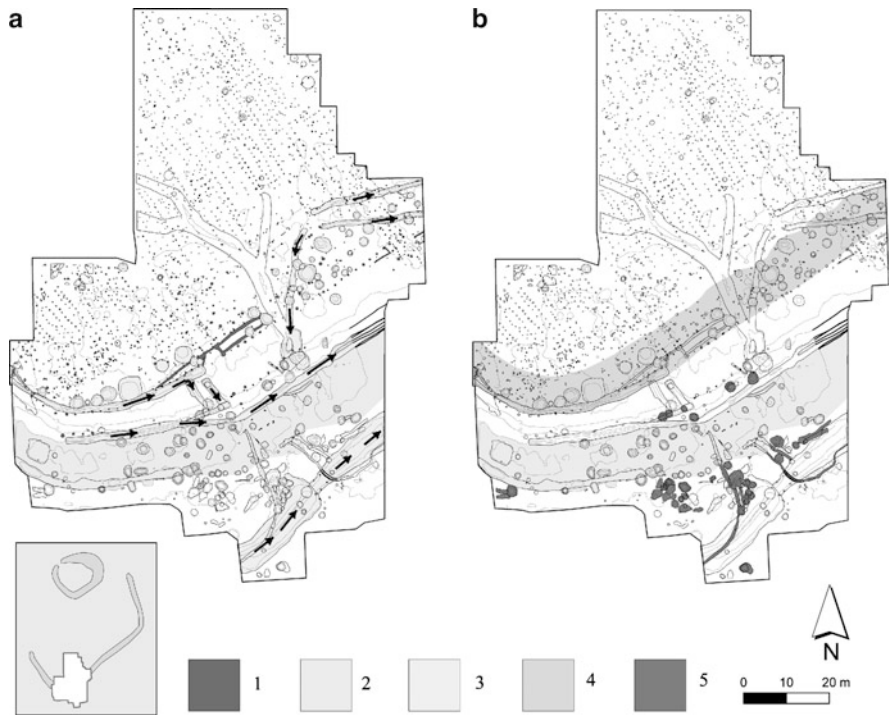


Fig. 2 Santa Rosa di Poviglio (RE), Villaggio Grande: 2007 survey. (a) the hydraulic system during the Recent Bronze Age; (b) the hydraulic system during the late Recent Bronze Age. (1) the door at the fringe of the village, (2) the moat, (3) channel and others hydraulic structures; *arrows* show the direction of the drainage, (4) the rampart during the Recent Bronze Age, (5) wells and channels during the late Recent Bronze Age

characteristics in time, as a consequence of the fluctuation of the water table, and indicate a reduction in terms of water availability towards the end of the period of occupation of the site (Cremaschi and Pizzi 2006), which was contemporary to the general collapse of the Terramare civilisation, around 1200 BC (Bietti Sestieri 1997; Bernabò Brea et al. 1997).

During its early phase (Fig. 2a), a large number of wells located on the fringe of the village (in coincidence with the fence) were dug to reach the water table, at a depth of three metres. They were kept in use for a long period of time and were re-excavated several times. The water extracted from them was not directed to the interior of the village: through a system of ditches, it was guided into the moat to flow into a channel excavated in its deepest part. The moat was rather large, but shallow and asymmetrical, steep and inaccessible at the inner bank, but smooth and gradual at the outer bank, as to permit access to the water from the countryside, which appears to be the real beneficiary for which the hydraulic system located on the fringe of the village was planned and constructed.

The fill of these water wells, clayey in texture, presents a complex stratigraphy consisting of organic material, laminated deposits and material fallen from the walls, which indicates that the wells collapsed and were re-excavated several times during the time they were in use. In the last phase, they were used as reservoirs and finally sealed by dump. The archaeological evidence found in them (Cremaschi et al. 2006) indicates that they were used for a long period of time, from the late Middle Bronze Age (about 1400–1330 BC), the period of the foundation of the Villaggio Grande, up to its apogee, in the Recent Bronze Age (1330–1170 BC).

Outside the moat, a large canal has been recently discovered. While its function is still unknown (it was probably meant to connect the moat to the adjoining palaeochannel of the Po River), its large size (6 m in width, 2 m in depth) and the sophisticated knowledge in hydraulic engineering required for this construction make it the first archaeological proof of large-scale water management during the Bronze Age.

During the last phase of the village (Fig. 2b), which has been dated on the base of the archaeological content to the late Recent Bronze Age, the wells of the fence and the canal were deactivated, and the flow inside the moat interrupted. Consequently, a large number of new wells were excavated, in a very short time, in the bottom of the moat. The dramatic need to find water is further attested by some superposed wells, the deepest of which is also the last to have been dug, indicating that they were frequently deepened with the purpose of following the descending water table. The water table that the wells in the moat sought to reach lies 5 m under the present surface, two metres deeper than the aquifers exploited by the wells of the fence during the early Recent Bronze age. This difference indicates an important drop of the aquifers in the last phase of the village, probably as a consequence of a dry period. The wells are surrounded by reservoirs connected by small ditches, allowing the available extracted water to be used on the spot; for instance, to water a flock descending into the moat.

4 Conclusive Remarks

The *Terramare* culture represented a unique experiment, while unsuccessful, in the context of the European Bronze Age. The people of this culture produced a systematic and intensive exploitation of the environment, quite early for northern Italy, characterised mainly by intensive agriculture and water management.

The moats surrounding most of the sites were probably conceived to concentrate water and redistribute it to the surrounding countryside through a network of irrigation ditches. The hydraulic system discovered on the fringe of the *terramara* of Santa Rosa suffered a clear drop in the level of the water table during the late Recent Bronze Age, and, in the final phase of occupation of the site, coincided with the abandonment of all the sites in the *Terramare* region. As the level of the local water table is strictly connected with the flow of the Po River, which is the main hydrological collector of a considerable part of the rivers and streams in northern Italy, the dry event observed in Poviglio is likely to have had at least a regional relevance. It may have played a role in the abandonment of the Santa Rosa site, and in the more general crisis of the *Terramare* system as well.

As water resources were strategic to supporting the agriculture on which the subsistence of the *Terramare* civilisation was based, it is not unrealistic to assume that a drop in water availability in a context of over-exploitation of resources and uncontrolled demographic pressure (and possibly other historical factors) may have represented the main factor in this specific case of civilisation collapse (Cremaschi et al. 2006).

References

- Balista C (1997) Fossati, canali e paleoalvei: connessioni nevralgiche per l'impianto e la sopravvivenza dei grandi siti terramaricoli di bassa pianura. In: Bernabò Brea M, Cardarelli A, Cremaschi M (eds) *Le terramare. La più antica civiltà padana*. Electa, Milano, pp 126–136
- Balista C (2002) La paleoidrografia dell'area terramaricola centro-padana verso la fine dell'età del Bronzo: inquadramento stratigrafico, cronologico e paleoclimatico. *Quaderni della Bassa Modenese* 42:7–48
- Balista C, De Guio A (1990) Il sito di Fabbrica dei Soci (Villabartolomea, VR): oltre la superficie. *Padusa* 26–27:111–117
- Balista C, De Guio A (1997) Ambienti ed insediamento nell'età del Bronzo nelle Valli Grandi Veronesi. In: Bernabò Brea M, Cardarelli A, Cremaschi M (eds) *Le terramare. La più antica civiltà padana*. Electa, Milano, pp 137–170
- Barfield L (1994) The Bronze Age of Northern Italy: recent work and social interpretation. In: *The Mediterranean Cultures during the Bronze*. In: Mathers C, Stoddart S (eds) *Development and decline in the Mediterranean Bronze Age*, Sheffield Archaeological Monographs 8. Collins J. R. Publications, Sheffield, pp 129–144
- Bernabò Brea M, Cardarelli A, Cremaschi M (1997) Il crollo del sistema terramaricolo. In: Bernabò Brea M, Cardarelli A, Cremaschi M (eds) *Le terramare. La più antica civiltà padana*. Electa, Milano, pp 745–756

- Bernabò Brea M, Cremaschi M (2004) La terramara di Santa Rosa di Poviglio nel corso del Bronzo Recente. In *Atti del Convegno L'età del Bronzo Recente in Italia (Lido di Camaiore 26–29 ottobre 2000)*, pp 101–111
- Bietti Sestieri AM (1997) Il territorio padano dopo le terramare. In: Bernabò Brea M, Cardarelli A, Cremaschi M (eds) *Le terramare. La più antica civiltà padana*. Electa, Milano, pp 757–772
- Chierici G (1871) *Le antichità preromane della provincia di Reggio nell'Emilia*, Reggio Emilia. Tipografia Artigianelli, Reggio Emilia
- Cremaschi M (1997) Terramare e paesaggio padano. In: Bernabò Brea M, Cardarelli A, Cremaschi M (eds) *Le terramare. La più antica civiltà padana*. Electa, Milano, pp 107–125
- Cremaschi M, Pizzi C (2006) I pozzi perimetrali del Villaggio Grande di Santa Rosa di Poviglio (RE). Uso delle risorse idriche tra la fine del Bronzo Medio e il Bronzo Recente, In *Studi di protostoria in onore di Renato Peroni*, Firenze, All'Insegna del Giglio, 50–61
- Cremaschi M, Pizzi C, Valsecchi V (2006) Water management and land use in the terramare and a possible climatic co-factor in their collapse. The case study of the terramara S. Rosa (Northern Italy). *Quat Int* 151:87–98
- Ferri R (1996) La fotografia aerea in zone di bassa pianura: iconografia analitica delle tracce fluviali ed evoluzione idrografica delle Valli Grandi Veronesi, In *La ricerca archeologica di superficie in area padana*. AGS Edizioni, Padova, pp 25–33
- Pearce M (1998) New research on the terramare of northern Italy. *Antiquity* 72:743–746
- Richard H, Gautier E (2007) Bilan des données pollinique concernant l'Âge du Bronze dans le Jura et le Nord des Alpes. In: Richard H, Magny M, Mordant C (eds) *Environnements et Cultures à l'Âge du Bronze en Europe occidentale*. Comité des Travaux Historiques et Scientifiques, Paris, pp 71–88

Cultural Landscapes of South-Eastern Rhodope: The Transition from Byzantine to Modern Times

M. Kampa, M.K. Sioliou, P. Kaparti, E. Tsirimona, and I. Ispikoudis

1 Introduction

The eleventh century AD monastery communities of the Papikion Mountain in Rhodope created cultural landscapes that reflect the traditional knowledge of a modern population. After the thirteenth century, monasteries began to decline, mostly due to fires. During post-Byzantine times, Papikion was not considered a monastic centre. However, the Islamized inhabitants of south-eastern Rhodope founded new settlements near the monasteries. The Pomaks, for example, are one of the few remaining traditional societies in Greece. They are part of the Muslim minority in Greece, as recognized by the Lausanne Treaty (1923). Pomak populations are also found in Bulgaria and Turkey. The historical origins of the Pomaks are obscure and there is little evidence about their evolution. Therefore, there are different “national histories” referring to them all over the Balkans.

The aim of this paper is to identify traditional practices in the cultural landscapes of the society of Pomaks in the area of south-eastern Rhodope, and to record the changes in the landscape.

2 Study Area

The study area is situated in Western Thrace. It comprises the mountainous area of the south-eastern Rhodope and covers around 13 km². It is situated at 25° 17' east longitude and 41° 13' north latitude. Its north-eastern end is located on the border between Greece and Bulgaria, while in the south-east it ends at the beginning of the Thracian plain (Fig. 1). The climate of the area is Mediterranean. The altitude varies

M. Kampa (✉), M.K. Sioliou, P. Kaparti, E. Tsirimona, and I. Ispikoudis
Laboratory of Rangeland Ecology (286), Aristotle University of Thessaloniki, 54124
Thessaloniki, Greece
e-mail: mariakampa97@hotmail.com

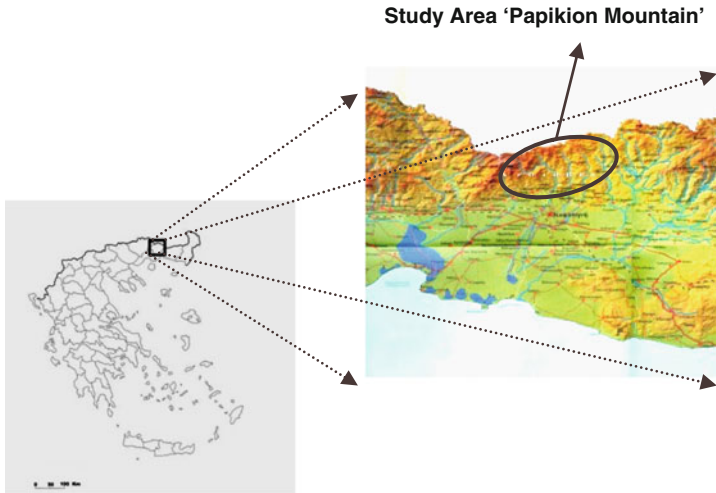


Fig. 1 Map of the study area

from 200 to 1,501 m. The morphology of the area is shaped by numerous river flows and slopes.

The Pomaks, an indigenous ethnic group from the mountains of Thrace, were selected for this study due to many reasons: first, they probably represent one of the last surviving traditional societies in Greece. This, in turn, is explained by the fact that they were almost completely isolated until the 1970s, due to historical and political reasons (Dalègre 1997). Even today, access to the Pomaks' villages is difficult. Pomaks still identify themselves as "mountain people" and carry out traditional practices, such as pollarding, shredding, multi-cultures, apiculture and semi-transhumance, conserving their unique landscapes (natural and cultural). Place names indicate the uses and functions of the areas. Customary law dictates the rights of each family. Lastly, their society is a characteristic example of how cultural landscapes associated with traditional practices can easily disappear because of modern management and social changes.

3 Methodology

In order to identify and record the changes in the cultural landscapes, data were gathered from different sources. Interviews with the majority of the Pomak population were conducted in the study area, with the help of a translator for both Pomak language and Turkish. More importance was given to the elder shepherds and farmers, since their testimonies were particularly valuable for recording traditional practices. The fieldwork covered the entire study area. Because the area is not

accessible during winter, fieldwork took place during the spring and summer, from 2003 to 2007. The main sources of statistical data were the National Statistical Service of Greece (N.S.S.G.) and the Forestry Service.

4 Results and Discussion

From the Byzantine era and until the 1970s, the mountainous area of south-eastern Rhodope represented the background for the creation of various cultural landscapes. The organization of spaces and of the vegetation is structured by the presence and the different functions of vegetal species and artefacts. Also, the successive producers of these landscapes – though with different cultural identities, first Christians (monks) and then, since the sixteenth century, Muslims – acted within a continuous historical and ecological framework. They preserved some basic landscape structures, adapting them to their cultural reality. Consequently the area is characterized by unity and continuity.

According to historical evidence, the first inhabitants of Mount Papikion were monks: historians' references to the numerous monasteries in the area date back to the twelfth century AD. The first establishment on the mountain dates back to the Iconomachy period (726–843 A.D.), when the icon worshipers took to mountainous areas far from the urban centres, where icon worshiping had been forbidden (Asdracha 1976; Papazotos 1980). The etymology of the place name “Papikion” probably derives from the term “pappos”, which in Greek means elder/monk.

The inhabitation of Mount Papikion primarily by anchorites and later on, the development of the monastic centre, can be explained on the one hand by the proximity to the Via Egnatia, that was revived as a key road of the Byzantine Empire since almost all Byzantine overland trade with western Europe traveled along the Via Egnatia, and on the other hand by the abundance of natural resources. The monasteries that were excavated or that are still visible as ruins are all located near water springs, either ravines or rivers. The monks had benefited from the water supply, using it for the operation of watermills and other buildings whose operation relies on water (baths, water towers, cisterns). Furthermore, the rivers supplied the monastery communities with Lenten food, fish and oysters.

It seems that after the destruction of the monasteries during the sixteenth century, the local Islamized people developed their villages or settlements on or near former monastery complexes. An abandoned settlement was called Chotzalar (hoca), meaning clergymen or priests, the Greek name for which was Monachoi (monks). These names indicate the subsequent use of the place. Six kilometres from today's village of Linos, the excavations brought to light a monastery complex; also, slightly higher up, in the location now known as Kilise Dere, a cistern and a watermill were found. In Turkish, Kilise means temple, church, while Dere means brook, rill. This latter name of the area reveals the subsequent use of windmills and cisterns, which were part of the previous monastery complex (Zikos 2001).

Three kilometres northward of the village of Sostis (=Saviour), during the excavations made by Zikos in 1983, a second monastery complex, and, slightly further to the north, between the settlements of Kerasia and Sostis, the nave and aisles of what was probably a third monastery were also found. During the same excavations, other two naves and aisles were brought to light, south-west of the settlement of Vronti, while in the south-eastern part of the area, Byzantine baths were found. The proximity of the Byzantine monuments both to the villages of Sostis and Linos and/or to other settlements is an example of the later establishment of settlements on or near monastery complexes. It is important to note that today's location of Linos is recent: the old Linos – known as Kiouplou or as Eski Kiouplou – is situated at a higher altitude, exactly next to the Byzantine monastery complex of Linos.

The majority of the local names are related to vine: “Linos” is “wine-press” in Greek, while Kiouplou (küplü) can be rendered into Greek as the “cheap wine shop” and Eski Kiouplou as the “old wine shop” (Eski = old, ancient) (Tunkany and Karatzas 2000). The name of Eski Kiouplou changed in 1967 to Palaiochori (=old village). Kiouplou exists up to date, as the village “was transferred” towards the lowlands at the beginning of the twentieth century.

Most monuments have been found in areas where remnants of vine and wheat cultivations had been noticed. However, the reforestations in the 1980s have covered pastures used by Pomaks, as well as lands where firewood had been gathered by the monks, and then by Pomaks, for the operation of the baths. These days, landscape units covered by these cultivations still exist, although the majority of them are on the verge of abandonment.

Only remnants of agroforestry systems related to vine cultivation were found. There are descriptions of how to use trees to support vines, reported as *anaden-drades ampeli* (=vines on trees), during classical times and in the Byzantine period, or as *ypoklima dendra* (=under-vine trees), in the Byzantine period and later (Delivoria 2002). According to the inhabitants of the area, this used to be a common form of multi-culture. However, it is important to note that, despite the fact that Muslims preserved the cultivations and traditional practices, the use of certain products was diversified due to their religious beliefs. Instead of producing wine, they produced *petmez* (treacle). Traditional techniques like pollarding and shredding continued to be used until their prohibition by the Forestry Service (Venetis 1985). The technique of pollarding certainly dates back to antiquity, given that it is mentioned by Theophrastus (Zaharis 1977).

The shortage of available space led the monks to build terraces, which were later used by the Pomaks. The terraces were constructed with stones (dry walls), collected from the river or the field itself. Today there are only few terraces left, mostly used for corn cultivation, or as pastures. In the past, terraces served as the ideal terrain for the agro-silvo-pastoral system (Fig. 2). Trees served not only as a source of forage, but also as espalier for the vine, planted around the fence.

Emigration was the main reason for the population decline in the study area. According to the N.S.S.G. (1961; 1971; 1981; 1991), the population in this area declined by 27.5% from 1951 to 1991. This change affected the mountainous villages



Fig. 2 Terraces with pollarded trees supported by dry stones

much more than the semi-mountainous ones. The number of sheep, goats, poultry and beehives in the area increased from 1961 to 1991, while the number of cattle, buffalos, mules and horses decreased.

Moreover, the area available for pasture has decreased, due to interdictions by the Forestry Service. During the interviews, all the remaining inhabitants of the villages strongly disagreed with the management of the Forestry Service, claiming their opinion was never asked and that they were gradually deprived of access to the forest.

5 Conclusions

The landscapes of the study area are the results of a complex religious, rural and ecological history. They are cultural landscapes, deriving both from human exploitation and ecological factors.

The main reason for the establishment of the monks on Mount Papikion was the availability of natural resources. The monastic centre formed the landscapes, by cultivating the land, creating terraces for vineyards and other multi-cultivations, setting up agroforestry systems. The Islamization of the inhabitants of the region and the destruction of the monastic centre led to the creation of new settlements that took advantage of the already shaped landscape.

Reforestation, combined with social causes (emigration) led to a decrease in population and to a gradual abandonment of traditional practices. The registration and evaluation of these cultural landscapes is urgent for many reasons. Not only they present ecological and economic advantages, but they also bear a high historical and cultural value, as relics of traditional landscapes. The key to the preservation of cultural landscapes are their creators: the local populations.

Acknowledgements This research was funded by the research program Pythagoras II-Environment, partially funded by the EU.

References

- Asdracha C (1976) Les Rhodopes au XIV^e siècle: Histoire administrative et prosopographie. *Revue des études Sud- Est Européennes* 34:175–209
- Dalègre J (1997) *La Thrace grecque: populations et territoire*. Paris: Ed. l’Harmattan
- Delivoria V (2nd edn) (2002) *Phytologion. Bank of Attica “Militos”*, (in Greek). Genus Press Ltd, p 347
- N.S.S.G. (National Statistical Service of Greece) (1961, 1971, 1981, 1991) *Katanomi tis ektaseos tis ellados kata basikes katigories gis* (classification of the Greek area into basic landuses). Athens
- Papazotos Th., (1980) *Pre-excavational Researches in Mount Papikion*. Thracian Annals, (in Greek)
- Tunkay F, Karatzas L (2000) *Turkish Greek dictionary*. Center of Eastern Languages and Culture, Athens, 865
- Venetis A (1985) *Forest management plan for forest area of Amaksades-Iasmos-Sostis- Asomatos, 1985–1994* (in Greek). Forestry Service Komotini, Komotini
- Zaharis SA (1977) *The forests of Crete from antiquity until today* (in Greek). Aspioti-ELKA, Athens
- Zikos N (2001) *Mount Papikion, Archaeological guide, Region and Regional bureau of Eastern Macedonia – Thrace*, (in Greek)

Part X
Metals and Metallurgical Ceramics
(Technology and Provenance)

XRF Analyses of Four Silver Gilded Hellenistic Epaulettes

E. Asderaki-Tzoumerkioti and A.G. Karydas

1 Introduction

The area today called Argitheia, in Karditsa territory, central Hellas (Greece), is located in the Pindos Mountains, where the ancient Athamanes used to live. In 1988–1989, excavation works were carried out in the eastern cemetery of the town. During these excavation works, 700 tombs were unearthed and more than 2,000 objects discovered (Chatziagellakis 2000). Among the finds, tomb 175 revealed a pair of silver gilded epaulettes (Fig. 1). They are longitudinal egg-shaped sheets, and one has embossed a head of Medusa covered with a gold leaf, while the other one has a thunderbolt.

A few years later, in 1995–1996, excavation works were carried out in the northern cemetery of ancient Demetrias, Magnesia. Demetrias was the second capital of the Macedonian Kingdom, one of the greatest economical centres of Thessaly, and the base for military and political control of the cities in southern Greece (Nikolaou 2000). During the excavation, 919 tombs were unearthed and 3,600 objects discovered. The cemetery was in operation from the Classical Age until Roman times. Here, we have also identified two similar silver gilded epaulettes (Fig. 2), which were found in tomb 419. They have the same shape as those from Argitheia, but are smaller in size. Both of them have embossed the image of god Eros.

This type of findings is not very common, and they might belong to special people. Although the objects originate from different sites, not close to each other, but however belonging to the wider area of Thessaly, we can assume that they are imported, and that they even originate from the same workshop, perhaps in Macedonia, as Thessaly was under Macedonian rule at that time. The epaulettes from

E. Asderaki-Tzoumerkioti (✉)
13th Ephorate of Prehistoric and Classical Antiquities, Athanassaki 1, 38222 Volos, Greece
e-mail: e.asderaki@gmail.com

A.G. Karydas
Institute of Nuclear Physics, NCSR “Demokritos”, 153 10 Aghia Paraskevi, Athens, Greece
e-mail: karydas@inp.demokritos.gr



Fig. 1 The two gilded epaulettes found in Argithea



Fig. 2 The two gilded epaulettes found in Demetrias

Demetrius were heavily corroded, as they were found in a location close to the sea, while the epaulettes from Argitheia are better preserved, as they were found at a remote site in the mountains. Both sites are dated to Hellenistic period.

2 Experimental

Macroscopic and non-destructive analyses were carried out for both sets of epaulettes using a stereomicroscope and a Portable X-ray Fluorescence (P-XRF) spectrometer (Karydas et al. 2004; Karydas 2007). The P-XRF spectrometer is composed of an Rh-anode side-window low power X-ray tube (50 Watt, 40 kV, 75 μm Be window), a PIN X-ray detector with 165 eV, FWHM at MnK_{α} , and 500- μm nominal crystal thickness, and a battery operated multichannel acquisition card. The element that represents the lower limit in the analytical range of the P-XRF spectrometer is aluminum ($Z = 13$). Two operational modes are implemented for optimum analytical and sensitivity performance: one “unfiltered”, with the high voltage set at 15 kV (for major and minor elements in samples of geological origin), and a “filtered” mode, with the high voltage set at 40 kV (for metal alloys and trace elements in samples of geological origin). In the “filtered” mode, the primary tube’s spectral distribution is modified by means of the insertion of a composite filter that reduces significantly the low energy bremsstrahlung continuum. For the proper alignment of the sample with respect to the exciting beam and the detector axis, two laser pointers were mounted in the spectrometer head in such a way as to allow for the intersection point of their beams to coincide with the cross-point of the X-ray beam and the detector axes, respectively. The beam spot at the sample position has a diameter of less than 3 mm. The quantitative analysis is supported by an in-house developed software based on first principles that describe the production of characteristic X-rays by an exciting polychromatic X-ray beam. Pure elements or compounds are used in order to deduce experimental calibration parameters, thus eliminating almost completely the inherent uncertainty in various atomic fundamental parameters, as well as the lack of precise description entailed by various instrumental and geometrical characteristics of the P-XRF spectrometer. The contribution induced by the secondary and ternary fluorescence enhancement processes to the fluorescence intensities is accounted for rigorously.

For the analysis of epaulettes, the P-XRF operational conditions were set as follows: 40 kV high voltage, filtered mode, and tube current of 50-100 μA . The silver alloy areas examined by the P-XRF spectrometer (four to five measurements per epaulette) were selected in such a way as to visually present the minimum surface alteration or gilding. Very few gilded areas presenting a rather good preservation state were also analysed. In the most of the silver alloy analyses, the detection of various amounts of Br indicated clearly the formation of a silver bromine layer of variable thickness. Furthermore, the copper peak intensity also showed significant variations among the positions analysed for each epaulette,

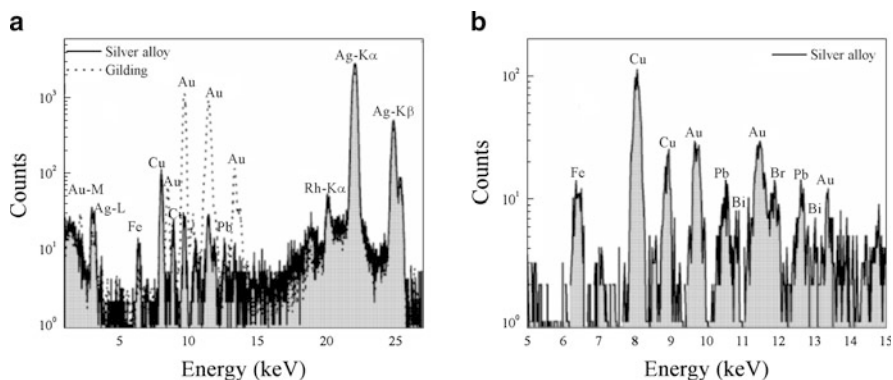


Fig. 3 (a) XRF spectra from the alloy and a gilded area of an Argithea epaulette. (b) Detail of the XRF spectrum from the alloy surface of an Argithea epaulette, indicating the detected minor elements in the alloy (Au, Pb, Bi)

possibly due to the formation of copper based alteration products in the respective areas. In both pairs of epaulettes, apart from Ag and Cu, minor amounts of Au, Pb and Bi were detected, associated with the raw mineral used for the processing and extraction of silver (Karydas et al. 2004). Two typical XRF spectra from an Argithea epaulette, from a gilded and an alloy area, respectively, are shown in Fig. 3.

It should be pointed out that the presence of gold could also be explained as a remnant of the gilding layer; however, its presence in minor amounts is rather common for a silver alloy, and it has been previously documented in the literature (Conophagos 1980; Williams and Ogden 1994). Few analyses of the silver alloy were selected for performing quantifications based on the absence of or minimum bromine signal, and of an Ag K/L intensity ratio that quantitatively resembled the respective ratio deduced experimentally for a pure silver target. Since even the criteria mentioned above do not ensure any homogeneity of the volume analysed by XRF, only indicative values or concentration ranges for the detected elements are reported.

3 Results

The copper concentration in the Argithea epaulettes is estimated to be in the range of 1–3%. In the case of the epaulettes from Demetrias, the copper content seems significantly higher, possibly due to the formation of copper based corrosion products. Gold and lead concentrations for both epaulettes range between 0.1 and 1%, whereas the Bi content is estimated to be below 0.1%.

An estimation of the thickness of the gilded layer was also carried out by evaluating the decrease of Ag-K α intensity from gilded areas of the two epaulettes (one from each pair). For the calculation, the geometrical parameters of the set-up were taken into account, whereas an effective excitation energy was introduced for the silver ionization in order to correct for the absorption of the exciting beam in the gilded layer. The thickness of the gold leaf in the Argitheia epaulettes was estimated to be $1.2 \pm 0.3 \mu\text{m}$, while in the ones from Demetrias $2.1 \pm 0.2 \mu\text{m}$.

4 Discussion and Conclusions

With regards to the gilding technique, the absence of mercury proves that the amalgam procedure was not used. Since the gold leaves were measured to be very thin, they could have been easily attached with organic glue directly onto the silver alloy surface; this method, however, does not provide durable gilding, because the adhesive is susceptible to biodeterioration (Oddy 1993). Another technique that could have been used is diffusion bonding, consisting of laying the gold leaf on the silver surface and then heating the object gently. This procedure produces an interdiffusion of the gold and the silver. The final step in this technique requires the burnishing of the gold leaf (Oddy 1993; Oddy et al. 1981).

The elemental patterns of the two pairs of epaulettes show similarities, in particular due to the presence of minor amounts of Au, Pb and Bi. For the Cu content, conclusions cannot be deduced with certainty. The fact that the epaulettes from Argitheia are soft might be explained by the rather small Cu concentration (1–3%); however, in any case, Cu seems to have been intentionally added in lesser or greater amount in both pairs of epaulettes. Indeed, if the copper content in native silver can range up to 1–2% (Ogden 1992), the usual concentration levels of this element do not commonly exceed 0.5% (Craddock 1995).

The application of P-XRF spectrometry was found useful for the non-invasive screening of the elemental composition of the silver alloy, for formulating hypotheses regarding the gilding technique(s), and for estimating the thickness of the gilded layer, thus supporting the conservation treatment. In the case of the epaulettes from Demetrias, for example, the gilded areas were covered by surface corrosion products and were not visible with the naked eye. Thus, a quick and not careful cleaning could have resulted in the loss of the remaining minute amounts of gold leaf. The portable XRF analysis was of great help in the identification of the gilded areas prior to any conservation treatment.

Acknowledgements We would like to thank L. Chatziagelakis, Director of the LD' EPCA, and E. Nikolaou, archaeologist of the AITHS, for providing us with the material for this study. Special thanks are due to Vicky Kantarelou, Institute of Nuclear Physics, NCSR "Demokritos", for her valuable help.

References

- Chatziagellakis L (2000) Works in the north-west part of Karditsa. In: Proceedings of the 1st Scientific Meeting, To ergo ton Eforion archaeotiton kai neoteron mnimion tou YPPO sti Thessalia kai tin evriteri periohi tis (1990–1998). (in Greek), Volos 2000. pp 381–394
- Conophagos CE (1980) *Le Laurium Antique*. Ekdotike Hellados, Athens
- Craddock PT (1995) *Early metal mining and production*. Edinburgh University Press, Edinburgh
- Karydas AG (2007) Application of a portable XRF spectrometer in the analysis of museum metal collections. *Annali di Chimica* 97(7):419–432
- Karydas A.G, Kotzamani D, Bernard R, Barrandon JN, Zarkadas Ch (2004) A compositional study of a museum jewellery collection (7th–1st BC) by means of a portable XRF spectrometer. *Nucl Instrum Methods B* 226:15
- Nikolaou E (2000) Excavation of the north cemetery of ancient Demetrias. In: Proceedings of the first Scientific Meeting, To ergo ton Eforion archaeotiton kai neoteron mnimion tou YPPO sti Thessalia kai tin evriteri periohi tis (1990–1998), (in Greek), Volos 2000. pp 309–314
- Oddy A (1993) Gilding of metals in the Old World. In: LaNiece S, Craddock P (eds) *Metal plating and patination: cultural, technical and historical development*. Butterworth-Heinemann, Oxford, pp 171–181
- Oddy WA, LaNiece S, Curtis JE, Meeks ND (1981) Diffusion bonding as a method of gilding in Antiquity. *MASCA Journal* 1(8):239–241
- Ogden J (1992) *Ancient jewellery*. British Museum Press, London
- Williams D, Ogden J (1994) *Greek gold: jewellery of the classical world*. British Museum Press, London

The Use of Industrial Computed Tomography in the Study of Archaeological Finds

A. Berdondini, R. Brancaccio, V. D'Errico, A. Miceli, M. Bettuzzi, F. Casali, M.P. Morigi, M. Senn, and A. Flisch

1 Introduction

The successful use of Computed Tomography (CT) as an efficient and powerful non-destructive tool for the study of archaeological artefacts has been reported by several authors (Rossi et al. 1999a, b; Rossi and Casali 2001; Applbaum and Applbaum 2005). The 3D reconstruction of the objects enables the archaeologists to carry out archaeological analyses; information about manufacturing and assembly techniques, as well as information useful for dating artefacts or determining the appropriate maintenance and restoration procedures can be obtained with this technique (Casali 2006). Most of the studies of archaeological artefacts reported in the literature are carried out using medical CT (Mazansky 1993; Anderson 1995; Allen 2007), whereas investigations performed with industrial CT systems are rather limited. The present study illustrates the results obtained with a high resolution CT system for industrial applications developed in our laboratories. The advantage of our system as compared to medical CT is the higher penetration capability that allows the investigation of high density objects. The system provides isotropic spatial resolution and fast data acquisition due to the cone-beam geometry employed. In this study, we have focused on demonstrating the potential of this procedure for extracting and analysing an item from a cluster. To this aim, we have investigated a ceramic vase with a diameter of 20 cm, filled with ancient coins.

A. Berdondini (✉), R. Brancaccio, V. D'Errico, M. Bettuzzi, F. Casali, and M.P. Morigi
Department of Physics, Università di Bologna, C.Berti Pichat 6/2, 40127 Bologna, Italy
e-mail: andrea.berdo@libero.it

A. Miceli
Department of Physics, Università di Bologna, C.Berti Pichat 6/2, 40127 Bologna, Italy
and
Empa – Swiss Federal Laboratories for Materials Testing and Research, Ueberlandstrasse 129,
8600 Duebendorf, Switzerland

M. Senn and A. Flisch
Empa – Swiss Federal Laboratories for Materials Testing and Research, Ueberlandstrasse 129,
8600 Duebendorf, Switzerland

2 Materials and Methods

In the framework of the European Project “DETECT” (New Product Design and Engineering Technologies Based on Next Generation Computed Tomography), the Physics Department of Bologna University has developed a detector with innovative characteristics, such as high spatial resolution and wide dynamic range. The resulting tomographic system is at present in operation at the Swiss Centre EMPA, and is mainly employed for industrial applications. Figure 1 shows an image of the developed tomographic system where it is possible to see all the main elements that constitute the system. The system consists of a 450 kVp X-ray tube, a manipulator, and a detector box composed by a scintillator and a CCD camera. The X-ray tube has a nominal voltage of 450 kV and effective focal spots of 5.0 mm (large focal spot) and 2.5 mm (small focal spot), respectively. The small focal spot was selected for performing the measurements presented in this study. The manipulator is able to move the object on four axes (three translation and one rotation axis) and is made of RHENOCAST mineral casting basis. The detector box is a structure which houses the mirror and the CCD camera. The CCD camera is further shielded by a shielding coffin. The visible photons enter the shielding coffin through a hole in which a lead glass can be inserted.

3 Results

In the present study, we have used this tomographic system to scan a ceramic vase filled with ancient coins. By means of CT, it is possible to create detailed cross-sectional images (slices) of an object, and these images can be fused together in order to obtain a 3D image. The 3D image can be analysed using specific software

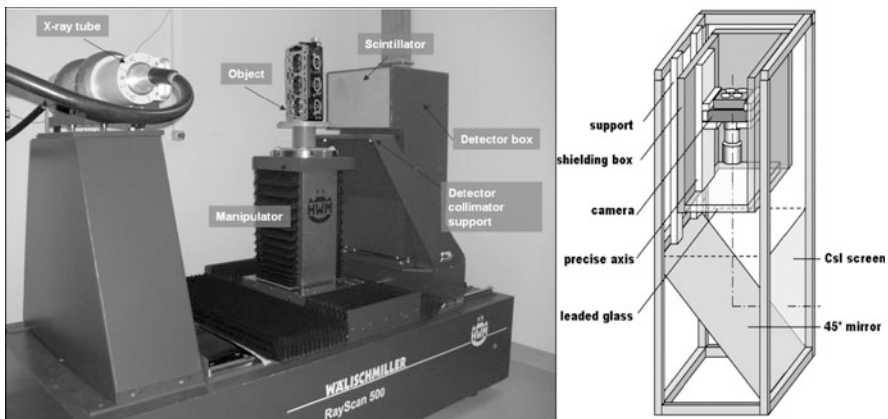


Fig. 1 On the *left*, an image of the CT system and on the *right*, a sketch of the detector box

and significant information can be drawn from the reconstructed image. The primary benefit of Computed Tomography lies in its ability to separate structures at different depths within the object. We have used this feature in order to extract and analyse an item (one ancient coin) from a cluster (ceramic vase filled with coins). Figure 2 shows several 3D CT images of the reconstructed object, where after different software manipulations it is possible to separate and extract one coin from the group.

With this type of procedure, it is possible to obtain a complete analysis of the scanned object and, due to the high resolution of the system, the details of the extracted coins are well-defined and it also becomes possible to see the inscriptions on the coins. All these pieces of information are useful for the restorer in order to identify the coins and to study their internal position within the object. Acquiring such information is of key importance for the restorer, in order to plan the extraction of the coins. Tables 1 and 2 report the parameters used during the acquisition and the reconstruction of the images; in order to have a high resolution, we used a small pixel size, with dimensions of 0.24 mm. The pixel size is the smallest element of an image that can be individually processed, and it is one of the most important parameters influencing the resolution of the system.

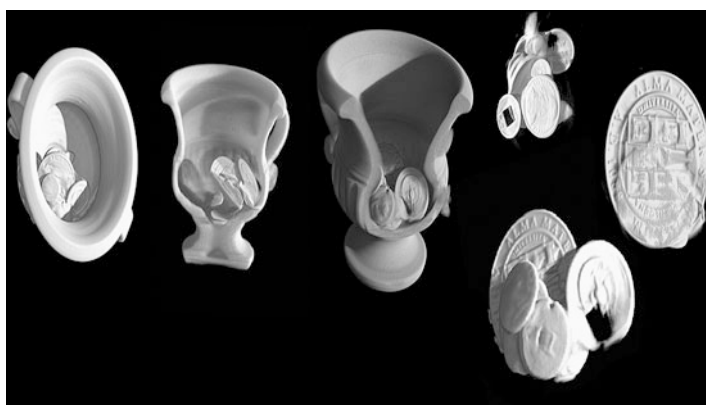


Fig. 2 Several 3D CT images of the reconstructed object (the ceramic vase and the ancient coins)

Table 1 Acquisition parameters

Focal spot	2.5
Number of projections	630
Filter	1 mm W
Pixels	2,184 × 1,472
Bits	12
Pixel size	0.24 × 0.24 mm ²
X-Ray tube voltage	450 kV
X-Ray tube current	5 mA
Acquisition time	132 min

Table 2 Reconstruction parameters

CT-filter	SHEPP-LOGAN
Volume	504 × 504 × 502 pixel
Voxel size	0.1339 × 0.1339 × 0.1339 mm ³

4 Conclusions

The excellent characteristics of the developed CT system made it possible to display the internal disposition of the investigated coins, confirming how an accurate analysis of archaeological finds can be carried out using this type of non-destructive technique. Due to the high spatial resolution provided by the CT system, it has been possible to read the inscriptions on the coins. Industrial CT appears therefore as a powerful non-destructive technique for the investigation of archaeological artefacts; in fact, the low energy source of the medical CT scanners can only be used on small objects. In conclusion, by using the developed industrial tomography system with high energy, it is possible to increase the dimension of the objects to be analysed and, at the same time, obtain high resolution images.

References

- Allen M (2007) Computed tomography of the Antikythera Mechanism. In: Proceedings of the 5th World Congress on Industrial Process Tomography. pp 29–37
- Anderson T (1995) Analysis of Roman cremation vessels by computerized tomography. *J Archaeol Sci* 22:609–617
- Applbaum N, Applbaum YH (2005) The use of medical computed tomography imaging in the study of ceramic and clay archeological artifacts from the ancient Near East, X-rays for archaeology. Springer, Heidelberg, pp 231–245
- Casali F (2006) X-ray digital radiography and computed tomography for cultural heritage. *Archeometriai Műhely* 1:24–28
- Mazansky C (1993) CT in the study of antiquities: analysis of a basket-hilted sword relic from a 400-year-old shipwreck. *Radiology* 186:55–61
- Rossi M et al (1999a) X-ray 3D computed tomography of bronze archeological samples. *IEEE Trans Nucl Sci* 46(4):897–903
- Rossi M, et al. (1999b) 3D computed tomography: a tool for analysis and conservation of archeological artifacts. In: 6th International conference on non-destructive testing and micro-analysis for the diagnostics and conservation of the cultural and environmental heritage, Rome. 17–19 May 1999
- Rossi M, Casali F (2001) 3D Computed Tomography for Archeometry. In: International Conference Archeometry in Europe in the Third Millennium, Rome. 29–30 Mar 2001

Arabic Coins as a Silver Source for Slavonic and Scandinavian Jewellers in the Tenth Century AD

N. Eniosova and R. Mitoyan

1 Introduction

It has long been known that during the Viking Age huge quantities of Islamic silver coins were exported from the Islamic world and deposited throughout European Russia, Ukraine, the Baltic lands and Scandinavia. A remarkable concentration of silver hoards was discovered at the Gnezdovo settlement, situated in the western part of Russia, along the river Dnepr, near the city of Smolensk. Two coin hoards and nine hoards of coins combined with ornaments were found at this important centre for merchants travelling between the Baltic and the Black Seas.

The hoards from Gnezdovo contain more than 1,100 Arabic coins. Samanid dirhams struck at the Samarkand, Shash, Bukhara, Andarabah, Balkh and Mádin mints in the first half of the tenth century AD are categorically prevalent in this selection. Abbasid and Buveihid coins, as well as Volga Bulgarian imitations, are very rare. The enormous wealth of Islamic silver in these assemblages provided us with a good opportunity to reveal some characteristic features for the chemical composition of the coins issued by the different Caliphate provinces during the ninth to tenth centuries, and evaluate them as a silver source for Slavonic and Scandinavian jewellers in the tenth century AD. By tracing the origin of the silver produced in the different regions and mine fields, we tried to analyse a series of coins with complete numismatic data, including the year and the place of issue, and the names of rulers.

N. Eniosova (✉)

Department of Archaeology, Moscow State University, Lomonosovsky prospect 27-4, 119992 Moscow, Russia
e-mail: eniosova@inbox.ru

R. Mitoyan

Department of Geochemistry, Moscow State University, Moscow, Russia
e-mail: mitoyan@geol.msu.ru

2 Methods of Investigation

Two hundred silver coins and 160 Slavonic and Scandinavian ornaments from the Gnezdovo deposits were analysed in the Moscow State Historical Museum and in the Golden Room of the Hermitage Museum in Saint Petersburg by a non-destructive method using portable ED XRF equipment. Calculation of the weight concentration of elements without standards has been carried out according to a method of fundamental parameters. Quantitative data were obtained for silver, copper, lead, gold, bismuth and mercury. Silver and copper were present in concentrations well above the detection limit in all analyses. Detection limits for gold, bismuth and lead were estimated to be 0.01% (Eniosova et al. 2002).

The surface corrosion and preferential loss of copper from the surface of silver objects present difficulties for non-destructive XRF. The consequent experimental abrasions and measurements of the metal of two unprovenanced dirhams with different silver fineness provided information on possible alteration of the results for pure and debased metal (Table 1).

The difference between metal surface and core is about 1% for fine silver and near 6% for debased silver. Despite the cleaning, gold and bismuth concentrations are almost the same. The concentration of lead increased by not more than 2%. The mercury detected on the surface of both samples was completely removed after abrasion. The presence of mercury in the Arabic silver coins possibly reflects one of the methods used to obtain silver, extracting the noble metal from slag and manufacturing waste (Craddock 1995).

In spite of the difficulties related to the surface enrichment, ED XRF provides useful information on the provenance of silver from different sources with different levels of impurities and trace elements.

3 Results and Discussion

3.1 Coins

For the most part of the selection, the minted silver was of a good quality (over 80% purity). There is a notable correlation between silver fineness and the mints.

Table 1 Surface and bulk silver composition before and after abrasive cleaning

Sample	Harun ar-Rashid, Ma'din as-Salam 798/99 AD		Nuch b. Nasr 943–954 AD	
	Before abrasive cleaning	After abrasive cleaning	Before abrasive cleaning	After abrasive cleaning
Ag	95.66	94.51	90.83	84.18
Cu	0.37	0.46	1.50	6.87
Pb	1.04	2.52	1.50	3.43
Bi	–	–	3.27	3.50
Au	0.6	0.67	0.46	0.42
Hg	0.25	–	0.32	–

A relatively high and stable concentration of silver was found for the mints of Andarabah. The most unstable and low silver concentrations are common for the coins struck in Shash and Samarkand.

This aspect suggests that galena or lead sulphide was one of the main sources of silver in the Islamic World. The argentiferous lead produced in the first smelting of galena would also contain some copper, bismuth and gold. Lumps of ancient unrefined silver found near the mines contain between 4 and 15% bismuth, which could be reduced only by repeated cupellation. However, this was not always carried out (Craddock 1995).

Laboratory experiments carried out by H. McKerrel and R. Stevenson revealed that copper, lead, tin and zinc were reduced or totally removed after extensive cupellation. Gold, on the other hand, survives cupellation completely. The bismuth content is unlikely to be reduced much below 1% by cupellation. Therefore, gold and bismuth seem to be the most appropriate elements for discriminating silver sources (McKerrel and Stevenson 1972).

M. Cowell and N. Lowick found that the silver minted in the Hindu Kush and derived from the Panjhir Valley galena deposits had a distinctive composition characterised by very low gold contents and relatively high bismuth contents (Cowell and Lowick 1988). However, the considerable recent contributions to the existing data show that some of the conclusions drawn on the basis of limited numbers of analyses may have to be revised.

The present study suggests that a high level of bismuth (above 0.1%) is detected in the coins struck in Transoxiana more often than in dirhams from the Hindu Kush region. The mints of Shash, Samarkand and Andarabah-Balkh issued silver coins with bismuth ranging from 0.5 up to 15% (Fig. 1).

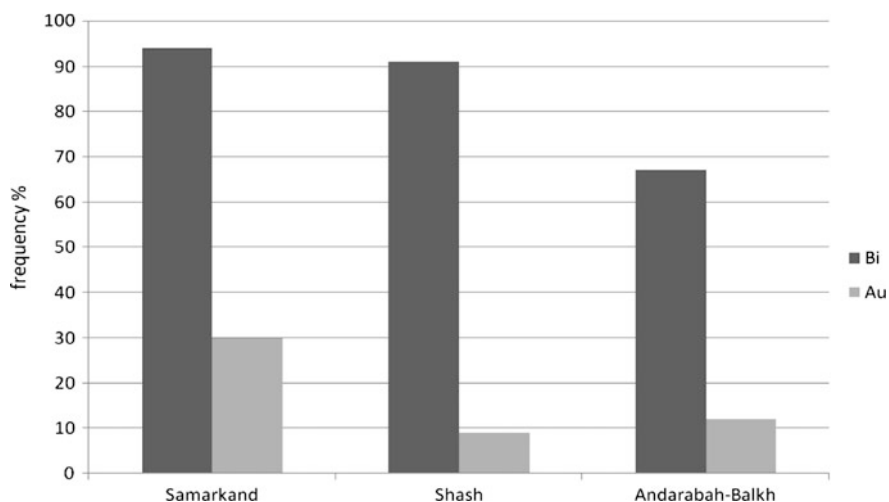


Fig. 1 Frequency distribution of bismuth and gold in the silver of coins (47, 55 and 24 coins were analysed from the Samarkand, Shash and Andarabah-Balkh mints, respectively)

Some coins from the two regions of the Eastern Caliphate contain relatively high gold concentrations. The most impressive results were obtained for the Samarkand selection. Fourteen of the 47 samples contain gold ranging from 0.3 up to 3%. This feature seems to indicate a possible separate silver source supplying a local mint.

Coins with a high content of bismuth, making the metal brittle, sometimes have broken edges and a rough surface with a grid of tiny wrinkles (Fig. 2a). However, the bismuth-in-silver ratio does not closely correspond to the quality of the coin. There are several fine coins with relatively high levels of bismuth (Fig. 2b).

Coin quality depends on dies or final polishing. Skilful coin makers were empirically aware of the difficulties inherent to this type of metal and used special methods of coin fabrication that reduced the dangerous influence of bismuth. More information about coin fabrication is provided by the Arabian writers. They describe the heating process applied before the steel stamp is pressed upon the dirham. The legends of those engravings appear on the coin clearly and correctly. According to the South-Arabian author al-Hamdani, the newly stamped coins were polished with a particular kind of sand, salt, and lastly with manure (Toll 1971).

Finally, the data obtained by the analyses of dirhams were supplemented by information from a geological survey in modern Uzbekistan. Rich argentiferous lead ores occur across an extensive area of Ilaq, known today as the Karamazar mining area, stretching over a huge distance within present day Tajikistan, Uzbekistan and Kyrgyzstan. Extensive archaeological excavations have revealed considerable evidence of silver extraction in the Ilaq region, including crashed ore, slag heaps, litharge, smelting ovens, cupels, and numerous tools of miners. This testifies to the broad scale of silver smelting in this area. The most impressive results were obtained for the Lashkerek mine, situated not far from the modern city of Tashkent. It was reported that 9,000 tons of slag containing 20% of lead were found here in 1929 (Masson 1953).

Geological research shows that the Lashkerek polymetallic ores are extremely rich in silver, containing sometimes about 3,000 ppm of silver. Native silver with 2% of copper and 0.1% of gold occurs as conglomerations of up to 1 cm in diameter, as well as thin veins and small disseminations in association with fahlore,



Fig. 2 (a) Nasr b. Achmad, Al-Shash, 938 AD (Ag 79.39%; Cu 9.7%; Pb 5.1%; Bi 5.81%); (b) Achmad b. Ismail, Balhk, 913 AD (Ag 96.04%; Cu 1.4%; Pb 1.38%; Bi 1.19%)

galena, sphalerite and bornite. Bismuth was also detected in all galena associations. Its quantity increases considerably with the depth of the mine. This aspect suggests that Lashkerek might be identified as the richest Kuchisim mine mentioned by Islamic Geographers (Dunin-Barkovsky 1959).

According to the Islamic writers, during the Samanid period, Central Asia was second only to the Panjhir region in silver production. It is clear today that the greatest part of the Samanid coins was issued by the mints of al-Shash and Samarkand using silver from the local mines. However, the silver dirhams declined in standard during the tenth and eleventh centuries over much of the Islamic World, from Spain to Central Asia (Steuer et al. 2002). The data chronologically arranged by mint over the period 892–953 AD shows a general downward trend from the middle of the tenth century. During the second half of the tenth century AD, the copper content reached 35–40%.

Apart from the economic and political reasons for this decline, a number of environmental problems were also influencing it, including the exhaustion of silver bearing ores, the almost complete depletion of the local forests, the lack of fuel, and the extreme depth of the mines. The depth of the Lashkerek mine in Uzbekistan reached up to 300 m (Buriakov 1974). Further mining operations were unlikely for technical reasons and also because of the high bismuth content in galena. Finally, the debased silver lost its value and the export of dirhams to Eastern and Northern Europe came to an end.

3.2 Jewellery

It is generally assumed that the most part of Viking Age jewellery was manufactured from Arabic silver. We tried to verify this hypothesis by comparing the silver content of the coins with that of the ornaments from the hoards found in Gnezdovo. A high quality of silver (over 90% Ag) was detected in the metal of the ornaments from the same hoards. Copper and lead contents of the objects are remarkably lower than the level found in coins. This indicates that silver cupellation was used in the workshops to produce jewellery. Nevertheless, the high bismuth content detected in the silver ornaments shows that Arabic coins were the main source of silver for Slavonic and Scandinavian craftsmen; this was detected in 65 of 160 samples. The bismuth concentrations in the ornaments are consistently lower than the concentrations found in coins. This feature also indicates the use of silver cupellation and the ability to control silver fineness. The silver content in the metal varies depending on the type of the ornaments. The lowest silver fineness is found in the cast and simply made jewellery, while the highest one is found in the ornaments with filigree and granulation.

We can thus conclude that analyses have shown that the situation under study here is quite complex. There appears to have been not only one source of silver for Scandinavian and Slavonic jewellery production in the tenth century. More information from trace-metal analyses is necessary. We hope that further projects aimed

at studying coins and other artefacts will help address the problems, questions and suggestions discussed in this paper.

Acknowledgments We would like to acknowledge the staff of the State Historical Museum, Moscow: Dr. Aleksej Fomin for his numismatic attribution, Dr. Natalia Nedoshivina and Svetlana Avdusina for their support in our study of the hoards. Dr. Rafail Minasyan from the Hermitage Museum in Saint Petersburg helped us to examine silver from the Golden Room. We wish to thank Dr. Tamara Pushkina from the Moscow State University for permission to study and publish the materials from her excavations in Gnezdovo. The English text was revised by Dr. Beate Reibold.

References

- Buriakov J (1974) Gornoe delo i metallurgija srednevekovogo Ilaka. Moscow, 110–112 (in Russian)
- Cowell MR, Lowick NM (1988) Silver from the Panjhir Mines. In: Oddy WA (ed) *Metallurgy in Numismatics II*. Royal Numismatic Society, London, pp 65–74
- Craddock PT (1995) Early metal mining and production. Edinburgh University press, Edinburgh, pp 214–221
- Dunin-Barkovsky RL (1959) K serebronostnosti mestorozdenija Lashkerek. *Uzbekski geologicheski zurnal* 2:62–67 (in Russian)
- Eniosova N, Koloskov S, Mitoyan R (2002) Application of non-destructive quantitative X-Ray fluorescent spectrometry to ancient non-ferrous alloys. In: Van Grieken R, Janssen K, Van't dack L, Meersman G (eds.) *Proceedings of 7th international conference on non-destructive testing and microanalysis for the diagnostics and conservation of the cultural and environmental heritage*. Antwerp, pp 1–6
- Masson ME (1953) K istorii gornogo dela na territorii Uzbekistana. *Izdatel'stvo akademii nauk UzSSR*. Tashkent, 24–32 (in Russian)
- McKerrel H, Stevenson RBK (1972) Some analyses of Anglo-Saxon and associated oriental silver Coinage. In: Hall ET, Metcalf DM (eds) *Methods of chemical and metallurgical investigation of Ancient Coinage*, Special Publications No 8. Royal Numismatic Society, London, pp 195–209
- Steuer H, Stern W, Goldenberg G (2002) Der Wechsel von der Münzgeld – zur Gewichtsgeldwirtschaft in Haithabu um 900 und die Herkunft des Münzsilbers im 9. Und 10. Jahrhundert, Haithabu und die frühe Städtenwicklung im nördlichen Europa. Neumünster, pp 143–145
- Toll C (1971) Minting technique according to Arabic literary sources. *Orientalia Suecana* 19–20 (1970–1971):125–139

Neutron-Based Analytical Methods for the Non-Invasive Characterisation of Iron Artefacts

E. Godfrey and W. Kockelmann

1 Introduction

Neutron-based methods can be used to characterise the bulk microstructure of archaeological iron and steel artefacts by completely non-invasive means. Time-of-flight neutron diffraction (ToF-ND) is a quantitative method that measures right through the thickness of an object, giving an average result. An entire object can be put in front of the neutron beam, in air, without any sample preparation. A far greater number of objects can thus be analysed than would ever be possible by traditional metallographic (i.e. destructive sampling) techniques. For this pilot study, only archaeological objects that were previously sampled for metallography are being analysed, along with bloomery iron and steel standards (Fig. 1). The ToF-ND work reported here is being carried out at the Isis Neutron Facility in the UK; the spectrographic analyses are being done at the Budapest Neutron Centre in Hungary. Imaging (radiography and tomography) of the objects will be done at SINQ in Switzerland (Paul Scherrer Institute, Villigen).

ToF-ND finds which metal, mineral, and intermetallic compounds are present in an object, down to a typical normalised fraction of around 0.5%. Average grain orientation can be seen in metals, allowing manufacturing techniques like casting and hammering to be identified and quantified. Quenching and tempering of steel can be detected as well, as these treatments produce distinctive changes in the neutron diffraction pattern (Fig. 2).

All of the material in the path of the neutron beam as it passes in one side and out the other side of an object is measured; corrosion products, both external and inside an object (i.e. inclusions, so long as they are present in sufficient volume to be detected), are thus analysed at the same time as the preserved metal. Each corrosion compound – e.g. magnetite, hematite, goethite – forms a separate mineral phase, which can be distinguished in the diffraction pattern. The volume of preserved metal that is present underneath the corrosion layers can be calculated. This

E. Godfrey (✉) and W. Kockelmann
STFC Rutherford Appleton Laboratory, Isis Neutron Facility, Harwell OX11 0QX, UK
e-mail: evelyn.godfrey@stfc.ac.uk

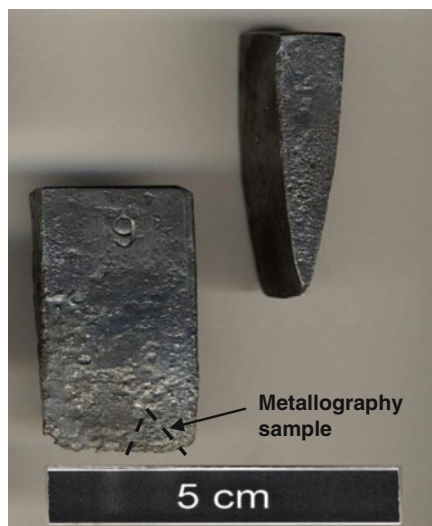


Fig. 1 Forged Bloomery Standard 9, which contained over 0.8 wt%C at the thin end of the wedge. White phosphorus-rich microstructures were visible as well. The authors analysed modern steel standards at ISIS, but the microstructures have little resemblance to archaeological bloomery iron. Iron was therefore smelted in an experimental bloomery furnace and a set of standards forged from the metal. The standards were then carburised to different extents following a steel-making procedure described in the Medieval text of Theophilus. The ToF-ND measurements were taken right next to the metallography sample-gaps. After sampling, the BS9 standard was quenched in water

information can be used in conjunction with radiographic imaging and tomography to assess the conservation state of the objects. It can also be extremely useful in selecting points for metallographic sampling if, for example, a large assemblage of objects is being examined, but destructive sampling can only be carried out on a very limited proportion, with just one or two sections cut from an individual object. Multiple data points can be collected by ToF-ND; this overcomes the interpretive problem of relying on a single small metallography section in order to characterise a whole – typically heterogeneous – ancient metal artefact.

2 Method

The pulsed thermal neutron beam used by the Isis diffractometers can be collimated to analyse a minimum volume of one cubic millimetre. Any crystalline material – metal, pigments, rock, ceramics – can be investigated by diffraction methods, and studies are being carried out by the authors on glassy materials as well (e.g. blast furnace slag). Neutron methods do not mark, heat, or alter the object. Iron containing carbon, phosphorus, and/or arsenic is not made radioactive by the neutron beam

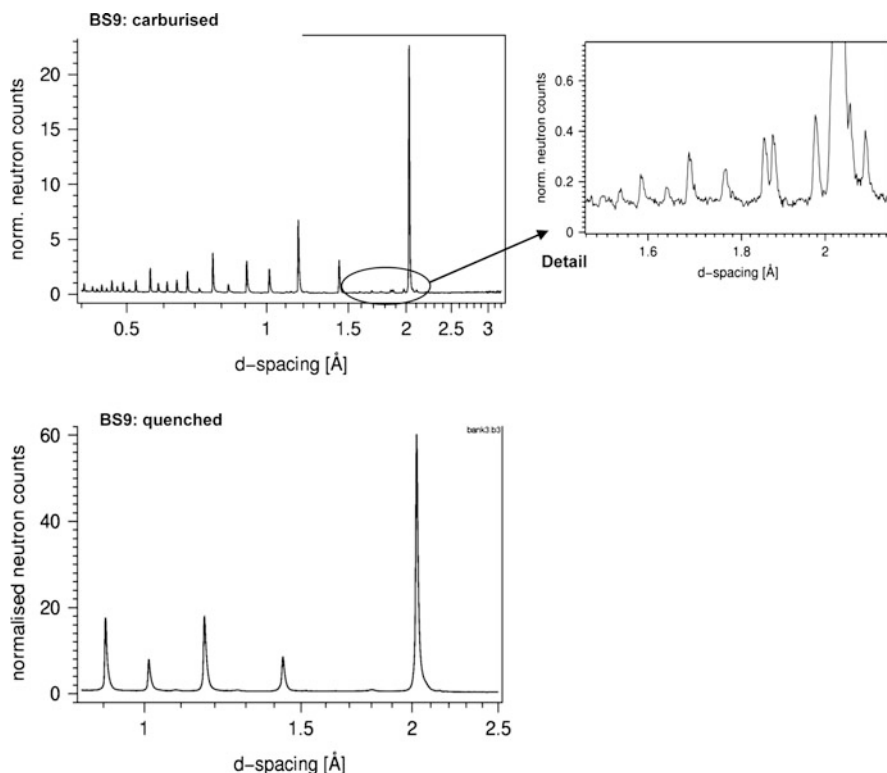


Fig. 2 Raw ToF-ND results for Bloomery Standard 9 (0.8–0.9% C), as carburised (*above*), and after quenching (*below*). Detail shows the characteristic double peak of cementite at 1.85 Å and 1.87 Å. The ToF-ND pattern after quenching shows martensite. The cementite peaks disappear in the “quenched” pattern. Martensite has a tetragonal crystal structure (as opposed to body-centred-cubic ferrite), but has major diffraction peaks in roughly the same positions as ferrite. Martensite can be measured by the distinctive broadening of the bases of the peaks seen here in the “BS9: quenched” pattern

at Isis. Manganese in iron can however be activated; after around two hours of exposure to neutrons, a manganese-containing sample might need two to three days before it can be handled. The manganese in high-Mn inclusions in archaeological iron can be activated by exposure on some neutron instruments (e.g. during prompt gamma activation spectrographic analysis at the Budapest facility), but the activation is low and very short-lived. Objects containing high-Mn slag inclusions have been measured by ToF-ND at ISIS, and no radioactivity was detected even immediately after analysis.

Multiple ToF-ND data points can be collected to produce a “map” of an object. The typical acquisition time on the ROTAX and ENGIN-X diffractometers at Isis is around 1 h per data point. The maximum dimensions of an object that can be analysed on ROTAX are 250 mm × 250 mm × 1,000 mm (height). ENGIN-X has a sample stage that can accommodate objects 1 m in width or depth, 3 m in height,

and one metric ton in weight. At Isis, ToF-ND data is normally processed using the GSAS programme (Larson and Von Dreele 1994), which is used to fit the diffraction peaks and perform Rietveld refinement.

Chemical concentrations can sometimes be calculated from ToF-ND data, by quantifying discrete phases. In steel for instance, carbon is present as an intermetallic compound, cementite (Fe_3C), that contains 6.7 wt% carbon. ToF-ND directly measures the amount of cementite in a volume of steel; this value is normalised and multiplied by 0.067 to find the bulk composition in terms of weight percent carbon. After carbon, phosphorus is the most common alloying element seen in iron that was made prior to the Industrial Revolution (Godfrey 2007). Phosphorus (and arsenic) phases are difficult to detect by ToF-ND, due to the low volume of these phases in typical bloomery iron objects. However, phosphorus in solid solution should in theory induce a shift in the ferrite peak position. When, for example, 1wt %P is present in solid solution, we can calculate that the measured ferrite lattice parameter value should change in the fourth decimal place. The authors are currently analysing phosphoric iron standards and archaeological objects by neutron and X-ray synchrotron diffraction in order to determine if such a small variation can indeed be measured. It is likely that segregated iron phosphide (as opposed to phosphorus in solid solution in ferrite) will not be visible by ToF-ND, due to the amount of this phase in the overall volume being so little.

3 Complementary Neutron Methods

Spatially-resolved elemental data can be acquired from objects using complementary non-invasive neutron-based techniques such as prompt gamma activation analysis [PGAA] (Molnár 2004) and neutron resonance capture analysis [NRCA] (Postma et al. 2004). PGAA is based on thermal and cold neutron capture using prompt gamma rays, which are measured in live-time, as opposed to the delayed measurement that is done with conventional instrumental neutron activation analysis. PGAA has high sensitivity for some light elements (e.g. H, B, Cl). The minimum volume that is usually analysed is a spot of 5 mm diameter. PGAA is best run on a continuous neutron source (i.e. at a reactor), although it is possible to build a PGAA set-up at a pulsed source such as Isis. NRCA on the other hand is based on higher energy epithermal neutron capture, and requires a pulsed source. NRCA has particularly good sensitivity for certain heavy elements (e.g. Au, As, Ag, Sb, Sn). The volume of material typically analysed by NRCA – with beam diameters of 50 to 70 mm – is much larger than with PGAA. However, the EU FP6 “Ancient Charm” Project has as one of its goals the development of a neutron resonance transmission detector that will allow the minimum volume analysed to be effectively reduced to 2×2 mm (Schooneveld et al. 2008). The Ancient Charm NRCA/NRT equipment development is planned for completion at Isis by mid-2009. Because of the different elemental sensitivities (with a number of overlaps), PGAA and NRCA can be usefully employed as complementary spectrographic techniques.

Work is currently underway to produce new instrument control and data visualisation software that will allow neutron diffraction and chemical analysis results to be integrated with tomographies and radiographies (whether X-ray or neutron). Neutron imaging detectors with a spatial resolution of 50–100 μm have already been developed; this is in the same range as current digital X-radiography. An advantage of the neutron-based method is the ability to do material phase imaging (by collecting radiographies at varying neutron energies), for example using the IMAT strain scanning and imaging instrument that is planned for development at Isis in 2009–2011.

4 Results

A series of modern engineering steel standards (compositions 1.1 wt%C; 0.9 wt%C; 0.8 wt%C; 0.5 wt%C; 0.4 wt%C; 0.2 wt%C; 0.1 wt%C) was analysed by ToF-ND, after metallographic sampling. The metal had been normalised from 800°C and was free from other alloying elements. The neutron diffraction results matched the expected carbon contents very closely: a composition of 1.1 wt%C was determined for the 1.1 wt%C standard; 0.9 wt%C for the 0.9 wt%C standard; 0.8 wt%C for the 0.8 wt%C standard; 0.4 wt%C for the 0.5 wt%C standard; 0.35 wt%C for the 0.4 wt%C standard; 0.2 wt%C for the 0.2 wt%C standard; and 0.03 wt%C for the 0.1 wt%C standard. The 0.1 wt%C and 0.9 wt%C standards were also found to contain minor amounts of austenite. The ToF-ND was performed with the large beamsize (10 × 10 mm × complete thickness of the object) that is possible when dealing with homogeneous materials.

It is clear that modern steel is quite different from the early iron and steel seen in the archaeological record. A second series of standards was therefore produced, by forging and heat-treating iron smelted in a charcoal-fuelled clay bloomery furnace (the smelting and smithing experiments will be described in Godfrey, Sauder and Williams, forthcoming). The ore used was phosphorus-rich goethite. A set of bloomery standards was made by Lee Sauder at Woods Creek Forge in Lexington, Virginia. The standards were analysed by metallography and scanning electron microscopy. All of the samples contained around 1 wt% phosphorus in heterogeneous solid solution. The highest carbon sample (0.8/0.9 wt%C) also had a very small volume of segregated phosphorus-rich phases. The bloomery standards were all ferrite to begin with; several were then carburised by smearing in fat, wrapping in leather, and heating with charcoal powder in a hearth for varying lengths of time at yellow heat. After metallographic sampling and ToF-ND analysis, the highest carbon standard was quenched in plain water from a bright orange heat. Two further high-carbon standards were produced for quenching in brine and oil. After sampling and ToF-ND analysis, the water-quenched sample was tempered and re-sampled.

ToF-ND of the bloomery standards on the ROTAX diffractometer confirmed the carbon contents: for example, the 0.8/0.9 wt%C bloomery standard gave a ToF-ND

result of 0.9 wt%C over the first 2.5 mm in from thin end of wedge and 0.7%C over first 5 mm; the 0.2 wt%C bloomery standard gave a ToF-ND result of 0.3 wt%C over first 2.5 mm and 0.2%C over first 5 mm; and Bloomery Standard 7, which metallography showed consisted of ferrite with a large area of fayalite and wüstite slag on the surface, gave a ToF-ND result of ferrite with 11% fayalite and 3% wüstite over the first 5 mm. The quenched high-carbon piece (Bloomery Standard 9) was solid martensite over the first 5 mm in from the edge (Fig. 2).

Several Late Roman-Iron Age and Early Medieval iron and steel objects (some high in phosphorus) that had already been sampled destructively are being analysed by ToF-ND, metallography and scanning electron microscopy as well. The carbon contents of the preserved metal areas in the objects have been successfully quantified by ToF-ND, the corrosion layers characterised, and cases of extreme cold-working distinguished (Godfrey and Kockelmann, forthcoming).

5 Conclusions

Modern steel and experimentally produced bloomery standards, along with a number of archaeological iron objects, have now been analysed by ToF-ND at Isis. This work has established that carbon contents and average bulk microstructures can be accurately measured in corroded, intact archaeological iron and steel objects without the need to remove a sample. Chemical analyses are being done on the same objects and standards now by PGAA and NRCA. This data will be combined with tomographic imaging (with neutrons and X-rays), with the aim of characterising the materials and manufacturing technology of a group of Early Medieval swords and knives. This non-destructive neutron-based methodology, combined with conventional typological studies and, where available, comparative metallographic data, presents the prospect for many larger-scale archaeometallurgical applications.

References

- Godfrey E (2007) The technology of ancient and medieval directly reduced phosphoric iron. PhD thesis, University of Bradford
- Larson AC, Von Dreele RB (1994) General structure analysis system (GSAS). Los Alamos National Laboratory Report LAUR; 86-748
- Molnár G (ed) (2004) Handbook of prompt gamma activation analysis. Springer, Heidelberg
- Postma H, Schillebeeckx P, Halbertsma RB (2004) Neutron resonance capture analysis of some genuine and fake Etruscan copper alloy statuettes. *Archaeometry* 46(4):635-646
- Schooneveld EM, Nakamura T, Rhodes NJ, Kockelmann WA, Tardocchi M, Perelli-Cippo E, Gorini G, Schillebeeckx P, Postma H (2008) NRT: a non-destructive bulk elemental analysis technique. Presented at the 37th International Symposium on Archaeometry, Siena. May 12th-16th, 2008

Corrosion Studies and Lead Isotope Analyses of Musket Balls from Scottish Battlefield Sites

A.J. Hall, R. Ellam, L. Wilson, T. Pollard, and N. Ferguson

1 Introduction

The recovery and analysis of musket balls and other lead projectiles, with a particular focus on their morphology and distribution in the ground, is an important aspect of seventeenth to nineteenth century battlefield archaeology (Pollard and Oliver 2003). However, one factor significant to the analysis of musket balls has not been given due attention by archaeologists, namely the sourcing of lead for their manufacture. Lead isotopes provide a means of characterising sources of lead (Pollard and Heron 1996) and although there have long been concerns about the use of this technique in archaeology, especially in relation to mixing of metal sources (Knapp 2000), this method does offer the potential of characterising the nearly pure lead found in musket balls. The technique may therefore have an important role to play in the identification of specific sources of lead and thus provide a valuable insight into the supply of armies in the seventeenth to nineteenth centuries.

In any investigation of archaeological artefacts, scientific analysis must be undertaken with minimal destruction. The question therefore arose: Could lead isotope analysis be undertaken on the corrosion products thus minimizing the possibility of damage to the musket ball itself? Archaeological surveys carried out on two major battlefields of the Jacobite Risings in Scotland, Killiecrankie (1689) and Culloden (1746), have recovered significant numbers of musket balls, all of which show variable degrees of surface corrosion and are therefore ideal for

A.J. Hall (✉)

Department of Archaeology, University of Glasgow, Glasgow, UK
e-mail: a.hall@archaeology.arts.gla.ac.uk

R. Ellam

Scottish Universities Environmental Research Centre, East Kilbride, UK

L. Wilson

Technical Conservation Group, Historic Scotland, Edinburgh, UK

T. Pollard and N. Ferguson

Department of Archaeology, Centre for Battlefield Archaeology, University of Glasgow, Glasgow, UK

this research. Not only will this research provide an important insight into lead sourcing during this period but will also, through the studies in lead corrosion, extend our understanding of lead survival in soil. Metallic lead is unstable in soils (Tylecote 1983) and lead musket balls will gradually corrode and dissolve in soil water. Once corrosion is complete or nearly complete, the ability to detect a lead musket ball using a metal detector, the only practical means of undertaking a systematic distribution survey (Pollard 2009), may no longer be possible. This is a major issue, not just for archaeological research on battlefields, but one that concerns the management and conservation of battlefield heritage as a whole.

2 Background

The Battle of Killiecrankie, 1689, is famed in Scottish history as the first battle of the Stuart Risings. This was to end in Jacobite defeat nearly 60 years later at the Battle of Culloden, close to Inverness, in 1746 after a series of unsuccessful campaigns stemming from political and religious upheaval (Duffy 2003). Fought along the main communication route from Perth into the Highlands, and within the enclosing landscape of the Pass of Killiecrankie, an army of *c.*4000 Government soldiers was to be defeated by *c.*2000 Jacobites, (Scots and some Irish). Although the basket-hilted broadsword and the older claymore may have been the Jacobite weapon of choice, firearms would have been used on both sides, in particular the flint-lock musket which, by 1689, would have replaced the unwieldy and less reliable matchlock musket (Pollard and Oliver 2003). At Culloden two distinct calibres of musket ball could be identified, allowing for the Brown Bess musket, predominantly used by the Government army, and the smaller French muskets, used by the Jacobites, to be distinguished in the assemblage. The same distinction cannot be made at Killiecrankie, where more variation in size was observed, thus making it more problematic to identify Jacobite from “redcoat” using the musket ball assemblage ($n = 67$) alone.

It is likely that lead used for musket balls in these battles, with such wide political scope and support, came from mixed sources all over Europe. However, it is possible that some lead, especially that used by the Jacobites, came from special sources in Scotland (Fig. 1a); for example, Tyndrum which was exploited from 1741 and was captured in 1745 by Government forces (Wilson 1921); Strontian which was blockaded by the English navy in 1745 (Parsons 2008); and Leadhills/Wanlockhead where lead was recovered from at least the sixteenth century (Porteus 1876). Mining activity in Scotland was stimulated by exemptions from export duties on lead following the Union in 1707 (Downs-Rose 1994). While sourcing musket ball lead has thus far not been a major concern in historic battlefield research, the potential to identify some specific Scottish sources is important and stimulated this research project. It is particularly noteworthy that Tyndrum has been confirmed to have a distinctive lead isotope signature (MacKenzie and Pulford 2002) as the one result in the Rohl (1996) database indicates (Fig. 2b).

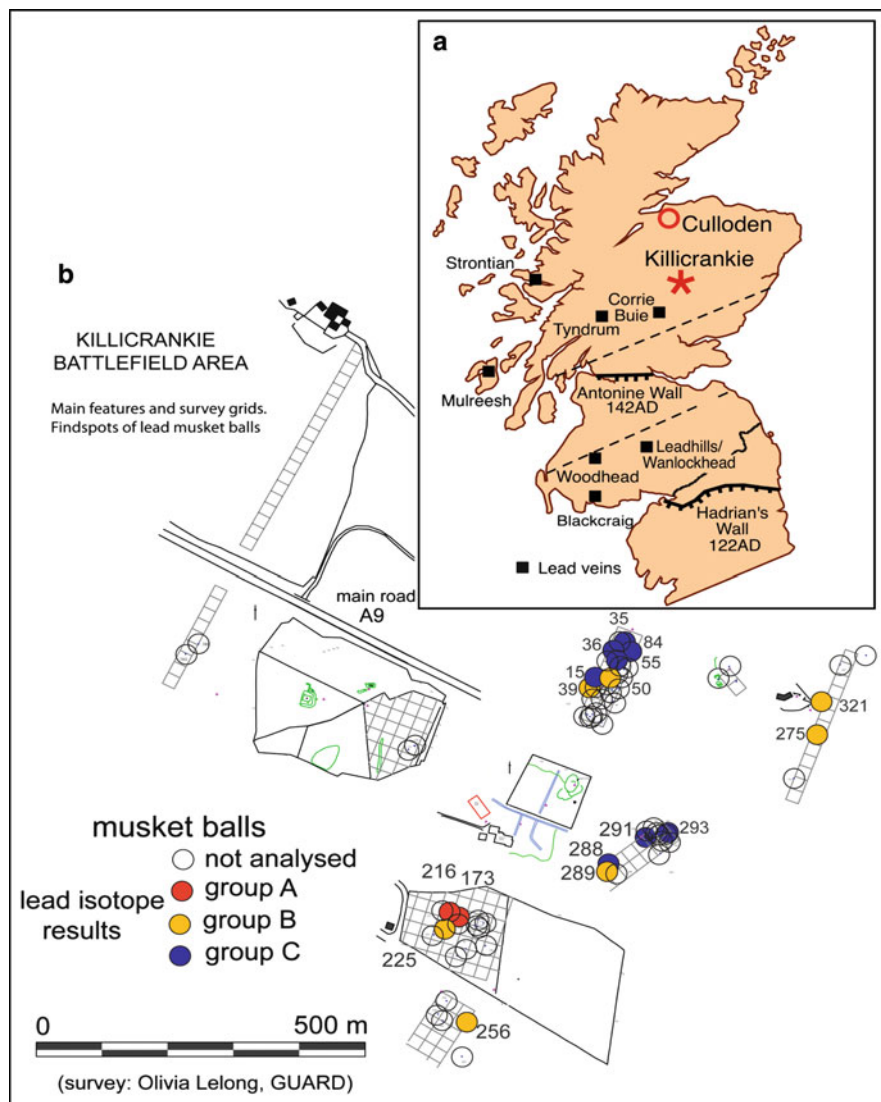


Fig. 1 (a) The inset map shows the location of the Killicrankie and Culloden battlefields and the major lead sources which were probably in production in Scotland during the eighteenth century. The Roman frontiers and the current England/Scotland border are shown for reference. The parallel *dashed lines* indicate the approximate boundaries of the Midland Valley of Scotland. (b) Killicrankie battlefield area showing the distribution of all musket balls recovered from survey grids. The analysed balls are numbered and colour-coded by provisional lead-isotope group (see Fig. 2a)

Geological studies of mining areas have mainly been concerned with the characterisation of minerals and understanding their origin. This contributes little directly to archaeological and historical interests. Nevertheless, archaeologists

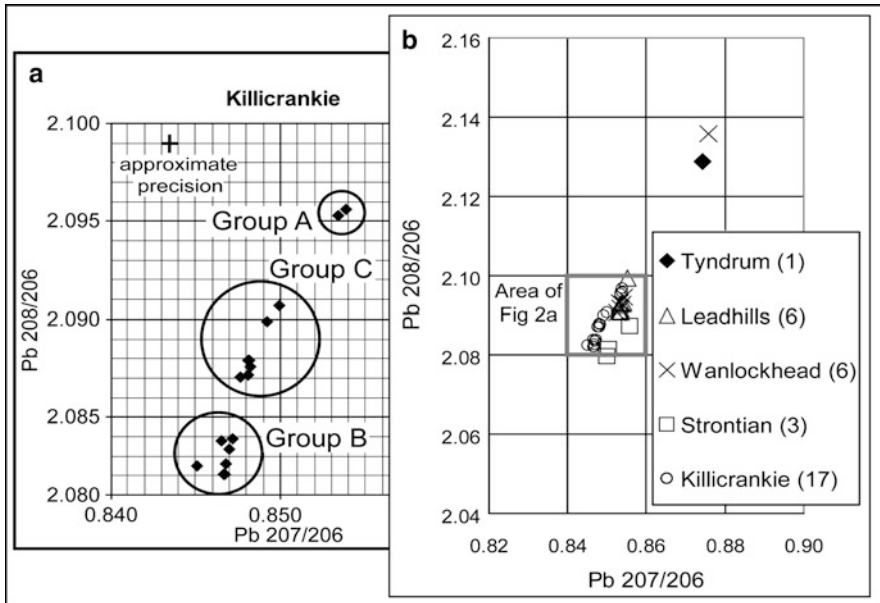


Fig. 2 (a) Lead isotope results showing three provisional groups of musket balls; the groups are very scattered on the battlefield (See Fig. 1b). (b) The Killicrankie musket ball results compared with data for Scottish mines (four) from Rohl (1996)

and historians have to turn to geological expertise in order to help establish the availability of lead in particular regions and fortunately this basic geological knowledge is now available. All known lead sources in the UK were incorporated into the lead isotope database of Rohl (1996), but the question remains as to which mines were in production in the seventeenth to nineteenth centuries.

3 Methods

Three non-destructive approaches have been used to investigate musket ball corrosion products:

3.1 Theoretical Computational Equilibrium Thermodynamics

This was used to understand the corrosion process and predict corrosion products. Geochemical modelling was undertaken using Geochemist's Workbench (Bethke 1996) and has the *ultimate aim* of estimating the lifetime of lead musket balls in the soil vadose zone. Analyses of soil-solution from battlefield sites is required for the

model and this was undertaken on Culloden soil-solution using ion chromatography and total inorganic carbon-total organic carbon (TIC-TOC) methods.

3.2 *Analyses of the Corrosion Products*

Powder X-ray diffraction spectrometry and scanning electron microscopy with energy dispersive X-ray analysis was used to determine the mineralogical and chemical components in the corrosion products. Both of these techniques can be used directly on musket balls without modification of the corrosion surface.

3.3 *Lead Isotope Analyses*

Non-destructive or more exactly, “minimally-invasive” analysis of the lead-rich corrosion layer was undertaken using a laser ablation ICP-MS. Errors estimated for Pb 208/206 and 207/206 are: ± 0.001 .

Whole samples were introduced to the ablation cell of a New Wave UP-213 laser system and supported on “plugs” of quartz wool. The laser, which is a frequency-quintupled Nd-YAG, was used to ablate Pb from the sample with a beam diameter of 5 μm . Ablated material was transported from the cell with a flow of Ar gas to a modified ICP-MS cyclonic spray chamber which was used to mix the sample material with a stream of Tl introduced from an Apex-Q desolvating nebuliser. The Pb-Tl mixture was then transported to the ion source of a Micromass IsoProbe MC-ICP-MS. Pb-isotope ratios were determined on 3 blocks of 20 5-s integrations while the laser beam was rastered over approximately $100 \times 100 \mu\text{m}$ squares, allowing a second pass to begin if the analysis time (5 min) required. No physical damage to the sample surface was discernable with the naked eye or the microscope optics of the laser system. Data quality was assessed by analyzing NBS981 Pb wire mounted in epoxy resin on a microscope slide. During the course of this study, this standard gave $^{208}\text{Pb}/^{206}\text{Pb} = 2.1688 \pm 18$ and $^{207}\text{Pb}/^{206}\text{Pb} = 0.91521 \pm 38$ (2 s.d., $n = 5$) which compare with the “triple spike” values of 2.16771 ± 10 and 0.914750 ± 35 (Galer and Abouchami 1998).

4 Results

4.1 *Theoretical Computational Equilibrium Thermodynamics*

Analysis of Culloden soil solution indicated this is a relatively corrosive environment, with a high chloride content and acidic pH. The theoretical calculations undertaken by simulating lead interaction with soil solution demonstrated that at

the Culloden battlefield site, there would be an initial period of lead dissolution, due to the corrosivity of soil solution. The model indicates however that while some mass would be lost from the musket balls, they would not dissolve completely. Instead they are likely to reach a thermodynamic equilibrium after approximately 170 years, whereupon lead carbonate minerals (cerussite, PbCO_3 and hydrocerussite, $\text{Pb}_2(\text{OH})_2\text{CO}_3$) are predicted to precipitate. These are typical lead corrosion products found in archaeological contexts and form a protective barrier layer which can prevent further corrosion. While the musket balls may not be lost to the archaeological record entirely, the mass loss predicted may be significant for this particular battlefield.

4.2 Analyses of the Corrosion Products

X-ray diffraction confirmed that cerussite is the major corrosion product as expected where rainwater with dissolved CO_2 is the main corrosive agent in soil.

4.3 Lead Isotope Analyses

Preliminary lead isotope analyses confirmed that the corrosion-layer lead can be used as a proxy for the lead metal of the musket ball with comparative results for Pb 208/206 and 207/206 better than ± 0.001 , i.e. within estimated analytical precision. This involved analysis of the metallic lead core and corrosion layer on a sliced section of a musket ball. Further analyses was undertaken only on corrosion surfaces.

The systematic results ($n = 17$) of balls selected to be representative of the size range (spanning pistol balls to musket balls) of the Killicrankie (Fig. 1b) archaeological assemblage ($n = 67$ of an estimated potential total of *c.* 1,000 fired) indicate provisionally on visual examination, that there are three groups of musket balls with similar lead isotope ratios (Fig. 2a). The overall range of data from Killicrankie compared with the UK Pb-isotope database of Rohl (1996) does not point to a single source; the detailed comparison with the Rohl (1996) data for Scotland is given in Fig. 2b.

5 Conclusion

It is confirmed that lead isotope analysis of lead corrosion products offers a means of characterising lead-rich archaeological materials and that this can be undertaken non-destructively using the laser ablation method.

Analyses of 17 representative musket balls from Killicrankie indicate that there are potentially three groups with significantly different isotopic ratios. However, understanding the significance of the groups and their distribution on the battlefield will require consideration of other archaeological data.

In order to recognise specific sources of lead used in the manufacture of musket balls recovered from Scottish battlefield sites, there is a need for historical information on Scottish lead production and also a more appropriate lead isotope database for historic lead sources, building on that of Rohl (1996) to include early European sources.

References

- Bethke CM (1996) *Geochemical reaction modeling: concepts and applications*. Oxford University Press, New York
- Downs-Rose G (1994) *A history of the New Glencrieff Vein, Wanlockhead, Dumfriesshire, 1603–1993, The museum of lead mining*. Wanlockhead Museum Trust, Wanlockhead
- Duffy C (2003) *The '45: Bonnie Prince Charlie and the untold story of the Jacobite Rising*. Cassell, London
- Galer SJG, Abouchami W (1998) Practical application of lead triple spiking for correction of instrumental mass discrimination. *Mineralogical Magazine* 62A:491–492
- Knapp AB (2000) Archaeology, science-based archaeology and the Mediterranean Bronze Age metals trade. *Eur J Archaeol* 3:31–56
- MacKenzie AB, Pulford ID (2002) Investigation of contaminant metal dispersal from a disused mine site at Tyndrum. *Appl Geochem* 17:1093–1103
- Parsons I (2008) Elemental history. *Elements* 4:216
- Pollard AM, Heron C (1996) *Archaeological chemistry*. Royal Society of Chemistry, Cambridge
- Pollard T (2009) The rust of time: metal detecting and archaeology. In: Thomas S, Stone PG (eds) *Metal detecting and archaeology*. Boydell, Woodbridge, pp 161–201
- Pollard T, Oliver N (2003) *Two men in a trench II: uncovering the secrets of british battlefields*. Penguin, London
- Porteus JM (1876) *God's treasure-house in Scotland; a history of times, mines, and lands in the Southern Highland*. Simpkin, Marshall, London
- Rohl BM (1996) Lead isotope data from the Isotrache Laboratory, Oxford: *Archaeometry data base 2 - Galena from Britain and Ireland*. *Archaeometry* 38:165–180
- Tylecote RF (1983) The behaviour of lead as a corrosion resistant medium undersea and in soils. *J Arch Sci* 10:397–409
- Wilson GV (1921) *Memoirs of the geological survey, Special reports on the mineral resources of Great Britain*. vol. xvii: The lead, zinc, copper and nickel ores of Scotland. HMSO, Edinburgh

Non-Destructive and Minimally Invasive Analyses of Bronze Seal Boxes from *Augusta Raurica* by Micro X-Ray Fluorescence Spectrometry, Raman Spectroscopy and FTIR Spectroscopy

K. Hunger, E. Hildbrand, V. Hubert, M. Wörle, A.R. Furger,
and M. Wartmann

1 Introduction

Augusta Raurica (Augst) is a vestige of a Roman town near Basel, Switzerland, which was built around the year 15 BC. Between 80 and 270 AD, the town spread to cover a surface of nearly 106 ha, and up to 20,000 inhabitants were living on the southern bank of the River Rhine. The zenith of town construction and activity at this location occurred in a period between the first and the early third century AD. Many remnants of Roman structures have been discovered at *Augusta Raurica*, such as the recently renovated scenic theatre, an amphitheatre, public baths, temples, private houses, a huge forum, and a 6.5 km aqueduct. More than 1,600,000 objects providing us with information about daily life in the town have been found (Derks and Roymans 2002). One special group of excavated objects consists of seal boxes. The assemblage from the Augst excavation site contains the highest number of bronze seal boxes (140) in the Roman world. Such boxes were used to hold writing tablets, coin purses, etc., for safekeeping, by enclosing these objects with a wax seal. Archaeological and technical questions that have been raised about these bronze seal boxes are the subject of an interdisciplinary project initiated by the archaeologists and conservators of the Roman Museum “Augusta Raurica” together with the scientists of the Laboratory for Conservation Research of the Collections Centre of the Swiss National Museum.

K. Hunger (✉), E. Hildbrand, V. Hubert, and M. Wörle
Swiss National Museum Zurich, Collection Centre, Lindenmoosstrasse 1, CH-8910 Affoltern a.A,
Switzerland
e-mail: katja.hunger@slm.admin.ch

A.R. Furger and M. Wartmann
Augusta Raurica, Giebenacherstrasse 17, CH-4302 Augst, Switzerland

2 Objects and Questions

We investigated a total of 29 seal boxes by carrying out 85 different analyses. The seal boxes were all ca. 2–3 cm wide (Fig. 1a, b, c).

The three main questions asked by conservators and archaeologists regarding these objects were as follows:

- (1). Which alloys were generally used and how were they made?
- (2). Were the box and lid made from the same metal, and are the hinge and catch cast together with the box or rather soldered?
- (3). Which materials were used for the variety of decorations present, and is there remaining debris from these materials?

3 Measurement Procedures

The investigation of the seal box alloys was carried out by X-ray fluorescence spectrometry, using an energy dispersive Eagle III spectrometer (EDAX, X-ray tube: rhodium target). This is a multi-elemental method (accuracy of the instrument is 0.01–0.05%) where the accuracy of the measurement depends upon the different elements and homogeneity of the samples. For the determination of the alloys, corrosion free areas are necessary for X-ray fluorescence analysis to be accurate, this being primarily a surface investigation method. Corrosion layers and the alloy itself do not have the same composition. For example, some elements (especially lead and tin) are enriched in the corrosion layer of ancient bronze artefacts. Most of the seal boxes required minimal invasive intervention so that the exact composition of the alloy could be determined without serious damage to the object. This necessitated the uncovering of very small areas, of approximately 0.5 mm², for the examination. On these scratched areas, ca. 30 measurement points (the diameter of the measurement spot was 50 µm) were selected and determined under the following conditions: voltage 20 kV, current 100 µA, and dwell time per point 200 s. According to this procedure, the average concentration, as well as the



Fig. 1 (a, b and c) Some examples of seal boxes from Augst/Augusta Raurica

standard deviation, were calculated. Because of the inhomogeneity of the alloy itself, only a semi-quantitative evaluation was carried out.

The investigation of the decorations, as well as of bolted areas, was carried out in a non-destructive or micro-destructive manner, because only a qualitative evaluation was necessary. The contents of the seal boxes were investigated with FTIR spectroscopy (Excalibur, Bio-Rad) and Raman analyses (LabRAM Aramis, Horiba Jobin Yvon). For infrared spectroscopy, small samples (ca. 1 mg) were taken from the objects. The Raman analyses were also non-destructive.

4 Results and Discussion

4.1 Alloys

The first question we addressed concerned the determination of the alloys. The results show that all of the seal boxes were made from a copper alloy or brass. The copper alloy is a lead tin bronze with a medial content of tin and lead, typical of compositions from Roman times (Riederer 2000). All of the copper alloy seal boxes were similar in terms of composition. Roman manufacturing procedures involved adding lead to the copper tin alloys in order to decrease the melting point, thus making the metal easier to cast. This special lead tin bronze made possible the addition of more ornamental details during the casting process, whereas a pure tin copper alloy would require a subsequent working of ornamental details after the casting (Deschler-Erb et al. 2005). The seals which were made from brass have medium to high zinc content, showing a shiny golden colour. An example is shown in the ternary plot of Fig. 2 for all the different parts of one seal box (lid, box, hinge and catch) that were investigated in order to determine whether they were cast or soldered.

Results of X-ray fluorescence spectroscopy for all these parts, as well as optical investigations, show that they were cast. The hinge, catch, lid and box have the same elemental composition indicating the presence of a lead tin bronze alloy within the error range. The use of a tin solder was not in evidence. An aspect that is interesting to note is that the riveted bolt, often seen in ornaments as an animal figure, has mostly the same alloy composition as the seal box itself. One can assume from this feature that the Roman metallurgists knew in detail how they would design their works before casting them. A model was evidently prepared initially for the seal box. For the lid, details such as hinges and catches were worked out in advance. A model was produced in the same way for the riveted bolt, and then the bronze or brass smelt carefully prepared, and all parts of the seal box cast with the same metal smelting process. Subsequently, all the finishing touches were added, rivets fixed, and the lid and box hinge connected with a small bolt made of iron.

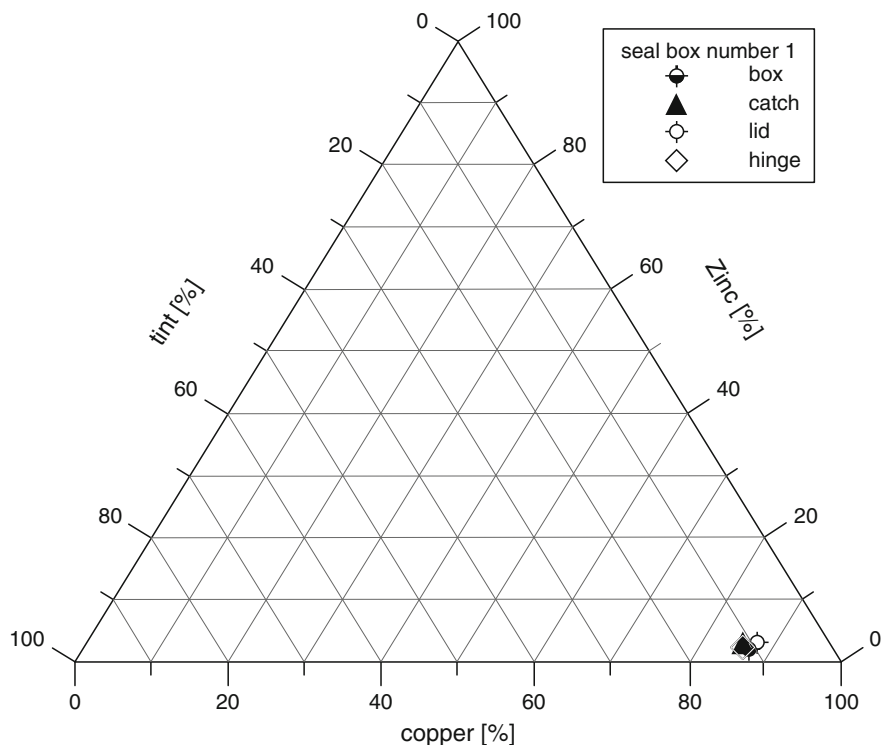


Fig. 2 Ternary plot of different (lid, box, hinge, catch) parts of seal box number 1. All parts show a very similar content of copper, tin and zinc

4.2 Decoration

The lid surfaces were designed according to different styles. Some of the seal boxes underwent a surface treatment, there being two types of surface treatment present. First, brass was often polished for a golden surface shine, with the surface being the same as the alloy itself (see Fig. 1a of seal box with gold, shiny surface and black decoration). Comparison of the zinc content of the surface ($18.1 \pm 0.5\%$) with that of the alloy ($17.9 \pm 0.8\%$) shows that there is no relevant difference between the two. This indicates that the golden shine has been obtained by polishing. There is no extra layer on the surface. Some of the bronze seal boxes have a tinned surface which is determined by a much higher content of tin than in the alloy itself (Fig. 1b showing a seal box with a tin content of $28.6 \pm 1.7\%$ in the alloy, and of $78.7 \pm 2.6\%$ in the shiny silver surface). Such a high content of tin indicates a tinned surface. Also noticeable are inlays made with niello. Niello is a grey to black material consisting of up to three metal sulphides. For decoration, the negative pattern is carved into the object, in this case in the lid of the seal box. Afterwards,

niello powder is filled into the grooves and the surface cleaned, the object being slowly heated as the powder melts. The last step entails polishing the surface in order to obtain a black pattern on the shiny metal background (Deschler-Erb 2002). The dark geometrical pattern seen in Fig. 1a is made with niello, the contents of copper ($75.7 \pm 0.5\%$) and sulphur ($18.6 \pm 0.5\%$) being characteristic for it (Deschler-Erb et al. 2004).

4.3 Content of the Seal Boxes

Some of the seal boxes are complete, shut tight and have remains of the original content inside. One example is shown in Fig. 1c. In order to investigate the contents of the seal boxes, small samples were taken from seven seals, the contents being mixtures of organic and inorganic material. First, FTIR spectroscopy was used, employing a diamond press cell. Five of the content materials could be determined as bee wax. The other samples were extracted with methylene chloride, and the extract was subsequently investigated. The content of these boxes could also be identified as bee wax. It was also possible to investigate the content of the seal boxes with micro Raman spectroscopy in order to determine which pigment was used to colour the wax. These measurements were non-destructive and could be carried out directly on the seal boxes. A 532 nm laser was used and peaks of $146 \pm 2 \text{ cm}^{-1}$ and $341 \pm 2 \text{ cm}^{-1}$ were identified, indicating a lead pigment (PbO).

5 Conclusion

This research project was an interdisciplinary work involving a cooperation between archaeologists and conservators from *Augusta Raurica* and scientists from the Laboratory of Conservation Research of the Collections Centre of the Swiss National Museum. In this project, non-destructive and minimal invasive micro XRF spectrometry, FTIR spectroscopy and Raman analysis were applied. Investigations were carried out on bronze seal boxes found at *Augusta Raurica*. The large number of analyses allowed answering many important questions related to the ancient bronze manufacture of seal boxes, as well as to the making of their decorative elements. Results show that the bronze seal boxes were made of either a lead tin copper alloy with a medial content of tin and lead, or of an alloy of brass with high zinc content for a golden shiny surface. All parts of the seals have been cast and there are no indications of soldering. Decorative elements are multifaceted, making the objects especially interesting. Moreover, with FTIR spectroscopy, we could identify bee wax in the contents of the seal boxes, after having been buried for ca. 2,000 years. The Raman spectroscopy showed that the wax was coloured (red) with a lead pigment (PbO).

References

- Derks T, Roymans N (2002) Seal-boxes and the spread of Latin literacy in the Rhine delta. In: Cooley AE (ed) *Becoming Roman, writing Latin? Literacy and epigraphy in the Roman west*. *J Rom Arch Supl Ser* 48, Portsmouth: 87–134
- Deschler-Erb E, Guggisberg M, Kaufmann-Heinimann A, Mit Beiträgen von Hunger K, Lehmann E, Vontobel P (2005) Eine Gorgo im Lararium? Zu einem Ensemble von Bronzestatuetten aus dem römischen Baden. *Grabungen der Gesellschaft Pro Vindonissa*
- Deschler-Erb E (2002) Niellierung auf Buntmetall, Ein Phänomen der frühen römischen Kaiserzeit. In: Thomas R (ed) *Akten zum 14. Internationalen Kongress zu Antiken Bronzen in Köln*. *Kölner Jahrbuch* 33(2000):383–396
- Deschler-Erb E, Lehmann E, Soares M, Hildbrand E, Hunger K, Kappeler A (2004) Alt heidnisch Bildlein von Ertz. *Archäologie der Schweiz* 27:3
- Riederer J (2000) Der Beitrag der Metallanalyse zur Bestimmung römischer Bronzewerkstätten. *KJ (Kölner Jahrbuch-Berlin)* 33:575–583

A Multi-Disciplinary Approach to the Study of An Assemblage of Copper-Based Finds Assigned to the Prehistory and Proto-History of Fucino, Abruzzo, Italy

M.L. Mascelloni, G. Cerichelli, and S. Ridolfi

1 Introduction

The present project aims to characterise, through a combination of archaeometric analyses, an assemblage of prehistorical and proto-historical copper-based finds known as “Fucino bronzes”; any data regarding context or specific provenance is lacking for most of these. The assemblage of Fucino bronzes includes artefacts that emerged during the drainage of Lake Fucino at the end of the nineteenth century, as well as bronzes acquired locally or excavated later by several collectors on behalf of the various Italian museums where the finds are currently located. Contextual and provenance data sometimes exist in varying degrees of completeness.

The Fucino bronzes are presently scattered throughout Italy: in Rome, at the L. Pigorini Pre-historic and Ethnographic Museum; Perugia, at the National Archaeological Museum of Umbria; Chieti, at the National Archaeological Museum; Sulmona, at the Civic Museum; Avezzano, at the Permanent Exhibition of Farming and Pastoral Culture in Torlonia Palace; and Firenze, at the Archaeological Museum. The bronzes in the Chieti Archaeological Museum have already been analysed in a similar project and are therefore excluded from the analytical phases of this particular study. As a long-term task, this research aims to extend its analyses to those finds emerging from current and regular excavations: bronzes, vitrified material, and smithing pottery.

This study is part of the current description of updates on the development of ancient metallurgy and proposes a broader re-evaluation of all the resources

M.L. Mascelloni (✉) and G. Cerichelli
Department of Chemistry, Chemical Engineering and Materials, University of L'Aquila, Via
Vetoio (Coppito 1), 67010 Coppito, L'Aquila, Italy
e-mail: mascelloni@hotmail.com; cerichel@univaq.it

S. Ridolfi
Ars Mensurae, Roma, Italy
e-mail: stefano@arsmensurae.it

available for the interpretation of metal finds, particularly as most of these are out of context. The present work explores the dynamics related to the production of objects and their assemblage, alongside relationships between production centres, local workshops, and the technological change from bronze to iron metallurgy. The study proceeds concurrently with various research and cataloguing phases:

- Quantification of finds
- Chemical characterisation of materials by ED-XRF
- Metallographic examination of samples by OM and SEM
- Development of a database

2 Experimental

For the quantification of materials, objects are grouped according to function in both classes and categories. At the same time, finds are also grouped typologically, technologically, chronologically and territorially, when appropriate, in order to derive customized models for data interpretation. The methodology aims to deduce the socio-technological conditions from the materials themselves, as theoretical constructs where data can be ordered and examined from a variety of perspectives. This procedure provides essential analyses that facilitate the development of a workable database.

Chemical analyses were carried out using a portable ED-XRF, which provides quantitative results that are comparable to the data produced by similar bronze characterisation projects, such as the San Francesco hoard in Bologna and a project of the Chieti Archaeological Museum, which also includes a number of the aforementioned Fucino bronzes.

The technical features of the portable X-ray Fluorescence system are:

- Tube: Tungsten anode, H_v max 38 kV anode, Power anode, max 0.5 mA, Air cooled; Size: 60(W) \times 200(D) \times 100(H) mm, Weight 2 kg; Collimator diameter: 1 mm. The tube avails of 35 kV tension and 0.2 mA power.
- Detector characteristics: SDD (Silicon Drift Detector) cooled by a Peltier cell. Resolution from 150 eV to 6.4 keV. A multi-channel: 1,024 channels.
- Pointing system: laser diode. A portable ACER computer with a self-made spectrum management program.

All the analysis points have been registered on the reverse side or the least visible points of the objects and the patinas have been removed.

In this research, the metallographic analysis was aimed at collecting data on the assemblage, maintenance and reparation of objects. This type of analysis could therefore be defined as macro-metallography, although this kind of definition is not universally recognized. The metallographic analysis of the finds was carried out with a stereo optical microscope (80 \times) and an SEM whenever possible. The

chemical analysis and metallographic examination of these finds were planned according to cross-sectional models:

- Analysis of *functional classes*
- Analysis of *technological classes*
- Analysis of selected *territories*

3 Results and Discussion

These objects are functionally grouped in 27 classes and three categories (Fig. 1): tools, ornaments and accessories, and weapons, narrowly defined as objects intended to harm others.

Chronologically, the bronzes show a common tendency of Bronze/Iron Age inventories, which generally include larger groups of weapons and tools from early periods and ornaments and accessories from more recent times. The Middle Iron Age in Italy reports a large peak in the ornaments/accessories category, with the use of rich gifts in the burial rituals of the rising IA communities.

One of the most interesting classes in the ornaments/accessories category are “kardiophylakes” (Fig. 2), bronze or bronze iron discs, which are the major group in

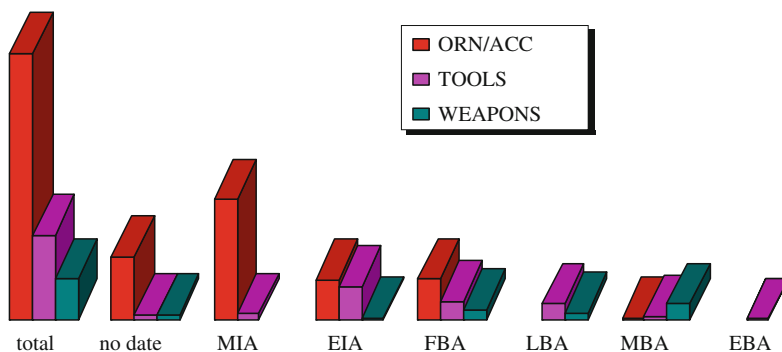


Fig. 1 Chart of chronological quantification of categories



Fig. 2 Kardiophylakes (n. 53832; n. 83114; n. 53833)

the functional classes and the most representative materials to be classified in terms of technology.

With 60 units, 26 in Rome and 34 in Perugia, kardiophylakes in this assemblage form one third of the known samples. They have been interpreted for a long time as parts of armours, but currently they are more widely linked to the expression of social and cultural belongings, and associated with both genders. Chronologically, geometrical discs of bronze are considered the earliest ones, and dated to the eighth century BC, while figurative discs of bronze back supported by iron sheets are considered the latest ones, and are dated to the sixth century BC (Colonna 2007)

Since most of these objects appear to have been frequently repaired, as products for consumption, with the addition of different metals and alloys, technological classes are based on their affinities in terms of constitutive elements and degree and types of maintenance and reparation. Particular attention was devoted to determining the chemical compositions and technologies employed for the various constituent elements of the artefacts or parts included in the reparation, in order to compare data both within the same artefact and among objects showing similar interventions.

Regarding kardiophylakes, for instance, the most frequent secondary interventions are on fractures along the rim or around the concave centre of the disc, with small sheets supported by two or more rivets. This kind of reparation may have been carried out with bronze sheets and rivets, iron sheets, and bronze and/or iron rivets, or by a complete intervention with iron, which actually led to a significant corrosion of the objects. This allows us to recognize technological sequences related to the widespread use of iron in the area, suggesting integrated chronologies for the objects and eventual links among the workshops or – along the line – metalwork traditions.

In this report, we discuss the results of a preliminary test of XRF-ED analysis (Table 1) on 6 kardiophylakes (Disc in Table 1), the group of 5 *aes ruda*e, 1 pendant, 7 beads and 1 spiral in the bead/spiral group.

As previously mentioned, all the samples are copper-based products, with Cu percentages ranging from 100% in one of the *aes ruda*e to 65.3% in one of the beads. The compositions of the 5 *aes ruda*e are nearly pure copper, except one showing iron and zinc with percentages of 7.2% and 2.8%, respectively.

All of the other samples are ternary bronze alloys (copper, tin and lead) with variable compositions, but for the time being, they appear to be consistent with the functional classes of the objects (Fig. 3).

The composition of spirals is more consistent with the composition of kardiophylakes than with the composition of beads; however, spirals are associated with the beads for inventory reasons and no other data indicates any further association than probably deposition. Moreover, beads originate from smithing operation chains that are very different from the ones used for spirals or kardiophylakes. The beads were made by one single casting operation, while the spirals and the discs needed prolonged cold working and annealing. Evidently, the presence of too much Pb made those objects too fragile to be intensely worked. By adding a massive quantity of lead, as in the case of beads (more than 20% of Pb in all of the samples), ancient workers first obtained a better fluidity for casting, and also

Table 1 Results of XRF-ED analysis

Object	Inv n	Cu	Sn	As	Pb	Sb	Ag	Fe	Zn	Ni	Bi
Disc	53832	85.3	13.1		1.5						
Disc	85251	85.1	10.1	0.5	3.9			0.5			
Disc	85250	89.6	5.2		5.2						
Disc patina	85253	87.5	10.9		1.6						
Disc sheet	85253	87.7	10.1		2.2						
Disc rivet	83114	81.5	11.9		2.5	0.9	0.1	3.1			
Disc sheet	83114	89.3	6.9		2.4			1.4			
Disc	53833	85.4	9.4		2.9		0.1	2.2			
Pendant	36458	70.7	7.0	2.1	14.9	2.7	0.1			2.5	
Aes rudaе	36465-5	88.8	0.2		1.0			7.2	2.8		
Aes rudaе	36465-2	98.4	0.2				0.1		1.3		
Aes rudaе	36465-3	100.0									
Aes rudaе	36465-1	99.3	0.1	0.1							0.4
Aes rudaе	36465-4	99.5						0.4			
Spiral	36466-10	87.3	7.8		4.8		0.1				
Bead	36466-2	72.2	6.0		21.8						
Bead	36466-7	71.3	5.6		23.1						
Bead	36466-6	74.7	4.5		20.8						
Bead	36466-5	69.0	5.4		25.6						
Bead	36466-3	72.3	5.9		21.0	0.7	0.1				
Bead	36466-1	71.9	6.4		21.7		0.1				
Bead	36466-4	65.3	8.0		26.7						
SRM ^a		87.4	4.3		4.2				4		

^aStandard Reference Material – NIST: Bronze, Phosphor (CDA 544)

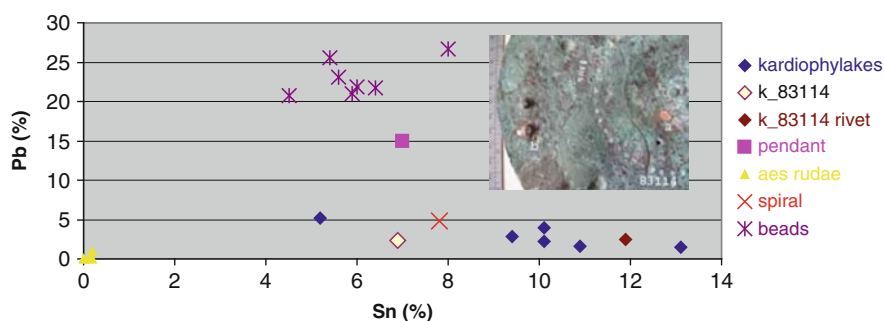


Fig. 3 Scatter plot diagram of lead vs. tin related to copper as major component

saved copper and tin, both being more expensive and much more difficult to recover than lead. In any case, it is worth adding that tin bronzes with high percentages of lead are common in the proto-history of continental Italy, emphasizing the occurrence of common metalwork traditions.

The plate, and also one of the rivets of disc n. 83114 have been analysed. The rivet composition, as shown in the diagram, includes a higher percentage of Sn as compared to the sheet and an unusual quantity of Fe (3.1%), and also considerable

traces of Sb and Ag. Such results strongly suggest that the different elements of the objects refer to different productions.

The objects referred to as “*aes ruda*” are unrefined bronze lumps involved in the exchange systems of the Italic proto-history. Their value was related only to their weight. The five lumps in the assemblage have been bought in stock and inventoried as slag. They are unusually light, and cannot be clearly interpreted as *aes ruda*, the heaviest one weighing only 16 g; however, the chemical composition of item n. five perfectly matches other *aes ruda* compositions: rich in iron and zinc, and with moderate percentages of lead and tin (Chiarantini et al. 2008). The five lumps show very similar patinas, which at least indicate their common deposition. Since antiquity, “quite pure copper” lumps were rarely lost, and they were eventually assembled for recycling.

For the territorial quantification of objects, two areas have been identified as working models: Ortucchio and Celano. Both archaeological areas are located on a dry lakebed and include several sites from the Mesolithic Age to the Early Iron Age, when they were both abandoned due to frequent flooding. Both areas have been recently excavated and report traces of substantial industrial activity. Both inventories appear to support the hypothesis of considerable industrial activity recently observed at the sites.

4 Conclusions

In a long-term perspective, the present research aims to extend its analyses to the other traces of industrial productions uncovered by current regular excavations. An assemblage of recent contextual finds from the Ortucchio and Celano sites will be analysed in order to compare it with other collections for purposes of data interpretation. This assemblage includes bronzes, one lump of copper, and some fragments of pottery, perhaps involved in some smelting or casting processes of domestic size.

The Fucino prehistoric and proto-historic archaeology did not provide clear contexts associated with metallurgic processes. However, on the other hand, the difficulty of finding such contexts earlier than the Iron Age is well known. Moreover, the Abruzzo region does not have significant mining resources that would suggest independent metallurgical traditions. Nevertheless, there is no reason to exclude a priori the possibility that local workshops existed and that they probably used their own strategies.

References

- Colonna G (2007) Dischi-corazza e dischi di ornamento femminile. *Archeologia Classica* 58(8)
- Chiarantini L, et al. (2008) Trace elements and isotopic tracers in archaeometallurgy: a contribution from the study of ‘*aes ruda*’ from the Etruscan sites. In: 37th International Symposium on Archeometry. Siena (Poster)

Copper-Based Kettles from Brador: A Contribution to the Study of Eastern Settlements of New France on the Northern Shore of the Estuary of the Saint-Lawrence (Quebec, Canada)

J.-F Moreau and R.G.V. Hancock

1 Introduction

Four centuries ago, in 1608, Samuel de Champlain founded Quebec City. In the next several decades, two other major towns, Montreal, then Trois-Rivières, were established west of Quebec City in the lowland valley of the Saint-Lawrence. Meantime, east of Quebec, small hamlets dotted the northern as well as the southern shore of the estuary of the Saint-Lawrence, as a result of lands ceded to people who distinguished themselves in the settling of New France. Such is the case for a soldier, Augustin Le Gardeur de Courtemanche (scholarly biography elaborated by Corley 1969), who in 1704 settled on land at Brador (Fig. 1). Archaeological investigations of his buildings were led respectively in 1968–1969 and 1982 (see Niellon 1996). Among the artefacts collected were fragments of copper-based kettles of which 74 samples were retrieved for instrumental neutron activation analyses (INAA) in 1997 (see Table 2).

2 INAA Method

Neutron activation analyses were performed following a modified methodology of Hancock et al. (1991a, b). Specimens of the order of 8–40 mg were first manually abraded in order to remove the outer layer of corrosion (Moreau and

J.-F. Moreau (✉)

Laboratoire d'Archéologie and Département des Sciences Humaines, Université du Québec à Chicoutimi, Chicoutimi, QC, Canada, G7H 2B1
e-mail: jfmoreau@uqac.ca

R.G.V. Hancock

Department of Medical Physics and Applied Radiation Sciences and Department of Anthropology, McMaster University, Hamilton, ON, Canada, L8S 4K1
e-mail: ronhancock@ca.inter.net



Fig. 1 Location of Brador site (Quebec, Canada)

Hancock 1999a). The cleaned samples were individually stored in 1.2 mL polyethylene vials and analyzed at the SLOWPOKE Reactor Facility of the University of Toronto. Following 1–5 min of neutron irradiation and a delay of about 1 h, the samples were assayed for zinc (Zn), copper (Cu), manganese (Mn) and indium (In), using a hyperpure germanium detector-based gamma ray spectrometer. The elemental concentrations were calculated using the comparator method (Hancock 1976).

Medium and long half-life radioisotope-producing elements were analyzed by batch irradiation of twenty to forty samples for 16 hours at a neutron flux of 2.5×10^{11} neutrons per square centimetre per second. Five to seven days later, samples were serially assayed for 500–2,000 s looking for gold (Au), copper (Cu), cadmium (Cd), arsenic (As), antimony (Sb), silver (Ag), zinc (Zn) and sodium (Na). A final counting was made ten to fourteen days after the irradiation, at which time the samples were counted for 4,000–60,000 s (depending on sample mass and relative trace elemental contents) to determine the concentration of tin (Sn), selenium (Se), mercury (Hg), gold (Au), arsenic (As), antimony (Sb), silver (Ag), nickel (Ni), scandium (Sc), iron (Fe), zinc (Zn) and cobalt (Co). This procedure produced replicate measurements of enough elements to guarantee no sample mix-ups. Analytical precisions ranged from $\pm 1\%$ to detection limits.

3 Previous Studies

Previous studies of copper-based kettles showed that when one such container is analyzed in detail the sheet making up the container body often presented a different chemical composition from pieces that were used to shape the two handle lugs, as well as that of the rivets (e.g. Moreau and Hancock 1999b).

Another study (Moreau and Hancock 1999c) comparing kettles from eleven archaeological sites in Ontario and Quebec, has shown that rivets composed of copper are far more numerous (see Table 1: $N = 33$) than rivets made from brasses ($N = 7$) with Zn in the order of 26%. In the same study, it was shown that copper-based kettles present a large variation in chemical compositions at the beginning of the seventeenth century (Zn from $\approx 1\%$ to $\approx 20\%$) while at the end of the French Regime, around 1750, kettles were made of brasses with variations in Zn contents between 18 and 30%.

4 Brador Data

How do these previous observations apply to the 74 samples retrieved from the Brador collection? In Table 1, we report the chemical composition of a subsample comprising the five groups of body-sheet/handle-lug/rivets sampled in the collection, sorted in decreasing content of copper for the sheet/lug. Two main observations can be made from Table 1. (1) When both body sheet and handle lug of a given group were sampled, their chemical composition is largely alike; (2) seven out of eight rivets from Brador are made up of copper ($>97\%$ Cu), only one of them being made of brass (Cu $\approx 69\%$ and Zn $\approx 30\%$). This ratio of one for seven rivets in brass alloy from Brador compares well with the other collections of rivets from Ontario and Quebec, with 33 rivets made of Cu compared to seven of brass. Hence, in as much as the decreasing ordering of the five groups of sheet/lug/rivet does more or less follow the general trend from high copper-based kettles to high Zn kettles throughout the French Regime from 1600 to 1750, the rivets were essentially made up of Cu during all this period.

The full collection of samples from Brador is reported in summary fashion in Table 2 according to the following breakdown: nine samples of copper with In not measurable); 13 samples of copper with In measurable; seven red brass: lower Zn samples; 14 fragments of yellow brass with higher Zn (24–28%); and 30 fragments of yellow brass with very high Zn (29–34%). As indicated by the arrow to the right of Table 2, the order of these groupings is akin to the observation reported as Moreau and Hancock (1999c) that suggests a shift from copper sheets making up the kettles when the French Regime was established (≈ 1600) to higher and higher Zn-brass sheets making kettles by the end of the French Regime around 1750.

Table 1 INAA data for sheets/lugs/rivets groups from Brador

Access No. ^a	Cu (%)	In (ppm)	Ag (ppm)	Au (ppm)	As (ppm)	Sb (ppm)	Sn (%)	Zn (%)
Brador copper group 1 unmeasurable In								
34S26	98	<0.7	1,250	1.7	3,980	175	<0.02	0.02
35R26	98	<1.2	1,040	1.6	3,570	147	<0.06	0.05
36R26	98	<0.7	990	1.5	3,820	173	<0.06	<0.01
Brador copper group 2 measurable In								
21L68	77	13	870	19.2	900	231	1.0	21
22L68	77	12	880	19.1	940	235	1.0	20
23R68	99	4	990	32.4	1,020	1,450	<0.11	0.12
Brador brass group 3 – lower Zn								
24S1572	75	2	690	1.8	450	28	<0.04	24
26S1572	73	3	800	1.6	480	35	<0.02	25
25Lout1572	71	9	610	4.8	980	109	1.4	27
27Lin1572	70	8	460	4.2	670	66	<0.04	31
28R1572	96	10	870	16.7	2,550	1,450	0.28	1.38
29R1572	97	5	760	15.4	3,840	1,550	1.0	0.99
Brador brass group 4 high Zn								
30S2572	71	2	770	2.1	450	42	<0.08	26
31L2572	66	4	830	2.6	540	42	<0.06	31
32R2572	96	6	700	34.1	1,970	1,380	<0.11	1.5
33R2572	97	6	750	15.0	4,340	1,560	<0.07	0.91
Brador brass group 5 – highest Zn								
41S28	67	35	280	5.9	590	45	0.05	32
42S28	70	43	280	5.6	580	41	0.03	29
43R28	69	37	290	5.4	790	45	0.04	30
All Brador copper rivets								
7 samples	97 ± 1	4.7 ± 3	870 ± 140	17 ± 13	3,020 ± 1,200	1,100 ± 650	0.2 ± 0.3	0.7 ± 0.6
Ontario/Quebec copper rivets ^b								
33 samples	97 ± 2	9.5 ± 9	900 ± 200	16 ± 14	3,000 ± 2,000	730 ± 600	0.2 ± 0.3	1.2 ± 1
Ontario/Quebec brass rivets ^b								
7 samples	71 ± 4	17 ± 7	760 ± 200	21 ± 9	660 ± 500	330 ± 500	0.7 ± 0.9	26 ± 4
<i>Orange</i> color enhances the Cu rivets of the sheet/lug/rivet groups from Brador, in order to compare their grouped statistics to those from collections from Ontario/Québec								
<i>Yellow</i> color enhances the brass rivet from the sheet/lug/rivet group 5 from Brador compared to the few low Cu rivet retrieved in collections from Ontario/Québec								

^aAccession numbers are composed of the analytical sample number; followed by a letter if the sample is a kettle sheet (S), a lug (L), out and in indicate outside and inside sheet of the lug) or a rivet (R); followed by the box number from which the sample was retrieved.

^bMoreau and Hancock 1999c, Tab.2, p. 334.

Table 2. INAA data for all Cu-based fragments retrieved from Brador

	Cu (%)	In (ppm)	Ag (ppm)	Au (ppm)	As (ppm)	Sb (ppm)	Sn (%)	Zn (%)	Zn time line ^a
N	0.05	<0.05	93	0.11	15	128	0.12	0.0	One Pb fragment
	9	9	9	9	9	9	9	9	In not measurable
Mean	98	0.9	1,090	1.7	4,320	162	0.1	0.03	Seven body sheets
SD	1	0.2	204	0.61	1,820	34	0.03	0.02	Two rivets
V	1	21	19	36	42	21	52	69	
N	13	13	13	13	13	13	13	13	In measurable
Mean	98	7.8	907	23.1	1,950	1,410	0.34	0.40	Eight body sheets
SD	1	4.6	228	10.6	1,340	840	0.56	0.57	Five rivets
V	1	60	25	46	69	60	164	143	
N	7	7	7	7	7	7	7	7	Red brass: lower Zn
Mean	82	10.1	870	18.8	4,180	2,510	1.71	15.1	Five body sheets
SD	6	4.3	390	11.5	5,550	4,810	0.94	6.1	Two handle lugs
V	7	42	44	61	133	192	55	41	
N	14	14	14	14	14	14	14	14	Yellow brass: high Zn
Mean	73	7.3	750	5.01	619	81	0.16	26.1	13 body sheets
SD	2	5.3	128	4.52	508	69	0.36	1.3	One handle lug
V	3	73	17	90	82	85	226	5	
N	30	30	30	30	30	30	30	30	Yellow brass: very high Zn
Mean	69	20	580	5.76	861	96	0.06	30.3	27 body sheets
SD	2	28	173	4.09	901	64	0.03	1.2	Two handle lugs
V	2	143	30	71	105	67	47	4	One rivet

^aTime line based on Zn contents as described in Moreau and Hancock 1999c: 330

5 Conclusions

Copper rivets were used in copper kettles and in earlier brass (with lower Zn) kettles. The highest occurrence of metal fragments, that of very high Zn-brass samples ($N = 30$) fits well with the late French Regime date from archival records for the Brador settlement (after 1704).

The high copper/lowest Zn (Table 2: unmeasurable and measurable In; 15 fragments, excluding the seven rivets), red brass (seven fragments) and high Zn yellow brass (14 fragments) could be an indication of older settlements in the same area as early as the 1600s and/or the result of the recycling of materials from older kettles, while very high Zn kettles were mainly in usage during the period of occupation of Brador.

References

- Corley NT (1969) Le Gardeur de Courtemanche, Augustin. In: Hayne D, Vachon A (eds) *Dictionnaire Biographique du Canada*. Vol 2, de 1701 à 1740, Québec et Toronto. Les Presses de l'Université Laval et University of Toronto Press
- Hancock RGV (1976) Low flux multi-element instrumental neutron activation analysis in archaeometry. *Anal Chem* 48:1443–1445
- Hancock RGV, Farquhar RM, Pavlish LA, Salloum R, Fox WA, Wilson GC (1991a) North American native copper and European trade copper analyses. In: Pernicka E, Wagner GA (eds) *Archaeometry-90*. Birkhäuser Verlag, Boston, pp 173–182
- Hancock RGV, Pavlish LA, Farquhar RM, Salloum R, Fox WA, Wilson GC (1991b) Distinguishing European trade Copper and North-Eastern North America native copper. *Archaeometry* 33 (1):69–86
- Moreau J-F, Hancock RGV (1999a) The effects of corrosion on INAA characterizations of brass kettles of the early European contact period in Northeastern North America. *J Archaeol Sci* 20 (8):1119–1125
- Moreau J-F, Hancock RGV (1999b) L'anatomie d'un chaudron. In: Moreau J-F (ed) *L'Archéologie sous la loupe*. Contributions à l'archéométrie, Montréal, Recherches amérindiennes au Québec, coll. Paléo-Québec n 29, 73–86
- Moreau J-F, Hancock RGV (1999c) Faces of European copper alloy cauldrons from Québec and Ontario “contact” sites. In: Young SMM, Pollard AM, Budd P, Ixer RA (eds) *Metals in antiquity*. BAR International series 792. Archaeopress, Oxford, pp 326–340
- Niellon F (1996) Du territoire autochtone au territoire partagé, Le Labrador, 1650–1830. In: Frenette P (dir) *Histoire de la Côte-Nord*, Québec, Les Presses de l'Université Laval and Institut québécois de recherche sur la culture. pp 135–177

On the Gold Adornments from Apahida-Fifth Century AD, Transylvania, Romania

G. Niculescu, R. Oanță-Marghitu, and M. Georgescu

1 Introduction

1.1 *Archaeological Material*

Three princely graves, all dating from the second half of the fifth century AD, were discovered at Apahida, in 1889, 1968, and 1979, respectively (Périn et al. 2000; Horedt and Protase 1972; Harhoiu 1998). Subsequently, the treasure of Cluj-Someșeni was found a few kilometres away (Périn et al. 2000; Harhoiu 1998). Both places are located close to the former Roman *municipium* of Napoca, in the proximity of an ancient Roman road connecting Napoca with the Roman camps (Gherla, Cășeiu, Ilișua) on the Someș valley. These four complexes, located outside the borders of the fifth century Roman Empire, exhibit inventories which are important documents for the archaeological discourse on the Early Middle Ages in the Middle Danube area. The most spectacular analogies for the items discovered at Apahida are found in the Childeric grave from Tournai, Belgium.

1.2 *Research Goals and Method*

By the XRF analysis of the elemental composition of different metallic elements assembled in the structure of several cloisonné decorated items (such as the ones

G. Niculescu (✉) and M. Georgescu
National Research Institute for Conservation and Restoration, 12 Calea Victoriei, 030026,
Bucharest, Romania
e-mail: niculescu.geo@gmail.com

R. Oanță-Marghitu
National History Museum of Romania, 12 Calea Victoriei, 030026 Bucharest, Romania
e-mail: rodicamarghitu@yahoo.com

shown in Fig. 1 and Fig. 2b), we aimed to verify if similar items found in different graves (such as the belt buckles) were fabricated with corresponding constructive elements with the same gold content. We also attempted to investigate if there was any correlation between the gold concentrations and the role of different elements in the structure of the artefacts. The results of the XRF measurements reported in this paper will be used at a further stage for reconstructing the entire technological chain (*chaîne opératoire*) employed in assembling these complicated cloisonné adorned objects.



Fig. 1 The purse-lid adornment from the Apahida II grave together with samples of gold patterned foils and garnets dismantled by the original discoverers

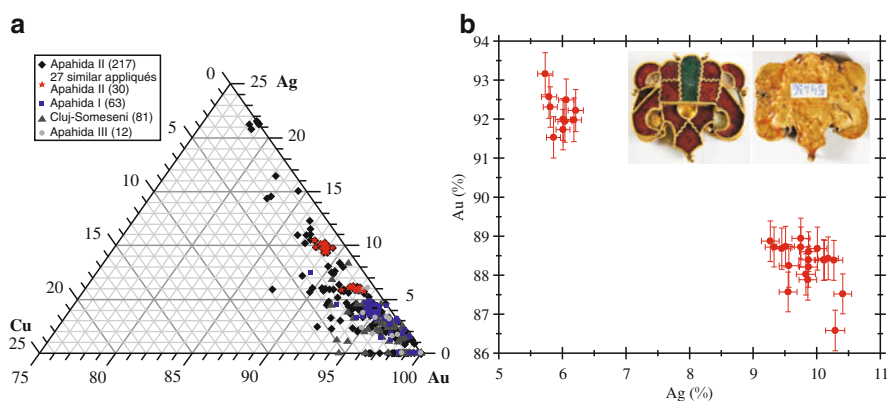


Fig. 2 (a) The results of XRF analyses carried out on gold objects from the inventories of Apahida graves and the Cluj-Someşeni treasure, (b) The results of XRF analyses carried out on the 27 similar harness adornments from the Apahida II grave

1.3 *Equipment*

The analyses of the gold objects were performed using an Innov-X Systems Alpha Series X-Ray Fluorescence (XRF) portable spectrometer, with an X-ray tube with W anode, operating at 35 kV and 40 μ A. The calibration of the spectrometer for quantitative analysis of gold alloys was carried out by the manufacturer of the instrument.

Due to the technical characteristics of the instrument, only those objects – or parts of objects – whose surfaces exceed the dimensions of the sampling window (approximately 17 mm diameter) were examined. By using this XRF analyser, we could also analyse small fragments – constructive components detached from the item in which they were initially assembled – such as the free patterned foils (Fig. 1 – bottom left and right, respectively) or the cell walls.

However, due to geometrical constraints – the measuring head of the spectrometer could not be advantageously positioned in order to allow all points of interest to be accessible for XRF measurements – we could not obtain valid information on the garnet inlaid parts. The results of the XRF measurements on gold objects are valid for the first micrometers from the surface of the analysed objects. Since no corrosion products were observed on the surface of the artefacts, no cleaning was carried out prior to the XRF analyses.

2 **Results and Discussion**

The cloisonné adorned items from Apahida and Cluj-Someşeni are complex structures composed of hundreds of gold fragments. An ideal investigation of such intricate objects would entail the analysis of each single element and of the assembling technique. Taking into account the above-mentioned characteristics of our XRF equipment and of the samples to be analysed, we have thus far only carried out a general evaluation of the objects' composition, measuring in as many different points as possible. Thus, we investigated several items from the above-mentioned four complexes, and we obtained results from 400 different spot measurements performed on different artefacts (Fig. 2a). The results of the XRF measurements carried out on the Apahida objects are discussed in what follows, and several correlations suggested by these results are also provided.

Each of the three Apahida graves contained an impressive, massive belt buckle. The multiple stylistic similarities between these three items indicate an identical pattern in their construction and decoration. Most likely, this aspect points out towards their having been manufactured in the same workshop. The belt buckles from the first and second Apahida grave are better preserved, but the belt buckle from the third grave is in a fragmentary state, almost completely dismantled. This particular condition allowed us to analyse all the different types of components

assembled together to form this item – link, pin, plate, cell walls, and patterned gold foils beneath the garnet inlays.

We also measured the concentrations of the main elements which compose the three buckles; the corresponding XRF results are presented in Table 1. No correlation between a specific alloy and a particular constructive element of the buckles (link or back plate) was observed. Moreover, similar elements of different buckles show different sets of values for the determined metal concentrations. A possible explanation for this might be the reusing of gold recovered from older objects. The available gold reserve was divided in several categories depending on the fragments' title; minor differences were not taken into account. The alloy was probably used without any other treatment, if its purity was within certain parameters – in these cases, high purity gold, with concentrations above 92%. On the basis of the values obtained for the patterned gold foils (Table 1, III, 6–12), we were able to assume that all these constructive elements were cut from the same large foil.

Table 1 The results of XRF analyses on the belt buckles found in the three graves from Apahida (I, II, III)

Analysed item	Au (%)	σ^a Au (%)	Ag (%)	σ Ag (%)	Cu (%)	σ Cu (%)	Fe (%)	σ Fe (%)
I.								
1. Back plate	96.0	0.6	3.1	0.1	0.5	0.1	0.4	0.1
2. Link	96.6	0.7	2.7	0.1	0.7	0.1	nd ^b	nd
3. Link	96.4	0.7	2.8	0.1	0.5	0.1	0.3	0.1
4. Link	96.4	0.5	2.6	0.1	0.7	0.1	0.3	0.0
II.								
1. Back plate	94.8	0.6	3.7	0.1	1.1	0.1	0.4	0.1
2. Link	98.1	0.6	1.4	0.1	nd	nd	0.5	0.1
3. Link	98.1	0.6	1.5	0.1	nd	nd	0.4	0.1
4. Pin	99.3	0.8	nd	nd	0.7	0.1	nd	nd
III.								
1. Pin	97.1	0.5	1.6	0.1	1.1	0.1	0.2	0.0
2. Pin's hook	95.9	0.7	1.8	0.1	2.3	0.1	nd	nd
3. Back plate	96.4	0.6	3.1	0.1	0.5	0.1	nd	nd
4. Link	93.4	0.6	5.8	0.1	0.8	0.1	nd	nd
5. Link	93.4	0.6	6.0	0.1	0.4	0.1	0.2	0.1
6. Patterned foil	99.7	0.8	nd	nd	nd	nd	0.3	0.1
7. Patterned foil	99.5	0.7	nd	nd	nd	nd	0.5	0.1
8. Patterned foil (rectangular)	99.1	0.8	nd	nd	nd	nd	0.9	0.1
9. Patterned foil (rectangular)	99.4	0.9	nd	nd	nd	nd	0.6	0.1
10. Patterned foil	99.1	0.7	nd	nd	nd	nd	0.9	0.1
11. Patterned foil	99.4	0.6	nd	nd	nd	nd	0.6	0.1
12. Patterned foil	99.6	0.8	nd	nd	nd	nd	0.4	0.1
13. Cell wall (omega)	97.2	1.0	nd	nd	1.2	0.1	1.6	0.2
14. Second back plate	92.6	0.8	2.3	0.1	2.6	0.1	2.5	0.2
15. Cell wall (S)	94.6	0.8	3.3	0.1	1.3	0.1	0.8	0.1

^a σ – standard deviation

^bnd – not detected

The high gold content and the low Ag and Cu concentrations – which were below the detection limits of our instrument – could also suggest an intentional choice, the result of the craftsman's intention to benefit from the special malleability of pure gold.

An important number of objects from the second Apahida grave were also damaged at the time of their discovery, and thus a lot of smaller fragments, such as gold patterned foils or cell walls, are available for analysis. One of the partially damaged objects is a large purse-lid adornment (Fig. 1). We analysed several gold patterned foils, usually mounted beneath the stones to enhance their lustre, in particular those preserving their initial omega or hexagonal shape (Table 2 and Fig. 1 – bottom left and right, respectively). While the patterned foils with the same shape seem to have been obtained from the same ingot, none of the omega shaped foils had a similar composition with the ones with hexagonal foil. This observation confirms the previously suggested hypothesis, i.e. that the small patterned foils were cut from the same large gold leaf.

On the other hand, it should also be emphasised that elements with similar function might have been obtained from different gold ingots. The elemental composition of the omega shaped patterned foils, with little more than 20% Ag, indicates that this type of elements could have been made by melting together different alloys, a high purity of gold not being a compulsory condition.

We also analysed the back supports of 27 similar harness adornments found in the second princely grave from Apahida. The results were grouped in two distinct

Table 2 The results of XRF analyses on the patterned foils detached from the purse-lid adornment (Apahida II)

Analysed item	Au (%)	σ^a Au (%)	Ag (%)	σ Ag (%)	Cu (%)	σ Cu (%)	Fe (%)	σ Fe (%)
1. hexagonal patterned foil	99.0	0.8	nd ^b	nd	nd	nd	1.0	0.1
2. hexagonal patterned foil	98.8	0.8	nd	nd	nd	nd	1.2	0.1
3. hexagonal patterned foil	97.5	0.8	nd	nd	nd	nd	2.5	0.2
4. hexagonal patterned foil	97.7	0.8	nd	nd	nd	nd	2.3	0.2
5. omega shape patterned foil	76.9	1.0	21.0	0.4	nd	nd	2.1	0.3
6. omega shape patterned foil	75.8	1.0	20.8	0.4	nd	nd	2.8	0.3
7. omega shape patterned foil	76.9	0.8	20.7	0.4	nd	nd	2.4	0.2
8. omega shape patterned foil	76.6	0.8	20.8	0.3	0.7	0.1	1.9	0.2

^a σ Standard deviation

^bnd not detected

clusters (the star-shaped dots in Fig. 2a, also shown in Fig. 2b, in which the Au/Ag diagram only for these 27 adornments is shown).

Again, this is a situation when elements with similar functions were made from different gold alloys; in this case, the back supports were cut perhaps from two larger gold plates.

3 Conclusion and Directions for Future Research

The variation in the composition of the gold points to the conclusion that, despite the proximity of the locations where the objects were found and stylistic similarities, most likely the manufacturing technology of the alloy, as well as the sources of raw materials, could have been different. This does not mean that the analysed objects were necessarily produced in different workshops, but it suggests that during the assembling process, fragments of different gold purity were used. Although the general aspect of the objects is similar, the alloys used for elements with similar structural function differ from one item to another, and elements with similar functions assembled in the same object could have been obtained from ingots of different purity. These findings provide us with a hint regarding the organisation and techniques used in the workshop – or workshops – where the cloisonné adornments from Apahida were manufactured. We can assume that old, recuperated metal was probably frequently used; this recycled metal was not necessarily re-melted to obtain a specific purity, as long as its title was already within certain limits. The main goal of the craftsman concerned the final aspect of the object, which could include elements of variable gold purity. It follows that the purity of the gold used to create such elaborated objects as the garnet inlaid adornments from Apahida was of secondary importance. The manufacturing process required a high technical background, a particular specialisation of the craftsman, and appropriate skills. Thus, the value of the object greatly exceeded that of the gold and gems built in it, the intrinsic material value blending with the much more important symbolic one.

This paper presents only a preliminary and partial interpretation of the results of an ongoing project. In the future, we intend to increase the number of analysed elements originating from the same items and to extend our research to the gem inlays.

References

- Harhoiu R (1998) Die frühe Völkerwanderungszeit in Rumänien. *Archaeologia Romanica I*, Bukarest
- Horedt K, Protase D (1972) Das Zweite Fürstengrab von Apahida (Siebenbürgen). *Germania* 50(1–2):174–220
- Périn P, Vallet F, Kazanski M (eds) (2000) *L'or des princes barbares. Du Caucase à la Gaule Ve siècle après J.-C.*, Éditions de la Réunion des musées nationaux, Paris

Non Destructive In Situ Analysis of Gold and Silver Artifacts from Tomb 7 of Monte Alban, Oaxaca, Mexico

G. Peñuelas, J.L. Ruvalcaba, J. Contreras, E. Hernández, and E. Ortiz

1 Introduction

Mesoamerican metallurgy began in the west of Mexico around 800 AD, perhaps due to interactions with people from South America, who first introduced metal technology in Mesoamerica at this time. However, Mixtecs and Zapotecs from the Oaxaca area, in the South of Mexico, probably established their own contacts with people from Central America and involved themselves in the production of metal objects around 1200 AD. During the late post-Classic period, from 1300 to 1521 AD, Mixtecs were well known for their metallurgy work; they manufactured exquisite assemblages of gold and silver objects to be deposited as offerings in burials.

The famous Tomb 7 was discovered in 1932 by Alfonso Caso in Monte Alban, in the Central Valley of Oaxaca. In this Zapotec tomb reused by the Mixtec people (c. 1250–1350 AD), one of the richest collections of offerings in Mesoamerica was found. Gold and silver artifacts, green stone pendants, turquoise decorated pieces, fine grained bone, obsidian and rock crystal objects, alabaster items, and other shells and coral fragments were recovered, together with the bone remains of three individuals. Concerning the metallic artifacts, very few analyses were performed on six objects in the 1960s (Easby 1969), most of them using micro-chemical tests and X-ray fluorescence (XRF). Additionally, in the last few years, scanning electron microscopy (SEM–EDS) analyses were carried out on a very limited number of samples (Camacho et al. 2005). While other collections of gold Mesoamerican

G. Peñuelas and J. Contreras

Escuela Nacional de Conservación, Restauración y Museografía, INAH, Mexico D.F., Mexico

J.L. Ruvalcaba (✉)

Instituto de Física, Universidad Nacional Autónoma de México (UNAM), Mexico city, Mexico
e-mail: sil@fisica.unam.mx

E. Hernández

Instituto de Investigaciones Estéticas, UNAM, Mexico city, Mexico

E. Ortiz

Instituto de Investigaciones Antropológicas, UNAM, Mexico city, Mexico

artifacts have been analyzed using non destructive techniques, such as Particle Induced X-ray Emission (PIXE) and XRF (Cesareo et al. 1994; Ruvalcaba et al. 1995; Rickards et al. 1999), this outstanding collection has never been analyzed in situ by non destructive methods before. Moreover, in the case of the pre-Hispanic silver items, scarce information concerning these objects existed. The study of this collection, one of the most important in Mexico with a well studied archaeological context, provides reliable information about technology and exchange of metallic items in Mesoamerica in the post-Classic period in Oaxaca (900–1521 AD). In this work, a representative set of artifacts (including unique pieces) was studied by an interdisciplinary team using a non destructive in situ methodology in the museum (Peñuelas 2008).

2 Methodology

The collection of Tomb 7 includes 121 gold artifacts – among these, rings, pendants and necklaces – and 24 pieces of silver, as well as two bimetallic discs. For this study, a representative set of 49 artifacts (consisting of 32 gold items, 15 silver objects and the two bimetallic discs) was analyzed.

First, all the artifacts were digitally photographed. The main features of manufacturing techniques were observed by optical microscopy using a 40× stereoscope with a digital camera. UV examinations were carried out with an 8 W UV lamp with long and short waves (365 and 254 nm, respectively) in order to determine the presence of bee wax, resins and polymers previously used for consolidation. All the images were recorded by digital photography as well. Finally, the artifacts were analyzed using our SANDRA XRF portable system. This device has a Mo X-ray tube and an Amptek CZT X-ray detector. The X-ray tube irradiation conditions were 0.30 mA and 45 kV, with a 1.5 mm diameter spot at the artifact's surface. About 700 measurements were carried out. The time required to collect one spectrum was 30 s. For quantitative analysis, reference gold alloys of 75% Au, 13% Ag, 12% Cu, and 58% Au, 34% Ag and 8% Cu, as well as 0.925 Ag and 0.725 Ag alloys were irradiated under the same conditions. As a result, matrix corrections were minimal. The quantitative analysis was performed following the procedure described by Karydas et al. (2004).

3 Results

UV examinations pointed out few punctual regions with remains of bee wax and resins used for mounting the artifacts in the museum displays. Fortunately, no polymers have been applied to the artifacts' surfaces for consolidation.

Figure 1 shows two of the best known and biggest artifacts of the collection, the pendant with dates and the Xipe-Totec god pendant. From the 32 gold artifacts, 23

were manufactured using the lost wax technique and the rest by hammering. In several objects, the remains of a black material were found in corners and in the interior parts. This corresponds to the mixture of carbon and clay used in the nucleus to support the wax model in the lost wax technique. In some cases, the formation of dendritic structures indicates a slow cooling (Fig. 1c). Also, a porous surface typical of the escape of gases during casting was observed for several artifacts.

On the other hand, the false filigree technique was used for most of the gold and silver artifacts. Several details of modeling can be observed in Fig. 1b, d. Defects and corrections in the models were detected.

XRF results indicate that, in general, Au–Ag–Cu alloys were used in the casting of gold artifacts, while the silver items were manufactured with Ag alloys with small amounts of Au and Cu (Fig. 1). The gold alloys are rich in gold (between 60 and 80% Au), with low amounts of copper (about 10–15%). Our results show lower gold contents as compared to previous SEM–EDS analyses (Camacho et al. 2005) that are affected by gold surface enrichment due to natural copper depletion effects. XRF provides elemental composition information from a thickness level about 20 times thicker than the one available by EDS for this type of materials.

Most of the artifacts are very homogeneous, and in very few cases several alloys were used to manufacture the various sections of the artifacts, but the casting of those pieces followed a row array order. In the collection, there are groups of pendants and finger ornaments with similar iconography and size, appearing almost identical. Nevertheless, they were modeled in wax and cast individually. The compositions of the set of pendants and other pieces are very similar and allow us to consider the possibility that these artifacts were produced in the same workshop, but that the complete burial offering consisted of items produced in very few workshops. Also, the similarity in the composition of the metallic pieces suggests that native sources from the same area were used as raw materials.

A general comparison of our results (in red in Fig. 2) with other gold collections from Oaxaca and other Mesoamerican areas shows a good agreement with the

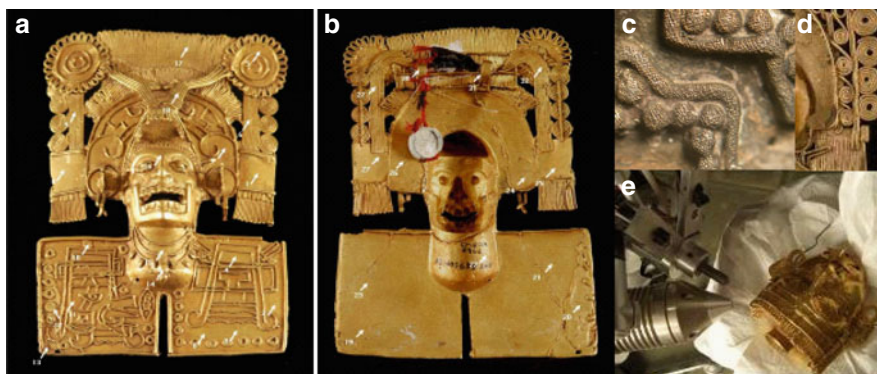


Fig. 1 Pendant with dates, (a) front and (b) reverse. Dendritic formation due to casting (c). False filigree technique (d). In situ XRF fluorescence analysis of the Xipe Totec (e)

composition of other artifacts from the Central Valleys of Oaxaca and Aztec items. However, the pieces from Tomb 7 are clearly different from the ones found in the Oaxaca Sierra and the Maya areas (Torres and Franco 1989; Rickards et al. 1999; Ortiz-Diaz et al. 2007). Maya pieces were traded from Panama cultures, while the Oaxaca Sierra pieces may correspond to a different locus of metal work. Thus, the gold artifacts from Tomb 7 were manufactured locally and were not imported from foreign regions.

In the case of the Ag alloys, the amount of gold is very low (less than 5%) and the silver content is higher than 90%. In few silver artifacts, manufactured by lost wax casting, the gold concentration is higher than 6%. The cast pieces are homogeneous, as in the case of the gold artifacts. We discovered that some parts of the ornaments were not correctly assembled after the excavations, since the composition of the bells does not correspond to the composition of the rest of the artifact. Finally, the rare bimetallic discs were manufactured using a rich gold alloy (85% Au, 15% Ag) and a silver alloy (92% Ag, 5% Au, 3% Cu). These artifacts appear fragile, perhaps due to the hammering procedure used to produce them, but the silver diffusion observed at the interphase suggests a thermal process carried out in order to join together the silver and gold parts.

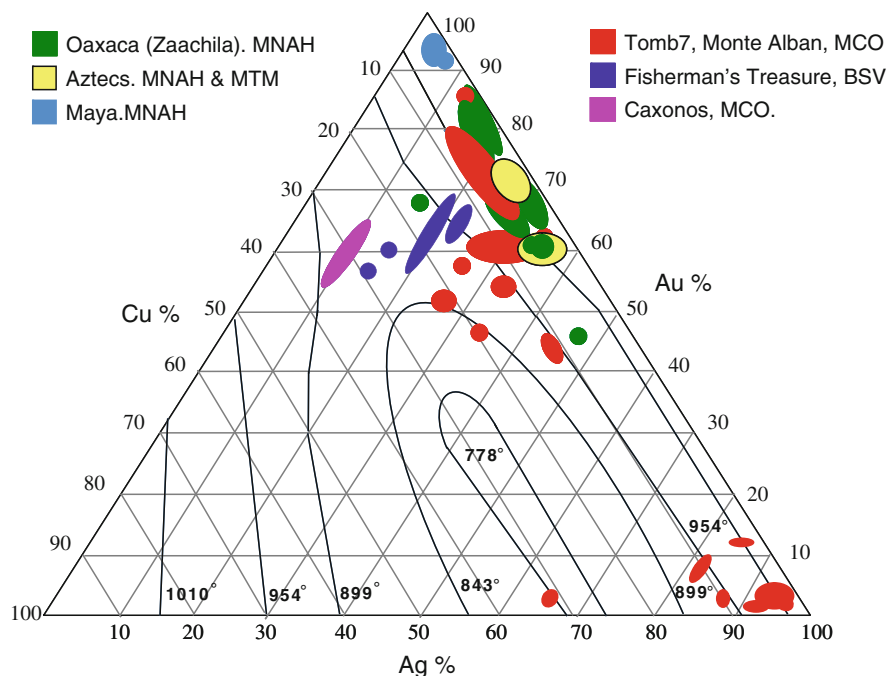


Fig. 2 Comparison of the elemental compositions of Monte Alban Tomb 7 artifacts (Peñuelas 2008) and other collections from various Mesoamerican areas and museum collections (MNAH Museo Nacional de Antropología e Historia, MTM Museo del Templo Mayor, MCO Museo de las Culturas de Oaxaca, BSV Baluarte de Santiago Veracruz)

4 Conclusions

The main analytical results indicate that most of the studied objects have a similar alloy composition with a high homogeneity. Gilding procedures and soldering were not observed. The more complex artifacts were produced by the lost wax casting technique. These results indicate that the Mixtec goldsmiths were able to produce large amounts of gold and silver alloys with similar composition, but also allow us to hypothesize the use of similar metals sources as well. Our results match the elemental composition of other gold artifacts from the Mixtec Central Valley of Oaxaca sites (high amounts of gold and low copper concentrations). Aztec pieces share the Mixtec metallurgical features. The conservation condition of the gold artifacts is very good due to the high gold and silver contents of the artifacts.

Acknowledgements The authors would like to thank the Museo de las Culturas de Oaxaca, as well as Oaxaca's INAH Centre, for providing the facilities used to carry out this study. This research has been supported by the Mexico CONACyT grant U49839-R.

References

- Camacho GA, Ortega-Aviles M, Velasco MA, José-Yacamán M (2005) A microstructural study of gold treasure from Monte Alban's tomb 7, *Journal of the Minerals, Metals Mater Soc* 57(7):19–24
- Cesareo R, Gigante GE, Iwanczyk JS, Rosales MA, Aliphat M, Ávila P (1994) Non destructive analysis of pre-Hispanic gold objects using energy dispersive X-ray fluorescence. *Revista Mexicana de Física* 40(2):301–308
- Easby D (1969) In *El Tesoro de Monte Alban, Memorias del Instituto Nacional de Antropología e Historia*, vol 3. INAH, Mexico, pp 353–370
- Karydas AG, Kotzamani D, Bernard R, Barrandon JN, Zarkadas Ch (2004) A compositional study of a museum jewellery collection (7th–1st BC) by means of a portable XRF spectrometer. *Nucl Instrum Methods Phys Res B* 226:15–28
- Ortiz-Díaz E, Ruvalcaba-Sil JL (2007) An historical approach to a gold pendant: The study of different metallurgic techniques in ancient Oaxaca, Mexico, during the late post classic period. In: 2nd International Conference on Archaeometallurgy in Europe, Associazione Italiana di Metallurgia, Milán. In CD. ISBN 88-85298-61-3
- Peñuelas G (2008) Caracterización por medio de análisis instrumentales de los materiales constitutivos de la orfebrería de la Tumba 7 de Monte Albán, Oaxaca. ENCRyM – INAH, Mexico
- Rickards J, Torres ML, Franco F, Flores MD (1999) Análisis por la técnica PIXE de artefactos de oro del Museo Nacional de Antropología. *Revista Antropológicas, IIA-UNAM* 15:71–74
- Ruvalcaba-Sil JL, Demortier G, Oliver A (1995) External beam analysis of gold pre-Hispanic jewelry items. *Int J PIXE* 5:273–288
- Torres Montes L, Franco Velázquez F (1989) La orfebrería prehispánica en el Golfo de México y el tesoro del pescador, en *Orfebrería Prehispánica*, Corporación Industrial San Luis. Ed. Patria, Mexico, pp 217–270

“Harvesting” the Ore: The Use of Iron Seepages in the Early Bloomery Furnace in Ireland

E. Photos-Jones and A.J. Hall

1 Introduction

In this paper we suggest that iron-seepages, a precursor form of bog iron ore, must have been among the earliest iron ores used in early bloomery furnaces in Ireland. This is because: of their bright orange colour; the dramatic red-staining of the associated water-red springs or *meinn* in Gaelic; their rapid regenerative nature which means that they would have been “harvested” on a cyclical basis rather than “mined”; and also because there is an absence of solid bog ore remains within the relict furnaces. Archaeological evidence for iron-seepage ore, consisting of fine powdery material, in early bloomery furnaces would be elusive on account of its clay-like pasty nature and the fact that it will easily merge into a background of soil and metallurgical waste. We assume that the original wet clay-like pasty mass would have been dried prior to charging in the furnace and purer than our modern sample; and also, possibly, but not necessarily, shaped into small lumps.

Given the above and based on the detailed investigation of the evidence from one early iron making site in Ireland, we suggest that in order for these elusive ores to be made archaeologically “visible” a methodology needs to be put in place that targets both the “soils” of the fills of the furnace as well as the metallurgical waste on a context-by-context basis.

Early iron making installations in Ireland are simple structures consisting often of nothing more than a hole in the ground now filled with the remains of slag and charcoal and embedded within local soil heated by the furnace (Fig. 1). The Iron Age site of Derrinsallagh IV, Co Laois, Ireland (Cal BC50-CalAD 250) was revealed in the course of a motorway (M7) extension. The site is situated in a flat

E. Photos-Jones (✉)

Analytical Services for Art and Archaeology (SASAA) Ltd, Glasgow, UK
and

Department of Archaeology, University of Glasgow, Glasgow, UK

A.J. Hall (✉)

Department of Archaeology, University of Glasgow, Glasgow, UK
e-mail: hall@archaeology.arts.gla.ac.uk

Fig. 1 View of cluster of excavated furnaces at Derrinsallagh IV. Note the colour halo of adjacent soil from black (*interior*) to red (*exterior*). Flat stones like the one shown here were probably used for resting bellows. (photo from Photos-Jones and Wilson, 2007)



plateau on an area of rising ground and forms part of a historic landscape consisting of many features of different dates (see http://d28272.n32.morsolutions.net/cms/publish/article_47.shtml). It was excavated by ACS Ltd, Ireland, in 2006 and consists of 42 small bowl furnaces within an area of 7,000 m². This is a phenomenal number of bowl furnaces at a single site. Its early date places it firmly within the Iron Age and provides a rare opportunity to examine iron making within the Celtic iron manufacturing tradition. The furnaces consist of holes in the ground without any major superstructure other than a short lip. Based on the size of the archaeological cut feature, they are *c.* 40 cm in diameter and about 30 cm deep; however, their actual working surface area would have been smaller. They occur singly or in clusters of two, three, four, or five (Photos-Jones and Wilson 2007).

2 Iron Seepages: Their Nature and Formation

Typical solid bog ore resembles macroscopically bloomery slag on account of its spongy texture; it is only distinguishable from slag on the basis of mineralogy and microscopic texture. Contrary to many places where remnants of solid bog ore, at various stages of reduction, are to be found within furnaces (Host-Madsen and Buchwald 1999), in Ireland and Scotland such specimens are rare (Photos-Jones et al. 1998; Hall and Photos-Jones 1998; Johnson et al. 2007); for the majority of sites, evidence for the use of iron-seepage ore would only come from the discovery of very small particles of relict ore within slag (Fig. 2). Given the powdery texture of the dried seepage, it is inevitable that a considerable amount of that powder could filter through the charcoal and be rendered unavailable for further reduction.

Solid bog ore is usually the product of natural drying and consolidation of iron-seepages (Bricker et al. 2003). Bog iron ores consist mainly of iron oxyhydroxides such as limonite FeOOH.nH₂O, which can originate from the sub-aerial oxidation and precipitation of iron in groundwater seepages ameliorated by iron-oxidising bacteria (Fig. 3). Iron seepages are visible today in Scotland and Ireland. The location of one such seepage (Fig. 4) was pointed out near Derrinsallagh IV by the local farmer, Mr Gerry Moylan, who alerted us to the existence of that and other

Fig. 2 Round particle of iron ore, about 400 μm , within slag in polished section, using SEM backscattered mode. SEM-EDAX analysis gave c. 87.5 wt.% FeO, 8% SiO₂, 1.5% MnO and 1% P₂O₅; Ni, As, Cu and Zn are below the level of detection (from Photos-Jones and Wilson 2007)

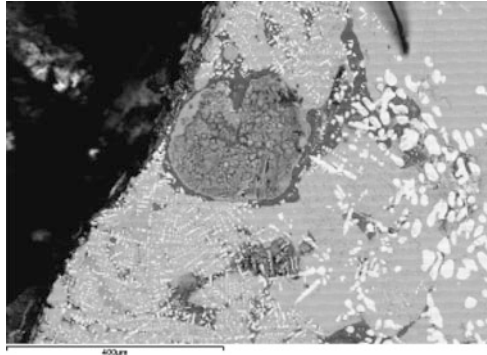


Fig. 3 Cartoon demonstrating the origin of iron-seepages at a spring and bog iron ore in the run-off. Chemical process is detailed in text

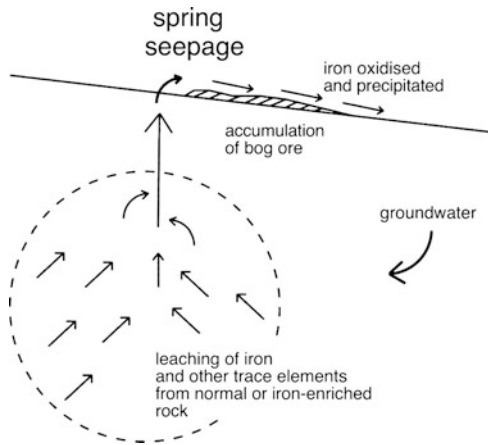
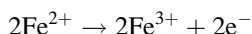


Fig. 4 A modern iron-seepage in the Derrinsallagh area and within a drainage channel. Note the bright orange colour of the iron oxyhydroxide precipitate (photo from Photos-Jones and Wilson 2007)

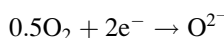


seepages within his land. Modern seepages often appear within drainage ditches at the interface between dry and boggy land. Reduced ferrous iron in groundwater which reaches the surface is oxidised to insoluble ferric iron precipitating colloidal iron oxyhydroxide and giving the acidic spring a rusty red colour, probably enhanced by the bacteria. The chemical process may be represented as follows:

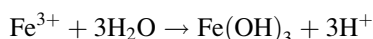
1. Oxidation of dissolved ferrous iron to ferric iron



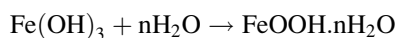
and



2. Precipitation of ferric iron as limonite



and



Two modern sources of iron-seepages were sampled from near the archaeological site. The analyses by portable XRF (Niton XLt-soil mode) of the dried material showed that they contained about 30–35 wt.% Fe and are enriched in Pb, Ca, As, Mn and Sr (Table 1). This iron content is commensurate with that found in bog iron ores.

3 Seeking the Seepages in the Fills of the Furnaces

The 42 furnaces excavated at the site contained 326 diverse fills which consisted of either slag alone, or “soils” with or without small inclusions of slag/charcoal. There was 100% recovery of the contents of the fills. The bags which contained only slag were weighed and put aside for further study with SEM-EDAX. The bags of “soils” were opened and spread out to dry. For those “soils” with slag/charcoal inclusions a qualitative assessment was carried out to establish relative quantities of different micro inclusions. XRF analysis with the portable XRF was carried out on all “soils”, a technique which facilitates processing of large numbers of samples.

XRF analyses of *some* “soils”/fills *containing no slag or other inclusions*, showed that they were highly ferruginous (see Table 2 for a number of contexts from different furnaces). Most “soil”/fills are expected to bear some “contamination” by powdered slag, but the high level of iron (ranging between 13–67% Fe) in these contexts cannot be considered “contamination”. Iron content in the soils averaged c 1.5% Fe (see analyses for control in Table 1). Control levels for each element reported in Table 1 were averaged over six samples retrieved from six different locations outwith the furnace structures and on the same stratigraphic level as the exposed archaeological features.

Table 1 XRF analyses (ppm) of two modern iron-seepages, and the Derrinsallagh IV Control soil sample

Iron-seepage	Pb	Sn	Sb	Sr	Rb	As	Zn	Cu	Ni	Fe	Mn	V	Ti	Ca	K
1	28	<D	<D	173	26	65	<D	<D	<D	346,036	1164	<D	588	43,744	4,930
2	21	<D	<D	165	19	62	<D	<D	<D	314,754	1845	55	848	82,190	7,374
Control	<D	26	<D	<D	19	49	<D	48	<D	12,780	961	<D	2,213	2,352	9,959

<D indicates the element is below detection limit

Table 2 XRF data for “soils” with high Fe content but with no evident slag inclusions

Feature furnace	Context 'soil'	Pb	Sb	Sr	Rb	As	Zn	Cu	Ni	Fe	Mn	V	Ti	Ca	K
5	371	<D	<D	12	24	102	<D	<D	314	231,125	30,495	109	1,466	8,576	8,212
14	276	27	<D	37	49	68	<D	<D	131	130,484	15,179	81	1,672	17,649	8,956
16	297	<D	<D	15	46	58	<D	<D	222	200,373	24,383	39	1,095	2,960	3,884
119	324	<D	<D	9	20	41	81	53	147	162,859	11,651	115	1,351	7,997	9,596
121	262	<D	<D	16	32	125	<D	<D	536	379,485	61,622	127	1,583	10,276	8,743
225	240	<D	<D	14	28	112	<D	<D	662	335,227	49,418	128	1,755	7,654	8,063
393	430	37	<D	23	47	<D	<D	<D	439	433,683	29,282	<D	1,098	4,713	4,037
428	296	<D	<D	17	27	168	<D	<D	824	677,091	49,382	144	1,707	14,862	9,627

Note: the high Mn and Ni in many samples; the sporadic high Pb; the sporadic high Zn, often with Cu in the same sample; and the frequent high As. These enrichments probably point to the use of ores from several localities. <D indicates the element is below detection limit. The Control for background values is given in Table 1

From the above we can only infer that the said “soils” were enriched in iron content from an iron rich source which could have only been the iron ore charged in the furnace. We suggest that this source was iron seepage, given that there were no visible slag/ore inclusions within these “soils”.

Manganese levels are also high as expected for this element which tends to follow iron geochemically. There is high Ni in many samples compared to other sporadically enriched elements like As, Zn, and Cu. The Ni-rich content points to a special source of ore be it seepage, bog or gossan but the modern iron-seepages sampled were not Ni-rich. Potential nickeliferous sources in the area are currently unknown. We suggest that the trace element pattern for seepages will vary depending on the source of the iron and the diverse enrichments observed at Derrinsallgh IV (Table 2) probably point to the use of ores from several localities. It is not possible to trace these original localities, only the ore type, since seepages could potentially “outcrop” at any location which fulfils the criteria for their formation.

4 Conclusions

We highlight here the potential use of iron seepages, as opposed to solid bog ore, in early iron making bloomery furnaces in Ireland based on our measurements of highly ferruginous “soils”/fills within some furnaces which were devoid of any slag or fragments of other materials and also on the basis of the evidence of small particle size inclusions within slag (Fig. 2). We suggest that these highly ferruginous fills contain powdery seepage ore which was never reduced. It would be desirable to carry out XRD of these “soils” (or magnetic concentrates thereof) in order to confirm the mineralogical state of the iron within and the presence/absence of fayalite or other slag related phase.

We cannot exclude the possibility of lumps of bog iron ore having been used *in addition* to seepages; however solid lumps thereof, in varying state of reduction, are the exception rather than the rule in the archaeo-metallurgical sites in Ireland and in Scotland; instead the *meinn* is ubiquitous both in the field and the documentary/oral record.

We suggest that iron seepages would have been “harvested”, resembling the lake ores of Scandinavia which “during the winter. . . (were) collected in boats by means of drags; and during winter. . . (they) were raked up through holes made in the ice” (Percy 1864). Lake ores were being dredged well into the twentieth century (Buchwald 2005). They regenerated themselves in the space of 20–30 years (Percy 1864). Bricker et al (2003) report that in the case of Eastern USA bog ores, these were able to regenerate themselves in only a year, the differentiation between the two being merely that of morphology rather than mineralogy.

Trace elements can be so diverse in iron oxyhydroxide ores that they are of little value in fingerprinting a type of ore or source unless direct comparison can be made with a potential source. For example, at Derrinsallgh IV, if a potential local source of iron ore proves to be Ni-enriched, it is very likely to have been a source for the

Iron Age furnaces. Some sources of ores used at Derrinsallagh had a Cu + Zn signature which is not be surprising on account of the diverse metalliferous deposits in Ireland. The high As-content of potential ore from furnace fills and the local modern seepage is surprising and justifies further study.

We suggest that iron seepages which would have been “harvested”, would fit well into a cycle of farming activities. Indeed the frequent presence of bloomeries within ringforts with evidence for domestic occupation suggests this (Photos-Jones 2004; Analytical data on CD by Photos-Jones in Carlin et al. 2008).

Chalybeate springs or iron-rich springs, called *meinn* in Gaelic (Photos-Jones 2004), were thought to have healing properties and in relatively recent times were often visited especially by patients who suffered from a number of ailments. There are various such springs reported in Scotland and Ireland (Beith 1995). It is not certain on what grounds they developed medicinal properties and whether or not these could have preceded use for iron making.

References

- Bricker O, Newell WL, Simon NS, Clark I (2003) Bog iron formation in the Nassawanto Watershed, Maryland. Accessed at: pubs.usgs.gov/of/2003/of03-346/
- Beith M (1995) Healing threads. Traditional medicines of the highlands and islands. Polygon, Edinburgh
- Buchwald VF (2005) Iron and steel in ancient times. Kongelige Danske Videnskaberne Selskab, Copenhagen
- Carlin N, Clarke L, Walsh F (2008) The archaeology of life and death in the boyne floodplain, the linear landscape of the M4. National Roads Authority, Ireland
- Hall A, Photos-Jones E (1998) The Bloomery mounds of the Scottish highlands Part 2: a review of iron mineralisation. *J Historical Metallurgical Soc* 32:54–66
- Host-Madsen L, Buchwald VF (1999) The characterization and provenancing of ore slag and iron from Iron Age settlement at Snorup. *J Historical Metallurgical Soc* 33:57–67
- Johnson ME, Photos-Jones E, Hickman S (2007) A medieval bloomery mound in Glen Docherty, Kinlochewe, Highland. *Scottish Archaeol J* 28:125–49
- Percy J (1864) *Metallurgy*. John Murray, London
- Photos-Jones E (2004) A site like “Kay”, An examination of metallurgical waste analysis from Killickaweeny Co. Kildare, Ireland, SASAA Report 112
- Photos-Jones E, Wilson L (2007) Derrinsallagh 4, Co. Laois, Eire, Holistic context analysis to further site understanding, SASAA Report 271
- Photos-Jones E, Atkinson JA, Hall AJ, Banks I (1998) The bloomery mounds of the Scottish highlands. Part I: The archaeological background. *J Historical Metallurgy Soc* 32:15–32

Analysis of Gold Jewellery by PIXE and SEM–EDS: A Comparison of Ancient and Modern Productions

V. Virgili and M.F. Guerra

1 Introduction

Gold jewellery produced in antiquity consists in many cases of a combination of gold parts joined together. During quite a few historical periods, these parts were multiple and minute, such as granulation, wires, leaves, die formed pendants, and so on. By copying and reproducing these tiny parts, modern goldsmiths were able to restore and reproduce ancient items, but could also produce jewellery ranging from the mere copy to the invented object. The difficulty of separating ancient items from modern objects depends on the skill of both the ancient and the modern goldsmiths, and on the degree of information about the ancient techniques we have access to nowadays. For this reason, scientific techniques of examination and analysis provide paramount information on the different steps of production of an object and allow comparing modern and ancient productions (Guerra 2005).

Requiring non-destructive analysis, rare and fragile gold jewellery items are usually submitted to elemental analysis – very often to X-ray based techniques, such as XRF, PIXE, SR-XRF (Guerra et al. 2008; Guerra 2008) – coupling, however, the examination of the items with elemental analyses of the alloys. According to such methods, relevant information pertaining to many of the production steps can be obtained. As such, SEM–EDS could be the best option for the study of gold jewellery if more than the very first surface layers of the alloy were analysed. As mechanical or chemical preparation is not allowed for the majority of these items, another technique, with a higher level of penetration and access to microanalysis, could be a good alternative. In the present work, we considered micro-PIXE as such a method. In order to assess the equivalence of the results obtained by PIXE and SEM-EDS, we analysed gold beads, both ancient (sixth

V. Virgili (✉)

CNR - Dipartimento Patrimonio Culturale, Innovation Relay Centre CIRCE, Rome, Italy

M.F. Guerra (✉)

Centre de Recherche et de Restauration des Musées de France, UMR 171 CNRS, Palais du Louvre, Paris, France

e-mail: maria.guerra@culture.gouv.fr

century BC) and modern (nineteenth century AD) ones produced in the ancient tradition, with similar typology, and produced by joining different sorts of wires; the study of the wires required the use of microanalysis.

2 Objects and Analytical Techniques

All the beads studied in this work belong to the Campana collection (Louvre Museum). The ancient sixth century BC beads, said to belong to an Etruscan necklace, were produced with beaded and strip-twisted wires joined together and supported by a gold tube. A plain circular section wire sustains all the elements at each side of the bead. Some of the joining regions were covered with granulation with diameters ranging from 120 to 200 μm (Fig. 1a). The modern beads, belonging to a necklace believed to be a construction of Castellani (a goldsmith's workshop in

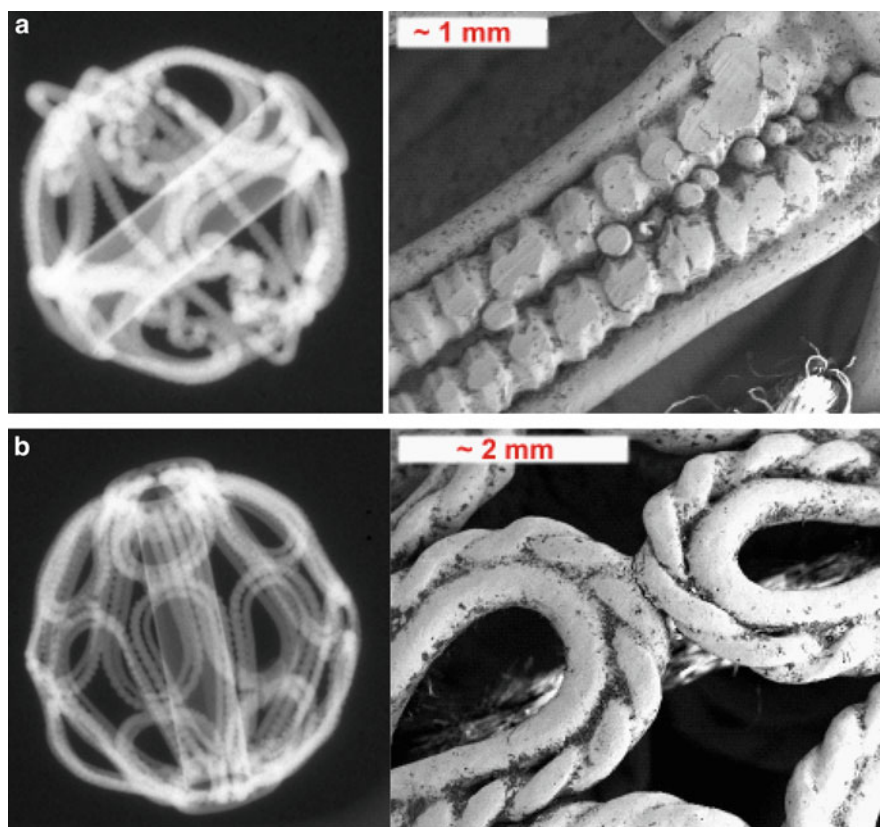


Fig. 1 X-ray radiography of the gold beads (©T. Borel, C2RMF) and SEM micrographs of the wires joined to form the beads (© M. F. Guerra, C2RMF): (a) ancient and (b) modern

Rome), were produced with drawn twisted wires and plain circular section wires joined together (Fig. 1b). Some of them present a supporting gold tube, while the others only present a thick soldering maintaining the wires together on both sides of the bead. The X-ray radiographies and SEM micrographs (Fig. 1a, b) show the difference in terms of production skill for the two types of beads: the fine work visible in the ancient beads in Fig. 1a (beaded wire finely joined together and decorated with powder granulation) contrasts with the poor work evident in the modern beads in Fig. 1b (large soldering and roughly twisted wire).

PIXE was carried out at the AGLAE accelerator of the C2RMF with a 3 MeV external proton beam. For this study, a micro-beam of 50 μm diameter and 40 nA intensity was used. Two Si(Li) detectors collected the X-rays emitted by the sample: one was dedicated to the identification of major elements and the other, with a copper absorber of 75 μm to absorb the gold L-lines, was used to determine trace elements (Guerra and Calligaro 2004). The quantification was performed with the GUPIX programme (Maxwell et al. 1988). The limits of detection reach 13 to 90 ppm for elements with atomic number between 20 and 60, and 100–300 ppm for elements with atomic numbers higher than 75 (Guerra 2004). SEM-EDS was carried out with a JSM 840 JEOL microscope associated with an Oxford Link ISIS energy dispersive X-ray system. Measurements were carried out on selected areas on the wires and junctions with an electron beam acceleration voltage of 20 kV. For both techniques, results were normalised to 100%.

3 Analytical Results

The selected wires from six modern and five ancient gold beads, typologically similar, were analysed for the quantitative evaluation of their elemental composition. Table 1 shows the results obtained by PIXE and SEM-EDS. The modern

Table 1 Composition of the alloys used in the fabrication of the ancient and modern gold beads by PIXE and SEM-EDS

Modern beads		Cu%	Ag%	Au%	Ancient beads		Cu%	Ag%	Au%
MB1	PIXE	0.9	1.9	96.8	GB1	PIXE	3.2	5.7	90.6
	EDS	0.8	0.9	98.2		EDS	2.5	6.8	90.7
MB2	PIXE	0.9	1.8	96.9	GB2	PIXE	2.9	5.8	90.9
	EDS	0.8	1.2	98.0		EDS	2.9	5.5	91.6
MB3	PIXE	0.9	1.6	96.5	GB3	PIXE	0.5	1.3	98.0
	EDS	1.1	1.7	97.2		EDS	0.1	1.0	98.9
MB4	PIXE	0.9	1.6	97.2	GB4	PIXE	0.8	1.5	97.4
	EDS	1.4	0.9	97.7		EDS	0.5	1.4	98.1
MB5	PIXE	0.5	2.1	96.8	GB5	PIXE	0.4	1.5	97.7
	EDS	0.4	1.8	97.8		EDS	0.2	1.1	98.7
MB6	PIXE	1.1	2.4	96.3	Joining				
	EDS	0.5	0.8	98.7					
Joining 1	PIXE	1.3	3.6	92.4	GB2	EDS	7.1	19.9	73.0
	EDS	0.5	5.5	93.0		GB4	EDS	1.8	1.0

beads have an average composition of $0.9 \pm 0.2\%$ Cu, $2.2 \pm 0.7\%$ Ag, $96.1 \pm 1.7\%$ Au as determined by PIXE, and of $0.8 \pm 0.4\%$ Cu, $1.8 \pm 0.4\%$ Ag, $97.2 \pm 0.5\%$ Au as determined by SEM-EDS. In spite of the small differences observed for the Ag contents, we can conclude that both techniques provide, on average, equivalent compositions for the gold wires. We can note that the concentrations of Cu and Ag determined for the modern beads are very close to the concentrations determined by Cesareo and von Hase (1976) for the copies of a few ancient gold fibulae and decorative plaques fabricated in Rome in the nineteenth century by the Castellani workshop. The assumption that our modern beads could be a production of the Castellani workshop appears thus to be confirmed. The compositions of these alloys are situated in the yellow-red region of the Au–Ag–Cu gold colour diagram (Rapson 1990). We can subsequently suggest that this is the type of alloy used in the nineteenth century to produce jewellery imitating the ancient style.

The ancient beads were produced with two different alloys: one with low Cu and Ag contents, and another with higher contents of these elements (Table 1).

For the first alloy, the average composition obtained is $0.5 \pm 0.2\%$ Cu, $1.4 \pm 0.1\%$ Ag, $97.7 \pm 0.3\%$ Au by PIXE, and $0.2 \pm 0.2\%$ Cu, $1.2 \pm 0.2\%$ Ag, $98.6 \pm 0.4\%$ Au by SEM-EDS. For the second alloy, the average composition obtained is $3.1 \pm 0.2\%$ Cu, $5.7 \pm 0.1\%$ Ag, $90.8 \pm 0.2\%$ Au by PIXE and $2.7 \pm 0.3\%$ Cu, $6.1 \pm 0.9\%$ Ag, $91.1 \pm 0.7\%$ Au by SEM-EDS. If we exclude some Cu contents, the concentrations obtained by both techniques are on average similar. When we compare the elemental compositions of the ancient and modern gold beads, we can assume that the ancient alloys can, in this particular case, be distinguished from the modern alloys by the detection of certain amounts of Cu and/or of Ag. We must, however, note that the standard deviations are higher by SEM-EDS, the results obtained by PIXE allowing an easier distinction of the beads, especially for low concentrations of those elements.

Finally, we also analysed the joining regions of three beads: one modern (MB1) and two ancient (GB2 and GB4). The results obtained for MB1 by PIXE and SEM-EDS are not in agreement, but both show that the joining alloy is obtained by an increase of the Ag content. In contrast, the joining alloy of the ancient beads, analysed by SEM-EDS, is obtained by the increase of either the Cu amount or both the Cu and Ag amounts. We must note that the analysis of the juncture by SEM-EDS is simplified by the fine selection of the region to be analysed, the diameter of the proton beam used for the PIXE analysis in this work being too large for the analysis of some high quality joining regions in the ancient work.

4 Conclusion

The use of PIXE and SEM-EDS to determine, without surface preparation, the composition of gold wires used in the production of necklace gold beads typologically similar, but some produced in the sixth century BC and others in the

nineteenth century AD following the ancient tradition, showed that both techniques provide, on average, equivalent elemental compositions. Both techniques are consequently adequate for distinguishing modern and ancient productions; however, for low concentrations of Cu and Ag, PIXE offers more reliable results.

We also established that, in contrast to ancient beads, modern beads were in this case all produced with the same alloy. The comparison of our results with the composition of copies of ancient objects produced in the nineteenth century in Rome by the Castellani workshop showed that our beads could also be suspected to represent productions of that workshop.

References

- Cesareo R, von Hase FW (1976) Analisi di ori etruschi del VII sec a.C. con uno strumento portatile che impiega la tecnica fluorescenza X eccitata da radioisotopo. *Atti dei Convegna Lincei* 11:259–296
- Guerra MF (2004) Fingerprinting ancient gold with proton beams of different energy. *NIM B* 226:185–198
- Guerra MF (2005) Etruscan gold jewellery pastiches of the Campana's collection revealed by scientific analysis. *Studia Archaeologica* 150, L'Erma Di Bretschneider: 103–128
- Guerra MF (2008) An overview on the ancient goldsmith's skill and the circulation of gold in the past: the role of X-ray based techniques. *X-ray Spectrom* 37–4:317–327
- Guerra MF, Calligaro T (2004) Gold traces to trace gold. *J Archaeol Sci* 31:1199–1208
- Guerra MF, Radtke M, Reiche I, Riesemeier H, Strub E (2008) Analysis of trace elements in gold alloys by SR-XRF at high energy at the BAMline. *NIM B* 266:2334–2338
- Maxwell JA, Campbell JL, Teesdale WJ (1988) The Guelph PIXE software: a description of the code package. *NIM B* 43:218–30
- Rapson RW (1990) The metallurgy of the coloured carat gold alloys. *Gold Bull* 23–4:128–133

Part XI
Integrated Site Studies

Reconstructing the Lost Moregine Site: A VR Based Approach to Simulate and Navigate an Inaccessible Archaeological Excavation

A.F. Abate, S.C. Nappo, T. Paduano, and S. Ricciardi

1 Introduction

The archaeological site of Moregine, discovered near Pompei during local highway maintenance works and mainly known for the beautiful paintings and jewels found within a very well preserved Roman villa, has been buried according to cost and convenience evaluations (Nappo 2003). As there are still a lot of unanswered questions which archaeologists can no longer address through field research, this site is paradigmatic of how computer generated images, real time interaction and stereoscopy can be of help for the further study of inaccessible locations. The methodology proposed in this study is aimed at achieving the most accurate and visually realistic virtual reconstruction of the site as it appeared to archaeologists after the completion of the excavation. In this sense, the resulting simulation is more focused on the archaeologists' interests than most of the available digital reconstructions, typically designed to address the request of cultural heritage dissemination for a wide audience. The object of the digital reconstruction is "building B" of the Moregine archaeological area (Mastroroberto 2003), more precisely "house D", which is part of a wider block consisting of *cauponae* located on the northern side of the ancient Sarno river bed (Di Maio and Stefani 2003). This compound house was originally buried by the eruption of the Vesuvio in 79 AD, and was first unearthed by a survey in the years 1880–1881. Overall, the excavation considered for virtual reconstruction covered an area of 20×10 m, with a floor level positioned 3 m below the present-day street level, exposed to the water table, the main reason behind the decision to rebury the site.

A.F. Abate (✉), S.C. Nappo, T. Paduano, and S. Ricciardi
Dipartimento di Matematica e Informatica, Università degli Studi di Salerno, 84084 Fisciano, (SA), Italy
e-mail: abate@unisa.it, scnappo@alice.it, t.paduano@libero.it, sricciardi@unisa.it

2 Approach Used

Since at the time of the excavation 3D scanning techniques were not available, the entire building has been modelled using measurements originating from the original survey maps and all the existing photographic material, referencing the first type of data to the latter. According to this technique, a reference grid of feature points is increasingly refined (Fig. 1), adding details retrieved from multiple sources (Debevec et al. 1996). The principal aim of this method is to allow the interactive realization of a rich virtual reconstruction, making content creators free to exploit even the most realistic (and computing expensive) techniques for modelling, animation and rendering, without any constraints in terms of scene or character complexity. On the other hand, since a pre-rendering based approach limits interactivity, we aimed to reduce this disadvantage through effective system design and an intuitive interface, using intelligent techniques derived from videogame development.

The foundation of our proposal was the development of a pre-rendered virtual world in which the user can navigate following pre-built paths and performing available actions through a context sensitive motion tracking based interface. The entire virtual world is a collection of video clips stored on a high performance server, including every scene, eventually viewed from any allowed angle, and every path, from one scene to another. In other terms, such a virtual world can be visualized as a graph whose nodes represent scenes and whose oriented arches represent available paths which take the user from scene to scene. Any node or arch is uniquely identified with a tag pointing to the start frame of the corresponding clip. There can be various types of scene-nodes and various types of path-arches. Every arch coming out from a scene-node is equivalent to an action available to the user at that precise moment of the virtual experience. Mono-directional arches only allow

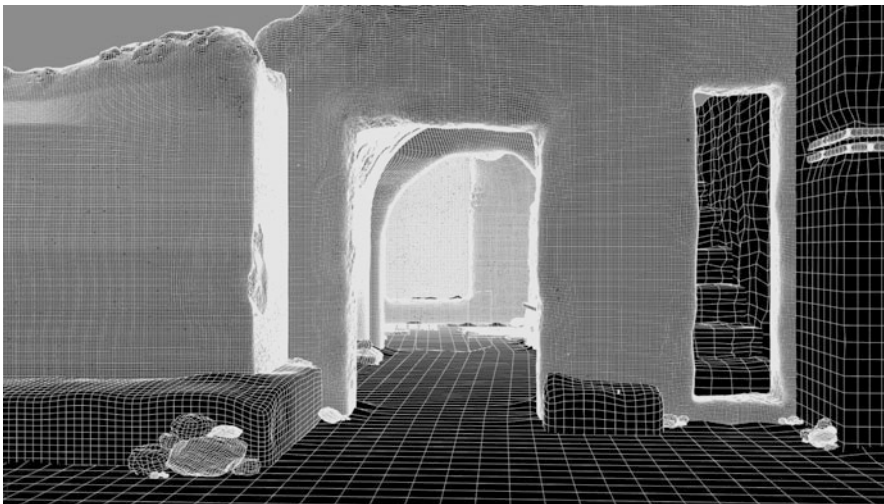


Fig. 1 Wireframe representation of the “B Building” highlighting multiple levels of detail

the user to move from the source node to the destination node according to the direction of the arrow, bi-directional arches represent a single clip that can be played in both directions, whereas two parallel mono-directional arches represent a path that is reversible, but only through two different clips. The heart of this system is the navigation engine, implementing a real time video editing application, which, based on the virtual world design and on the user's input, plays the correct video clip for a given context (Kwatra et al. 2003). Due to the underlying hardware technology, clips previously rendered to be jointed at specific time positions are seamlessly played. This way, the navigation and interaction results in a pseudo real-time experience. For instance, since the hardware architecture is able to play a video sequence in both directions, user can smoothly change his viewpoint (on a given axis) by simply playing a circular seamless pre-rendered animation if that option is available for that particular scene-node.

The hardware equipment necessary for this architecture to work effectively is closely related to the requested image resolution and to the number of clips present in the World-Graph (including all layers, if any). A typical system configuration (for an output resolution of up to 2K+ pixels) requires a RAID-0 server equipped with an array of SATA or Ultra SCSI hard-disks, each one featuring high RPMs and 8–16 Mbytes buffers for more efficient read and write operations. As the RAID-0 operative modality implements a parallel access to all mounted drives, this results in a single virtual disk whose capacity and transfer rate are the sum of the corresponding values of all physical drives. A total of 2–3 Tbytes of storage space is not unusual, allowing the simulation to play up to hours of high resolution uncompressed content with a sustained transfer rate of up to 300+ Mbytes/s. The navigation software runs on the video server, as it has a very low computing load since images are stored uncompressed, and therefore does not require special hardware or powerful processors. However, as high speed data exchange between storage sub-systems and video frame-buffers is crucial for this architecture, 2 Gbytes of RAM (used as content buffer) and a fast system bus (PCI-Express) are required. The graphic subsystem is based on a workstation class graphic board, which is not used for polygon processing but for its high pixel fill-rate, driving simultaneously two monitors or projectors in passive stereo, or just one in active stereo through a quad buffered output.

User interaction is accomplished through a motion tracking system, which detects the hand and/or head position in 3D space, plus their rotation on three axes for up to 6° of freedom (Christopoulos et al. 2003). In our experiments, we used the IS 900 ultrasonic based motion tracking hardware from Intersense Inc., able to precisely acquire and process motion data coming from each of the two wireless devices the user can wear: a head tracker and a joypad (Fig. 2). The keypad features a programmable multi button interface and an analogous joystick which can be used to trigger specific actions. In our implementation, we developed an iconic context dependent on the graphical interface showing either actions or camera options available at a given stage of navigation. These icons appear as an overlay drawn in real time over the video content, and allow the user to visualize not only which option is available (to change the viewpoint, to move forward or backward, to choose a new



Fig. 2 User wearing wireless trackers and stereoscopic goggles during navigation through the reconstructed environment

path, etc.), but even how to select it. In fact, the user can select the desired action by simply moving the head toward the corresponding icon and confirming the selection via the wireless keypad (a button-icon colour based correspondence and an animated confirmation simplify this task). With regard to the rendering issues, advanced computer graphics techniques like depth-map based modelling and high resolution displacement mapping have been exploited in order to render the aspect of most surface typologies, not how they originally appeared, but again respecting the state in which they were found. As we did not need real-time calculations, we were free to use even the most demanding lighting algorithms, like global illumination, and the most realistic shaders. Finally, the model has been optimised and made available for active stereoscopic visualization (Sawhney et al. 2001). During the completion of the system, additional info such as text, actual photos or drawings can be visualized onto the rendered scene, augmenting it, if requested by the user.

References

- Christopoulos D, Papaioannou G, Gaitatze A (2003) Enhancing virtual walkthroughs of archaeological sites. In: Proceedings of ACM/Eurographics VAST 2003, Brighton, UK
- Debevec P, Taylor CJ, Malik J (1996) Modeling and rendering architecture from photographs: a hybrid geometry and image-based approach. In: SIGGRAPH 96 Conference Proceedings

- Di Maio G, Stefani G (2003) Sulla linea di costa, il corso del fiume Sarno e gli insediamenti del quartiere fluviale: Considerazioni sulla linea di costa del 79 d.C. e sul porto dell'antica Pompei. *Rivista di Studi Pompeiani* 14:141–245
- Kwatra V, Schödl A, Essa I, Turk G, Bobick A (2003) Graphcut textures: image and video synthesis using graph cuts. In: *ACM Proceedings of SIGGRAPH*
- Mastroroberto M (2003) Un caseggiato del quartiere sul Sarno (Edificio B), in *Storia da un'eruzione. Pompei Ercolano Oplontis*, Milano, pp 464–472
- Nappo SC (2003) L'edificio "B" di Murecine a Pompei. Un esempio di architettura ricettiva alla foce del Sarno. In: *Archeologia e Storia I*, Salerno, 5–17
- Sawhney HS, Guo Y, Hanna K, Kumar R, Adkins S, Zhou S (2001) Hybrid stereo camera: an IBR approach for synthesis of very high resolution stereoscopic image sequences. In: *Proceedings of SIGGRAPH 2001*

The Study of the Fourth Millennium Mud-Bricks at Arslantepe: Malatya (Turkey): Preliminary Results

C. Alvaro, M. Frangipane, G. Liberotti, R. Quaresima, and R. Volpe

1 Introduction

Arslantepe is located in the Malatya plain (Eastern Anatolia), an oasis in the Anti-Taurus Mountains, 15 km south-west of the River Euphrates. The site is an artificial mound (*tell*), approximately 30 m high and covering a surface of 4 ha, formed by the overlapping deposits of many occupations, built for millennia in the same place. Arslantepe has been occupied without interruption at least from the sixth millennium BC until the Roman and Byzantine periods (Fourth to sixth centuries AD).

The beginning of the excavations (carried out in the 1930s by a French mission) is linked with the discovery of some interesting structures from the twelfth to eighth centuries BC, when Arslantepe/Melid was the capital of a Neo-Hittite Kingdom. From 1961 onwards, the investigations have been carried out by the Italian Archaeological Expedition of the University of Rome “La Sapienza”, presently directed by Marcella Frangipane under regular permission from the Turkish government.

The earliest settlement levels that have been reached so far date to the Late Chalcolithic, Periods VIII (4200–3800 BC), VII (3800–3350 BC) and VIa (3350–3000 BC) of the site sequence. Finds from these periods have shed new light on the origin of cities and on the process of state formation, as monumental mud-brick buildings have come to light on the western side of the mound. In particular, the ones dated to the period VIa have demonstrated the key role of

C. Alvaro (✉), and M. Frangipane

Department of Historical, Archaeological and Anthropological Sciences, University of Rome “La Sapienza”, P.le Aldo Moro 5, 00185 Roma, Italy
e-mail: jovina@inwind.it

G. Liberotti, R. Quaresima, and R. Volpe

Department of Chemistry, Chemical Engineering and Materials, University of L’Aquila, Monteluco di Roio, 67100 L’Aquila, Italy

Arslantepe in the period marking the origin of “cities” and of early state organisations. Arslantepe was in fact one of the main proto-state centres at the end of the fourth millennium BC, and one of the “poles” of “urbanisation” in the north-Mesopotamian region (Frangipane 1993).

The study of the constructions and of the materials used is aimed at the reconstruction of the technologies employed (mud-brick raw material provenance, production process, relation between material properties and “know-how”) and their cultural context. In this paper, the study of buildings excavated from period VII is reported, including data on building function, distribution, function of rooms, as well as on building technology.

2 Archeological Features

A large complex of monumental structures from period VIa had both an administrative and religious function, and testifies to the important development of the centre during this time. In the north side of this public complex, the presence of residential buildings in a topographically high position suggests that there may have existed forms of diversification within the settlement, perhaps with an architecturally predominant area in the south-western zone. What is certain, in any case, is the significant extent of the Late Chalcolithic settlement, which seems to cover the entire area now occupied by the *tell* (Alvaro 2004).

Some very large monumental buildings, with stout mud-brick walls and a stone base, seem to date back to the previous period, VII (Fig. 1), and were discovered in a direct sequence under the structures from period VIa. In the north-eastern area of the mound, at the periphery of the site, there are one- or two-roomed mud brick dwellings, working areas with ovens, and burials under the floorings of the houses.

Higher up, at the top of the mound, impressive official buildings were located, grouped together in different sectors: in the northernmost parts of the settlement were situated the working and storage areas, and the “private” elite buildings; south of these structures, a large tripartite ceremonial building (according to the Mesopotamian architectural traditions) was found, which was probably a temple. Thus, it might be said that period VII is characterized by a large number of superimposed building levels, a considerable extension and an interesting differentiation of building and room functions. The extensive excavation that has been carried out in the last 20 years allows the identification, by means of diachronic reading, of the changes occurring in the localization, type, function and use of internal and external spaces. Hence, on the basis of these observations, coupled with the analytical study of the materials used in the constructions, it will be possible to shed new light on the architectural characteristics and reconstruction hypotheses in the crucial periods of the formation of monumental public areas.

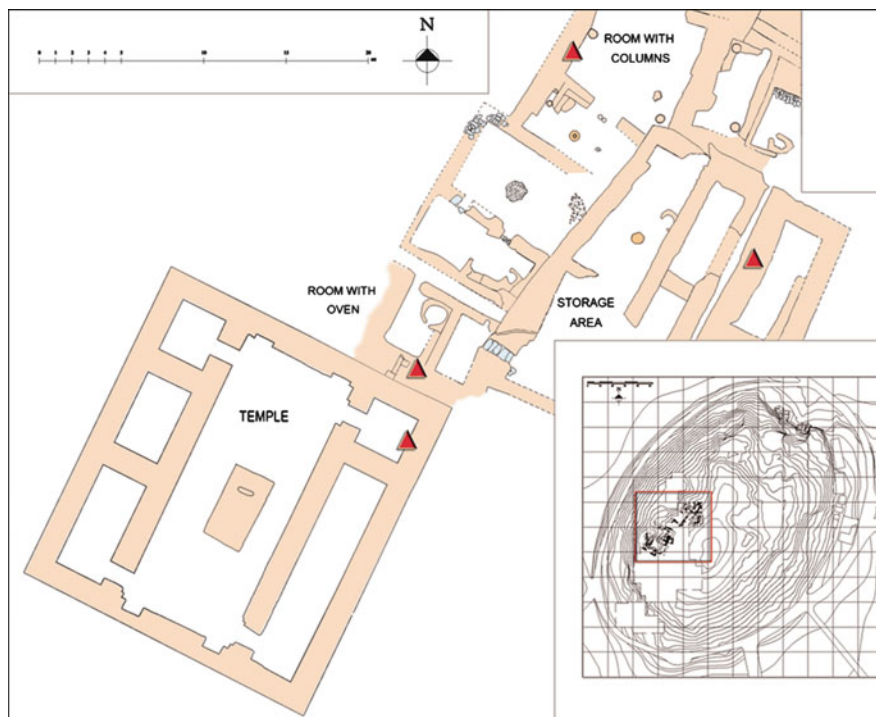


Fig. 1 Map of some buildings from period VII. *Red triangles* indicate the sampling locations

Table 1 Sample numbers of the mud-bricks and characteristics of the setting

Sample number	Characteristics
1–8	Square E6(1), Room A582: huge wall room (1–1.20 m thick) with double rows of mud-bricks varying in texture along the edges and presence of columns made of mud or of mud and pieces of mud-bricks. The building, walls and columns are plastered and painted, and should have had an important function (dwelling of chiefs or high rank families).
9–10	Square D7(3), Room A853: smaller room, distinct owing to the fact that it contains a large oven. With respect to the previous room, these walls are thicker, with traces of red and black painting plaster.
11–12	E6(11), Room A842: very long room which belongs to a probable storage area with other similar proximate rooms. Here the mud-bricks were laid down more regularly than in the other cases.
13–16	Square D7(7), Room A950: small room of a large tripartite ceremonial building, measuring 22 × 20 m, probably a temple, standing on a platform of huge stone slabs and wooden poles.

3 Characterization of the Mud-Bricks

During the last two excavation campaigns (2006 and 2007), 16 samples of mud-bricks have been selected, according to the Nor.Ma.L Recommendation (Nor.Ma.L 1980), from four different walls belonging to the Late Chalcolithic Period VII context. The features of the samples collected are reported in Table 1.

The samples collected were characterised by means of:

- Light microscopy (LM) for the observation of the macroscopic aspect, as well as of the fine particles
- X-ray powder diffraction (XRD), in order to characterize the main mineralogical phases of random and oriented samples

Table 2 XRD results: mineralogical phases of the random and oriented samples

Sample number	Crystalline and clayey phases
1	Calcite, quartz, anorthoclase, plagioclase (§), ankerite, gypsum, halite, phyllosilicates (palygorskite, smectite, chlorite, illite, kaolinite, mixed layers illite/smectite)
2	Calcite, quartz, plagioclase, ankerite, dolomite, halite, phyllosilicates (palygorskite, smectite, chlorite, illite, kaolinite, mixed layers illite/smectite)
3	Calcite, quartz, anorthoclase, plagioclase (§), dolomite, halite, phyllosilicates (palygorskite, smectite, chlorite, illite, kaolinite, mixed layers illite/smectite)
4	Calcite, quartz, plagioclase, ankerite, gypsum, halite, phyllosilicates (palygorskite, smectite, chlorite, illite, kaolinite, mixed layers illite/smectite)
5	Calcite, ankerite, quartz, plagioclase, halite, phyllosilicates (palygorskite, smectite, chlorite, illite, kaolinite, mixed layers illite/smectite)
6	Calcite, quartz, plagioclase, halite (§), phyllosilicates (palygorskite, chlorite, kaolinite)
7	Calcite, quartz, ankerite, dolomite, plagioclase (§), halite (§), phyllosilicates (palygorskite, smectite, chlorite, illite, kaolinite, mixed layers illite/smectite)
8	Calcite, quartz, plagioclase, halite (§), ankerite (§), dolomite (§), magnesioriebeckite (§#), phyllosilicates (palygorskite, smectite, chlorite, illite, kaolinite, mixed layers illite/smectite)
9	Calcite, quartz, plagioclase (§), halite (§), gypsum (§), dolomite (§), phyllosilicates (palygorskite, smectite, chlorite, illite, kaolinite, mixed layers illite/smectite)
10	Calcite, quartz, plagioclase, halite (§), gypsum (§), phyllosilicates (palygorskite, smectite, chlorite, illite, kaolinite, mixed layers illite/smectite)
11	Calcite, quartz, plagioclase, ankerite, dolomite, gypsum (§), sylvite (#), phyllosilicates (palygorskite, smectite, chlorite, illite, kaolinite, mixed layers illite/smectite)
12	Calcite, quartz, plagioclase (§), ankerite, dolomite (§), halite (§), gypsum (§), phyllosilicates (palygorskite, smectite, chlorite, illite, kaolinite, mixed layers illite/smectite)
13	Calcite, quartz, plagioclase, phyllosilicates (palygorskite, smectite, chlorite, illite, kaolinite, mixed layers illite/smectite)
14	Calcite, quartz, plagioclase, phyllosilicates (palygorskite, smectite, chlorite, illite, kaolinite, mixed layers illite/smectite)
15	Calcite, quartz, plagioclase, gypsum (§), phyllosilicates (palygorskite, smectite, chlorite, illite, kaolinite, mixed layers illite/smectite)
16	Quartz, calcite, plagioclase (§), gypsum (§), phyllosilicates (palygorskite, smectite, chlorite, illite, kaolinite, mixed layers illite/smectite)

Legend: (§) traces; (#) possible attribution

- Determination of the water content (oven drying at 105°C)
- Helium pycnometry and dry flow porosimetry to measure density and porosity
- Scanning electron microscopy (SEM) with energy dispersive system (EDS), in order to assess morphological and chemical features
- X-ray fluorescence (XRF), in order to determine the chemical composition

Microscopy showed that the addition of natural fibres was a common practice. It is known that such addition was carried out in order to increase the performance of the mud-bricks (to increase the tensile strength and to decrease the quantity of raw material). The additions also created an interconnected system of macro- and mesoporoses able to contribute to the durability of both the mud-bricks and the structure as a whole. For these reasons, the water content in the samples is also very low (around 2%).

XRD results, reported in Table 2, showed that all samples have the same mineralogical composition (calcite, quartz, plagioclase, phyllosilicate, gypsum and/or dolomite), but in different proportions. The raw materials are extracted from calcareous soils (Palmieri and Morbidelli 2007; Palmieri and Marcolongo 1993; Palmieri and Cellai 1983) around Arslantepe which contain quartz and phyllosilicates. The different plasticity of samples is correlated with the nature and quantity of the phyllosilicates detected (kaolinite, smectite, chlorite, illite and palygorskite).

The presence of gypsum in some samples, even as traces, must be carefully interpreted: was this compound usually present in the raw material due to the origin of the soil, or was it used to stabilize the mud-bricks? Analyses on soils of the mound and from the surrounding area are in progress. XRF results show that the elemental composition of the samples is similar, but with some variation. This

Table 3 Chemical and physical characteristics of the sampled mud-bricks from Arslantepe (Malatya)

Sample number	Al %	Mg %	Fe %	Si %	Cl %	K %	Ca %	Porosity %	Density (g/cm ³)	Bulk density (g/cm ³)
1	5.9	4.9	7.2	29.4	3.8	6.4	40.3	27.9	2.618	1.192
2	4.0	4.6	4.5	17.8	9.0	5.1	53.7	38.3	2.651	1.635
3	5.8	7.2	5.4	28.3	3.1	7.0	41.9	41.5	2.633	1.552
4	6.2	7.7	5.9	29.6	2.2	6.5	40.1	29.0	2.651	1.882
5	4.5	10.9	5.9	25.2	2.3	5.4	43.8	36.4	2.651	1.685
6	4.1	6.0	5.0	19.5	12.1	6.2	45.9	40.4	2.651	1.580
7	5.2	9.2	6.6	27.7	2.4	5.9	41.2	28.6	2.654	1.883
8	7.3	6.5	8.7	31.5	2.5	7.2	34.4	22.0	2.665	2.079
9	6.0	5.3	6.2	25.4	1.4	4.5	49.5	a ₋	a ₋	a ₋
10	9.7	5.4	8.6	37.9	0.9	5.8	29.8	36.6	2.830	1.681
11	6.9	6.1	7.1	29.8	4.1	6.4	37.7	38.5	2.651	1.631
12	6.8	6.5	6.6	29.1	1.2	4.7	43.8	38.9	2.714	1.651
13	9.9	5.5	7.7	37.8	0.8	6.1	30.7	a ₋	a ₋	a ₋
14	8.7	5.3	8.5	34.8	5.1	6.8	28.5	23.2	2.651	2.023
15	8.3	5.2	8.1	35.8	0.8	5.6	34.3	a ₋	a ₋	a ₋
16	11.1	4.7	11.3	41.1	2.8	7.0	19.4	23.5	2.714	2.077

^aNot determined, due to insufficient sample available

aspect must be investigated further. Much of the work currently in progress is aimed at developing an interdisciplinary method based on an integrated historical and scientific approach, in order to assess archaeological issues, but also to design materials and technologies for the conservation of the entire area. Part of the chemical and physical results is reported in Table 3.

References

- Alvaro C (2004) Il più antico complesso palatino: architettura del palazzo di Arslantepe. In: Frangipane M (ed) *Alle origini del potere, Arslantepe, la collina dei leoni*. Electa, Milano, pp 60–61
- Frangipane M (1993) Local components in the development of centralized societies in Syro-Anatolian regions. In: Frangipane M, Hauptmann H, Liverani M, Matthiae P, Mellink M (eds) *Between the rivers and over the mountains, archeologica Anatolica et Mesopotamica Alba Palmieri dedicata*, Dipartimento di Scienze Storiche, Archeologiche ed Antropologiche dell'Antichità. Università degli Studi di Roma "La Sapienza", Roma, pp 133–161
- Nor Ma L (1980) *Materiali Lapidèi: campionamento*, Doc. n.3/80,CNR-ICR (eds) Roma
- Palmieri AM, Cellai L (1983) Sedimentological data for the history of tell. *Origini* XII/2:629–636
- Palmieri AM, Marcolongo B (1993) Environment, water supply and cultural development at Arslantepe (Malatya Turchia). *Origini* 2:619–628
- Palmieri AM, Morbidelli P (2007) XRD and ICP analyses of some Arslantepe *Cretulae* fragments and clay samples from the region: characterization and archaeological implications. In: Frangipane M (ed) *Arslantepe Cretulae. An early centralized administrative system before writing*, Università di Roma "La Sapienza" Dip. Scienze Storiche. Archeologiche e Antropologiche dell'Antichità, Roma, pp 406–414

Intra-Site Testing Using Magnetometry and Shovel Test Pits in the Podere Funghi near Poggio Colla (Florence, Italy)

R. Sternberg and S. Bon-Harper

1 Introduction

The Podere Funghi is an Etruscan ceramic production site adjacent to Poggio Colla, a hilltop ritual center in the Mugello Valley (Vicchio, FI). Prior to our study a workshop and set of kilns had been excavated at the Podere Funghi, and an adjacent dump and surface scatters suggested additional occupation and ceramic producing activities elsewhere in the field (Warden 2007; Fedeli and Warden 2006; Warden et al. 2005; Warden and Thomas 2003; Gleba 2003). The present study, conducted in 2007 and 2008, combined subsurface archaeological testing with geophysics in an attempt to investigate other evidence of past activity on the site. At the same time, our work in adjacent fields explored the extent of ceramic-related industries of this and other time periods.

Subsurface archaeological testing on this project included the excavation of 50 cm shovel test pits (STPs) in the plow-disturbed deposits, or plowzone, at five meter intervals across the site. The recovery of artifacts at this interval provides evidence for the extent of occupation and its temporal and spatial variability. The success of identifying occupation remains with this method of sub-surface testing is based on the integrity of spatial relationships of artifacts in plowzone and the ability to detect those artifacts, in this case by using shovel test pits of an appropriate size at an appropriate interval (Bon-Harper et al. 2003; Dunnell and Simek 1995; Lightfoot 1986; O'Brien and Lewarch, 1981; Shott 1995). The testing interval and pit size were established considering the spatial autocorrelation indicated by a preliminary grid of thirty STPs in the field and with consideration for the time and labor needed to dig the grid of STPs across the remaining portions of the field (Schiffer et al. 1978). Shovel-testing is an established method of site detection used particularly in forested areas of the eastern United States (Lightfoot 1986; Shott 1985). However,

R. Sternberg (✉)

Department of Earth and Environment, Franklin & Marshall College, Lancaster, PA 17603, USA
e-mail: rob.sternberg@fandm.edu

S. Bon-Harper

Monticello Department of Archaeology, PO Box 316, Charlottesville, VA 22902, USA

STPs are rarely employed in the heavily agricultural Mediterranean, where surface visibility allows site detection from pedestrian surveys (cf. Alcock and Cherry 2004; Terrenato 1996). In addition, the application of shovel-testing to intra-site spatial analysis is innovative in both the U.S. and Italy.

Archaeological geophysics is commonly used to locate archaeological sites and to identify structures and artifacts within sites (Gaffney and Gater 2003; Sarris and Jones 2000). We initiated magnetometry in the Podere Funghi primarily to search for buried kilns and piles of kiln wasters. However, magnetics can also be used to search for soil disturbance, burning related to domestic activities, and concentrations of magnetized artifacts, either metals or fired clay. The co-examination of the magnetic and STP data sets, which reveal related signatures of human activity through independent methods, might provide additional insight into identification of use areas and an even more comprehensive landscape archaeology (Kvamme 2003; Venter et al. 2006).

2 Methods

Shovel-test sampling: We excavated a 50 cm round shovel test pit every 5 m on an orthogonal grid. Each pit was excavated to the base of plowzone, whether it ended on bedrock or non-plowed archaeological strata beneath. All sediment was screened through quarter-inch (6 mm) mesh, and artifacts collected.

Magnetics: We used a hand-carried cesium vapor magnetometer for our survey instrument, and a proton precession magnetometer as a base station. Line spacings were 0.5–2.0 m, and measurements were taken every 0.2 s. Eight grids were done, five in the Podere Funghi (two overlapping, only one of which is reported here), and three more in adjacent areas (not reported here), for a total of more than 78,000 measurements over an area of 1.1 ha. Positions were determined with a combination of GPS and total station measurements.

3 Results

The shovel-test sampling and magnetometry yield independent views of the same study area (Fig. 1).

Overlapping areas of interest identified by both methods are a robust indication of archaeological potential, particularly the presence of kilns.

High-density points in the artifact scatter may include domestic middens and also kiln dumps, likely adjacent to kilns themselves. The magnetics reveal a dipole anomaly in one of the highest-density artifact concentrations (1065 N, 1010 E). This area along the western edge of the site is adjacent to an excavated midden that also contained kiln wasters. Our methods have likely identified elements that could be the remains of a kiln and nearby dump of kiln wasters.

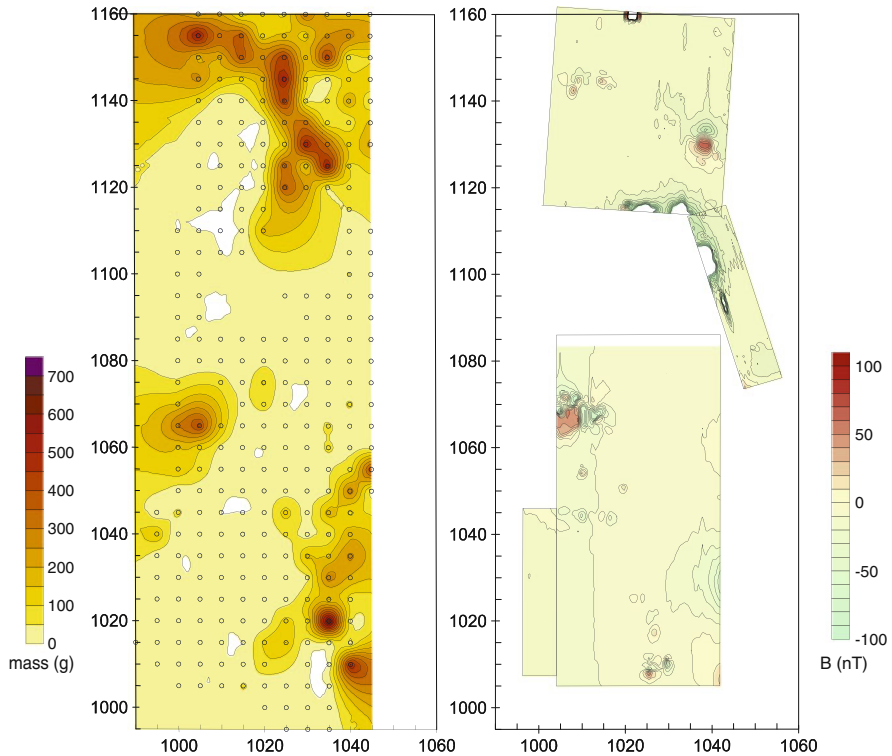


Fig. 1 Contour maps from the Podere Funghi of artifact distribution and magnetometer results. Grid coordinates given in meters. Grid north, which is approximately true north (also downhill), towards *top of page*. Blank areas on both maps indicate areas excavated during previous archaeological campaigns

Further magnetic anomalies along the eastern edge and in the southeastern corner of the field also correspond to relatively high concentrations of artifacts and confirm knowledge already gained from the surface scatters of artifacts while the field was still under cultivation. One additional area of correspondence is in the northeast quadrant of the site, just downhill from the excavated ceramic workshop (1130 N, 1040 E). This may be a kiln or high concentration of kiln debris.

Comparison of the two datasets allows us to interpret an artifact concentration on the hillslope (1140 N, 1025 E) without correspondence to a magnetic feature as downslope artifact movement from the building or the scatter discussed just above.

A final area of interest is in the northwestern corner of the field at the foot of a short, steep slope. A concentration of artifacts occurs here (at approximately 1155 N, 1010 E). It may be a scattering of debris relocated from the known workshop by gravity and plowing. However, the location of this concentration near several small magnetic anomalies (at 1145 N, 1010 E) may suggest that there was occupation or production activity on that part of the site as well.

4 Discussion

The returns from systematic sub-surface testing and artifact recovery concurrent with geophysical survey exceed those from simply ground-truthing following the detection of magnetic anomalies. Such combined work has the capability to provide chronological and contextual evidence for any geophysical anomalies, and to create side-by-side datasets for comparison. An example from the adjacent field to the north underscores the importance of integrating these two testing methods. Magnetic survey in that field indicated a large dipolar magnetic anomaly of approximately 12×13 m (Fig. 2). Archaeological coring in 2007 initially suggested a level of fill and reddening of the soil by burning. Further test excavations in the 2008 season revealed an eighteenth or nineteenth century tile dump. Excavation did not continue to sterile layers, but the most parsimonious explanation is that the modern tile dump overlies a kiln of the same period, and the burning evidenced in the 2007 core was due to a recent tile kiln rather than an Etruscan-period one. Simultaneous geophysical and sub-surface archaeological testing with the recovery of artifacts would have readily provided evidence to date the anomaly. The lesson to be learned from this example is that the combination of these methods adds to the strength and speed of interpretation.

A few of the high amplitude, short wavelength magnetic anomalies on the map were identified during the 2008 field season as being due to the presence of rebar

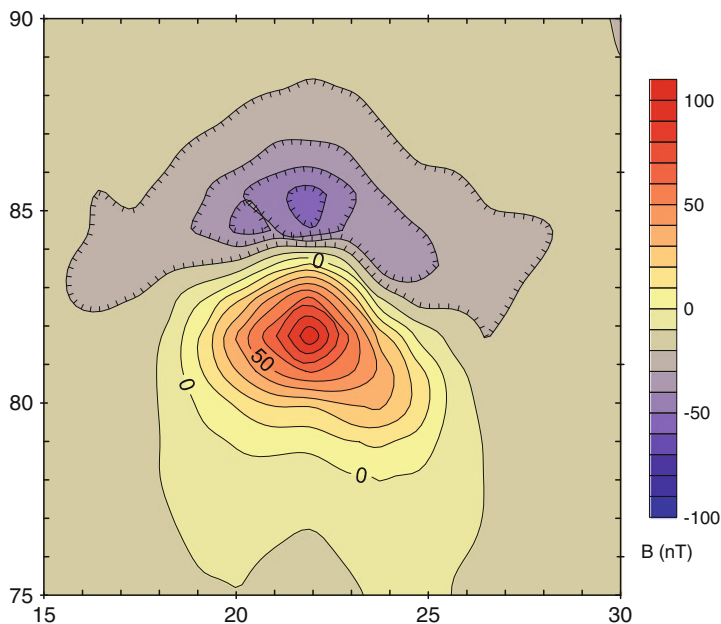


Fig. 2 Dipolar anomaly contour map from the field north of the Podere Funghi. Relative grid coordinates given in meters. Grid north, which is approximately true north, towards *top* of page

stakes. These anomalies do not correlate with STP artifact anomalies, as would be expected. Future data reduction will smooth the anomalies due to identified rebar, and include improved magnetics data collected during the 2008 season.

5 Implications

This combination of testing methods provides a glimpse of archaeological resources across the entire field surrounding an excavated ceramic workshop in the Podere Funghi. The extent of the remains is known within a certain resolution. We have learned enough to direct future excavations (in the southeastern corner of the field and off the northeastern corner of the excavated building), and we have established that there were not other large workshop buildings similar to the one previously excavated.

Our research in the adjacent field did not reveal additional Etruscan kilns. It did show a diachronic component in local clay extraction and the production of ceramic tile. Based on evidence of kilns on the flanks of Poggio Colla and in the fields adjacent to the Podere Funghi (Winkler et al. 2005), we suspect that this part of the valley may have functioned as a locus of extensive clay-related industries throughout its settlement history. Our future research will continue to investigate other industrial installments in adjacent fields, perhaps finding contemporary Etruscan ones, and perhaps finding other more recent elements. Our combined methods will prove effective tools in this task.

6 Conclusions

The correlation between artifact scatters and magnetic anomalies may suggest causative features that produced them both. Large magnetic anomalies could be kilns, and smaller amplitude magnetic anomalies may relate to habitation or other activity areas. The concentration of fine wares, which were produced in the known kilns at the Podere Funghi, is highest near the suspected kiln. Concentrations of all artifacts show peaks in the same area, and also in the southeast and western edge of the test area.

The layering of additional independent methods may provide further methodological direction for archaeological research. Our fieldwork in 2008 included research supported by the Keck Geology Consortium by a team of six undergraduate geosciences students. These students further examined the Podere Funghi using magnetometry, magnetic susceptibility, soil phosphate analysis, chemical and clay characterizations, and geomorphological interpretation, as well as contributing to the excavation of the completed grid of STPs discussed here. Combined, these data sets will provide a layering of research methods that may be able to further identify common areas of interest.

Acknowledgments We gratefully acknowledge the support of the Mugello Valley Archaeological Project and its directors. The Etruscan Foundation provided support for fieldwork with its 2008 Research Fellowship awarded to SB-H. The Keck Geology Consortium provided support for the 2008 field season, including some of the STP work. We also thank Franklin & Marshall College for financial support for RS.

References

- Alcock SE, Cherry JF (eds) (2004) *Side-by-side survey: comparative regional studies in the mediterranean world*. Oxbow Books, Oxford
- Bon-Harper S, Wheeler D, Neiman F (2003) Adjusting the focus: site detection at Monticello. In: Poster presented at the annual meeting of the Society for American Archaeology, Milwaukee, WI
- Dunnell RC, Simek J (1995) Artifact size and Plowzone Process. *J Field Archaeology* 22:305–319
- Fedeli L, Warden PG (2006) Recenti Scavi a Poggio Colla (Vicchio). *Notiziario della Soprintendenza per i Beni Archeologici della Toscana*. Firenze, Soprintendenza Archeologica Toscana: 334–337
- Gaffney C, Gater J (2003) *Revealing the buried past: geophysics for archaeologists*. Tempus Publishing, Stroud
- Gleba M (2003) Archaeology in Etruria 1995–2002. *Archaeological Reports* 49:89–103
- Kvamme KL (2003) Geophysical surveys as landscape archaeology. *Am Antiquity* 68:435–457
- Lightfoot KG (1986) Regional surveys in the Eastern United States: the strengths and weaknesses of implementing subsurface testing programs. *Am Antiquity* 51:484–504
- O'Brien MJ, Lewarch DE (eds) (1981) *Plowzone archaeology: contributions to theory and technique*, 27. Vanderbilt University, Nashville, TN
- Sarris A, Jones RE (2000) Geophysical and related techniques applied to archaeological survey in the Mediterranean: a review. *J Mediterranean Archaeol* 13:3–75
- Shott M (1985) Shovel-test sampling as a site discovery technique: a case study from Michigan. *J Field Archaeol* 12:457–68
- Shott MJ (1995) Reliability of archaeological records on cultivated surfaces: a Michigan case study. *J Field Archaeol* 22:475–90
- Schiffer MB, Sullivan AP, Klinger TC (1978) The design of archaeological surveys. *World Archaeol* 10:1–28
- Terrenato N (1996) Field survey methods in central Italy (Etruria and Umbria): between local knowledge and regional traditions. *Archaeological Dialogues* 3:216–30
- Venter ML, Thompson VD, Reynolds MD, Waggoner JC Jr (2006) Integrating shallow geophysical survey: archaeological investigations at Totogal in the Sierra de los Tuxtles, Veracruz, Mexico. *J Archaeological Sci* 33:767–777
- Warden PG (2007) Poggio Colla: Campagna di Scavo 2006. *Notiziario della Soprintendenza per i Beni Archeologici della Toscana*. Firenze, Soprintendenza Archeologica Toscana: 38–40
- Warden PG, Thomas ML, Steiner A, Meyers G (2005) Excavations at Poggio Colla (1998–2004 excavations). *J Roman Archaeol* 18:252–266
- Warden PG, Thomas ML (2003) Sanctuary and settlement: archaeological work at Poggio Colla (Vicchio di Mugello). *Etruscan Studies* 9:97–108
- Winkler JJ, Tykot RH, Warden PG (2005) Ceramic production and distribution in late iron age Etruria: an example from the Mugello Basin. *Geo- and Bioarchaeological Studies* 3:283–286